Antenna Modeling Notes

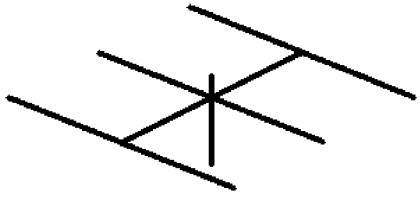

Volume 3

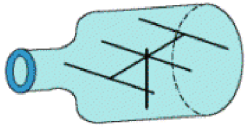

L. B. Cebik, W4RNL

Antenna Modeling Notes

Volume 3

L. B. Cebik, W4RNL

Published by
antenneX Online Magazine
http://www.antennex.com/
POB 271229
Corpus Christi, Texas 78427-1229 USA

Copyright 2004 by **L. B. Cebik** jointly with ***antenneX Online Magazine***. All rights reserved. No part of this book may be reproduced or transmitted in any form, by any means (electronic, photocopying, recording, or otherwise) without the prior written permission of the author and publisher jointly.

ISBN: 1-877992-62-3

Table of Contents

Dedication 6
Preface 7
51. Testing the Fringes of Modeling Programs 9
52. Flipping Among NEC Programs 24
53. Voltage and Current Sources: How? 44
54. GC: Wire Segment Length and Radius Tapering 58
55. Parallel Sources, Angular Junctions, and Average Gain: Correcting "Weaknesses" 73
56. When MININEC is Superior to NEC 92
57. Some Comments on Comments 107
58. Some Basic Guideline Graphics for NEC 120
59. MININEC and NEC: A Design Case Study 135
60. NVIS Antenna Models and the Ground Type 154
61. GM: Coordinate Transformation 176
62. GH: Helix-Spiral Specification 204
63. GH and GM: The NEC-4 Versions 226
64. An Orientation to the NEC Output File 246
65. The 1/2-WL Resonant Dipole as a Core Test Instrument . 265
66. State of the Art? 282
67. Wire Grids 1: Plane and Simple 294
68. Wire Grids 2: Angular and Awkward 310
69. 4-8-16-Infinite Sided Loops 325
70: Refining Physical Transmission-Line Models 341
71: The Average Gain Test Revisited 357
72. The GX or Symmetry Geometry Input 368

73. Source-to-Feedline Matching Techniques 386
74. Some Numerical Green's Function Rudiments 400
75. NEC: Power Efficiency vs. Radiation Efficiency 416
Appendix: Antenna Models 431
Other Publications 433

Dedication

This volume of studies of antenna modeling is dedicated to the memory of Jean, who was my wife, my friend, my supporter, and my colleague. Her patience, understanding, and assistance gave me the confidence to retire early from academic life to undertake full-time the continuing development of my personal web site at the URL, http://www.cebik.com. The site is devoted to providing, as best I can, information of use to radio amateurs and others--both beginning and experienced--on various antenna and related topics. This volume grew out of that work--and hence, shows Jean's help at every step.

Preface

This collection of antenna modeling notes continues the compilation of the series that I began in 1998 in *antenneX*. It contains numbers 51 through 75 of the long-running series that is running even today. The time has come to collect these columns into a more convenient form for the reader. There is just too much material for a single volume, so I have broken the collection into three 25-column units. I have reviewed the text and graphics for each column to ensure as much accuracy as I can muster. However, I have also reviewed the sample models used in each column. That process permitted me to add something to these volumes that is not available in *antenneX* or at my own web site. The Appendix to each of these volumes contains a collection of antenna modeling files in three formats: .NEC (ASCII), .EZ (EZNEC), and .NWP (NEC-Win Plus). I have revised the text to include a file name for the applicable model in the Appendix. Therefore, should you wish to do so, you will be able to read a column in front of your computer and to test for yourself the ideas involved.

This volume includes a potpourri of basic and advanced modeling techniques. At the basic level, there is a collection of graphic charts enumerating many of the DOs and DON'Ts of NEC modeling so that you may extract and keep handy a series of reminders as you construct a model. As well, I have revisited a number of topics to expand the coverage and go a bit more deeply into detail. The episodes on the Average Gain Test (AGT) and the overall contents of the NEC output file are examples.

Several columns devote themselves to comparisons between NEC and MININEC. There are types of models in which one or the other modeling core is superior, and the columns attempt to explore when you should use one or the other. The key limiting factors include both geometry and ground calculation concerns. Although NEC cores are highly uniform in performance, MININEC cores have undergone extensive modification by software developers and are not equally capable over a variety of modeling tasks.

This volume also includes introductions to the use of some of the geometry and command inputs that are not available on most low-end commercial versions of NEC-2. We shall examine the rudiments of the GC (Wire Segment Length and Radius Tapering), GH (Helix-Spiral Specification), GM (Coordinate Transformation), and GX (Symmetry) geometry input cards, as well as introduce the use of the commands related to the use of Numerical Green's Function files. For some of these model inputs, there are differences between the required NEC-2 and NEC-4 entries, and we shall explore some of those differences.

In addition to mastering the various commands, potentials, and limitations of the basic modeling cores, there are a number of fundamental modeling tips and techniques that can be useful in the construction of ever better models. Columns appear in this series in response, normally, to questions that come my way. In this volume, we shall look at the simulation of circular loops by using the required NEC straight wires. Also included is a discussion of using parallel sources in place of complex geometries when two or more wires come together to form a single source wire or segment. A perennial question is how to incorporate into a model frequency-nimble complex impedance matching sections that physically apply directly to the source of an antenna: we shall look at a usable but not universal technique. We shall also explore a small bit of the territory called wire-gridding, the use of wire-grid structures to simulate both simple and complex conductive surfaces.

Although the list of topics seems to grow more advanced and complete, the appearance is an illusion. Indeed, the topics carry us into the use of advanced programs using the NEC and MININEC cores. However, the command set is far too large for coverage even in 3 volumes. As well, good antenna simulations depend as much on the ingenuity of modelers as they do on simply knowing how to apply various commands. Hence, the list of techniques by which to improve our models may well be endless. Mastering antenna modeling software has a further dimension that this volume does not cover: the use of the software to educate ourselves on the capabilities of various types of antennas. If we add this dimension of the use of NEC and MININEC to further mastery of the command structures and additional modeling techniques, then we may fairly predict that the series is far from its final episode.

51. Testing the Fringes of Modeling Programs

In episodes 2 and 3 of this continuing series, I outlined briefly the nature and limitations of programs using NEC cores and those using MININEC cores for antenna modeling calculations. Special limitations applicable to NEC-4 that do not appear in the core manual were outlined in "NEC-4.1: Limitations of Importance to Hams," *QEX* (May/June, 1998), 3-16, and these limitations also apply to NEC-2 as well. The ARRL NEC-2 antenna modeling continuing education course has two lessons specifically devoted to modeling core limitations. Note that I specifically call them core limitations, since a given limitation would apply to every commercial implementation of a given core unless the programmer adds specific correctives. For example, the NEC-2 difficulty—largely corrected in NEC-4—of handling stepped diameter elements is overcome by the introduction of Leeson corrections (calculated substitute elements of uniform diameter) in both EZNEC and NEC-Win Plus. The correctives are programmer additions to the core.

Often, it is difficult to appreciate the nature and extent of core limitations without having access to a variety of programs on which to make comparisons. As well, for simple modeling projects in the HF range, almost any one of the program cores will do a good job. If we combine these ideas, then it might be useful to look at a couple of models that press the cores to their limits—and sometimes beyond—in order to see what various programs do with them. The results can be useful in evaluating the suitability of a given program for the particular range of projects that the modeler has in mind.

The following notes will include these programs:

EZNEC 3.0 Professional Version: NEC-2, NEC-4, and NEC4-D (double-precision)
NEC-Win Plus: NEC-2
NEC-Win Pro: NEC-2
GNEC: NEC-4D
ELNEC: MININEC 3.13 (DOS)
AO: MININEC 3.13 (DOS)
Antenna Model: MININEC 3.13 (Windows)

NEC4WIN-VM: MININEC 3.13 (Windows)
MMANA: MININEC 3.13 (Windows) (freeware)

Although the NEC-4 and NEC-2 cores may seem to be fixed items, they are not. They continue to evolve as new methods emerge for speeding up routines in the dense matrix calculations in the compiled FORTRAN core. As well, because MININEC 3.13 is a public domain program, it has been translated into compiled BASIC, DOS machine coding, and into C++ for Windows operation. The latter steps have largely removed the older 256-segment limitation of earlier implementations. Hence, we can expect some slight variation in results, since implementing the core code in various ways opens the program to the use of various correctives for its other limitations. Expert MININEC, a proprietary newer version of the code with new algorithms, was not accessible for this set of tests.

A Simple Folded Dipole Test

Let's begin with a simple antenna that every core can effectively run: a folded dipole that does not press program limitations. **Fig. 51-1** shows the outlines of the model. See model 51-1.

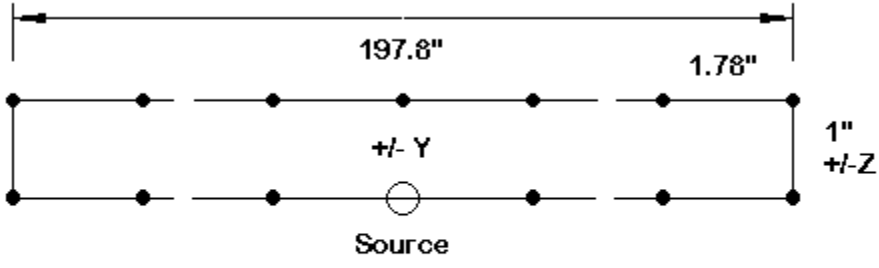

Standard Folded Dipole for 28.5 MHz: MININEC Version
Wire Diameter: AWG #18 Copper

Fig. 51-1

Each long wires is 197.9" (5.0242 m or 0.4776 wavelength) long at the test frequency of 28.5 MHz. The end wires are 1" (0.0254 m or 0.002415 wavelength) long. The end wires have 1 segment each, while the long wires each use 111 segments for NEC models and 110 segments for MININEC models. The heavy segmentation essentially overcomes the MININEC tendency to truncate corner junctions. (NEC4WIN limited the number of segments for the long wires to 50.) The odd-even segmentation difference, of course, relates to source placement. A NEC source appears in the middle of a segment, calling for an odd number of segments for center placement. A MININEC source appears on a pulse or junction of two segments, calling for an even number of segments for center placement on the wire. The source type—voltage or current—makes no difference to the outcome.

The length of the segments is about 0.004 wavelength on the long wires and about 0.0024 wavelength on the end wires, for a segment length ratio of 1.78:1. This value falls within the recommended 2:1 ratio of segment lengths for adjacent segments. The wire diameter is 0.0403", corresponding to AWG #18. This diameter is 1.0236 mm or about 9.73E-5 wavelength, well within recommended limits.

The models were set as Y-coordinate values, with the space between the folded dipole wires appearing on the Z-axis. This orientation presents a “broadside” for the azimuth pattern from which I took gain readings. Had I set the wire spacing on the X-axis, the maximum gain readings would have appeared to be about 0.05 dB higher than those in the table, with an approximate 0.1 dB “front-to-back” ratio. This differential occurs because the wires do not have equal current magnitudes and phase angles at corresponding points. The wire conductivity or resistivity value is for copper wire, although NEC4WIN in Version 3.1 of the program does not have user choices for material losses. Hence, its gain values will be for lossless or “perfect” wire.

The initial model was pruned to resonant length using NEC-4 as the standard. The defined model was then run in programs using other cores. The following table provides the results. Note that AO and NEC4WIN offer several possible combinations of loop and frequency correctives and will have multiple entries. All gain and impedance values are presented in the degree of precision used by the individual programs. NEC-4D means the double-precision version of the NEC-4 core.

Standard Folded Dipole at 28.5 MHz

Program and Core	Free-Space Gain dBi	Source Impedance R +/- jX Ohms
A. NEC Cores		
EZNEC 3.0		
NEC-4	2.10	288.6 - j 0.5613
NEC-4D	2.10	288.5 + j 0.1557
NEC-2	2.10	288.5 + j 0.1875
NEC-Win Plus		
NEC-2	2.10	288.488 + j 0.1597
NEC-Win Pro		
NEC-2	2.10	288.488 + j 0.160
GNEC		
NEC-4D	2.10	288.487 + j 0.153
B. MININEC 3.13 Cores		
ELNEC 3.0	2.098	288.28 - j 4.5420
AO 6.5		
No Corrections	2.09	288 - j 3
Frequency Cor.	2.09	290 + j 7
Bent-Wire Cor.	2.09	288 - j 4
Fr. + B-W Cor.	2.09	290 + j 6
Antenna Model	2.10	288.68 + j 0.6826
NEC4WIN-VM 3.1		
No Corrections	2.13	286.13 - j 2.33
NEC Freq. Cor.	2.13	287.76 + j 10.88
Loop-Wire Cor.	2.15	306.61 + j 104.96
Fr. + Loop Cor.	2.15	308.16 + j 111.01
MMANA	2.06	291.158 - j 4.915

The coincidence of values for both NEC cores illustrates the degree to which the model is well within core guidelines. The ELNEC MININEC result shows a slight capacitive reactance owing to the fact that this program does not implement a frequency corrective. Uncorrected AO results in a similar figure, although with correctives, the impedance values fluctuate around resonance in ways that would be operationally insignificant. The MMANA result appears to reflect a wire conductivity or resistivity assignment that is slightly high, which reduces gain in the hundredths column and increases the resistive component of the source impedance. Although differentials are not operationally significant, the Antenna Model result most closely coincides with the NEC-4 and NEC-4D reports.

The NEC4WIN-VM numbers require further interpretation, since they are for lossless wire. The basic NEC-4 model returns a gain of 2.14 dBi and a source impedance of 286.4 - j 2.47 for this same condition. The uncorrected NEC4WIN numbers correspond well with this value set. The frequency correction offsets the values in a similar way to the frequency correction in AO. (We shall look at frequency issues in a subsequent model.) Clearly, the loop wire correction is not designed for use with closely spaced wires, such as in a folded dipole.

Now let us contrast these results with those for a folded dipole that challenges the limits of the cores. **Fig. 51-2** shows the outlines of the new folded dipole model. We shall retain the 28.5-MHz test frequency. However, we shall reduce the wire diameter to AWG #22, that is, 0.0253", 0.6426 mm, or 6.11E-5 wavelength. As well, we shall reduce the spacing between wires to yield end wires that are much shorter: 0.375", 0.009525 m, or 9.06E-4 wavelength. The basic NEC-4 model became resonant within +/- j 1 Ohm with a length of 199.04", 5.0556 m, or 0.4806 wavelength. See model 51-2.

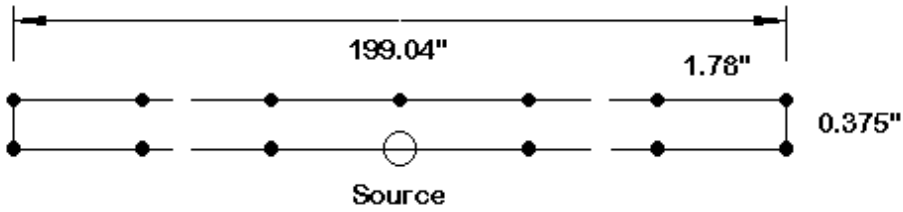

Test Narrow Folded Dipole for 28.5 MHz
MININEC Version
Wire Diameter: AWG #22 Copper

Fig. 51-2

Retaining the 110/111 segmentation density for the long wires and single segments for the end wires, we wind up with segment lengths of 4.33E-3 wavelength and 9.06E-4 wavelength, respectively, for a ratio of 4.78:1. This value exceeds the recommended ratio for adjacent segments in both cores. Further limitations of the cores become apparent when we tabulate the results for all programs.

Narrow Folded Dipole at 28.5 MHz

Program and Core	Free-Space Gain dBi	Source Impedance R +/- jX Ohms
A. NEC Cores		
EZNEC 3.0		
NEC-4	2.07	290.0 - j 0.7181
NEC-4D	2.08	289.8 + j 0.2772
NEC-2	2.08	289.8 + j 0.3964
NEC-Win Plus		
NEC-2	2.08	289.808 + j 0.2683
NEC-Win Pro		
NEC-2	2.08	289.808 + j 0.268
GNEC		
NEC-4D	2.08	289.807 + j 0.264
B. MININEC 3.13 Cores		
ELNEC 3.0	2.074	289.544 - j 6.4580
AO 6.5		
No Corrections	-.09	7.81 - j 61.5
Frequency Cor.	-.27	7.46 - j 59.8
Bent-Wire Cor.	-.09	7.81 - j 61.5
Fr. + B-W Cor.	-.27	7.46 - j 59.8
Antenna Model	2.08	289.459 - j 2.04
NEC4WIN-VM 3.1		
No Corrections	2.19	9.60 - j 73.90
NEC Freq. Cor.	2.20	6.74 - j 62.36
Loop-Wire Cor.	2.31	1.74 - j 46.76
Fr. + Loop Cor.	2.32	1.29 - j 40.10
MMANA	-.51	14.626 - j 58.674

The NEC core values hold up well under the limit pressure applied in this model. Since the wires have a smaller diameter, the gain reduction relative to the model of a standard folded dipole is reasonable. The source impedance for any pair of wires in a folded dipole is approximately 4 times the value of the source impedance for a single wire of the same diameter. Hence, the impedance values are quite sensible as well.

For the most part, the implementations of public domain MININEC yield wholly unreliable results, indicating that the model has exceeded core limitations by an excessive amount. The completely unrealistic source impedance values make any inspection of the gain values otiose. However, the fact that the NEC4WIN gain values are out of line with the AO and MMANA values, even for uncorrected MININEC

calculations, suggests that in redoing the algorithms for Windows, some alteration has occurred.

The ELNEC and Antenna Model value sets, however, are exceptions to the MININEC rule. Both ELNEC and Antenna Model contain close-wire correction factors not used by the other programs. The results are sets of both gain and impedance values that are quite coincident with the values produced by NEC models.

Although we have looked at only two models—folded dipoles that are within and outside normal core limitations—the exercise does indicate the value of comparative modeling. There are differences between the limitations of the cores surveyed. As well, there are also limitations and correctives within implementations of those cores, some of which involve core reprogramming and some of which involve supplemental correction factors. Even correctives bearing similar names in different programs may operate differently. Therefore, it pays to explore the programs by using a series of models that press the limitations to discover just where a given program's limits actually lie.

A UHF Model of a 4-Element Yagi

We have noted a frequency corrective applied to some implementations of MININEC. As we increase frequency, MININEC 3.13 develops a frequency inaccuracy that AO, Antenna Model, and NEC4WIN attempt to correct. ELNEC and MMANA apparently do not have such correction factors.

Interestingly, the AO MININEC correction factors are calibrated to NEC-2. However, NEC-2 also exhibits a frequency-based deviation from the results obtained from NEC-4 models of the same antenna. The deviation become more pronounced in the upper VHF area and above. It is likely that the differences in reports result from changes made for the NEC-4 core in the treatment of the source "gap" and the element end calculations.

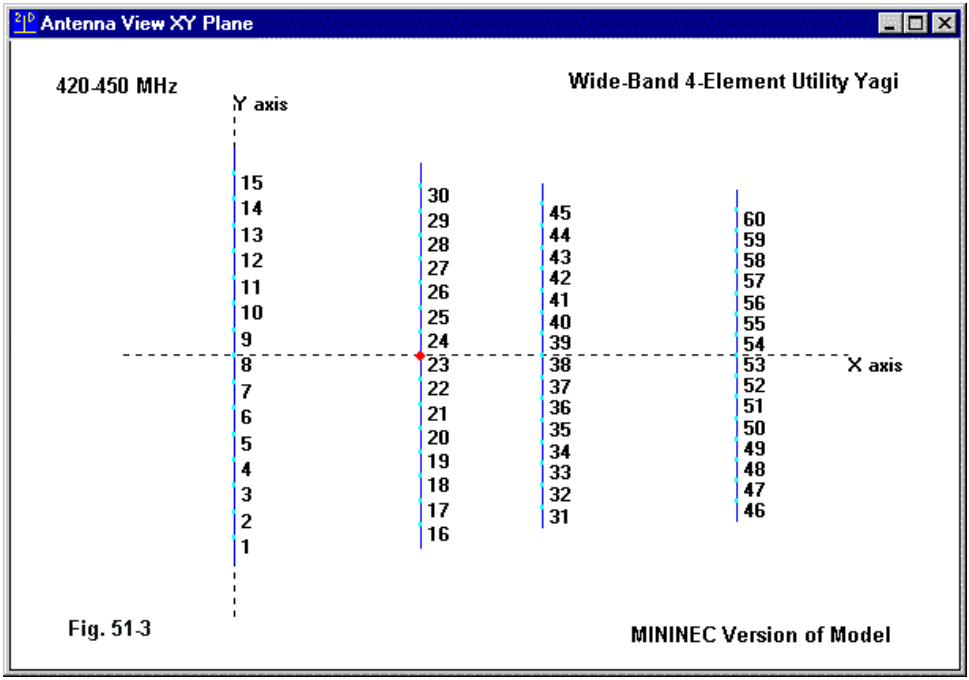

Let's see to what extent the programs display the deviations. **Fig. 51-3** shows the outline of a 4-element utility Yagi designed to have a very low (under 1.25:1) 50-Ohm SWR across the 420-450 MHz band. **Fig. 51-4** shows the NEC-4 SWR curve for the antenna.

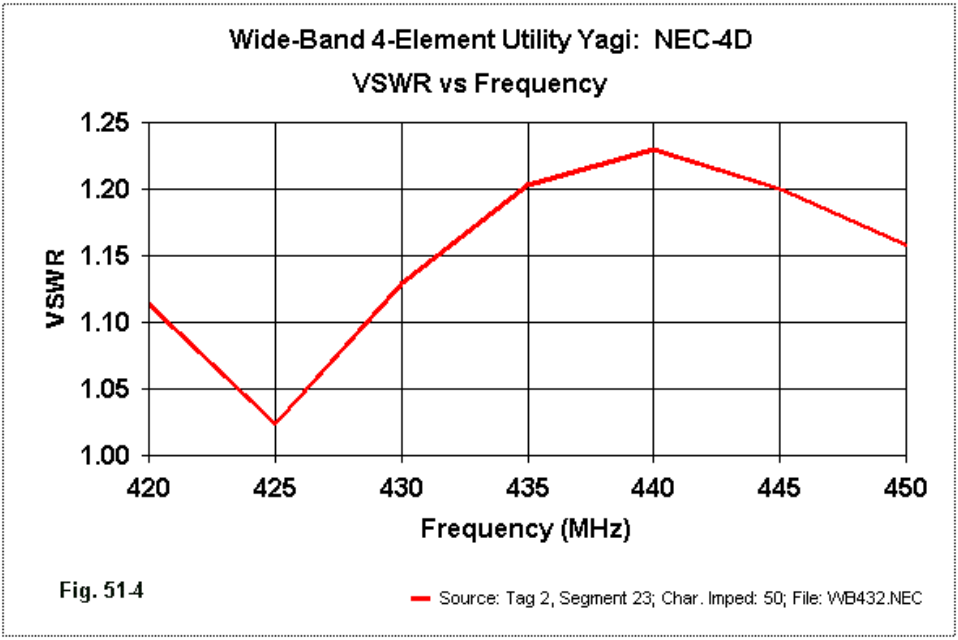

Fig. 51-4

The following listings of EZNEC wire tables provide the dimensions for the antenna in inches, in meters, and in wavelengths. See model 51-3.

```
W4RNL 432 WB Yagi                Frequency = 432  MHz.

Wire Loss: Aluminum — Resistivity = 4E-08 ohm-m, Rel. Perm. = 1
                  ———————— WIRES ————————
Wire Conn.— End 1 (x,y,z : in) Conn.— End 2 (x,y,z : in)   Dia(in) Segs

1          0.000, -6.575,  0.000         0.000,  6.575,  0.000 5.00E-01  15
2          5.807, -6.083,  0.000         5.807,  6.083,  0.000 5.00E-01  15
3          9.626, -5.453,  0.000         9.626,  5.453,  0.000 5.00E-01  15
4         15.748, -5.256,  0.000        15.748,  5.256,  0.000 5.00E-01  15
```

```
Wire Conn.— End 1 (x,y,z : m ) Conn.— End 2 (x,y,z : m )   Dia(mm) Segs

1          0.000, -0.167,  0.000         0.000,  0.167,  0.000 1.27E+01  15
2          0.147, -0.154,  0.000         0.147,  0.154,  0.000 1.27E+01  15
3          0.244, -0.139,  0.000         0.244,  0.139,  0.000 1.27E+01  15
4          0.400, -0.133,  0.000         0.400,  0.133,  0.000 1.27E+01  15
              ———————— WIRES ————————

Wire Conn.— End 1 (x,y,z : wl) Conn.— End 2 (x,y,z : wl)   Dia(wl) Segs

1          0.000, -0.241,  0.000         0.000,  0.241,  0.000 1.83E-02  15
2          0.213, -0.223,  0.000         0.213,  0.223,  0.000 1.83E-02  15
3          0.352, -0.200,  0.000         0.352,  0.200,  0.000 1.83E-02  15
4          0.576, -0.192,  0.000         0.576,  0.192,  0.000 1.83E-02  15

              ———————— SOURCES ————————

Source    Wire      Wire #/Pct From End 1    Ampl.(V, A)  Phase(Deg.)  Type
          Seg.     Actual      (Specified)
1           8     2 / 50.00   (  2 / 50.00)      1.000       0.000       I

Ground type is Free Space
```

The worst case segment length to wire radius ratio is 2.62:1, reasonably well within most program limitations for linear elements with no odd geometric features. The shortest segment is 0.024 wavelength long (with the longest 0.03231 wavelength). MININEC models of the same antenna used 16 segments per element to center the source on wire 2.

In tabulating the results for this model using various programs, it is necessary to sample them at 10 MHz intervals across the 420-450 MHz span. Therefore, each entry consists of four lines forming a progression that will be useful in evaluating the results. Because each data entry is larger, values have been truncated wherever they exceed the column allowance.

Wide-Band 4-Element Yagi for 420-450 MHz

Program and Core	Freq. MHz	Free-Space Gain dBi	Front-Back Ratio dB	Source Impedance R +/- jX Ohms	50-Ohm SWR
A. NEC Cores					
EZNEC 3.0					
NEC-4	420	9.12	11.56	45.81 - j 2.99	1.114

	430	9.23	12.14	56.30 + j 1.51	1.130
	440	9.34	12.73	61.22 - j 2.38	1.230
	450	9.55	14.31	49.46 - j 7.28	1.158
NEC-4D	420	9.12	11.56	45.81 - j 2.99	1.114
	430	9.23	12.14	56.30 + j 1.51	1.130
	440	9.34	12.73	61.22 - j 2.38	1.230
	450	9.55	14.31	49.47 - j 7.28	1.158
NEC-2	420	9.17	11.69	47.77 - j 1.14	1.053
	430	9.27	12.20	58.14 + j 1.51	1.166
	440	9.40	12.92	59.93 - j 4.57	1.221
	450	9.64	14.99	42.72 - j 6.56	1.236
NEC-Win Plus					
NEC-2	420	9.17	11.69	47.77 - j 1.14	1.053
	430	9.27	12.19	58.14 + j 1.50	1.166
	440	9.40	12.92	59.93 - j 4.57	1.221
	450	9.64	14.99	42.72 - j 6.56	1.236
NEC-Win Pro					
NEC-2	420	9.17	11.69	47.77 - j 1.15	1.05
	430	9.27	12.19	58.14 + j 1.50	1.17
	440	9.40	12.92	59.93 - j 4.57	1.22
	450	9.64	14.99	42.73 - j 6.57	1.24
GNEC					
NEC-4D	420	9.12	11.56	45.81 - j 3.00	1.11
	430	9.23	12.14	56.30 + j 1.51	1.13
	440	9.35	12.74	61.22 - j 2.38	1.23
	450	9.55	14.31	49.47 - j 7.29	1.16
B. MININEC 3.13 Cores					
ELNEC 3.0	420	8.95	10.42	38.11 - j 12.47	1.480
	430	9.10	11.58	48.22 - j 3.96	1.092
	440	9.20	12.21	57.67 - j 1.27	1.156
	450	9.33	13.00	59.82 - j 5.36	1.227
(	460	9.58	14.95	46.49 - j 7.08	1.178)
AO 6.5					
No Corrections					
	420	8.95	10.74	39.3 - j 11.4	1.44
	430	9.09	11.81	49.6 - j 3.5	1.07
	440	9.20	12.39	58.6 - j 1.5	1.18
	450	9.34	13.24	59.4 - j 5.7	1.22
Frequency Cor.					
	420	9.02	11.86	47.7 - j 2.8	1.08

	430	9.13	12.30	58.4 + j 1.2	1.17
	440	9.26	12.85	62.6 - j 2.9	1.26
	450	9.49	14.58	49.3 - j 6.3	1.14
Ant. Model	420	9.00	11.55	44.90 - j 4.87	1.160
	430	9.12	12.13	55.80 + j 0.92	1.117
	440	9.24	12.61	62.51 - j 1.39	1.252
	450	9.44	13.96	53.65 - j 6.89	1.162
NEC4WIN-VM 3.1					
No Corrections					
	420	8.95	10.43	38.13 - j 12.49	1.48
	430	9.10	11.58	48.25 - j 3.96	1.09
	440	9.20	12.21	57.74 - j 1.26	1.16
	450	9.33	13.00	59.91 - j 5.38	1.23
Frequency Cor.					
	420	9.45	10.86	48.22 - j 5.77	1.13
	430	9.54	11.59	53.32 + j 12.77	1.29
	440	9.67	12.85	42.13 - j 18.51	1.54
	450	9.92	15.58	23.44 - j 7.82	2.20
MMANA					
	420	8.94	10.41	38.16 - j 12.53	1.48
	430	9.09	11.57	48.28 - j 3.99	1.09
	440	9.19	12.20	57.75 - j 1.28	1.16
	450	9.32	12.99	59.93 - j 5.35	1.23

If we compare MININEC results to the NEC-2/-4 results, we obtain an interesting picture. Uncorrected MININEC gives consistent results in all implementations. However, as the extra line in the ELNEC entry shows, there is nearly a 10 MHz offset in the 420-450 MHz band relative to NEC values. This amounts to an approximate 2- to 2.5-percent difference.

The frequency offset correction operations differ between AO 6.5 and Antenna Model on the one hand and NEC4WIN-VM 3.1 on the other. The AO and Antenna Model corrected values tend to track the NEC-2 figures very well, although there is a slight gain deficit in the MININEC values despite calibration to NEC-2. In contrast, the NEC4WIN corrected values appear to push the NEC-2 values by a frequency offset that is 10% in the other direction than uncorrected MININEC. For example, the source impedance value for 450 MHz (23.44 - j 7.82 Ohms) is not reached by

the NEC models until the frequency is near 470 MHz. As well, the NEC4WIN gain values may be as much as two 10 MHz steps off.

However, we should not neglect the fact that there is also a difference between the NEC-2 and NEC-4 figures. Since all NEC-2 values coincide and all NEC-4 (including both single and double precision) values also coincide, we can glimpse the differentials from looking at the EZNEC values, which are clustered in the table. There is about a 5 MHz frequency offset between NEC-2 and NEC-4. The NEC-2 values for 420 MHz approach those reached in NEC-4 at about 425 MHz, and the progression continues through the passband of the antenna. The progression applies to all of the figures for gain, front-to-back ratio, and source impedance.

The 1+% frequency offset between NEC-2 and NEC-4 at UHF may not seem like much for a wide-band utility Yagi design. However, for a long-boom, narrow-band array that requires precise dimensions for each element, that degree of offset may prove quite significant.

The frequency offset is a function of the fact that the element diameter (0.5") is approaching the length of a segment (average 0.8"). Whenever this condition exists, NEC-2 will return offset results unless one invokes the EK command. This command is not presently available on entry-level software, except for NEC2GO, where it is invoked automatically. However, the command is available on advanced NEC-2 software, such as NEC-Win Pro. If we add the “fat-wire” command (actually labeled the “extended thin wire kernel”), which uses a more complex algorithm for the core calculations, we obtain the following results for a NEC-2 model.

Wide-Band 4-Element Yagi for 420-450 MHz

Program and Core	Freq. MHz	Free-Space Gain dBi	Front-Back Ratio dB	Source Impedance R +/- jX Ohms	50-Ohm SWR
A. NEC Cores					
NEC-Win Pro with EK					
NEC-2	420	9.12	11.52	45.64 - j 2.99	1.12
	430	9.23	12.11	56.12 + j 1.64	1.13
	440	9.35	12.72	61.11 - j 1.23	1.23
	450	9.55	14.29	49.40 - j 7.23	1.16

The end product is a table of values very close to the NEC-4 values. The revised algorithms in NEC-4 resulted in dropping the EK command from the list, since it was no longer required. Whenever the wire diameter is more than half the length of the segments in a NEC-2 model, it is usually wise to invoke the EK command if it is available.

Returning to the MININEC 3.13 programs, we should note that of all the commercial implementations, only Antenna Model yields results in both the close-spaced wire test and the UHF test that track closely with NEC results. AO has an effective frequency corrective and ELNEC has an effective close-wire corrective: Antenna Model has both, plus reported correctives for both standard (quad-type) corner junctions and very narrow (less than 28 degrees) angular junctions. These latter features would require additional tracking tests, with the caution that for very narrow angular junctions, there may be differences in NEC-2 and NEC-4 results.

As with all offsets among programs and program cores, the degree of offset allowable relative to a particular standard depends upon the range of tasks, frequencies, and antenna geometry complexities that define our modeling needs. These notes are designed simply to bring some of the fringe-area phenomena into the open for inspection. The relative importance of each differential is, in the end, a user judgment.

Special Note: The calculating cores supplied with NEC and MININEC are continuously evolving. MININEC cores may undergo changes in the correctives or changes in the program language. NEC cores are compiled Fortran, and compilation programs change and improve from time to time. Hence, for this episode and all of the following ones, you may encounter slight differences in the results you obtain from a model and those in the tables. The tables show the values obtained at the time the column was written. For simple changes in the compilation or programming language of a core, your results should coincide with the tables to about 3 significant digits. More radical differences may indicate (usually with MININEC programs) revisions to the core itself.

* * * * *

Models included: 51-1 through 51-3. (.NEC and .NWP model dimensions in meters; .EZ model dimensions in inches. Due to the variability of systems used to save a MININEC model, only NEC models can be supplied with this volume.)

52. Flipping Among NEC Programs

As the use of antenna modeling software becomes more and more common, it is becoming less unusual to find modelers who possess more than one program. Some earlier DOS-based programs have been supplanted by Windows programs, not always from the same source. For example, the highly respected AO for MININEC 3.13 was a DOS program that is no longer sold (although still widely used). In its place have emerged, in Windows garb, NEC4WIN and MMANA from Canada and Japan, respectively. In addition, there is the highly refined version of MININEC called Antenna Model, from Terisoft in the U.S.

Among NEC users, the most common programs we encounter are EZNEC 3.0 for Windows from W7EL and NEC-Win Plus (one of a collection of programs from Nittany Scientific, with the others being NEC-Win Pro and GNEC for NEC-2 and NEC-4, respectively). In the following notes, we shall confine ourselves to NEC programs, since our topic will be flipping from one program to another: how to do it and what to watch out for. Most of the MININEC programs use file formats that are not directly convertible from one program to the other. However, NEC4WIN can handle some NEC files, while ELNEC MININEC files can be directly read by EZNEC. Nonetheless, we shall have our hands full just converting from one NEC program to another.

The basic file format for the NEC core (-2 or -4) has the extension .NEC. It is an ASCII file, a sample of which appears in **Fig. 52-1**. See model 52-1.

The file is a simple ASCII file that one can produce on almost any simple text editor. To a large degree—but not completely—NEC-2 and NEC-4 files are interchangeable. NEC-4 introduces some new input potentials and revises a few ways of handling some program control cards. However, mainline work involving the sorts of things new users are likely to do rarely involve the differences between core potentials. Hence, moving files from one core to the other is 90% flawless.

```
CM 6-el 2M Yagi
CE
GW 1 21 0 -0.514604 0 0 0.514604 0 0.0023813
GW 2 21 0.257302 -0.50419 0 0.257302 0.50419 0 0.00635
GW 3 21 0.363728 -0.474726 0 0.363728 0.474726 0 0.0023813
GW 4 21 0.658622 -0.461264 0 0.658622 0.461264 0 0.0023813
GW 5 21 0.946912 -0.461264 0 0.946912 0.461264 0 0.0023813
GW 6 21 1.377188 -0.443992 0 1.377188 0.443992 0 0.0023813
GS 0 0 1
GE 0
EX 0 2 11 0 1 0
LD 5 1 1 21 25000000
LD 5 2 1 21 25000000
LD 5 3 1 21 25000000
LD 5 4 1 21 25000000
LD 5 5 1 21 25000000
LD 5 6 1 21 25000000
FR 0 1 0 0 146 1
RP 0 1 361 1000 90 0 1 1
EN
```

Standard Form ASCII .NEC Model File Sample
Fig. 52-1

However, EZNEC and NEC-Win Plus each use proprietary file formats. The .EZ model file is in a format specifically developed by W7EL to fit the needs of his programming of the interface between the model specification and the core. The .NWP file format is based on a spreadsheet input system that allows the program to have some special functions. Bridging the gap Between EZNEC and NEC-Win Plus requires reversion to a .NEC file.

NEC-Win Plus permits saving any model in .NEC format. Some things saved in the .NWP files, such as model-by-equation spreadsheet entries, cannot appear in the .NEC file. The .NEC file is always the file of a specific model with a certain wire table having numeric entries, along with program control cards that reflect these values.

Standard EZNEC 3.0 does not have a provision to import files in .NEC format, nor a provision to save files in this format. However, the Pro version of the program has both potentials. Whether or not one needs the NEC-4 core, if one reaches the point of investing in multiple programs, upgrading to the Pro version of EZNEC may make sense.

The Utility of Multiple Programs

Why bother going from one program to the other? For one reason, the tabular and graphical outputs of the two programs have different styles. We might well find one style more suited to certain data collections or presentations than the other, even if we had done the initial work on the other program.

For example, EZNEC presents data on current magnitudes and phase angles in tables that subdivide the model elements into wires and segments within those wires. For some purposes, this format may be clearer than the NEC-Win tables that use absolute segment numbers. As well, EZNEC presents current data using RMS values, while NEC-Win adheres to the NEC core use of peak values. Often, we find presentation needs that arise only after we have done some modeling work, and Murphy's Law dictates that we shall have done the initial modeling and data collection in the program that does not meet current presentation needs.

Fig. 52-2 and **Fig. 52-3** present partial current data for the model shown in **Fig. 52-1** in EZNEC and NEC-Win format, respectively. The numbers are the same, since the EZNEC source used 1 volt RMS, while the NEC-Win source used 1 volt peak. Hence, the respective RMS and peak values of output data will have the same numerical values.

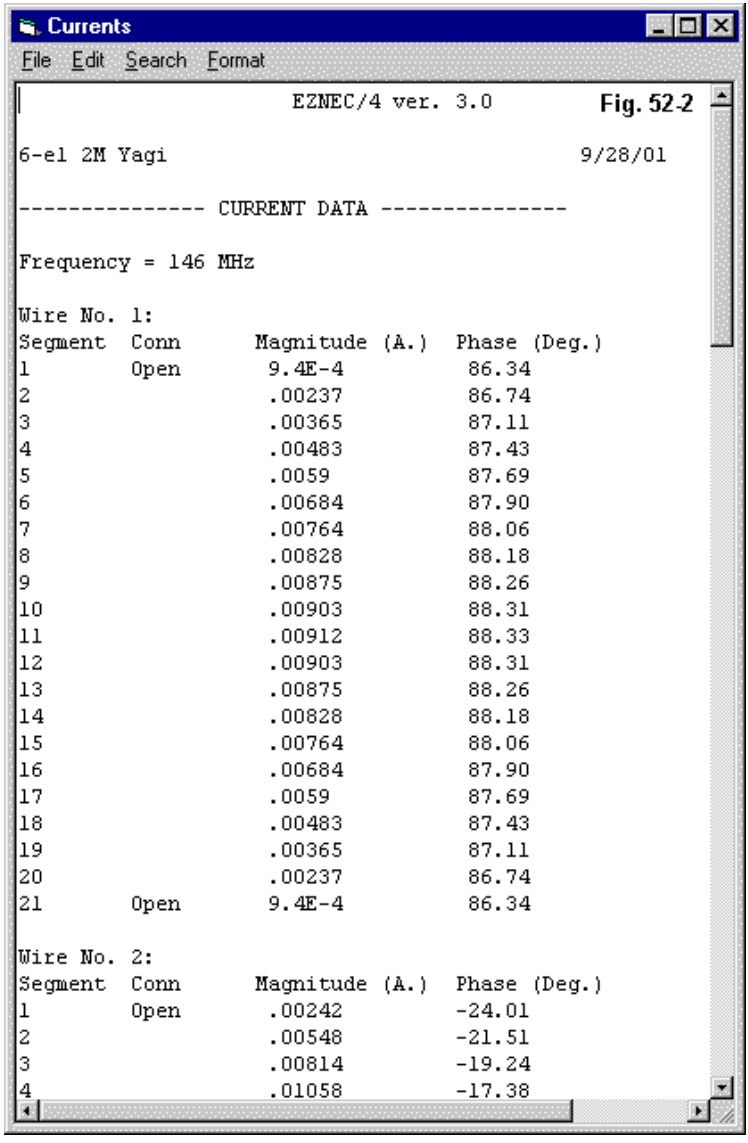
Currents
File Edit Search Format
EZNEC/4 ver. 3.0
Fig. 52-2
6-el 2M Yagi
9/28/01
---------- CURRENT DATA ----------
Frequency = 146 MHz
Wire No. 1:
Segment Conn Magnitude (A.) Phase (Deg.)
1 Open 9.4E-4 86.34
2 .00237 86.74
3 .00365 87.11
4 .00483 87.43
5 .0059 87.69
6 .00684 87.90
7 .00764 88.06
8 .00828 88.18
9 .00875 88.26
10 .00903 88.31
11 .00912 88.33
12 .00903 88.31
13 .00875 88.26
14 .00828 88.18
15 .00764 88.06
16 .00684 87.90
17 .0059 87.69
18 .00483 87.43
19 .00365 87.11
20 .00237 86.74
21 Open 9.4E-4 86.34
Wire No. 2:
Segment Conn Magnitude (A.) Phase (Deg.)
1 Open .00242 -24.01
2 .00548 -21.51
3 .00814 -19.24
4 .01058 -17.38

There are also reasons of convenience for switching programs. Consider **Fig. 52-4**, the wire table from an EZNEC model of a 6-element 2-meter Yagi. My goal was to examine the patterns of this antenna at a height of 20' over real ground with the antenna horizontally oriented and with the antenna vertically oriented. Making the adjustments to the model, initially horizontal, for real ground analysis requires only that I change the antenna height and set up the ground. However, changing the orientation from horizontal to vertical requires a large number of individual wire coordinate-value changes in the Y and Z columns at both ends of each wire.

Wires

Wire Other

Fig. 52-4

☐ Coord Entry Mode ☐ Preserve Connections

Wires

	No.	End 1				End 2				Diameter	Segs
		X (in)	Y (in)	Z (in)	Conn	X (in)	Y (in)	Z (in)	Conn	(in)	
▶	1	0	-20.26	0		0	20.26	0		0.1875	21
	2	10.13	-19.85	0		10.13	19.85	0		0.5	21
	3	14.32	-18.69	0		14.32	18.69	0		0.1875	21
	4	25.93	-18.16	0		25.93	18.16	0		0.1875	21
	5	37.28	-18.16	0		37.28	18.16	0		0.1875	21
	6	54.22	-17.48	0		54.22	17.48	0		0.1875	21
✳											

Fig. 52-5 shows a simpler solution. I saved the free-space horizontal model as a .NEC file and then opened it in NEC-Win Plus. It is immaterial that EZNEC saves files in .NEC format only in meters. Everything will return to inches when we are done. The key is the simple rotation along an axis permitted by NEC-Win Plus. The figure shows the effect on one of the elements of the rotation, although all elements will follow suit, since all were blocked together for the operation.

Note: The technique being described applies to EZNEC 3.0. However, with the release of EZNEC 4.0, users should have access to full wire movement and rotation controls within the Wires table options, as well as the potential for moving wire orientations within the Antenna View system.

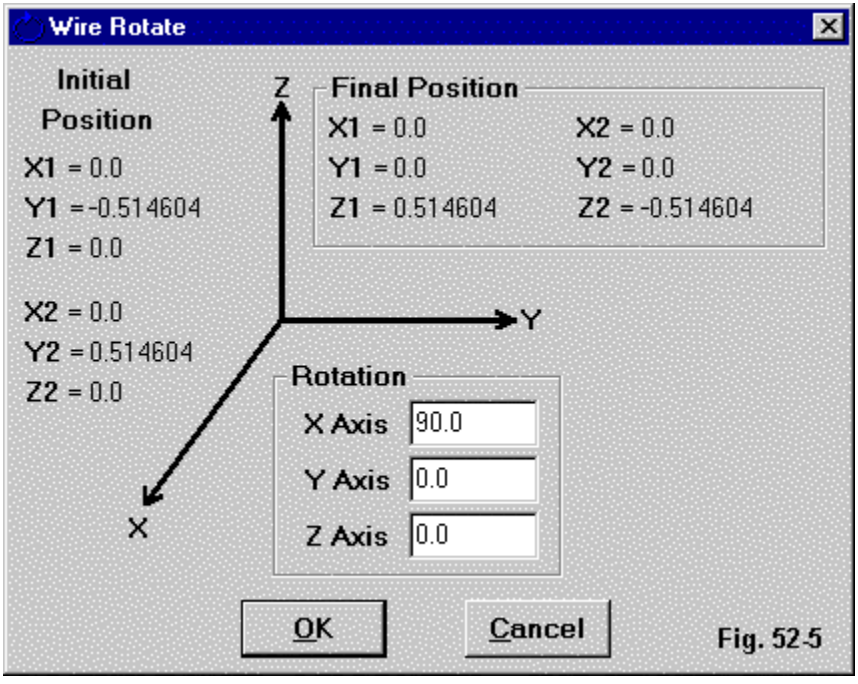

After the rotation operation, I again saved the file in .NEC format from within NEC-Win Plus and reopened it in EZNEC. I then changed the unit of measure back to inches to arrive at the wire table shown in **Fig. 52-6**. I then used the same set-up steps to place the boom of the antenna 20' above real ground.

Not only did I save time, but as well, I saved all of those errors resulting from misplacing and transposing numbers. While the time saving for this model was not great, it mounts up when changing orientations with UHF Yagis up to 43 elements total.

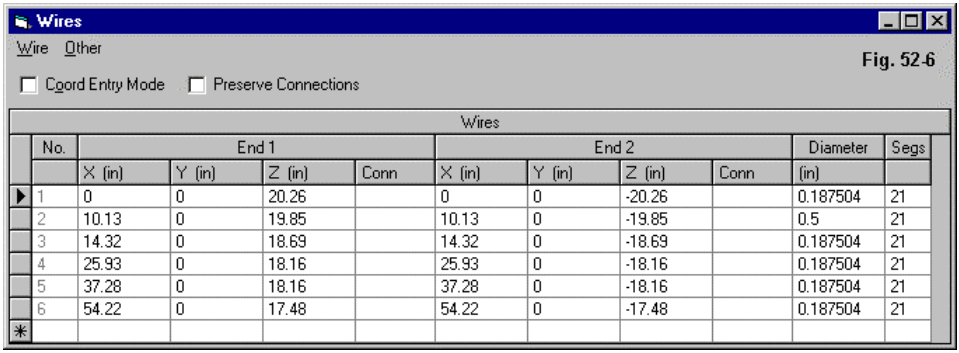

Wires

Wire Other

Fig. 52-6

☐ Coord Entry Mode ☐ Preserve Connections

Wires

No.	End 1				End 2				Diameter	Segs
	X (in)	Y (in)	Z (in)	Conn	X (in)	Y (in)	Z (in)	Conn	(in)	
1	0	0	20.26		0	0	-20.26		0.187504	21
2	10.13	0	19.85		10.13	0	-19.85		0.5	21
3	14.32	0	18.69		14.32	0	-18.69		0.187504	21
4	25.93	0	18.16		25.93	0	-18.16		0.187504	21
5	37.28	0	18.16		37.28	0	-18.16		0.187504	21
6	54.22	0	17.48		54.22	0	-17.48		0.187504	21

Another instance in which switching from one program to another makes good sense is in data collections that can be done more readily on one program than the other. For example, EZNEC permits only one RP0 request, that is a single polar pattern request. Suppose we have created a model in EZNEC and wish now to gather free-space data for both azimuth and elevation patterns (in free-space, E-plane and H-plane patterns) over a frequency sweep of considerable proportions. Since NEC-Win permits the user to specify multiple pattern requests, transporting the model to this program makes sense. As well, the data set is saved in a durable file, so that the output file for a single frequency sweep run can be recalled later for further examination. Such potentials exist for any .NEC file, whether using NEC-Win Plus, Pro, or GNEC.

Going the other way, I sometimes have occasion to need to exactly frequency scale a model. If the model has not been set up in NEC-Win Plus using the model by equation facility, then scaling becomes a manual operation. However, by saving the file in .NEC format and opening it in EZNEC Pro, I can use the automated frequency scaling option in that program. Saving again in .NEC format permits a return to NEC-Win for subsequent operations. A 3-element array is no problem for manual re-scaling. However, suppose we wished to scale a 25-element Yagi originally designed for 432 MHz into a version centered on 224 MHz. The benefits of having both programs available become evident.

These applications for program "flipping" only sample the potential available. However, they will suffice to illustrate the benefits and the process.

Observing Program Limitations

As important as knowing some of the applications for flipping from one program to another is observing and expecting the limitations of moving a model from one program to the other. The programs each have limitations in accepting a .NEC file from the other source.

When opening a .NEC file within EZNEC Pro, the file undergoes a conversion into the standard EZNEC format. Some of the unique characteristics of that format and the program structure require the conversion process to set aside some lines and even to reject a file. For example, it is possible to create and save a .NEC file that lacks an EX line, that is a specification of source conditions. EZNEC will reject such files as incomplete. A basically complete file will require a set of wire geometry lines (GW), a source (EX), a frequency (FR), and a pattern request (RP).

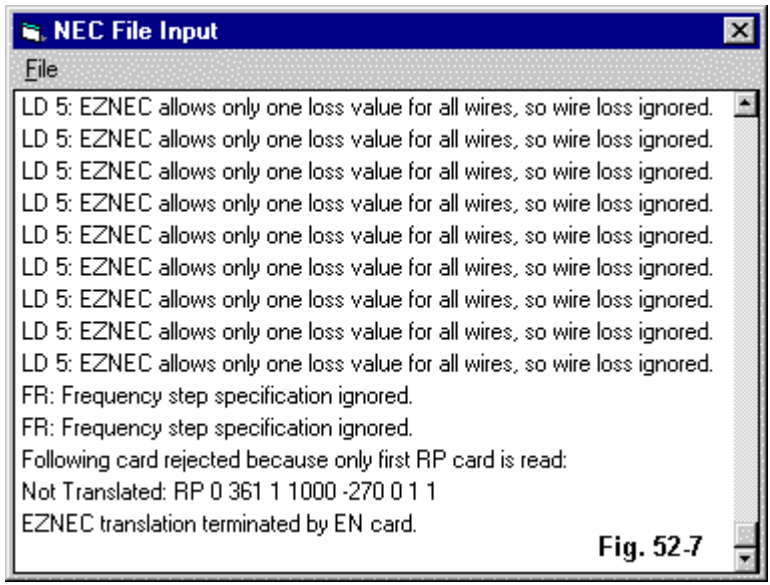

Fig. 52-7

Fig. 52-7 summarizes for a particular model most of the cases in which EZNEC either ignores or modifies a line to meet its structural needs. Although it is possible to directly create an LD5 line—the line that specifies the material conductivity of a wire—that covers all wires in a model, NEC-Win wire-creation facilities assign conductivity values to each line individually. The user can therefore have different values of conductivity for each wire in the model. In contrast, EZNEC allows only one loss value for all wires. Therefore, it ignores LD5 entries. Following the conversion process, the user must re-enter the desired material loading value into a special sub-screen in the program.

Since frequency sweeping is a special function within EZNEC, single frequency core runs are the norm. If the conversion process encounters a sweep step value in the FR entry, it will omit it from the resulting EZNEC file. If the .NEC file has multiple frequency entries, as is common when NEC-Win models request multiple radiation patterns, only one of those frequency steps—modified if necessary to register only the start frequency—will remain in the EZNEC file. The user must set up a frequency sweep from a special screen within EZNEC.

EZNEC also provides for only one radiation pattern request at a time. Therefore, the program retains only the first request labeled RP and does not accept further such requests. Another small change involves the wire diameter. The original file may specify the wire as an AWG gauge from a special table. However, the .NEC file will register that wire size as a numerical wire radius, and that value will appear as a wire numerical wire diameter within the EZNEC wire table. If the user desires to use the EZNEC AWG entry, he or she must do a single or wire-group modification in the wire table.

The upshot is simply this: when opening a .NEC format model within EZNEC Pro, the automatic conversion process does not accomplish every necessary model set-up step. The user must survey the main screen and verify that all model values are the ones desired.

As we earlier noted, saving a model from within EZNEC Pro in .NEC format also has a limitation. All wire dimensions of the saved file will be in meters, the basic unit used by the core for all calculations. NEC-Win will open the files and show metric values.

The conductivity-resistivity values used for the two programs are not everywhere identical. Therefore, a NEC-Win Plus wire screen will normally show a numerical conductivity value. If the user prefers to specify a value from the program list, he or she must change the individual entries or perform a master block change. If one uses a .NEC file exported from EZNEC from DOS versions of the program, the user should also check the establish the desired type of R-L-C load, since the earlier versions of EZNEC may convert all such loads to R+/-jX loads in the .NEC file.

Because EZNEC permits only a single pattern request at a time, the .NEC file opened within NEC-Win Plus will show only that single pattern. However, the user should also determine that the pattern meets the NEC-Win pattern request requirements so that the user can request an "Analysis" to determine the maximum gain, front-to-back ratio, and beamwidth data.

Fig. 52-8 shows a failed NEC-Win Plus pattern resulting from an unmodified model converted from another program. Note that the pattern is present, but the request for the analysis is denied. The data is still available, but will have to be extracted from the NEC output file in tabular form. Extracting a front-to-back value (whether 180-degree or worst-case) will require user calculation from forward and rearward gain values. Determining the -3-dB beamwidth will also require user calculation of the relevant gain values and then a scan of the RP0 data to find the bearings at which the calculated values most closely approach the reported values. Since the output file will report in terms of the phi-theta conventions, rather than the casual modeler's accustomed azimuth-elevation conventions, one may have to make further adjustments to arrive at the correct values.

The failed pattern also provides a reminder of the correct minimum requirements to be able to obtain a pattern analysis in NEC-Win Plus. Azimuth patterns must run (at least) between 0 and 359 degrees, while elevation patterns must run (at least) between 0 and 180 degrees.

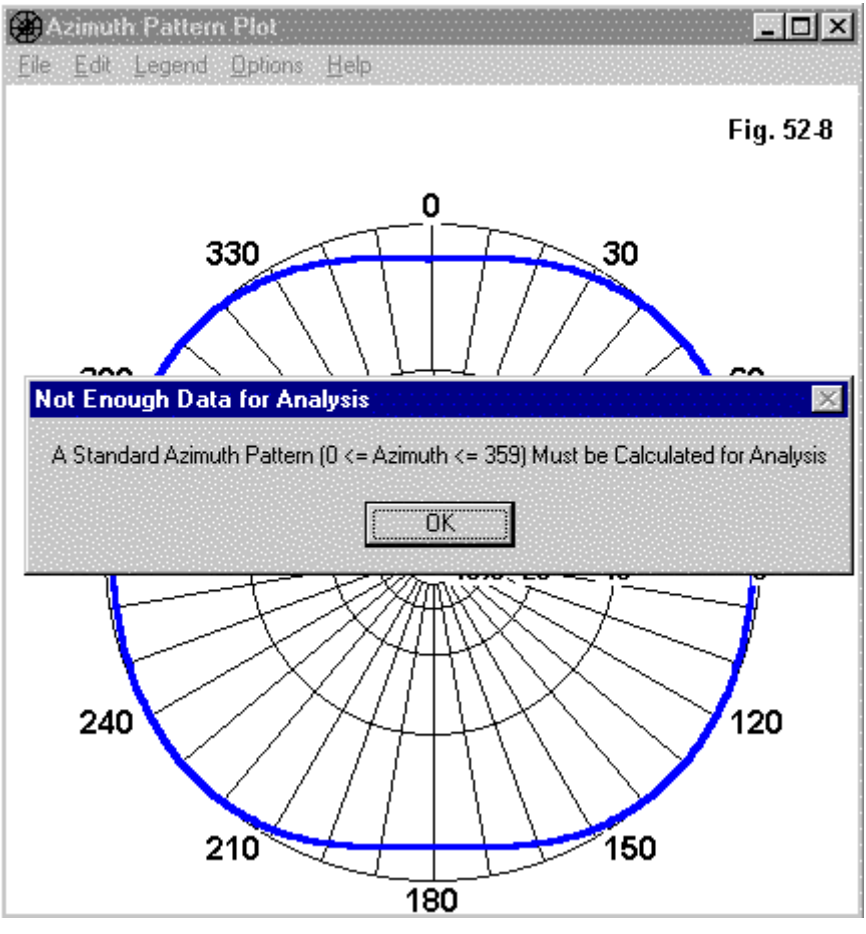

However, since the NEC-Win user may desire multiple patterns, there is a tendency to simply request the missing pattern, as shown in **Fig. 52-9**. The added

pattern is the elevation pattern, using the default values offered by the program. However, the user will be disappointed in two respects by the resulting elevation pattern. First, it will be at right angles to the axis of the forward lobe. The user must examine the model to determine the orientation of the antenna before accepting or modifying the pattern values. In this case, the requested azimuth angle for the pattern should be along the 90-270-degree line.

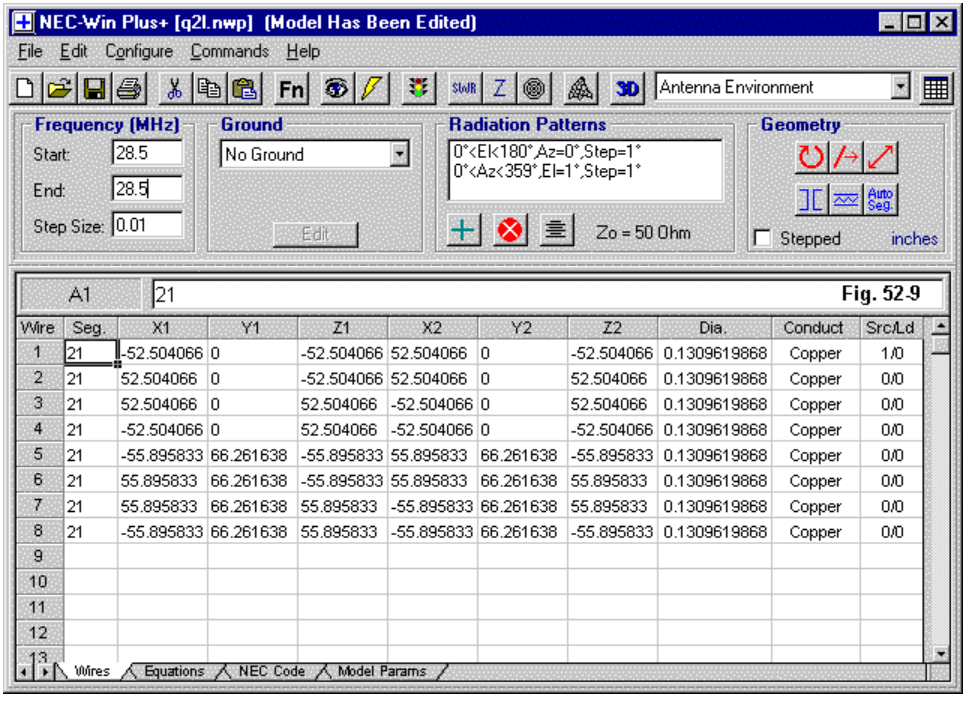

Wire	Seg.	X1	Y1	Z1	X2	Y2	Z2	Dia.	Conduct	Src/Ld
1	21	-52.504066	0	-52.504066	52.504066	0	-52.504066	0.1309619868	Copper	1/0
2	21	52.504066	0	-52.504066	52.504066	0	52.504066	0.1309619868	Copper	0/0
3	21	52.504066	0	52.504066	-52.504066	0	52.504066	0.1309619868	Copper	0/0
4	21	-52.504066	0	52.504066	-52.504066	0	-52.504066	0.1309619868	Copper	0/0
5	21	-55.895833	66.261638	-55.895833	55.895833	66.261638	-55.895833	0.1309619868	Copper	0/0
6	21	55.895833	66.261638	-55.895833	55.895833	66.261638	55.895833	0.1309619868	Copper	0/0
7	21	55.895833	66.261638	55.895833	-55.895833	66.261638	55.895833	0.1309619868	Copper	0/0
8	21	-55.895833	66.261638	55.895833	-55.895833	66.261638	-55.895833	0.1309619868	Copper	0/0
9										
10										
11										
12										
13										

Second, the requested pattern will produce only half a free-space elevation of H-plane pattern. The default value for elevation patterns is a 180-degree sweep to cover all cases over real ground. The range for the elevation pattern requires an

increase to 360 degrees for a full free-space pattern. In a similar way, the default elevation angle for azimuth patterns is 1-degree elevation to ensure that the polar plot will yield a pattern over ground. For free-space patterns, this angle should be set at zero degrees.

As we have noted, standard EZNEC operation is for a single frequency. This situation will be reflected in the .NEC file exported for use with NEC-Win programs. If a frequency sweep is needed, then the user must modify the frequency input data.

Throughout these notes on flipping from one program to another, we have not mentioned something so obvious that—without mention—it may go unnoticed. File keeping is as important to regular program flipping as any other facet of the process. Suppose that I begin with a file called QUAD.EZ. If I create a QUAD.NEC version of the file and open it in NEC-Win Plus, I shall likely save a file called QUAD.NWP. However, if I wish to transport the file with some modifications back to EZNEC, saving the file as QUAD.NEC will result in a different model than the earlier one.

Therefore, it is useful to develop some regular scheme for naming the transport .NEC files. A simple way is to designate files saved in .NEC format from EZNEC as QUAD-E.NEC and files saved from NEC-Win Plus in .NEC format as QUAD-P.NEC. This practice honors the tradition of the 8+3 filename. However, current versions of Windows allow for very extended filenames. Therefore, some users have adopted the "complete description" theory of filenames, for example, 2-EL-QUAD-EZ-VER.NEC or 2-EL-QUAD-NWP-VER.NEC, or something similar.

Adjunct Program and Their Exports

Adjunct programs to assist in developing NEC models are on the rise. Perhaps the most common one in the U.S. is NEC-Win Synth, a program that allows the user to synthesize complex shapes into wire-grid models. The program is primarily designed to meld with NEC-Win Plus. However, one may do a number of things with the synthesized wire table: save it an import it as a NEC-file into NEC-Win Pro/GNEC or EZNEC Pro, or export it as a wire table in a format acceptable for importation by all versions of EZNEC within the Wire Table.

However, Synth produces incomplete files, lacking a source (EX) and other data necessary to make a complete model file. Although a program like GNEC will open the file, the user cannot run it as an antenna model file until he or she has made the proper additions. Since the file is incomplete, the EZNEC Pro .NEC input conversion system will reject the file. However, the system will accept the file once it is complete as a model.

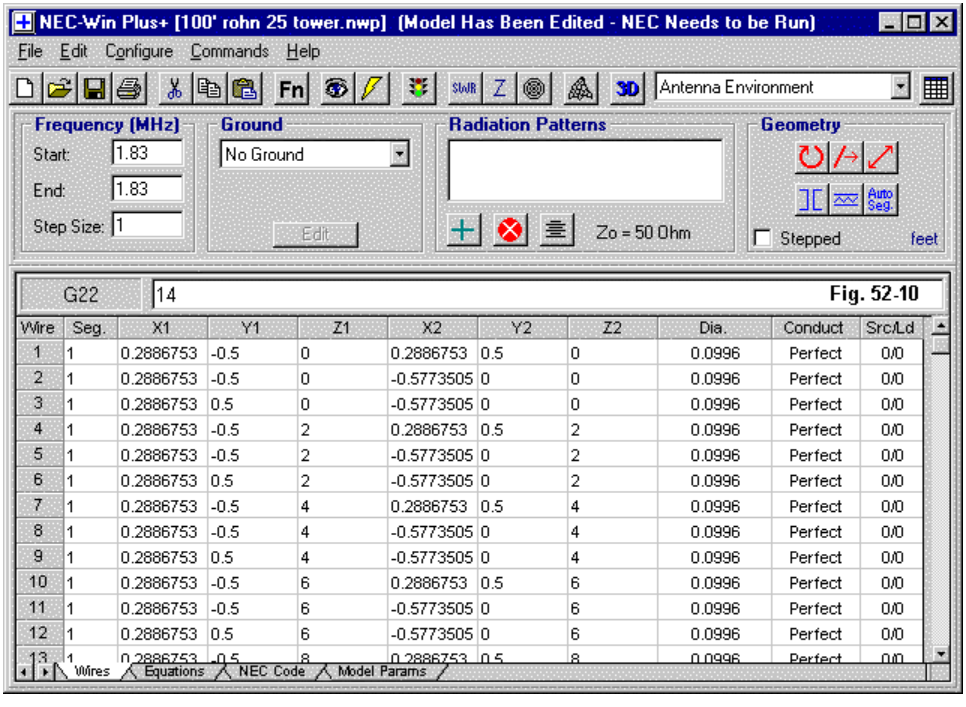

Wire	Seg.	X1	Y1	Z1	X2	Y2	Z2	Dia.	Conduct	Src/Ld
1	1	0.2886753	-0.5	0	0.2886753	0.5	0	0.0996	Perfect	0/0
2	1	0.2886753	-0.5	0	-0.5773505	0	0	0.0996	Perfect	0/0
3	1	0.2886753	0.5	0	-0.5773505	0	0	0.0996	Perfect	0/0
4	1	0.2886753	-0.5	2	0.2886753	0.5	2	0.0996	Perfect	0/0
5	1	0.2886753	-0.5	2	-0.5773505	0	2	0.0996	Perfect	0/0
6	1	0.2886753	0.5	2	-0.5773505	0	2	0.0996	Perfect	0/0
7	1	0.2886753	-0.5	4	0.2886753	0.5	4	0.0996	Perfect	0/0
8	1	0.2886753	-0.5	4	-0.5773505	0	4	0.0996	Perfect	0/0
9	1	0.2886753	0.5	4	-0.5773505	0	4	0.0996	Perfect	0/0
10	1	0.2886753	-0.5	6	0.2886753	0.5	6	0.0996	Perfect	0/0
11	1	0.2886753	-0.5	6	-0.5773505	0	6	0.0996	Perfect	0/0
12	1	0.2886753	0.5	6	-0.5773505	0	6	0.0996	Perfect	0/0
13	1	0.2886753	-0.5	8	0.2886753	0.5	8	0.0996	Perfect	0/0

Saving the file as a wire table for use with the EZNEC wire table import feature also requires care. **Fig. 52-10** shows a Synth product absorbed into NEC-Win Plus.

Note that the wire diameter is in feet, the chosen unit of measure. The diameter corresponds to a value just below 1.2".

Had we exported the same table to EZNEC for importing within the wire table, we would obtain the partial wire table shown in **Fig. 52-11**. Note that all of the numerical values are the same as we found in the NEC-Win Plus table. However, EZNEC always uses inches for wire diameters whatever the selected English unit of measure and always uses millimeters for the wire diameter whatever the selected metric unit of measure.

Wires

Wire Other

Fig. 52-11

☐ Coord Entry Mode ☐ Preserve Connections

Wires

No.	End 1				End 2				Diameter	Segs
	X (ft)	Y (ft)	Z (ft)	Conn	X (ft)	Y (ft)	Z (ft)	Conn	(in)	
1	0.288675	-0.5	0	W2E1	0.288675	0.5	0	W3E1	0.0996	1
2	0.288675	-0.5	0	W155E1	-0.577351	0	0	W3E2	0.0996	1
3	0.288675	0.5	0	W154E1	-0.577351	0	0	W156E1	0.0996	1
4	0.288675	-0.5	2	W5E1	0.288675	0.5	2	W6E1	0.0996	1
5	0.288675	-0.5	2	W159E1	-0.577351	0	2	W6E2	0.0996	1
6	0.288675	0.5	2	W157E2	-0.577351	0	2	W158E2	0.0996	1
7	0.288675	-0.5	4	W8E1	0.288675	0.5	4	W9E1	0.0996	1
8	0.288675	-0.5	4	W162E1	-0.577351	0	4	W9E2	0.0996	1
9	0.288675	0.5	4	W160E2	-0.577351	0	4	W161E2	0.0996	1
10	0.288675	-0.5	6	W11E1	0.288675	0.5	6	W12E1	0.0996	1
11	0.288675	-0.5	6	W165E1	-0.577351	0	6	W12E2	0.0996	1
12	0.288675	0.5	6	W163E2	-0.577351	0	6	W164E2	0.0996	1
13	0.288675	-0.5	8	W14E1	0.288675	0.5	8	W15E1	0.0996	1
14	0.288675	-0.5	8	W168E1	-0.577351	0	8	W15E2	0.0996	1
15	0.288675	0.5	8	W166E2	-0.577351	0	8	W167E2	0.0996	1

Therefore, when importing a Synth wire table into EZNEC as a wire table function, the user must be prepared to change the wire diameter(s). The exceptions, of course, are when the Synth unit of measure is either inches or millimeters.

This situation is only a sample of the care we must use in moving from one program to another. Not all conversions or importations will work perfectly, nor

should we expect them to do so. Importations and conversions are largely a user convenience, and some supplemental effort by the modeler is to be expected. At a minimum, the modeler should always carefully read the imported material to ensure that everything is correct relative to the model design.

NEC and MININEC Files

Back in **Fig. 52-1**, we looked at a standard-form .NEC file. For the most part, .NEC files are the common thread among almost all implementations of NEC cores. The model files are similar to, but not identical with, MININEC model files. The development of MININEC derived from the need to be able to run antenna models on early PCs with very limited memory capabilities. Hence, some of the MININEC conventions are offshoots of early predecessors to NEC-2. The requirements of the more compact algorithms and other goals of MININEC, of course, required significant deviations from the Fortran-based code that was to become NEC.

Some MININEC program implementations have limited ability to accept and convert .NEC files to their own formats. However, MININEC model files are not especially interchangeable from one implementation of the public domain core to another—even though most use an ASCII input file (with ELNEC and Antenna Model being exceptions).

Fig. 52-12 shows a typical NEC4WIN model file. The programmer has structured the wire table so that its parts correspond to those of a .NEC file. However, there are numerous functions that NEC handles with program control cards that MININEC handles with verbal entries. The CM (comment) and the GW (wires) entries are familiar enough. However, the entries for ground-related matters, the unit of measure, and the position of the excitation (Source or S) are all significant departures from the NEC-2-style file entry. The “height” entry is unique to MININEC, which separates the calculation of the source impedance (always over perfect ground) from the far-field calculations that employ the ground quality specification in a simplified reflection coefficient calculation.

NEC4Win Model File Sample
Fig. 52-12

```
CM
CM  ************  Beam 144 *************
CM               Vertical Polarization
CM
CM       Plot Azimuth to get a nice pattern
CM
CM    lots of segments, lots of calculations
CM

CE
GND Reference
UNITS Meters
Height 10.00
Over Ground  13  5 (Diel. - Cond. µSiemens)
Circular Boundary
F  144.500
GW  1   6    -0.411   0.000  -0.522  -0.411   0.000   0.522   0.010
GW  2   6     0.000   0.000  -0.488   0.000   0.000   0.488   0.010
GW  3   6     0.246   0.000  -0.463   0.246   0.000   0.463   0.010
GW  4   6     0.532   0.000  -0.459   0.532   0.000   0.459   0.010
GW  5   6     0.864   0.000  -0.454   0.864   0.000   0.454   0.010
GW  6   6     1.248   0.000  -0.450   1.248   0.000   0.450   0.010
GW  7   6     1.695   0.000  -0.445   1.695   0.000   0.445   0.010
GW  8   6     2.212   0.000  -0.441   2.212   0.000   0.441   0.010
GW  9   6     2.812   0.000  -0.436   2.812   0.000   0.436   0.010
GW  10   6     3.509   0.000  -0.432   3.509   0.000   0.432   0.010
GW  11   6     4.317   0.000  -0.428   4.317   0.000   0.428   0.010
S   1 8    100    0
Coax  50
```

The MMANA model file, a sample of which appears in **Fig. 52-13**, uses a different order for the entries, with only the wire table showing a good correlation to the NEC4WIN file. However, MMANA does not identify the wires by GW-numbers. The MMANA file contains a pattern request, but the NEC4WIN model file does not. This is only one of many major differences between the two implementations of MININEC. One of the major programming decisions required by MININEC concerns which

commands to include within the model file itself and which to implement as overall program functions selected as needed by the user.

MMANA Model File Sample
Fig. 52-13

```
Omni dipol 144 with gamma-match, by DL2KQ
*
145.0
***Wires***
13
0.0,  0.06, -0.145,     0.0,  0.0075,     -0.145,     0.003,      -1
0.0,  -0.058,     -0.145,     0.0,  -0.15,      -0.062,     0.003,      -1
0.0,  -0.15,      -0.062,     0.0,  -0.15,      0.062,      0.003,      -1
0.0,  -0.15,      0.062,      0.0,  -0.062,     0.15, 0.003,      -1
0.0,  -0.062,     0.15, 0.0,  -0.006,     0.15, 0.003,      -1
0.0,  0.062,      0.15, 0.0,  0.15, 0.062,      0.003,      -1
0.0,  0.15, 0.062,      0.0,  0.15, -0.062,     0.003,      -1
0.0,  0.15, -0.062,     0.0,  0.06, -0.145,     0.003,      -1
0.0,  0.062,      0.15, 0.0,  0.006,      0.15, 0.003,      -1
0.0,  0.0075,     -0.145,     0.0,  -0.058,     -0.145,     0.003,      -1
0.0,  0.06, -0.145,     0.0,  0.06, -0.125,     0.001,      -1
0.0,  0.06, -0.125,     0.0,  0.0075,     -0.125,     0.001,      -1
0.0,  0.0075,     -0.125,     0.0,  0.0075,     -0.145,     0.001,      -1
*** Source ***
1,    1
w13c, 0.0,  1.0
***   Load   ***
1,    1
w13b, 0,    0.0,  18.0, 0.0
**Segmentation**
400,  40,   2.0,  1
*GH/??/R/AzEl/X*
0,    5.0,  4,    50.0, 120,  60,   0
```

Classic AO (6.5, for the sample shown in **Fig. 52-14**) uses still another format, one permitting the introduction of variables and their definitions. The file may be viewed as perhaps the most compact format of all ASCII MININEC files. NEC2GO, a version of NEC-2, can read most AO files with their native .ANT extension.

With a suitable text editor and a template to guide us in moving items around, it is possible to convert most MININEC files from one program to another without re-entering everything from scratch. However, this ability does not extend to versions of MININEC using non-ASCII file formats.

AO 6.5 Model File Sample Fig. 52-14

```
4-Element WB Yagi
Free Space Symmetric
28.8 MHz
4 6060-t6 wires, inches
a = 107
b = 102.5
c = 94.5
d = 91.414
bs = 49.5
cs = 53
ds = 96
di = .5
20    0   -a    0    0    a    0    di
20   bs   -b    0   bs    b    0    di
18   cs   -c    0   cs    c    0    di
16   ds   -d    0   ds    d    0    di
1 source
Wire 2, center
```

In the end, familiarizing ourselves with more than one program can allow us to move a model to the program that will best accomplish a particular task. However, when flipping from one program to another, we must always be aware of all the pitfalls to avoid. If we make the necessary adjustments in advance of running the transported model, we can usually save ourselves considerable time and energy. In contrast, if we must always back track to pick up pieces that we forgot to adjust, we

may end up spending more time in flipping than in patiently working through a modeling exercise wholly within one program.

* * * * *

Model included: 51-1. (.NEC and .NWP model dimensions in meters; .EZ model dimensions in inches. Due to the variability of systems used to save a MININEC model, only NEC models can be supplied with this volume.)

53. Voltage and Current Sources: How?

Programs such as NEC-Win Plus and EZNEC have a special feature that is not inherent to the NEC-2 core: the current source. In past columns, we have reviewed some of the significant uses of a current source. For example, by placing a current magnitude of 1.0 at a phase angle of 0.0 degrees on the source segment of the driver wire of a Yagi antenna, we can conveniently explore the relative current magnitude and phase angle at the center of each parasitic wire. For another example, if we have a phased array, we can simulate its operation by using multiple current sources, each set for the correct magnitude and phase angle. These two applications alone would justify the availability of a current source.

However, NEC-2 and NEC-4 do not include a current source of the type used in these examples of applications. In fact, of all the potential modes of excitation, EZNEC and NEC-Win Plus implement only one: the standard voltage source that is in series with the wire segment on which we place it. So the question arises: how do we implement a current source?

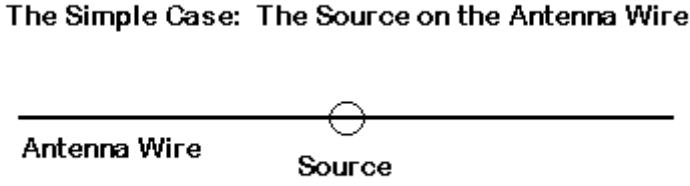

Fig. 53-1

Let's begin with the simplest case, a simple dipole with a single source at its center. **Fig. 53-1** shows an outline of our model. To set up this model, say in NEC-Win Plus, we would develop a simple wire entry, such as the one shown in **Fig. 53-2**. This particular example happens to be at a frequency of 50.5 MHz, with suitable

wire diameter and wire material load values, but these will not play a significant role in this exercise.

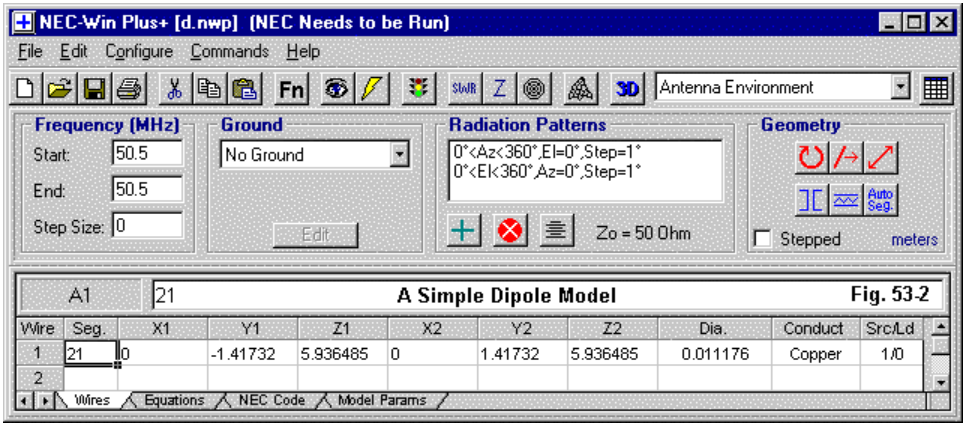

More relevant to our interests is the registry of a single source for the model, at the far right of the wire entry screen. If we click on that entry, we open the source screen, shown in **Fig. 3**. Our entry for this model is a very standard default entry of a voltage magnitude of 1.0 and a voltage phase angle of 0.0 degrees. Indeed, for the model at hand, there is no good reason to use any other value pair.

The standard .NEC-format file for this model would look like the following lines of ASCII entries:

```
CM 6m dipole
CE
GW 1 21 0 -1.41732 5.936485 0 1.41732 5.936485 0.005588
GS 0 0 1
GE 0
EX 0 1 11 0 1 0
LD 5 1 1 21 5.8001E7
FR 0 1 0 0 50.5 1
RP 0 1 361 1000 90 0 1 1
RP 0 361 1 1000 -270 0 1 1
EN
```

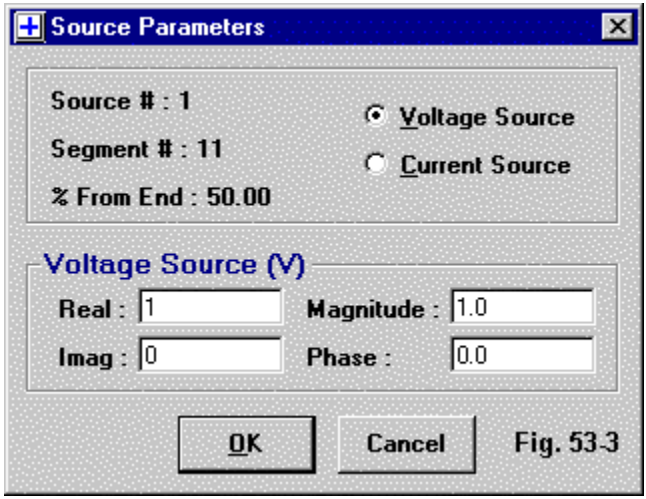

The GW entry is our wire, with the last entry giving the wire size as a radius. The EX entry is the source information, showing a source on segment 11 (out of 21) on wire 1 with a voltage value (at the far right) of 1.0 and a phase angle of 0.0 (minus the decimal places).

The output data of most relevance for our concerns is the "Antenna Input Parameters" section of the NEC output file. We normally encounter this information in tables that are easier to read, but let's look at the entries as they occur in the NEC-2 output file.

```
                    - - - ANTENNA INPUT PARAMETERS - - -

TAG    SEG.      VOLTAGE (VOLTS)           CURRENT (AMPS)
NO.    NO.     REAL          IMAG.        REAL          IMAG.
1      11    1.00000E+00   0.00000E+00 1.36049E-02  -9.46163E-04

           IMPEDANCE (OHMS)          ADMITTANCE (MHOS)          POWER
          REAL          IMAG.        REAL          IMAG.       (WATTS)
        7.31493E+01   5.08723E+00  1.36049E-02  -9.46163E-04  6.80244E-03
```

This one line of data (split into two lines for ease of reading) is the basis for a number of entries that we can find in the output data from NEC-Win Plus and EZNEC. The input or source consists of a voltage of 1.0 + j 0.0 volts. The resultant current is 0.0136 -j 0.000946 amps. Of course, by using the square root of the sum of squares, plus a tangent, we can convert these values into voltage and current magnitudes and their associated phase angles.

The source impedance is normally given in real and imaginary terms, which translate into a resistance and a reactance: 73.149 + j 5.087 Ohms.

The utility of using real and imaginary numbers for the impedance is that we can easily calculate the power at the source. Remember that NEC uses peak voltage and current values. NEC-Win Plus follows this procedure, so the source voltage that we entered was 1.0 volts peak. (EZNEC uses RMS entries for voltages and currents and internally correlates these with NEC input and output values.) Since power is I^2 R, but in RMS terms, we must multiply the current by 0.7071068, or the current squared by 0.5. Hence, the power at the input is 0.00680 watts. (For maximum precision, we should convert the current into a magnitude and phase angle.)

This data also provides all that we need to determine the SWR relative to any standard impedance that we wish to input. NEC does not provide this data. Instead, the programs we have mentioned do the calculation using the data that we have just given.

With this much background on using a voltage source, we are ready to change the source to a current source. The input process is simple enough: we simply mark a box or (in EZNEC) change a letter in the source entry line. **Fig. 53-4** shows the relevant source box for our model.

The user changes from a voltage to a current source with great ease, and sees no visible sign on the wire table that anything but a simple check-mark has changed. However, the model has changed significantly. In fact, if we look at the .NEC-format model generated by NEC-Win Plus, we can see considerable revision of the model. See model 53-1.

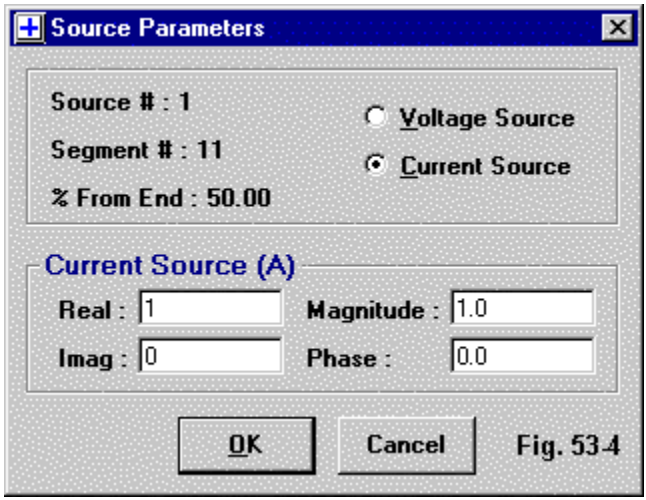


```
CM 6m dipole
CE
GW 1 21 0 -1.41732 5.936485 0 1.41732 5.936485 0.005588
GW 30901 1 9901.0000 9901.0000 9901.0000 9901.0001 9901.0001 9901.0001 .00001
GS 0 0 1
GE 0
EX 0 30901 1 0 0.0 1.0
LD 5 1 1 21 5.8001E7
NT 30901 1 1 11 0 0 0 1 0 0
FR 0 1 0 0 50.5 1
RP 0 1 361 1000 90 0 1 1
RP 0 361 1 1000 -270 0 1 1
EN
```

The first revision on the list of lines is the introduction of a new wire, #30901. NEC-Win Plus uses numbers above 30,000 for wires that will remain hidden from the user's view on the regular screens. However, the wires can always be viewed by tabbing to the "NEC Code" page of the spreadsheet input system. In EZNEC, the file remains hidden unless one has the Pro version, which permits saving the model file in .NEC format.

The wire is a remote wire that is very short, very thin, and has only 1 segment. Like the wires that we use to terminate transmission lines, it is short, thin, and remote enough to not contribute detectably to the overall radiation of the essential wire geometry of the antenna.

The other new entry in the list is labeled NT, for network. A network is a two-port non-radiating construct that employs short-circuit matrix elements. We place a network between any two wire segments in the overall wire geometry and enter real and imaginary short-circuit admittance values. One of the wire segments may be a remote wire, such as 30901, which the NT line registers at the left as the first of the wires. The other wire is the former source segment on the dipole, segment 11 of wire 1.

Let's expose the hidden portions of the current source model fully by revising the usual model. Everywhere we see the entry 30901, we shall write 2. This involves the second GW card, the NT card, and the EX card. If we then import this file into NEC-Win Plus, we obtain a main screen that looks like **Fig. 53-5**.

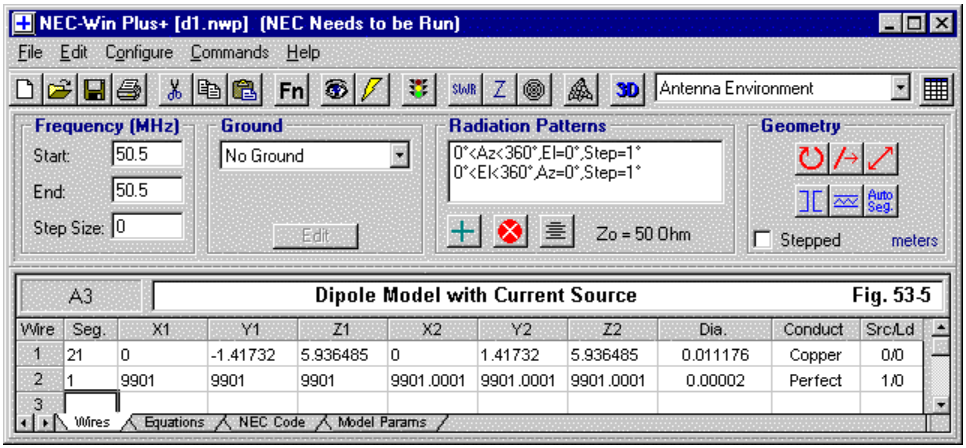

Now the model file looks normal. We see that wire 2 has a source, to which we shall turn momentarily. Although the main screen does not show it, we now have a network whose entries can be viewed.

The ports of a network are labeled Y1 and Y2. If we place a set of admittance values across the Y1 terminals, we have Y11. Likewise, if we place values across the terminals of Y two, we have a Y22 value. A set of admittance values going from one port to the other bear the label Y12. **Fig. 53-6** shows the conventional sketch for such a port set up for the current source.

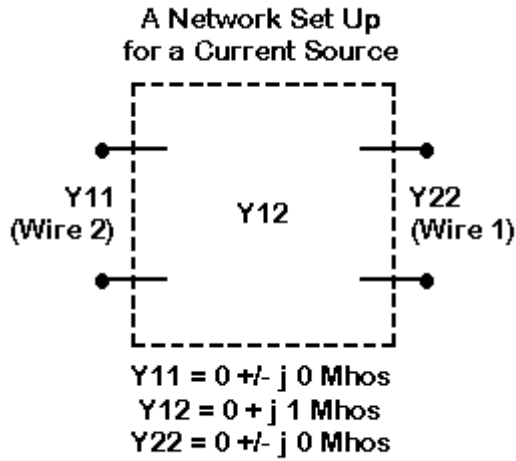

Fig. 53-6

The entries on the NT card following the wire and segment places are, in order, Y11, Y12, Y22, with a real and an imaginary value (conductance and susceptance, in usual electrical terms) for each entry. Note that the current source requires only a Y12 entry, with a value of 1 Mho (or 1 siemen) in the imaginary slot. Networks, like transmission lines (TL), are in series with the wire segment and any LD load on it, but in parallel with other networks and sources.

By clicking on the network symbol on the main screen, we can see the network port entries, as shown in **Fig. 53-7**. We place zeroes where there are no entries. Since the admittance matrix is symmetric, we need not have an entry labeled Y21. Y12 does all the work. There we find the 1-Mho imaginary admittance entry.

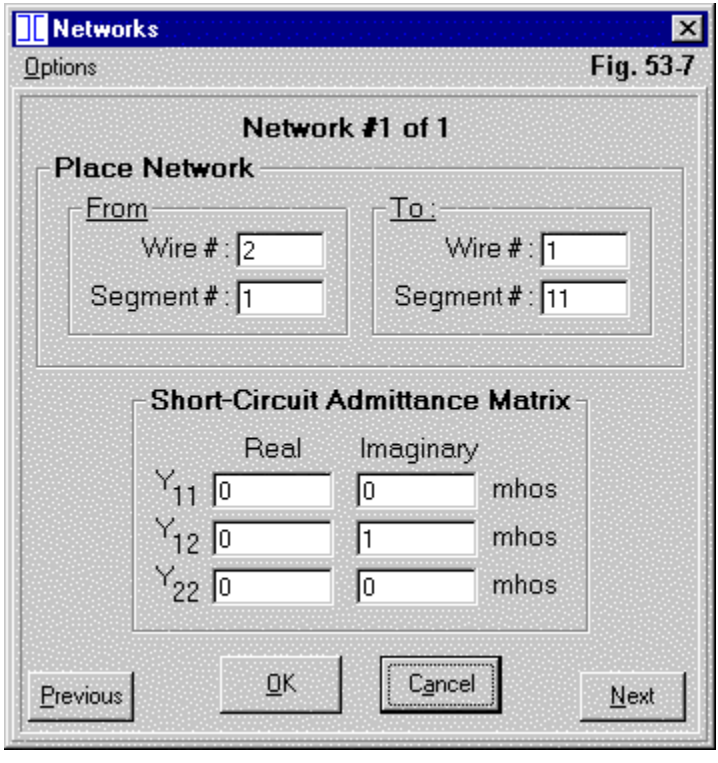

The current source requires one further revision to the standard voltage source entry, and we find this by opening the source screen for our revised model, shown in

Fig. 53-8. Instead of entering a real value of 1.0 and an imaginary value of 0.0—which is equivalent to entering a voltage magnitude of 1.0 and a phase angle of 0.0 degrees—we enter a real voltage value of 0.0 and an imaginary value of 1.0, yielding a voltage magnitude of 1.0 at a phase angle of 90 degrees.

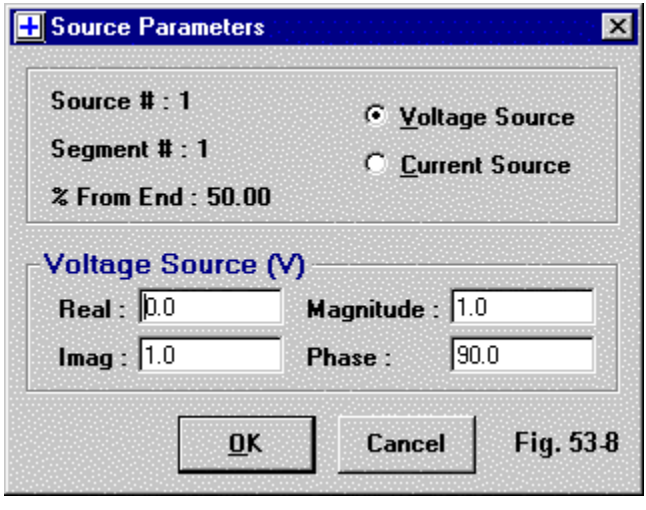

The fully revised model in .NEC format has the following appearance:

```
CM 6m dipole
CE
GW 1 21 0 -1.41732 5.936485 0 1.41732 5.936485 0.005588
GW 2 1 9901.0000 9901.0000 9901.0000 9901.0001 9901.0001 9901.0001 .00001
GS 0 0 1
GE 0
EX 0 2 1 0 0.0 1.0
LD 5 1 1 21 5.8001E7
NT 2 1 1 11 0 0 0 1 0 0
FR 0 1 0 0 50.5 1
RP 0 1 361 1000 90 0 1 1
RP 0 361 1 1000 -270 0 1 1
EN
```

By standard network theorems, the combination of the specified source and the network will yield a current of 1.0 at a phase angle of 0.0 degrees on the segment of the dipole that the user thought he or she had designated as the source in the original current-source model. Our substitute model has simply shown what goes on behind the scenes in a NEC program offering current sources.

With a voltage source, we were able to take data on the source voltage, current, impedance, and power directly from the "Antenna Input Parameters" line of the NEC output report. Now everything will surely look different and prevent us from picking up the data so easily without further calculation. In fact, the "Antenna Input Parameter" line of the new current-sourced model has the following appearance (once more split into two lines for ease of reading):

```
                    - - - ANTENNA INPUT PARAMETERS - - -

TAG    SEG.      VOLTAGE (VOLTS)             CURRENT (AMPS)
NO.    NO.     REAL          IMAG.          REAL          IMAG.
 2     22    0.00000E+00  1.00000E+00  -5.08723E+00   7.31493E+01

               IMPEDANCE (OHMS)          ADMITTANCE (MHOS)          POWER
             REAL          IMAG.         REAL          IMAG.       (WATTS)
          1.36049E-02  -9.46163E-04  7.31493E+01  5.08723E+00 3.65746E+01
```

The process of picking up data from the NEC output file for redisplay and possible reformatting in a program output is simply a matter of selecting the data needed. In fact, the data needed is fully present on the input parameter line, although not where we expect to find it. Let's do some label swapping. Swap the labels on the admittance and impedance entry pairs—but keep the real and imaginary parts as given. The impedance becomes 73.149 + j 5.087 Ohms.

Next, reverse the column labels of the voltage and the current. Convert each value into a magnitude and phase angle and subtract 90 degrees. (For our quick look at these tables, we may re-label the voltage as current and the current as voltage. Then, for each of these entry pairs, swap the real and imaginary labels. We would not use this short cut if we were actually calculating voltages and currents in the program.) The result is a voltage of 73.148 - j 5.087 volts, and a current of 1.0 + j 0.0 amps.

Since the current is 1.0 peak, to find the power we take half the square of the current (that is, 0.5) and multiply it by the real part of the impedance, for a result of 36.575 watts, which is the value shown in the power column. If you prefer to take the magnitudes of I and E, multiplying them after converting from peak to RMS values, you will also get half of 73.149 or 36.575 watts. (A phase angle difference must also be taken into account, but it is too slight to affect the outcome significantly in this crude check calculation.)

It is possible to go through the network calculations, but the results will be the same as for our entry label-swapping scheme. Although I do not have the internal program coding at hand, it is likely that most programs simply change flags for picking up certain data when a current source has been designated by the user.

Before leaving the subject, let's see if the system pans out with a few more models. For example, suppose that we have a turnstile antenna composed of two dipoles at right angles. Next, let us feed the two dipoles using current sources. In a perfect turnstile antenna, the two sources should have identical magnitudes and a 90-degree current phase shift between the two dipole sources. Except for a slight displacement owing to the need to make the two dipole wires pass each other without touching, we should obtain the same impedance for each dipole.

The following model, a hybrid of EZNEC and NEC-Win Plus, shows the structure of our turnstile dipole antenna. See model 53-2.

```
CM 6m dipole turnstile
CE
GW 1,21,0.,-1.4351,6.096,0.,1.4351,6.096,.0008138
GW 2,21,-1.4351,0.,6.1214,1.4351,0.,6.1214,.0008138
GW 3,2,593.6486,593.6486,593.6486,593.6605,593.6605,593.6605,5.9365E-4
GE 1
LD 5,1,0,0,5.7471E+7,1.
LD 5,2,0,0,5.7471E+7,1.
FR 0,1,0,0,50.5
GN 2,0,0,0,13.,.005
EX 0,3,1,0,0.,1
EX 0,3,2,0,-1,0
NT 3,1,1,11,0.,0.,0.,1.,0.,0.
NT 3,2,2,11,0.,0.,0.,1.,0.,0.
RP 0,1,361,1000,76.,0.,0.,1.,0.
EN
```

Notice that EZNEC creates only one wire for the termination of the networks, but it has two segments, one for each source. The sources (EX lines) have been converted to 1.0 voltage peak value maximums. Since the current source that we specified as 1.0 at 0.0 degrees requires a remote voltage source of 0.0 at 90 degrees (or 0.0 + j 1.0 volts), the source that we specified as 1.0 at 90 degrees advances a further 90 degrees. Hence, its value is 1.0 at 180 degrees or -1.0 + j 0.0 volts. The network inputs for each source remain constant except for the terminating wire segment numbers.

The "Antenna Input Parameter" line of the NEC output report is the following entry:

```
                    - - - ANTENNA INPUT PARAMETERS - - -

TAG   SEG.      VOLTAGE (VOLTS)            CURRENT (AMPS)
NO.   NO.     REAL          IMAG.         REAL          IMAG.
3     43    0.00000E+00  1.00000E+00   2.01009E+00  6.98866E+01
3     44   -1.00000E+00  0.00000E+00  -6.96795E+01  1.83212E+00

          IMPEDANCE (OHMS)          ADMITTANCE (MHOS)          POWER
         REAL          IMAG.       REAL          IMAG.       (WATTS)
       1.42971E-02  4.11214E-04  6.98866E+01  -2.01009E+00  3.49433E+01
       1.43415E-02  3.77089E-04  6.96795E+01  -1.83212E+00  3.48398E+01
```

The impedance for each dipole is about 69.87 and 69.68 Ohms, respectively—as read from the admittance column. With the current magnitude squared and halved (after reading it from the voltage columns), the power is 34.94 and 34.84 watts, respectively, using the real portion of the impedances. Again, reading current from the voltage columns (while reversing the real and imaginary headings) we can see that the currents are 90 degrees apart. If in fact, programs do use the data flagging technique for picking up values (and, as noted, I do not assert that they do in the absence of access to proprietary codes), it is likely that they convert the real and imaginary values as given into a magnitude and phase for each and then subtract 90 degrees.

One more example should suffice for our rudimentary demonstration of how we obtain current sources from voltage source. Consider a dipole, just as we have

been working with, but having one addition. The center of the dipole connects through a transmission line (TL) to a short source wire. We shall treat the short wire as a current source segment. The resulting .NEC-format file looks like the following one. See model 53-3.

```
CM 6m dipole with 1/4-wl TL
CE
GW 1 21 0 -1.41732 5.936485 0 1.41732 5.936485 0.005588
GW 2 1 -0.0127 0 2.54 0.0127 0 2.54 0.000635
GW 30901 1 9901.0000 9901.0000 9901.0000 9901.0001 9901.0001 9901.0001 .00001
GS 0 0 1
GE 0
EX 0 30901 1 0 0.0 1.0
LD 5 1 1 21 5.8001E7
NT 30901 1 2 1 0 0 0 1 0 0
TL 1 11 2 1 70 1.484122 0 0 0 0
FR 0 1 0 0 50.5 1
RP 0 1 361 1000 90 0 1 1
RP 0 361 1 1000 -270 0 1 1
EN
```

The now-familiar remote source wire, 30901, is evident, as are the network and excitation entries. The 70-Ohm transmission line is 1.484 meters long (about 0.25 wavelength), as we read the TL card. The interesting part of this model is the fact that we have two remote wires—a visible one that is the user source wire and a normally invisible one that is the program source because the user has selected a current source. By virtue of the fact that a 70-Ohm line is not a perfect match for a nearly resonant dipole, we should expect some transformation in the impedance at the source.

Again, we can turn to the “Antenna Input Parameters” line for values.

```
                        - - - ANTENNA INPUT PARAMETERS - - -

TAG     SEG.      VOLTAGE (VOLTS)            CURRENT (AMPS)
NO.     NO.     REAL          IMAG.         REAL          IMAG.
30901   23    0.00000E+00   1.00000E+00   4.73228E+00   6.66507E+01

            IMPEDANCE (OHMS)           ADMITTANCE (MHOS)          POWER
           REAL          IMAG.        REAL           IMAG.       (WATTS)
         1.49283E-02   1.05993E-03   6.66507E+01   -4.73228E+00   3.33253E+01
```

Reading the impedance from the admittance position, we find a 66.65-Ohm real part and a -4.73-Ohm imaginary part. I^2R gives us 33.33 watts of power. We reversed the heading of the voltage and current columns, converting each to a magnitude and phase angle, and then subtracting 90 degrees. However, because the real part of the impedance is more than an order of magnitude greater than the imaginary part, any further calculations we might make with these values would not be seriously hurt by a simplified scan of values. This easy situation, of course, will not always—indeed, not even commonly—be the case for examples more complex than our simple dipole system.

The reason for setting forth the last model is that there is another section of the NEC output report that we can sometimes confuse with the "Antenna Input Parameters" portion. The "Structure Excitation" section contains some values that appear to be candidates for our source calculations using a current source. However, they are not suitable for the task.

If these notes familiarize you with the terms of a current source—as constructed out of a voltage source and a network—then they will have served their purpose.

* * * * *

Models included: 53-1 through 53-3. (.NEC and .NWP model dimensions in meters; .EZ model dimensions in inches.)

54. GC: Wire Segment Length and Radius Tapering

There are numerous occasions on which we wish to taper either the segment length or the radius (diameter) of a wire along its length. Entry-level programs restrict users to the GW, GS, and GE geometry cards, and this restriction makes tapering a complex procedure involving many wires. However, versions of NEC-2 and NEC-4 that make the entire set of geometry entries available to the user considerably simplify the procedure—and result in faster run times for the resulting model.

The key is the GC or geometry continuation card. Perhaps the best way to illustrate the use of the card is with a small example.

```
CM bi-conical dipole—tapered radius and tapered segment lengths
CE
GW 1 5 0 0 -5.85 0 0 -0.336 0
GC 0 0 .8 .5 .0833
GW 2 1 0 0 -0.336 0 0 0.336 .0833
GW 3 5 0 0 0.336 0 0 5.85 0
GC 0 0 1.25 .0833 .5
GS 0 0 .3048
GE 0
EX 0 2 1 0 1 0
LD 5 1 1 5 3.0769E7
LD 5 2 1 1 3.0769E7
LD 5 3 1 5 3.0769E7
FR 0 1 0 0 31.6 1
RP 0 1 361 1000 90 0 1 1
EN
```

In almost all respects, everything about the model is standard. We have a dipole composed of 3 wires, each of which has some material loss (the LD5 entries). Wire 2 in the center has a standard voltage excitation, and the frequency of operation is 31.6 MHz. The model requests a single azimuth/phi pattern. The GS entry conversion constant tells us that the dimensions are in feet, and from the GW entries, we can see that the antenna extends along the Z-axis +/-5.85'.

However, we want to look closely at the GW1 and GW3 entries. They have a zero in the final radius column. The zero-entry for radius is NEC's method of alerting the program to a following or continuation card, namely the GC entry. (If you use an entry other than zero and have a following GC line, the core will alert you to a geometry error, but will not tell you exactly what it is.)

The GC card permits you to taper both the radius and the segment length within the specified number of segments in the preceding GW line. Both GW1 and GW3 specify 5 segments, mostly to allow me to present short tables in what follows.

The GC entry allows three different ways of handling the segment-length tapering, as shown in the triple screen grab of **Fig. 54-1**, taken from GNEC. Before we explore the differences among the three variations in segment length handling, note that the radius entry is the same for all three. NEC uses a single equation to taper the element radius, and it is not a simple linear taper. Given a starting and end segment radius, along with the number of segments in the wire, the radius will taper according to the following equation:

$$R_{RAD} = \left(\frac{RAD2}{RAD1} \right)^{\frac{1}{NS-1}} \qquad (1)$$

R_{RAD} is the ratio of two adjacent segment radii, RAD1 is the first specified segment radius, RAD2 is the specified last segment radius, and NS is the specified number of segments. Once the ratio is determined, the program simply multiplies each segment radius by the ratio to arrive at the next in the sequence.

In the sample .NEC file, the GC entry for GW3 in the final 2 columns shows .0833 and .5. These are the first and last radii values for a wire that increases in diameter along its length. The final two columns for the GC entry following GW1 are in reverse order, indicating a wire that decreases in diameter along its length. For the moment, it is incidental, but note that the radius of GW2, a 1-segment wire, is the same as the end radius for GW1 and as the start radius for GW3.

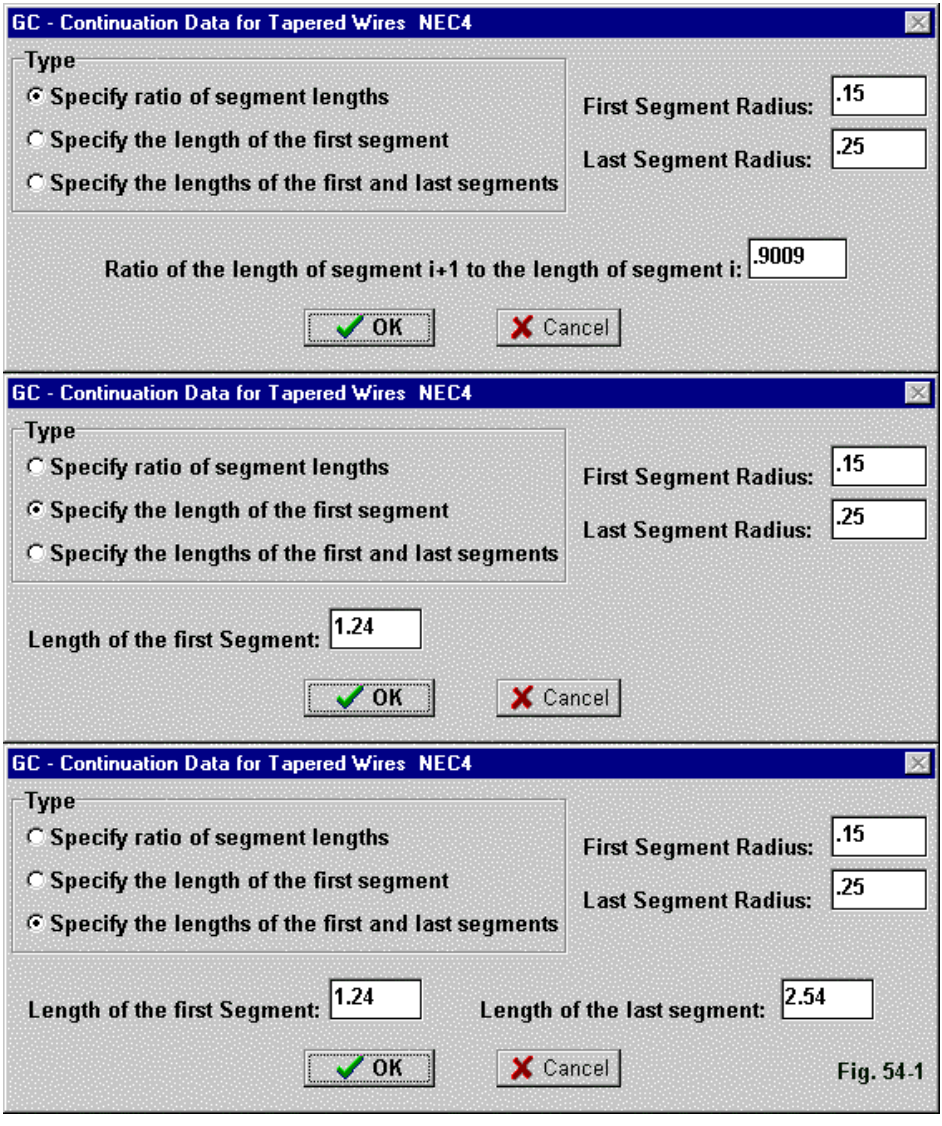
GC - Continuation Data for Tapered Wires NEC4
Type
Specify ratio of segment lengths
Specify the length of the first segment
Specify the lengths of the first and last segments
First Segment Radius: .15
Last Segment Radius: .25
Ratio of the length of segment i+1 to the length of segment i: .9009
OK
Cancel
GC - Continuation Data for Tapered Wires NEC4
Type
Specify ratio of segment lengths
Specify the length of the first segment
Specify the lengths of the first and last segments
First Segment Radius: .15
Last Segment Radius: .25
Length of the first Segment: 1.24
OK
Cancel
GC - Continuation Data for Tapered Wires NEC4
Type
Specify ratio of segment lengths
Specify the length of the first segment
Specify the lengths of the first and last segments
First Segment Radius: .15
Last Segment Radius: .25
Length of the first Segment: 1.24
Length of the last segment: 2.54
OK
Cancel

Fig. 54-1

With respect to the tapering of segment lengths, we have three options, one of which we must specify in the first integer place on the GC line:

0 Used to specify a ratio between each adjacent segment on the wire
1 Used to specify the length of the first segment on the wire, with the remaining segments calculated by the program
2 Used to specify the length of the first segment and the last segment on the wire, with the remaining segments calculated by the program

The sample model uses Type 0 segment length specifications. Had we desired only to change the wire radius but use equal length segments, we would have specified a ratio of 1.0, which would appear in the third column (first floating decimal place) in the GC line. **Fig. 54-1** shows a ratio of 0.9009 as the requested ratio for a Type 0 GC entry, while the sample model shows a value of 0.8 for GW1 and 1.25 for GW3. A value less than 1 indicates decreasing segment lengths along the wire, while a value greater than 1 indicates increasing segment lengths along a wire. Since 0.8 is the inverse of 1.25, we receive the clue that GW1 and GW3 will vary their segment lengths so that the resulting total dipole element is exactly symmetrical about the source segment/wire.

Let L be the total wire length, i be the segment number, and R_v be the ratio of adjacent segment lengths. Then the length of the first segment, v_1, emerges from the following equation:

$$v_1 = \frac{L(1 - R_v)}{1 - R_v^{NS}} \qquad (2)$$

The program then applies the user-selected ratio to the initial segment length value to determine the remaining segment lengths.

If we choose a Type 1 GC entry and specify the length of the first segment, we would refer to the middle panel of **Fig. 54-1**. The first-segment length selection, if there is one, always goes in the column to the right of the last radius entry in the GC

line. The program then solves equation 2 for R , the length ratio, by iteration and then proceeds as in a Type 0 GC line to calculate the successive segment lengths.

Both Type 0 and Type 1 segment-length calculations use the value in the GW line for the number of segments on the wire. However, the situation changes if we use a Type 2 GC line and specify the length of the first and last segments. In this case, the GC calculations determine both the ratio of a segment length to the next and the number of segments in the wire. Let v be the length of the first segment and v be the length of the last segment. R will be the ratio of adjacent segment lengths and N will be the number of segments in the wire.

$$R_v = \frac{L - v_1}{L - v_2} \qquad N = 1 + \frac{\log(v_2 / v_1)}{\log R_v} \qquad (3)$$

Since N is rounded to an integer to populate the wire with an integral number of segments, the program recalculates R . Thus, the final segment length may depart slightly from the requested value to accommodate the rounding without changing the requested wire length.

(Note: the NEC manuals employ a *delta* wherever I have written *v* to indicate a segment length. The use of a letter simplifies the HTML encoding, the original format of these columns.)

With this background, we may explore a couple of examples of GC use.

Creating a Bi-conical Dipole

To a limited degree, we may simulate a bi-conical dipole, that is, a wire element whose radius increases continuously from the element center outward. However, the simulation has several restrictions. First, without resorting to wire-cage assemblies, the simulation will use a stepped-diameter element. Instead of decreasing the radius of the wire with each outward movement, we increase the radius. The use of this technique in NEC-2 is subject to the well-known limitation of the program

when encountering any stepped-diameter element: it is unreliable. NEC-4 is more reliable so long as the stepping increment is not too large.

Second, the source segment should not change radius or length relative to the immediately adjacent segments. By making the last segment of the first wire and the first segment of the third wire the same length and diameter as the single-segment source wire, we preserve this condition. **Fig. 54-2** shows the central portion of a bi-conical simulation using 3 wires and GC entries.

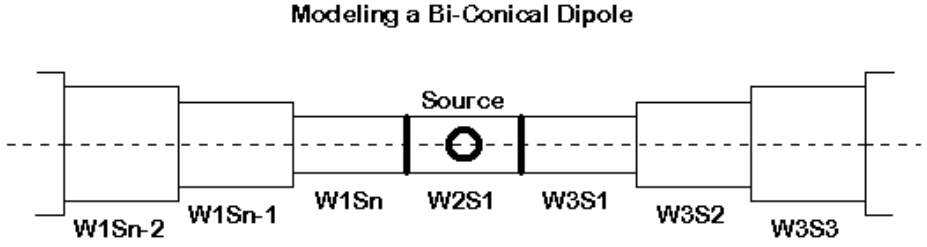

Fig. 54-2

If we specify a Type 0 GC entry for both wires 1 and 3, we might initially set the segment length ratio to 1.0, insuring the production of equal segment lengths. We can easily pre-calculate the resulting segment lengths from the GW1 or GW3 entries and set the center wire to the same length in a reasonable number of iterations. The following chart from the NEC output file shows the resulting segment lengths and radii. The internal units of measure in NEC are meters, but the numbers correspond to our 11.7' dipole. See model 54-1.

```
                    - - - - SEGMENTATION DATA - - - -
                         COORDINATES IN METERS
               I+ AND I- INDICATE THE SEGMENTS BEFORE AND AFTER I

SEG.  COORDINATES OF SEG. CENTER     SEG.     WIRE     CONNECTION DATA  TAG
NO.       X         Y         Z     LENGTH   RADIUS     I-    I    I+    NO.
 1   0.00000   0.00000  -1.62098   0.32420   0.15240     0    1    2      1
 2   0.00000   0.00000  -1.29678   0.32420   0.09737     1    2    3      1
```

3	0.00000	0.00000	-0.97259	0.32420	0.06220	2	3	4	1
4	0.00000	0.00000	-0.64839	0.32420	0.03974	3	4	5	1
5	0.00000	0.00000	-0.32419	0.32420	0.02539	4	5	6	1
6	0.00000	0.00000	0.00000	0.32419	0.02539	5	6	7	2
7	0.00000	0.00000	0.32419	0.32420	0.02539	6	7	8	3
8	0.00000	0.00000	0.64839	0.32420	0.03974	7	8	9	3
9	0.00000	0.00000	0.97259	0.32420	0.06220	8	9	10	3
10	0.00000	0.00000	1.29678	0.32420	0.09737	9	10	11	3
11	0.00000	0.00000	1.62098	0.32420	0.15240	10	11	0	3

Note that the program counts segments in absolute numbers. The Tag numbers to the far right indicate the wire to which the segment numbers are assigned. The equality of segment lengths is clear from the near-middle column. As well, we can see the segment radius tapering performed by program calculations in the Wire Radius column.

A 3-wire model of the bi-conical simulation is nearly indistinguishable internally in NEC from a model composed of individual wires, each 1 segment long and each having an assigned radius. The following segmentation table shows just such a model.

- - - - SEGMENTATION DATA - - - -
COORDINATES IN METERS
I+ AND I- INDICATE THE SEGMENTS BEFORE AND AFTER I

SEG. NO.	COORDINATES OF SEG. CENTER X	Y	Z	SEG. LENGTH	WIRE RADIUS	CONNECTION DATA I-	I	I+	TAG NO.
1	0.00000	0.00000	1.62100	0.32420	0.15200	0	1	2	1
2	0.00000	0.00000	1.29680	0.32420	0.12100	1	2	3	2
3	0.00000	0.00000	0.97260	0.32420	0.08890	2	3	4	3
4	0.00000	0.00000	0.64840	0.32420	0.05710	3	4	5	4
5	0.00000	0.00000	0.32420	0.32420	0.02540	4	5	6	5
6	0.00000	0.00000	0.00000	0.32420	0.02540	5	6	7	6
7	0.00000	0.00000	-0.32420	0.32420	0.02540	6	7	8	7
8	0.00000	0.00000	-0.64840	0.32420	0.05710	7	8	9	8
9	0.00000	0.00000	-0.97260	0.32420	0.08890	8	9	10	9
10	0.00000	0.00000	-1.29680	0.32420	0.12100	9	10	11	10
11	0.00000	0.00000	-1.62100	0.32420	0.15200	10	11	0	11

Almost the only clue that we have a different model appears in the TAG NO. column, where we see 11 different wire numbers. However, we do have a second clue: the assignment to each segment of a radius that reflects linear stepping. Sim-

ply as a matter of interest, you may wish to compare the radius values in this table to those calculated by using the GC card. The linear steps are each 0.03165 m, and the result is a continuously variable ratio between steps, one that decreases with increasing wire radius. In contrast, the earlier GC-calculated set of steps uses a ratio of about 1.565 for each step larger or smaller.

One question to consider when selecting a 1.0 ratio between successive segment lengths concerns the changing segment-length-to-radius ratio along the wire. Some modelers may prefer to use a more nearly constant or at least a slower changing ratio of segment length to radius. In the initial segmentation table, the length-to-radius ratio varies from 12.769 at the center to 2.127 at the outer ends of the dipole. To bring those ratios some distance—but far from all the way—together, we may implement a changing segment length by specifying a ratio value other than 1.0. The original model shows a pair of rates: 0.8 for the decreasing radius side of the dipole and 1.25 for the increasing radius side. These values do not coincide with the radius ratio of 1.565, but they may go some distance in closing the gap. How much they close the distance appears in the following segmentation table. See model 54-2.

- - - - SEGMENTATION DATA - - - -
COORDINATES IN METERS
I+ AND I- INDICATE THE SEGMENTS BEFORE AND AFTER I

SEG. NO.	COORDINATES OF SEG. CENTER X	Y	Z	SEG. LENGTH	WIRE RADIUS	CONNECTION DATA I-	I	I+	TAG NO.
1	0.00000	0.00000	-1.53310	0.49996	0.15240	0	1	2	1
2	0.00000	0.00000	-1.08314	0.39997	0.09737	1	2	3	1
3	0.00000	0.00000	-0.72316	0.31997	0.06220	2	3	4	1
4	0.00000	0.00000	-0.43519	0.25598	0.03974	3	4	5	1
5	0.00000	0.00000	-0.20480	0.20478	0.02539	4	5	6	1
6	0.00000	0.00000	0.00000	0.20483	0.02539	5	6	7	2
7	0.00000	0.00000	0.20480	0.20478	0.02539	6	7	8	3
8	0.00000	0.00000	0.43519	0.25598	0.03974	7	8	9	3
9	0.00000	0.00000	0.72316	0.31997	0.06220	8	9	10	3
10	0.00000	0.00000	1.08314	0.39997	0.09737	9	10	11	3
11	0.00000	0.00000	1.53310	0.49996	0.15240	10	11	0	3

The segment length to radius ratio is 8.067 at the center and 3.278 at the outer end. How much importance this factor may have will depend upon the particular

modeling project at hand. Had we doubled the number of segments in GW1 and GW3, adjusting the center segment length accordingly, the outer segments would have violated the conservative recommendation for a 4:1 segment length to radius ratio, and the revised model would not quite meet the recommendations. However, judicious use of the segment length ratio facility would ease the problem of meeting that recommendation—or any other applicable to a particular model.

Creating a Buried Radial System

NEC-4 offers the user the ability to place wires below the surface of the ground. The buried-wire capability allows more accurate modeling of vertical monopoles and related antennas that use buried ground-plane radial systems. Modeling such systems in the most economic manner relative to core run time without shortcuts that threaten the accuracy of the results is another good exercise for the GC entry.

Fig. 54-3 sketches a radial system of 120-128 radials, as might be used in either an advanced amateur or commercial broadcast antenna system. (Many such systems employ secondary short radial systems close to the antenna base.) Let's set the vertical monopole at a maximum height of 40 m and give it a 25-mm diameter. The radials will be 2-mm in diameter and extend a full 1/4 wavelength from the antenna base or 40.9553 m.

The rules for ground penetration of the monopole require that the Z=0 level coincide with a segment junction, and to minimize chances for error, many experts recommend that this also be a wire junction. The radial system will be 0.16382 m below ground, which dictates that the wire length from Z=0 to the radial junction be that length. Equally important for accuracy is that the source segment and the segments adjoining it be of equal length. Since we wish the source to be on the lowest segment above ground, that segment must be 0.16382-m long, and as well, the segment above it.

These requirements would suggest that we construct the entire model from segments that are 0.16382-m long. The result would be an exceptionally large model in terms of segment numbers. However, a technique developed for MININEC can reduce the model size to manageable proportions. Some programs, such as EZNEC, implement a form of element length-tapering that calculates from a specified end 1 (or both ends toward the middle) increasing lengths on a 2:1 length ratio, starting

from a user-specified shortest length to a user specified longest length. The result is a smaller model with no significant loss of accuracy (assuming judicious application of the tapering feature). The lower half of **Fig. 54-3** shows the general tapering principle involved.

The cost of tapering is a very significant increase in the number of individual wires, although this increase in no way matches the decrease in the total number of segments. A 128-radial version of the monopole, with element length-tapering applied to the main element as well as to the radials, results in 776 wires and 1550 segments. This is about the best one might do with an implementation of NEC that uses only the GW, GS, and GE geometry inputs. However, if the basic, pre-tapered, model had been transferred to NEC-4 in a program allowing the use of the GC entry, we might have saved about 645 of the wires. Since run time is an exponential function of both the number of segments and the number of wires, in many very large problems, we might save a significant amount of time.

Let's illustrate the differences between a hand-tapered model and a GC-tapered model using a somewhat smaller system. We shall take the same monopole and place it over only 4 radials. This move will shrink the repetitive radial portion of the model to readable proportions. An external tapering of the elements would present the following wire table (without the associated program control entries).

```
CM 160-m 1/4 wl vert-4 bur radial
CE
GW 1,7,0.,0.,40.,0.,0.,5.242276,.0125
GW 2,1,0.,0.,5.242276,0.,0.,2.621138,.0125
GW 3,1,0.,0.,2.621138,0.,0.,1.31057,.0125
GW 4,1,0.,0.,1.31057,0.,0.,.6552857,.0125
GW 5,1,0.,0.,.6552857,0.,0.,.3276435,.0125
GW 6,1,0.,0.,.3276435,0.,0.,.163821,.0125
GW 7,1,0.,0.,.163821,0.,0.,0.,.0125
GW 8,1,0.,0.,0.,0.,0.,-.163821,.0125
GW 9,1,0.,0.,-.163821,.1638211,0.,-.163821,.001
GW 10,1,.1638211,0.,-.163821,.4914632,0.,-.163821,.001
GW 11,1,.4914632,0.,-.163821,1.146747,0.,-.163821,.001
GW 12,1,1.146747,0.,-.163821,2.457316,0.,-.163821,.001
GW 13,1,2.457316,0.,-.163821,5.078453,0.,-.163821,.001
GW 14,7,5.078453,0.,-.163821,40.95526,0.,-.163821,.001
GW 15,1,0.,0.,-.163821,1.2368E-8,.1638211,-.163821,.001
GW 16,1,1.2368E-8,.1638211,-.163821,3.7104E-8,.4914632,-.163821,.001
GW 17,1,3.7104E-8,.4914632,-.163821,8.6577E-8,1.146747,-.163821,.001
```

```
GW 18,1,8.6577E-8,1.146747,-.163821,1.8552E-7,2.457316,-.163821,.001
GW 19,1,1.8552E-7,2.457316,-.163821,3.8341E-7,5.078453,-.163821,.001
GW 20,7,3.8341E-7,5.078453,-.163821,3.092E-06,40.95526,-.163821,.001
GW 21,1,0.,0.,-.163821,-.1638211,2.4736E-8,-.163821,.001
GW 22,1,-.1638211,2.4736E-8,-.163821,-.4914632,7.4209E-8,-.163821,.001
GW 23,1,-.4914632,7.4209E-8,-.163821,-1.146747,1.7315E-7,-.163821,.001
GW 24,1,-1.146747,1.7315E-7,-.163821,-2.457316,3.7104E-7,-.163821,.001
GW 25,1,-2.457316,3.7104E-7,-.163821,-5.078453,7.6683E-7,-.163821,.001
GW 26,7,-5.078453,7.6683E-7,-.163821,-40.95526,6.1841E-6,-.163821,.001
GW 27,1,0.,0.,-.163821,1.9535E-9,-.1638211,-.163821,.001
GW 28,1,1.9535E-9,-.1638211,-.163821,5.8606E-9,-.4914632,-.163821,.001
GW 29,1,5.8606E-9,-.4914632,-.163821,1.3675E-8,-1.146747,-.163821,.001
GW 30,1,1.3675E-8,-1.146747,-.163821,2.9303E-8,-2.457316,-.163821,.001
GW 31,1,2.9303E-8,-2.457316,-.163821,6.056E-08,-5.078453,-.163821,.001
GW 32,7,6.056E-08,-5.078453,-.163821,4.8839E-7,-40.95526,-.163821,.001
GE -1
```

The length-tapering of each element uses 32 wires. However, a GC-tapered equivalent model would use only 8 wires (including the untouched wires in the vicinity of the ground penetration).

```
CM 160-m 1/4 wl vert-4 bur radial
CE
GW 1,11,0.,0.,40.,0.,0.,.327644,0
GC 2 0 0 .0125 .0125 13 .16328
GW 2,1,0.,0.,.327644,0.,0.,.163821,.0125
GW 3,1,0.,0.,.163821,0.,0.,0.,.0125
GW 4,1,0.,0.,0.,0.,0.,-.163821,.0125
GW 5,12,0.,0.,-.163821,40.9553,0.,-.163821,0
GC 2 0 0 .001 .001 .163281 13.5
GW 6,12,0.,0.,-.163821,0.,40.9553,-.163821,0
GC 2 0 0 .001 .001 .163281 13.5
GW 7,12,0.,0.,-.163821,-40.9553,0.,-.163821,0
GC 2 0 0 .001 .001 .163281 13.5
GW 8,12,0.,0.,-.163821,0.,-40.9553,-.163821,0
GC 2 0 0 .001 .001 .163281 13.5
GE -1
```

We have added to each long element a GC entry. The main element entry, below GW1, works from the top of the monopole downward, while the radial entries work from the junction outward for GW5 through GW8. The model specifies a Type 2 GC entry, with both the starting and ending segment lengths specified: 0.16281

and 13.5 for the radials. The main element begins with a 13.0-m first segment and works down to the 0.16281-m length.

The essential internal calculations appear in the geometry specification section of the NEC output file. (Unfortunately, the NEC output file format is too large for the page format, and all lines are broken. I recommend that you examine the actual on-screen output file for model 54-3. Note that the model includes only wires and hence will not produce a pattern. But the NEC output file will record the wire structure.)

```
                          - - - STRUCTURE SPECIFICATION - - -
                             COORDINATES MUST BE INPUT IN
                             METERS OR BE SCALED TO METERS
                            BEFORE STRUCTURE INPUT IS ENDED
 WIRE                                                                    NO.
OF    FIRST  LAST     TAG
  NO.        X1         Y1         Z1         X2         Y2         Z2     RADIUS
SEG.      SEG.   SEG.      NO.
     1     0.00000     0.00000    40.00000      0.00000     0.00000     0.32764
0.00000      11         1    11        1
         ABOVE WIRE IS TAPERED.  REQUESTED INITIAL AND FINAL SEG. LENGTHS =
13.00000  0.16328
                                  RADIUS FROM  0.01250 TO  0.01250
                                 COMPUTED NUMBER OF SEGMENTS =    12   LENGTH
RATIO =  0.67526
     2     0.00000     0.00000     0.32764      0.00000     0.00000     0.16382
0.01250       1        13    13        2
     3     0.00000     0.00000     0.16382      0.00000     0.00000     0.00000
0.01250       1        14    14        3
     4     0.00000     0.00000     0.00000      0.00000     0.00000    -0.16382
0.01250       1        15    15        4
     5     0.00000     0.00000    -0.16382     40.95530     0.00000    -0.16382
0.00000      12        16    27        5
         ABOVE WIRE IS TAPERED.  REQUESTED INITIAL AND FINAL SEG. LENGTHS =
0.16328 13.50000
                                  RADIUS FROM  0.00100 TO  0.00100
                                 COMPUTED NUMBER OF SEGMENTS =    12   LENGTH
RATIO =  1.49568
     6     0.00000     0.00000    -0.16382      0.00000    40.95530    -0.16382
0.00000      12        28    39        6
         ABOVE WIRE IS TAPERED.  REQUESTED INITIAL AND FINAL SEG. LENGTHS =
0.16328 13.50000
                                  RADIUS FROM  0.00100 TO  0.00100
```

```
                                  COMPUTED NUMBER OF SEGMENTS =    12   LENGTH
RATIO =  1.49568
     7    0.00000    0.00000   -0.16382   -40.95530    0.00000   -0.16382
0.00000     12       40    51       7
         ABOVE WIRE IS TAPERED.  REQUESTED INITIAL AND FINAL SEG. LENGTHS =
0.16328 13.50000
                                   RADIUS FROM  0.00100 TO  0.00100
                                  COMPUTED NUMBER OF SEGMENTS =    12   LENGTH
RATIO =  1.49568
     8    0.00000    0.00000   -0.16382     0.00000  -40.95530   -0.16382
0.00000     12       52    63       8
         ABOVE WIRE IS TAPERED.  REQUESTED INITIAL AND FINAL SEG. LENGTHS =
0.16328 13.50000
                                   RADIUS FROM  0.00100 TO  0.00100
                                  COMPUTED NUMBER OF SEGMENTS =    12   LENGTH
RATIO =  1.49568

   GROUND PLANE SPECIFIED.

  TOTAL SEGMENTS USED=   63    NO. SEG. IN A SYMMETRIC CELL=   63    SYMMETRY
FLAG=  0
```

Note that each GC request for tapering specifies the same radius for the starting and stopping segments. In this instance, we are interesting only in length-tapering the segments. The result uses shorter segment lengths closer into the junction and longer ones further out than the manually tapered model. To give a one-radial example, the following table tracks the segment lengths of a radial from this model in the geometry structure section of the NEC output file, immediately following the input request section that we have just viewed.

SEG. NO.	COORDINATES OF SEG. CENTER X	Y	Z	SEG. LENGTH	WIRE RADIUS	CONNECTION DATA I-	I	I+	TAG NO.
16	0.08164	0.00000	-0.16382	0.16328	0.00100	-28	16	17	5
17	0.28539	0.00000	-0.16382	0.24422	0.00100	16	17	18	5
18	0.59013	0.00000	-0.16382	0.36527	0.00100	17	18	19	5
19	1.04592	0.00000	-0.16382	0.54632	0.00100	18	19	20	5
20	1.72765	0.00000	-0.16382	0.81712	0.00100	19	20	21	5
21	2.74728	0.00000	-0.16382	1.22215	0.00100	20	21	22	5
22	4.27232	0.00000	-0.16382	1.82794	0.00100	21	22	23	5
23	6.55330	0.00000	-0.16382	2.73400	0.00100	22	23	24	5
24	9.96489	0.00000	-0.16382	4.08919	0.00100	23	24	25	5
25	15.06753	0.00000	-0.16382	6.11610	0.00100	24	25	26	5

```
26  22.69944   0.00000  -0.16382   9.14771    0.00100    25   26   27    5
27  34.11430   0.00000  -0.16382  13.68201    0.00100    26   27    0    5
```

Whether from idle curiosity or some other purpose, we may contrast this scheme with the manually tapered comparable radial.

```
SEG.    COORDINATES OF SEG. CENTER      SEG.      WIRE    CONNECTION DATA    TAG
NO.        X          Y          Z      LENGTH    RADIUS    I-    I    I+    NO.
15   0.08191   0.00000  -0.16382   0.16382    0.00100   -27   15   16    9
16   0.32764   0.00000  -0.16382   0.32764    0.00100    15   16   17   10
17   0.81911   0.00000  -0.16382   0.65528    0.00100    16   17   18   11
18   1.80203   0.00000  -0.16382   1.31057    0.00100    17   18   19   12
19   3.76788   0.00000  -0.16382   2.62114    0.00100    18   19   20   13
20   7.64108   0.00000  -0.16382   5.12526    0.00100    19   20   21   14
21  12.76634   0.00000  -0.16382   5.12526    0.00100    20   21   22   14
22  17.89160   0.00000  -0.16382   5.12526    0.00100    21   22   23   14
23  23.01686   0.00000  -0.16382   5.12526    0.00100    22   23   24   14
24  28.14211   0.00000  -0.16382   5.12526    0.00100    23   24   25   14
25  33.26737   0.00000  -0.16382   5.12526    0.00100    24   25   26   14
26  38.39263   0.00000  -0.16382   5.12526    0.00100    25   26    0   14
```

The differences in output reports between the two systems of tapering—one continuous, the other with a user-specified limit to outer segment length—are not great. Both models show a theta angle of 73 degrees (17-degree elevation angle). The manually tapered model shows a gain of 2.10 dBi in contrast to the 2.06 figure for the GC-tapered model. The corresponding source impedance reports are 47.4 + j 14.5 Ohms and 47.5 + j 14.0 Ohms.

Although the 4-radial model saves us only 24 wires and hence little run-time on a modern PC, it is likely that a 128-radial model would save noticeable time. As well, more complex models, perhaps involving the shorter radials as well as the full size ones, might save enough time to make a difference in the course of a project.

Nevertheless, our foray into the use of the GC entry has been primarily to examine its capabilities and how to implement them. Ultimately, the aptness of the entry for a particular model is a judgment call by the modeler.

* * * * *

Models included: 54-1 through 54-3. (Models available in .NEC format only.)

55. Parallel Sources, Angular Junctions, and Average Gain: Correcting "Weaknesses"

The following notes emerged from conversations with Dean Straw of ARRL over a problematical model. By the time I finished investigating the problem, NEC had involved me with several problems simultaneously:

1. The parallel sourcing of two wires simultaneously, as the model attempted to capture the geometry that might actually be used in the physical antenna;

2. The angular junction of the two wires as they might meet at a common wire section on which we might place the source; and

3. The results of the average gain test and what they might indicate about the model and its improvement.

Let's begin with a review, starting with the Average Gain Test.

AGT

Essentially, we only need two numbers to perform the Average Gain Test (AGT): the input power and radiated power. For a lossless antenna, the input power and the average radiated power should be equal. Whatever the gain in one or more favored directions, it will be offset by nulls in other directions. Over the entire sphere of free space, the total amount of radiated power can never exceed the power supplied to the antenna. Hence, the ratio of average radiated power to supplied power should be 1. If the ratio differs by more than a small amount from 1, then the model may be considered suspect.

The conditions under which an adequate model will show an Average Power Gain (G_{ave}) of 1 also establishes the conditions for performing the Average Gain test. The model is set in free space for a k of 1 and over perfect ground for a k of 2. The wire material must be perfect or lossless. All "real" or resistive parts of loads,

networks, and transmission lines must also be set to zero (which may require in a parallel R-L-C load a very high value for the parallel resistance).

For test purposes, the model is run by taking a regular sample of the radiation pattern every few degrees, and the results are averaged. The result is a fair reading of the average radiated power. To calculate the average power gain, we simply apply the following simple equation:

$$G_{AVE} = \frac{kP_{RAD}}{P_{IN}} \qquad G_{AVE(dB)} = 10\log(G_{AVE}) \qquad 1$$

P_{rad} is the radiated power as averaged and P_{in} is the input power as calculated from source information.

The average gain figure that results from the test may be higher or lower than 1.0. One proposed gradation of model merit uses the following dividing points:

G_{ave} Value Range	Significance
0.95 - 1.05	Model is considered to have passed the test and is likely to be highly accurate.
0.90 - 0.95 and 1.05 - 1.10	Model is quite usable for most purposes.
0.80 - 0.90 and 1.10 - 1.20	Model may be useful, but adequacy can be improved.
<0.80 and >1.20	Model is subject to question and should be refined.

The user may develop more strict limits for the adequacy of a model based on the specific tasks within which the model plays a role.

Most models that deviate in the test from an average gain of 1 show an inverse correlation between errors in gain and in the resistive component of the source impedance. As the gain climbs, the source impedance decreases, and vice versa. For limited purposes, the average gain value derived from the test can be used to correct both figures, using the following equations:

$$\textit{Corrected Input Resistance} = \frac{\textit{Computed}R_{IN} \times G_{AVE}}{k} \qquad 2$$

and

$$\textit{Corrected Gain} = \frac{\textit{Computed Gain} \times k}{G_{AVE}} \qquad 3$$

Obviously, an average gain value that is greater than 1 will increase the input resistance and decrease the gain. Values less than 1 will do the opposite.

Parallel-Fed Driven Elements

When we develop a model of two or more elements that use a common source, the most common modeling configuration appears at the top of **Fig. 55-1**. We bring the element wires together at a common wire. Normally, we use 3 segments to ensure that the source segment and the adjacent segments have the same length. This technique is especially apt for center feeding, since the current levels on the segments on either side of the source segment will be equal.

Fig. 1 also shows an alternative sourcing scheme. We create independent elements, each with its own sourcing wire, with the two wires closely spaced and parallel to each other. However, we place the source on only one wire. From that wire, we run a TL transmission line from one ostensible sourcing segment to the truly sourced segment. By making the TL length very short—for example a fraction of an inch—we obtain negligible impedance transformation, effectively connecting the two source segments in parallel. Moving the actual source from one wire to the other normally yields a difference in impedance that show up only in the hundredths columns of the resistance and reactance. Although the TL length may be only a small fraction of an inch, the actual spacing of the parallel source wires may be somewhat larger. How much larger is part of the story to come.

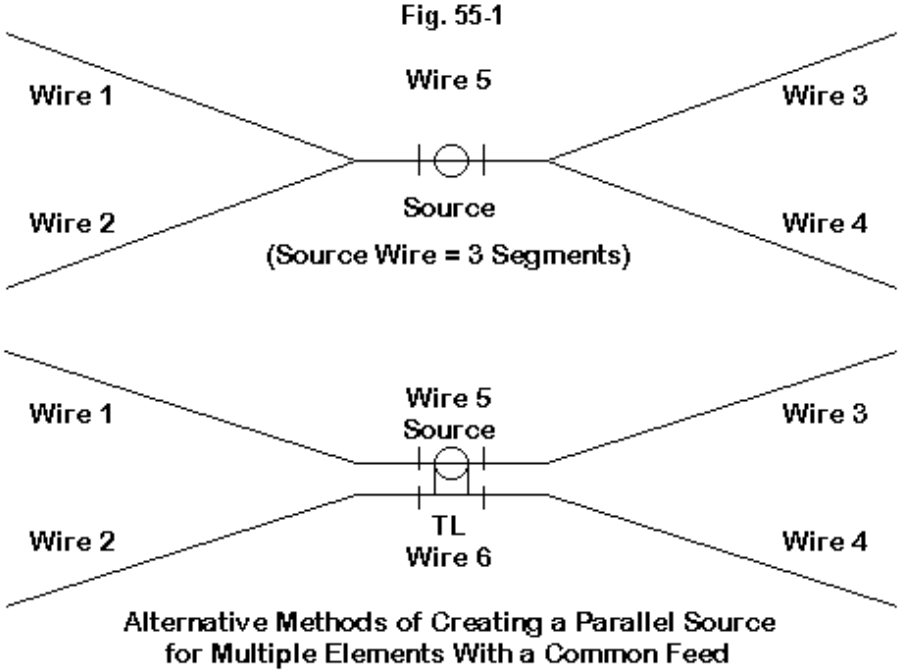

The question that emerges from this abstract presentation is this: when do we need to resort to the second mode of feeding parallel sources? The answer is not simple, but the Average Gain Test can help us decide on a case-by-case basis.

Some NEC Limitations

The alternative parallel source systems and the AGT come together in guiding our modeling, because NEC has some limitations. Moreover, some of those limita-

tions may affect NEC-2 more than NEC-4. The two most important limitations for the present situation are these:

1. The sensitivity of NEC to very closely spaced wires, especially where we cannot practically establish exacting parallelism between the segment junctions of the wires; and

2. Angular junctions of wires, as we decrease the angle between them.

NEC-2 and NEC-4 appear to be equally susceptible to the first limitation. However, NEC-2 is much more sensitive than NEC-4 to the second limitation. As a foreshadowing of notes to come, in numerous cases of the type we are dealing with, NEC-2 and NEC-4 will yield divergent output reports and AGT values using the upper configuration in **Fig. 55-1**. In some cases, we shall be able to achieve a better AGT value and a close coincidence of NEC-2 and NEC-4 reports by using the alternative feed system. Since I have no specific formula to offer as to when we might benefit from moving from one feed system to the other, a set of test cases may have to suffice to give fair warning instead.

Dipole Elements

Let's first look at a series of models of dipole elements. Each model will consist of a 28.5-MHz dipole in free space. However, each antenna will have two dipoles fed in parallel. The differences among the models will consist of the angle that each of the two dipoles takes toward the other. In all of the examples, the angular divergence of wires will occur on the X-Y plane.

Fig. 55-2 shows our initial case, where the two dipole elements are at 90 degrees to each other. The outline and the wire table show the modeling convention used. A leg from each dipole meets its counterpart at a common section of wire, using the technique at the top of **Fig. 55-1**. From this model, we obtained the following NEC-2 and NEC-4 results. (In all dipole listings, gain is the free-space gain and the source resistance is in Ohms.) See model 55-1.

Fig. 55-2

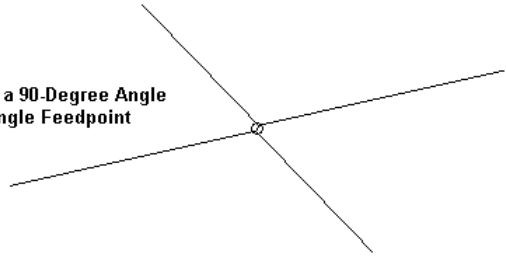

Dipoles Crossed at a 90-Degree Angle and Joined to a Single Feedpoint

Wires

Wire Other

DP10-90

Coord Entry Mode Preserve Connections

Wires

No.	End 1				End 2				Diameter	Segs
	X (in)	Y (in)	Z (in)	Conn	X (in)	Y (in)	Z (in)	Conn	(in)	
1	-97.3	0	0		-1.5	-1.5	0	W2E2	#8	50
2	0	-97.3	0		-1.5	-1.5	0	W5E1	#8	50
3	1.5	1.5	0	W4E1	97.3	0	0		#8	50
4	1.5	1.5	0	W5E2	0	97.3	0		#8	50
5	-1.5	-1.5	0	W1E2	1.5	1.5	0	W3E1	#8	3
*										

DP10-90	Max Gain dBi	Source Resistance	AGT Values Ratio	dB
NEC-4	1.17	34.62	0.997	-0.01
NEC-2	1.24	34.07	1.013	0.06

Both AGT ratings fall well within the highly accurate range. However, let's perform the corrective calculations in equations 2 and 3 as an exercise. The NEC-4 reading is 0.01 dB low, for a corrected value of 1.18 dBi. The NEC-2 gain reading is 0.06 dB high, for a corrected reading of 1.18 dBi. Using the AGT ratio as a multiplier on the resonant source resistance, we get a correct NEC-4 source resistance of 34.52 Ohms and a NEC-2 correct value of 34.51 Ohms. One could not wish for a better starting example.

Fig. 55-3

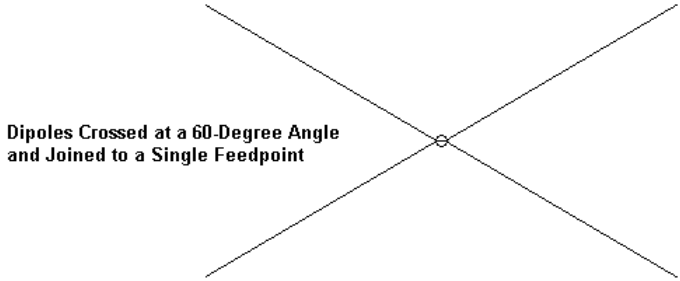

Dipoles Crossed at a 60-Degree Angle
and Joined to a Single Feedpoint

Wires

Wire Other

DP10-60

Coord Entry Mode Preserve Connections

Wires

No.	End 1				End 2				Diameter	Segs
	X (in)	Y (in)	Z (in)	Conn	X (in)	Y (in)	Z (in)	Conn	(in)	
1	47.5	-82.2	0		0	-1.5	0	W2E2	#8	50
2	-47.5	-82.2	0		0	-1.5	0	W5E1	#8	50
3	0	1.5	0	W4E1	47.5	82.2	0		#8	50
4	0	1.5	0	W5E2	-47.5	82.2	0		#8	50
5	0	-1.5	0	W1E2	0	1.5	0	W3E1	#8	3
*										

In **Fig. 55-3**, we have a model that closes the angle between dipole wires to about 60 degrees, with the element lengths adjusted for resonance within +/-1 Ohm of remnant reactance. Again, the model uses the single common wire system of parallel feeding. In this case, we obtain the following results. See model 55-2.

DP10-60	Max Gain	Source	AGT Values	
	dBi	Resistance	Ratio	dB
NEC-4	1.65	49.37	0.999	-0.00
NEC-2	1.86	47.05	1.049	0.21

Although the NEC-2 AGT value of 1.049 appears to fall within the highly accurate range, it represents a 0.21 dB over-estimate of the maximum gain. Corrected, the gain become 1.65 dBi, the same value as reported by NEC-4. Correcting the

NEC-2 source resistance yields a value of 49.36 Ohms, a match for the NEC-4 value. Whether or not the differences in NEC-2 and NEC-4 reports makes any operational difference, the example provides some insight into the fact that as we close the angle between the dipole element wires, NEC-2 more rapidly departs from a perfect AGT report than does NEC-4.

Fig. 55-4

Dipoles Crossed at a 20-Degree Angle and Joined to a Single Feedpoint

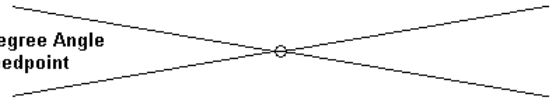

Wires

Wire Other DP10-20

☐ Coord Entry Mode ☐ Preserve Connections

Wires

No.	End 1				End 2				Diameter	Segs
	X (in)	Y (in)	Z (in)	Conn	X (in)	Y (in)	Z (in)	Conn	(in)	
1	15	-90.4	0		0	-1.5	0	W2E2	#8	50
2	-15	-90.4	0		0	-1.5	0	W5E1	#8	50
3	0	1.5	0	W4E1	15	90.4	0		#8	50
4	0	1.5	0	W5E2	-15	90.4	0		#8	50
5	0	-1.5	0	W1E2	0	1.5	0	W3E1	#8	3
*										

Fig. 55-4 closes the angle still further—to between 19 and 20 degrees. Once more, the element lengths have changed to obtain resonance. From this model, still using the single common feed wire, we obtain the following reports. See model 55-3.

DP10-20	Max Gain	Source	AGT Values	
	dBi	Resistance	Ratio	dB
NEC-4	2.32	57.45	1.069	0.29
NEC-2	2.96	49.62	1.238	0.93

The 20-degree angle between element wires yields gain values that exceed the possible gain of a dipole in free space for both cores. Moreover, we see a continuing more rapid departure from an ideal AGT value in the NEC-2 report than the

NEC-4 report. However, even the NEC-4 report has fallen out of the ostensible "highly accurate" range.

Corrected, the NEC-4 maximum gain is 2.03 dBi, the same value as the corrected NEC-2 maximum gain value. The corrected NEC-4 source resistance is 61.41 Ohms, while correcting NEC-2 yield 61.42 Ohms. Once more, the AGT permits us to correct the values listed, but we have a remnant difficulty. The NEC-4 source impedance shows a reactance of +0.33 Ohms, while the NEC-2 report shows +1.40 Ohms. The AGT provides no guidance on handling the reactance.

The divergence of the initially reported values for the two cores for the 20-degree dipole case suggests that it is time to try the alternative feed system. See **Fig. 55-5** and model 55-4.

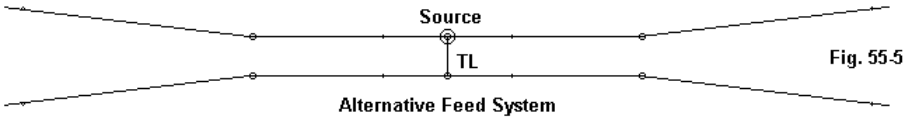

Fig. 55-5

Wires

Wire Other DP10-20-A

Coord Entry Mode Preserve Connections

Wires

No.	End 1				End 2				Diameter	Segs
	X (in)	Y (in)	Z (in)	Conn	X (in)	Y (in)	Z (in)	Conn	(in)	
1	15	-90.4	0		0	-1.5	0.25	W5E1	#8	50
2	-15	-90.4	0		0	-1.5	-0.25	W6E1	#8	50
3	0	1.5	0.25	W5E2	15	90.4	0		#8	50
4	0	1.5	-0.25	W6E2	-15	90.4	0		#8	50
5	0	-1.5	0.25	W1E2	0	1.5	0.25	W3E1	#8	3
6	0	-1.5	-0.25	W2E2	0	1.5	-0.25	W4E1	#8	3
*										

The figure shows only the feed portion of the model. The AWG #8 wires are 0.1285" in diameter and are spaced 0.5" apart. Because this model is highly symmetrical, the close spacing is possible, but wider spacing may be necessary for other types of models. The element ends remained at their original positions, even

though separating the two feed sections slightly shortens each modeled element's total length. The transmission line length is 0.01". From this model, we obtain the following results.

DP10-20A	Max Gain dBi	Source Resistance	AGT Values Ratio	dB	Reactance
NEC-4	2.07	60.72	1.010	0.04	-j 5.39
NEC-2	2.07	60.74	1.009	0.04	-j 5.31

Most notable in the table is the exacting coincidence of NEC-2 and NEC-4 reports, including the AGT values. Correction of the gain to 2.03 dBi and the source resistance to 61.3 Ohms in both cases is simple. However, with slightly wider spacing, one can bring the AGT value close to 1.000 for the model on both cores.

The alternative parallel sourcing system, then, can overcome some of the divergence in reports between NEC-2 and NEC-4. In this case, the greater sensitivity of NEC-2 to small angular junctions of wires disappears in the alternative system, because it removes the tight angular junctions altogether.

Closed Geometry Cases

A second test that we might perform on the angular junction situation occurs with multi-band quad beams that use a common feedpoint. Let's look at two cases, the first of which involves quads for 14 and 28 MHz. **Fig. 55-6** shows the basic layout where the drivers come together in a single 3-segment wire that lies in the plane of the 10-meter driver loop wire. Hence, only the 20-meter loop shows significant departure from a standard square quad loop. See model 55-5.

The wire table reveals that the two quads are concentric and spaced from driver to reflector at 0.16 wavelength. Thus, the 20-meter reflector is behind the 10-meter reflector and the 20-meter driver is forward of the 10-meter driver. The angle made by the lower (fed) 20-meter wire is correspondingly complex.

The following table of results gives both 14 and 28 MHz values for both cores. Since the antenna is 35' over real ground, the gain value includes a Take-Off angle or elevation angle of maximum radiation. The driven elements are not resonant, so the source impedance gives an R +/- jX value in Ohms.

Fig. 55-6

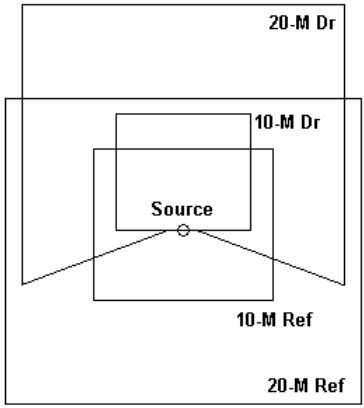

Concentric 10 and 20 Meter 2-Element Quad Beams With a Common Feedpoint at the 10-Meter Driver Source

Wires

Wire Other

QU10-20

☐ Coord Entry Mode ☐ Preserve Connections

Wires

No.	End 1				End 2				Diameter	Segs
	X (ft)	Y (ft)	Z (ft)	Conn	X (ft)	Y (ft)	Z (ft)	Conn	(in)	
1	-8.4	5.55	26.6	W5E2	-0.75	2.75	31.5	W10E2	#14	8
2	0.75	2.75	31.5	W11E2	8.4	5.55	26.6	W3E1	#14	8
3	8.4	5.55	26.6	W2E2	8.4	5.55	43.4	W4E1	#14	15
4	8.4	5.55	43.4	W3E2	-8.4	5.55	43.4	W5E1	#14	15
5	-8.4	5.55	43.4	W4E2	-8.4	5.55	26.6	W1E1	#14	15
6	-9.27	-5.55	25.85	W9E2	9.27	-5.55	25.85	W7E1	#14	15
7	9.27	-5.55	25.85	W6E2	9.27	-5.55	44.15	W8E1	#14	15
8	9.27	-5.55	44.15	W7E2	-9.27	-5.55	44.15	W9E1	#14	15
9	-9.27	-5.55	44.15	W8E2	-9.27	-5.55	25.85	W6E1	#14	15
10	-3.5	2.75	31.5	W15E2	-0.75	2.75	31.5	W11E1	#14	4
11	-0.75	2.75	31.5	W1E2	0.75	2.75	31.5	W12E1	#14	3
12	0.75	2.75	31.5	W2E1	3.5	2.75	31.5	W13E1	#14	4
13	3.5	2.75	31.5	W12E2	3.5	2.75	38.5	W14E1	#14	7
14	3.5	2.75	38.5	W13E2	-3.5	2.75	38.5	W15E1	#14	7
15	-3.5	2.75	38.5	W14E2	-3.5	2.75	31.5	W10E1	#14	7
16	-4.65	-2.75	30.42	W19E2	4.65	-2.75	30.42	W17E1	#14	7
17	4.65	-2.75	30.42	W16E2	4.65	-2.75	39.58	W18E1	#14	7
18	4.65	-2.75	39.58	W17E2	-4.65	-2.75	39.58	W19E1	#14	7
19	-4.65	-2.75	39.58	W18E2	-4.65	-2.75	30.42	W16E1	#14	7

QU10-20	Freq. MHz	Max Gain dBi	Source Impedance	AGT Values Ratio	dB
NEC-4	14	11.49/24	97.6-j43.6	1.005	0.02
	28	6.57/33	211.4+j14.3	1.006	0.03
NEC-2	14	11.86/24	90.3-j36.6	1.089	0.37
	28	6.93/33	195.1+j21.0	1.095	0.39

According to gradation scales, the NEC-4 model is highly accurate, while the NEC-2 model is reasonably accurate. The corrected gain is 6.54 and 6.55 dBi for NEC-2 and NEC-4 at 28 MHz and 11.49 and 11.47 dBi for NEC-2 and NEC-4 at 14 MHz. Corrected source resistances are about 213 Ohms at 28 MHz and 98 Ohms at 14 MHz for both cores.

The question we might pose is to what degree we can trust these corrected values, since the model deals with a closed geometry. To perform a test, I developed the alternative feed structure for the drivers, as shown in **Fig. 55-7**.

The trial spacing of the source wires, using AWG #14 (0.0641" diameter) wire, was 0.05' or 0.6". This spacing had proven adequate for the 20-degree dipoles and was worth a try. The TL line was set at 0.01' or 0.12". Swapping feedpoints at the ends of the line yielded a difference in the source impedance only in the 4th significant digit. The results that emerged are in the following table. See model 55-6.

QU10-20A	Freq. MHz	Max Gain dBi	Source Impedance	AGT Values Ratio	dB
NEC-4	14	11.11/24	101.8-j43.2	0.920	-0.36
	28	6.30/33	247.8-j15.4	0.915	-0.38
NEC-2	14	11.13/24	101.9-j43.5	0.920	-0.36
	28	6.29/33	248.4-j15.6	0.915	-0.38

Alternative Drive System

Fig. 55-7

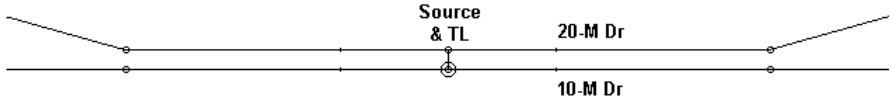

Wires

Wire Other

QU10-20A

Coord Entry Mode Preserve Connections

Wires

No.	End 1				End 2				Diameter	Segs
	X (ft)	Y (ft)	Z (ft)	Conn	X (ft)	Y (ft)	Z (ft)	Conn	(in)	
1	-8.4	5.55	26.6	W6E2	-0.75	2.8	31.5	W2E1	#14	8
2	-0.75	2.8	31.5	W1E2	0.75	2.8	31.5	W3E1	#14	3
3	0.75	2.8	31.5	W2E2	8.4	5.55	26.6	W4E1	#14	8
4	8.4	5.55	26.6	W3E2	8.4	5.55	43.4	W5E1	#14	15
5	8.4	5.55	43.4	W4E2	-8.4	5.55	43.4	W6E1	#14	15
6	-8.4	5.55	43.4	W5E2	-8.4	5.55	26.6	W1E1	#14	15
7	-9.27	-5.55	25.85	W10E2	9.27	-5.55	25.85	W8E1	#14	15
8	9.27	-5.55	25.85	W7E2	9.27	-5.55	44.15	W9E1	#14	15
9	9.27	-5.55	44.15	W8E2	-9.27	-5.55	44.15	W10E1	#14	15
10	-9.27	-5.55	44.15	W9E2	-9.27	-5.55	25.85	W7E1	#14	15
11	-3.5	2.75	31.5	W16E2	-0.75	2.75	31.5	W12E1	#14	4
12	-0.75	2.75	31.5	W11E2	0.75	2.75	31.5	W13E1	#14	3
13	0.75	2.75	31.5	W12E2	3.5	2.75	31.5	W14E1	#14	4
14	3.5	2.75	31.5	W13E2	3.5	2.75	38.5	W15E1	#14	7
15	3.5	2.75	38.5	W14E2	-3.5	2.75	38.5	W16E1	#14	7
16	-3.5	2.75	38.5	W15E2	-3.5	2.75	31.5	W11E1	#14	7
17	-4.65	-2.75	30.42	W20E2	4.65	-2.75	30.42	W18E1	#14	7
18	4.65	-2.75	30.42	W17E2	4.65	-2.75	39.58	W19E1	#14	7
19	4.65	-2.75	39.58	W18E2	-4.65	-2.75	39.58	W20E1	#14	7
20	-4.65	-2.75	39.58	W19E2	-4.65	-2.75	30.42	W17E1	#14	7

The coincidence of all reports between the two cores confirms that the use of separate feed wires with a very short TL overcomes the differential sensitivity between NEC-2 and NEC-4 to the angular junction of wires. However, the AGT values suggest there remains a problem that is common to both cores, relative to an ideal report. The most likely culprit is the spacing between the source/TL wires. There-

fore, I increased the spacing from 0.6" to 3", while leaving the TL length at 0.12". The reports that emerged from model 55-7 were as follows.

QU10-20B	Freq. MHz	Max Gain dBi	Source Impedance	AGT Values Ratio	dB
NEC-4	14	11.47/24	97.0-j44.1	1.000	0.00
	28	6.697/33	228.9-j30.5	1.000	0.00
NEC-2	14	11.49/24	93.1-j44.4	1.000	0.00
	28	6.69/33	229.5-j30.8	1.000	0.00

The 20-meter gain values from this version of the model coincide exactly with the corrected values for the original model and for the first try at using the alternative feed system. The 10-meter gain values are slightly higher than the original model corrected values and in line with the correct values for the first try at the alternative system. As we expected, the NEC-2 and NEC-4 models remained closely coincident.

As well, the corrected first try and the second try source resistance values are closely aligned. However, they both depart somewhat from the common feed-wire system model, even when corrected. As well, we have no guidance as to what set of reactance values may apply. However, the major changes toward capacitive reactance occur at 14 MHz, and that wire has grown shorter with each alternative feed system maneuver.

In general, this exercise on the original 14-28-MHz model has aimed to identify aspects of the sourcing situation that are divergent between cores and those that are common to both cores. Nothing in the original model was so far out of line with reality to make it wholly unusable. However, we may sample a more extreme case.

Fig. 55-8 shows the driver feed section and wire table for a combined 2-element quad for both 12 and 10 meters. The principles are identical to those of the 14-28-MHz original model with one exception. The angular junction of feed wires is much smaller. The results clearly show what happens. Once more, the antenna is centered 35' above real ground. See model 55-8.

10/12-Meter Quads With
a Common Driver Source

Fig. 55-8

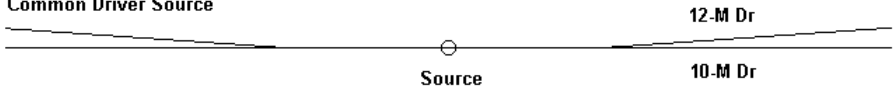

Wires

Wire Other

QU10-12

☐ Coord Entry Mode ☐ Preserve Connections

Wires

	No.	End 1				End 2				Diameter	Segs
		X (ft)	Y (ft)	Z (ft)	Conn	X (ft)	Y (ft)	Z (ft)	Conn	(in)	
▶	1	-4.5	2.155	30.5	W6E2	-0.75	2.155	30.5	W2E1	#14	7
	2	-0.75	2.155	30.5	W11E2	0.75	2.155	30.5	W3E1	#14	3
	3	0.75	2.155	30.5	W12E1	4.5	2.155	30.5	W4E1	#14	7
	4	4.5	2.155	30.5	W3E2	4.5	2.155	39.5	W5E1	#14	17
	5	4.5	2.155	39.5	W4E2	-4.5	2.155	39.5	W6E1	#14	17
	6	-4.5	2.155	39.5	W5E2	-4.5	2.155	30.5	W1E1	#14	17
	7	-4.65	-2.155	30.35	W10E2	4.65	-2.155	30.35	W8E1	#14	17
	8	4.65	-2.155	30.35	W7E2	4.65	-2.155	39.65	W9E1	#14	17
	9	4.65	-2.155	39.65	W8E2	-4.65	-2.155	39.65	W10E1	#14	17
	10	-4.65	-2.155	39.65	W9E2	-4.65	-2.155	30.35	W7E1	#14	17
	11	-4.9	2.465	30.1	W15E2	-0.75	2.155	30.5	W1E2	#14	20
	12	0.75	2.155	30.5	W2E2	4.9	2.465	30.1	W13E1	#14	20
	13	4.9	2.465	30.1	W12E2	4.9	2.465	39.9	W14E1	#14	20
	14	4.9	2.465	39.9	W13E2	-4.9	2.465	39.9	W15E1	#14	20
	15	-4.9	2.465	39.9	W14E2	-4.9	2.465	30.1	W11E1	#14	20
	16	-5.1	-2.465	29.9	W19E2	5.1	-2.465	29.9	W17E1	#14	20
	17	5.1	-2.465	29.9	W16E2	5.1	-2.465	40.1	W18E1	#14	20
	18	5.1	-2.465	40.1	W17E2	-5.1	-2.465	40.1	W19E1	#14	20
	19	-5.1	-2.465	40.1	W18E2	-5.1	-2.465	29.9	W16E1	#14	20
*											

QU10-12	Freq. MHz	Max Gain dBi	Source Impedance	AGT Values Ratio	dB
NEC-4	24.94	12.04/15	109.9-j 3.0	1.095	0.40
	28.5	10.43/13	1378+j1644	1.198	0.78
NEC-2	24.94	12.96/15	89.8+j15.4	1.356	1.32
	28.5	11.31/13	1042+j1315	1.464	1.66

The corrected gain values for each core show 11.64 dBi at 24.94 MHz and 9.65 dBi at 28.5 MHz. However, the 28.5-MHz impedance values are almost unbelievable. Therefore, I introduced the alternate feed system, shown in **Fig. 55-9**.

10/12-Meter Quads With an Alternative Driver Source System **Fig. 55-9**

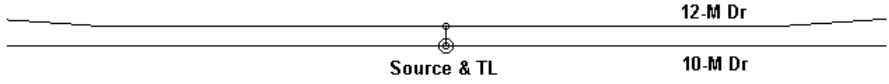

Wires

Wire Other QU10-12A

Coord Entry Mode Preserve Connections

Wires

No.	End 1				End 2				Diameter	Segs
	X (ft)	Y (ft)	Z (ft)	Conn	X (ft)	Y (ft)	Z (ft)	Conn	(in)	
1	-4.5	2.155	30.5	W6E2	-0.75	2.155	30.5	W2E1	#14	7
2	-0.75	2.155	30.5	W1E2	0.75	2.155	30.5	W3E1	#14	3
3	0.75	2.155	30.5	W2E2	4.5	2.155	30.5	W4E1	#14	7
4	4.5	2.155	30.5	W3E2	4.5	2.155	39.5	W5E1	#14	17
5	4.5	2.155	39.5	W4E2	-4.5	2.155	39.5	W6E1	#14	17
6	-4.5	2.155	39.5	W5E2	-4.5	2.155	30.5	W1E1	#14	17
7	-4.65	-2.155	30.35	W10E2	4.65	-2.155	30.35	W8E1	#14	17
8	4.65	-2.155	30.35	W7E2	4.65	-2.155	39.65	W9E1	#14	17
9	4.65	-2.155	39.65	W8E2	-4.65	-2.155	39.65	W10E1	#14	17
10	-4.65	-2.155	39.65	W9E2	-4.65	-2.155	30.35	W7E1	#14	17
11	-4.9	2.465	30.1	W16E2	-0.75	2.2	30.5	W12E1	#14	9
12	-0.75	2.2	30.5	W11E2	0.75	2.2	30.5	W13E1	#14	3
13	0.75	2.2	30.5	W12E2	4.9	2.465	30.1	W14E1	#14	9
14	4.9	2.465	30.1	W13E2	4.9	2.465	39.9	W15E1	#14	20
15	4.9	2.465	39.9	W14E2	-4.9	2.465	39.9	W16E1	#14	20
16	-4.9	2.465	39.9	W15E2	-4.9	2.465	30.1	W11E1	#14	20
17	-5.1	-2.465	29.9	W20E2	5.1	-2.465	29.9	W18E1	#14	20
18	5.1	-2.465	29.9	W17E2	5.1	-2.465	40.1	W19E1	#14	20
19	5.1	-2.465	40.1	W18E2	-5.1	-2.465	40.1	W20E1	#14	20
20	-5.1	-2.465	40.1	W19E2	-5.1	-2.465	29.9	W17E1	#14	20
*										

The feed-wire spacing is 0.045' or .54", with a TL length of 0.01' or 0.12". Using this system, model 55-9 returned the following results.

QU10-12A	Freq.	Max Gain	Source	AGT Values	
	MHz	dBi	Impedance	Ratio	dB
NEC-4	24.94	11.67/15	118.9-j30.8	1.002	0.01
	28.5	12.04/13	134.3+j71.7	1.001	0.01
NEC-2	24.94	11.65/15	119.7-j31.0	1.002	1.01
	28.5	12.04/13	134.4+j71.8	1.001	1.01

The alternate feed system is a necessity in this case to yield values that are sensible. However, had we not had the AGT to alert us to the distortions in the model reports occasioned by the very narrow angle at the driver wire junctions, we might well have interpreted the results as suggesting that interactions among the elements in a physical antenna would make the combination quad impossible to construct.

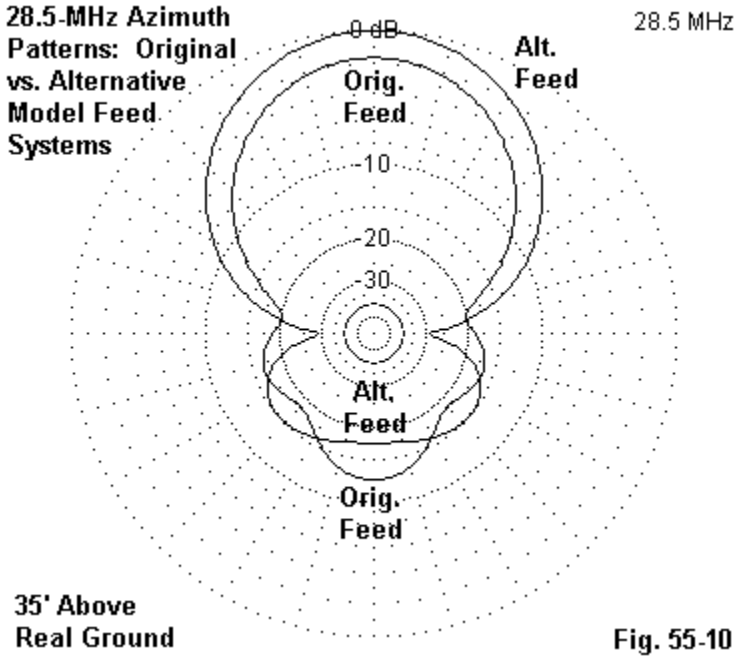

Fig. 55-10

The differences show up most clearly in the overlaid NEC-4 azimuth patterns for 28.5 MHz for the two versions of the model, shown in **Fig. 55-10**. The disparity between the patterns calls for little comment.

Conclusion

The exercises included in these notes only sample the many facets of modeling that we have touched upon so far. We have looked at differential sensitivities between NEC-2 and NEC-4. We have also looked at sample problems common to both cores. We have used the Average Gain Test to uncover both types of difficulties. And we have employed an alternative scheme for parallel feeding elements from a common source as one route to overcoming those problems.

The variations on the many themes are endless. In the end, the individual modeler must use all of the tests at hand to detect problems and to devise solutions that offer a route to more precise and accurate models. As we have seen in at least one case, a failure to exercise such care may lead to completely misleading results.

* * * * *

Models included: 55-1 through 55-9. (.NEC and .NWP model dimensions in meters; .EZ model dimensions in inches or feet.)

56. When MININEC is Superior to NEC

Although NEC (-2 or -4) has become the *de facto* stand for modeling LF through VHF wire antennas, we should be aware that there are cases in which public domain MININEC, especially in its corrected and improved versions, may yield superior results. In an earlier column, I compared some results using NEC-4 and various implementations of public domain MININEC. However, in that column, I used NEC-4 as a standard against which to compare the various versions of MININEC. The models used were selected on the basis of the known accuracy of NEC-4 relative to the model geometries involved.

NEC-2/-4 Weaknesses

There are, however, a number of model geometries, which neither NEC-2 nor NEC-4 handle very well. NEC-2 has its well-documented weakness with any stepping of element diameter. When elements are linear, the Leeson corrections provide accurate results. However, the Leeson corrections actually provide the user with a substitute constant-diameter element having the same electrical properties as the original stepped diameter element. Moreover, the use of a Leeson-substitute is applicable only when the element is a. linear, b. within about 15% of half-wavelength resonance (1/4-wavelength resonance for vertical monopoles), and c. not loaded except at the element center (if horizontal) or at the element base (if a 1/4-wavelength monopole). Although exceptionally useful for monoband Yagis, the Leeson corrections have limitations when we try to model arrays with loaded elements or arrays that intermix elements for many frequencies.

NEC-4 has to a major extent overcome the NEC-2 weakness with stepped-diameter elements. However, the results grow more inaccurate as the diameter step grows larger. In most cases, the potential for error shows up on the average gain test as a value that departs considerably from the ideal 1.00 (for horizontal elements—2.00 for monopoles touching the ground). Therefore, when using even NEC-4, running the average gain test after removing all resistive loading from the antenna and placing it in free space (or over perfect ground for monopoles touching the ground) is a crucial step in assessing the appropriate confidence level in a model.

Both NEC-2 and NEC-4 retain weaknesses in related model geometries where no easy correctives current exist. One such area is an angular junction of wires that have dissimilar diameters. This form of construction is common in LF through VHF antenna construction. At lower frequencies, wire extensions may emanate from a tower. At higher frequencies, antenna elements may begin as aluminum tubing and end as copper wire.

The errors that accrue to angular junctions of dissimilar diameter wires tend to disappear with at least one type of structure. Consider an element with a symmetrical hat structure (or a ground-plane radial structure). If the structure of wires is truly symmetrical, then the net radiation from the structure is (nearly) zero. With these types of structures, the angular junction errors tend to disappear.

A second type of error that appears in both NEC-2 and NEC-4 models appears when we closely space elements of different diameters. The common folded dipole may use length-wise wires of differing diameters to control the impedance step-up over a standard dipole. The ratio is 4:1 only if both wires are the same diameter—and NEC handles this case very well if the segment junctions are well aligned for the two wires. However, if the unfed wire is significantly thicker or thinner than the fed wire, then NEC yields results that are prone to error.

The wires need not be connected at the ends for the errors to appear. In open-sleeve coupling situations, the fed element and the slaved element may be a. in very close proximity and b. of different lengths and diameters. Depending upon the lengths, the diameters, and the spacing, considerable error may creep into the NEC output. The closer the spacing, the higher the error.

For a more complete review of these weakness, see “NEC-4.1: Limitations of Importance to Hams,” *QEX* (May/June, 1998), pp. 3-16.

MININEC 3.13 Strengths and Weaknesses

MININEC 3.13 is the public domain version of the program. As such, it has been subject to numerous modifications by those implementing the core within more user-friendly interfaces. In its initial form, MININEC has a series of known weaknesses.

1. MININEC requires an excessively high level of segmentation to overcome errors at angular junctions of wires.

2. There is a known limit to the smallest angle that MININEC may handle with a wire junction at any level of segmentation

3. As one increases frequency, MININEC shows a frequency offset of increasing proportions.

4. As one decreases the spacing between wires, inaccuracies increase.

Each of these inadequacies has been addressed by at least one implementation of MININEC. However, the latest incarnation of public domain MININEC—Antenna Model—has addressed all of them and returns results that are very consistent with NEC-4 models through the lower UHF region (the limits of my testing so far).

Thus far, no one has managed to weld the highly accurate Sommerfeld ground calculation system to MININEC. Hence, the simple reflection coefficient system remains in all current implementations of the program. Any wire with a horizontal component (meaning both horizontal and tilted wires) will show increasing inaccuracy of results when the wire is less than about 0.2 wavelength high at its lowest point. MININEC thus shows its greatest strengths when the model is in free space or at a relatively high position relative to the ground.

(We shall by-pass in this column the use of a MININEC ground as a substitute for ground-plane radials for monopoles touching the ground. I did a series of articles "Some Facts of Life About Modeling 160-Meter Vertical Arrays" for *The National Contest Journal* in 200-2001 the explore this territory in considerable detail.)

MININEC 3.13 tends to show its strength in just the areas where NEC displays its weaknesses. Linear elements with a stepped diameter produce accurate results without need for any correctives. Indeed, the original Leeson correctives were calibrated to MININEC results using the same elements. (See Chapter 8 of *Physical Design of Yagi Antennas* by David B. Leeson, especially section 8.5.) Moreover, angular junctions of dissimilar-diameter wires can be routinely handled once correctives are introduced for the basic angular junction difficulty in MININEC. Fi-

nally, MININEC shows an ability to yield accurate results with closely spaced wires of differing diameters once the basic close-spaced wire inadequacy has been corrected.

Note that many of the MININEC strengths—excepting the ability to handle directly stepped-diameter wires—depend upon the introduction of correctives to initial MININEC weaknesses. Hence, the reliability of MININEC 3.13 depends to a great degree upon the adequacy and number of correctives introduced into the calculating core. AO has a good frequency corrective and ELNEC has a good close-wire corrective. As noted, however, Antenna Model has introduced the most thoroughgoing collection of corrections and will be used as the MININEC program in a couple of sample exercises.

A VHF Rectangle as a Sample Comparison between MININEC and NEC

As an exercise for which I have actually built a physical antenna to check models against reality, let's consider a 2-meter rectangle designed for 146.0 MHz. **Fig. 56-1** shows the model, its segmentation, and feedpoint. The model shape was dictated by the task specification of arriving at an antenna having a feedpoint impedance that yields a low SWR with 50-Ohm coaxial cable feedline. The model uses (in the MININEC version) 16 segments in the horizontal legs and 34 segments in the vertical legs.

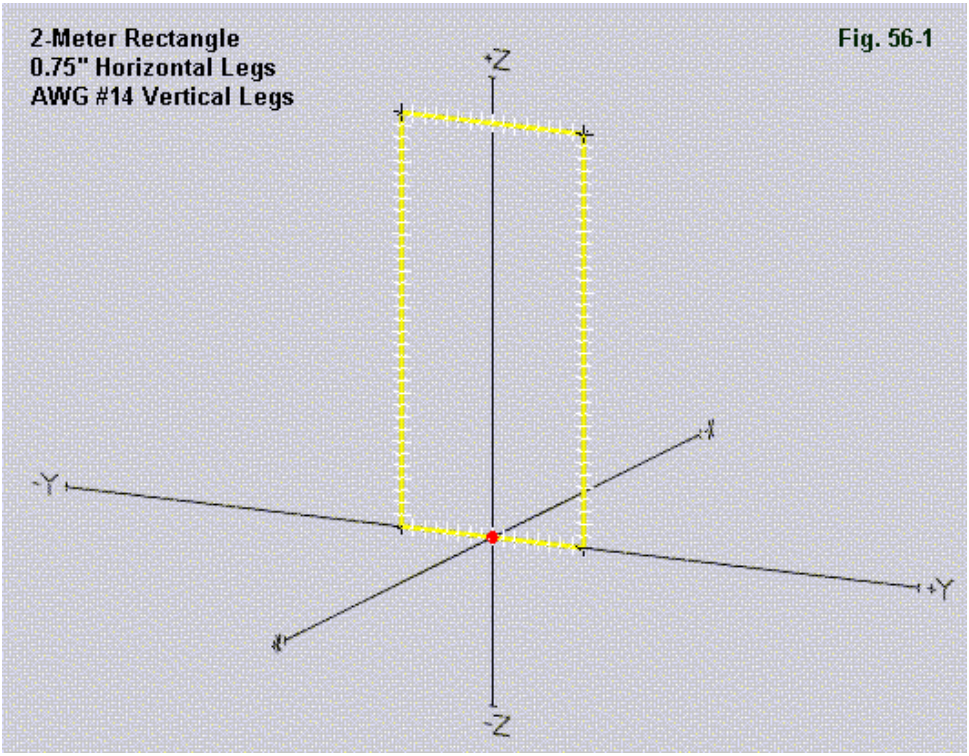

The physical construction of the antenna appears in outline form in **Fig. 56-2**. The horizontal legs consist of 0.75" diameter aluminum tubing 16.0" long. The lower horizontal leg is split for direct connection of a female UHF connector. The vertical legs each use 33.75" of AWG #14 wires (0.0641" diameter). The wires are bare copper. The test antenna itself used a simple PVC vertical center support and small blocks of wood to support the horizontal legs. The vertical PVC support used two different nesting sizes of PVC to allow for adjustment of the vertical height during tests. See model 56-1.

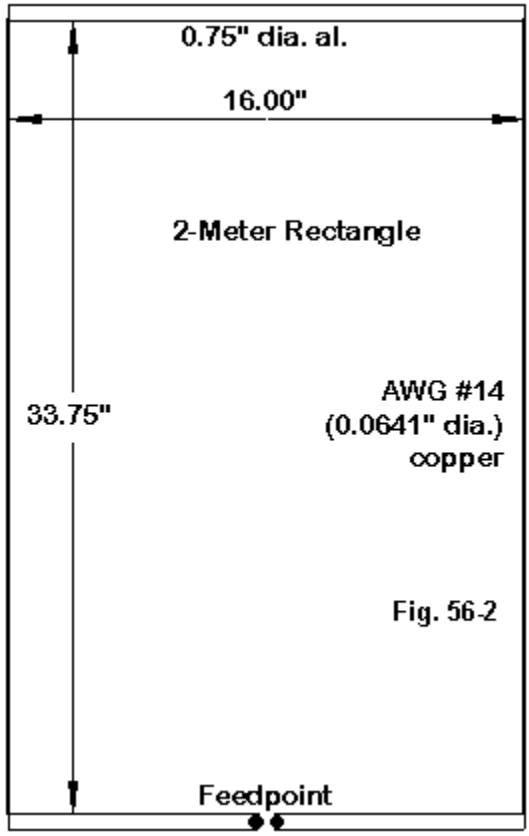
0.75" dia. al.
16.00"
2-Meter Rectangle
33.75"
AWG #14
(0.0641" dia.)
copper
Feedpoint

Fig. 56-2

The free-space pattern for the antenna appears in 3-dimensional form in **Fig. 56-3**. For those more used to seeing 2-dimensional patterns for the antenna, **Fig. 56-4** provides the azimuth or E-plane pattern for the antenna. Note that the nulls at 90 degrees to broadside to the antenna are not as deep as those on a dipole placed in free space. There is significant radiation from the vertical legs of any quad loop, square or rectangular—at least enough to diminish the nulls off the edge of the array.

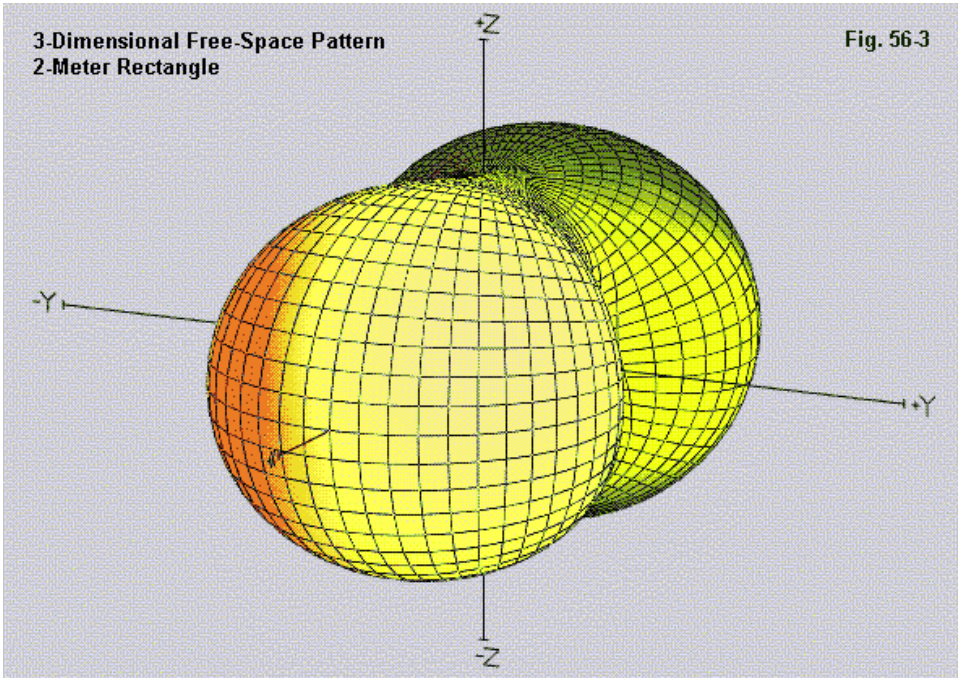

I ran this antenna at 146.0 MHz using Antenna Model's corrected MININEC and on various implementations of NEC-2 and NEC-4. The following table summarizes the results. There was no difference between single and double precision NEC-4 values.

Core	Impedance R+/-jX Ohms	Free-Space Gain dBi	AGT Gain/dB
MININEC (AM)	53.1 + j 0.7	5.04	0.9871/-0.06
NEC-4	65.2 + j68.6	5.01	0.9780/-0.10
NEC-2	83.8 + j152	4.82	0.9470/-0.24

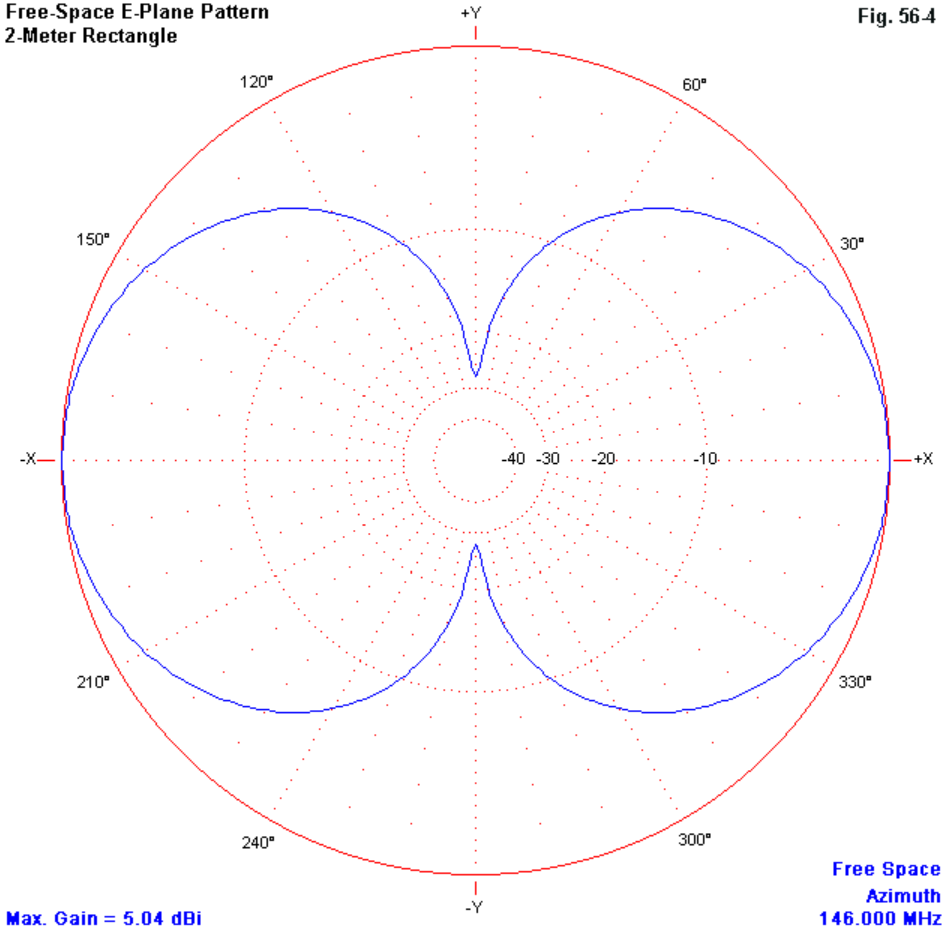

There are several facets to explore in this table. Although one might view some aspects as unnecessarily subtle, the results form an interesting composite.

First, the average gain test (AGT) values emerge from both EZNEC and NEC-Win Plus for the NEC-2 test—and are consistent in both. EZNEC shares in common with Antenna Model the ability to arrive at an AGT value even if the elements have material loading (LD5 in NEC). These values are of little or no use, since they do not differentiate between material losses and a failure to achieve an ideal 1.0 AGT value due to the antenna geometry in relationship to core calculations. Therefore, one must use care to use perfect or lossless wire for the test. NEC-Win Plus does this automatically in its implementation of the test.

The AGT value can be translated into a gain deficit (as in the example) or a gain surplus by multiplying the common log of the AGT value by 10. In all three cases, the corrected gain value (the reported value minus the AGT in dB) becomes something very close to 5.1 dBi.

The AGT value itself may be used to correct source impedances having negligible reactance. Multiply the source resistance by the AGT. The MININEC report becomes about 52.4 Ohms, a difference too small for my instruments to measure. However, the high reactance associated with the NEC source impedance reports voids the use of the AGT to correct the source resistance values.

In fact, adjusting the vertical legs of the NEC models to yield a source impedance close to resonant provided me with a simple test of which program provided the most accurate results. NEC-4 required vertical legs of 32" to yield a source impedance of about 57 Ohms, while NEC-2 needed vertical legs 29.6" long to report a resonant source impedance of about 65 Ohms. The significant difference between the length of the vertical legs with no change of the horizontal legs allowed a simple test to determine the most accurate modeling result.

The physical antenna was within about 0.2" of the MININEC results and showed a source impedance very close to 50 Ohms—allowing for instrument error. It is interesting to note that ELNEC, which does not use a frequency corrective for its MININEC core, reported a gain of 5.1 dBi and a source impedance of 50.8 - j 4.0 Ohms, indicating that the frequency drift of raw MININEC has not surpassed usability at the 146-MHz range.

A Step-Up Folded Dipole as a Sample Comparison between NEC and MININEC

A folded dipole that is resonant on any given frequency will exhibit the familiar 4:1 impedance set-up relative to a single wire resonant dipole only if the long wires are of equal diameter. If the fed wire is larger in diameter than the unfed wire, then the impedance will increase by less than 4:1, but in no case will it be less than 1:1. If the unfed wire is larger in diameter than the fed wire, then the impedance ratio relative to a single-wire resonant dipole will be greater than 4:1.

The theoretical impedance transformation is given by the following equation:

$$R = \left(1 + \frac{\log \frac{2s}{d_1}}{\log \frac{2s}{d_2}} \right)^2 \qquad (1)$$

R is the impedance transformation ratio, s is the wire spacing, center-to-center, d_1 is the diameter of the fed wire, and d_2 is the diameter of the second wire, and where s, d_1, and d_2 are given in the same units.

Suppose that we create a folded dipole using AWG #12 wire (0.0808" dia.) for the fed wire and 0.5" diameter for the unfed wire. Let's also space the wires 3" (0.25') center-to-center. The impedance transformation predicted by the equation is 7.47. If a single wire dipole has an impedance of abut 71 Ohms, then the anticipated folded dipole impedance would be about 530 Ohms. The equation does not take into account the connecting end wires, so we may expect some variance from the value, but not by more than a few percent. As well, the impedance of a dipole will vary slightly depending upon the diameter and type of material, so we should expect perhaps a range of +/-5 Ohms for the set-up folded dipole relative to calculations.

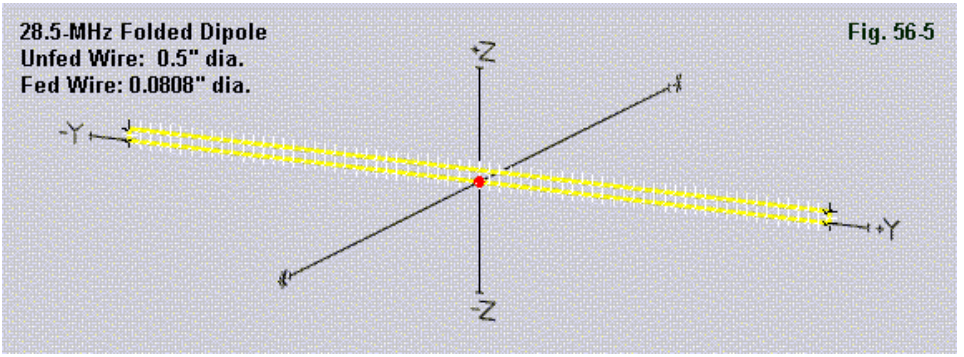

Now let's make a model of the step-up folded dipole. If we choose 28.5 MHz as the test frequency, we can segment a folded dipole as shown in **Fig. 56-5**. The long wires have 68 segments in MININEC and 67 segments in NEC—to ensure proper centering of the feedpoint. The AWG #12 end wires use 2 segments per wire.

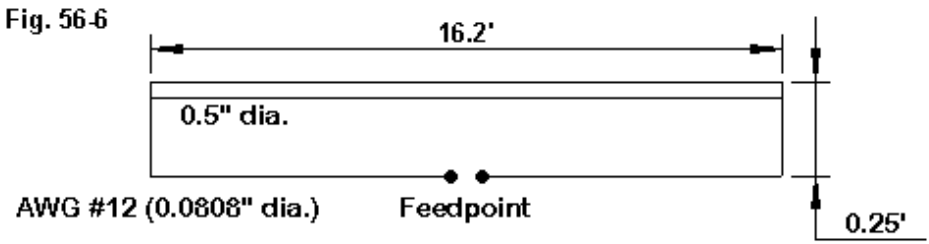

Test Folded Dipole for 28.5 MHz

Fig. 6 shows the general physical outlines of the antenna. For the test frequency, the long wires are 16.2' long. For this test, the end wires extend along the Z-axis. If we lay the folded dipole along the X-Y axes, there will be a slight gain difference in the resulting two azimuth lobes amounting to about 0.1 dB. Using the

Z-axis for the two long wire displacement equalizes the gain in the lobes. See model 56-2.

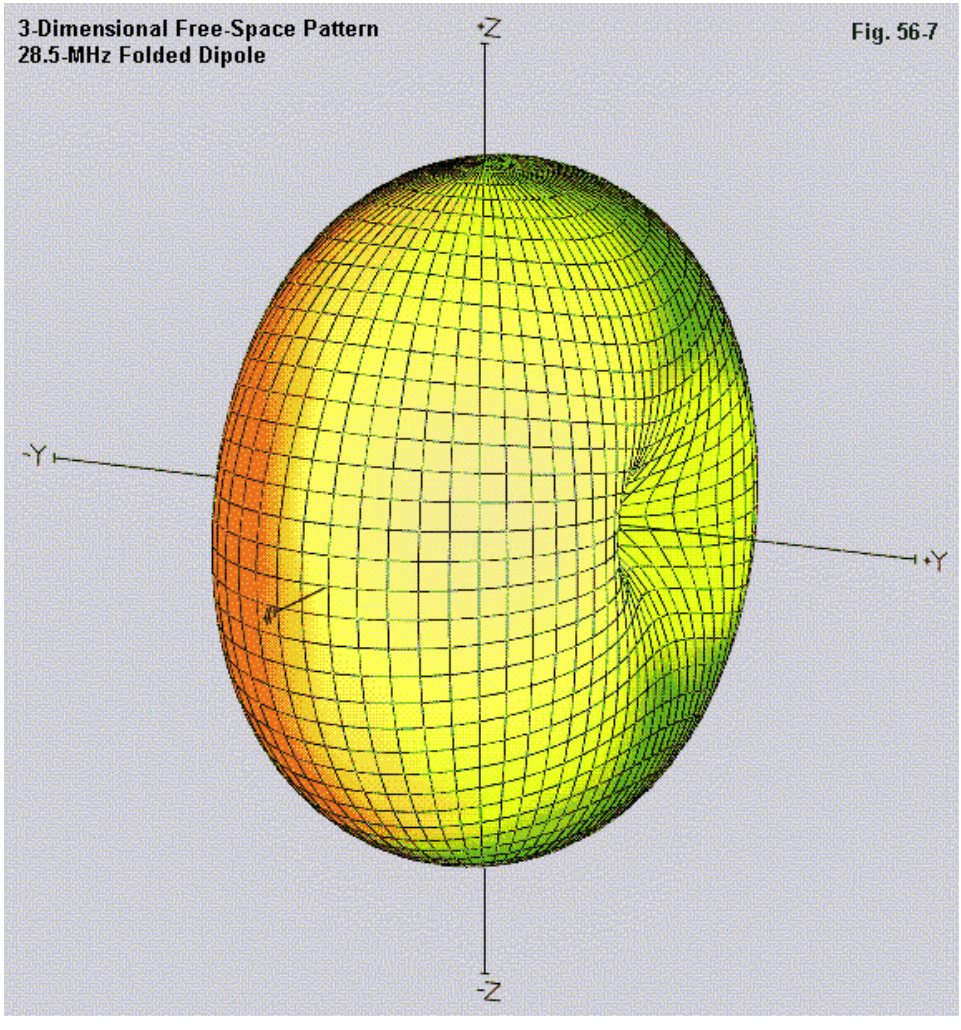

Fig. 56-7 shows the 3-dimensional free-space pattern of the antenna and the familiar donut shape applicable to dipoles, whether folded or unfolded. Those who prefer 2-dimensional patterns may look at **Fig. 56-8**, which records the E-plane pattern of the antenna in free space. Incidentally, all patterns and segmentation graphics in this column come from Antenna Model. Hence, the recorded gain is that of the MININEC model.

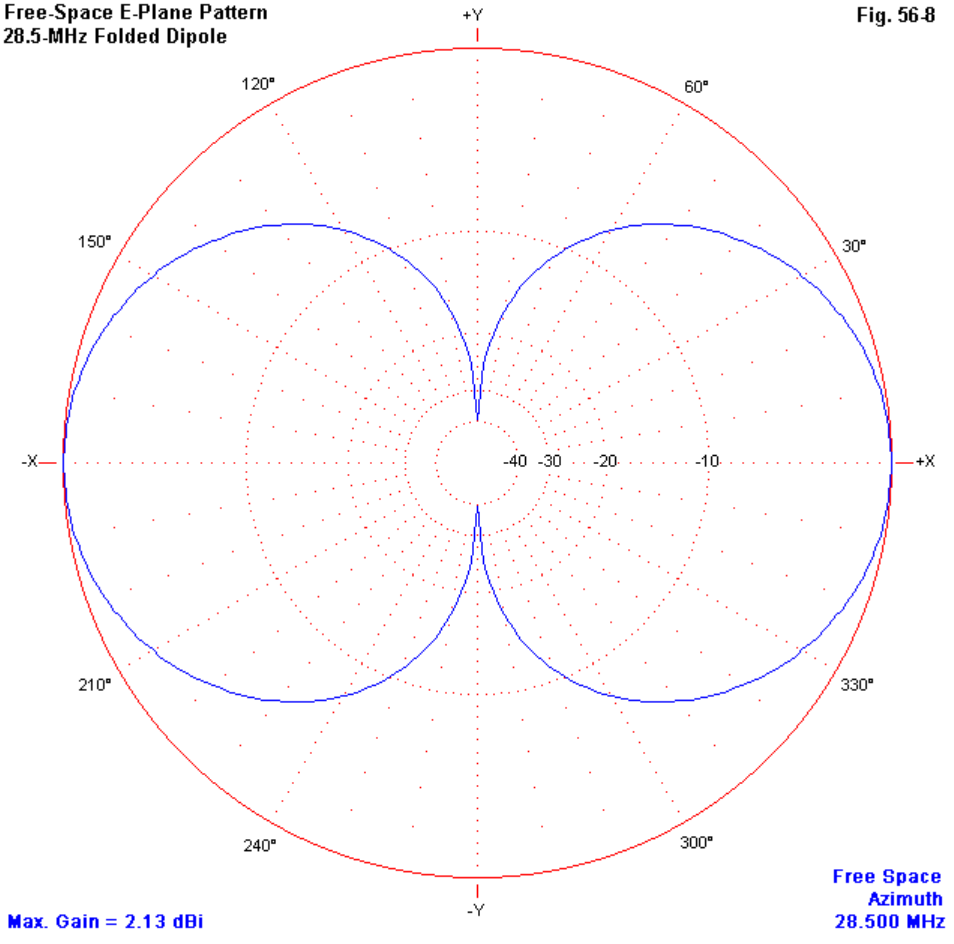

The crux of our investigation hinges upon how well MININEC fares over and against NEC-2 and NEC-4 models of the same antenna. The only difference between models will be in the segmentation of the long wires: 68 vs. 67.

Core	Impedance R+/-jX Ohms	Free-Space Gain dBi	AGT Gain/dB
MININEC (AM)	530.5 + j 2.0	2.13	0.9988/-0.01
NEC-4	463.0 + j17.5	1.50	0.8660/-0.62
NEC-2	375.2 + j25.8	0.60	0.7030/-1.53

The MININEC model produces highly credible numbers for both the source impedance and the gain. As well, it yields a very good AGT value. In contrast, the NEC-4 and NEC-2 numbers fall well outside the range of credibility. (As with the first test, there is no significant difference between NEC-4 single and double precision values.) Although NEC-4 comes closer to believable numbers, as witnessed by the higher AGT value, the model still falls into the range of the unusable. However, if we adjust the gain values by the AGT deficit in dB, we come close to the value reported directly by the MININEC model.

Both NEC-2 and NEC-4 provide excellent results when the two long wires of the folded dipole have the same diameter. The limitation faced by NEC lies in its calculations when the wires have different diameters. Indeed, making the end wires equal in diameter to the unfed wire does not change the results. MININEC is the preferred core for antenna design and analysis when antennas have geometries resembling the one in the step-up folded dipole.

Conclusion

There are, then, antenna wire geometries for which MININEC is the preferred modeling core, especially if that core has been adjusted to overcome past known weaknesses. This is the case with Antenna Model, although if VHF and upward frequencies are not used, ELNEC will handle close-spaced wires quite well and if no close-spaced geometries are involved, AO will handle VHF and UHF frequencies well. See column #50 for further specific comparisons among MININEC cores.

These notes are not intended in any way as a criticism or indictment of NEC-2 or NEC-4. Quite the opposite: we obtain the best results in our modeling tasks when we apply the right tool to the right job. For many tasks, NEC-2 and NEC-4 are the right tools. However, corrected MININEC is also available for certain special jobs that NEC-2 and NEC-4 do not do well. And, for a large class of modeling tasks, both NEC and MININEC are equally apt as modeling cores.

* * * * *

Models included: 56-1 through 56-2. (.NEC and .NWP model dimensions in meters; .EZ model dimensions in inches or feet.)

57. Some Comments on Comments

NEC (-2 and -4) allows the user to introduce at the very beginning of a model file the CM input or card. CM means comment, and the user can introduce as many CM lines as needed to say anything that he or she wishes to say about the model. Each 80-character line allows 77 text characters (allowing for the necessary CM and space at the beginning of each line). With a virtually unlimited number of lines, one might come close to writing a full report on the model.

The string of CM cards requires a closing line entry line, CE, which may also contain a comment. This entry terminates the comments and must be followed by a geometry entry, such as a GW wire entry. The NEC output report will print all of the CM lines at the beginning of the file. CM lines have no affect on any computation made by the NEC core.

Various commercial implementations of NEC handle the CM inputs in different ways. For example, EZNEC has two different CM-relevant entries: the antenna model title, which is saved within the .EZ model file, and the antenna notes, which are saved in a separate .TXT file having the same file name as the model itself. The title is visible whenever the user calls up the model. As shown in **Fig. 57-1**, the comments appear in a separate window only when called. In the Pro version of the program, when the user converts an .EZ file to .NEC format, both the title and the notes become CM lines in the converted file.

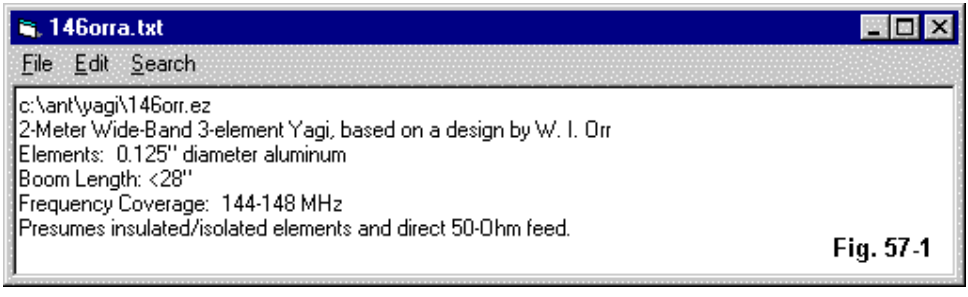

Fig. 57-1

NEC-Win Plus also has a special screen for comments, a sample of which appears in **Fig. 57-2**. Since this screen contains the file name and location, adding that data to the comments is unnecessary unless conversion of the .NWP file to .NEC format is anticipated. There is no separate model title, so that information must be included in the comments. All of the data in the special "Comments" box becomes a set of CM lines in a file saved in the .NEC format.

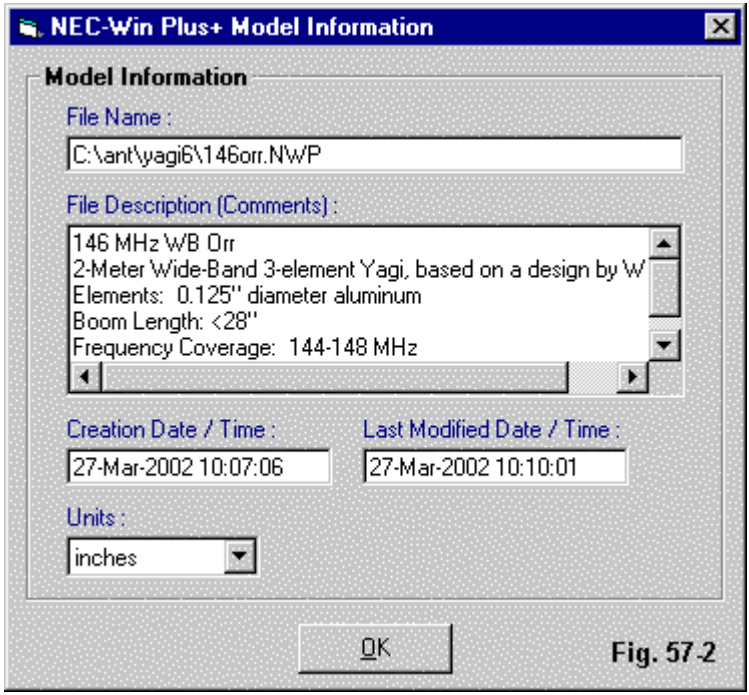

Fig. 57-2

Programs such as NEC-Win Pro and GNEC present the user with a standard ASCII page of lines making up a .NEC-format model file. Hence, the user intro-

duces comments by opening a new line, labeling it CM, and then filling the remaining spaces, as needed, with whatever the user views as an appropriate comment.

Why Dwell on Comments?

A natural question is why I should linger over a calculationally non-functional aspect of NEC. Perhaps the answer may become obvious from **Fig. 57-3**, a simple model file (of a 3-element 2-meter Yagi) in .NEC format.

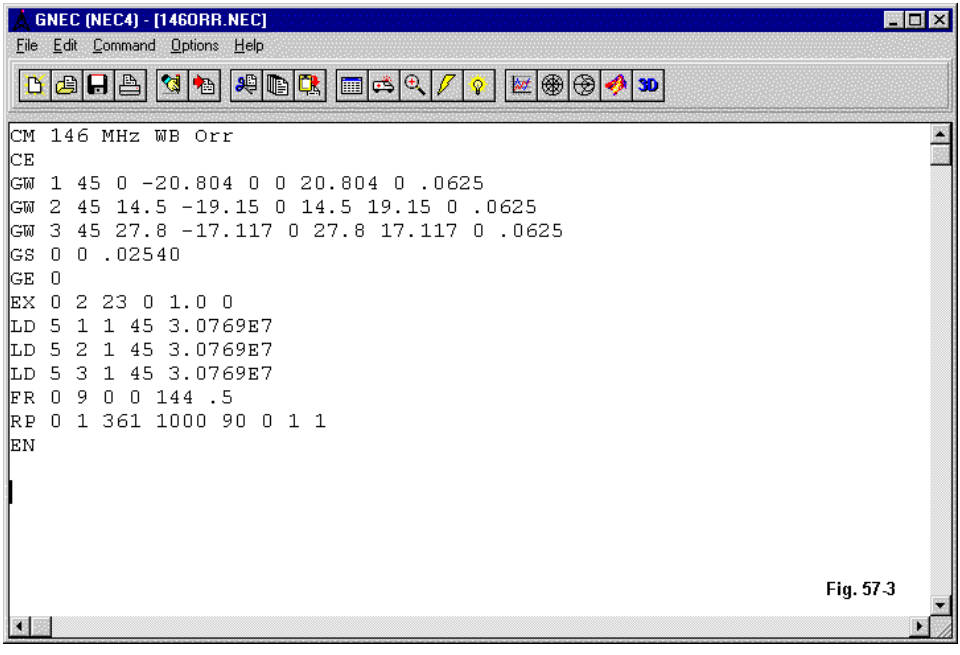

Fig. 57-3

The sole CM line yields a model title, and in highly truncated form at that. Perhaps the only clear information is the design frequency: 146 MHz. Missing is the

antenna type—which we may glean from examining the GW lines—and any other data about the antenna.

This style of model file used to be common in my directories, and is typical of files from others that have come my way. Indeed, I have stored reams of paper with information about the models that I have constructed and evaluated. Correlating the paperwork with an actual model on file has often been a laborious task—even when I remembered to write down the location of the file.

Gradually, I began to realize that I was passing up a potentially important NEC facility. So over a period of time, I developed a system of using the CM lines to encapsulate the most important model data. The system that I developed is based on the main lines of work that I do. Hence, it will not be satisfactory for every modeler. However, it might set the wheels in motion for the development of your own system.

The main categories of CM entries that I use are the following ones.

1. Model file location and file name.

2. Full modeling task specifications and/or origin of the antenna modeled.

3. Overview of the basic construction of the model.

4. Special features of the model.

5. A basic performance report.

6. Commentary on the model, including reactions, potential uses, comparisons, etc.

These categories are fully functional for my work, which focuses on models of antennas with energy sources, where the key data include the source impedance, the far field information, sometimes the near-field information, and sometimes the relative current magnitudes and phase angles on the antenna elements. There are numerous other applications of NEC, including electromagnetic compatibility analyses, radar profiles, receiving tests using plane-wave excitation, etc. These applica-

tions may require the development of different categories of information to place within the CM lines of the model.

The key benefit of developing a standard list of information categories is that one may simply label the information group with the category number and save a good bit of typing. As well, the information will be consistent from one model to the next, allowing direct comparisons. In fact, one may type the information into an editor, such as Notepad, and block copy it into the model later.

Some Details of the Category Contents

Let's look at each category in a bit more detail.

1. *Model file location and file name*: This information may seem otiose, since it is buried in the model itself and not outside of the system of directories where the models lie in storage. Granted, I do keep an external list of models, with a basic title and their locations. However, I often have the occasion to move a model from one directory to another to group it with relevantly similar or comparative models. In each case, I add the new location to the old within the model CM lines, including any file name changes that might occur due to the new use of the model. I also add to the list any direct scalings of a model from one frequency range to another to give me the ability to track the heritage of a model.

2. *Full modeling task specifications and/or origin of the antenna modeled*: This category has 2 functions owing to the different reasons for which I may approach a model. One reason for modeling is either to develop a working design or to analyze an existing design. These tasks do not occur in a vacuum, but are often parts of a specific task. Listing both the task and the task parameters provides insight into later remarks in category 6, the reactive commentary to the model. Hence, the task specification should be as complete as possible within the limitations of truncated entries. If the task involves analysis for the achievement of certain levels of gain, beam width, bandwidth, rear pattern performance, etc., all of these should be noted. Comparing two models many moons later becomes simpler when the performance of the models is read in the context of the original tasks that generated the models.

Many models have their basis in existing antennas or antenna designs. Listing the essential particulars of the design origin is critical to avoiding errors in model

reports, to re-inventing already existing designs, and to finding other details about the antenna design. Notes should also include revisions to an original or basic design, so that a sequence of models—perhaps versions A through G—reveals the evolution of a modified design.

3. *Overview of the basic construction of the model*: An overview of the model's basic construction can save a good bit of time ferreting out the information from the lines of a model (or from the various windows in some implementations of NEC). The data should include the units of measure used in the GW lines. These units may be different from the units used to express construction details and, hence, may allow the correlation of numbers without calculation between some source material for the antenna and the actual model entries. The basic data should also include the element diameter, if that is the most usual wire measure used in your design work, since the .NEC wire entries will use the radius. (Numerous implementations of NEC provide a wire construction table that employs the wire diameter.) The element material should find a place in this list as a check on subsequent LD5 entries. As well, one should note the level of segmentation used, whether expressed in terms of the number of segments per element or segments per (half-)wavelength.

Of course, we should not omit a set of element dimensions. The format that we use for these dimensions may vary with the system that we use to enter coordinates. For free-space simple (1-antenna) models, one might use element lengths expressed in terms of the "+/-" values of half-lengths. If we model a system of antennas where the overall dimensions might be opaque due to scattering the multiple antennas throughout a coordinate system, full-length measurements of elements may prove more useful. The separation of elements in a multi-element antenna can follow whatever convention one uses for constructing the model. Some modelers center such antennas equally behind and ahead of one of the coordinate system axes. Others count from zero for the rearmost element, with positive values for the other elements. Still others place the driven element at zero and count fore and aft of that element. A consistent convention from one model to the next—or a second data set if a certain task forces one to use a non-normal convention—generally saves interpretation time. Amassing data is only useful if it simplifies interpretation. If the data concentration complicates interpretation, it is likely time for a re-evaluation of system of recording it.

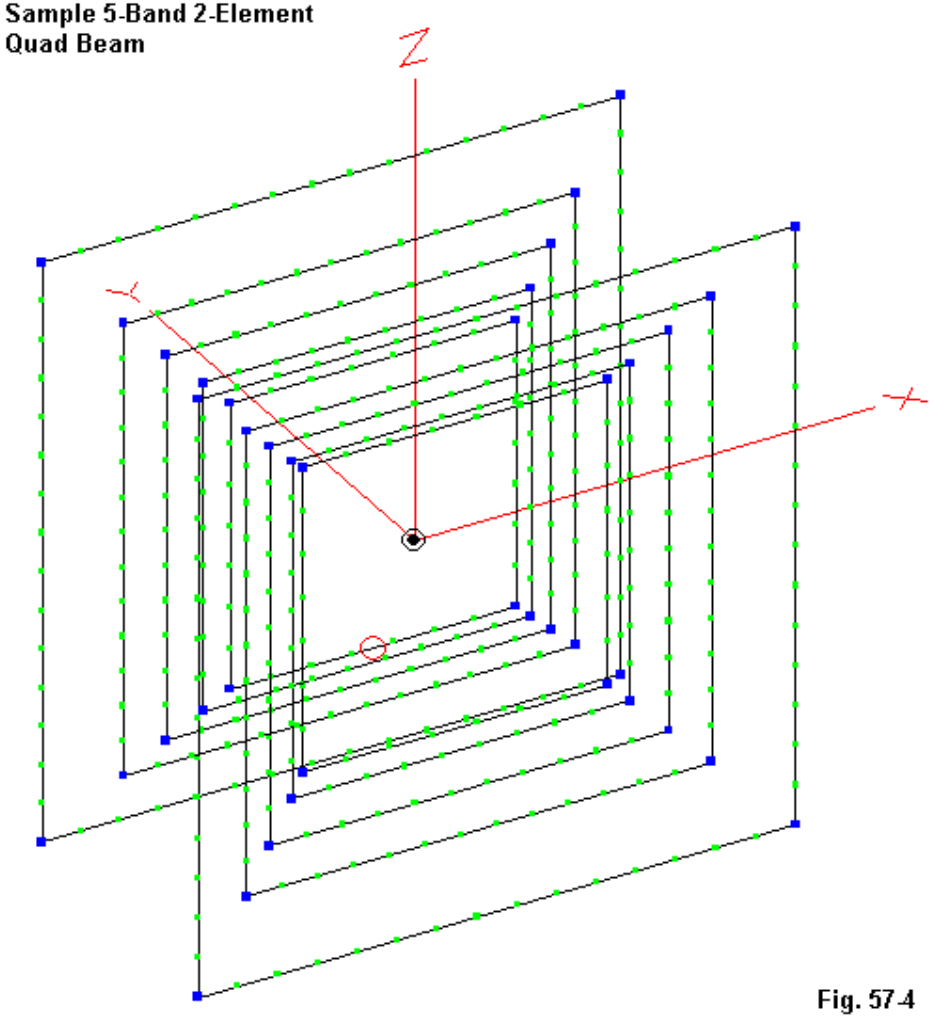

Fig. 57-4

4. *Special features of the model*: Every data collection system needs a catch-all bin for data that just seem to have no home but are important to a model. The lack of a home is usually a function of the fact that the data involved are model-specific and do not appear with all models within a roughly coherent collection. So I created a home for all such data.

The data that I almost always include in this category cover the antenna environment (free-space, *x* WL above *y* ground, etc.), structural aspects of the antenna (such as the element relationship to a supporting boom), the specified feed system, and any matching systems used to obtain a specific feedpoint impedance. However, many antennas have specific data applicable almost only to them.

For many models, there are special data pertaining to sources, loads, and/or transmission lines that may be apt for this category. To give just one example, consider **Fig. 57-4**, the outline of a 5-band 2-element quad beam using a separate feedpoint for each band.

Quad loops require 4 wires each, and there are two sets of loops per band. Keeping track of the source wires and segment numbers for each band can be daunting, especially if the model does not use a strictly progressive mode of construction. In this case, the wire order is 20, 15, and 10 meters (driven, then reflector wires) followed by 17 and 12 meters (driven and director wires). I know this instantly from the comments, where I stored the requisite source information, recorded in **Fig. 57-5**. Gleaning this information from the GW wires would take a good bit of time, especially if I had not worked with the model for some months.

Of course, there is more than one way of handling the sources in cases like this. We may keep a single EX (excitation) input line and change the requisite details. However, in some programs, such as EZNEC, one enters the source information in a table. In such cases, we might wish to use the lower portion of **Fig. 57-5** as a means of source entry. We enter the location of all of the sources and then activate only one of them by assigning a source magnitude that is greater than zero.

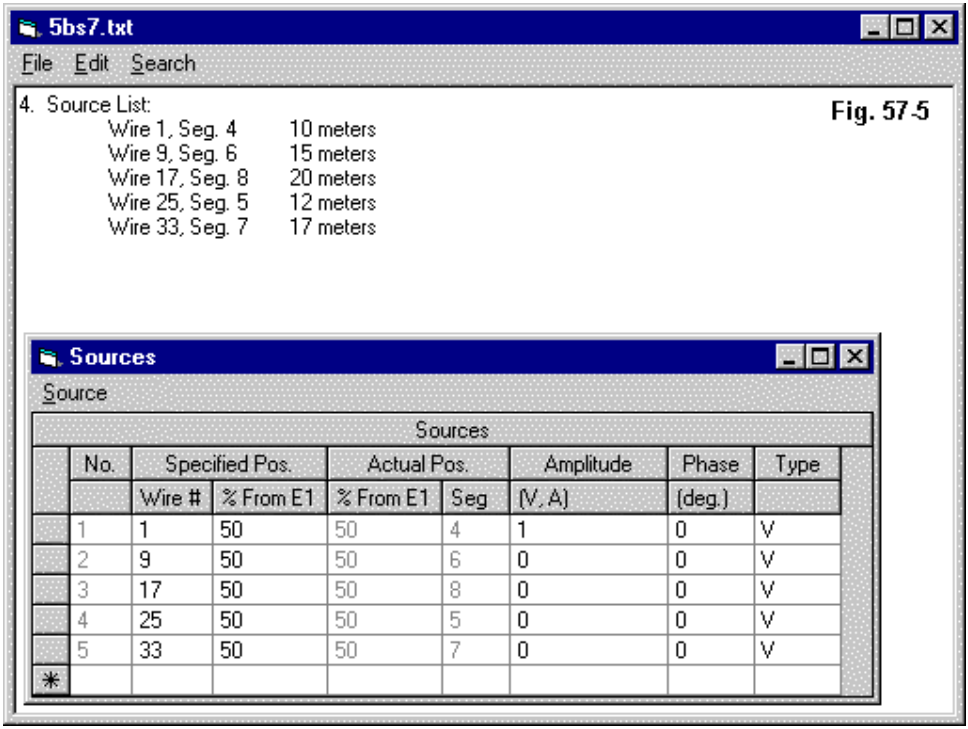

Sources

No.	Specified Pos.		Actual Pos.		Amplitude	Phase	Type
	Wire #	% From E1	% From E1	Seg	(V, A)	(deg.)	
1	1	50	50	4	1	0	V
2	9	50	50	6	0	0	V
3	17	50	50	8	0	0	V
4	25	50	50	5	0	0	V
5	33	50	50	7	0	0	V
*							

Load data for load types LD0 and LD1 show the value of inductance or capacitance. We might wish to enter in category 4 the corresponding reactance value at the center design frequency. Alternatively, a load type LD4 uses a reactance value, and we might enter here the corresponding value of inductance or reactance.

Transmission lines have many functions, including their use simply as transmission lines. However, open and shorted stubs are often common features of models used for impedance matching and phasing lines in collinear arrays. Horizontal and vertical phased arrays also require transmission lines. Category 4 is a convenient

place to record the functions of each transmission line (TL) in the model, with such other particulars as may be useful to sort out a potentially confusing morass of TL constructs.

Although our original sample model Yagi is in free space, it might well be placed at a specific height in terms of a wavelength above a ground of a certain type, whether simple or complex. Entries in category 4 can obviate the need to interpret the numeric entries on GN or GD lines in the model.

How many more special entries you might need depends on the model particulars. The useful data will emerge in part from the model parameters and in part from the overall modeling task. However, if a large series of models that are part of a long-term general task have consistently used data elements, then you might consider creating an additional regular or major CM data category.

5. *A basic performance report*: The CM lines are not likely the best place to store complete frequency sweep data for a given model. However, a truncated performance report at the center design frequency may be useful when surveying models. For the class of antennas that I typically model, far field and source data generally form the core of my needs. For the Yagi in **Fig. 57-3**, the gain, front-to-back ratio, beamwidth at -3 dB points, source impedance, and 50-Ohm SWR comprise the central data. Since the antenna is a wide-band unit, my interest would extend to the band edges as well as including the mid-band frequency. Hence, I might record a short data table for 144, 146, and 148 MHz.

The results of all of our data summarizing appear in a revision of **Fig. 57-3**, shown in **Fig. 57-6**. The CM lines now occupy more space in the file than the geometry and control inputs that affect calculations. However, ASCII files are very small, and the added data requires very little storage space. Hence, adding the information costs little more than the time it takes to record it.

Having the data within the model file allows me to re-learn what I originally learned by running the model. Now I need to run the model only if there are additional data that I find a need to accumulate. Whether to include some of the new data in the CM lines becomes a real time decision based upon an estimate of my later needs for seeing that new data.

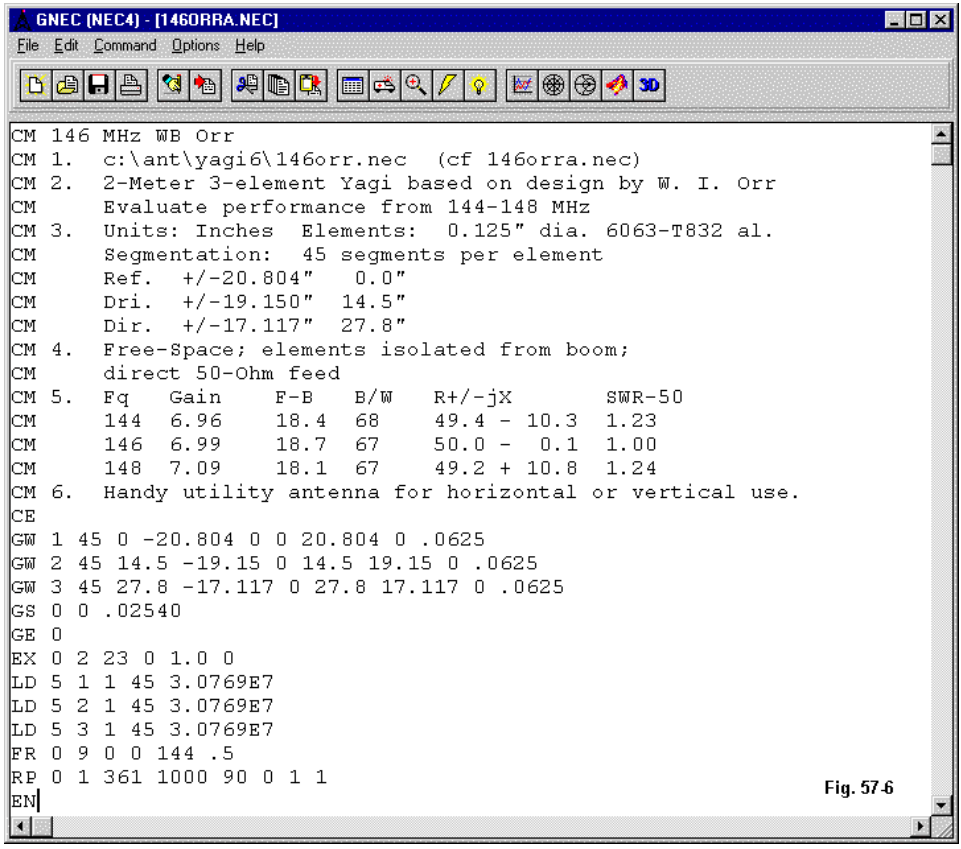

Fig. 57-6

6. *Commentary on the model, including reactions, potential uses, comparisons, etc.*: We have so far omitted category 6. from the list to this point, because it is perhaps the most task-driven entry of all. The comment shown in **Fig. 57-6** indicates my initial interest in the Yagi, as a possible directional utility antenna for the 2-

meter amateur band. The boom length (under 28") promised a lightweight antenna that one might construct using a non-conductive boom material and supporting from the rear. Hence, with a suitably flexible support system, one might easily change the orientation from horizontal to vertical and back again, a desirable feature in a utility antenna. I might also add to the simple remark in **Fig. 57-6** open questions about transforming the model into a real antenna. For example, any implementation of the antenna would require a split driven element for direct feed, and this fact promises to complicate construction relative to the simple mounts required by the parasitic elements.

Since the exact information suited to this category is task specific, it is impossible to say in general what sorts of entries would be most useful. In a series of models set up for comparison, one might record the ranking of the given model—or a series of rankings within the series based upon a list of critical parameters. It likely is also useful to record reactions, especially if they result from surprise—perhaps at how well or how poorly an antenna performs in one or another department of concern. As well, one might enter here what model modifications are envisioned, and the file name and location of the model that incorporates those revisions.

Equally important to recording evaluative remarks that fit within the task at hand is to enter comments that are relevant to the model but which fall outside a defined task. To see a potentially new use for an antenna type is significant, even if not within the scope of work.

Printing

The utility of the CM lines as a basic data storage medium can be lost if we only save the model file and never refer to it again. Therefore, my practice has been to print a copy of the model file and include it in the sheaf of papers recording output data. This practice requires attention to the provisions of the modeling program used. In EZNEC, one may print the comments from one screen and print an antenna model description from another. NEC-Win Pro permits saving a model in .NEC format, and thus printing can be a single step. Generic NEC programs would use the input file as the basis for printing.

Very often, printing the input file can save reams of paper often necessary to print the NEC output file. A number of programs permit one to print selected sec-

tions of the output file and thus avoid having to waste paper on portions of the NEC output file that serve little function relative to an assigned task. Of course, in very large models, the input file itself may run to many pages, especially if one does not take legitimate shortcuts. For example, a 200-wire model with all wires having identical material loads (type LD5) requires in many set-ups an extra 200 lines of LD entries. We may truncate these to a single line using techniques spelled out in the NEC manuals. (Not all programs permit conversion of LD5 lines into a single line, while others permit only a single material load entry for an entire antenna structure.)

We have explored one systematic way of using the CM lines as an aid to modeling. The system shown is one that suits a specific modeler, namely, me. It may require anywhere from minor to major revision to be suitable to some other modeler. In a departmental setting, I can imagine the situation devolving into a series of interminable meetings trying to decide the best set of categories for everyone involved in the modeling enterprise. One can only hope that simple rationality will prevail over modern group dynamics.

Nevertheless, the sample system that we have explored does demonstrate that the CM lines represent a resource that we can too easily overlook. If these notes make you aware of the potential for these lines, then they will have done their work.

* * * * *

Models included: none

58. Some Basic Guideline Graphics for NEC

Over the years since I started this column, I have had requests for a listing of basic guidelines and limits applicable to NEC. I have had occasion to create some presentation graphics covering some of this information, and I shall present them in this column.

The .GIF graphics in the original (HTML) text can be extracted from the document and placed in a Word or Word Perfect document, one per page at full paper width. Then the result may be printed or saved. Only the ones useful to you should be extracted. As well, you may run them through a graphic program, such as Paint Shop Pro or equivalent, for printing—and even revising to suit your specific needs. Alternatively, you may take notes on aspects of NEC limitations and guidelines as they apply to your projected modeling work. When extracting graphics from this version of the text, you may print a single page or transfer the graphic to another program for any manipulation that you desire.

The set of graphics is neither comprehensive nor complete in detail. Most of the sheets are taken from the NEC-2 manual, but apply also generally to NEC-4. The key exception is the fact that NEC-4 permits wires underground, with rules for the penetration of a wire into the ground. **Fig. 58-7** below covers the NEC-4 situation in an example of a monopole with buried radials.

Since the graphics themselves contain the text, little commentary is required. Actually, each graphic requires a full column of commentary, but that has mostly appeared in past columns.

For fuller information, there are several useful sources. Of course, the NEC-2 and NEC-4 user manuals are the primary sources. For modeling with NEC-2, *Basic Antenna Modeling: A Hands-On Tutorial* is available from Nittany-Scientific (http://www.nittany-scientific.com). As well, ARRL offers an on-line course in modeling with NEC-2. Both of these latter sources offer exercise model files.

Since most of the graphics require a full page, I shall introduce several, followed by the graphics themselves.

Fig. 58-1: *Some Absolute NEC Limits for Wires and Segmentation*: Although few MF and HF models will approach these limitations, they become especially important in the modeling of antennas for VHF and upward, where the anticipated element diameter may become a very appreciable fraction of a wavelength. See column #3 for more information on NEC limitations.

Fig. 58-2: *Some Conservative Wire and Segmentation Recommendations for Newer Modelers*: The experienced modeler may safely by-pass these recommendations, although most models should remain within these guidelines in order to achieve an AGT (Average Gain Test) value that is close to ideal. See **Fig. 58-11** for further information on the AGT.

Fig. 58-3: *Some Modeling Practices to Embrace*: Not all good practices appear in this brief set of guidelines, but the listed suggestions may help you develop your own extended list of good practices. Good practices do not ensure a good model, but they do help to eliminate oversights that seem to defy detection once the full model is complete.

Fig. 58-4: *Some Modeling Practices to Avoid*: As with the list of good practices, this list of practices to avoid is incomplete, but a potential foundation for a user-specific list of things to avoid. Some practices, such as using a stepped-diameter element, have correction features in some implementations of NEC-2. NEC-4 has overcome much of the inaccuracy involved in stepped diameter elements, but AGT values for large diameter changes may still be disappointing. The remaining practices to avoid apply equally to NEC-2 and NEC-4, with the exception of the ground warning, which applies to NEC-2 only.

Wire Modeling and Segmentation Guidelines

Fig. 58-1

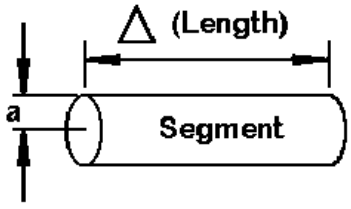

Δ = Segment Length

a = Wire Radius

d = 2a = Wire Diameter

Key Parameter: Segment Length relative to a Wavelength

$\Delta < 0.1\ \lambda$	for accuracy in most cases	10 segments per λ
$\Delta < 0.05\ \lambda$	in critical regions (complex shapes)	20 segments per λ
$\Delta < 0.2\ \lambda$	on long straight wires	5 segments per λ

Limit: $\Delta > 10^{-4}$ Wavelength

Note: Some programs input Diameter (d),
but NEC calculates from Radius (a).

a -- Must be small relative to both λ and Δ: $a < 0.5\,\Delta$ $a < \sim 0.1\ \lambda$

Fig. 58-2

Some Conservative Segmentation Recommendations for Beginning Modelers

Relatively "thin" linear elements:
11 segments / 1/2 λ minimun

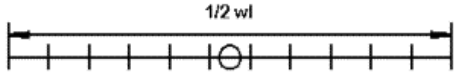

Square ("quad") 1 λ loops:
5 segments per 1/4 λ side minimum

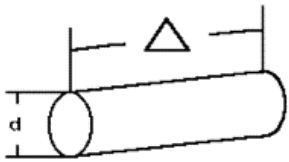

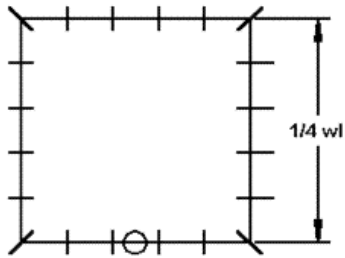

Segment Length to Diameter ratio: 4:1

Stretch "beginner" limits toward "absolute" limits in small steps.

Fig. 58-3

Modeling Practices to Embrace

1. Use adequate segmentation.

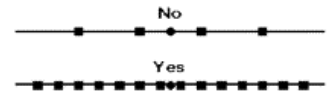

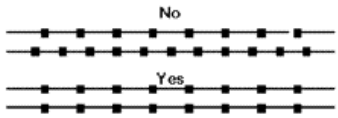

2. For parallel wires, align segment junctions.

3. Connect wires only at ends. Wire connections at segment junctions are allowable, but not recommended.

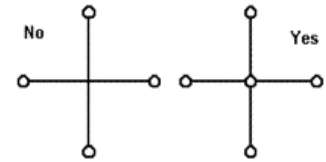

4. Connected wires ideally should have the same radius/diameter.

5. Except for a "Perfect" Ground, keep all wires above ground (Z>0). **(Nec-2)**
   See Fig. 7 for NEC-4 Rules.

6. Plan your models in advance (on paper).

7. Keep output record data in greater-than-required precision and truncate values for the presentation audience.

   Ex.: Recorded: 52.385 Ohms Presented: 52.4 or 52 Ohms

Modeling Practices to Avoid

Fig. 58-4

1. Crossing wires at "mid-points."

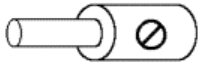

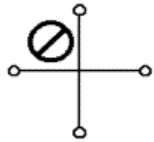

2. Large changes of radius/diameter

3. Wires that overlap (surfaces penetrate each other).

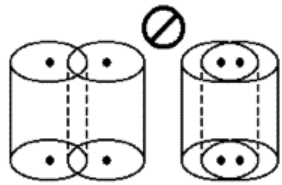

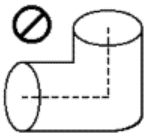

4. Sharp bends in thick wires (where the radius of one wire may penetrate the middle third or more of the other wires).

5. Closely spaced wires of different diameters, whether or not connected at the ends.

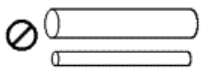

6. Angular junctions of wires having dissimilar diameters.

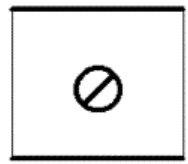

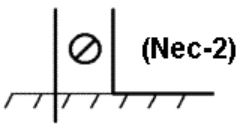

7. Except for a Perfect Ground, do NOT let wires touch or penetrate the ground (Z=0; Z<0).

Fig. 58-5: *Limits for Wires Near the Ground*: The Sommerfeld-Norton ground calculation system is very accurate for wires very near the ground, and the limits for wire proximity to ground are small. However, a ground radial system very near the ground in NEC-2 provides only a crude indication of the buried ground radial system for which it may substitute and which is available in NEC-4. See column #11 for more on ground radial systems. The increased speed of current-generation PCs has largely made the use of the reflection coefficient method of calculating ground effects irrelevant, since the S-N ground calculations do not significantly slow the calculation process down.

Fig. 58-6: *Selecting the Right Ground for the Right Job*: In NEC-2, a wire (vertical monopole) touching the ground may not yield correct results with either the S-N or the reflection coefficient ground. Hence, resorting to a perfect ground for comparative results between models may be necessary. However, for more accurate results that take into account the properties of the ground, NEC-4 is preferred, since one may directly model a buried ground radial system.

Fig. 58-7: *NEC-4 Ground Penetration Rules, Using a Vertical Monopole and Radials as a Sample Case*: The sample in this figure combines the rules for ground penetration in NEC-4 with an example of element length tapering to avoid adjacent segments that differ too much in length. The method shown uses manual tapering with separate wires for each segment length. However, it is possible to use the GC input to automate the process within single wires for each element. Whichever system is used, the source wire and the wire between Z=0 and the junction of the radials should be individual wires to allow for maximum control over the model and to avoid junction errors as one modifies the model. Although the wire penetrating ground may have a segment junction at the required Z=0 point, users achieve maximum model control by making Z=0 a wire junction.

Fig. 58-8: *Transmission Line (TL) Limitations*: As non-radiating elements of the model, transmission lines are subject to many limitations. Where a model requires transmission lines outside regions of high current and low rates of current change, many lines may be modeled using physical (GW) wires. See column #21 and #22 for more on transmission lines.

Wires Near the Ground

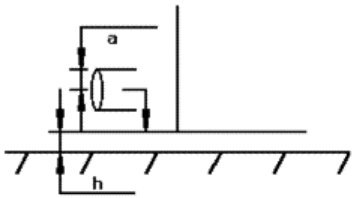

a = wire radius
h = height above ground
ground = Z = 0

Sommerfeld-Norton Ground or Perfect Ground

Height (h) should be several times the radius (a): $h > \sim 3\ a$

$(h^2 + a^2)^{½} > 10^{-6}\ \lambda$ If a is very small compared to h, wires may approach 10-6 λ toward ground.

Note: h = height from ground (Z=0) to center-line of wire (Z coordinate).

. . . . . .

Reflection Coefficient Approximation

Vertical wires should be at least 0.1 to 0.2 λ above ground.
Horizontal wires should be at least 0.4 λ above ground.

Fig. 58-5

Selecting the Ground

Fig. 58-6

1. Free Space or No Ground:

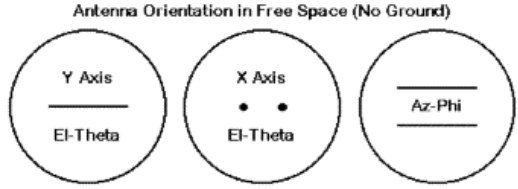

Applications:
- Basic Design
- Comparing Similar Antenna Types

2. Grounds (at Z = 0):

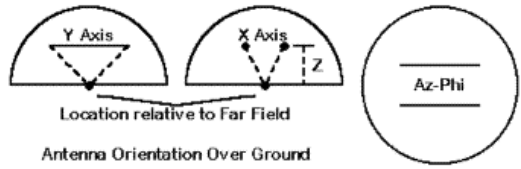

a. Perfect: use for comparing vertical antennas/arrays and for theoretical studies

b. Reflection Coefficient: calculates rapidly but less accurate close to ground–a "real" ground with ground losses

c. Sommerfeld-Norton: calculates more slowly, but accurate very close to ground–a "real" ground with ground losses

Note: For all grounds, antenna Z>0 (except for vertical monopoles touching perfect ground) with NEC-2. See Fig. 7 for NEC-4 Rules.

Fig. 58-7

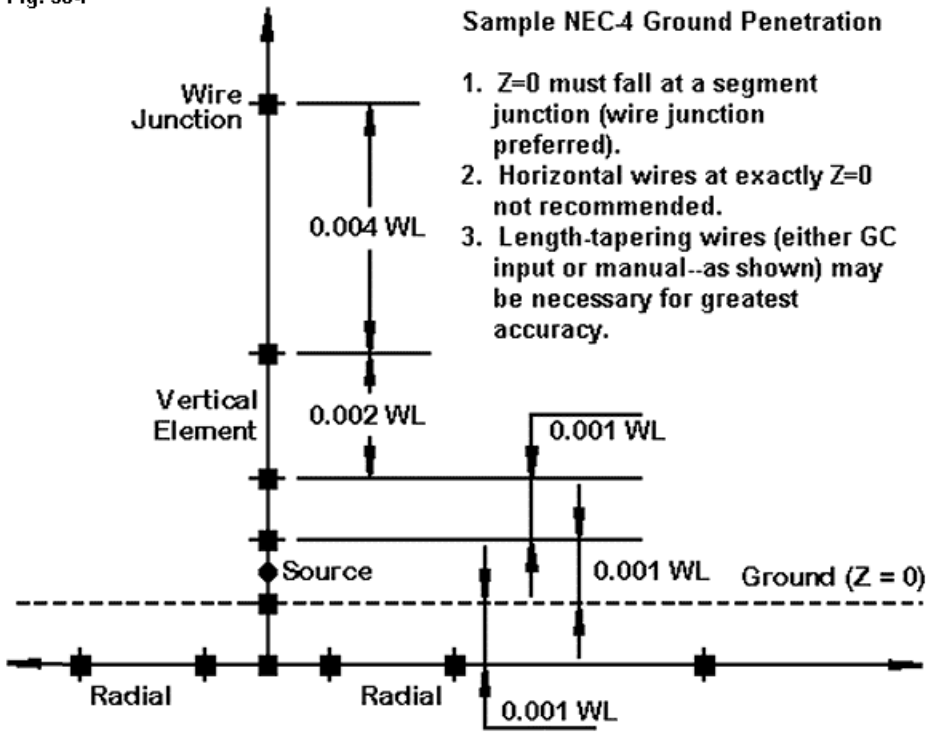
Sample NEC-4 Ground Penetration
1. Z=0 must fall at a segment junction (wire junction preferred).
2. Horizontal wires at exactly Z=0 not recommended.
3. Length-tapering wires (either GC input or manual--as shown) may be necessary for greatest accuracy.
Wire Junction
0.004 WL
Vertical Element
0.002 WL
0.001 WL
Source
0.001 WL
Ground (Z = 0)
Radial
Radial
0.001 WL

TL (Transmission Line) Basics: Limitations

Fig. 58-8

1. For highest accuracy, TL transmission lines must be balanced. Balance is most nearly assured when the current on the segments adjacent to each TL "leg" is the same (as is the case at the center of a ½ λ dipole or similar antenna).

2. Departure from exact balance increases inaccuracies.

3. Modeling situations to avoid with TL lines:

Mid-element stub/linear loading

Collinear array inter-element phasing stubs

Off-center-fed doublet feedline simulations

For these and similar situations, construct parallel feedlines with actual wires.

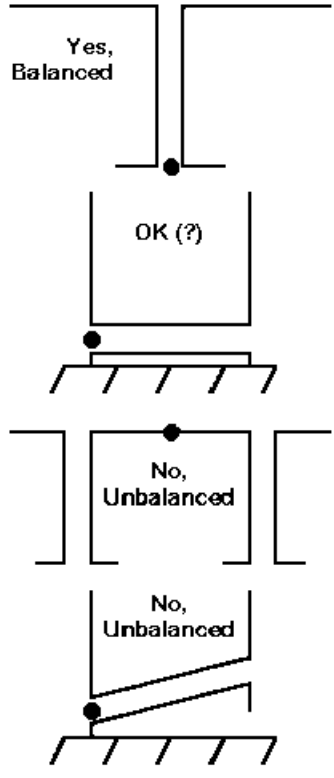

Fig. 58-9: *Connections of Loads, Sources, and Transmission Lines on the Same Segment*: Applying multiple loads, sources, and/or transmission lines on a single segment is often a source of confusion. (In addition, some implementations of NEC may permit only a single load and/or a single source on a chosen segment.) See columns #4 and #5 for more on sources. See columns #6, #13-#17, and #46 for more on loads. Since a load is in series with a transmission line, placing a load on the wire used to terminate a transmission line will not place the load in parallel with a source at the near end of the transmission line. One must use the admittance facilities of the TL entry, although these values are not frequency nimble. To obtain a load in parallel with a source that will change reactance as the frequency changes requires other types of work-arounds.

Fig. 58-10: *The Convergence Test*: For a fuller account of the convergence test, see column #1. The convergence test, like the AGT, is a necessary but not a sufficient condition of model adequacy.

Fig. 58-11: *The Average Gain Test*: For a fuller account of the average gain test, see column #20. Since both the convergence test and the average gain test are necessary but not sufficient conditions of model adequacy, they together yield at best a good indication of model adequacy, but not a decisive judgment. The use of experimental results, as well as a full evaluation of the model in terms of all program limits, remain recommended additional checks on models.

Converting the AGT number into a value in decibels is simply a matter of 10 times the common log of the AGT value. Use only the AGT value obtained in free-space (or over perfect ground) for lossless wires and no resistive components to any loads in the model. If the source impedance is very close to having no reactance, then the basic AGT value times the reported source resistance value will provide a more correct source resistance value. The positive AGT value in dB may be subtracted from the reported gain value and a negative AGT value in dB may be added to the reported gain value to yield a more nearly correct gain figure for many models.

Connections of Loads, Sources, and Transmission Lines on the Same Segment

	Load	Source	Tr. Line
Load	Series	Series	Series
Source	Series	Series	Parallel
Tr. Line	Series	Parallel	Parallel

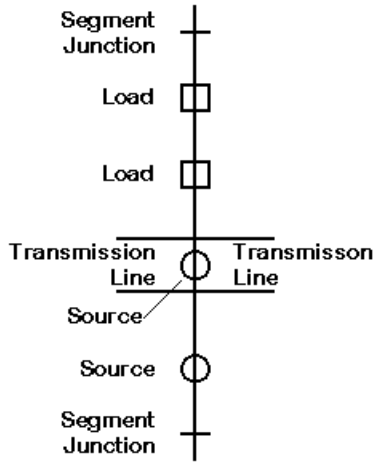

Fig. 58-9

Convergence Testing

To determine an adequate level of segmentation for an antenna model, uniformly increase the number of segments on each wire and examine the most critical output reports. Repeat as necessary.

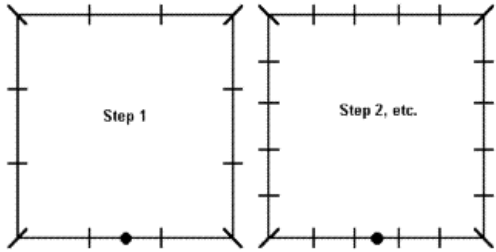

1. Does the gain (and, where relevant, front-to-back) value change excessively between steps? If so, continue increasing segmentation.

2. Does the source impedance value change excessively between steps? If so, continue increasing segmentation.

There is no preset definition of "excessive;" it is task-directed.

Some models may show a range of segmentation where changes are minimal, with greater changes for both more and fewer segments per unit of wire length. Some models may never converge.

The convergence test is a necessary, but not a sufficient condition of model adequacy.

Fig. 58-10

Average Gain Test

Fig. 58-11

Perfect loss-free antenna: $G_{ave} = k*P_{rad}/P_{in}$ where k=1 in free space
(G_{ave} = average power gain; k=2 for perfect ground
P_{rad} = radiated power; and P_{in} = input power)

Integrate/average P_{rad} over either a free-space sphere or a perfect ground hemisphere, using sufficient sampling points.

Obtain a value for G_{ave}. This value

a. Is a figure of merit for the model, and/or
b. Can be used to correct the gain and source impedance of the model.

NEC-Win Plus suggests merit values, but final decisions of model adequacy are task driven.

0.95 to 1.05	Highly accurate
0.85-0.95 and 1.05-1.15	Reasonably accurate and usable
0.80-0.85 and 1.15-1.20	Usable, but can be improved
<0.80 and >1.20	Questionable and requires refinement

The average gain test is a necessary, but not a sufficient, condition of model adequacy.

There are additional rules and provisions within NEC. There are, as well, numerous very specific situations that might create a problem if not modeled carefully. Nevertheless, I hope this collection of graphics—whether in whole or in part—provides a few handy reminders that help you avoid potential pitfalls.

* * * * *

Models included: none

59. MININEC and NEC: A Design Case Study

In past columns, I have had occasion to suggest that, within the limitations of wire antenna modeling as a whole, one should select the program best suited to a design or analysis task. Of course, the generic choices are NEC (-2 or -4) on the one hand, and MININEC on the other. The choice of programs rests on working to the strengths of a core and away from its weaknesses.

NEC, of course, has the Sommerfeld-Norton ground, and wherever wires with a horizontal far field component must reach below the 0.2-wavelength level, NEC is the obvious selection. The MININEC ground system inflates gain values below the 0.2-wavelength level and only calculates the source impedance based on a perfect ground. Likewise, NEC is the obvious choice for antenna structures involving coaxial or other low-impedance transmission lines. The TL facility creates non-radiating (non-wire geometry) lines that do not add to the segment burden of the model. MININEC lacks this feature.

NEC-4 improves upon NEC-2 in several ways. First, it can better handle linear elements with stepped diameter schedules than can NEC-2. However, both tend to have access to the Leeson substitute constant diameter element correction feature that has proven very accurate. Still, that feature applies only to linear elements that (when horizontal) meet certain standards with respect to load and transmission-line placement.

NEC-4 also permits wires underground and is the current default standard for the simulation of buried ground radial system. NEC-4 is also more accurate at mid-VHF frequencies and upward. As well, NEC-4 has improved surface patch facilities and the ability to handle wire permeability, as well as conductivity. The core also accepts insulated sheaths and upper medium inputs for greater flexibility in modeling.

In contrast, MININEC 3.13 (the public domain version) has lost many of its limitations through creative programming. While NEC-2 cores and NEC-4 cores tend all to yield very similar results within their types, MININEC cores tend to vary in results,

depending upon the correctives introduced by the programmer. At present, Antenna Model by Teri Software yields results that most closely correlate with those of NEC-4 over a range of models falling well within the capabilities of both types of programs. See column 51 of this series for a detailed comparison of MININEC programs in current use by many modelers.

Virtually all Windows implementations of MININEC have lost the DOS-based limitation of 256 segments (or double that number for programs implementing symmetry). As well, MININEC needs no correction factor for stepped-diameter elements. Indeed, the Leeson corrections were initially calibrated against MININEC modeling results. MININEC does require correction factors for very closely spaced elements, for frequencies above about 30 MHz, and for wires forming tight angles. Not all implementations are equally successful in providing such correctives.

Angular junctions of wires of different diameter form a limitation on NEC that is worse in NEC-2 than in NEC-4. See column #56 in this series for some test cases. I want to return to this type of model to present a design case study. It will reveal some temptations to think that a model is OK, when it may not be. It will also show some ways to tell the difference. Those ways may not all be inherent in the modeling process when we examine that process in isolation.

A "Large" Triangle Omni-Directional Antenna for 2 Meters

The search for a horizontally polarized omni-directional antenna has persisted over many years. The triangle came into being in the 1950s and has recently been re-developed by Par Electronics for VHF and UHF use. These triangles are of the "small" variety, and a sample version is included in the AO software package by K6STI. "Small" means that the total circumference is under 0.6 wavelengths, the feedpoint impedance is in the 8-12 Ohm range, and the inductive reactance runs from 70 to 170 Ohms, depending upon the exact design. It thus requires both reactance compensation and impedance transformation. The loop is interrupted and has a gap of about an inch (at 2 meters) opposite the feedpoint.

There is also a larger version of the 2-meter triangle, with a circumference of about 0.75 wavelength. It uses a larger gap—something in the 3-4" range. The benefits of the larger interrupted loop include a feedpoint resistance close to 50 Ohms, but still offset by an inductive reactance in the 350-Ohm range. The disadvantage of the larger loop is about a 0.1 dB gain deficit relative to the small loop,

although one would not likely notice that deficit in operation. Both types of triangles tend to surpass the more traditional turnstiled dipole array by about a dB in gain and by achieving a much more circular pattern. Unlike a turnstile, the pattern of which quickly devolves into a distinct oval even when only a small amount off the design frequency, the triangle tends to preserve its nearly perfect omni-directional pattern over it operating bandwidth.

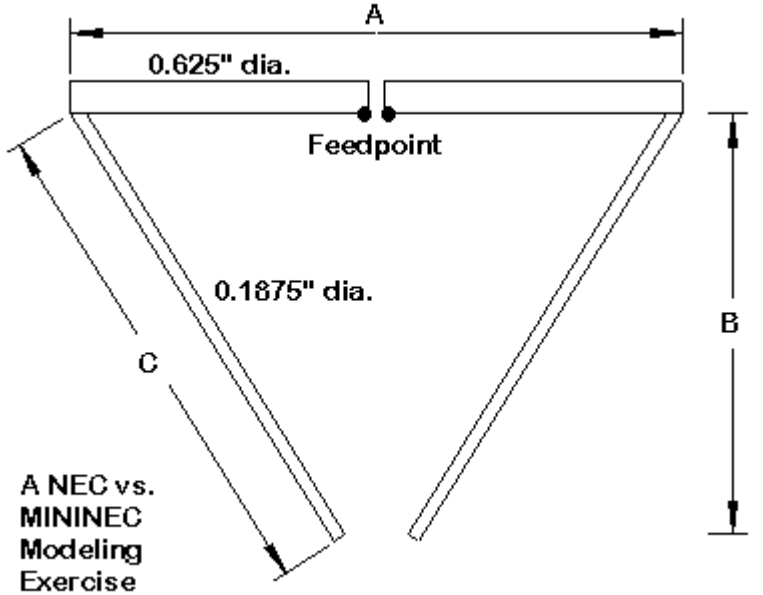

Fig. 59-1

The design issue facing the triangle builder is supporting the antenna. Ordinarily, one would support the structure at the feedpoint, using a large diameter element for the main arms and thinner material for the legs that extend to the gap. The basic mechanical structure results in a design model that requires two angular junc-

tions of wires having dissimilar diameters. **Fig. 59-1** provides the key dimensional elements of the antenna.

The overall arm length (dimension A) for the design exercise uses 0.625" (5/8") diameter aluminum. At element the diameters used, there is no performance difference among any of the alloys of aluminum. The legs will use 0.1875" (3/16") diameter rods. The model requires us to calculate on the basis of dimension B, but it is simple to move between the arm length (dimension C) and the required coordinates indicated by dimension B.

The key is to find a set of dimensions, including the gap between leg tips, that yields an omni-directional pattern. Only with a tightly designed combination of arm length, leg length, and gap will the array yield a circular polar plot. This requires a balance between the radiation from the arms and the legs. Since the current and the consequential field strength are not constant along the element, a simple symmetrical arrangement, such as an equilateral triangle, will not achieve the goal. The best way to determine the exact element dimensions is by trial-and-error modeling. (Remember that we also must adjust the gap along the way to achieve a 50-Ohm resistance at the feedpoint.)

The MININEC model of the antenna appears in **Fig. 59-2**. The white crosses represent pulses or segment junctions. The arm wire of the model uses an even number of segments to ensure that the source is placed at the exact center of the wire. A fuller description of the model, in AM (Antenna Model) format, appears at the end of the column.

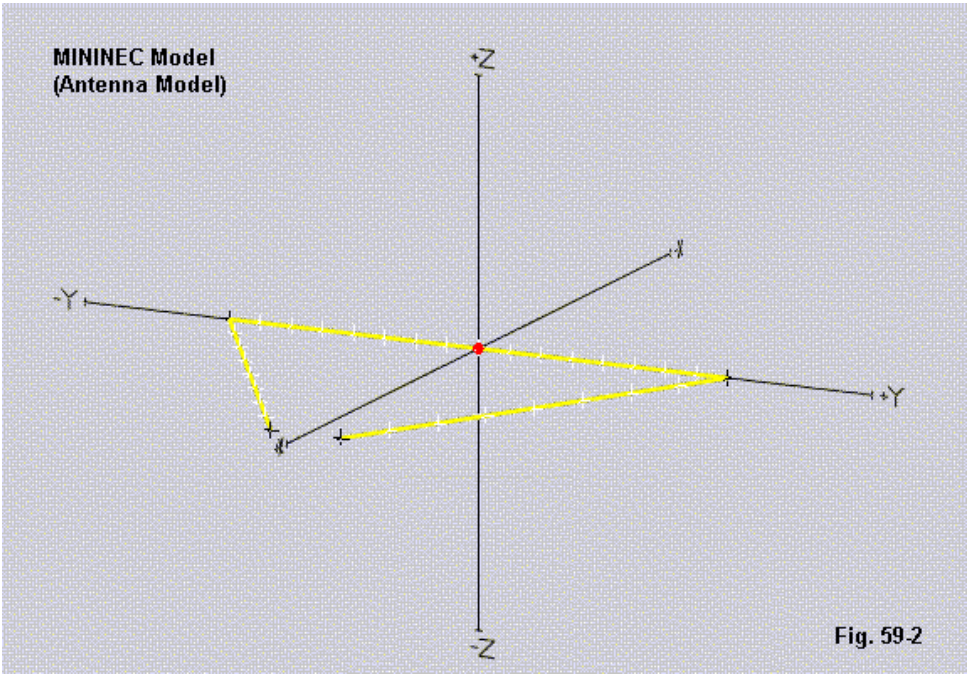

Fig. 59-2

The NEC model is shown in **Fig. 59-3**. EZNEC Pro/4 is the software I used for this exercise, although any version of NEC-4 would do as well. The models are not distinguishable from the graphic views provided by the software. However, what is apparent is that when a user moves from one software package to another, he or she must become familiar with the graphic conventions used in the current software. The EZNEC antenna view is shifted laterally by 180 degrees relative to the Antenna Model view. With the axes showing, the shift is not problematical.

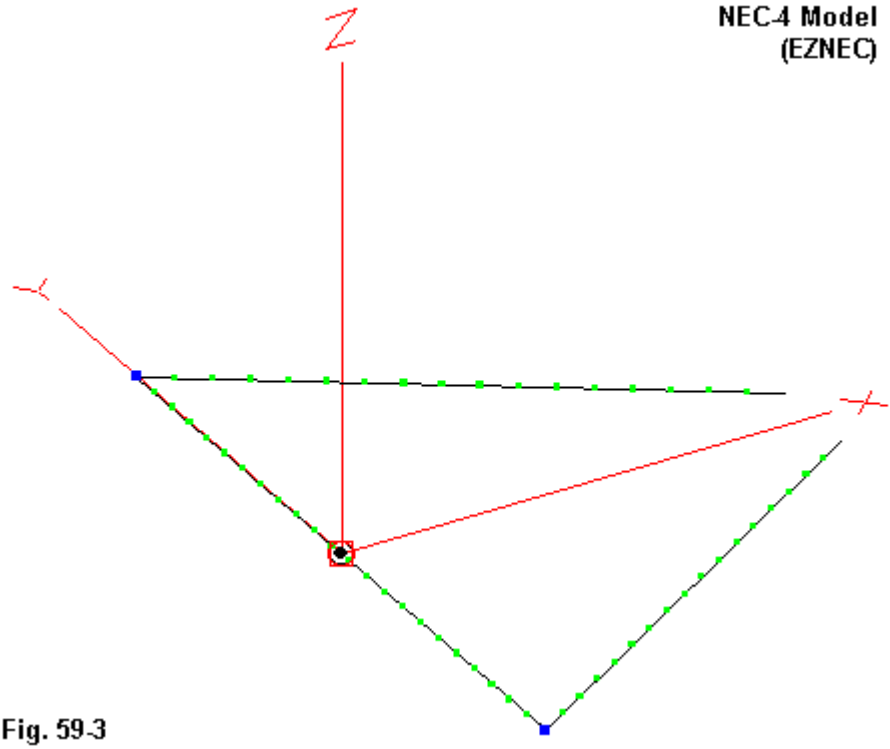

Fig. 59-3

The key differences between the models surround the dimensions required to obtain as close to a perfectly circular pattern as possible. The MININEC model in AM results in the following values—referenced to **Fig. 59-1**. Recall that the arms (A) use 5/8" diameter tubing and the legs (C) use 3/16" rod.

Dimension	Length in Inches	Dimension	Length in Inches
A	22.8	C	18.9
B	16.2	Gap	3.2

Using these dimensions, the AM model yields a feedpoint impedance of 49.5 + j357.3 Ohms. Eliminating the reactance for a 50-Ohm feedline is an exercise beyond the scope of this modeling study.

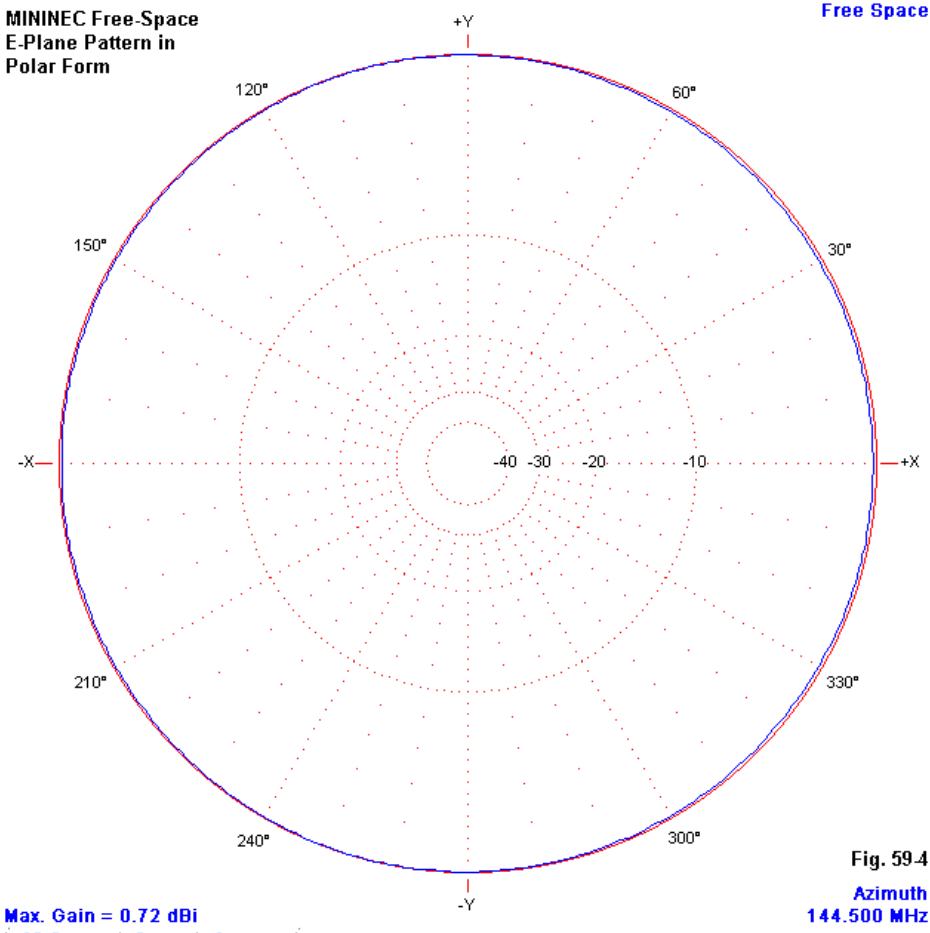
MININEC Free-Space
E-Plane Pattern in
Polar Form
Free Space
+Y
120°
60°
150°
30°
-X
+X
-40
-30
-20
-10
210°
330°
240°
300°
-Y
Max. Gain = 0.72 dBi
Azimuth
144.500 MHz

Fig. 59-4

Fig. 59-4 shows in polar form the free-space E-plane pattern of the resulting antenna. Maximum gain occurs approximately at a 90-degree angle to the line running from the feedpoint through the center of the gap. The antenna feedpoint is to the left, with the gap to the right, with the arms pointing straight up and down relative to the figure plane.

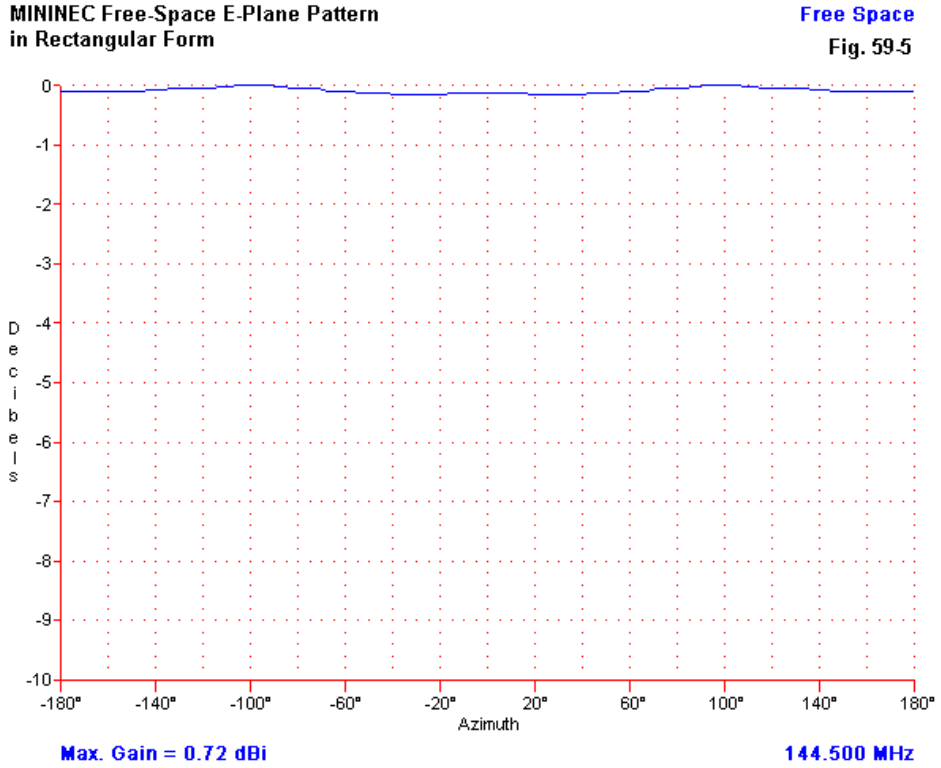

The maximum free-space gain is 0.72 dBi, with about a 0.2 dB maximum variation in gain around the circle. The gain to the antenna "rear," that is, behind the feedpoint, is slightly higher than the gain in the direction of the gap, although the difference is about 0.1 dB. The rectangular plot on **Fig. 59-5** provides a slightly greater resolution of the pattern variations.

The pattern centerline from the feedpoint to and through the gap is centered on the X-axis. Note that as we move in either direction away from this center line by about 20 degrees, we reach a double "null" in the pattern at about 0.2 dB down from the maximum or 0-dB line. (The nulls would be more exacting with higher resolution, but -10 dB is the highest resolution permitted by the program.) The double null means that the actual maximum-gain points are not at precise right angles, but further back in the vicinity of 100 degrees off the centerline. As a consequence, the radiation in the direction of the feedpoint is only about 0.1 dB down from the maximum gain.

The NEC-4 model of the same antenna (model 59-1), optimized as closely as possible to a perfectly circular E-plane pattern, results in the following dimensions.

Dimension	Length in Inches	Dimension	Length in Inches
A	23.6	C	18.75
B	15.75	Gap	3.2

The feedpoint impedance reported by NEC-4 is 53.2 + j 390.4 Ohms.

The free-space E-plane pattern derived from EZNEC appears in **Fig. 59-6**. I have moved data into the polar plot field for easier reference. The data includes in tabular form much of the information that we gleaned from the AM rectangular plot. The maximum reported gain is 0.76 dBi, and the two maximum gain points lie on bearings further to the rear of the antenna, given an orientation identical to the one used with the AM model. Hence, the 0.26-dBi gain deficit in the direction of the gap is halved in the direction of the feedpoint.

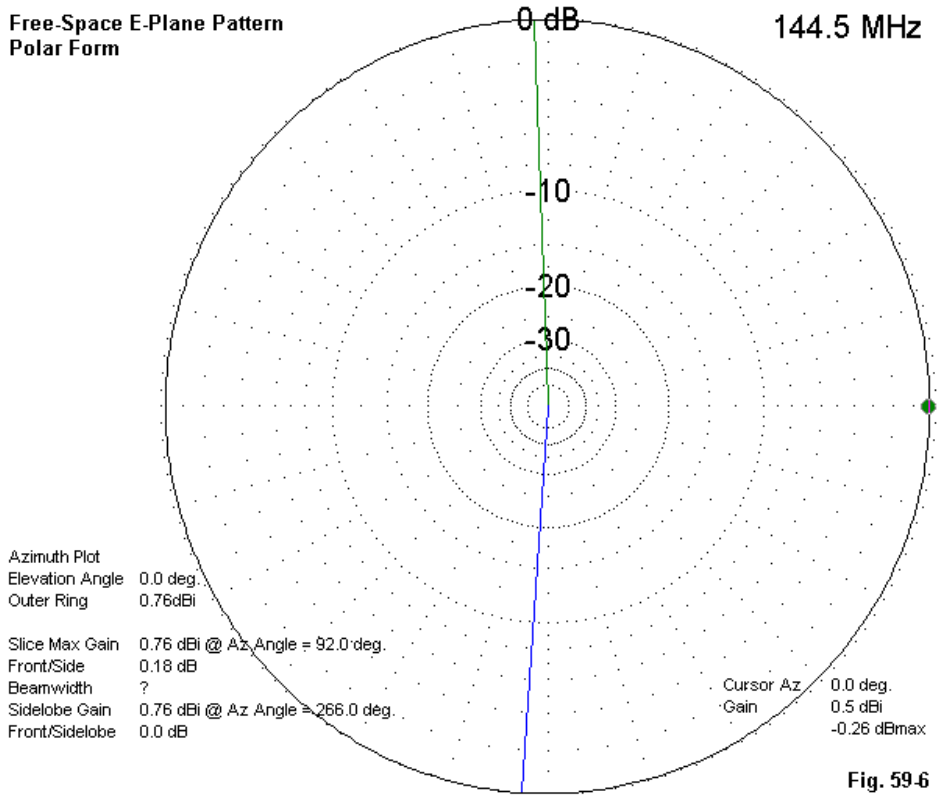

Fig. 59-6

There are two indicators that tell use something about which of the two models is the more accurate. First, NEC-4 improves upon the performance of NEC-2 with respect to angular junctions of wires having different diameters. The NEC-2 report on the model using NEC-4 dimensions shows a maximum gain of 0.72 dBi and a minimum gain of 0.32 dBi, a variation of 0.4 dB. Second, the reported feedpoint

impedance is 57.1 + j 411.7 Ohms. If we are aware in advance of the deficit in accuracy of NEC-2 relative to NEC-4 under the modeling parameters used in this structure, and if we know as well that NEC-4 advances accuracy without attaining full precision, then we have an indication of potential problems with the NEC-4 dimensions.

The average gain test (AGT), which is available in all three programs used in this case study, provides a means of turning suspicions into a measure of model adequacy. A perfect model would yield an AGT value of 1.0 with the model in free space and using zero-loss wires. The NEC-2 model returns a value of 0.947, while the NEC-4 model shows a value of 0.977. The AM MININEC model returns a value of 0.9955.

Some charts of AGT values suggest that the range from 0.95 through 1.05 represents very adequate and accurate models, remembering that the AGT is a necessary but not a sufficient condition of model adequacy. (None of the factors that tend to produce models with high AGT values but known inadequacies occur with these models. Many of the model types that show good AGT results but remain inadequate models involve parallel wire structures with essentially self-canceling radiation or inequalities of current on each side of the source position.)

In essence, the *a priori* charts recording model quality by reference to AGT values would show that both the AM and NEC-4 models are fully accurate, despite the differences in their dimensions. For some purposes, the charts might be adequate, but in this instance, the precision that we have imposed on the modeling task requires that we use a higher standard. For example, using a contrast between a perfect 1.0 AGT value and a 0.95 values yields more than a 0.22 difference in the gain report, which is as great or greater than the gain variations we have discussed relative to pattern perfection.

The acid test for the models involves a different exercise, suggested by the fact that the dimensions for the triangle indicated by each program are different. Let's apply these dimensions across programs.

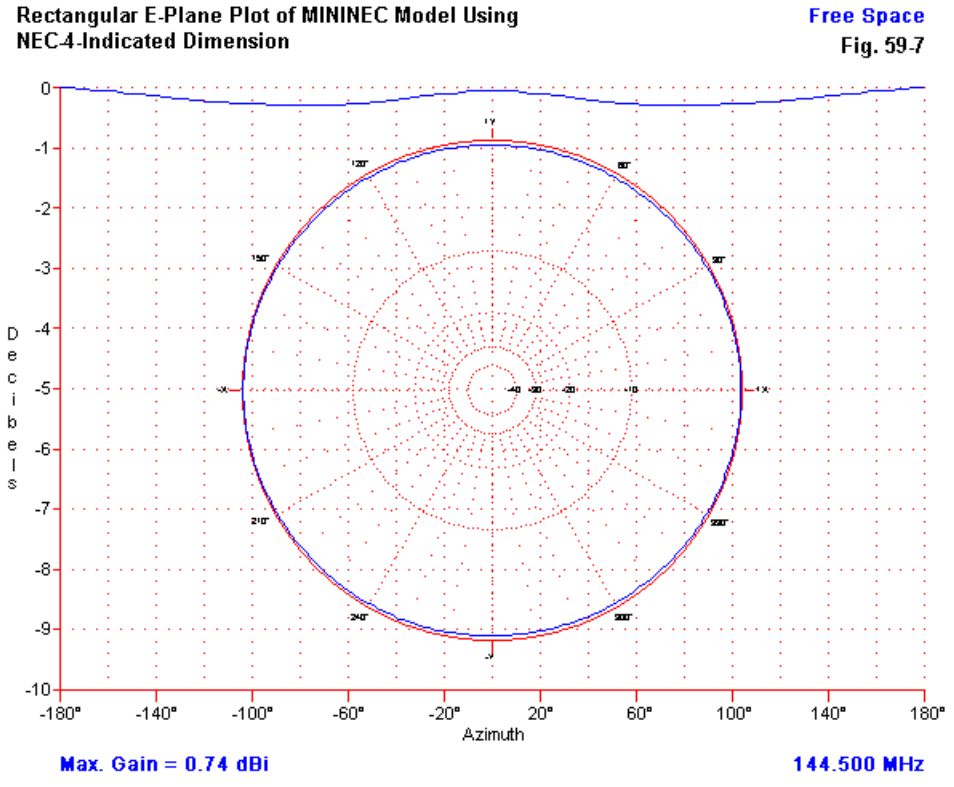

Fig. 59-7 shows both the polar and the rectangular E-plane plots for the free-space model using the dimensions developed in the NEC-4 portion of the exercise. The maximum gain of 0.74 dBi is accompanied by an increase in imperfection in the plot that now is approaches 0.3 dB. As well, the maximum and minimum gain positions have now reversed, with minimum gain at right angles to the line running from the feedpoint through the triangle's gap. The reported feedpoint impedance is

50.9 + j 355.2 Ohms. Although the resistive portion of the impedance is only about 2 Ohms different from the NEC-4 report, the inductive reactance shows a 10% difference from the NEC-4 figure.

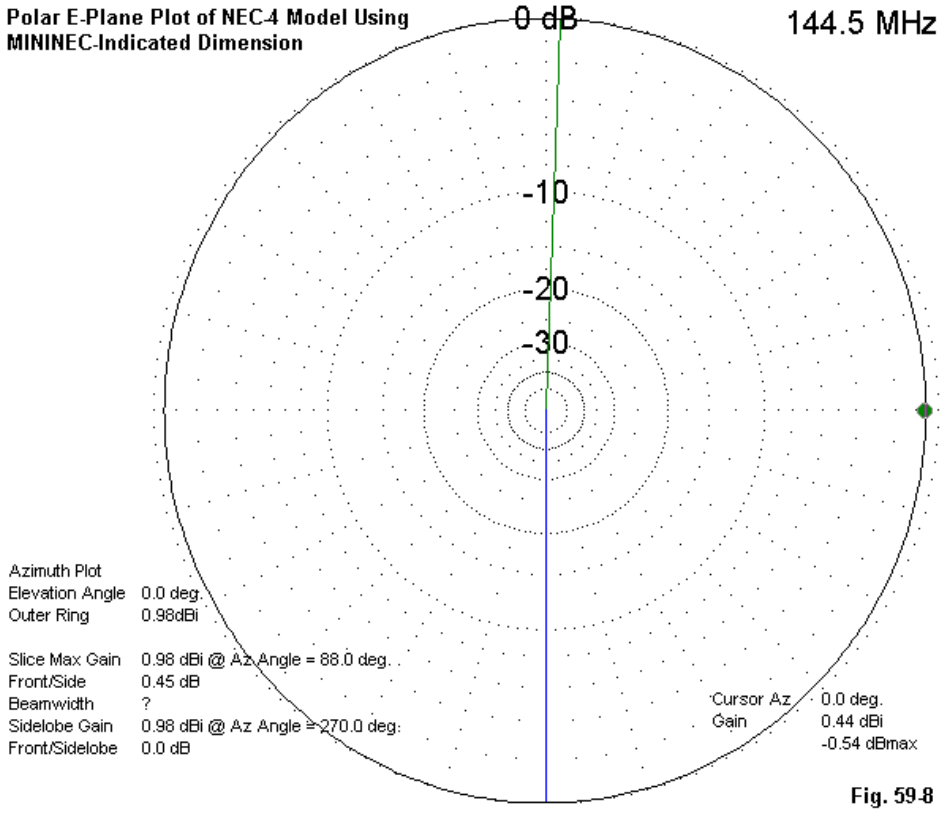

Fig. 59-8

For the sake of contrast, the NEC-4 report on the dimensions developed via MININEC appears in **Fig. 59-8**. The maximum reported gain is 0.98 dBi and occurs

at right angles to the line from the feedpoint through the gap. Minimum gain occurs along the feedpoint-gap line and is least in the direction of the gap. The maximum variation in gain is over 0.5 dB. The reported feedpoint impedance is 51.2 + j 389.1 Ohms. Once more, the resistive component difference is about 2 Ohms, but the difference in reactance approaches 10%. However, the differences are less than those we encountered when running the NEC-4 dimensions on MININEC.

It is interesting to note that the NEC-4 model using MININEC dimension shows a greater pattern difference but a smaller feedpoint impedance difference than the MININEC model using NEC-4 dimensions. Of greater significance for the modeler are the indications offered by the dimensional changes. If the arms are too long relative to the legs, the pattern distorts along the line from feedpoint to the gap. If the legs are too long relative to the arms, the pattern distorts at roughly right angles to the line.

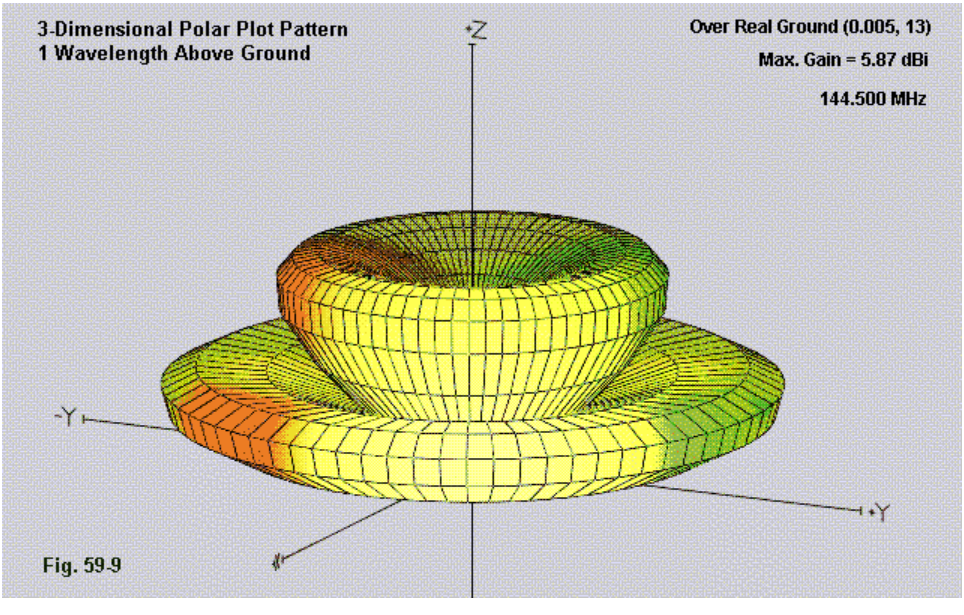

Fig. 59-9

Although it may be a bit gratuitous, **Fig. 59-9** shows a 3-dimensional pattern for the triangle when we place it 1 wavelength above real ground, the height that generally corresponds to a mobile installation. Relative to a turnstiled-dipole array, the triangle exhibits higher gain within the lower elevation lobe. This gain is largely the result of a reduction in the gain of the higher-angle lobe. A stack of 2 such triangles with 1/2-wavelength spacing and fed in phase is capable of about 2.4 dB further gain with the lower triangle at 1 wavelength above ground.

What, If Anything, Does the Case Study Show?

The importance of the differences between using NEC-4 and corrected-MININEC for the design of the triangle may vary from insignificance to high import. The weight of the differences depends upon two major factors: the operational parameters assigned to the design effort and the degree to which manufacture can replicate the model.

If variations of as much as 1 dB in the omni-directional pattern are acceptable, then the differences in the design results make little or no difference. Either program's dimensions will yield a pattern within the assigned specification limit.

However, if the design specifications call for the least possible variation in the pattern gain, then the higher AGT score of the MININEC model (when derived from an adequately corrected version of MININEC 3.13) yields higher confidence in the dimensions produced by that model. Note, however, that the adequacy of the version of MININEC used must be established in advance.

A very tight design specification is only relevant where the construction of the actual antenna is capable of replicating the modeled conditions very closely. Every model is subject to differentials between model and reality that result from a manufacturing process and a modeling process that can only approximate each other. The differentials become an ever-growing burden as we model in the VHF and UHF range. Nuts and bolts that make no difference to the HF performance of an array become more appreciable factors at much higher frequencies.

For a home-brew or garage type assembly, it is likely that the differences between models make no difference at all. For a precision shop having the goal of

producing many such antennas with repeatable performance from unit-to-unit, beginning with the most reliable design may be more crucial.

There are several factors that the models do not show. For example, the models do not show any projections of either the arms or the legs beyond the corresponding portion of the element at the corners. Such projections would be almost inevitable for most proto-types, although one might eliminate them in final production models. Moreover, the models do not show the effects of splitting the feedpoint region of the arms and adding a feedline connector (as well as adding any type of matching components). The fatter the conductor, the greater the capacitance at the feedpoint split. Hence, its dimensions may affect the remnant inductive reactance. As well, feedline connectors and the leads from the connector to the element will also have an affect on the impedance.

The final factor in the mix involves the ability to test the pattern precisely. The average backyard builder is unlikely to have more than a receiver with an S-meter as a guide to the omni-directionality of the pattern. Chamber tests used by engineering and manufacturing firms are much more likely to uncover small variations in the pattern's circularity.

For the backyard builder and casual user, then, there is likely to be no discernable difference between antennas built up from each of the models. For the precision shop, the corrected-MININEC model is more likely to yield the better results. What is clear, however, even for the casual modeler and builder, is that the use of NEC-2 is more likely to result in an antenna that falls far short of the desired results. Its ability to handle angular junctions of wires having different diameters falls far short of NEC-4, which the AGT values suggest is still shy of corrected MININEC.

One last question might arise here: why is the differential between MININEC and NEC models so much less dramatic than the types of case examined in column #56 of this series? The answer is straightforward. The greater the differential of wire diameters at the junction, the greater the error level in NEC. The differential between wires in this design exercise is 3.3:1. In column #56, the differential was 6.2:1. In that exercise, it was clear that the NEC models were seriously deficient. In this exercise, we have been working with borderline differences the weight of which depends upon factors external to the modeling process itself. Clear deficiencies show themselves vividly once we know what to look for. However, the borderline

cases are less self-evident. It is important to understand the borderline cases and what is involved in their evaluation. That has been part of the design case study.

```
================================================================================
                              ANTENNA MODEL
                    Copyright (C) 1992-2002 Teri Software Co.
                    05-04-2002                        3:39 PM

                            Antenna File: il6fs.def

                   2-meter interrupted loop hor. pol. antenna

                                  Free Space

                  Lowest Frequency of Operation: 144.0000 megahertz
                  Center Frequency of Operation: 144.5000 megahertz
                 Highest Frequency of Operation: 145.0000 megahertz

                Dimensions below are in inches unless otherwise noted

Wire Statements

              End Coordinates, Wire #1                Wire
          X           Y           Z          Diameter  Segments     Material

End 1:   0.000000   -11.40000    0.000000   0.625000    16        6063-T832
End 2:   0.000000    11.40000    0.000000                           Alloy

              End Coordinates, Wire #2                Wire
          X           Y           Z          Diameter  Segments     Material

End 1:  16.20000     -1.600000   0.000000   0.187500     8        6063-T832
End 2:  0.000000     -11.40000   0.000000                           Alloy

              End Coordinates, Wire #3                Wire
          X           Y           Z          Diameter  Segments     Material

End 1:  0.000000     11.40000    0.000000   0.187500     8        6063-T832
End 2:  16.20000     1.600000    0.000000                           Alloy

   Approximate near-field/far-field boundary is 3.55210 meters or 1.71211
wavelengths
```

```
Source Statements
     Source #1
                Pulse              Voltage             Phase
                 No.               (Volts)             (Deg)

                   8               1.00000           0.00000

============================================================================

============================================================================
EZNEC/4 ver. 3.0

2-m large triangle 144.5 MHz                        5/4/02     3:44:58 PM

        ———————— ANTENNA DESCRIPTION ————————

Frequency = 144.5 MHz
Wire Loss: Aluminum (6061-T6) — Resistivity = 4E-08 ohm-m, Rel. Perm. = 1

              ———————— WIRES ————————

No.      End 1   Coord. (in)         End 2   Coord. (in)        Dia (in)  Segs
    Conn.    X         Y     Z     Conn.    X        Y     Z
1   W3E2     0,      -11.8,  0     W2E1     0,      11.8,  0     0.625     17
2   W1E2     0,       11.8,  0              15.75,   1.6,  0     0.1875     8
3            15.75, -1.6,    0     W1E1     0,     -11.8,  0     0.1875     8

Total Segments: 57

              ———————— SOURCES ————————

No.       Specified Pos.      Actual Pos.       Amplitude    Phase    Type
       Wire #  % From E1  % From E1  Seg       (V/A)     (deg.)
1       1        50.00      50.00    12        1           0         I

           ———————— LOADS (RLC Type) ————————

Load Specified Pos.     Actual Pos.       R      L      C       R Freq Type
     Wire #  % From E1  % From E1  Seg   (ohms) (uH)   (pF)     (MHz)
1    1       50.00      50.00      12     Short  Short  2.82415  0      Ser

No transmission lines specified

Ground type is Free Space
============================================================================
```

* * * * *

Models included: 59-1. (.NEC and .NWP model dimensions in meters; .EZ model dimensions in inches. The MININEC model is not included.)

60. NVIS Antenna Models and the Ground Type

In past columns, we have noted some of the deficiencies of the systems of ground calculations associated with MININEC and with the fast or reflection coefficient system in NEC (-2 and -4). These two ground calculation systems both use (although not in exactly the same way) a simplified algorithm for the rapid calculation of ground effects on the far field of a signal. The NEC reflection coefficient system also applies the ground calculations to the source impedance calculations. However, MININEC always calculates the source impedance as if the antenna is over perfect ground.

The simplified calculation systems for ground effects emerged for various reasons. The original MININEC system had to do its calculations within the restrictions of early desktop computer systems with as little as 640 KB of RAM. The NEC reflection coefficient system held a speed advantage over a more complete ground analysis system, a strong consideration with large models in the days of CPU speeds below 10 MHz.

NEC also incorporates the Sommerfeld-Norton (S-N) ground calculation system, which is the most accurate calculation system available on wire-based antenna simulation packages. While very accurate, it requires considerably more time to execute within a model, relative to the reflection coefficient system. However, for any NEC implementation, modern CPU speeds ranging from 200 MHz to 2 GHz tend to make the extra time required for execution of the S-N system less than significant. Indeed, perhaps the only use remaining for the reflection coefficient system in NEC is to make comparisons among ground effect calculation systems. For a comparison of the mathematical foundations of the various ground systems, the appropriate NEC manuals contain full information.

The limitations of the MININEC ground system and the NEC ground reflection system are matters of the height of the antenna wires above ground. Both systems begin to yield inaccurate results when any wire in the antenna system is at or below about 0.2 wavelengths and has any horizontal component to the radiation. Because the error gradually develops as we lower the wire closer to the earth, we may easily

overlook it. As well, we cannot mark a clear and distinct point or height at which errors begin. Nonetheless, well below the boundary region, the errors are vivid, if one has some experience with what values are sensible at very low antenna heights.

In episode 37 of this series, we performed a small exercise with tilted dipoles with one end very close to the ground. As we tilted the dipole away from the vertical and toward the horizontal, the disparity between MININEC results and NEC-4 S-N results grew in proportion to the horizontal component of the tilted dipole radiation. The S-N system in either NEC-2 or NEC-4 is considered accurate down to several wire radii from the earth's surface.

NVIS Antennas and Models

Near Vertical Incidence Skywave (NVIS) propagation makes use of the fact that near-vertical signals do not all penetrate the ionospheric layers and disappear into space. Instead, a usable amount of signal is ordinarily reflected or refracted downward. A good brief account of the general parameters of NVIS propagation appears in Jaques d'Avignon, VE3VIA, "The NVIS Propagation Mode and the Ham," *The ARRL Antenna Compendium*, Vol. 5, pp. 129-134.

The most common form of NVIS antenna is a simple wire array placed relatively close to the earth's surface. The antenna types used include dipoles, loops, and in-phase fed pairs of dipoles or folded dipoles. Heights range from a few feet to about 1/4 wavelength. Above that height, the elevation angle of maximum radiation lowers enough to reduce the vertical radiation significantly. The object of a NVIS antenna is to radiate vertically as strongly as possible.

Antenna modelers are always interested in how much gain and what feedpoint impedance an antenna has. Hence, curiosity about NVIS antenna models goes back to the early days of MININEC. The models are simple—well within the 256-segment limitation of the original DOS-based MININEC program. Although Windows implementations of MININEC have removed the segmentation limit on models, they have not yet overcome the limitations of the MININEC ground calculation system.

Virtually by definition, all NVIS antennas use a height that places horizontal wires below the threshold for accurate results using the MININEC or NEC reflection coef-

ficient ground systems. Hence, it is not out of place to present two modeling rules for NVIS antennas.

1. NEVER use MININEC to model a NVIS antenna.

2. NEVER use the NEC reflection coefficient ground system to model a NVIS antenna.

By default, we are left with a third rule:

3. Always use the NEC S-N ground system when modeling NVIS antennas.

The question these rules leave us is this: how much error can we expect if we use the "forbidden" ground or modeling systems with a NVIS antenna? Since a NVIS antenna may have wires ranging from virtually at the earth's surface to about 1/4 wavelength above the ground, there is no single answer. However, we can perform a series of exercises to show the growth of the error under varying conditions with various kinds of models. Since this column is finite, we can only sample a few cases. For convenience, all examples will use 3.9 MHz as the operating frequency.

A Wire Dipole

One common antenna that amateurs press into service for NVIS operations is the simple dipole. **Fig. 60-1** shows the basic outline of a #14 copper wire dipole, cut to 121' for the test frequency. See model 60-1.

At 3.9 MHz, a wavelength is 252.2', placing a quarter wavelength just below the 70' height mark. We can test the antenna at 10, 30, 50, and 70 feet above ground and compare the results that we get using different ground systems. EZNEC allows one to use NEC-2 (or NEC-4 in the Pro version) with not only the reflection coefficient and S-N systems, but as well with the MININEC ground system. The MININEC ground results correlate extremely well with the same ground system in its MININEC antenna property calculation environment. Therefore, we may conveniently make comparisons among ground system effects of reported antenna properties without leaving a single program.

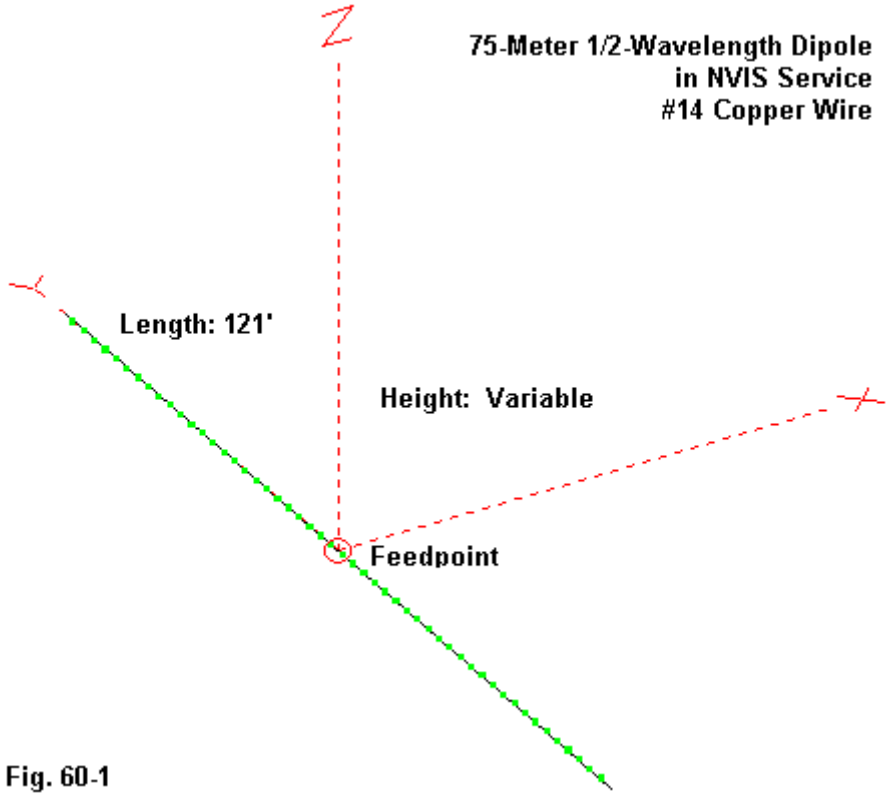

Fig. 60-1

The following table lists the results of modeling our NVIS dipole at the test heights using each of the ground systems.

```
MININEC Ground
Height              Gain         TO angle       Feedpoint Impedance
(feet)              (dBi)        (degrees)          (R +/- jX Ohms)
 10                 9.40         89                   5 - j 36
 30                 8.04         90                  30 + j  0
 50                 6.91         86                  66 + j  9
 70                 5.90         52                  91 - j  6

NEC Reflection Coefficient Ground
Height              Gain         TO angle       Feedpoint Impedance
(feet)              (dBi)        (degrees)          (R +/- jX Ohms)
 10                 1.78         88                  31 - j 35
 30                 6.15         88                  47 - j  4
 50                 6.47         86                  72 - j  1
 70                 6.03         52                  87 - j 15

NEC S-N Ground
Height              Gain         TO angle       Feedpoint Impedance
(feet)              (dBi)        (degrees)          (R +/- jX Ohms)
 10                 -.51         88                  53 - j  8
 30                 5.64         88                  52 - j  4
 50                 6.40         87                  73 - j  3
 70                 6.04         52                  87 - j 16
```

If we model the NVIS dipole using a MININEC ground, we shall draw all of the wrong conclusions. The antenna height for maximum gain appears to be as close to the ground as we can manage and certainly no higher than about 10'. As well, we shall have a very low feedpoint impedance to consider when developing a system to match the antenna to the feedline and the feedline to the equipment.

However, even the reflection coefficient system of NEC shows how inaccurate the MININEC ground is under these circumstances. It correctly shows that the optimum height is somewhere around 50' or about 0.2 wavelengths above ground. The S-N system is more dramatic in its results (and more accurate). The gain of the dipole at a 10' height at 3.9 MHz is about 10 dB lower than the MININEC ground illusion. As well, the feedpoint impedance is an easily managed 50 Ohms.

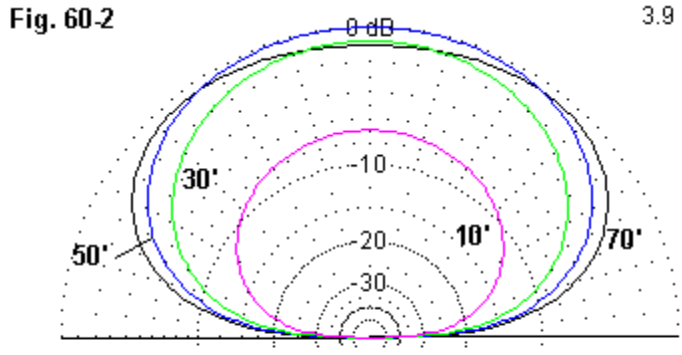

Elevation Patterns of a 75-Meter Dipole for NVIS Service at 10, 30, 50, and 70 Feet Above Average Soil

Fig. 60-2 shows the comparative elevation patterns for the dipole at the 4 heights sampled in this modeling test. For NVIS work, the 50' height is closest to the optimum value in terms of radiation directed vertically. At slightly lesser gain, the 30' height is also usable—and, of course, anything between and around these values. The 70' height sacrifices vertical radiation for radiation at a lower angle. The 10' height is simply deficient in gain from any perspective.

Fig. 60-3 shows the azimuth patterns of the dipole with an elevation angle of 60 degrees. Although the gain deficit of the 10' height is clear, perhaps the more important aspect of the azimuth patterns is their oval shape. Even though one thinks about NVIS work in terms of a circular pattern, operating needs in terms of target stations or areas may make an oval pattern more desirable on occasion than a purely circular one.

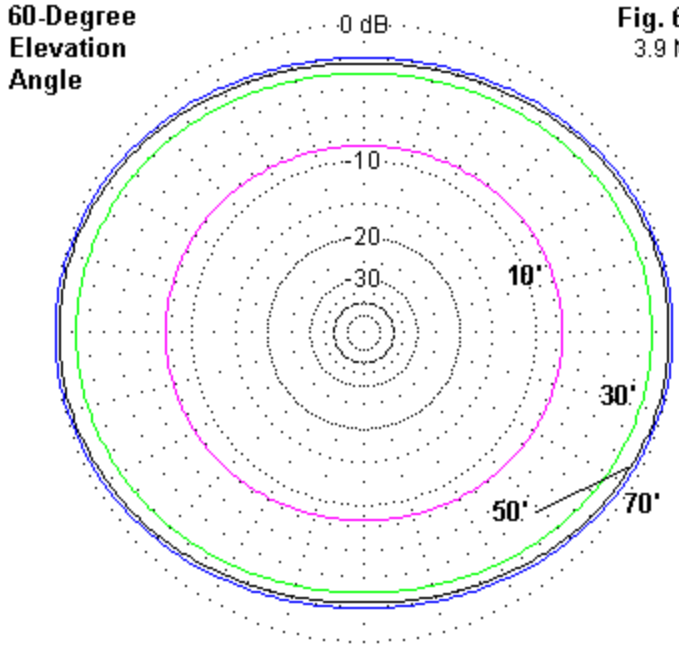

Azimuth Patterns of a 75-Meter Dipole for NVIS Service at 10, 30, 50, and 70 Feet Above Average Soil

A Wire Loop

One technique used to obtain a more circular pattern in NVIS operation is to use a 1-wavelength loop instead of a dipole. **Fig. 60-4** shows the rudiments of such an antenna. See model 60-2.

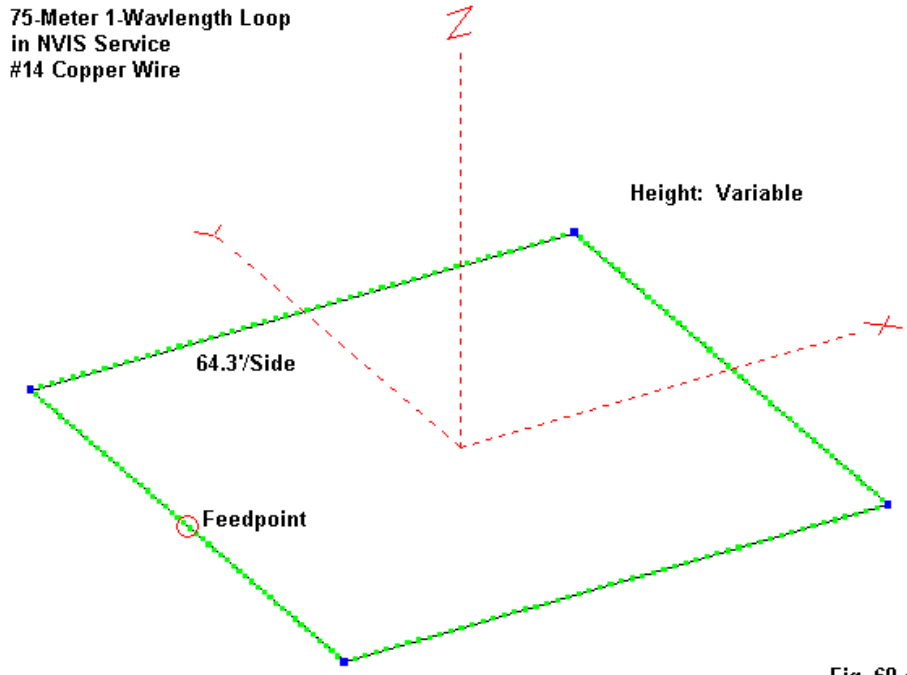

Fig. 60-4

The dimensions shown are somewhat arbitrary but close to correct for the 3.9-MHz operating frequency. The diagram shows a side-fed loop, although we might as easily have chosen a feedpoint at the loop corner or anywhere between. The results of comparing ground systems for this antenna at the test heights appear in the following table.

```
MININEC Ground
Height              Gain         TO angle       Feedpoint Impedance
(feet)              (dBi)        (degrees)          (R +/- jX Ohms)
 10                 10.15        90                   10 + j  8
 30                  8.60        90                   58 + j  2
 50                  7.48        90                  124 - j  4
 70                  6.05        101                 167 - j 45

NEC Reflection Coefficient Ground
Height              Gain         TO angle       Feedpoint Impedance
(feet)              (dBi)        (degrees)          (R +/- jX Ohms)
 10                 4.46         90                   36 - j 52
 30                 7.11         90                   81 - j 16
 50                 7.17         90                  132 - j 27
 70                 6.26         101                 158 - j 63

NEC S-N Ground
Height              Gain         TO angle       Feedpoint Impedance
(feet)              (dBi)        (degrees)          (R +/- jX Ohms)
 10                 0.42         90                   95 + j 48
 30                 6.32         90                   98 - j 12
 50                 7.04         90                  136 - j 30
 70                 6.26         102                 158 - j 65
```

Once more, the MININEC ground system yields unbelievably optimistic reports of antenna performance at very low heights. The loop gain is reportedly almost 10 dB higher than the same antenna calculated using the S-N system. As well, the feedpoint resistance reported by the MININEC system is about a tenth of the value yielded by the S-N system. Of course, there is a relationship between the errors produced by the MININEC ground system at very low heights. The extremely low source impedance indicates erroneously high current levels that yield a high gain value.

Unfortunately, the ground errors cannot show themselves in the average gain test, since this test requires the use of free space (or a perfect ground for ground-mounted monopoles). All of these tests place the NVIS antennas above average ground (conductivity: 0.005 S/m; dielectric constant: 13).

The reflection coefficient system in NEC lowers the amount of error for any given low height, but still yields inaccurate results. If we compare the excess gain at 10' with the low feedpoint impedance, relative to the S-N report, we find the same pattern as in the MININEC results. The S-N system finds the best height for the loop to be in the vicinity of 50' at 3.9 MHz or about 0.2 wavelength above ground.

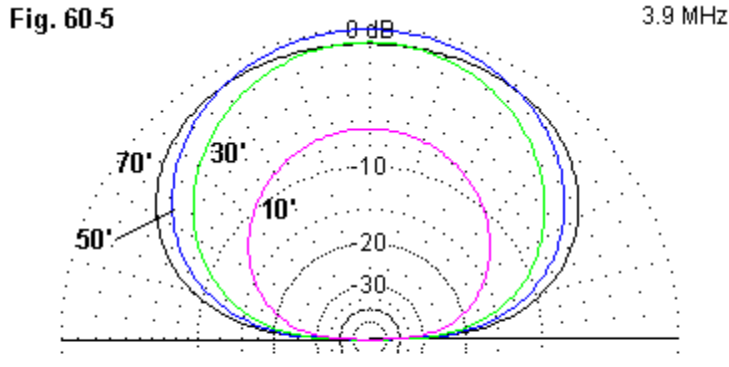

Elevation Patterns of a 75-Meter Loop for NVIS Service at 10, 30, 50 and 70 Feet Above Average Soil

The elevation patterns in **Fig. 60-5** show the same general properties as those for the dipole. The 50' height gives us the highest gain straight up of all of the test heights. 70' shows its highest gain somewhat off vertical, and 10' simply yields insufficient gain relative to what it might be at a better height.

The azimuth patterns in **Fig. 60-6** reveal that the use of a loop does indeed circularize the pattern compared to the pattern of a dipole. The 60-degree elevation angle applies to these patterns as well as to those of the dipole in **Fig. 60-3**. The departure from a circle is a little over 1 dB for heights from 30' to 70', with the stronger directions being in line with the feedpoint.

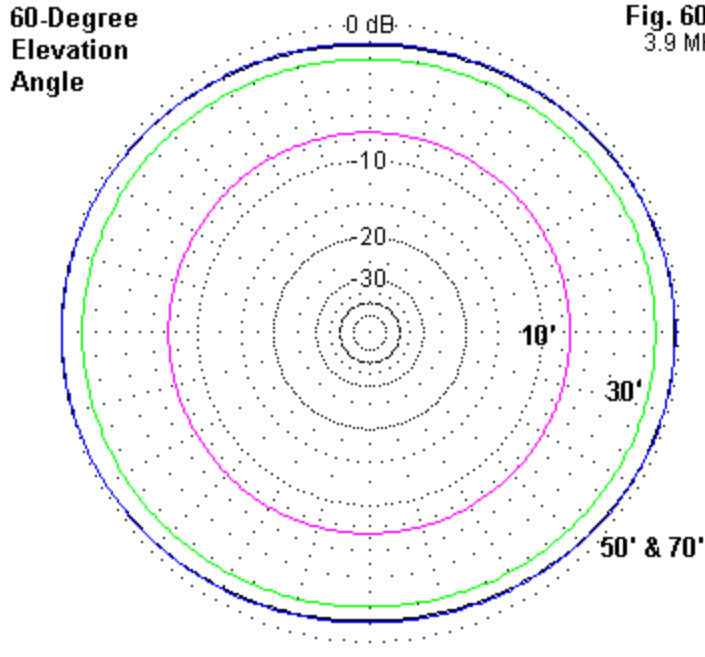

Azimuth Patterns of a 75-Meter Loop for NVIS Service at 10, 30, 50 and 70 Feet Above Average Soil

A Dipole and a Low Reflector

One type of antenna recommended by some for NVIS service consists of a dipole at about 1/4 wavelength above ground, with a low wire in line with the driven dipole. To simulate this type of antenna, I took the dipole we previously examined, placed it at 70' above average soil, and added a second wire the same length (121')

at a height of 5' above ground. **Fig. 60-7** shows the general outline of the model. See model 60-3.

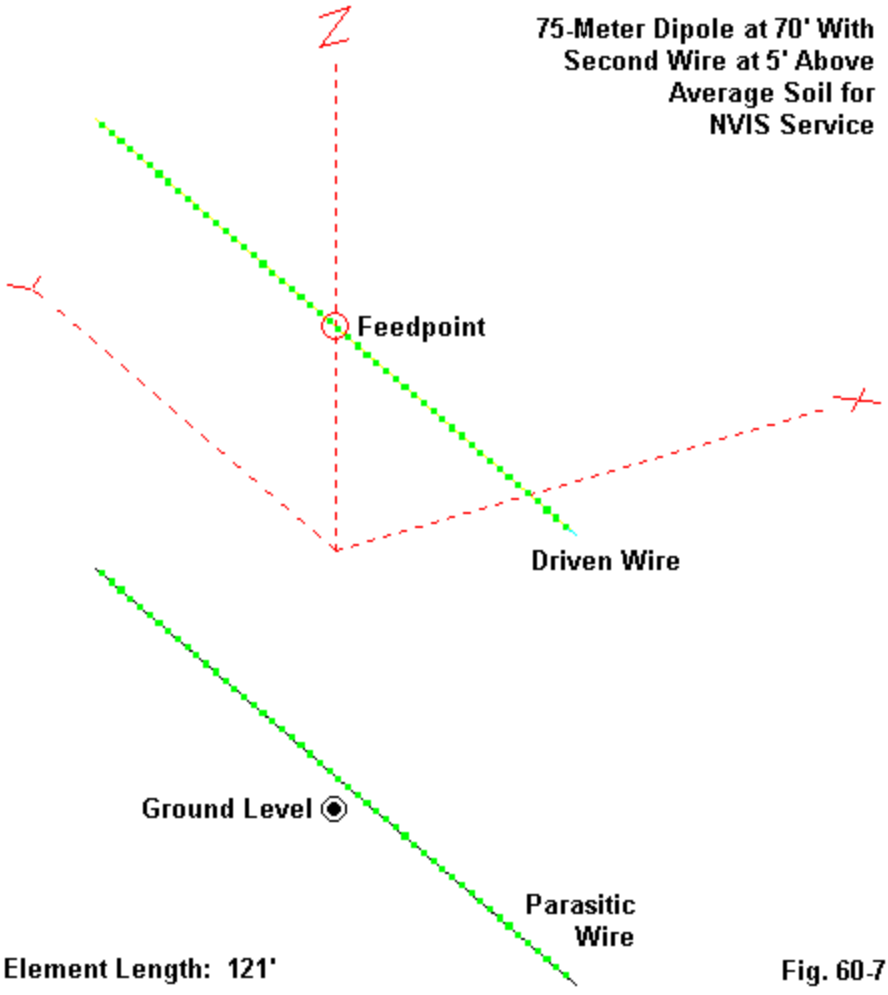

Fig. 60-7

The results for the antenna appear in the following table, which includes both NEC-2 and NEC-4 reported values and the values for the earlier dipole at 70' without a parasitic wire below it.

```
MININEC Ground:  70' and 5'
Model              Gain         TO angle       Feedpoint Impedance
                   (dBi)        (degrees)          (R +/- jX Ohms)
NEC-4              5.75         52                  92 - j  8
NEC-2              5.75         53                  92 - j  8
Dipole only        5.90         52                  91 - j  6

NEC Reflection Coefficient Ground:  70' and 5'
Model              Gain         TO angle       Feedpoint Impedance
                   (dBi)        (degrees)          (R +/- jX Ohms)
NEC-4              5.67         50                  81 - j 20
NEC-2              6.22         55                  88 - j 11
Dipole only        6.03         52                  87 - j 15

NEC S-N Ground:  70' and 5'
Model              Gain         TO angle       Feedpoint Impedance
                   (dBi)        (degrees)          (R +/- jX Ohms)
NEC-4              6.09         53                  79 - j 11
NEC-2              6.09         53                  79 - j 11
Dipole only        6.04         52                  87 - j 16
```

In the case of the dipole with its low parasitic reflector, the MININEC results are at odds with the NEC-4 S-N results in showing a lower gain with a higher source impedance. As noted earlier, these error directions are consistent with each other. The reflection coefficient results are interesting insofar as there are more distinct differences between NEC-2 and NEC-4 than for the other two cases.

Fig. 60-8 shows the azimuth and elevation patterns for the array, which are remarkable similar to those for the dipole alone at 70' without the extra wire. The extra wire does little that the average ground beneath the driven element cannot do with respect to the far field radiation pattern or the feedpoint impedance.

The tightness of the figures for NEC-2, NEC-4, and the dipole alone in NEC-4 contrast with the somewhat wider span of numbers between the two-and one-wire arrays using a MININEC ground. The differential suggests that even if the driven

wire is above the region of inaccuracy for MININEC ground, the almost functionless second wire close to the earth in the array does have an affect on the reported results.

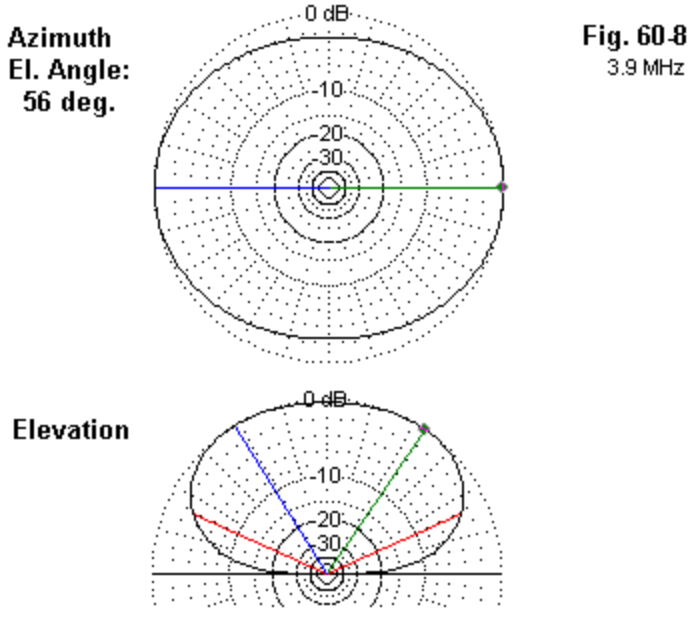

Fig. 60-8
3.9 MHz

75-Meter Dipole at 70'
With Second Wire at 5' Above Average Soil
for NVIS Service

A correspondent took me to task for using an example with the reflector wire the same length as the driver wire. So I surveyed the situation by leaving the driver as

is and gradually lengthening the reflector wire. The following chart shows the results of the survey.

NEC-4 S-N Ground: Refl. Length (ft)	70' and 5': Gain (dBi)	Driver 121' TO angle (degrees)	Feedpoint Impedance (R +/- jX Ohms)
121'	6.09	53	79 - j 11
122'	6.14	52	80 - j 10
123'	6.18	52	82 - j 10
124'	6.20	52	83 - j 7
125'	6.21	53	84 - j 10
126'	6.21	52	85 - j 10
127'	6.21	53	85 - j 11
128'	6.21	53	86 - j 11
129'	6.20	53	86 - j 11
130'	6.20	54	86 - j 12
131'	6.19	53	86 - j 12
132'	6.19	53	86 - j 16

The reflector plays a very small role in increasing the gain of the dipole + reflector combination—0.12 dB relative to the initial model and 0.17 dB relative to the dipole alone, as modeled in NEC-4 using the SN ground system. Of course, this survey is in many ways beside the point, which is to compare the performance of modeling software with respect to the ability to adequately model various types of NVIS arrays when one or more of the wires is close to the ground.

A Wire Loop and a Low Reflector

I repeated the modeling experiment using the 1-wavelength perimeter wire loop at 70' with a second loop at the 5' level. **Fig. 60-9** shows the general outlines of the model. See model 60-4.

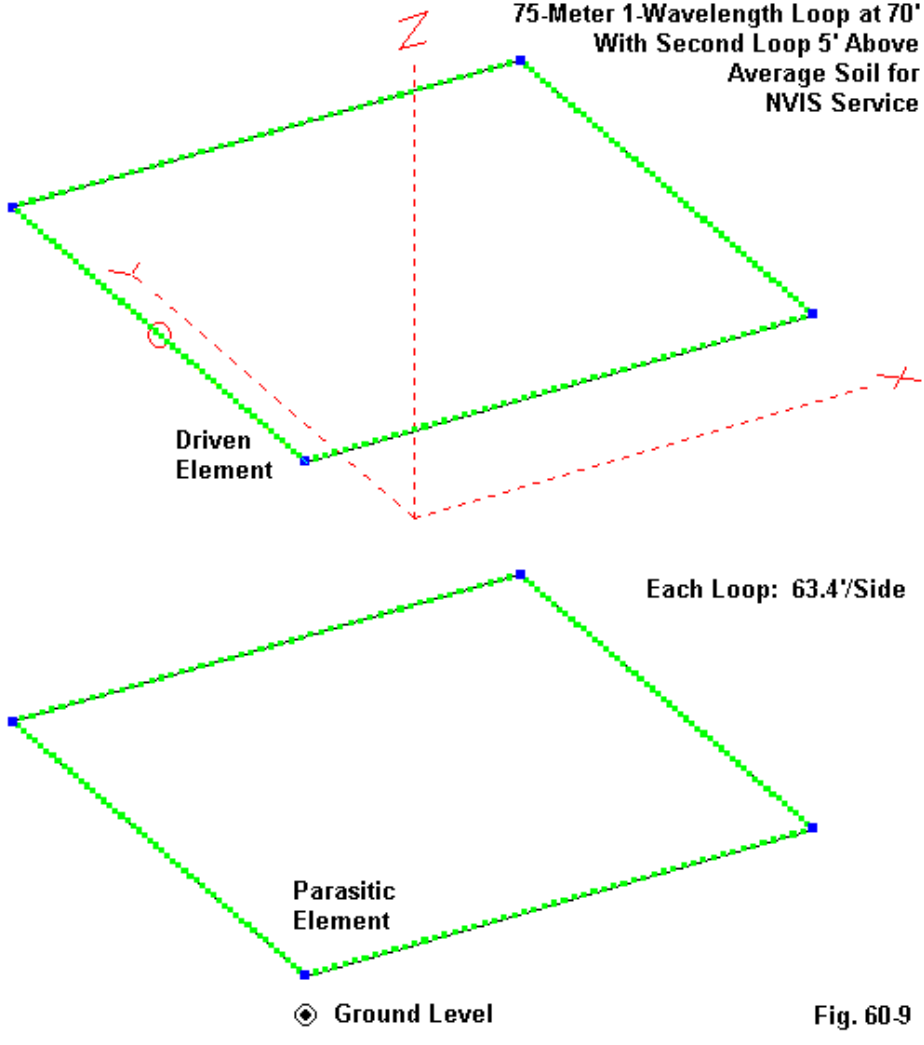
75-Meter 1-Wavelength Loop at 70'
With Second Loop 5' Above
Average Soil for
NVIS Service
Z
Y
X
Driven
Element
Each Loop: 63.4'/Side
Parasitic
Element
Ground Level

Fig. 60-9

The following table follows the reflected-dipole format, but with data for the reflected loop.

```
MININEC Ground:  70' and 5'
Model              Gain         TO angle       Feedpoint Impedance
                   (dBi)        (degrees)          (R +/- jX Ohms)
NEC-4              6.90          92                164 - j 34
NEC-2              6.90          95                164 - j 34
Loop only          6.05         101                167 - j 45

NEC Reflection Coefficient Ground:  70' and 5'
Model              Gain         TO angle       Feedpoint Impedance
                   (dBi)        (degrees)          (R +/- jX Ohms)
NEC-4              5.76         108                144 - j 66
NEC-2              6.50         100                159 - j 57
Loop only          6.26         101                158 - j 63

NEC S-N Ground:  70' and 5'
Model              Gain         TO angle       Feedpoint Impedance
                   (dBi)        (degrees)          (R +/- jX Ohms)
NEC-4              6.47          97                159 - j 51
NEC-2              6.47         100                159 - j 51
Loop only          6.26         102                158 - j 65
```

The loop situation shows something significant to modeling: once a source impedance has a relatively high reactive component, the pattern that we have observed of gain moving in one direction while the resistive part of the impedance moves in the other may no longer hold. The MININEC ground model shows excess gain relative to the NEC-4 S-N ground version, but the resistive impedance relationship does not hold. Nevertheless, the considerable size of the low reflector apparently increases the gain above the S-N model by a greater amount than the reflector did with the dipole.

The reflection coefficient model again shows significant variations between NEC-2 and NEC-4 core runs of the model. These variations apply both to the gain and to the source impedance. As well, the 8-degree difference in the elevation angle of maximum radiation occasions differences between the far field patterns, although the amount of variation would not likely be measurable in the field.

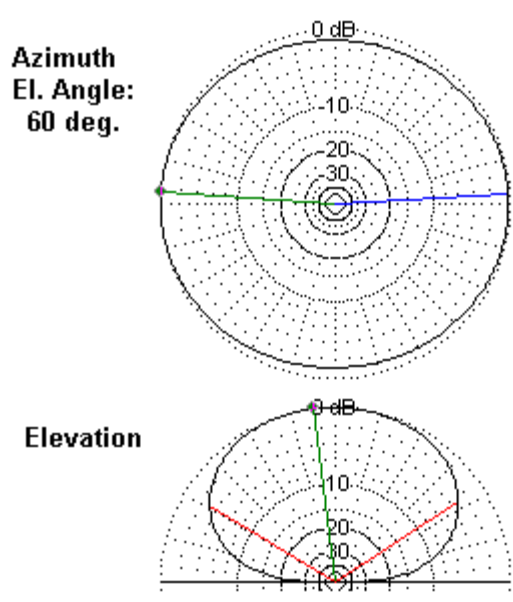

Fig. 60-10 shows the S-N azimuth and elevation patterns for array with its reflector, patterns that do not differ noticeably from those for the loop alone.

Conclusion

The lower the wires of a NVIS antenna, the more unreliable will be the results from a model using either a NEC reflection coefficient ground or a MININEC ground. The inaccuracies of the MININEC ground system affect mainly the gain and feedpoint impedance reports, although those errors will also show up in the reported currents on the antenna elements. In some cases, the errors may slightly affect the far field pattern shape, although such distortions will normally be very slight.

The level of error becomes very seriously misleading with a MININEC ground in two respects. First, when the wires of a MININEC model are brought below about 0.1 wavelength, the gain increases and the source impedance decreases so that the result is wholly unrealistic. Second, the MININEC ground system error curve is such as to lead the idea that the lowest possible antenna height yields the strongest signal. Even the unreliable reflection coefficient system in NEC more correctly identifies the best height as falling in the region of about 0.2 wavelengths.

Those who wish to pursue studies of modeled ground calculation systems and low wires with a horizontal component may use the model descriptions below as starters.

```
                    EZNEC/4 ver. 3.0

75-meter NVIS dipole                          5/18/02     10:40:54 AM

         ———————— ANTENNA DESCRIPTION ————————

Frequency = 3.9 MHz
Wire Loss: Copper — Resistivity = 1.74E-08 ohm-m, Rel. Perm. = 1

               ———————— WIRES ————————

No.      End 1   Coord. (ft)       End 2   Coord. (ft)       Dia (in)  Segs
    Conn.     X      Y      Z Conn.     X      Y      Z
1             0, -60.5,    50           0,  60.5,    50       #14      51

Total Segments: 51

               ———————— SOURCES ————————

No.      Specified Pos.     Actual Pos.      Amplitude   Phase    Type
       Wire #  % From E1  % From E1  Seg       (V/A)     (deg.)
1       1        50.00      50.00    26       1           0         V

No loads specified

No transmission lines specified

Ground type is Real, High-Accuracy

               ———————— MEDIA ————————

No.    Cond.    Diel. Const.  Height    R Coord.
```

```
       (S/m)                  (ft)      (ft)
1      0.005     13           0         0

 . . . . . . . . . . . . . . . . . . . . . . . . . . . . . . . . . . . . .

                      EZNEC/4 ver. 3.0

75-m loop for NVIS                            5/18/02     10:43:12 AM

          ──────── ANTENNA DESCRIPTION ────────

Frequency = 3.9 MHz
Wire Loss: Copper — Resistivity = 1.74E-08 ohm-m, Rel. Perm. = 1

               ──────── WIRES ────────

No.       End 1   Coord. (ft)       End 2   Coord. (ft)       Dia (in)  Segs
    Conn.      X       Y       Z Conn.      X       Y       Z
1   W4E2       0,      0,     30  W2E1      0,64.2564,    30       #14       51
2   W1E2       0,64.2564,     30  W3E1   64.2564,64.2564,30       #14       51
3   W2E2 64.2564,64.2564,   30  W4E1   64.2564,   0,     30       #14       51
4   W3E2 64.2564,     0,    30  W1E1      0,      0,     30       #14       51

Total Segments: 204

               ──────── SOURCES ────────

No.       Specified Pos.      Actual Pos.       Amplitude    Phase    Type
       Wire #  % From E1  % From E1  Seg       (V/A)     (deg.)
1       1        50.00      50.00    26       1           0         I

No loads specified

No transmission lines specified

Ground type is Real, High-Accuracy

               ──────── MEDIA ────────

No.    Cond.    Diel. Const.  Height    R Coord.
       (S/m)                  (ft)      (ft)
1      0.005     13           0         0

 . . . . . . . . . . . . . . . . . . . . . . . . . . . . . . . . . . . . .
```

```
                        EZNEC/4 ver. 3.0

75-m dipole/parasitic NVIS                    5/18/02     10:42:10 AM

          ———————— ANTENNA DESCRIPTION ————————

Frequency = 3.9 MHz
Wire Loss: Copper — Resistivity = 1.74E-08 ohm-m, Rel. Perm. = 1

                ———————— WIRES ————————

No.      End 1   Coord. (ft)       End 2   Coord. (ft)       Dia (in)  Segs
    Conn.     X      Y      Z Conn.     X      Y      Z
1             0, -60.5,    70           0,  60.5,    70       #14      51
2             0, -60.5,     5           0,  60.5,     5       #14      51

Total Segments: 102

                ———————— SOURCES ————————

No.      Specified Pos.     Actual Pos.      Amplitude    Phase    Type
       Wire #  % From E1  % From E1  Seg       (V/A)     (deg.)
1       1        50.00      50.00    26       1          0         V

No loads specified

No transmission lines specified

Ground type is Real, High-Accuracy

                ———————— MEDIA ————————

No.    Cond.    Diel. Const.  Height    R Coord.
       (S/m)                  (ft)      (ft)
1      0.005     13           0         0

 . . . . . . . . . . . . . . . . . . . . . . . . . . . . . . . . . . . . . . . .

                        EZNEC/4 ver. 3.0

75-m loop + parasitic NVIS                    5/18/02     10:44:11 AM

          ———————— ANTENNA DESCRIPTION ————————

Frequency = 3.9 MHz
Wire Loss: Copper — Resistivity = 1.74E-08 ohm-m, Rel. Perm. = 1
```

```
                ──────── WIRES ────────

No.       End 1   Coord. (ft)        End 2   Coord. (ft)        Dia (in)  Segs
    Conn.      X       Y       Z Conn.      X       Y       Z
1   W4E2       0,      0,     70  W2E1      0,64.2564,    70        #14       51
2   W1E2       0,64.2564,     70  W3E1   64.2564,64.2564,70        #14       51
3   W2E2 64.2564,64.2564,   70  W4E1   64.2564,   0,     70        #14       51
4   W3E2 64.2564,     0,    70  W1E1      0,      0,     70        #14       51
1   W4E2       0,      0,     5  W2E1      0,64.2564,     5        #14       51
2   W1E2       0,64.2564,     5  W3E1   64.2564,64.2564, 5        #14       51
3   W2E2 64.2564,64.2564,   5  W4E1   64.2564,   0,     5        #14       51
4   W3E2 64.2564,     0,    5  W1E1      0,      0,     5        #14       51

Total Segments: 408

                ──────── SOURCES ────────

No.       Specified Pos.      Actual Pos.       Amplitude    Phase    Type
        Wire #  % From E1  % From E1  Seg       (V/A)     (deg.)
1        1        50.00      50.00    26        1          0         I

No loads specified

No transmission lines specified

Ground type is Real, High-Accuracy

                ──────── MEDIA ────────

No.     Cond.     Diel. Const.  Height     R Coord.
        (S/m)                   (ft)       (ft)
1       0.005      13           0          0
```

* * * * *

Models included: 60-1 through 60-4. (.NEC and .NWP model dimensions in meters; .EZ model dimensions in feet.)

61. GM: Coordinate Transformation

Most NEC-2 readers of this series employ entry-level programs, such as EZNEC or NEC-Win Plus. These programs limit the wire inputs available to the user to GW (Wire Geometry), GS (Scale Structure Dimensions), and GE (End Geometry Inputs) for the geometry portion of the model. Moreover, to one degree or another, these lines are invisible, as the user focuses on a wire table, supplemented by a "unit of measure" input. The end result, however, is a standard NEC input file (or its equivalent).

Consider a dipole made from AWG #14 (0.0641" diameter) wire set up as a model using +/-7.96' as the length. We shall arbitrarily use 21 segments for the wire and place the voltage source on segment 11 of our one wire. For those who have not read the NEC manual itself, wire numbers are called "tags." The tag number is a convenience, since the program itself will calculate according to absolute segment numbers. Hence, the first segment of wire or tag 2 would have an absolute segment number of 22.

Fig. 61-1 shows the NEC input file for our dipole, taken from NEC-Win Pro. The GW input line specified the coordinates of the wire and the radius in the same unit as the unit of length. Hence, our #14 wire has a radius of 2.67E-3 feet. The GS input provides the scaling factor to translate these values into meters, the basic unit used by NEC. Any input line beyond the GS card that scales for a coordinate, length, or radius dimension must be specified in meters. The GE card ends the geometry section of our simply model. See model 61-1.

The geometry information from the input file appears in the NEC output file (extension .NOU in NEC-Win Pro). The following lines are extracted from the output file as a point of reference for what is to come. Due to format limitations, most of the single report lines are split into 2 lines here.

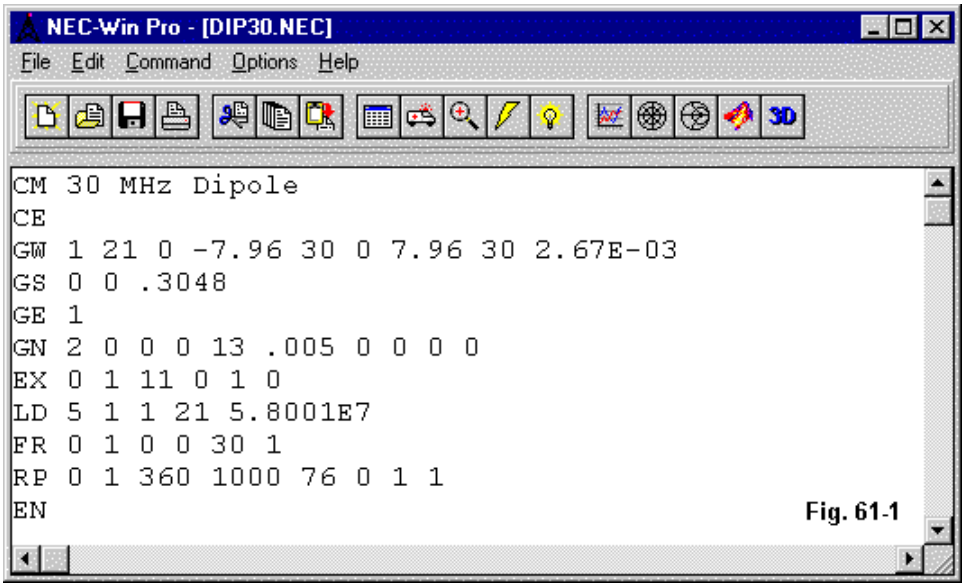

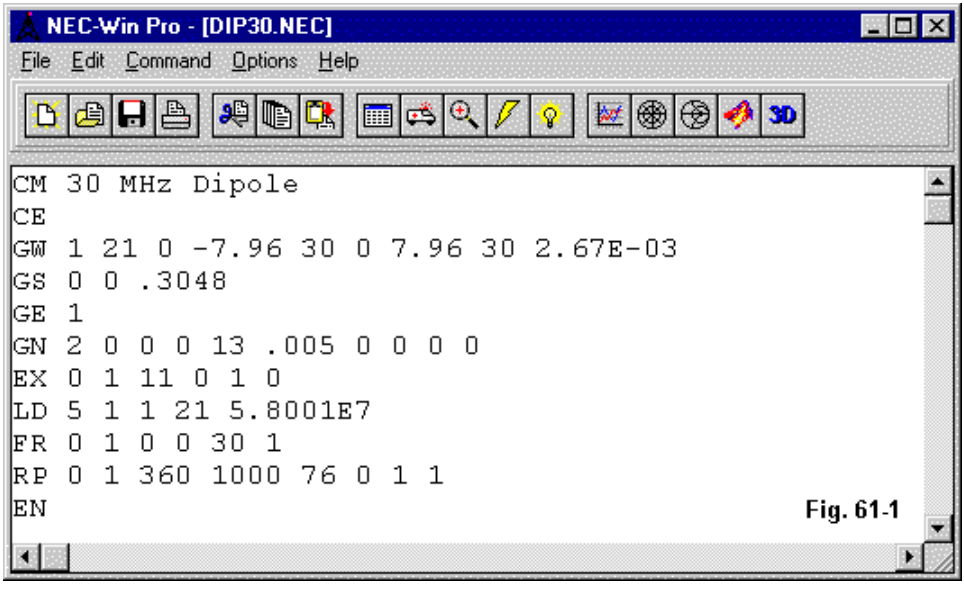
NEC-Win Pro - [DIP30.NEC]
File Edit Command Options Help
3D
CM 30 MHz Dipole
CE
GW 1 21 0 -7.96 30 0 7.96 30 2.67E-03
GS 0 0 .3048
GE 1
GN 2 0 0 0 13 .005 0 0 0 0
EX 0 1 11 0 1 0
LD 5 1 1 21 5.8001E7
FR 0 1 0 0 30 1
RP 0 1 360 1000 76 0 1 1
EN
Fig. 61-1

```
                    - - - STRUCTURE SPECIFICATION - - -

  WIRE                                                                    NO.
OF    FIRST  LAST     TAG
  NO.        X1         Y1         Z1         X2         Y2         Z2      RADIUS
SEG.      SEG.    SEG.      NO.
  1   0.00000   -7.96000   30.00000    0.00000   7.96000   30.00000   0.00267
21        1    21       1
      STRUCTURE SCALED BY FACTOR   0.30480

   GROUND PLANE SPECIFIED.

  TOTAL SEGMENTS USED=   21    NO. SEG. IN A SYMMETRIC CELL=   21    SYMMETRY
FLAG=  0



                      - - - - SEGMENTATION DATA - - - -
                            COORDINATES IN METERS
                I+ AND I- INDICATE THE SEGMENTS BEFORE AND AFTER I


  SEG.     COORDINATES OF SEG. CENTER       SEG.     ORIENTATION ANGLES    WIRE
CONNECTION DATA   TAG
  NO.        X          Y          Z        LENGTH     ALPHA     BETA      RADIUS
I-    I     I+    NO.
    1   0.00000   -2.31067   9.14400   0.23107   0.00000  90.00000  0.00081
0     1     2       1
    2   0.00000   -2.07961   9.14400   0.23107   0.00000  90.00000  0.00081
1     2     3       1
    3   0.00000   -1.84854   9.14400   0.23107   0.00000  90.00000  0.00081
2     3     4       1
    4   0.00000   -1.61747   9.14400   0.23107   0.00000  90.00000  0.00081
3     4     5       1
    5   0.00000   -1.38640   9.14400   0.23107   0.00000  90.00000  0.00081
4     5     6       1
    6   0.00000   -1.15534   9.14400   0.23107   0.00000  90.00000  0.00081
5     6     7       1
    7   0.00000   -0.92427   9.14400   0.23107   0.00000  90.00000  0.00081
6     7     8       1
    8   0.00000   -0.69320   9.14400   0.23107   0.00000  90.00000  0.00081
7     8     9       1
    9   0.00000   -0.46213   9.14400   0.23107   0.00000  90.00000  0.00081
8     9    10       1
   10   0.00000   -0.23107   9.14400   0.23107   0.00000  90.00000  0.00081
9    10    11       1
```

```
   11   0.00000   0.00000   9.14400   0.23107   0.00000  90.00000   0.00081
10   11   12      1
   12   0.00000   0.23107   9.14400   0.23107   0.00000  90.00000   0.00081
11   12   13      1
   13   0.00000   0.46213   9.14400   0.23107   0.00000  90.00000   0.00081
12   13   14      1
   14   0.00000   0.69320   9.14400   0.23107   0.00000  90.00000   0.00081
13   14   15      1
   15   0.00000   0.92427   9.14400   0.23107   0.00000  90.00000   0.00081
14   15   16      1
   16   0.00000   1.15534   9.14400   0.23107   0.00000  90.00000   0.00081
15   16   17      1
   17   0.00000   1.38640   9.14400   0.23107   0.00000  90.00000   0.00081
16   17   18      1
   18   0.00000   1.61747   9.14400   0.23107   0.00000  90.00000   0.00081
17   18   19      1
   19   0.00000   1.84854   9.14400   0.23107   0.00000  90.00000   0.00081
18   19   20      1
   20   0.00000   2.07961   9.14400   0.23107   0.00000  90.00000   0.00081
19   20   21      1
   21   0.00000   2.31067   9.14400   0.23107   0.00000  90.00000   0.00081
20   21    0      1
```

The structure specification serves as a check on the entries in the input file. The segmentation data provides a listing of the wire segments created by this structure. Although we tend normally to overlook these basic features of the NEC output file, we shall have occasion to make significant use of them before we complete our work.

As a further reference, the model—set over average S-N ground—yields a source impedance of 77.4 + j 0.4 Ohms.

We have in past columns looked at some supplementary geometry input cards, most notably, the GC input that allows tapering the segment lengths or the radius of the wire. See column #54. These cards are normally available only on more advanced programs, such as NEC-Win Pro (NEC-2) or GNEC (NEC-4). In this episode, we shall examine the basics of using the GM input, labeled in the NEC Manual as “Coordinate Transformation.” We shall confine ourselves to NEC-2 because the NEC-4 input equivalent has a few differences relative to its NEC-2 predecessor. The differences result from the fact that NEC-2 restricted itself to 7 floating decimal entry places, while NEC-4 observes no such limit. With 10 floating decimal entry

positions in the GM line, it is able to allow the user some finer divisions of the GM work. However, if we become clear on some basic ways in which we can use the NEC-2 entry, we can easily master the NEC-4 counterpart.

The GM line is subdivided as follows:

```
GM   ITG1   NRPT   ROX   ROY   ROZ   XS   YS   ZS   IMOV
     I1     I2     F1    F2    F3    F4   F5   F6   F7
```

I1 and I2 are integer entries, and the series, F1 through F7 are floating decimal entries. Not all floating decimal entries necessarily function as the decimal values of one or another parameter. As we shall see, the F7 entry will use the decimal to separate two integers as a means of expanding the number of entries allowed by the line.

The meanings of the entries follow from the general functional definition of the GM entry: to translate or rotate a structure with respect to the coordinate system or to generate new structures translated or rotated from the original. In other words, we may set up a structure in very simplified terms relative to the coordinate system and then follow one of two main options. 1. We may move the structure from its starting points to another set of coordinates based either on rotating the structure around one or more of the axes or upon incrementing all X or all Y, or all Z values by a specified amount. 2. We may create a structure identical to the original, but displaced along one or more axes or rotated (or both), leaving the original in its specified position. Of course, with multiple GM cards, we may do both.

Within this context, the entries take on the following meanings:

ITG1: This entry specifies the tag (wire) number increment to be applied either to the present structure or to the created structure. If we leave everything else in the line at zero, we simply increase the tag numbers by the indicated amount.

NRPT: The second integer entry specifies the number of new structures to be generated. If NRPT is zero, then any other instructions apply to the original structure. Since the instructions will either rotate or displace the structure, nothing will remain in its original place. If NRPT is 1 or higher, then the instructions apply to the new structure, and the original structure remains in its original place.

ROX, ROY, ROZ: These floating decimal entries specify the angle in degrees through which the structure (new or original, depending on the value of NRPT) will be rotated around the indicated axis. A positive value causes a right-hand rotation. Since rotation is around a specified axis, a set of values displaced from a centered position across a given axis will rotate around the axis, not around the center of the structure.

XS, YS, ZS: These entries specify the amount be which the structure is translated or moved along or parallel to a given axis with respect to the coordinate system.

Note: The order of operation always begins with rotation in the order X, Y, and Z, followed by translation in the order X, Y, and Z. If you wish to move a structure before rotating it, use two GM entries.

IMOV: IMOV uses the decimal point to separate two separate integer fields: IMOV1 and IMOV2. IMOV1 indicates the first tag/wire number to which the instructions apply. IMOV2 indicates the ending tag/wire.

Note: I am indebted to Arie Voors for calling my attention to the fact that early versions of the NEC-2 core used ITS for F7, with a seemingly different procedure. Hence, if using a public domain core of unknown vintage, check the applicable edition of the NEC-2 manual for applicable instructions.

NEC-4 introduces a refinement to this system of specifying the start and stop tag numbers for the geometry rotation and translation maneuvers within the GM input. Floating decimal entry places 7 through 10 are used to specify individually the start tag and segment numbers and the stop tag and segment numbers.

Once we grow familiar with the GM card capabilities, using it gradually becomes second nature. A couple of simple transformations may help us move from just reading the manual to actually using the input line.

GM-1: A Simple Rotation and Translation

Suppose that we wish to perform two operations on our original dipole. First, we want to rotate the dipole so that it extends along the X-axis rather than as at present along the Y-axis. This maneuver requires a 90-degree rotation around the Z-axis, since the antenna is centered at 0, 0, 0 on the coordinate system.

Second, suppose that we wish to change the antenna height by 10'. This move requires a translation of +10 feet along the Z-axis.

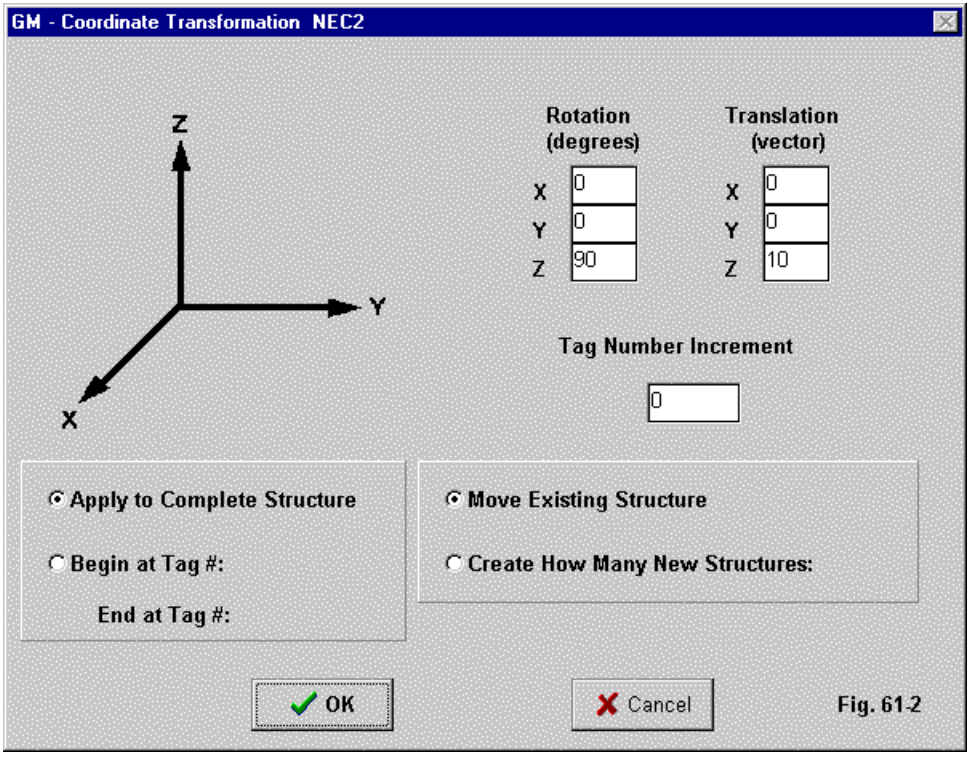

Fig. 61-2

Before we make a move to create a GM line, we should ask whether the order of operations will make a difference to the outcome. By reference to the rules above,

we determine that the order of operations will not affect the outcome. Therefore, we may use a single GM card. It will have the general appearance of the following line:

```
GM    0      0      0     0     90    0     0   10    0
GM   ITG1   NRPT   ROX   ROY   ROZ   XS    YS  ZS   IMOV
     I1     I2     F1    F2    F3    F4    F5  F6   F7
```

I have adjusted the entry spacing so that I can repeat the identification of the entries below the actual GM line that we would type to show clearly that we are rotating around the Z-axis (ROZ) and translating along the Z-axis (ZS). The combination of the integer entries and IMOV specify that the operations will not create a new structure, but will involve the entirety of the existing structure.

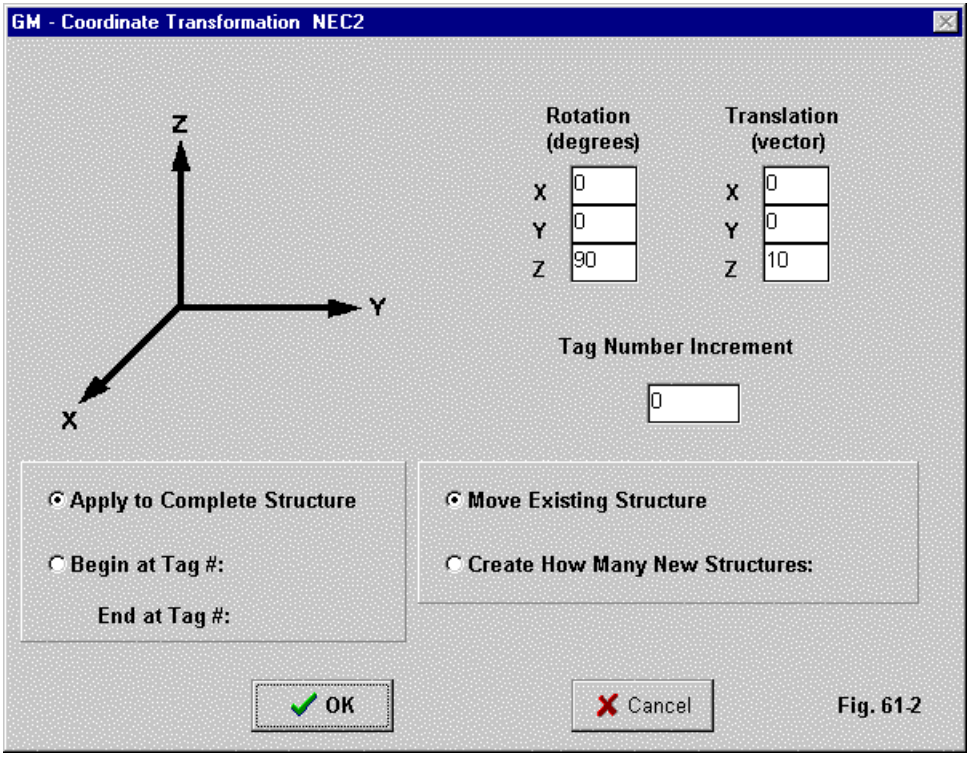

Fig. 61-2

Some implementations of NEC-2 offer line-aides, that is, windows that permit the user to enter data without concern for the spacing and separation of the entries in the final line. **Fig. 61-2** shows the NEC-Win Pro GM window, with our data entered. When we OK the window, it creates the desired line in our model, which appears in its entirety in **Fig. 61-3**. See model 61-2.

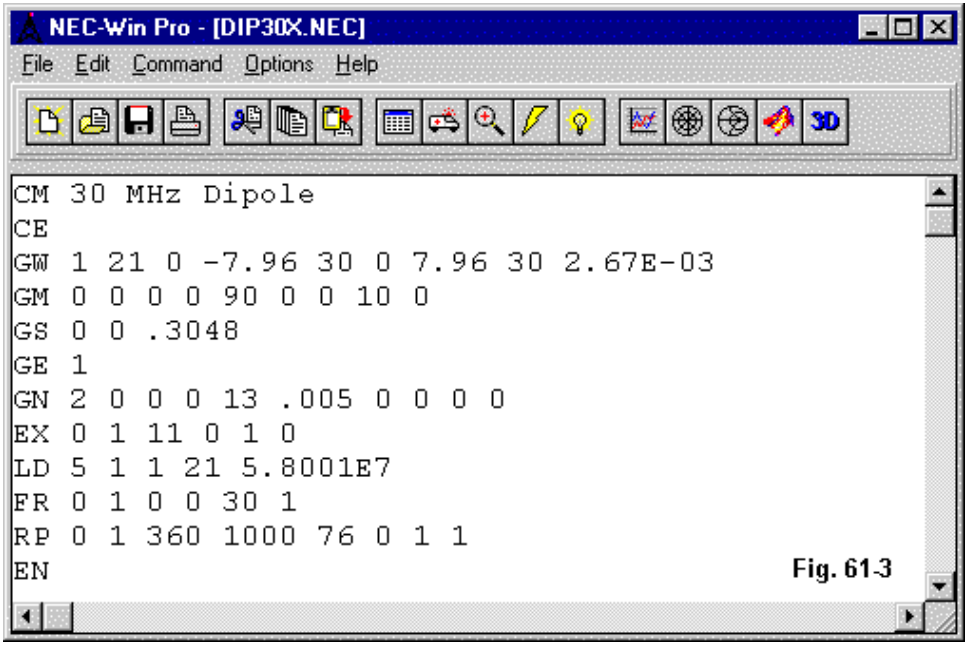

Fig. 61-3

Note that the only difference between this model and the one we used earlier is the insertion of the GM line. Since the GM line appears before the GS (scaling) line, we enter the desired translation moves in the same units that we used for the GW or wire line. In this case, we are using feet. (Getting used to the requisite scaling

factors shown in the GS line provides the necessary data to determine what the unit of measure is in the GW line, since the scaling factor will always be the value necessary to translate the GW units into meters.)

To see what actually happened to our model, we must refer to the NEC output file. The following extracts give us the information, especially when we compare this data to the data for the original model.

```
                    - - - STRUCTURE SPECIFICATION - - -

  WIRE                                                                    NO.
OF    FIRST  LAST     TAG
  NO.       X1        Y1        Z1         X2        Y2        Z2     RADIUS
SEG.     SEG.   SEG.     NO.
  1   0.00000   -7.96000   30.00000    0.00000   7.96000   30.00000   0.00267
21        1    21       1
      THE STRUCTURE HAS BEEN MOVED, MOVE DATA CARD IS -
        0    0   0.00000   0.00000  90.00000   0.00000   0.00000  10.00000
0.00000
       GM command acting on tag #'s            0 through            0
  inclusive.
      STRUCTURE SCALED BY FACTOR   0.30480

   GROUND PLANE SPECIFIED.

   WHERE WIRE ENDS TOUCH GROUND, CURRENT WILL BE INTERPOLATED TO IMAGE

                    - - - - SEGMENTATION DATA - - - -
                          COORDINATES IN METERS
              I+ AND I- INDICATE THE SEGMENTS BEFORE AND AFTER I


  SEG.    COORDINATES OF SEG. CENTER      SEG.     ORIENTATION ANGLES    WIRE
CONNECTION DATA   TAG
  NO.       X         Y         Z       LENGTH     ALPHA     BETA      RADIUS
I-   I    I+    NO.
      1     2.31067     0.00000    12.19200     0.23107     0.00000-180.00000
0.00081   0    1    2      1
      2     2.07961     0.00000    12.19200     0.23107     0.00000-180.00000
0.00081     1    2    3      1
      3     1.84854     0.00000    12.19200     0.23107     0.00000-180.00000
0.00081     2    3    4      1
      4     1.61747     0.00000    12.19200     0.23107     0.00000-180.00000
0.00081     3    4    5      1
```

```
     5    1.38640     0.00000    12.19200     0.23107     0.00000-180.00000
0.00081     4    5    6      1
     6    1.15534     0.00000    12.19200     0.23107     0.00000-180.00000
0.00081   5    6    7      1
     7    0.92427     0.00000    12.19200     0.23107     0.00000-180.00000
0.00081     6    7    8      1
     8    0.69320     0.00000    12.19200     0.23107     0.00000-180.00000
0.00081   7    8    9      1
     9    0.46213     0.00000    12.19200     0.23107     0.00000-180.00000
0.00081     8    9   10      1
    10    0.23107     0.00000    12.19200     0.23107     0.00000-180.00000
0.00081     9   10   11      1
    11    0.00000     0.00000    12.19200     0.23107     0.00000-180.00000
0.00081    10   11   12      1
    12   -0.23107     0.00000    12.19200     0.23107     0.00000-180.00000
0.00081    11   12   13      1
    13   -0.46213     0.00000    12.19200     0.23107     0.00000-180.00000
0.00081    12   13   14      1
    14   -0.69320     0.00000    12.19200     0.23107     0.00000-180.00000
0.00081    13   14   15      1
    15   -0.92427     0.00000    12.19200     0.23107     0.00000-180.00000
0.00081    14   15   16      1
    16   -1.15534     0.00000    12.19200     0.23107     0.00000-180.00000
0.00081    15   16   17      1
    17   -1.38640     0.00000    12.19200     0.23107     0.00000-180.00000
0.00081    16   17   18      1
    18   -1.61747     0.00000    12.19200     0.23107     0.00000-180.00000
0.00081    17   18   19      1
    19   -1.84854     0.00000    12.19200     0.23107     0.00000-180.00000
0.00081    18   19   20      1
    20   -2.07961     0.00000    12.19200     0.23107     0.00000-180.00000
0.00081    19   20   21      1
    21   -2.31067     0.00000    12.19200     0.23107     0.00000-180.00000
0.00081    20   21    0      1
```

There are a few items in the extract worth noting. First, the input structure specifications simply note the presence and parameters of the GM input but do not alter the original line in this section of the report. Instead, the transformations appear in the segmentation data that follows.

Second, we note that the values that formerly were in the Y-column of the original model are now in the X-column. However, note that the segment-1 value is positive, whereas it had been negative in the initial model. Had we needed to specify

a negative value for segment-1, then we would have entered -90 under ROZ. The difference makes no difference for this simple file. However, with more complex structures, it might make a difference. Hence, growing accustomed to the conventions governing the rotation entries and their consequences is important.

Third, our original model showed Z-values of 9.144 (meters). The new Z-value is 12.192 m or 3.048 meters higher than the original model, that is, 10'. The segmentation data this provides confirmation that our GM entry has indeed done what we intended to request.

For reference, the output report returns a source impedance of 72.9 + j 9.1 Ohms. This value is sensible in light of the 1/3-wavelength by which we increased the antenna height above average ground.

Translating a structure has many rationales. With the GM line, we may revise the height of the antenna with a single numerical revision. Although this does not represent much of a saving for our simple dipole, it certainly might shorten the work of evaluating a 5-band 4-element quad (80 wires) at a series of heights above ground. Similarly, the rotation might not seem significant for the dipole. However, suppose that we had a stack of two Yagis and wished to evaluate the influence of one upon the other at different and divergent angles of orientation. We can use the GM line to rotate one of the Yagis by any angle whatsoever—and change that angle by simply altering one entry within the line. We may also rotate an antenna along its bore sight (assuming that it is centered on an axis) in order to evaluate the antenna's performance over ground when both horizontally and vertically polarized. If we have an array of 4 long-boom Yagis for weak-signal use, we may alter the spacing among them to obtain the best results using GM entries. As well, we can change from a flat square to a diamond arrangement by rotating the arrays about a common centerline. These are but a few of the potential applications for rotating and translating part or all of a wire structure using the GM entry.

GM-2: A Simple Replication Example

We may also use the GM entry to replicate wire structures without further GW lines in the input model. Let's try a simple case: we shall replicate our dipole 3 more times at 16' intervals from the original model. We might do such things to create phased arrays or for any number of other reasons.

Fig. 61-4 shows the help screen. We have chosen to create 3 new complete structures and to translate each of them by an interval of 16 (feet) along the X-axis. When we OK this screen, we obtain the input model shown in **Fig. 61-5**.

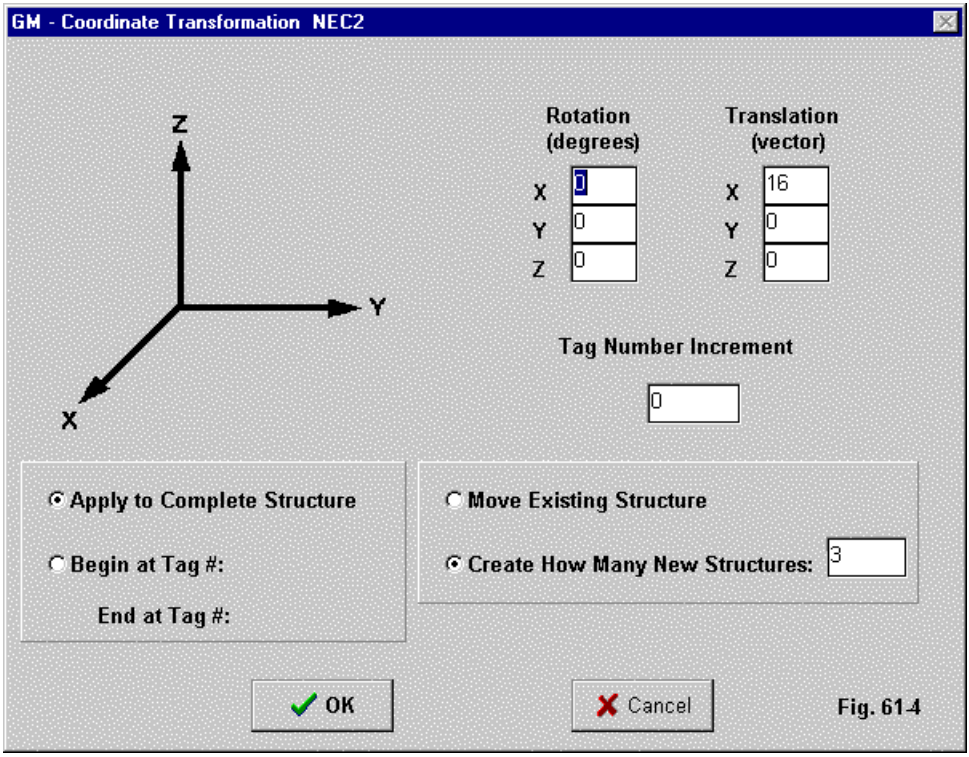

See model 61-3.

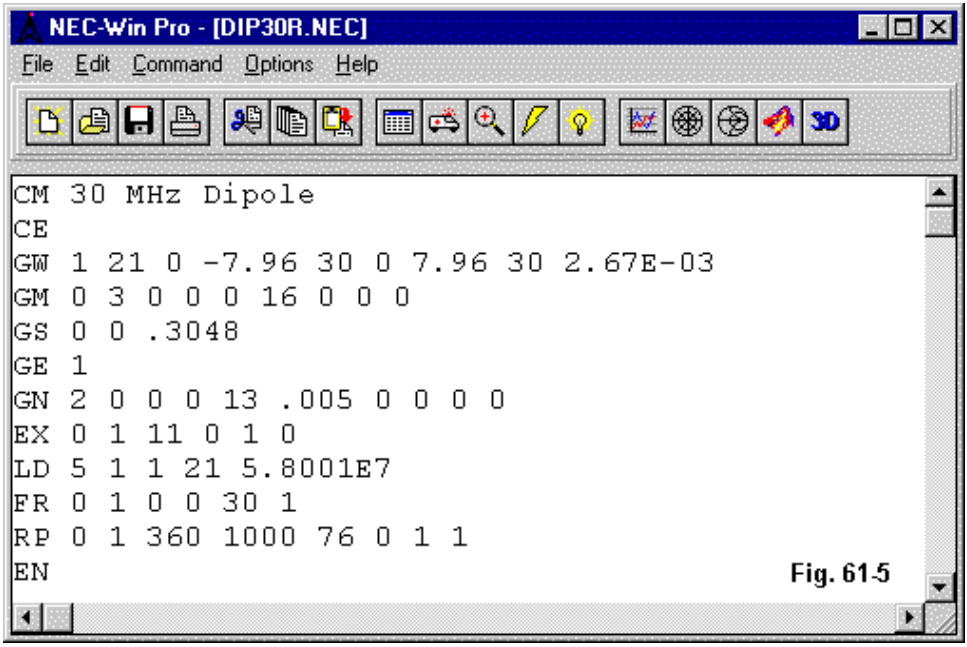

Fig. 61-5

The only difference between this model file and the one for the original dipole is the GM line. In this case, we are leaving the original structure intact and creating 3 additional structures, each one a dipole having the same dimensions and wire radius. A view of the total wire structure appears in **Fig. 61-6**.

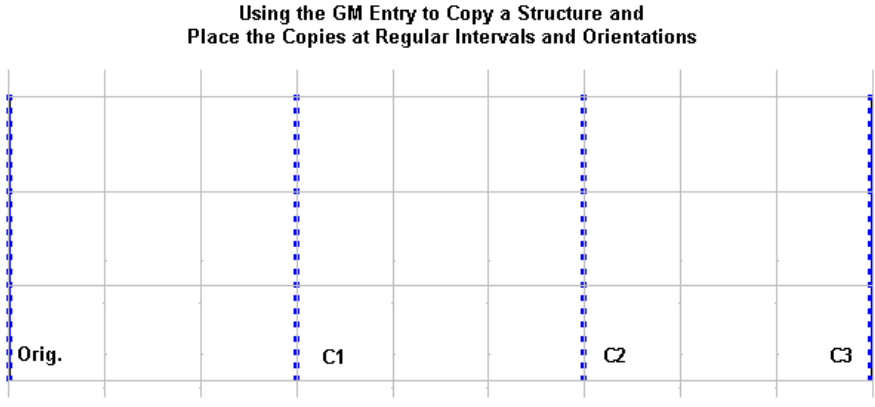

Fig. 61-6

If we look at the NEC output file, we obtain the following extract of data.

```
                    - - - STRUCTURE SPECIFICATION - - -

  WIRE                                                                    NO.
OF    FIRST  LAST     TAG
  NO.        X1         Y1         Z1         X2         Y2         Z2      RADIUS
SEG.      SEG.    SEG.      NO.
  1    0.00000   -7.96000   30.00000    0.00000    7.96000   30.00000    0.00267
21         1    21       1
      THE STRUCTURE HAS BEEN MOVED, MOVE DATA CARD IS -
        0    3   0.00000    0.00000    0.00000   16.00000    0.00000    0.00000
0.00000
       GM command acting on tag #'s            0 through            0
  inclusive.
      STRUCTURE SCALED BY FACTOR   0.30480

   GROUND PLANE SPECIFIED.
```

- - - - SEGMENTATION DATA - - - -
COORDINATES IN METERS
I+ AND I- INDICATE THE SEGMENTS BEFORE AND AFTER I

SEG. NO.	COORDINATES OF SEG. CENTER X	Y	Z	SEG. LENGTH	ORIENTATION ANGLES ALPHA	BETA	WIRE RADIUS	CONNECTION DATA I-	I	I+	TAG NO.
1	0.00000	-2.31067	9.14400	0.23107	0.00000	90.00000	0.00081	0	1	2	1
2	0.00000	-2.07961	9.14400	0.23107	0.00000	90.00000	0.00081	1	2	3	1
3	0.00000	-1.84854	9.14400	0.23107	0.00000	90.00000	0.00081	2	3	4	1
4	0.00000	-1.61747	9.14400	0.23107	0.00000	90.00000	0.00081	3	4	5	1
5	0.00000	-1.38640	9.14400	0.23107	0.00000	90.00000	0.00081	4	5	6	1
6	0.00000	-1.15534	9.14400	0.23107	0.00000	90.00000	0.00081	5	6	7	1
7	0.00000	-0.92427	9.14400	0.23107	0.00000	90.00000	0.00081	6	7	8	1
8	0.00000	-0.69320	9.14400	0.23107	0.00000	90.00000	0.00081	7	8	9	1
9	0.00000	-0.46213	9.14400	0.23107	0.00000	90.00000	0.00081	8	9	10	1
10	0.00000	-0.23107	9.14400	0.23107	0.00000	90.00000	0.00081	9	10	11	1
11	0.00000	0.00000	9.14400	0.23107	0.00000	90.00000	0.00081	10	11	12	1
12	0.00000	0.23107	9.14400	0.23107	0.00000	90.00000	0.00081	11	12	13	1
13	0.00000	0.46213	9.14400	0.23107	0.00000	90.00000	0.00081	12	13	14	1
14	0.00000	0.69320	9.14400	0.23107	0.00000	90.00000	0.00081	13	14	15	1
15	0.00000	0.92427	9.14400	0.23107	0.00000	90.00000	0.00081	14	15	16	1
16	0.00000	1.15534	9.14400	0.23107	0.00000	90.00000	0.00081	15	16	17	1
17	0.00000	1.38640	9.14400	0.23107	0.00000	90.00000	0.00081	16	17	18	1
18	0.00000	1.61747	9.14400	0.23107	0.00000	90.00000	0.00081	17	18	19	1

```
   19   0.00000   1.84854   9.14400   0.23107   0.00000  90.00000  0.00081
18   19   20      1
   20   0.00000   2.07961   9.14400   0.23107   0.00000  90.00000  0.00081
19   20   21      1
   21   0.00000   2.31067   9.14400   0.23107   0.00000  90.00000  0.00081
20   21    0      1
   22   4.87680  -2.31067   9.14400   0.23107   0.00000  90.00000  0.00081
0   22   23      1
   23   4.87680  -2.07961   9.14400   0.23107   0.00000  90.00000  0.00081
22   23   24      1
   24   4.87680  -1.84854   9.14400   0.23107   0.00000  90.00000  0.00081
23   24   25      1
   25   4.87680  -1.61747   9.14400   0.23107   0.00000  90.00000  0.00081
24   25   26      1
   26   4.87680  -1.38640   9.14400   0.23107   0.00000  90.00000  0.00081
25   26   27      1
   27   4.87680  -1.15534   9.14400   0.23107   0.00000  90.00000  0.00081
26   27   28      1
   28   4.87680  -0.92427   9.14400   0.23107   0.00000  90.00000  0.00081
27   28   29      1
   29   4.87680  -0.69320   9.14400   0.23107   0.00000  90.00000  0.00081
28   29   30      1
   30   4.87680  -0.46213   9.14400   0.23107   0.00000  90.00000  0.00081
29   30   31      1
   31   4.87680  -0.23107   9.14400   0.23107   0.00000  90.00000  0.00081
30   31   32      1
   32   4.87680   0.00000   9.14400   0.23107   0.00000  90.00000  0.00081
31   32   33      1
   33   4.87680   0.23107   9.14400   0.23107   0.00000  90.00000  0.00081
32   33   34      1
   34   4.87680   0.46213   9.14400   0.23107   0.00000  90.00000  0.00081
33   34   35      1
   35   4.87680   0.69320   9.14400   0.23107   0.00000  90.00000  0.00081
34   35   36      1
   36   4.87680   0.92427   9.14400   0.23107   0.00000  90.00000  0.00081
35   36   37      1
   37   4.87680   1.15534   9.14400   0.23107   0.00000  90.00000  0.00081
36   37   38      1
   38   4.87680   1.38640   9.14400   0.23107   0.00000  90.00000  0.00081
37   38   39      1
   39   4.87680   1.61747   9.14400   0.23107   0.00000  90.00000  0.00081
38   39   40      1
   40   4.87680   1.84854   9.14400   0.23107   0.00000  90.00000  0.00081
39   40   41      1
   41   4.87680   2.07961   9.14400   0.23107   0.00000  90.00000  0.00081
40   41   42      1
```

```
   42   4.87680   2.31067   9.14400   0.23107   0.00000  90.00000  0.00081
41   42    0      1
   43   9.75360  -2.31067   9.14400   0.23107   0.00000  90.00000  0.00081
0   43   44      1
   44   9.75360  -2.07961   9.14400   0.23107   0.00000  90.00000  0.00081
43   44   45      1
   45   9.75360  -1.84854   9.14400   0.23107   0.00000  90.00000  0.00081
44   45   46      1
   46   9.75360  -1.61747   9.14400   0.23107   0.00000  90.00000  0.00081
45   46   47      1
   47   9.75360  -1.38640   9.14400   0.23107   0.00000  90.00000  0.00081
46   47   48      1
   48   9.75360  -1.15534   9.14400   0.23107   0.00000  90.00000  0.00081
47   48   49      1
   49   9.75360  -0.92427   9.14400   0.23107   0.00000  90.00000  0.00081
48   49   50      1
   50   9.75360  -0.69320   9.14400   0.23107   0.00000  90.00000  0.00081
49   50   51      1
   51   9.75360  -0.46213   9.14400   0.23107   0.00000  90.00000  0.00081
50   51   52      1
   52   9.75360  -0.23107   9.14400   0.23107   0.00000  90.00000  0.00081
51   52   53      1
   53   9.75360   0.00000   9.14400   0.23107   0.00000  90.00000  0.00081
52   53   54      1
   54   9.75360   0.23107   9.14400   0.23107   0.00000  90.00000  0.00081
53   54   55      1
   55   9.75360   0.46213   9.14400   0.23107   0.00000  90.00000  0.00081
54   55   56      1
   56   9.75360   0.69320   9.14400   0.23107   0.00000  90.00000  0.00081
55   56   57      1
   57   9.75360   0.92427   9.14400   0.23107   0.00000  90.00000  0.00081
56   57   58      1
   58   9.75360   1.15534   9.14400   0.23107   0.00000  90.00000  0.00081
57   58   59      1
   59   9.75360   1.38640   9.14400   0.23107   0.00000  90.00000  0.00081
58   59   60      1
   60   9.75360   1.61747   9.14400   0.23107   0.00000  90.00000  0.00081
59   60   61      1
   61   9.75360   1.84854   9.14400   0.23107   0.00000  90.00000  0.00081
60   61   62      1
   62   9.75360   2.07961   9.14400   0.23107   0.00000  90.00000  0.00081
61   62   63      1
   63   9.75360   2.31067   9.14400   0.23107   0.00000  90.00000  0.00081
62   63    0      1
    64   14.63040   -2.31067    9.14400    0.23107    0.00000  90.00000
0.00081     0   64   65      1
```

```
     65    14.63040    -2.07961     9.14400     0.23107     0.00000   90.00000
0.00081     64    65    66       1
     66    14.63040    -1.84854     9.14400     0.23107     0.00000   90.00000
0.00081     65    66    67       1
     67    14.63040    -1.61747     9.14400     0.23107     0.00000   90.00000
0.00081     66    67    68       1
     68    14.63040    -1.38640     9.14400     0.23107     0.00000   90.00000
0.00081     67    68    69       1
     69    14.63040    -1.15534     9.14400     0.23107     0.00000   90.00000
0.00081     68    69    70       1
     70    14.63040    -0.92427     9.14400     0.23107     0.00000   90.00000
0.00081     69    70    71       1
     71    14.63040    -0.69320     9.14400     0.23107     0.00000   90.00000
0.00081     70    71    72       1
     72    14.63040    -0.46213     9.14400     0.23107     0.00000   90.00000
0.00081     71    72    73       1
     73    14.63040    -0.23107     9.14400     0.23107     0.00000   90.00000
0.00081     72    73    74       1
    74  14.63040    0.00000   9.14400   0.23107   0.00000  90.00000   0.00081
73    74    75       1
    75  14.63040    0.23107   9.14400   0.23107   0.00000  90.00000   0.00081
74    75    76       1
    76  14.63040    0.46213   9.14400   0.23107   0.00000  90.00000   0.00081
75    76    77       1
    77  14.63040    0.69320   9.14400   0.23107   0.00000  90.00000   0.00081
76    77    78       1
    78  14.63040    0.92427   9.14400   0.23107   0.00000  90.00000   0.00081
77    78    79       1
    79  14.63040    1.15534   9.14400   0.23107   0.00000  90.00000   0.00081
78    79    80       1
    80  14.63040    1.38640   9.14400   0.23107   0.00000  90.00000   0.00081
79    80    81       1
    81  14.63040    1.61747   9.14400   0.23107   0.00000  90.00000   0.00081
80    81    82       1
    82  14.63040    1.84854   9.14400   0.23107   0.00000  90.00000   0.00081
81    82    83       1
    83  14.63040    2.07961   9.14400   0.23107   0.00000  90.00000   0.00081
82    83    84       1
    84  14.63040    2.31067   9.14400   0.23107   0.00000  90.00000   0.00081
83    84     0       1
```

We easily note that the structure replicates itself along the Y-axis, but at 4.8768 m (16') intervals along the X-axis. If we run this model, we obtain a source impedance of 89.7 - j 11.1 Ohms.

We have possibly forgotten something, especially if we intended to make the total structure into a phased array of 4 dipoles fed in phase. Our model in **Fig. 61-5** showed a single source (EX line). The GM entry replicates only the wire structure. It does NOT replicate any sources or loads applied to that structure. Let's correct part of that situation, as shown in **Fig. 61-7**. See model 61-4.

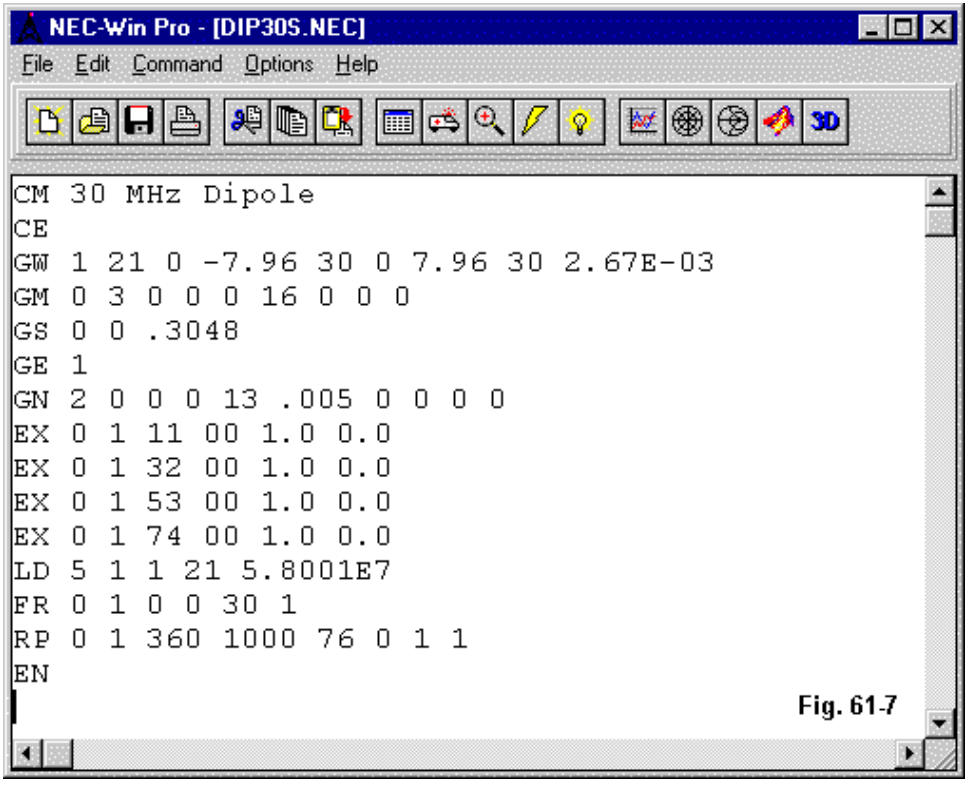

Fig. 61-7

The model now contains 4 sources or EX entries, each a voltage source having the same magnitude and phase angle. We may use the antenna view function to check on the placement of the sources, as shown in **Fig. 61-8**.

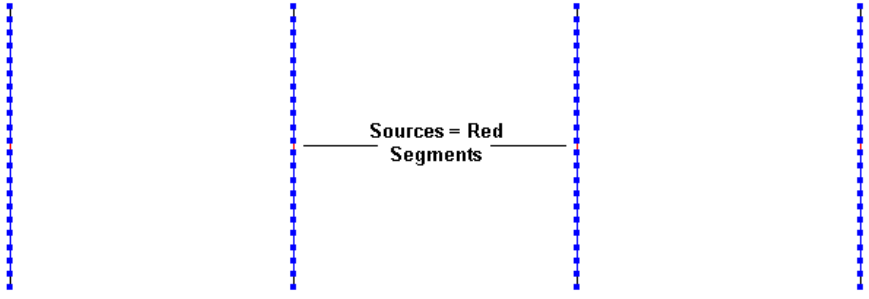

Fig. 61-8

Note that we did not revise the LD line. Therefore, only the original structure is copper and has that less-than-perfect conductivity. The new wires have perfect conductivity. Therefore, when we run this model, we should not expect perfect symmetry among the source values. Indeed, we obtain the following values for sources 1-4:

1. 69.7 - 33.9 Ohms
2. 50.7 - 49.8 Ohms
3. 50.4 - 50.0 Ohms
4. 69.0 - 34.1 Ohms

The model has another peculiarity. We did not increment the tag number for each new structure. Therefore, the segmentation data shows a “1” for the tag number throughout. This result has several implications.

First, there is a difference between a tag number and a wire number. The two are the same only when, after all operations in the geometry section, there is a different tag number for each length of wire having open ends or junctions with other wires in the model. Many geometry input cards use a single tag number for a collection of wires that, if we had entered each one separately, would have had different

tag numbers. The GC, GH, and GA inputs are typical. The equation of tag and wire numbers applies only if all wires are GW entries.

Second, we might have specified copper conductivity for all wires by a simple revision of the LD5 entry. Instead of ending the load at segment 21 (in Fig. 7), we could have specified segment 84.

The loading specification just noted would not work had we replicated the dipole with an increment in the tag number. See **Fig. 61-9**.

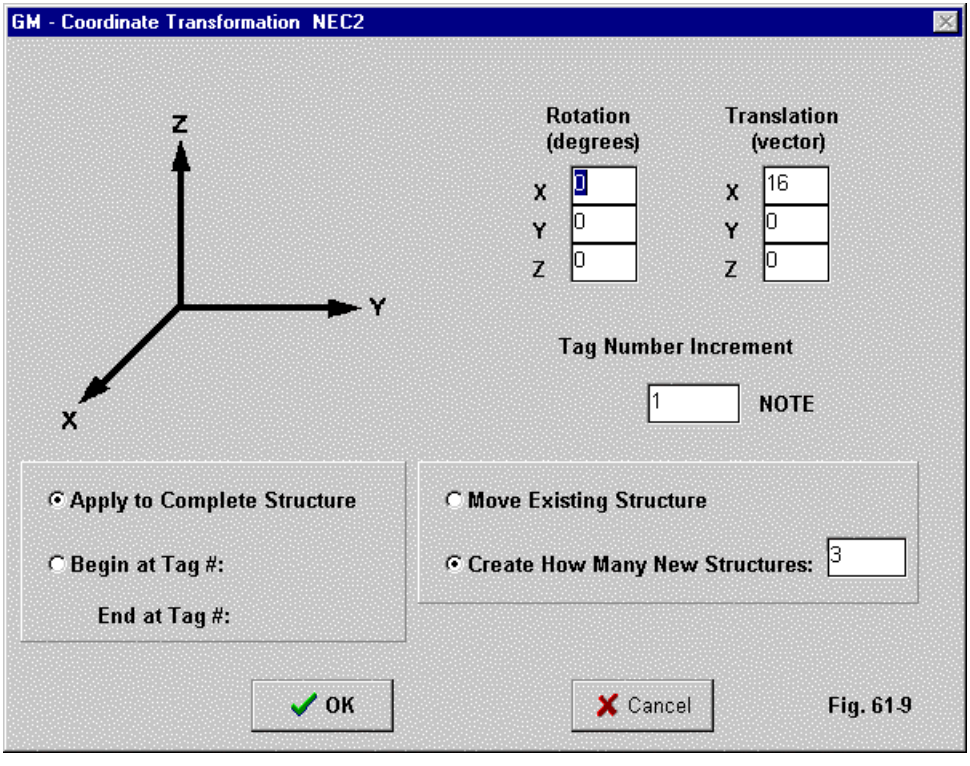

Fig. 61-9

The help screen in **Fig. 61-9** is identical to the one in **Fig. 61-4** with one exception. Note that the Tag Number Increment is now 1 (rather than zero). The result of this change appears in the GM line in the model shown in **Fig. 61-10**.

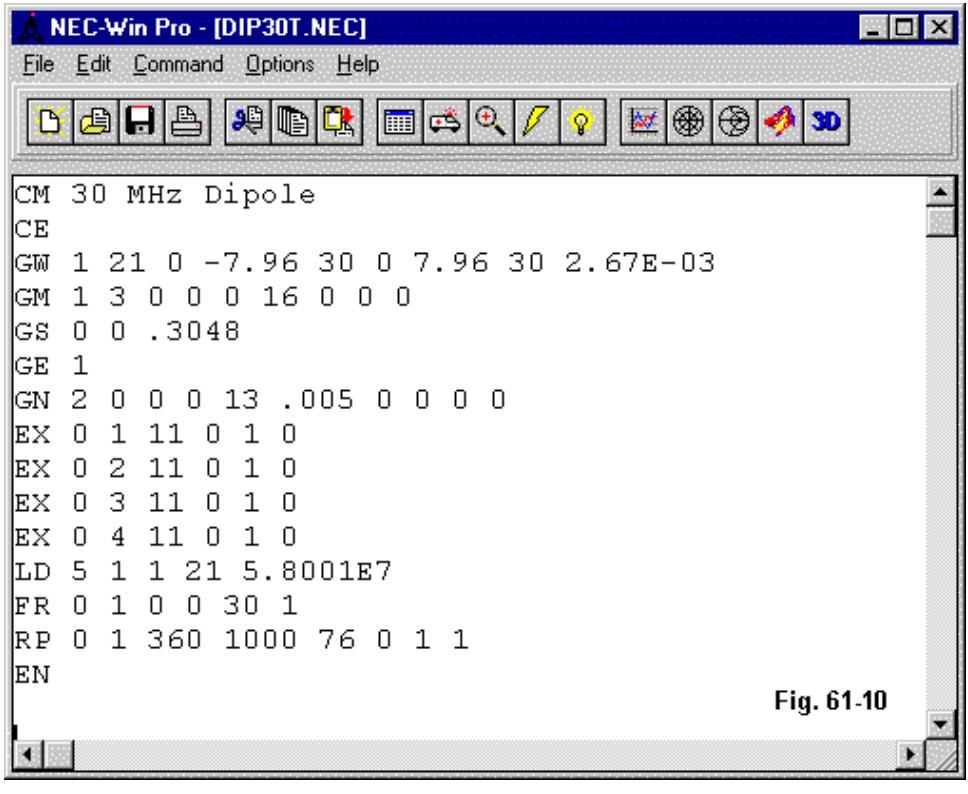

For simplicity, I have left the LD5 entry as it was. See model 61-5. Thus the only change required in addition to the GM line is a re-specification of the positions of the sources in the EX entries. Each one now specifies the same segment number, but for different wire/tag numbers. The antenna view would be identical to the one shown in **Fig. 61-8**, which serves as a quick check in advance of running the model. Once we do run the model, we come up with the following data extract.

```
                    - - - STRUCTURE SPECIFICATION - - -

WIRE                                                                    NO.
OF    FIRST  LAST     TAG
  NO.       X1        Y1        Z1         X2        Y2        Z2     RADIUS
SEG.     SEG.   SEG.     NO.
     1    0.00000   -7.96000   30.00000     0.00000    7.96000   30.00000
0.00267     21        1    21       1
      THE STRUCTURE HAS BEEN MOVED, MOVE DATA CARD IS -
        1    3   0.00000   0.00000   0.00000  16.00000   0.00000   0.00000
0.00000
       GM command acting on tag #'s            0 through            0
  inclusive.
      STRUCTURE SCALED BY FACTOR   0.30480
   GROUND PLANE SPECIFIED.

                    - - - - SEGMENTATION DATA - - - -
                         COORDINATES IN METERS
              I+ AND I- INDICATE THE SEGMENTS BEFORE AND AFTER I

  SEG.     COORDINATES OF SEG. CENTER      SEG.     ORIENTATION ANGLES    WIRE
CONNECTION DATA   TAG
  NO.        X         Y         Z       LENGTH     ALPHA     BETA      RADIUS
I-    I    I+    NO.
1    0.00000   -2.31067    9.14400    0.23107    0.00000  90.00000   0.00081
0    1    2      1
    2   0.00000   -2.07961    9.14400    0.23107    0.00000  90.00000   0.00081
1    2    3      1
    3   0.00000   -1.84854    9.14400    0.23107    0.00000  90.00000   0.00081
2    3    4      1
    4   0.00000   -1.61747    9.14400    0.23107    0.00000  90.00000   0.00081
3    4    5      1
    5   0.00000   -1.38640    9.14400    0.23107    0.00000  90.00000   0.00081
4    5    6      1
    6   0.00000   -1.15534    9.14400    0.23107    0.00000  90.00000   0.00081
5    6    7      1
    7   0.00000   -0.92427    9.14400    0.23107    0.00000  90.00000   0.00081
6    7    8      1
    8   0.00000   -0.69320    9.14400    0.23107    0.00000  90.00000   0.00081
7    8    9      1
    9   0.00000   -0.46213    9.14400    0.23107    0.00000  90.00000   0.00081
8    9   10      1
   10   0.00000   -0.23107    9.14400    0.23107    0.00000  90.00000   0.00081
9   10   11      1
   11   0.00000    0.00000    9.14400    0.23107    0.00000  90.00000   0.00081
10   11   12      1
```

```
   12   0.00000   0.23107   9.14400   0.23107   0.00000  90.00000  0.00081
11   12   13      1
   13   0.00000   0.46213   9.14400   0.23107   0.00000  90.00000  0.00081
12   13   14      1
   14   0.00000   0.69320   9.14400   0.23107   0.00000  90.00000  0.00081
13   14   15      1
   15   0.00000   0.92427   9.14400   0.23107   0.00000  90.00000  0.00081
14   15   16      1
   16   0.00000   1.15534   9.14400   0.23107   0.00000  90.00000  0.00081
15   16   17      1
   17   0.00000   1.38640   9.14400   0.23107   0.00000  90.00000  0.00081
16   17   18      1
   18   0.00000   1.61747   9.14400   0.23107   0.00000  90.00000  0.00081
17   18   19      1
   19   0.00000   1.84854   9.14400   0.23107   0.00000  90.00000  0.00081
18   19   20      1
   20   0.00000   2.07961   9.14400   0.23107   0.00000  90.00000  0.00081
19   20   21      1
   21   0.00000   2.31067   9.14400   0.23107   0.00000  90.00000  0.00081
20   21    0      1
   22   4.87680  -2.31067   9.14400   0.23107   0.00000  90.00000  0.00081
0   22   23      2
   23   4.87680  -2.07961   9.14400   0.23107   0.00000  90.00000  0.00081
22   23   24      2
   24   4.87680  -1.84854   9.14400   0.23107   0.00000  90.00000  0.00081
23   24   25      2
   25   4.87680  -1.61747   9.14400   0.23107   0.00000  90.00000  0.00081
24   25   26      2
   26   4.87680  -1.38640   9.14400   0.23107   0.00000  90.00000  0.00081
25   26   27      2
   27   4.87680  -1.15534   9.14400   0.23107   0.00000  90.00000  0.00081
26   27   28      2
   28   4.87680  -0.92427   9.14400   0.23107   0.00000  90.00000  0.00081
27   28   29      2
   29   4.87680  -0.69320   9.14400   0.23107   0.00000  90.00000  0.00081
28   29   30      2
   30   4.87680  -0.46213   9.14400   0.23107   0.00000  90.00000  0.00081
29   30   31      2
   31   4.87680  -0.23107   9.14400   0.23107   0.00000  90.00000  0.00081
30   31   32      2
   32   4.87680   0.00000   9.14400   0.23107   0.00000  90.00000  0.00081
31   32   33      2
   33   4.87680   0.23107   9.14400   0.23107   0.00000  90.00000  0.00081
32   33   34      2
   34   4.87680   0.46213   9.14400   0.23107   0.00000  90.00000  0.00081
33   34   35      2
```

```
   35   4.87680   0.69320   9.14400   0.23107   0.00000  90.00000  0.00081
34   35   36      2
   36   4.87680   0.92427   9.14400   0.23107   0.00000  90.00000  0.00081
35   36   37      2
   37   4.87680   1.15534   9.14400   0.23107   0.00000  90.00000  0.00081
36   37   38      2
   38   4.87680   1.38640   9.14400   0.23107   0.00000  90.00000  0.00081
37   38   39      2
   39   4.87680   1.61747   9.14400   0.23107   0.00000  90.00000  0.00081
38   39   40      2
   40   4.87680   1.84854   9.14400   0.23107   0.00000  90.00000  0.00081
39   40   41      2
   41   4.87680   2.07961   9.14400   0.23107   0.00000  90.00000  0.00081
40   41   42      2
   42   4.87680   2.31067   9.14400   0.23107   0.00000  90.00000  0.00081
41   42    0      2
   43   9.75360  -2.31067   9.14400   0.23107   0.00000  90.00000  0.00081
0   43   44      3
   44   9.75360  -2.07961   9.14400   0.23107   0.00000  90.00000  0.00081
43   44   45      3
   45   9.75360  -1.84854   9.14400   0.23107   0.00000  90.00000  0.00081
44   45   46      3
   46   9.75360  -1.61747   9.14400   0.23107   0.00000  90.00000  0.00081
45   46   47      3
   47   9.75360  -1.38640   9.14400   0.23107   0.00000  90.00000  0.00081
46   47   48      3
   48   9.75360  -1.15534   9.14400   0.23107   0.00000  90.00000  0.00081
47   48   49      3
49    9.75360  -0.92427   9.14400   0.23107   0.00000  90.00000  0.00081
48   49   50      3
   50   9.75360  -0.69320   9.14400   0.23107   0.00000  90.00000  0.00081
49   50   51      3
   51   9.75360  -0.46213   9.14400   0.23107   0.00000  90.00000  0.00081
50   51   52      3
   52   9.75360  -0.23107   9.14400   0.23107   0.00000  90.00000  0.00081
51   52   53      3
   53   9.75360   0.00000   9.14400   0.23107   0.00000  90.00000  0.00081
52   53   54      3
   54   9.75360   0.23107   9.14400   0.23107   0.00000  90.00000  0.00081
53   54   55      3
   55   9.75360   0.46213   9.14400   0.23107   0.00000  90.00000  0.00081
54   55   56      3
   56   9.75360   0.69320   9.14400   0.23107   0.00000  90.00000  0.00081
55   56   57      3
   57   9.75360   0.92427   9.14400   0.23107   0.00000  90.00000  0.00081
56   57   58      3
```

```
   58   9.75360   1.15534   9.14400   0.23107   0.00000  90.00000  0.00081
57   58   59      3
   59   9.75360   1.38640   9.14400   0.23107   0.00000  90.00000  0.00081
58   59   60      3
   60   9.75360   1.61747   9.14400   0.23107   0.00000  90.00000  0.00081
59   60   61      3
   61   9.75360   1.84854   9.14400   0.23107   0.00000  90.00000  0.00081
60   61   62      3
   62   9.75360   2.07961   9.14400   0.23107   0.00000  90.00000  0.00081
61   62   63      3
   63   9.75360   2.31067   9.14400   0.23107   0.00000  90.00000  0.00081
62   63    0      3
    64   14.63040   -2.31067    9.14400    0.23107    0.00000  90.00000
0.00081     0   64   65      4
    65   14.63040   -2.07961    9.14400    0.23107    0.00000  90.00000
0.00081    64   65   66      4
    66   14.63040   -1.84854    9.14400    0.23107    0.00000  90.00000
0.00081    65   66   67      4
    67   14.63040   -1.61747    9.14400    0.23107    0.00000  90.00000
0.00081    66   67   68      4
    68   14.63040   -1.38640    9.14400    0.23107    0.00000  90.00000
0.00081    67   68   69      4
    69   14.63040   -1.15534    9.14400    0.23107    0.00000  90.00000
0.00081    68   69   70      4
    70   14.63040   -0.92427    9.14400    0.23107    0.00000  90.00000
0.00081    69   70   71      4
    71   14.63040   -0.69320    9.14400    0.23107    0.00000  90.00000
0.00081    70   71   72      4
    72   14.63040   -0.46213    9.14400    0.23107    0.00000  90.00000
0.00081    71   72   73      4
    73   14.63040   -0.23107    9.14400    0.23107    0.00000  90.00000
0.00081    72   73   74      4
   74  14.63040   0.00000   9.14400   0.23107   0.00000  90.00000  0.00081
73   74   75      4
   75  14.63040   0.23107   9.14400   0.23107   0.00000  90.00000  0.00081
74   75   76      4
   76  14.63040   0.46213   9.14400   0.23107   0.00000  90.00000  0.00081
75   76   77      4
   77  14.63040   0.69320   9.14400   0.23107   0.00000  90.00000  0.00081
76   77   78      4
   78  14.63040   0.92427   9.14400   0.23107   0.00000  90.00000  0.00081
77   78   79      4
   79  14.63040   1.15534   9.14400   0.23107   0.00000  90.00000  0.00081
78   79   80      4
   80  14.63040   1.38640   9.14400   0.23107   0.00000  90.00000  0.00081
79   80   81      4
```

```
   81   14.63040    1.61747    9.14400    0.23107    0.00000   90.00000   0.00081
80    81    82       4
   82   14.63040    1.84854    9.14400    0.23107    0.00000   90.00000   0.00081
81    82    83       4
   83   14.63040    2.07961    9.14400    0.23107    0.00000   90.00000   0.00081
82    83    84       4
   84   14.63040    2.31067    9.14400    0.23107    0.00000   90.00000   0.00081
83    84     0       4
```

The tag numbers increment according to the GM-line instruction. Otherwise, the structure and segmentation data is identical to the preceding model. So, too, is the source data for sources 1 through 4. Incrementing the tag number is useful, but not always necessary to obtain correct results from the model using a GM entry.

These simple models function only to acquaint the new modeler with the facilities of the GM entry. Many more applications are possible. We can create a cube with a single wire and then a least-necessary number of GM lines. What we can do to a cube, we can also do to virtually any geometric shape that we simulate with straight lines.

The exercise has also aimed at revealing a few cautions about the use of the GM facility, especially with respect to control inputs, such as EX and LD, that we may have to replicate along with the geometry structure.

In the final analysis, how useful the GM entry is may depend upon the imagination of the modeler. However, we should remember that each wire created by a GM entry is in fact a wire that participates in the matrix calculations. We may save a considerable amount of modeling time with the GM card, but we do not effect a saving in the calculation time.

* * * * *

Models included: 61-1 through 63-5. (Models available in .NEC format only.)

62. GH: Helix-Spiral Specification

In episode 29 of this series, we explored the construction of a model of a helical dipole for 28.5 MHz. The techniques used there combined the model-by-equation facility of NEC-Win Plus with its spreadsheet blocking capabilities to produce the model solely by using the GW (wire geometry) input. In entry level programs, such as EZNEC and NEC-Win Plus, the GW input is the only way to create the individual wires and segments out of which a NEC model emerges.

Advanced NEC-2 and NEC-4 programs sacrifice some of the convenience of the spreadsheet functions in order to provide the user with all of the core input capabilities. So we shall examine a new way to create our helical dipole using the GH input—and then combine it with the GM input that we examined in the preceding episode.

The Old Helical Dipole

If we translate the NEC-Win Plus model into a standard ASCII format .NEC file, we shall obtain the following model. See model 62-1.

```
CM 28,5-MHz helical dipole
CM radius 4", length 112", 1t=12"
CE
GW 1 3 0 4 0 2 2 3.4641 0.0404331
GW 2 3 2 2 3.4641 4 -2 3.4641 0.0404331
GW 3 3 4 -2 3.4641 6 -4 0 0.0404331
GW 4 3 6 -4 0 8 -2 -3.4641 0.0404331
GW 5 3 8 -2 -3.4641 10 2 -3.4641 0.0404331
GW 6 3 10 2 -3.4641 12 4 0 0.0404331
GW 7 3 12 4 0 14 2 3.4641 0.0404331
GW 8 3 14 2 3.4641 16 -2 3.4641 0.0404331
GW 9 3 16 -2 3.4641 18 -4 0 0.0404331
GW 10 3 18 -4 0 20 -2 -3.4641 0.0404331
GW 11 3 20 -2 -3.4641 22 2 -3.4641 0.0404331
```

```
GW 12 3 22 2 -3.4641 24 4 0 0.0404331
GW 13 3 24 4 0 26 2 3.4641 0.0404331
GW 14 3 26 2 3.4641 28 -2 3.4641 0.0404331
GW 15 3 28 -2 3.4641 30 -4 0 0.0404331
GW 16 3 30 -4 0 32 -2 -3.4641 0.0404331
GW 17 3 32 -2 -3.4641 34 2 -3.4641 0.0404331
GW 18 3 34 2 -3.4641 36 4 0 0.0404331
GW 19 3 36 4 0 38 2 3.4641 0.0404331
GW 20 3 38 2 3.4641 40 -2 3.4641 0.0404331
GW 21 3 40 -2 3.4641 42 -4 0 0.0404331
GW 22 3 42 -4 0 44 -2 -3.4641 0.0404331
GW 23 3 44 -2 -3.4641 46 2 -3.4641 0.0404331
GW 24 3 46 2 -3.4641 48 4 0 0.0404331
GW 25 3 48 4 0 50 2 3.4641 0.0404331
GW 26 3 50 2 3.4641 52 -2 3.4641 0.0404331
GW 27 3 52 -2 3.4641 54 -4 0 0.0404331
GW 28 3 54 -4 0 56 -2 -3.4641 0.0404331
GW 29 3 56 -2 -3.4641 58 2 -3.4641 0.0404331
GW 30 3 58 2 -3.4641 60 4 0 0.0404331
GW 31 3 60 4 0 62 2 3.4641 0.0404331
GW 32 3 62 2 3.4641 64 -2 3.4641 0.0404331
GW 33 3 64 -2 3.4641 66 -4 0 0.0404331
GW 34 3 66 -4 0 68 -2 -3.4641 0.0404331
GW 35 3 68 -2 -3.4641 70 2 -3.4641 0.0404331
GW 36 3 70 2 -3.4641 72 4 0 0.0404331
GW 37 3 72 4 0 74 2 3.4641 0.0404331
GW 38 3 74 2 3.4641 76 -2 3.4641 0.0404331
GW 39 3 76 -2 3.4641 78 -4 0 0.0404331
GW 40 3 78 -4 0 80 -2 -3.4641 0.0404331
GW 41 3 80 -2 -3.4641 82 2 -3.4641 0.0404331
GW 42 3 82 2 -3.4641 84 4 0 0.0404331
GW 43 3 84 4 0 86 2 3.4641 0.0404331
GW 44 3 86 2 3.4641 88 -2 3.4641 0.0404331
GW 45 3 88 -2 3.4641 90 -4 0 0.0404331
GW 46 3 90 -4 0 92 -2 -3.4641 0.0404331
GW 47 3 92 -2 -3.4641 94 2 -3.4641 0.0404331
GW 48 3 94 2 -3.4641 96 4 0 0.0404331
```

```
GW 49 3 96 4 0 98 2 3.4641 0.0404331
GW 50 3 98 2 3.4641 100 -2 3.4641 0.0404331
GW 51 3 100 -2 3.4641 102 -4 0 0.0404331
GW 52 3 102 -4 0 104 -2 -3.4641 0.0404331
GW 53 3 104 -2 -3.4641 106 2 -3.4641 0.0404331
GW 54 3 106 2 -3.4641 108 4 0 0.0404331
GW 55 3 108 4 0 110 2 3.4641 0.0404331
GW 56 3 110 2 3.4641 112 -2 3.4641 0.0404331
GS 0 0 .02540
GE 0
EX 0 28 3 0 1 0
EX 0 29 1 0 1 0
LD 5 1 1 3 5.8001E7
LD 5 2 1 3 5.8001E7
LD 5 3 1 3 5.8001E7
LD 5 4 1 3 5.8001E7
LD 5 5 1 3 5.8001E7
LD 5 6 1 3 5.8001E7
LD 5 7 1 3 5.8001E7
LD 5 8 1 3 5.8001E7
LD 5 9 1 3 5.8001E7
LD 5 10 1 3 5.8001E7
LD 5 11 1 3 5.8001E7
LD 5 12 1 3 5.8001E7
LD 5 13 1 3 5.8001E7
LD 5 14 1 3 5.8001E7
LD 5 15 1 3 5.8001E7
LD 5 16 1 3 5.8001E7
LD 5 17 1 3 5.8001E7
LD 5 18 1 3 5.8001E7
LD 5 19 1 3 5.8001E7
LD 5 20 1 3 5.8001E7
LD 5 21 1 3 5.8001E7
LD 5 22 1 3 5.8001E7
LD 5 23 1 3 5.8001E7
LD 5 24 1 3 5.8001E7
LD 5 25 1 3 5.8001E7
```

```
LD 5 26 1 3 5.8001E7
LD 5 27 1 3 5.8001E7
LD 5 28 1 3 5.8001E7
LD 5 29 1 3 5.8001E7
LD 5 30 1 3 5.8001E7
LD 5 31 1 3 5.8001E7
LD 5 32 1 3 5.8001E7
LD 5 33 1 3 5.8001E7
LD 5 34 1 3 5.8001E7
LD 5 35 1 3 5.8001E7
LD 5 36 1 3 5.8001E7
LD 5 37 1 3 5.8001E7
LD 5 38 1 3 5.8001E7
LD 5 39 1 3 5.8001E7
LD 5 40 1 3 5.8001E7
LD 5 41 1 3 5.8001E7
LD 5 42 1 3 5.8001E7
LD 5 43 1 3 5.8001E7
LD 5 44 1 3 5.8001E7
LD 5 45 1 3 5.8001E7
LD 5 46 1 3 5.8001E7
LD 5 47 1 3 5.8001E7
LD 5 48 1 3 5.8001E7
LD 5 49 1 3 5.8001E7
LD 5 50 1 3 5.8001E7
LD 5 51 1 3 5.8001E7
LD 5 52 1 3 5.8001E7
LD 5 53 1 3 5.8001E7
LD 5 54 1 3 5.8001E7
LD 5 55 1 3 5.8001E7
LD 5 56 1 3 5.8001E7
FR 0 1 0 0 28.5 1
RP 0 1 360 1000 89 0 1 1
RP 0 181 1 1000 -90 0 1 1
EN
```

I have purposely listed the entire set of 56 wires and 56 loads, since assigning a material conductivity to individual wires is standard for programs such as NEC-Win Plus. Once in .NEC form, I could replace all of the LD5 lines with a single line, since the entire helical dipole is constructed from AWG #12 copper wire. The length is 112", which gives us 9.33 turns of the helix. The helix is uniform throughout, using 12" per complete turn. Since each of the 56 wires has 3 segments, we end up with a total segment count of 168.

The model uses a split source which yields a free-space source impedance of 25.4 + j 5.4 Ohms and a gain of 1.74 dBi.

Recreating the Helical Dipole with GH

Initially, we shall use a single line to create the basic free-space helical dipole. The only entry will look like the top line of the following entry.

```
GH   1    168   12   106   4    4    4    4    .0404
GH   ITG  NS    S    HL    A1   B1   A2   B2   RAD
     I1   I2    F1   F2    F3   F4   F5   F6   F7
```

The line structure, like most other NEC-2 geometry entries, consists of 2 integer places and 7 floating decimal places. The use of integers in many of those entries is simply a function of using rounded numbers to keep the example easy-to-read and to have the new model correspond as closely as possible with the old. Here is a list of the entries and their explanations.

ITG: This entry assigns a tag number to all of the segments making up the helix (or spiral). For simplicity, we assign a 1 here.

NS: The number of segments into which the helix (or spiral) will be divided. Note that the new helical dipole will be constructed of a single wire composed of many segments. We shall retain the 168 value from the old model.

S: The turn spacing, as measured from a consistent point on successive turns. In NEC-2, the turn spacing for helixes and spirals will be constant or linear. The model assigns a 12" spacing between turns, the same value as used in the old model.

HL: The total length of the helix. Here we assign—for reasons that we shall discover—a value of 106" instead of the 112" of the initial model. If HL is zero, then we obtain a flat spiral. Some implementations of NEC-2 may yield a division-by-zero error if HL=0. However, one may always give HL a very low value to avoid this problem and retain an essentially flat spiral. If HL is negative, the output is a left-handed spiral; if positive, the helix is right-handed. Since the helical dipole does not care about its hands, we have assigned a positive number.

The following 4 entries rest on the fact that NEC-2 grows its helices along the Z-axis. For a free-space model, this presents no problems, even for our HF helical dipole, since we can always use a theta pattern instead of a phi pattern to obtain the typical dipole figure-8 pattern. As well, we shall look at ways to reorient the helix once we have finished constructing it.

A1: The radius of the helix along the X-axis at Z=0 (the helix starting point). Since we used a “radius” of 4" from center to hexagon point in our old model, we shall use 4 as the radius.

B1: The radius of the helix along the Y-axis at Z=0 (the helix starting point). Once more, we assign a 4.

A2: The radius of the helix along the X-axis at Z=HL (the terminating point of the helix). Since our helix is uniform in radius, we assign another 4.

B2: The radius of the helix along the Y-axis at Z=HL (the terminating point of the helix). Since our helix is uniform in radius, we assign another 4.

RAD: The wire radius. Since we are using AWG #12, the radius is 0.0404.

If we were designing a flat spiral, then HL would be zero or virtual zero, and A2 and B2 would not have the same values as A1 and B1. However, A2 and B2 must grow or shrink together to prevent intersecting wires within the spiral. In a helix, it is not necessary to maintain a constant radius, although that is the most common form. We can create a spiral helix by using different values for A1/B1 and A2/B2 while using a non-zero value for HL. The result will be roughly conical, with the more open end higher or lower depending on our selection of A and B values.

A limitation of the NEC-2 helix creation line is that it does not permit variation of the pitch as we move along the helix. This limitation has no effect on our simple model.

The GH input does not appear in the original (1981) NEC-2 user's manual. It is classified as a non-official addition to NEC-2. Nonetheless, it is a highly useful addition.

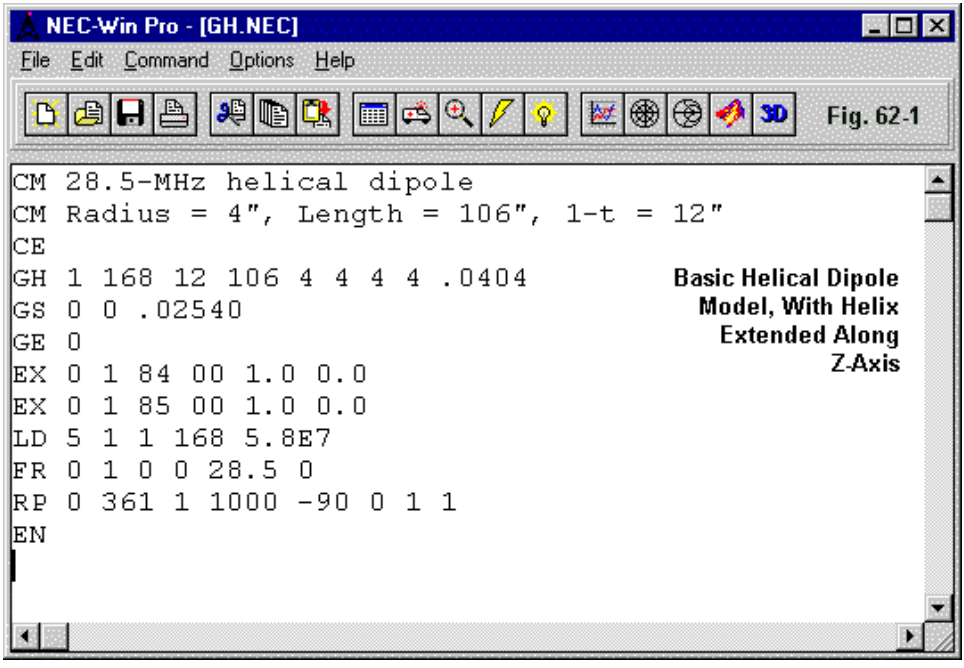

Fig. 62-1 shows the complete simple helix model. Since the wire units are in inches, we add the scaling line (GS) to convert them to meters. As well, since we specified a total of 168 segments in the model to coincide roughly with the original model, we use a split-feed system. However, rather than occurring on adjacent wires, as in the original, they occur on adjacent segments of our single tag: segments 84 and 85, specifically. As well, a single load (LD5) line suffices to give the

model wire copper's conductivity. The RP0 line specifies a theta pattern. See model 62-2.

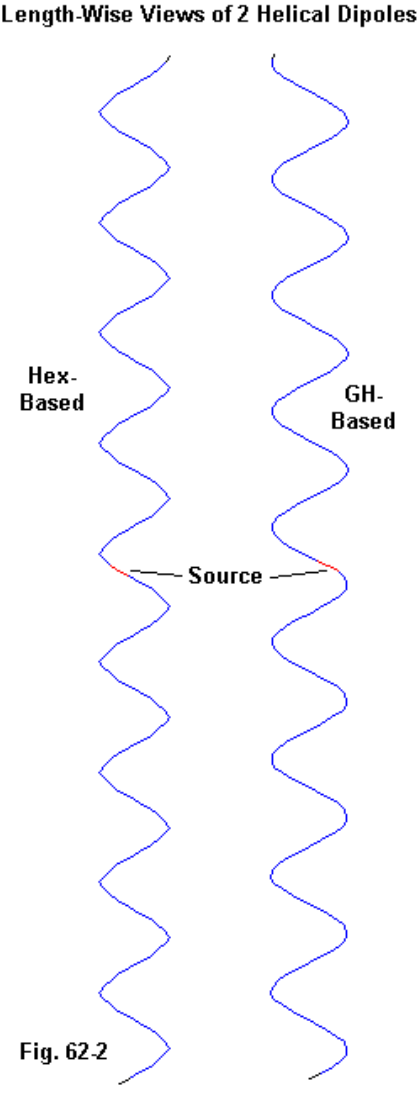

Fig. 62-2

Fig. 62-2 places the two helices side by side, but not perfectly to scale. The old model has 9.33 turns, while the new one has 8.83 turns, given the fixed 12-inch turn spacing in each model. If the new model curves seem smoother than the old, that is no illusion. The old model uses 3 segments per straight line, while the new model has a new angle for each segment.

The new model returns a free-space gain of 1.73 dBi and a source impedance (combining the split-feed in series) of 22.6 - j 1.9 Ohms. But it does so with a length of 106" rather than the original 112".

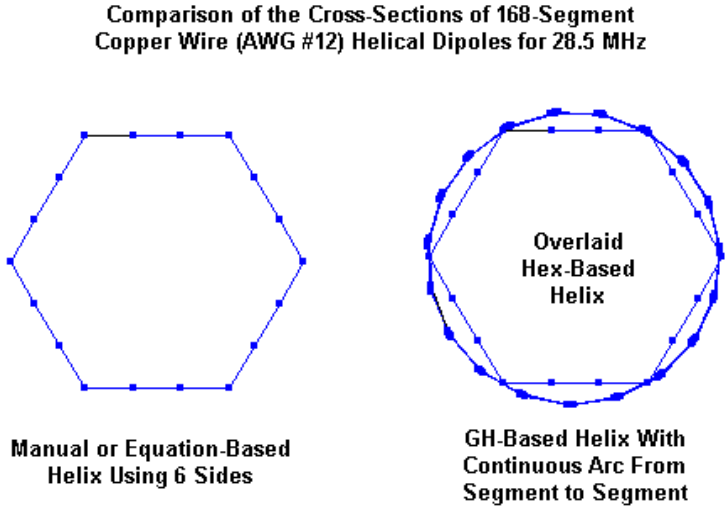

Fig. 62-3

We can capture something of the reason for the length difference from the views of **Fig. 62-3**. The original model used a hexagon to simulate a circle. For general building guidance, the simulation is reasonable. However, with a radius to a point of 4", the circumference of the hexagon is somewhat shorter than that of a circle with

the same radius. Hence, we would require greater length to equal the total wire in the much more circular helix created by the GH entry.

One modeling benefit of using the GH facility is that we can prune our helix model to length simply by changing 1 number in the GH line (HL). Changing the length of the original model requires that we add, remove, or modify one or more GW entries.

The NEC output report on the helix provides some useful information not readily available from the original model. The following extract from the output file for our simple "GH" model is helpful in checking our design or finding out some of its properties.

```
                    - - - STRUCTURE SPECIFICATION - - -

  WIRE
           NO. OF    FIRST  LAST     TAG
  NO.        X1          Y1          Z1          X2          Y2          Z2
RADIUS   SEG.     SEG.    SEG.     NO.
     HELIX STRUCTURE-   AXIAL SPACING BETWEEN TURNS =  12.000 TOTAL AXIAL
LENGTH = 106.000
  1  RADIUS OF HELIX =     4.000     4.000     4.000     4.000
0.04040     168        1   168       1
     THE PITCH ANGLE IS   25.5228
     THE LENGTH OF WIRE/TURN IS   27.8506
      STRUCTURE SCALED BY FACTOR   0.02540

                    - - - - SEGMENTATION DATA - - - -
                         COORDINATES IN METERS
       I+ AND I- INDICATE THE SEGMENTS BEFORE AND AFTER I

  SEG.     COORDINATES OF SEG. CENTER       SEG.     ORIENTATION ANGLES
WIRE    CONNECTION DATA   TAG
  NO.        X          Y          Z        LENGTH     ALPHA     BETA
RADIUS    I-   I    I+    NO.
     1    0.09885    0.01648    0.00801    0.03706   25.62438  99.46429
0.00103     0    1    2      1
     2    0.08816    0.04765    0.02404    0.03706   25.62438 118.39286
0.00103     1    2    3      1
     3    0.06794    0.07368    0.04007    0.03706   25.62438 137.32143
0.00103     2    3    4      1
     4    0.04036    0.09173    0.05609    0.03706   25.62438 156.25000
0.00103     3    4    5      1
```

```
     5    0.00842    0.09986    0.07212    0.03706   25.62438 175.17857
0.00103    4    5    6      1
     6   -0.02443    0.09719    0.08814    0.03706   25.62438-165.89286
0.00103    5    6    7      1
     7   -0.05463    0.08402    0.10417    0.03706   25.62438-146.96429
0.00103    6    7    8      1
     8   -0.07893    0.06175    0.12020    0.03706   25.62438-128.03572
0.00103    7    8    9      1
     9   -0.09470    0.03280    0.13622    0.03706   25.62438-109.10715
0.00103    8    9   10      1
    10   -0.10022    0.00031    0.15225    0.03706   25.62438 -90.17857
0.00103    9   10   11      1
    11   -0.09490   -0.03221    0.16828    0.03706   25.62438 -71.25000
0.00103   10   11   12      1
    12   -0.07932   -0.06126    0.18430    0.03706   25.62438 -52.32143
0.00103   11   12   13      1
—
    80    0.04264    0.09070    1.27408    0.03706   25.62438 154.82140
0.00103   79   80   81      1
    81    0.01091    0.09962    1.29011    0.03706   25.62438 173.74997
0.00103   80   81   82      1
    82   -0.02200    0.09777    1.30613    0.03706   25.62438-167.32145
0.00103   81   82   83      1
    83   -0.05252    0.08535    1.32216    0.03706   25.62438-148.39288
0.00103   82   83   84      1
    84   -0.07737    0.06370    1.33819    0.03706   25.62438-129.46431
0.00103   83   84   85      1
    85   -0.09385    0.03516    1.35421    0.03706   25.62438-110.53574
0.00103   84   85   86      1
    86   -0.10018    0.00281    1.37024    0.03706   25.62438 -91.60717
0.00103   85   86   87      1
    87   -0.09567   -0.02984    1.38627    0.03706   25.62438 -72.67860
0.00103   86   87   88      1
    88   -0.08082   -0.05926    1.40229    0.03706   25.62438 -53.75003
0.00103   87   88   89      1
    89   -0.05723   -0.08227    1.41832    0.03706   25.62438 -34.82146
0.00103   88   89   90      1
—
   157    0.01339    0.09932    2.50810    0.03706   25.62438 172.32138
0.00103  156  157  158      1
   158   -0.01955    0.09829    2.52412    0.03706   25.62438-168.75005
0.00103  157  158  159      1
   159   -0.05038    0.08663    2.54015    0.03706   25.62438-149.82148
0.00103  158  159  160      1
   160   -0.07576    0.06561    2.55618    0.03706   25.62438-130.89291
0.00103  159  160  161      1
```

```
   161    -0.09294     0.03748     2.57220     0.03706    25.62438-111.96434
0.00103   160  161  162      1
   162    -0.10008     0.00531     2.58823     0.03706    25.62438 -93.03577
0.00103   161  162  163      1
   163    -0.09639    -0.02744     2.60426     0.03706    25.62438 -74.10720
0.00103   162  163  164      1
   164    -0.08227    -0.05723     2.62028     0.03706    25.62438 -55.17862
0.00103   163  164  165      1
   165    -0.05926    -0.08082     2.63631     0.03706    25.62438 -36.25005
0.00103   164  165  166      1
   166    -0.02984    -0.09567     2.65233     0.03706    25.62438 -17.32148
0.00103   165  166  167      1
  167   0.00281   -0.10018   2.66836   0.03706   25.62438   1.60709   0.00103
166  167  168      1
   168     0.03516    -0.09385     2.68439     0.03706    25.62438   20.53566
0.00103   167  168    0      1
```

I have left only 3 turns—the two ends and the turn in the source region—in this report to reveal the segment-by-segment change of angle in a GH helix. The helix extends from Z=0 to Z=2.6924 m (106"). The values in the Z column do not match these terminal values, since they are values for the center of each segment.

Among the useful data provided in the NEC output report is the pitch angle (25.522 degrees) and the length of wire per turn (27.8506"). From the latter value, knowing that we have 8.833 turns, we can derive the total length of wire in the helix: 246". (Since each wire in the original model is 4.47" long—allowing for the pitch of the turns—and we have 56 wires, the total wire length in that model is 250".)

Manipulating the Helical Dipole

The helical dipole that we just created is vertical and extends from Z=0 to Z=HL. It is unlikely that this position is what we might desire for the finished product. However, we may change a number of positional features of the structure by using the GM input that we reviewed in episode 61.

Let's begin by rotating the structure reactive to the X-axis. Our goal will be to set the structure into what would be a horizontal orientation extending from Y=0 to Y=HL. A single entry on a GM card placed just after the GH card will do the job.

Fig. 62-4 shows the revised model. Note that we have entered a -90-degree rotation in order to come up with positive values for the Y-axis entries. See model 62-3.

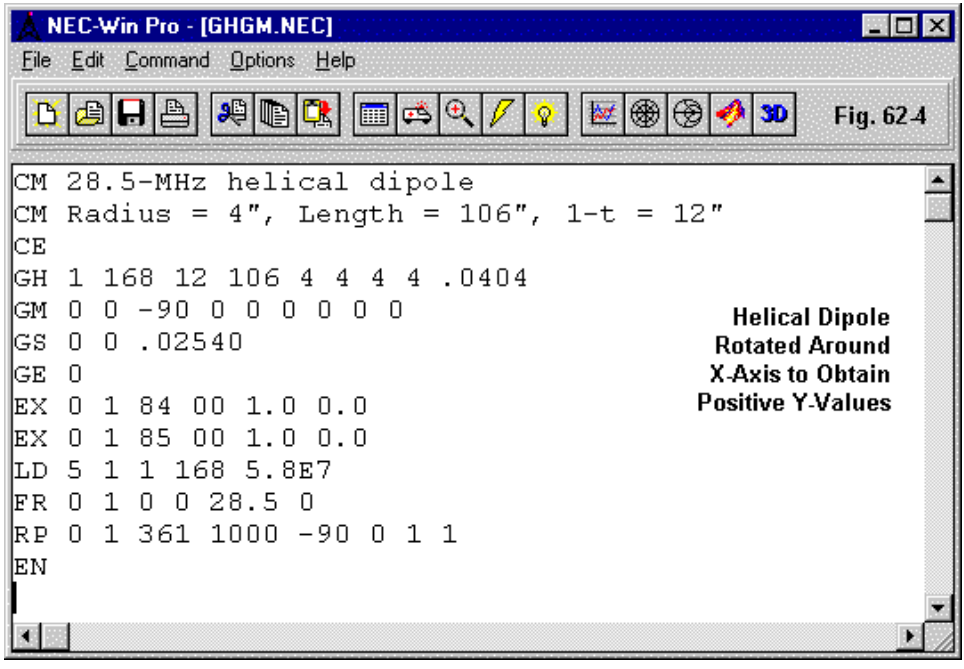

The following extract from the NEC output file gives us a view of what we accomplished.

```
                    - - - STRUCTURE SPECIFICATION - - -

                      COORDINATES MUST BE INPUT IN
                     METERS OR BE SCALED TO METERS
                    BEFORE STRUCTURE INPUT IS ENDED


  WIRE
          NO. OF    FIRST  LAST     TAG
  NO.       X1         Y1         Z1          X2         Y2         Z2
RADIUS   SEG.     SEG.   SEG.     NO.
```

```
     HELIX STRUCTURE-    AXIAL SPACING BETWEEN TURNS =  12.000 TOTAL AXIAL
LENGTH = 106.000
  1  RADIUS OF HELIX =     4.000     4.000     4.000     4.000          0.04040
168        1   168       1
     THE PITCH ANGLE IS   25.5228
     THE LENGTH OF WIRE/TURN IS   27.8506
      THE STRUCTURE HAS BEEN MOVED, MOVE DATA CARD IS -
        0     0 -90.00000   0.00000   0.00000   0.00000   0.00000   0.00000
0.00000
       GM command acting on tag #'s            0 through            0
  inclusive.
     STRUCTURE SCALED BY FACTOR   0.02540

                    - - - - SEGMENTATION DATA - - - -
                         COORDINATES IN METERS
               I+ AND I- INDICATE THE SEGMENTS BEFORE AND AFTER I

  SEG.      COORDINATES OF SEG. CENTER       SEG.     ORIENTATION ANGLES
WIRE    CONNECTION DATA   TAG
  NO.         X          Y          Z        LENGTH     ALPHA     BETA
RADIUS    I-   I    I+    NO.
      1     0.09885     0.00801    -0.01648     0.03706   -62.79489 108.92291
0.00103     0    1    2      1
      2     0.08816     0.02404    -0.04765     0.03706   -52.48438 134.75235
0.00103     1    2    3      1
      3     0.06794     0.04007    -0.07368     0.03706   -37.67732 146.87851
0.00103     2    3    4      1
      4     0.04036     0.05609    -0.09173     0.03706   -21.29291 152.34449
0.00103     3    4    5      1
      5     0.00842     0.07212    -0.09986     0.03706    -4.34627 154.29633
0.00103     4    5    6      1
      6    -0.02443     0.08814    -0.09719     0.03706    12.69518 153.68493
0.00103     5    6    7      1
      7    -0.05463     0.10417    -0.08402     0.03706    29.44213 150.22438
0.00103     6    7    8      1
      8    -0.07893     0.12020    -0.06175     0.03706    45.24815 142.10108
0.00103     7    8    9      1
      9    -0.09470     0.13622    -0.03280     0.03706    58.42714 124.31185
0.00103     8    9   10      1
     10    -0.10022     0.15225    -0.00031     0.03706    64.37504  90.37230
0.00103     9   10   11      1
     11    -0.09490     0.16828     0.03221     0.03706    58.62722  56.17144
0.00103    10   11   12      1
     12    -0.07932     0.18430     0.06126     0.03706    45.52954  38.12186
0.00103    11   12   13      1
```

```
     80     0.04264     1.27408    -0.09070     0.03706   -22.55676 152.07639
0.00103    79   80   81      1
     81     0.01091     1.29011    -0.09962     0.03706    -5.63323 154.24218
0.00103    80   81   82      1
     82    -0.02200     1.30613    -0.09777     0.03706    11.41387 153.81986
0.00103    81   82   83      1
     83    -0.05252     1.32216    -0.08535     0.03706    28.19972 150.61245
0.00103    82   83   84      1
     84    -0.07737     1.33819    -0.06370     0.03706    44.11424 142.96058
0.00103    83   84   85      1
     85    -0.09385     1.35421    -0.03516     0.03706    57.60257 126.18023
0.00103    84   85   86      1
     86    -0.10018     1.37024    -0.00281     0.03706    64.32867  93.34651
0.00103    85   86   87      1
     87    -0.09567     1.38627     0.02984     0.03706    59.40185  58.17066
0.00103    86   87   88      1
     88    -0.08082     1.40229     0.05926     0.03706    46.64632  39.04739
0.00103    87   88   89      1
     89    -0.05723     1.41832     0.08227     0.03706    30.98812  30.29621
0.00103    88   89   90      1
     90    -0.02744     1.43434     0.09639     0.03706    14.29458  26.50571
0.00103    89   90   91      1
```

———

```
    155     0.07152     2.47605    -0.07020     0.03706   -40.05297 145.59858
0.00103   154  155  156      1
    156     0.04488     2.49207    -0.08960     0.03706   -23.81736 151.78846
0.00103   155  156  157      1
    157     0.01339     2.50810    -0.09932     0.03706    -6.91952 154.17381
0.00103   156  157  158      1
    158    -0.01955     2.52412    -0.09829     0.03706    10.13116 153.93953
0.00103   157  158  159      1
    159    -0.05038     2.54015    -0.08663     0.03706    26.95272 150.97652
0.00103   158  159  160      1
    160    -0.07576     2.55618    -0.06561     0.03706    42.96780 143.77073
0.00103   159  160  161      1
    161    -0.09294     2.57220    -0.03748     0.03706    56.74142 127.94738
0.00103   160  161  162      1
    162    -0.10008     2.58823    -0.00531     0.03706    64.20849  96.30074
0.00103   161  162  163      1
    163    -0.09639     2.60426     0.02744     0.03706    60.13300  60.27703
0.00103   162  163  164      1
    164    -0.08227     2.62028     0.05723     0.03706    47.74811  40.02946
0.00103   163  164  165      1
    165    -0.05926     2.63631     0.08082     0.03706    32.21882  30.74262
0.00103   164  165  166      1
```

```
   166    -0.02984     2.65233     0.09567     0.03706    15.57208   26.67626
0.00103   165  166  167      1
  167   0.00281   2.66836   0.10018   0.03706  -1.44899  25.63317   0.00103
166  167  168      1
   168     0.03516     2.68439     0.09385     0.03706   -18.43868   27.12110
0.00103   167  168    0      1
```

The entries make it clear that the extension of the helical dipole that formerly appeared in the Z-column now appears in the Y-column.

Since it is also unlikely that we would want the helical dipole to lie partially above and partially below ground when we add a ground system to the model later on, we should likely raise the antenna in the Z-axis. Perhaps 30' or 360" will do as a start. As well, many modelers prefer to have their antennas centered, with equal amounts extending + and - relative to the axis at right angles to them. This move would require that we move the structure along the Y-axis by -53 (a 53" move toward the negative portion of the Y-axis).

We need not add a second GM card. Our total revision involves a rotation first, followed by two translations. Since the GM card rotates before translating—our desired order of operation—we may include all 3 requests on a single card, as shown in **Fig. 62-5**.

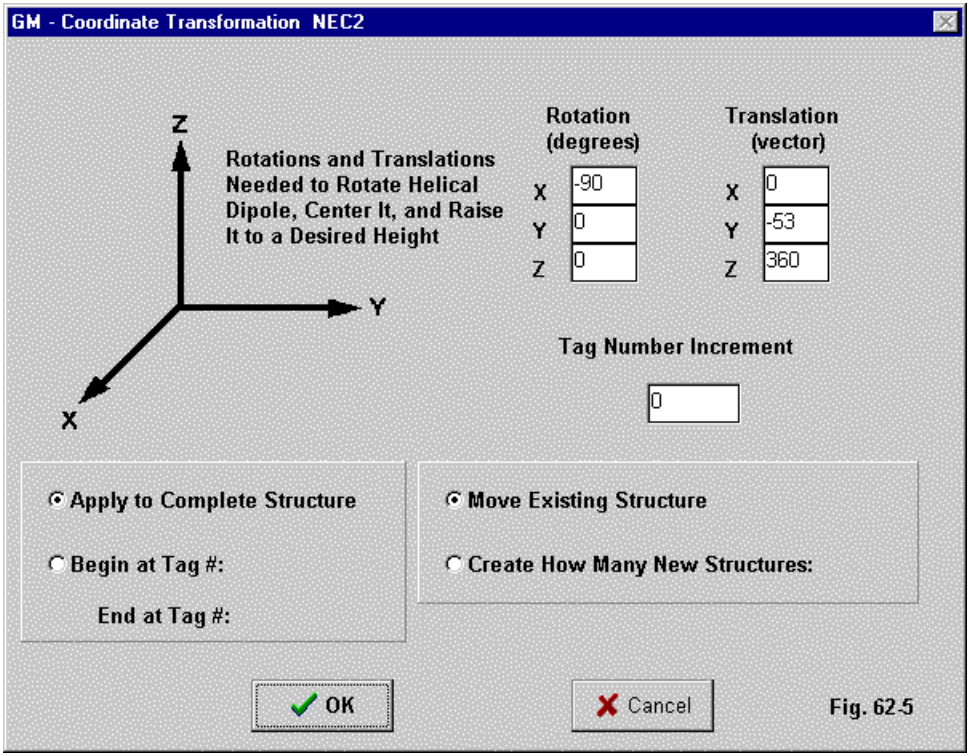

Fig. 62-5

Since the GM card will precede the GS or scaling card, we may make all entries in the unit of measure that we used for the GH line. The final model (at least for this exercise) appears in **Fig. 62-6**. See model 62-4.

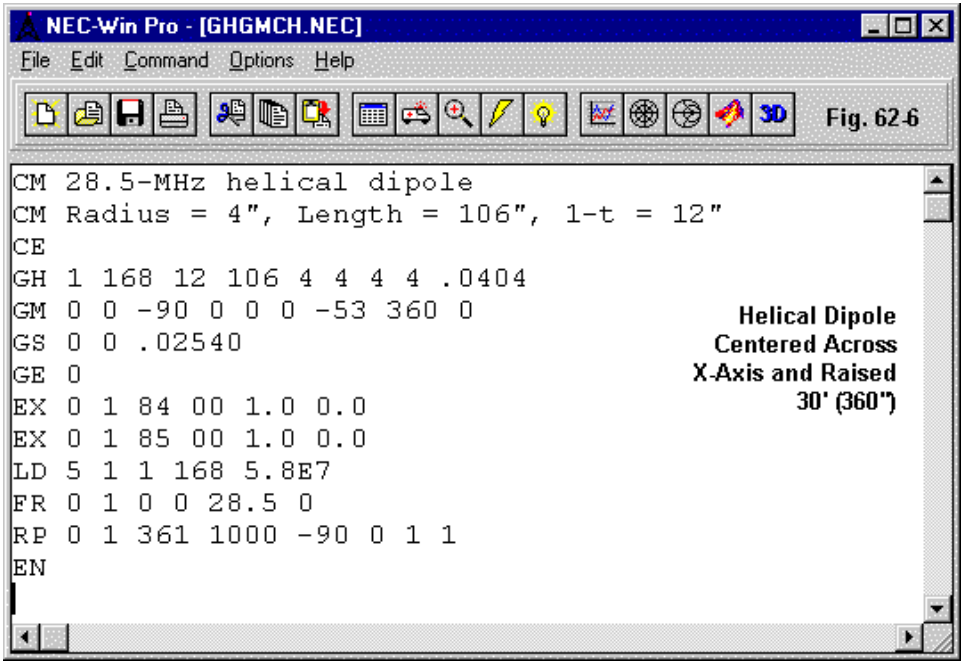

We need only look at an extract from the NEC output file to see if we succeeded in all of our moves.

```
                    - - - STRUCTURE SPECIFICATION - - -

  WIRE
NO. OF    FIRST  LAST     TAG
  NO.        X1         Y1         Z1          X2         Y2         Z2
RADIUS   SEG.     SEG.   SEG.     NO.
     HELIX STRUCTURE-   AXIAL SPACING BETWEEN TURNS =  12.000 TOTAL AXIAL
LENGTH = 106.000
     1  RADIUS OF HELIX =     4.000     4.000     4.000     4.000
0.04040     168        1   168
```

```
1
     THE PITCH ANGLE IS   25.5228
     THE LENGTH OF WIRE/TURN IS   27.8506
      THE STRUCTURE HAS BEEN MOVED, MOVE DATA CARD IS -
        0    0 -90.00000   0.00000   0.00000   0.00000 -53.00000 360.00000
0.00000
       GM command acting on tag #'s            0 through            0
  inclusive.
      STRUCTURE SCALED BY FACTOR   0.02540

                    - - - - SEGMENTATION DATA - - - -
                         COORDINATES IN METERS
          I+ AND I- INDICATE THE SEGMENTS BEFORE AND AFTER I

  SEG.     COORDINATES OF SEG. CENTER       SEG.     ORIENTATION ANGLES
WIRE    CONNECTION DATA   TAG
  NO.        X          Y          Z        LENGTH     ALPHA     BETA
RADIUS    I-   I    I+    NO.
      1     0.09885    -1.33819     9.12752     0.03706   -62.79489 108.92291
0.00103     0    1    2      1
      2     0.08816    -1.32216     9.09635     0.03706   -52.48438 134.75235
0.00103     1    2    3      1
      3     0.06794    -1.30613     9.07032     0.03706   -37.67732 146.87851
0.00103     2    3    4      1
      4     0.04036    -1.29011     9.05227     0.03706   -21.29291 152.34449
0.00103     3    4    5      1
      5     0.00842    -1.27408     9.04414     0.03706    -4.34627 154.29633
0.00103     4    5    6      1
      6    -0.02443    -1.25806     9.04681     0.03706    12.69518 153.68493
0.00103     5    6    7      1
      7    -0.05463    -1.24203     9.05998     0.03706    29.44213 150.22438
0.00103     6    7    8      1
      8    -0.07893    -1.22600     9.08225     0.03706    45.24815 142.10108
0.00103     7    8    9      1
      9    -0.09470    -1.20998     9.11120     0.03706    58.42714 124.31185
0.00103     8    9   10      1
     10    -0.10022    -1.19395     9.14369     0.03706    64.37504  90.37230
0.00103     9   10   11      1
     11    -0.09490    -1.17792     9.17621     0.03706    58.62722  56.17144
0.00103    10   11   12      1
     12    -0.07932    -1.16190     9.20526     0.03706    45.52954  38.12186
0.00103    11   12   13      1
————
     80     0.04264    -0.07212     9.05330     0.03706   -22.55676 152.07639
0.00103    79   80   81      1
```

```
     81     0.01091    -0.05609     9.04438     0.03706    -5.63323 154.24218
0.00103    80   81   82      1
     82    -0.02200    -0.04007     9.04623     0.03706    11.41387 153.81986
0.00103    81   82   83      1
     83    -0.05252    -0.02404     9.05865     0.03706    28.19972 150.61245
0.00103    82   83   84      1
     84    -0.07737    -0.00801     9.08030     0.03706    44.11424 142.96058
0.00103    83   84   85      1
     85    -0.09385     0.00801     9.10884     0.03706    57.60257 126.18023
0.00103    84   85   86      1
     86    -0.10018     0.02404     9.14119     0.03706    64.32867  93.34651
0.00103    85   86   87      1
     87    -0.09567     0.04007     9.17384     0.03706    59.40185  58.17066
0.00103    86   87   88      1
     88    -0.08082     0.05609     9.20326     0.03706    46.64632  39.04739
0.00103    87   88   89      1
     89    -0.05723     0.07212     9.22627     0.03706    30.98812  30.29621
0.00103    88   89   90      1
     90    -0.02744     0.08814     9.24039     0.03706    14.29458  26.50571
0.00103    89   90   91      1
————
    156     0.04488     1.14587     9.05440     0.03706   -23.81736 151.78846
0.00103   155  156  157      1
    157     0.01339     1.16190     9.04468     0.03706    -6.91952 154.17381
0.00103   156  157  158      1
    158    -0.01955     1.17792     9.04571     0.03706    10.13116 153.93953
0.00103   157  158  159      1
    159    -0.05038     1.19395     9.05737     0.03706    26.95272 150.97652
0.00103   158  159  160      1
    160    -0.07576     1.20998     9.07839     0.03706    42.96780 143.77073
0.00103   159  160  161      1
    161    -0.09294     1.22600     9.10652     0.03706    56.74142 127.94738
0.00103   160  161  162      1
    162    -0.10008     1.24203     9.13869     0.03706    64.20849  96.30074
0.00103   161  162  163      1
    163    -0.09639     1.25806     9.17144     0.03706    60.13300  60.27703
0.00103   162  163  164      1
    164    -0.08227     1.27408     9.20123     0.03706    47.74811  40.02946
0.00103   163  164  165      1
    165    -0.05926     1.29011     9.22482     0.03706    32.21882  30.74262
0.00103   164  165  166      1
    166    -0.02984     1.30613     9.23967     0.03706    15.57208  26.67626
0.00103   165  166  167      1
  167   0.00281   1.32216   9.24418   0.03706  -1.44899  25.63317   0.00103
166  167  168      1
```

```
   168     0.03516     1.33819     9.23785     0.03706   -18.43868   27.12110
0.00103   167  168    0      1
```

The average Z value is 9.144 m or 30'. The model extends from Y=-1.3462 m to +1.3462 m (that is, -53" to +53"). The values shown for segments 1 and 168, of course, represent the Y coordinates of the segment center, so their values will be just shy of the tag end coordinates.

Conclusions and Cautions

This little exercise set in using the GH entry—along with the GM entry—to create helical structures has aimed at familiarization with some of the modeling economies that are available in implementations of NEC-2 that make all of the geometry cards available to the user. The original model of our helical dipole used 56 GW entries, while the revised model used only 1 GH and eventually 1 GM entry to do the same work. As well, we need only one LD5 entry to provide the dipole with copper's conductivity throughout.

For our efforts, we received the benefit of having a helix that better simulates a spiral curvature. The angle changes with every segment, rather than with every third segment, as in the original. The result is a structure that yields a slightly different required length for resonance and a slightly different source impedance.

When constructing models of helical structures, we need to remain aware of all NEC limitations. If we make the radius of the helix too small for the wire radius used, then we may run against the segment-length-to-wire-radius limits of NEC. If we confine the space required by 1 turn to a value that is too low, then the wire proximity may violate NEC limitations. Proximity errors may increase if the parallel segment junctions are not in very close alignment. Most of these problems will show up within one of two tests. First, most NEC implementations have some sort of error checking routine to pre-test a model relative to many of the NEC guidelines. Second, we can perform an average gain test as a check on model adequacy.

The limitations on helical models do not impinge on the design and modeling of most helical antenna designs for the VHF region and above. In these antennas, turns are relatively widely spaced with a large radius to the spiral. However, the

limitations will often be approached and surpassed in attempts to model compact helical dipoles for HF service. Typically, such dipoles use fairly closely spaced wires on forms with under a 2" diameter. The GH facility can create the requisite wire structure, but the user must be cautious with the results.

These notes apply only to the NEC-2 implementation of the GH entry. The NEC-4 version of the entry has a different format, so that a NEC-2 model with a GH entry does not import directly into NEC-4. By shrinking the helix radius entries into single values for the start and end, the entry opens room for specifying differential start and stop wire radii. As well, instead of asking for the spacing of a full turn and the total length of the helix, the NEC-4 entry asks for the total length and the number of turns. Finally, the NEC-4 version of GH allows two different types of spirals. Since both NEC-2 and NEC-4 use only 7 floating decimal entries, entry meanings will change when moving from one program to the other.

* * * * *

Models included: 62-1 through 62-4. (Models available in .NEC format only.)

63. GH and GM: The NEC-4 Versions

We have examined in the past two episodes the basic uses of the GH (Helix-Spiral Specification) and the GM (Coordinate Transformation) inputs in their NEC-2 incarnations. Along the way, we had occasion to briefly note that in certain particulars, the NEC-4 versions of these geometry input lines differed from the NEC-2 counterparts. Some modelers may have occasion to use NEC-4, and so it may be useful to trace the way in which this core employs these input lines.

Although the inputs are a function of the NEC-2 and NEC-4 cores, implementing software provides the user with certain helps. Therefore, we shall examine the GH and GM cards through NEC-Win Pro (NEC-2) and GNEC (NEC-4), both by Nittany Scientific. The screens of these programs will have similar appearances, since they are roughly counterpart programs. However, it will be the differences that most interest us.

The Helical Dipole for 28.5 MHz

Let's begin be re-creating the helical dipole from the preceding column. In **Fig. 63-1**, we have the ASCII inputs that define this model. See model 63-1.

There are only two lines in the model versions that differ. One is the LD5 material conductivity line. In the NEC-2 version, places 2, 3, and 4 specify the tag number, the start segment, and the stop segment of the wire to be loaded. The NEC-4 versions uses a shortcut: these same places all contain zeroes, indicating that all segments in the model will be loaded by the conductivity value (in S/m) listed in the last entry position. We have noted this shortcut in past columns, but likely have not illustrated its use until now.

The more germane difference lies in the GH line that defines the helical dipole. The basic design consists of AWG #12 wire (0.0808" diameter) would in a helix in which the turns occupy 12" each. The radius is 4", and the overall length is 106" or 8.8333 turns.

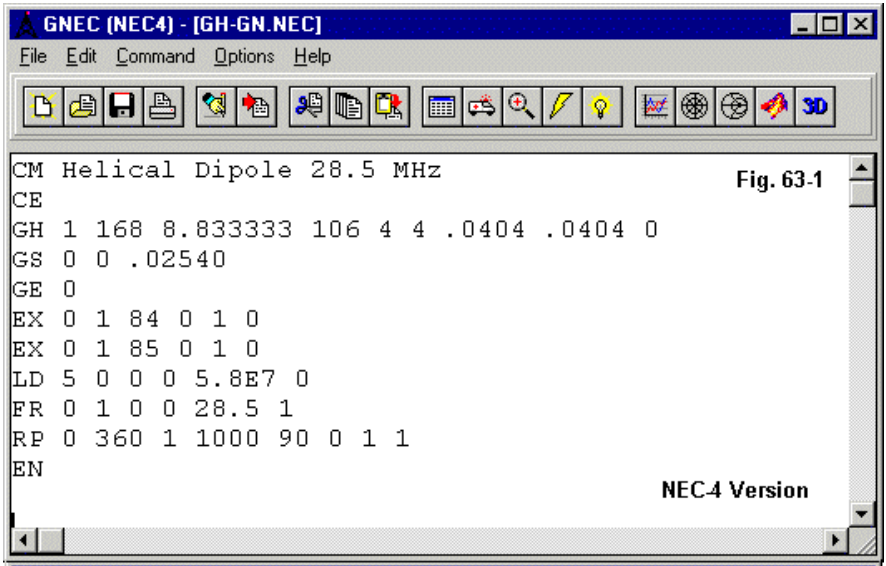
GNEC (NEC4) - [GH-GN.NEC]
File Edit Command Options Help
3D
CM Helical Dipole 28.5 MHz
CE
GH 1 168 8.833333 106 4 4 .0404 .0404 0
GS 0 0 .02540
GE 0
EX 0 1 84 0 1 0
EX 0 1 85 0 1 0
LD 5 0 0 0 5.8E7 0
FR 0 1 0 0 28.5 1
RP 0 360 1 1000 90 0 1 1
EN
Fig. 63-1
NEC-4 Version

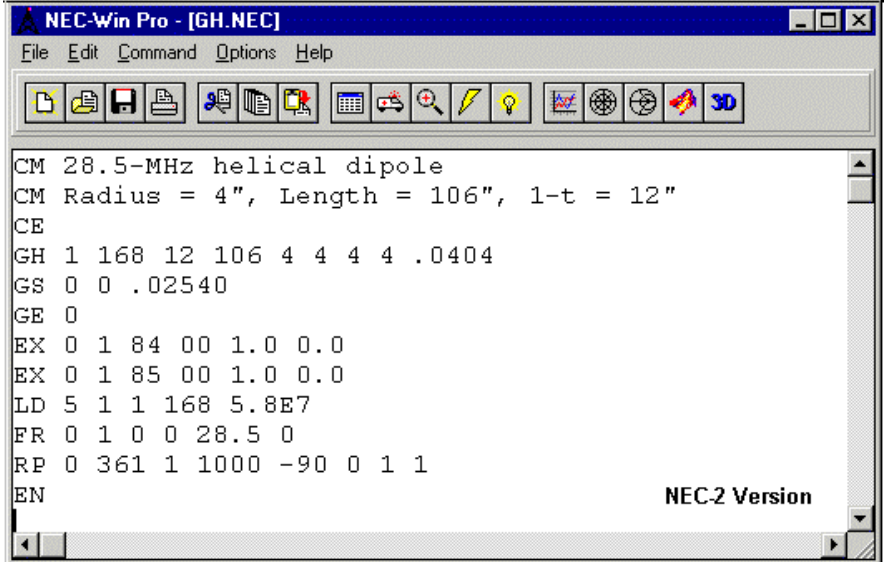
NEC-Win Pro - [GH.NEC]
File Edit Command Options Help
3D
CM 28.5-MHz helical dipole
CM Radius = 4", Length = 106", 1-t = 12"
CE
GH 1 168 12 106 4 4 4 4 .0404
GS 0 0 .02540
GE 0
EX 0 1 84 00 1.0 0.0
EX 0 1 85 00 1.0 0.0
LD 5 1 1 168 5.8E7
FR 0 1 0 0 28.5 0
RP 0 361 1 1000 -90 0 1 1
EN
NEC-2 Version

NEC-2 enters the data in this format:

```
GH   1     168   12   106   4    4    4    4    .0404
GH   ITG   NS    S    HL    A1   B1   A2   B2   RAD
     I1    I2    F1   F2    F3   F4   F5   F6   F7
```

Note that we use the space between turns and the total length to define the helix, where both values are in the unit of measure chosen for the model and transformed to meters by the GS line.

In contrast, the basic defining data required by the NEC-4 version is the number of turns, where the number of turns may be a decimal value rather than a simple integer, and the total length of the helix. Hence, the line input format undergoes a reshaping.

```
GH   1     168   8.3333   106     4     4     .0404   .0404   0
GH   ITG   NS    TURNS    ZLEN    HR1   HR2   WR1     WR2     ISPX
     I1    I2    F1       F2      F3    F4    F5      F6      F7
```

The integer entries retain the same meanings to indicate the tag number of the spiral and the total number of segments with the helix. F1 and F2 contain the number of turns and the total length. The length is designated ZLEN, because—common to both cores—the initial helix is grown along the Z-axis from zero to a positive limit. If ZLEN is negative, the output is a left-handed spiral; if positive, the helix is right-handed. Since the helical dipole does not care about its hands, we have assigned a positive number.

Whereas in NEC-2, we might assign different values to the radius along the X-axis and the Y-axis (allowing an oval), HR1 and HR2 assign a single radius value to the Z=0 end and to the Z=ZLEN ends of the spiral, respectively. WR1 and WR2 refer to the wire radius at each end of the helix. If we enter different values for two entries, then the program automatically scales the radii of the segments logarithmically.

The final entry, ISPX is effective only when HR2 and HR1 are not equal—which creates a spiral structure. When HR1=HR2, values of 0 or 1 make no difference.

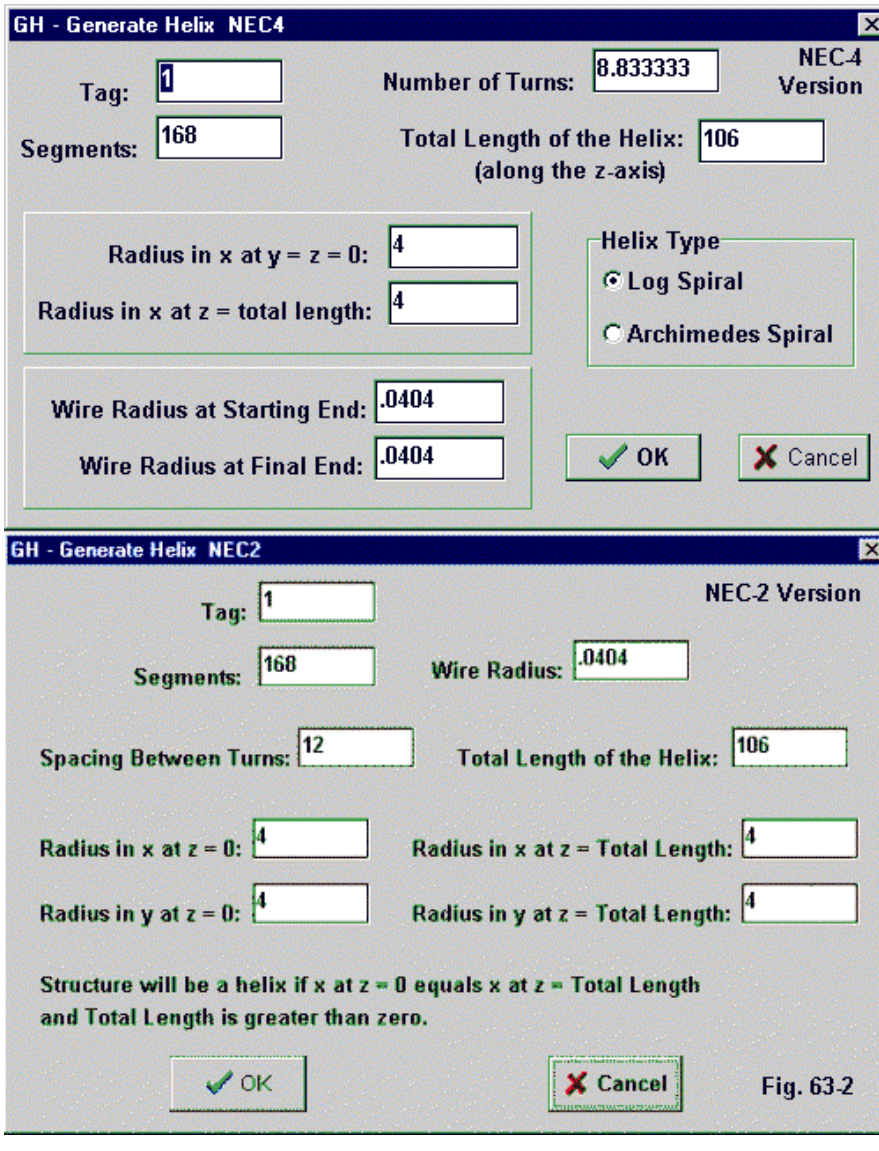
GH - Generate Helix NEC4
Tag:
1
Number of Turns:
8.833333
NEC-4 Version
Segments:
168
Total Length of the Helix: (along the z-axis)
106
Radius in x at y = z = 0:
4
Radius in x at z = total length:
4
Helix Type
Log Spiral
Archimedes Spiral
Wire Radius at Starting End:
.0404
Wire Radius at Final End:
.0404
OK
Cancel
GH - Generate Helix NEC2
Tag:
1
NEC-2 Version
Segments:
168
Wire Radius:
.0404
Spacing Between Turns:
12
Total Length of the Helix:
106
Radius in x at z = 0:
4
Radius in x at z = Total Length:
4
Radius in y at z = 0:
4
Radius in y at z = Total Length:
4
Structure will be a helix if x at z = 0 equals x at z = Total Length and Total Length is greater than zero.
OK
Cancel

Fig. 63-2

However, when we have a spiral, 0 defines a log spiral and 1 defines an Archimedes spiral.

Fig. 63-2 shows the NEC-2 and NEC-4 GH-help screens to further identify the differences between the GH geometry input lines. The help screens simply provide places to enter the line data in order (or to revise individual entries), so correlation to the respective model lines should be straightforward.

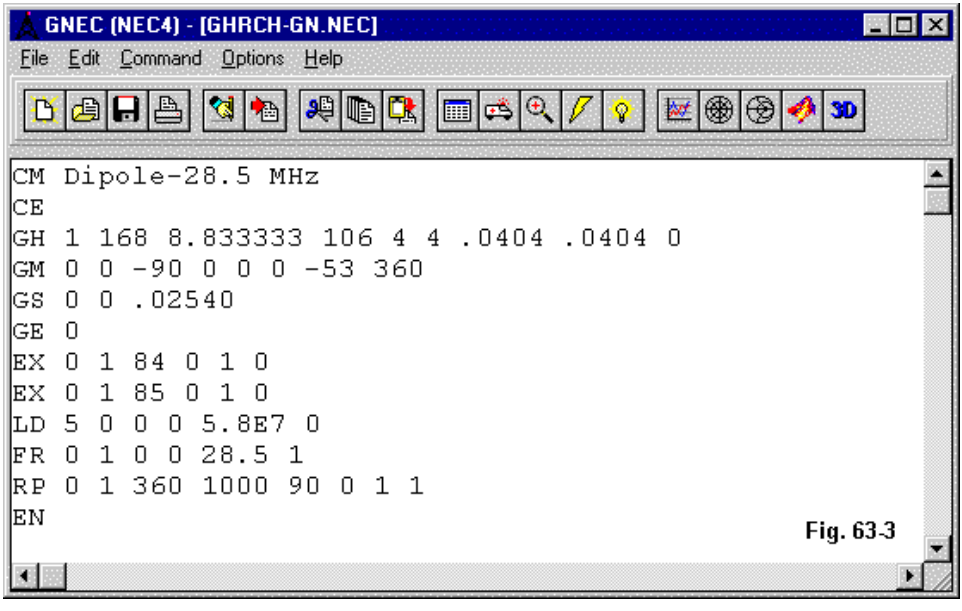

In the original model, we were not content to leave the helix extending from Z=0 to Z=106 (inches). Therefore, we rotated the helix -90 degrees on the X-axis, dis-

placed it by -53" on the Y-axis, and elevated it 360" on the Z-axis. We accomplished all of this with a single GM line input. For operations that act upon the entirety of the tags and segments within a model, there is no difference between the NEC-2 and the NEC-4 GM inputs. Therefore, in the final helical dipole model, the NEC-4 version will appear as in **Fig. 3**. See model 63-2.

To verify that the resulting model is identical to the one we produced in NEC-2 in the preceding column, we may take a truncated look at the NEC output file.

```
                    - - - STRUCTURE SPECIFICATION - - -

  WIRE                                                                    NO.
OF    FIRST  LAST     TAG
  NO.        X1        Y1        Z1         X2        Y2        Z2     RADIUS
SEG.     SEG.   SEG.     NO.
  1     THIS WIRE IS A LOG-SPIRAL OR HELIX                                168
1   168       1
 SPIRAL DATA: TURNS=     8.8333   LENGTH=   1.0600E+02   H.RAD=   4.0000E+00
4.0000E+00  W.RAD=  4.0400E-02  4.0400E-02
          TOTAL LENGTH OF WIRE IN THE SPIRAL =  2.45104E+02
      THE STRUCTURE HAS BEEN MOVED, GM COMMAND DATA IS -
       0    0 -90.00000   0.00000   0.00000   0.00000 -53.00000 360.00000    0
1    0  168
      STRUCTURE SCALED BY FACTOR   0.02540

                    - - - - SEGMENTATION DATA - - - -

  SEG.   COORDINATES OF SEG. CENTER     SEG.     ORIENTATION ANGLES    WIRE
CONNECTION DATA   TAG
  NO.       X         Y         Z       LENGTH     ALPHA     BETA      RADIUS
I-   I    I+    NO.
     1   0.09885  -1.33819   9.12752   0.03706  -62.79489 108.92291   0.00103
0    1    2      1
     2   0.08816  -1.32216   9.09635   0.03706  -52.48438 134.75235   0.00103
1    2    3      1
     3   0.06794  -1.30613   9.07032   0.03706  -37.67732 146.87851   0.00103
2    3    4      1
     4   0.04036  -1.29011   9.05227   0.03706  -21.29291 152.34449   0.00103
3    4    5      1
     5   0.00842  -1.27408   9.04414   0.03706   -4.34628 154.29633   0.00103
4    5    6      1
     6  -0.02443  -1.25806   9.04681   0.03706   12.69518 153.68493   0.00103
5    6    7      1
```

```
     7  -0.05463  -1.24203   9.05998   0.03706   29.44213 150.22438   0.00103
6    7    8      1
     8  -0.07893  -1.22600   9.08225   0.03706   45.24814 142.10108   0.00103
7    8    9      1
     9  -0.09470  -1.20998   9.11120   0.03706   58.42714 124.31186   0.00103
8    9   10      1
    10  -0.10022  -1.19395   9.14369   0.03706   64.37504  90.37231   0.00103
9   10   11      1
    11  -0.09490  -1.17792   9.17621   0.03706   58.62722  56.17145   0.00103
10  11   12      1
    12  -0.07932  -1.16190   9.20526   0.03706   45.52955  38.12187   0.00103
11  12   13      1
-------
    80   0.04264  -0.07212   9.05330   0.03706  -22.55679 152.07638   0.00103
79  80   81      1
    81   0.01091  -0.05609   9.04438   0.03706   -5.63326 154.24218   0.00103
80  81   82      1
    82  -0.02200  -0.04007   9.04623   0.03706   11.41384 153.81986   0.00103
81  82   83      1
    83  -0.05252  -0.02404   9.05865   0.03706   28.19970 150.61245   0.00103
82  83   84      1
    84  -0.07737  -0.00801   9.08030   0.03706   44.11422 142.96060   0.00103
83  84   85      1
    85  -0.09385   0.00801   9.10884   0.03706   57.60255 126.18027   0.00103
84  85   86      1
    86  -0.10018   0.02404   9.14119   0.03706   64.32866  93.34658   0.00103
85  86   87      1
    87  -0.09567   0.04007   9.17384   0.03706   59.40187  58.17071   0.00103
86  87   88      1
    88  -0.08082   0.05609   9.20326   0.03706   46.64635  39.04741   0.00103
87  88   89      1
    89  -0.05723   0.07212   9.22627   0.03706   30.98815  30.29622   0.00103
88  89   90      1
    90  -0.02744   0.08814   9.24039   0.03706   14.29461  26.50571   0.00103
89  90   91      1
-------
   157   0.01339   1.16190   9.04468   0.03706   -6.91958 154.17381   0.00103
156 157  158      1
   158  -0.01955   1.17792   9.04571   0.03706   10.13111 153.93953   0.00103
157 158  159      1
   159  -0.05038   1.19395   9.05737   0.03706   26.95266 150.97653   0.00103
158 159  160      1
   160  -0.07576   1.20998   9.07839   0.03706   42.96775 143.77077   0.00103
159 160  161      1
   161  -0.09294   1.22600   9.10652   0.03706   56.74138 127.94746   0.00103
160 161  162      1
```

```
   162  -0.10008   1.24203   9.13869   0.03706   64.20848  96.30087   0.00103
161  162  163      1
   163  -0.09639   1.25806   9.17144   0.03706   60.13303  60.27713   0.00103
162  163  164      1
   164  -0.08227   1.27408   9.20123   0.03706   47.74816  40.02950   0.00103
163  164  165      1
   165  -0.05926   1.29011   9.22482   0.03706   32.21887  30.74264   0.00103
164  165  166      1
   166  -0.02984   1.30613   9.23967   0.03706   15.57213  26.67627   0.00103
165  166  167      1
   167   0.00281   1.32216   9.24418   0.03706   -1.44894  25.63317   0.00103
166  167  168      1
   168   0.03516   1.33819   9.23785   0.03706  -18.43862  27.12109   0.00103
167  168    0      1
```

The values are essentially the very same as those we developed in the NEC-2 model for the helical dipole. Indeed, NEC-4 returned a source impedance of 22.6 - j 2.1 Ohms, with a free-space gain of 1.73 dBi. The NEC-2 model returned the same gain with a source impedance of 22.6 - j 1.9 Ohms.

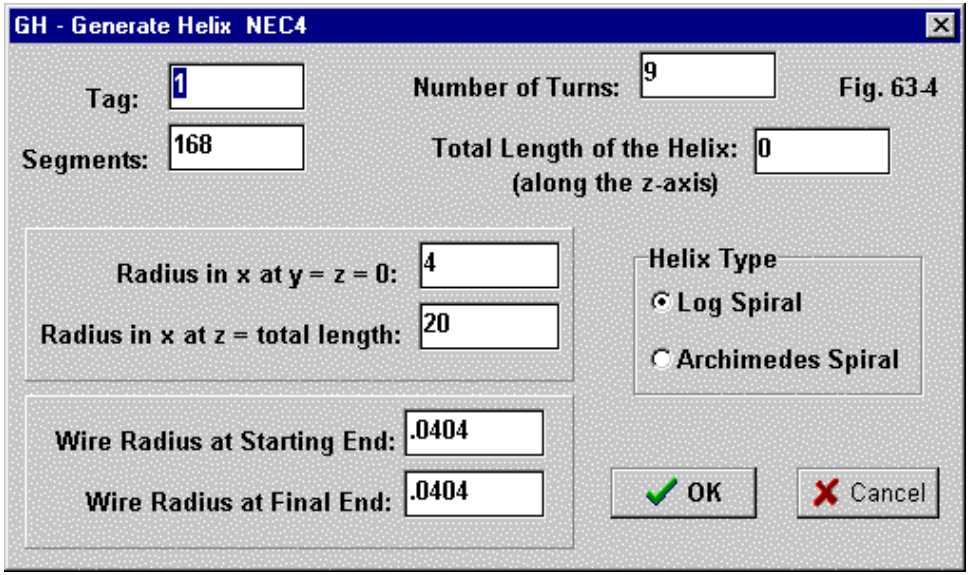

Log vs. Archimedes Spirals

If we set HR1 and HR2 to different values, we obtain a spiral structure. Only if we set the helix length (ZLEN) to zero will we obtain a flat spiral. Just for the exercise, lets create a flat spiral with a starting radius of 4" and a final radius of 20". In fact, either HR1 or HR2 may be the larger or the smaller figure. However, if HR2=0, then its values becomes the value of HR1. Hence, for a nearly closed end to HR2, we must use a very low number, but one greater than zero.

For the sake of simplicity, we shall use a constant wire radius throughout and retain the 168 total segment count. In addition, we shall specify 9 turns for our spiral. The resulting help screen version of the new GH line will look like **Fig. 63-4**.

The only remaining option is whether to choose a log spiral (entry = 0) or an Archimedes spiral (entry = 1) in the ISPX position. The differences in the ways of calculating rate of spiraling lie in the development of a new radius based on the preceding radius using a program-calculated constant.

$$\textit{log spiral}\,(0): r = r_1\, a^{\theta} \qquad \textit{Archimedes spiral}\,(1): r = r_1 + a\theta$$

In practical terms, alternately selecting between the two spirals and leaving the other spiral-determining factors constant results in the two spirals shown in **Fig. 63-5**.

The differential in spacing between the successive rings of the two spirals is clearly apparent. However, there are other features worth noting. In both spirals, the segment lengths increase at the same rate from the innermost point to the outer limit. The selection of the number of turns and the number of total segments results in segment junctions that do not align particularly well. For the highest accuracy when using closely spaced wire segments, segment junction should be aligned as closely as possible. With 171 segments, the junctions would align at 19 segments per turn.

All other recommendations and limitations applicable to wires set up with the GW input apply to the GH input. The user should be especially aware of these limitations when using closely spaced spiral rings in conjunction with sizable wire

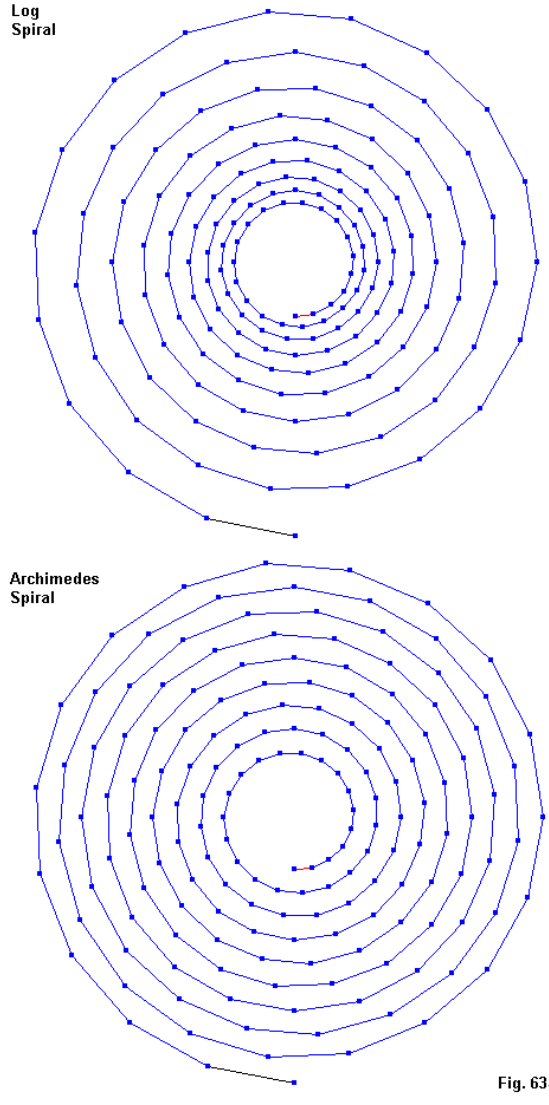

Fig. 63-5

radii. The log spiral may prove tricky unless the modeler pays close attention to the innermost rings and their spacing. The following extract from the NEC output report tracks the first 2 and the final 2 rings of the log spiral in our example as a sample of the ring-spacing differentials that may emerge.

```
                    - - - STRUCTURE SPECIFICATION - - -

  WIRE                                                                    NO.
OF    FIRST  LAST     TAG
  NO.       X1        Y1        Z1         X2        Y2        Z2     RADIUS
SEG.     SEG.   SEG.     NO.
  1     THIS WIRE IS A LOG-SPIRAL OR HELIX                                168
1   168       1
 SPIRAL DATA: TURNS=     9.0000   LENGTH=   0.0000E+00   H.RAD=   4.0000E+00
2.0000E+01  W.RAD=  4.0400E-02  4.0400E-02
          TOTAL LENGTH OF WIRE IN THE SPIRAL =  5.59747E+02
      STRUCTURE SCALED BY FACTOR   0.02540

   TOTAL SEGMENTS USED=  168    NO. SEG. IN A SYMMETRIC CELL=  168    SYMMETRY
FLAG=  0

                - - - - SEGMENTATION DATA - - - -

                        COORDINATES IN METERS

  SEG.   COORDINATES OF SEG. CENTER     SEG.     ORIENTATION ANGLES    WIRE
CONNECTION DATA   TAG
  NO.       X         Y         Z       LENGTH     ALPHA     BETA      RADIUS
I-   I    I+    NO.
     1   0.09921   0.01694   0.00000   0.03421    0.00000  98.02802   0.00103
0    1    2      1
     2   0.08890   0.04923   0.00000   0.03454    0.00000 117.31374   0.00103
1    2    3      1
     3   0.06830   0.07655   0.00000   0.03488    0.00000 136.59945   0.00103
2    3    4      1
     4   0.03956   0.09573   0.00000   0.03521    0.00000 155.88516   0.00103
3    4    5      1
     5   0.00578   0.10442   0.00000   0.03555    0.00000 175.17088   0.00103
4    5    6      1
     6  -0.02931   0.10143   0.00000   0.03589    0.00000-165.54341   0.00103
5    6    7      1
     7  -0.06176   0.08689   0.00000   0.03624    0.00000-146.25769   0.00103
6    7    8      1
```

```
     8  -0.08783   0.06221   0.00000   0.03659    0.00000-126.97198   0.00103
7    8    9       1
     9  -0.10444   0.03000   0.00000   0.03694    0.00000-107.68626   0.00103
8    9   10       1
    10  -0.10953  -0.00624   0.00000   0.03730    0.00000 -88.40055   0.00103
9   10   11       1
    11  -0.10230  -0.04247   0.00000   0.03765    0.00000 -69.11484   0.00103
10  11   12       1
    12  -0.08333  -0.07459   0.00000   0.03802    0.00000 -49.82912   0.00103
11  12   13       1
    13  -0.05454  -0.09886   0.00000   0.03838    0.00000 -30.54341   0.00103
12  13   14       1
    14  -0.01900  -0.11240   0.00000   0.03875    0.00000 -11.25769   0.00103
13  14   15       1
    15   0.01937  -0.11345   0.00000   0.03913    0.00000   8.02802   0.00103
14  15   16       1
    16   0.05629  -0.10166   0.00000   0.03950    0.00000  27.31374   0.00103
15  16   17       1
    17   0.08754  -0.07810   0.00000   0.03988    0.00000  46.59945   0.00103
16  17   18       1
    18   0.10947  -0.04524   0.00000   0.04027    0.00000  65.88516   0.00103
17  18   19       1
    19   0.11941  -0.00661   0.00000   0.04065    0.00000  85.17088   0.00103
18  19   20       1
    20   0.11599   0.03352   0.00000   0.04105    0.00000 104.45659   0.00103
19  20   21       1
    21   0.09936   0.07062   0.00000   0.04144    0.00000 123.74231   0.00103
20  21   22       1
    22   0.07114   0.10043   0.00000   0.04184    0.00000 143.02802   0.00103
21  22   23       1
    23   0.03430   0.11943   0.00000   0.04224    0.00000 162.31374   0.00103
22  23   24       1
    24  -0.00714   0.12525   0.00000   0.04265    0.00000-178.40055   0.00103
23  24   25       1
    25  -0.04857   0.11698   0.00000   0.04306    0.00000-159.11484   0.00103
24  25   26       1
    26  -0.08529   0.09529   0.00000   0.04347    0.00000-139.82912   0.00103
25  26   27       1
    27  -0.11305   0.06236   0.00000   0.04389    0.00000-120.54341   0.00103
26  27   28       1
    28  -0.12853   0.02173   0.00000   0.04431    0.00000-101.25769   0.00103
27  28   29       1
    29  -0.12973  -0.02215   0.00000   0.04474    0.00000 -81.97198   0.00103
28  29   30       1
    30  -0.11625  -0.06437   0.00000   0.04517    0.00000 -62.68626   0.00103
29  30   31       1
```

```
    31  -0.08931  -0.10011   0.00000   0.04561    0.00000 -43.40055   0.00103
30   31   32      1
    32  -0.05173  -0.12518   0.00000   0.04605    0.00000 -24.11484   0.00103
31   32   33      1
    33  -0.00756  -0.13654   0.00000   0.04649    0.00000  -4.82912   0.00103
32   33   34      1
    34   0.03833  -0.13264   0.00000   0.04694    0.00000  14.45659   0.00103
33   34   35      1
    35   0.08076  -0.11362   0.00000   0.04739    0.00000  33.74231   0.00103
34   35   36      1
    36   0.11485  -0.08135   0.00000   0.04784    0.00000  53.02802   0.00103
35   36   37      1
```

```
   133   0.29053   0.20650   0.00000   0.12117    0.00000 123.74231   0.00103
132  133  134      1
   134   0.20801   0.29367   0.00000   0.12234    0.00000 143.02802   0.00103
133  134  135      1
   135   0.10030   0.34922   0.00000   0.12352    0.00000 162.31374   0.00103
134  135  136      1
   136  -0.02087   0.36624   0.00000   0.12471    0.00000-178.40055   0.00103
135  136  137      1
   137  -0.14201   0.34206   0.00000   0.12591    0.00000-159.11484   0.00103
136  137  138      1
   138  -0.24940   0.27862   0.00000   0.12712    0.00000-139.82912   0.00103
137  138  139      1
   139  -0.33057   0.18235   0.00000   0.12834    0.00000-120.54341   0.00103
138  139  140      1
   140  -0.37583   0.06354   0.00000   0.12958    0.00000-101.25769   0.00103
139  140  141      1
   141  -0.37934  -0.06477   0.00000   0.13082    0.00000 -81.97198   0.00103
140  141  142      1
   142  -0.33991  -0.18822   0.00000   0.13208    0.00000 -62.68626   0.00103
141  142  143      1
   143  -0.26116  -0.29271   0.00000   0.13335    0.00000 -43.40055   0.00103
142  143  144      1
   144  -0.15127  -0.36603   0.00000   0.13464    0.00000 -24.11484   0.00103
143  144  145      1
   145  -0.02210  -0.39926   0.00000   0.13593    0.00000  -4.82912   0.00103
144  145  146      1
   146   0.11208  -0.38785   0.00000   0.13724    0.00000  14.45659   0.00103
145  146  147      1
   147   0.23614  -0.33223   0.00000   0.13856    0.00000  33.74231   0.00103
146  147  148      1
   148   0.33582  -0.23787   0.00000   0.13990    0.00000  53.02802   0.00103
147  148  149      1
```

```
   149   0.39934  -0.11470   0.00000   0.14124    0.00000  72.31374   0.00103
148  149  150      1
   150   0.41881   0.02386   0.00000   0.14260    0.00000  91.59945   0.00103
149  150  151      1
   151   0.39115   0.16239   0.00000   0.14398    0.00000 110.88516   0.00103
150  151  152      1
   152   0.31861   0.28519   0.00000   0.14536    0.00000 130.17088   0.00103
151  152  153      1
   153   0.20852   0.37802   0.00000   0.14676    0.00000 149.45659   0.00103
152  153  154      1
   154   0.07266   0.42978   0.00000   0.14817    0.00000 168.74231   0.00103
153  154  155      1
   155  -0.07407   0.43379   0.00000   0.14960    0.00000-171.97198   0.00103
154  155  156      1
   156  -0.21524   0.38869   0.00000   0.15104    0.00000-152.68626   0.00103
155  156  157      1
   157  -0.33473   0.29864   0.00000   0.15250    0.00000-133.40055   0.00103
156  157  158      1
   158  -0.41857   0.17298   0.00000   0.15396    0.00000-114.11484   0.00103
157  158  159      1
   159  -0.45656   0.02527   0.00000   0.15545    0.00000 -94.82912   0.00103
158  159  160      1
   160  -0.44352  -0.12817   0.00000   0.15694    0.00000 -75.54341   0.00103
159  160  161      1
   161  -0.37992  -0.27003   0.00000   0.15845    0.00000 -56.25769   0.00103
160  161  162      1
   162  -0.27201  -0.38402   0.00000   0.15998    0.00000 -36.97198   0.00103
161  162  163      1
   163  -0.13116  -0.45666   0.00000   0.16152    0.00000 -17.68626   0.00103
162  163  164      1
   164   0.02729  -0.47892   0.00000   0.16307    0.00000   1.59945   0.00103
163  164  165      1
   165   0.18570  -0.44730   0.00000   0.16464    0.00000  20.88516   0.00103
164  165  166      1
   166   0.32612  -0.36434   0.00000   0.16623    0.00000  40.17088   0.00103
165  166  167      1
   167   0.43228  -0.23845   0.00000   0.16783    0.00000  59.45659   0.00103
166  167  168      1
   168   0.49146  -0.08309   0.00000   0.16944    0.00000  78.74231   0.00103
167  168    0      1
```

Another advantage of aligning the segment junctions is that one can more easily calculate the spacing between rings by using aligned segment centers from the table.

A Reversible Yagi: The NEC-4 GM Input

We have so far overlooked the final 4 entry positions in the NEC-4 GM card. The structure of the GM input follows this model:

```
GM   ITG1   NRPT   ROX   ROY   ROZ   XS   YS   ZS   IT1   IS1   IT2   IS2
     I1     I2     F1    F2    F3    F4   F5   F6   F7    F8    F9    F10
```

Up through floating decimal input F6, the GM input line is identical to the NEC-2 version. However, NEC-4 uses 4 final places to input the start and stop tag numbers and segments numbers for the structure to be copied and replicated at a new position (and orientation). Omission of these 4 entries results in the movement or duplication of all segments in the model. We used this feature in our first example.

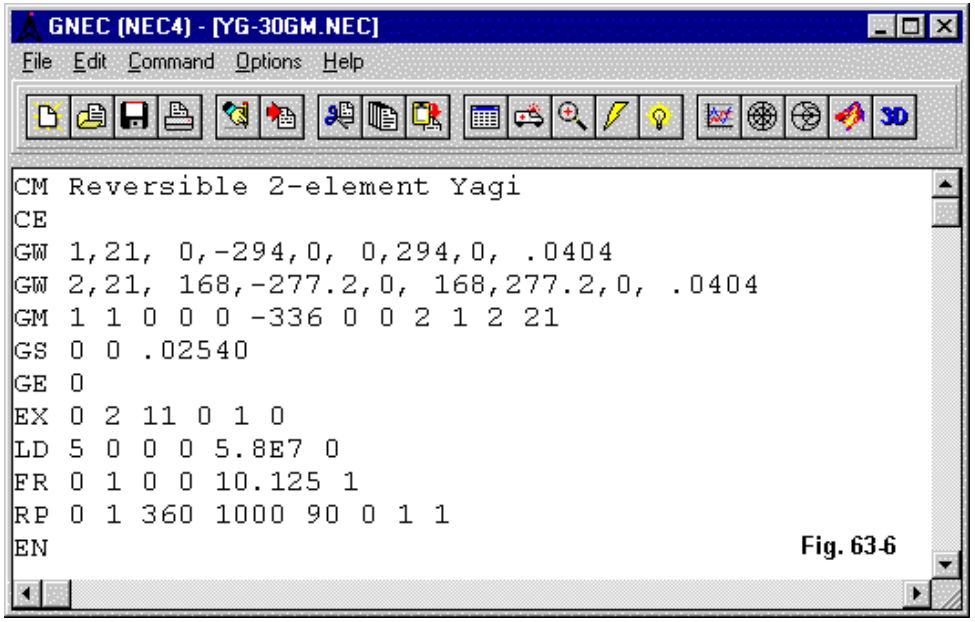

Fig. 63-6

If IT1 is zero, then IS1 refers to the absolute segment number in the model. If IT1 is greater than zero, then IS1 refers to the relative (tag-number-related) segment number specified, except that an IS1 value of zero in this case becomes a value of 1. Similar rules apply to IS2, with IT2 referring to the last tag number in the range. If IT2 and IS2 are both zero, the range extends to the last segment defined in the model up to the entry of the GM line.

Let's use a simple example of a reversible 2-element Yagi. Such antennas are sometimes used in the lower HF range and made from wire. A permanent installation would not be rotatable, and so one might install alternative driver elements, one on each side of a common reflector wire. The unused driver would have small effects on the overall pattern of the antenna, relative to its omission.

Fig. 63-6 shows the model to be used for this antenna. We create two wires by standard GW entries. The longer wire (GW 1) is obviously the reflector. The shorter

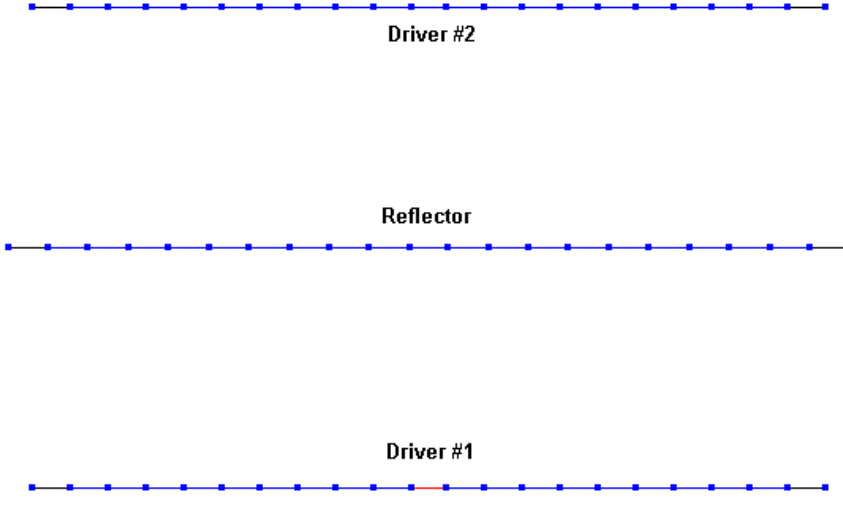

Fig. 63-7

wire (GW 2) defines one driver, spaced 168" from the reflector for this 10.125-MHz array. See model 63-3.

Although we save no modeling space, let's use the GM input to define the third wire, that is, the alternate driver. We shall want this driver to be a new structure and

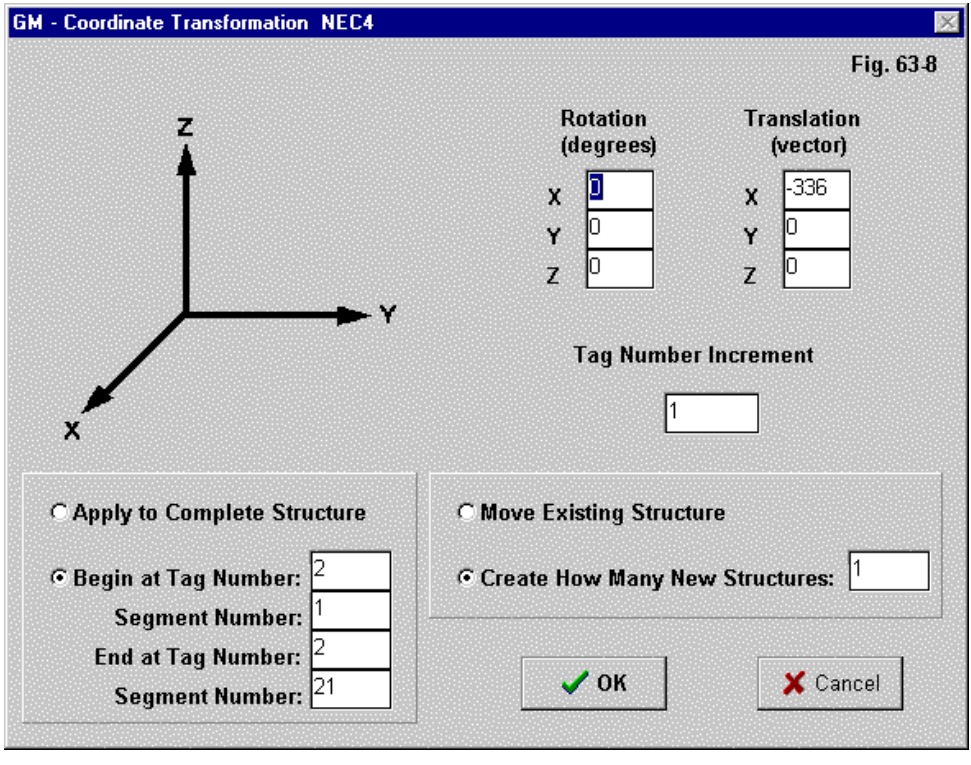

to have its own tag number. There, we specific a tag increment of 1 and also 1 new structure. Since we wish to space the wire equally distant from the reflector, but on the opposite side, we order a translation of 336" along the X-axis.

The final 4 entries show the tag and segment numbers for the start and stop of the existing wire to be duplicated and moved. If we look at the antenna view graphic,

we get a picture of the total final model shown in **Fig. 63-7** (minus the identifications of the element functions).

The addition of the 4 places to the GM line offers some interesting possibilities for the modeler. In NEC-2, we could only duplicate and move entire structures defined by a tag number. However, NEC-4 permits us to duplicate partial structures within the limits of a given tag number. Indeed, there is no restriction against beginning in the middle of one tag number and ending in the middle of another.

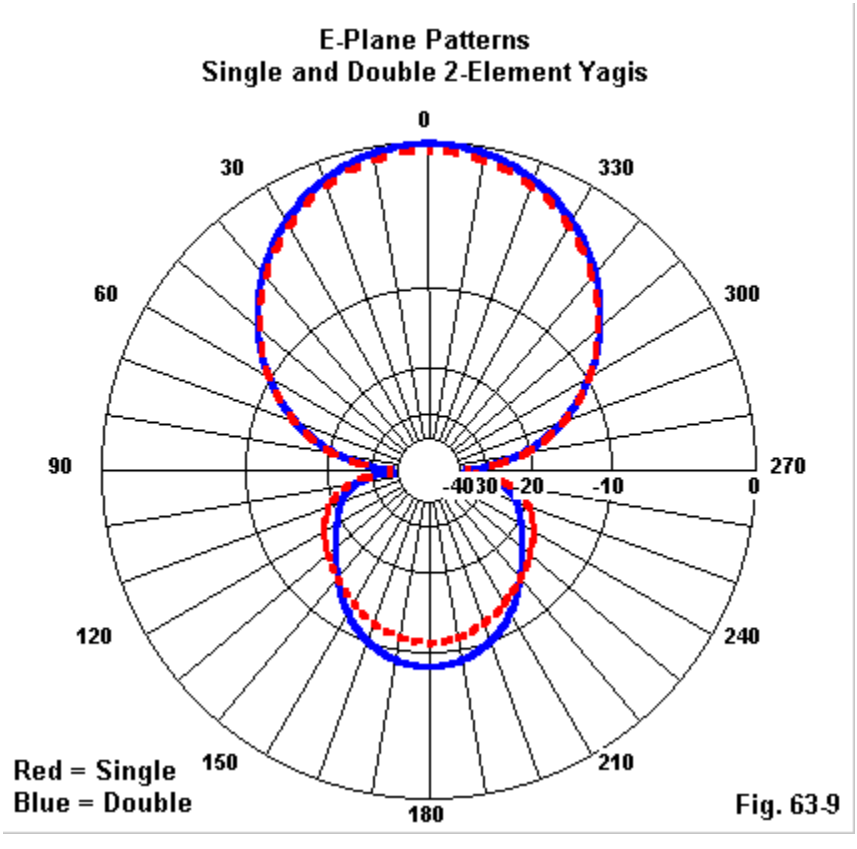

Fig. 63-9

Fig. 63-8 shows the GM help screen with the start-stop entries opened. We might have begun with tag 1, segment 11 and ended with tag 2, segment 8 (although in the context of our example, I cannot think of a reason for doing so). (Those interested may wish to open the help screen for the GM line in our first example. There we only rotated and translated an existing structure. The differences between that help screen and the present one may be useful in becoming accustomed to the differing appearances of the GM lines in that example and this one.)

Since we have only specified a single source, we may run the model both with and without the GM input line. **Fig. 63-9** compares the free-space E-plane pattern for the original 2-element wire Yagi and the new reversible model. The effects of the undriven alternate driver are clear in its slight addition to gain and the slight decrease in front-to-back ratio.

In order to obtain the reverse-direction pattern, we need only alter the source location on the EX input line. Instead of specifying tag 2, we would enter tag 3 in the second entry position. (See **Fig. 63-6**.)

Conclusion

We have used simple models in this exercise because our aim was to illustrate the differences between the NEC-4 and the NEC-2 formats and functions for the GH and GM entries. The true utility of these geometry entry lines begins to emerge when our structures become far more complex. Consider creating a rectangular grid of wires. First, create 3 sides of one grid square with 3 GW entries. Then duplicate the second 2 wires in a single GM line as many times as it takes to make a single row of grid squares, each with an open bottom edge. Now, with a second GM line, duplicate the entire row as many times as it takes to fill the rectangular plane. Since the bottoms of the last row of squares are all open, let's enter a GW line to close the first square. Now add a final GM line to duplicate this line and close the remaining square bottoms. The model remains at a constant ASCII input size whether we are creating a 5-by-5 grid or a 50-by-50 grid. However, since every new GM structure replicates wires and segments, the core run times will be quite different for the two sizes of wire grids.

One common practice among modelers is to run the same model on both NEC-2 and NEC-4, sometimes to detect any differences between results and thereby catch any sensitivity of the model to limitations of the programs. We may perform such tests only where the entry lines for the model are the same for both NEC-2 and NEC-4. A model using only GW entries for the wire geometry and simple control input entries are amenable to being run in both programs without modification. (As an example of a control card difference, the LD 5 entry, which handles material conductivity, has an extra entry for permeability in the NEC-4 version. It is best to remove that final entry before running the NEC-4 model in NEC-2.)

However, there are many subtle differences in the advanced input structures for lines having the same identification letters within NEC-2 and NEC-4. We have sampled a few of those differences as they relate to the GH and GM inputs. There are many others, and numerous ones apply to the control inputs. If these small exercises have made you a bit self-conscious about the input line differences among the NEC cores, then they will have done some useful work.

* * * * *

Models included: 63-1 through 63-3. (Models available in .NEC format only and will run correctly only in NEC-4.)

64. An Orientation to the NEC Output File

Most beginning NEC modelers employ one of the entry-level programs, such as EZNEC or NEC-Win Plus. These programs are amazing pieces of software for a number of reasons. They ease the task of inputting the information necessary to create a model. As well, they provide a mass of distilled output data that the user most wants and re-forms it into tables and graphics that make it the most readable. One cost of having so much convenience is that the entry-level programs must restrict the number of wire geometry and control inputs made available to the user.

Because the entry-level programs are so convenient, many users have little idea of what is going on behind the scenes to create the graphics and tables. They may never look at the output file produced by the NEC core that is doing the calculating (except for some post-run additional calculations for user convenience). So I thought that we might take a look at an output file and see what it can tell us—or at least show us from where the output functions of our modeling program gets their information.

EZNEC (short of the Pro version) does not give the user easy access to the NEC output file. The most recent output file is accessible via the "View File" facility. However, the NEC output file is stored for each model and is always accessible in NEC-Win Plus and in advanced programs. So we shall be looking at NEC-Win programs in this exercise. We shall use both NEC-Win Plus and NEC-Win Pro, although both produce an output file with the extension .NOU to save the core-run output. (A core "run" is simply the operation of the NEC calculating portion of the overall program, which shows only as thermometer bars in EZNEC and as a temporary sub-screen in NEC-Win software.)

Let's begin with a small model, the one shown in NEC-Win Plus format in **Fig. 64-1**. The wire layout consists of 2 wires for a 30-meter Yagi. The wire has a diameter of 2 mm (0.0787"), and the dimensions are all in meters. The wire is copper, and the source is at the center of wire 1. The upper left corner lets us know that we shall run the antenna at 10.125 MHz only. The "No Ground" label tells us the antenna is in free space. We have requested 2 radiation patterns. Modeling con-

ventions designate them as azimuth and elevation patterns, but in free space, they are best termed E-plane and H-plane patterns, respectively. See model 64-1.

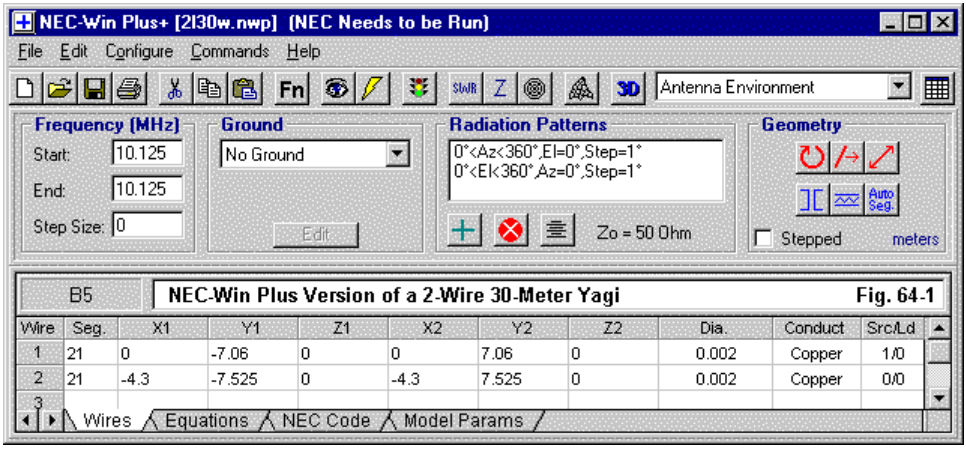

Fig. 2 shows the modeling outline of the array. Each element has 21 equal-length segments. The red source segment is at the center of the element designated as the driver. Since the remaining element is longer, it functions as a reflector.

NEC functions with neither of these forms of model set-up. The .NWP file for the model in **Fig. 64-1** is in spreadsheet format, while the outline is a graphic. NEC requires a simple ASCII file consisting of lines of characters meeting certain standards. The standards for input data vary according to the type of line.

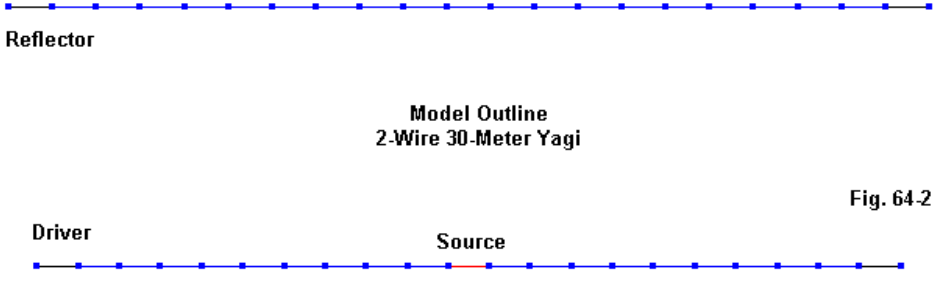

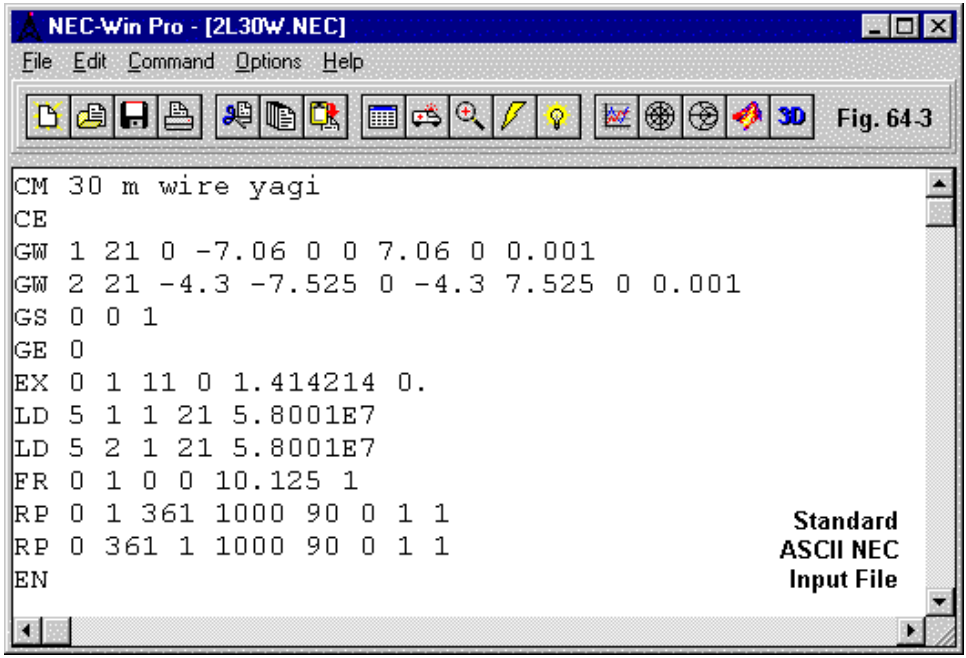

NEC-Win Plus creates an input file for the model that has the very same form as one that we might create by typing into a simple text editor. This file has the format used by NEC-Win Pro and other advanced programs that give the user access to all of the geometry and control inputs that are usable with NEC. (See **Fig. 64-3**.) The GW lines provide the coordinates of the wires, the number of segments in them, and the wire radius (1 mm). Since all dimensions are already in meters, the GS or scaling line uses a factor of 1.

The EX line provides data for the voltage source, specifying its location on wire or tag 1, segment 11, with a magnitude of 1.414 and a phase angle of zero. Each wire or tag has a corresponding LD5 line to specify that the wires have the conductivity of copper (5.8E7 s/m). The FR line sets the single frequency of the calculations, while the two RP0 lines request standard azimuth and elevation patterns. The former is at zero degrees elevation, while the latter is at an azimuth angle of zero degrees. However, these patterns—in basic NEC terms—are really phi and theta

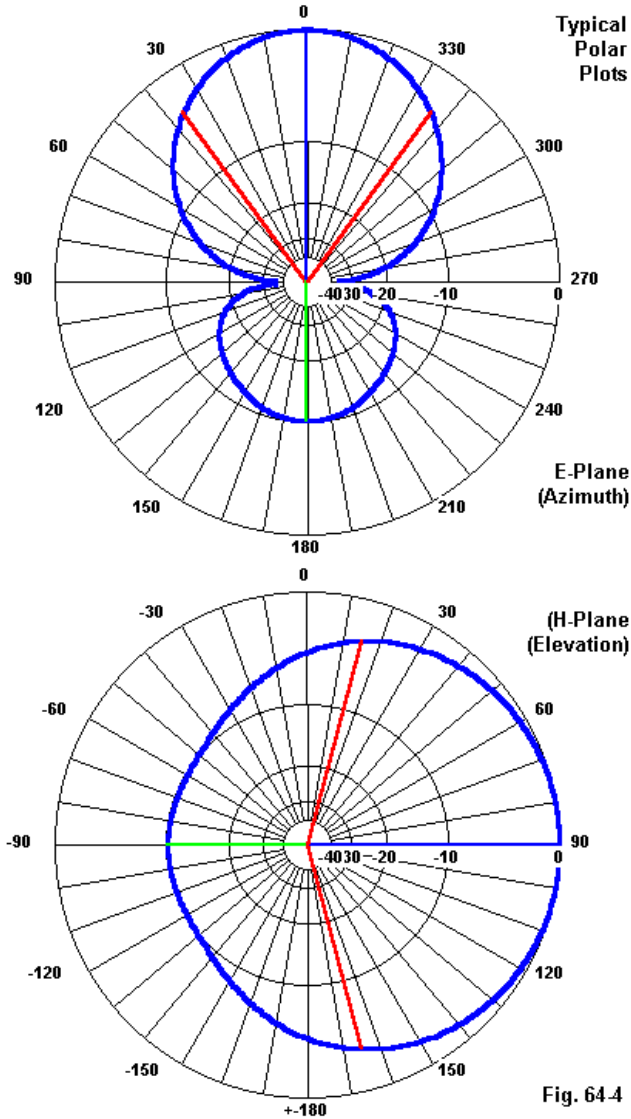
Typical
Polar
Plots
0
30
330
60
300
90
270
120
240
150
210
180
-40
-30
-20
-10
0
E-Plane
(Azimuth)
0
-30
30
(H-Plane
(Elevation)
-60
60
-90
90
-120
120
-150
150
+-180

Fig. 64-4

patterns. The give-away is the "90" entry, which specifies the theta angle for the phi, counting from overhead to the horizon. In the theta pattern itself, the 90-degree entry simply specifies the starting point for the pattern data. Both patterns request 361 data points so that the total pattern will close on itself and not leave a 1-degree gap.

Fig. 64-4 shows the resulting E-plane and H-plane (azimuth/phi and elevation/theta) patterns that emerge from the core calculations. The E-plane pattern counts degrees in a counter-clockwise direction, indicating a phi rather than a true azimuth pattern. The H-plane pattern shows 90 degrees at the virtual horizon, with 0 degrees at the top, indicating its true identity as a theta and not an elevation pattern.

Fig. 64-5

```
---- VSWR ----
Source at Tag 1, Segment 11
Frequency = 10.125
Characteristic Impedance = 50.00  Ohms
Input Impedance:
  Real(Z) = 49.498   , Imag(Z)  = 1.713
  Mag(Z)  = 49.528   , Phase(Z) = 1.982
VSWR = 1.04
```

Typical Partial Data Readout

Most programs provide the user with selected tabular data. **Fig. 64-5** shows the VSWR report from NEC-Win Pro. Invisible to the user is the fact that only some of the reported data comes from the NEC calculations directly: the information on the input impedance. The VSWR figure comes from a post-run calculation made by the program and dependent upon the user's insertion of an impedance reference figure.

What the Core Output Looks Like and Tells Us

With this much orientation, let's turn to the actual NEC output file for this model and see what it looks like and what it has to tell us—and where it is silent. The report is an ASCII document, making it convenient for moving part or all of the data into

other programs for viewing or manipulation. The best place to begin is at the beginning of the file created by the core run.

```
 ********************************************
    NUMERICAL ELECTROMAGNETICS CODE (NEC-2D-P)
 ********************************************
 Enhanced version, copyright 1997-2001 Nittany Scientific
 Run date:  08:39:25 on 04-JUN-2002

 Parameter dimensions:
   NEC2D Version:  2.5
   Maximum # of segments:            42
   Maximum # of segments in core:            42
   Maximum # of new connections to NGF segments:           180
   Maximum # of sources:             1
   Maximum # of degrees of symmetry:             1
   Maximum # of networks:             0
   Maximum # of segments at a junction:             1
   Maximum # of loads:             2
   Maximum # of frequencies or angles:           361

 ********************************************
```

The NEC calculation core operates best when certain parameters are at least as large as required by the size of the model but not so much larger that they slow down the speed of the matrix and other calculations made by the core. Originally set by a separate file, most implementations of NEC-2 use an automated system of setting the parameters.

```
                    - - - STRUCTURE SPECIFICATION - - -

                       COORDINATES MUST BE INPUT IN
                       METERS OR BE SCALED TO METERS
                      BEFORE STRUCTURE INPUT IS ENDED

  WIRE                                                                    NO.
OF    FIRST  LAST     TAG
  NO.       X1         Y1         Z1         X2         Y2         Z2      RADIUS
SEG.     SEG.    SEG.     NO.
  1   0.00000   -7.06000   0.00000    0.00000   7.06000   0.00000   0.00100
21        1    21       1
```

```
  2   -4.30000   -7.52500    0.00000    -4.30000    7.52500    0.00000    0.00100
21        22     42        2
      STRUCTURE SCALED BY FACTOR    1.00000

   TOTAL SEGMENTS USED=   42     NO. SEG. IN A SYMMETRIC CELL=   42     SYMMETRY
FLAG=  0
```

The first entry in the output file is a record of the wire geometry of the model. Due to format limitations, the individual report lines are broken into 2 text lines. This section serves as an important check for the modeler to discover whether the intended model actually materialized. Note that the core assigns each wire a tag number. These will normally be the same as the wire numbers, but not when implementing certain complex structures.

As well, the structure section of the report assigns to each segment in the model an absolute segment number. The tag number serves as a way of tracking the location of the absolute segments within the model.

```
                        - - - - SEGMENTATION DATA - - - -
                              COORDINATES IN METERS
                  I+ AND I- INDICATE THE SEGMENTS BEFORE AND AFTER I


  SEG.     COORDINATES OF SEG. CENTER       SEG.     ORIENTATION ANGLES    WIRE
CONNECTION DATA    TAG
  NO.         X          Y          Z        LENGTH     ALPHA     BETA      RADIUS
I-    I     I+     NO.
     1    0.00000   -6.72381    0.00000    0.67238    0.00000  90.00000   0.00100
0     1     2       1
     2    0.00000   -6.05143    0.00000    0.67238    0.00000  90.00000   0.00100
1     2     3       1
     3    0.00000   -5.37905    0.00000    0.67238    0.00000  90.00000   0.00100
2     3     4       1
     4    0.00000   -4.70667    0.00000    0.67238    0.00000  90.00000   0.00100
3     4     5       1
     5    0.00000   -4.03429    0.00000    0.67238    0.00000  90.00000   0.00100
4     5     6       1
     6    0.00000   -3.36190    0.00000    0.67238    0.00000  90.00000   0.00100
5     6     7       1
     7    0.00000   -2.68952    0.00000    0.67238    0.00000  90.00000   0.00100
6     7     8       1
     8    0.00000   -2.01714    0.00000    0.67238    0.00000  90.00000   0.00100
7     8     9       1
```

```
    9   0.00000  -1.34476   0.00000   0.67238   0.00000  90.00000  0.00100
8    9   10      1
   10   0.00000  -0.67238   0.00000   0.67238   0.00000  90.00000  0.00100
9   10   11      1
   11   0.00000   0.00000   0.00000   0.67238   0.00000  90.00000  0.00100
10  11   12      1
   12   0.00000   0.67238   0.00000   0.67238   0.00000  90.00000  0.00100
11  12   13      1
   13   0.00000   1.34476   0.00000   0.67238   0.00000  90.00000  0.00100
12  13   14      1
   14   0.00000   2.01714   0.00000   0.67238   0.00000  90.00000  0.00100
13  14   15      1
   15   0.00000   2.68952   0.00000   0.67238   0.00000  90.00000  0.00100
14  15   16      1
   16   0.00000   3.36190   0.00000   0.67238   0.00000  90.00000  0.00100
15  16   17      1
   17   0.00000   4.03429   0.00000   0.67238   0.00000  90.00000  0.00100
16  17   18      1
   18   0.00000   4.70667   0.00000   0.67238   0.00000  90.00000  0.00100
17  18   19      1
   19   0.00000   5.37905   0.00000   0.67238   0.00000  90.00000  0.00100
18  19   20      1
   20   0.00000   6.05143   0.00000   0.67238   0.00000  90.00000  0.00100
19  20   21      1
   21   0.00000   6.72381   0.00000   0.67238   0.00000  90.00000  0.00100
20  21    0      1
    22   -4.30000   -7.16667    0.00000    0.71667    0.00000  90.00000
0.00100     0   22   23      2
    23   -4.30000   -6.45000    0.00000    0.71667    0.00000  90.00000
0.00100    22   23   24      2
    24   -4.30000   -5.73333    0.00000    0.71667    0.00000  90.00000
0.00100    23   24   25      2
    25   -4.30000   -5.01667    0.00000    0.71667    0.00000  90.00000
0.00100    24   25   26      2
    26   -4.30000   -4.30000    0.00000    0.71667    0.00000  90.00000
0.00100    25   26   27      2
    27   -4.30000   -3.58333    0.00000    0.71667    0.00000  90.00000
0.00100    26   27   28      2
    28   -4.30000   -2.86667    0.00000    0.71667    0.00000  90.00000
0.00100    27   28   29      2
    29   -4.30000   -2.15000    0.00000    0.71667    0.00000  90.00000
0.00100    28   29   30      2
    30   -4.30000   -1.43333    0.00000    0.71667    0.00000  90.00000
0.00100    29   30   31      2
    31   -4.30000   -0.71667    0.00000    0.71667    0.00000  90.00000
0.00100    30   31   32      2
```

```
   32   -4.30000    0.00000    0.00000    0.71667    0.00000  90.00000   0.00100
31   32   33       2
   33   -4.30000    0.71667    0.00000    0.71667    0.00000  90.00000   0.00100
32   33   34       2
   34   -4.30000    1.43333    0.00000    0.71667    0.00000  90.00000   0.00100
33   34   35       2
   35   -4.30000    2.15000    0.00000    0.71667    0.00000  90.00000   0.00100
34   35   36       2
   36   -4.30000    2.86667    0.00000    0.71667    0.00000  90.00000   0.00100
35   36   37       2
   37   -4.30000    3.58333    0.00000    0.71667    0.00000  90.00000   0.00100
36   37   38       2
   38   -4.30000    4.30000    0.00000    0.71667    0.00000  90.00000   0.00100
37   38   39       2
   39   -4.30000    5.01667    0.00000    0.71667    0.00000  90.00000   0.00100
38   39   40       2
   40   -4.30000    5.73333    0.00000    0.71667    0.00000  90.00000   0.00100
39   40   41       2
   41   -4.30000    6.45000    0.00000    0.71667    0.00000  90.00000   0.00100
40   41   42       2
   42   -4.30000    7.16667    0.00000    0.71667    0.00000  90.00000   0.00100
41   42    0       2
```

The segmentation information is useful in determining whether all aspects of the geometric structure wind up where you intend. The present straight-wire model offers no question marks, but catenary wires, arcs, and helices can present many questions that an examination of the segmentation can answer. Note, however, that the information specifies the center point of each segment on the cartesian coordinate system—not the segment ends or junctions. However, the +/-I list provides a list of connections, which can be useful in determining whether all segments having a desired junction actually hit the junction point.

The presence of a GE entry indicates the end of the geometry section. At this point, the output report records the control inputs as a series of line entries. Note that all of the numeric entries that fall into floating decimal positions take on engineering notation. Hence, the frequency in the FR line is no longer 10.125, but 1.01250E+01.

```
 ***** DATA CARD NO.   1 EX     0     1    11     0  1.41421E+00  0.00000E+00
0.00000E+00  0.00000E+00
0.00000E+00  0.00000E+00
```

```
 ***** DATA CARD NO.   2 LD     5     1     1    21  5.80010E+07  0.00000E+00
0.00000E+00  0.00000E+00
0.00000E+00  0.00000E+00
 ***** DATA CARD NO.   3 LD     5     2     1    21  5.80010E+07  0.00000E+00
0.00000E+00  0.00000E+00
0.00000E+00  0.00000E+00
 ***** DATA CARD NO.   4 FR     0     1     0     0  1.01250E+01  1.00000E+00
0.00000E+00  0.00000E+00
0.00000E+00  0.00000E+00
 ***** DATA CARD NO.   5 RP     0     1   361  1000  9.00000E+01  0.00000E+00
1.00000E+00  1.00000E+00
0.00000E+00  0.00000E+00
```

The frequency holds sufficient significance to receive a separate region of the output report to itself.

```
                        - - - - - - FREQUENCY - - - - - -
                           FREQUENCY= 1.0125E+01 MHZ
                          WAVELENGTH= 2.9610E+01 METERS
 APPROXIMATE INTEGRATION EMPLOYED FOR SEGMENTS MORE THAN   1.000 WAVELENGTHS
APART
```

Following the frequency, the report lists any loads, whether they specify RLC, R-X, or simple element conductivity.

```
                    - - - STRUCTURE IMPEDANCE LOADING - - -
      LOCATION          RESISTANCE   INDUCTANCE  CAPACITANCE       IMPEDANCE
(OHMS)     CONDUCTIVITY    TYPE
     ITAG FROM THRU           OHMS         HENRYS        FARADS         REAL
IMAGINARY    MHOS/METER
     1   1  21                                                    5.8001E+07
WIRE
     2   1  21                                                    5.8001E+07
WIRE
```

The report will also record the antenna environment, which is simple in this model (free-space). As well, it records the time expended so far on basic matrix calculations—a very brief time for this simple model. Often, examining the timing—especially of a model that has been left unattended during its run—can provide clues either to the adequacy of the model or to the computer set-up on which one runs the model.

```
                    - - - ANTENNA ENVIRONMENT - - -
                                FREE SPACE

                        - - - MATRIX TIMING - - -
                FILL=    0.110 SEC.,  FACTOR=    0.000 SEC.
```

The core has so far calculated the mutual impedances among all of the segments in the model. However, before it can calculate the currents on each segment—a necessary prerequisite to determining the antenna power gain in any chosen direction—it must account for the source or excitation. Therefore, it records all of the source input data, along with calculations predicated on the source and factors already calculated. Only then can the program calculate the segment currents.

```
                    - - - ANTENNA INPUT PARAMETERS - - -

TAG   SEG.    VOLTAGE (VOLTS)         CURRENT (AMPS)         IMPEDANCE (OHMS)
ADMITTANCE (MHOS)      POWER
NO.   NO.     REAL        IMAG.       REAL        IMAG.       REAL        IMAG.
REAL        IMAG.     (WATTS)
1   11 1.41421E+00 0.00000E+00 2.85369E-02-9.87696E-04 4.94981E+01 1.71318E+00
2.01786E-02-6.98406E-04 2.01787E-02

                    - - - CURRENTS AND LOCATION - - -
                        DISTANCES IN WAVELENGTHS

  SEG.  TAG    COORD. OF SEG. CENTER     SEG.            - - - CURRENT (AMPS)
- - -
  NO.   NO.     X        Y        Z      LENGTH     REAL        IMAG.       MAG.
PHASE
      1     1    0.0000   -0.2271    0.0000   0.02271    2.5339E-03 -1.9134E-04
2.5411E-03   -4.318
      2     1    0.0000   -0.2044    0.0000   0.02271    7.0345E-03 -5.1543E-04
7.0533E-03   -4.191
      3     1    0.0000   -0.1817    0.0000   0.02271    1.1146E-02 -7.8904E-04
1.1174E-02   -4.049
      4     1    0.0000   -0.1590    0.0000   0.02271    1.4929E-02 -1.0156E-03
1.4963E-02   -3.892
      5     1    0.0000   -0.1362    0.0000   0.02271    1.8343E-02 -1.1912E-03
1.8381E-02   -3.716
      6     1    0.0000   -0.1135    0.0000   0.02271    2.1338E-02 -1.3112E-03
2.1378E-02   -3.516
      7     1    0.0000   -0.0908    0.0000   0.02271    2.3866E-02 -1.3714E-03
2.3905E-02   -3.289
```

```
     8     1    0.0000   -0.0681    0.0000   0.02271    2.5881E-02 -1.3682E-03
2.5917E-02   -3.026
     9     1    0.0000   -0.0454    0.0000   0.02271    2.7347E-02 -1.2979E-03
2.7378E-02   -2.717
    10     1    0.0000   -0.0227    0.0000   0.02271    2.8238E-02 -1.1534E-03
2.8262E-02   -2.339
    11     1    0.0000    0.0000    0.0000   0.02271    2.8537E-02 -9.8770E-04
2.8554E-02   -1.982
    12     1    0.0000    0.0227    0.0000   0.02271    2.8238E-02 -1.1534E-03
2.8262E-02   -2.339
    13     1    0.0000    0.0454    0.0000   0.02271    2.7347E-02 -1.2979E-03
2.7378E-02   -2.717
    14     1    0.0000    0.0681    0.0000   0.02271    2.5881E-02 -1.3682E-03
2.5917E-02   -3.026
    15     1    0.0000    0.0908    0.0000   0.02271    2.3866E-02 -1.3714E-03
2.3905E-02   -3.289
    16     1    0.0000    0.1135    0.0000   0.02271    2.1338E-02 -1.3112E-03
2.1378E-02   -3.516
    17     1    0.0000    0.1362    0.0000   0.02271    1.8343E-02 -1.1912E-03
1.8381E-02   -3.716
    18     1    0.0000    0.1590    0.0000   0.02271    1.4929E-02 -1.0156E-03
1.4963E-02   -3.892
    19     1    0.0000    0.1817    0.0000   0.02271    1.1146E-02 -7.8904E-04
1.1174E-02   -4.049
    20     1    0.0000    0.2044    0.0000   0.02271    7.0345E-03 -5.1543E-04
7.0533E-03   -4.191
    21     1    0.0000    0.2271    0.0000   0.02271    2.5339E-03 -1.9134E-04
2.5411E-03   -4.318
    22     2   -0.1452   -0.2420    0.0000   0.02420   -8.7033E-04  1.1146E-03
1.4141E-03  127.985
    23     2   -0.1452   -0.2178    0.0000   0.02420   -2.4453E-03  3.1118E-03
3.9576E-03  128.161
    24     2   -0.1452   -0.1936    0.0000   0.02420   -3.9163E-03  4.9537E-03
6.3148E-03  128.329
    25     2   -0.1452   -0.1694    0.0000   0.02420   -5.2948E-03  6.6605E-03
8.5086E-03  128.483
    26     2   -0.1452   -0.1452    0.0000   0.02420   -6.5590E-03  8.2103E-03
1.0509E-02  128.620
    27     2   -0.1452   -0.1210    0.0000   0.02420   -7.6828E-03  9.5767E-03
1.2278E-02  128.738
    28     2   -0.1452   -0.0968    0.0000   0.02420   -8.6411E-03  1.0734E-02
1.3780E-02  128.835
    29     2   -0.1452   -0.0726    0.0000   0.02420   -9.4114E-03  1.1659E-02
1.4984E-02  128.911
    30     2   -0.1452   -0.0484    0.0000   0.02420   -9.9753E-03  1.2334E-02
1.5863E-02  128.965
```

```
    31     2   -0.1452   -0.0242    0.0000   0.02420   -1.0319E-02   1.2744E-02
1.6398E-02  128.998
    32     2   -0.1452    0.0000    0.0000   0.02420   -1.0435E-02   1.2882E-02
1.6578E-02  129.009
    33     2   -0.1452    0.0242    0.0000   0.02420   -1.0319E-02   1.2744E-02
1.6398E-02  128.998
    34     2   -0.1452    0.0484    0.0000   0.02420   -9.9753E-03   1.2334E-02
1.5863E-02  128.965
    35     2   -0.1452    0.0726    0.0000   0.02420   -9.4114E-03   1.1659E-02
1.4984E-02  128.911
    36     2   -0.1452    0.0968    0.0000   0.02420   -8.6411E-03   1.0734E-02
1.3780E-02  128.835
    37     2   -0.1452    0.1210    0.0000   0.02420   -7.6828E-03   9.5767E-03
1.2278E-02  128.738
    38     2   -0.1452    0.1452    0.0000   0.02420   -6.5590E-03   8.2103E-03
1.0509E-02  128.620
    39     2   -0.1452    0.1694    0.0000   0.02420   -5.2948E-03   6.6605E-03
8.5086E-03  128.483
    40     2   -0.1452    0.1936    0.0000   0.02420   -3.9163E-03   4.9537E-03
6.3148E-03  128.329
    41     2   -0.1452    0.2178    0.0000   0.02420   -2.4453E-03   3.1118E-03
3.9576E-03  128.161
    42     2   -0.1452    0.2420    0.0000   0.02420   -8.7033E-04   1.1146E-03
1.4141E-03  127.985
```

The excitation data is needed for the current calculations. If you look closely at the impedance entries, you will see—in slightly different notation—the impedance report that went into the VSWR table shown in an earlier figure. NEC does not calculate VSWR values, but those are simple enough to implement in a post core-run action.

I have included the entire current listing for this small model to provide you with a sense of how the internal parts of the output report interrelate. Note that the entries list the center coordinates for each segment, corresponding to the list we viewed in the segmentation data. For each segment, we find a current given in two forms: by the real and imaginary components and by a magnitude and phase angle. Some programs provide facilities for creating a rectangular plot of the current along a wire or sequence of wires. This data—in either tabular or graphical form—can be useful in determining the properties of elements within an antenna array. As well, the current level at the center of each wire is often useful data for understanding especially the operations of arrays using elements in the neighborhood of 1/2 wave-

length. Hence, it is important to be able to locate a wire center segment by reference to its absolute segment number. (Some programs, such as EZNEC, translate the current table into a format that restores the original wire and segment numbers used in the creation of GW entries.)

Note that the current levels are very low, making it difficult in some cases to clearly see the relative current level along an element. Using a current source (discussed in an earlier column in this series) can provide a basis for showing all current levels relative to a source current magnitude of 1.0. Such a source is also convenient in phased arrays for setting each source with a specific current magnitude and phase angle. As we have shown in earlier columns, we may also calculate for a voltage source the magnitude necessary to produce a power of a given level—taking into account that NEC uses and reports peak values of voltage and current, whereas power is always an RMS calculation. This calls for a revision of the user-input for the voltage magnitude and a rerun of the core—unless the program has a provision for calculating this value after the user specifies a desired power level (EZNEC). Using different power levels or equalizing them for all revisions of the model does not affect the power gain calculations that appear in the radiation patterns under an RP0 request. However, setting a power level is very useful to near field and ground wave calculations.

```
    - - - POWER BUDGET - - -

INPUT POWER   = 2.0179E-02 WATTS
RADIATED POWER= 1.9644E-02 WATTS
STRUCTURE LOSS= 5.3508E-04 WATTS
NETWORK LOSS  = 0.0000E+00 WATTS
EFFICIENCY    =  97.35 PERCENT
```

Some programs omit some aspects of the power budget. However, the total input power is useful as a check on any manual adjustment of the voltage magnitude to achieve a desired power level. The radiated power is subject to two types of subtractions from the input power. Structure losses are those losses owing to LD5 (wire conductivity) loads. One reason that I chose a wire array is to let you change the wire conductivity from a perfect or lossless wire to a copper wire to an aluminum wire, etc. You will observe changes in the radiated power and the overall efficiency of the antenna.

Network losses owe to the use of any RLC or R-X loads that have a resistive component. As well, networks with less than unlimited conductance will also create losses. Since such loads and networks may be anywhere along the elements, the same load will not necessarily show the same overall loss at every position. Any loads created by the use of transmission lines (such as open or shorted stubs) will be lossless (in contrast to the same types of loads in their physical implementations). In addition, external losses created by matching networks that are not part of the model will not show up in the efficiency report.

We are finally ready to read out the pattern requests. However, I shall truncate the two reports to only a few lines each.

```
[Phi pattern]         - - - RADIATION PATTERNS - - -

  - - ANGLES - -          - POWER GAINS -       - - - POLARIZATION - - -    -
- - E(THETA) - - -    - - - E(PHI) - - -
  THETA     PHI         VERT.    HOR.     TOTAL       AXIAL      TILT    SENSE
MAGNITUDE    PHASE       MAGNITUDE    PHASE
 DEGREES  DEGREES      DB     DB     DB       RATIO    DEG.            VOLTS/
M    DEGREES       VOLTS/M    DEGREES
   90.00      0.00     -999.99     5.65     5.65     0.00000     90.00  LINEAR
0.00000E+00     0.00    2.10773E+00   -64.63
   90.00      1.00     -999.99     5.65     5.65     0.00000    -90.00  LINEAR
1.87706E-13   115.37    2.10715E+00   -64.63
   90.00      2.00     -999.99     5.64     5.64     0.00000    -90.00  LINEAR
3.75218E-13   115.38    2.10542E+00   -64.62
   90.00      3.00     -999.99     5.63     5.63     0.00000    -90.00  LINEAR
5.62342E-13   115.39    2.10254E+00   -64.61
   90.00      4.00     -999.99     5.61     5.61     0.00000    -90.00  LINEAR
7.48885E-13   115.41    2.09851E+00   -64.59
   90.00      5.00     -999.99     5.59     5.59     0.00000    -90.00  LINEAR
9.34656E-13   115.43    2.09334E+00   -64.57
   90.00      6.00     -999.99     5.56     5.56     0.00000    -90.00  LINEAR
1.11946E-12   115.45    2.08703E+00   -64.55
   90.00      7.00     -999.99     5.53     5.53     0.00000    -90.00  LINEAR
1.30312E-12   115.48    2.07961E+00   -64.52
   90.00      8.00     -999.99     5.50     5.50     0.00000    -90.00  LINEAR
1.48545E-12   115.52    2.07107E+00   -64.48
   90.00      9.00     -999.99     5.46     5.46     0.00000    -90.00  LINEAR
1.66625E-12   115.56    2.06143E+00   -64.44
   90.00     10.00     -999.99     5.41     5.41     0.00000    -90.00  LINEAR
1.84536E-12   115.60    2.05070E+00   -64.40
```

```
   90.00    351.00     -999.99     5.46     5.46     0.00000     90.00  LINEAR
1.66625E-12   -64.44    2.06143E+00   -64.44
   90.00    352.00     -999.99     5.50     5.50     0.00000     90.00  LINEAR
1.48545E-12   -64.48    2.07107E+00   -64.48
   90.00    353.00     -999.99     5.53     5.53     0.00000     90.00  LINEAR
1.30312E-12   -64.52    2.07961E+00   -64.52
   90.00    354.00     -999.99     5.56     5.56     0.00000     90.00  LINEAR
1.11946E-12   -64.55    2.08703E+00   -64.55
   90.00    355.00     -999.99     5.59     5.59     0.00000     90.00  LINEAR
9.34656E-13   -64.57    2.09334E+00   -64.57
   90.00    356.00     -999.99     5.61     5.61     0.00000     90.00  LINEAR
7.48885E-13   -64.59    2.09851E+00   -64.59
   90.00    357.00     -999.99     5.63     5.63     0.00000     90.00  LINEAR
5.62342E-13   -64.61    2.10254E+00   -64.61
   90.00    358.00     -999.99     5.64     5.64     0.00000     90.00  LINEAR
3.75218E-13   -64.62    2.10542E+00   -64.62
   90.00    359.00     -999.99     5.65     5.65     0.00000     90.00  LINEAR
1.87706E-13   -64.63    2.10715E+00   -64.63
   90.00    360.00     -999.99     5.65     5.65     0.00000    -90.00  LINEAR
2.19582E-22   115.37    2.10773E+00   -64.63

[Theta pattern]         - - - RADIATION PATTERNS - - -

  - - ANGLES - -           - POWER GAINS -       - - - POLARIZATION - - -    -
- - E(THETA) - - -    - - - E(PHI) - - -
  THETA      PHI         VERT.    HOR.     TOTAL       AXIAL      TILT    SENSE
MAGNITUDE    PHASE      MAGNITUDE    PHASE
 DEGREES  DEGREES       DB     DB     DB       RATIO    DEG.             VOLTS/
M    DEGREES       VOLTS/M    DEGREES
   90.00      0.00     -999.99     5.65     5.65     0.00000     90.00  LINEAR
0.00000E+00     0.00    2.10773E+00   -64.63
   91.00      0.00     -999.99     5.65     5.65     0.00000     90.00  LINEAR
0.00000E+00     0.00    2.10762E+00   -64.62
   92.00      0.00     -999.99     5.65     5.65     0.00000     90.00  LINEAR
0.00000E+00     0.00    2.10729E+00   -64.62
   93.00      0.00     -999.99     5.64     5.64     0.00000     90.00  LINEAR
0.00000E+00     0.00    2.10673E+00   -64.61
   94.00      0.00     -999.99     5.64     5.64     0.00000     90.00  LINEAR
0.00000E+00     0.00    2.10596E+00   -64.59
   95.00      0.00     -999.99     5.64     5.64     0.00000     90.00  LINEAR
0.00000E+00     0.00    2.10496E+00   -64.57
   96.00      0.00     -999.99     5.63     5.63     0.00000     90.00  LINEAR
0.00000E+00     0.00    2.10374E+00   -64.54
   97.00      0.00     -999.99     5.63     5.63     0.00000     90.00  LINEAR
0.00000E+00     0.00    2.10230E+00   -64.51
```

```
   98.00      0.00     -999.99     5.62     5.62     0.00000     90.00  LINEAR
0.00000E+00     0.00     2.10064E+00   -64.47
   99.00      0.00     -999.99     5.61     5.61     0.00000     90.00  LINEAR
0.00000E+00     0.00     2.09876E+00   -64.43
  100.00      0.00     -999.99     5.60     5.60     0.00000     90.00  LINEAR
0.00000E+00     0.00     2.09665E+00   -64.39
```

```
  441.00      0.00     -999.99     5.61     5.61     0.00000     90.00  LINEAR
0.00000E+00     0.00     2.09876E+00   -64.43
  442.00      0.00     -999.99     5.62     5.62     0.00000     90.00  LINEAR
0.00000E+00     0.00     2.10064E+00   -64.47
  443.00      0.00     -999.99     5.63     5.63     0.00000     90.00  LINEAR
0.00000E+00     0.00     2.10230E+00   -64.51
  444.00      0.00     -999.99     5.63     5.63     0.00000     90.00  LINEAR
0.00000E+00     0.00     2.10374E+00   -64.54
  445.00      0.00     -999.99     5.64     5.64     0.00000     90.00  LINEAR
0.00000E+00     0.00     2.10496E+00   -64.57
  446.00      0.00     -999.99     5.64     5.64     0.00000     90.00  LINEAR
0.00000E+00     0.00     2.10596E+00   -64.59
  447.00      0.00     -999.99     5.64     5.64     0.00000     90.00  LINEAR
0.00000E+00     0.00     2.10673E+00   -64.61
  448.00      0.00     -999.99     5.65     5.65     0.00000     90.00  LINEAR
0.00000E+00     0.00     2.10729E+00   -64.62
  449.00      0.00     -999.99     5.65     5.65     0.00000     90.00  LINEAR
0.00000E+00     0.00     2.10762E+00   -64.62
  450.00      0.00     -999.99     5.65     5.65     0.00000     90.00  LINEAR
0.00000E+00     0.00     2.10773E+00   -64.63
```

The radiation reports—whether for phi or theta—offer a variety of data for each bearing defined by a combination of phi and theta angles. For the reports selected here, the format is for a 2-dimensional pattern in which one angular system is progressively calculated while holding the other constant. Other patterns are possible, including 3-dimensional patterns that sample the entire sphere around the antenna at specified intervals.

The reports offer, of course, the total power gain—recorded in dBi using an isotropic radiator as a comparator—and its vertical and horizontal components. The report also offers polarization information, which is not especially useful in this particular model using linear elements. Finally, we find a record of the electrical fields tangential to the X-Y axes (theta) and parallel to it (phi). Although many general modelers focus only upon the antenna power gain, the other data has extensive

applications, depending upon the type of antenna and upon the properties of highest interest.

We should note a few seeming oddities in the report. First, the theta pattern ends at an angle of 450 degrees. This ending point stems from the starting point on the virtual horizon (90 degrees) and the fact that the core counts in a positive direction. The polar H-plane plot that we earlier observed has done a post-run reset of the angles to correspond to something more familiar.

Since the antenna is in free space and is composed of linear elements, it is polarized in parallel to the X-Y axes. There is no significant radiation at right angles to this orientation. Hence, the vertical power gain is virtually zero. NEC records such a power gain—in dBi—as -999.99, an insignificantly low but non-zero value.

```
 ***** DATA CARD NO.   7 EN     0     0     0     0  0.00000E+00  0.00000E+00
0.00000E+00  0.00000E+00
0.00000E+00  0.00000E+00

 RUN TIME =     0.330
```

The EN entry marks the end of the core run. Note that we obtain a registration of the total run time. This value happens for the present entry to be 3 times the value of the matrix fill and factor value recorded earlier. Those who implement versions of NEC commercially are ever on the search for ways of compiling the original FORTRAN program so that it calculates faster. In conjunction with the latest 2 GHz, fast memory bus machines, these techniques have converted runs that took overnight into runs that barely allow one to inhale properly.

We have taken you through the structure of the NEC output report for a simple model on which we placed equally simple demands. However, I hope the exercise orients you to the output report sufficiently well so that you can navigate around more complex reports—perhaps involving plane wave sources, requests for ground waves or near field data, and those making use of one or more of the supplementary geometry inputs. The next step is to transfer the output report to a spreadsheet on which you may manipulate the data in further useful ways. The output tables and graphics of any given implementation of NEC may cover most of the important data, but they cannot cover all possible present and future interests. The only way to

make full use of the NEC output data is to return to the output report itself. The more comfortable you are in navigating that report, the more interesting and useful information you can draw from it.

* * * * *

Model included: 64-1. (All dimensions in meters.)

65. The 1/2-WL Resonant Dipole as a Core Test Instrument

In the course of creating models, we occasionally enter into gray areas that border upon the limitations of the calculating core, whether that is NEC-2, NEC-4, or MININEC. Very often we simply plunge ahead with the model, despite that fact that it may be quite complex. We hope that any difficulties will show themselves.

Actually, the more complex the model, the more likely it is to mask the difficulties that we encounter. Consider a model of a log periodic dipole array (LPDA) that uses physical wires as the phase line. For normal phase lines using wires ranging from AWG #18 to AWG #10 or so, the phase line separation will be under 2". However, some element sections of the LPDA may be over 2" in diameter.

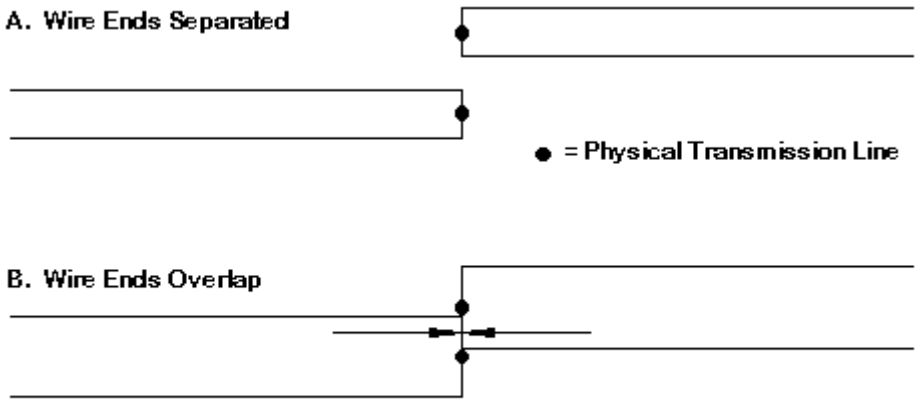

The Initial Problem Area for Investigation

Fig. 65-1

As shown in **Fig. 65-1**, the most ordinary way to model an LPDA with physical wires as the phase line is to set the two wires of the line vertically. Each LPDA element is split in the center, with half connected to each line. For thinner LPDA elements, we encounter no potential problems, as evidenced by the upper portion of the sketch.

However, large-diameter center sections of an element can result in the case shown in the lower half of the figure. The element centerlines are separated by a large enough space that the core does not interpret them as forming a wire junction. However, the surface boundaries of each element pass each other and touch at the ends.

Modeling rules prohibit wires that penetrate the surface area of another wire. Had we used crossing wires, the surfaces of the two wires would have penetrated each other and we would have had an error in geometry. Even if we have a core that allows the run, the results would have been useless. I once encountered a model of an antenna with such errors that seemed to yield over 35-dBi gain. Only when I examined the model did I find the surface penetrations. The AGT for the model was over 1,000.0 (when perfection would have been 1.0), indicating that the true gain was minuscule.

However, our present case uses wires that abut at the ends. There is no end cap invoked, since the wires make a junction with another wire. The situation invokes no warnings or errors, and the core runs look sensible at first sight. Our question is whether these results are reliable.

To answer that question, we should go back to the simplest model possible and perform a series of tests on the situation itself. For that purpose, the dipole is ideal.

Some NEC Tests

The construction of a modeling test scenario requires some thought. Just making a resonant dipole will not do the job. There are numerous questions to pose.

1. *What type of test will do the job?* Since the initial problem involves an LPDA phase line, which is an application of a transmission line, we shall eventually need to construct a physical transmission line connected to the center of a dipole. If we

compare the source impedance of a simple model of a dipole of a given diameter with the impedance of any transmission line that is 1/2-wavelength long, we should be able to detect any significant problems created by the situation in **Fig. 65-1**.

2. *What transmission line and what diameter dipole elements?* We need to be able to approach and then pass the limit of the two dipole halves abutting at the centerline of the dipole. If we use 0.5", 1.0", and 1.5" dipoles, we shall need a transmission line whose wires are separated by perhaps a little over an inch. If we use AWG #16 (0.0508" diameter) wire for the lines, we can obtain an impedance of 450 Ohms with a spacing of about 1.084". With a vertically oriented transmission line, the 0.5" dipole will be well short of overlap. The 1" element will almost but not quite touch. The 1.5" diameter element will overlap. For reference, we shall add a #16 wire dipole to the list as a baseline.

We shall use perfect or lossless wires for all parts of the test dipole models. A lossless transmission line wire will most closely approach a true velocity factor of 1.0, allowing us to use calculated values of 1/2 wavelength.

3. *What frequency?* Since the problem arose in connection with models of LPDAs in the HF range, we may arbitrarily select 14 MHz as the test frequency. The test is not frequency dependent, but a middle HF frequency has some modeling advantages. First, it allows us to make fine discriminations in length simply by measuring everything in inches. Second, for the element diameters used, we have potentially sufficient numbers of segments available, given the recommended limit that the length of a NEC segment should be at least as large as the element diameter. For some tests, 1" long segments to match the separation of the transmission line wires will be possible. Since a dipole model converges far below this level of segmentation, we may use fewer segments for some initial models.

A wavelength at 14 MHz is 843.061". We shall use 1/2-wavelength transmission lines that are 421.531" long. The resonant length of the perfect-wire dipole, of course, will vary with the diameter of the element.

4. *What test models should we generate?* **Fig. 65-2** shows the range of models that we shall examine.

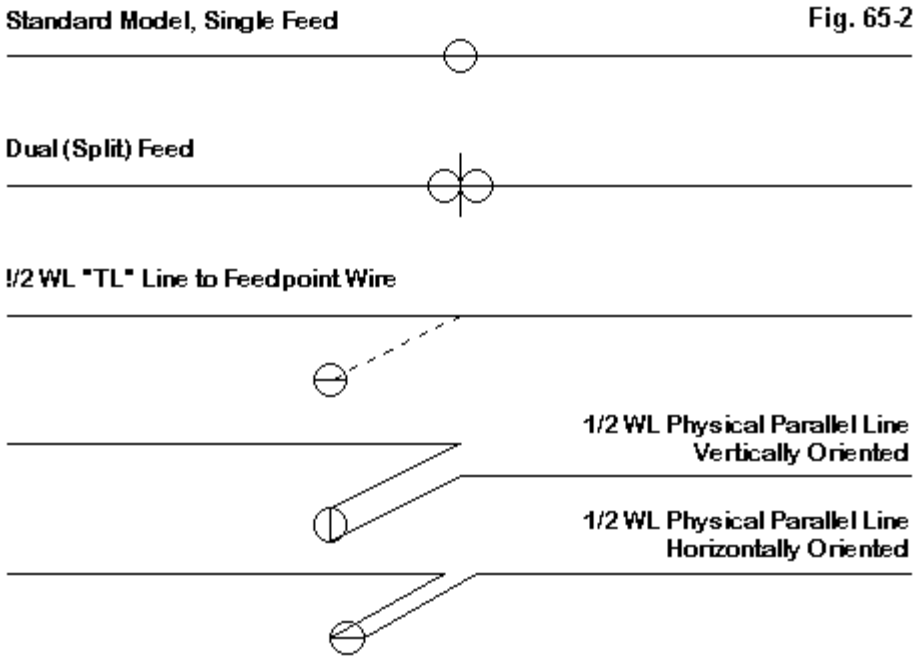

Test Configurations for a Dipole and Transmission Line
NEC-4 Models

Since we are working initially with NEC—specifically NEC-4—we shall look at two ways of feeding a dipole for reference. The simple dipole model will have 41 segments with the feedpoint or source at the center segment, in accord with the NEC system wherein the current center is the segment center. We shall also examine the same dipole using a dual-feed or split-feed system. Here, we shall use 42 segments, feeding the segments on either side of the centerline. This test will tell us something about the sensitivity of the model to minor changes in segmentation and feed arrangements.

We shall then apply to our simple single-feed dipole a 1/2-wavelength transmission line, which we shall terminate in the shortest practical wire. We shall place the source on this 1-segment wire.

Finally, we shall construct two types of physical transmission lines. The first will be a vertically oriented or Z-axis line corresponding to modeling practices for LPDAs. The element inner ends will be displaced by 1.084" at their wire centerlines, and each inner end will terminate at 0.0 on its axis. This set-up will ensure that the 1.5" diameter elements will overlap as they touch at their ends, but will not form a wire junction. The second type of physical transmission line—used only as a check—will consist of two wires spaced horizontally in the plane of the length of the dipole. This line will effect a center spacing of 1.084" in the dipole.

The simple model results: The following table summarizes the results obtained for the simple models of a dipole using both single and split feed systems. See models 65-1 and 65-2, versions a through d. Each dipole was resonated to under +/-0.01 Ohm reactance, and the dipole length (listed as a +/- value in inches) is carried out to more decimal places than we would ever need in practical modeling. However, we are not modeling a practical antenna, but checking the modeling system for certain sensitivities. Hence, the excess precision is warranted.

The table lists the dipole length, the resonant source impedance, and the Average Gain Test (AGT) value, given as both a relative gain value and in dB. The AGT value yields a relative merit rating, where 1.0 indicates perfection, and a set of correctives. The test is a necessary but not a sufficient condition of model adequacy. Hence, a perfect AGT rating suggests but does not guarantee an adequate model. For AGT values less than 1.0, the conversion of the value into a value in dB indicates how much the reported gain is below the likely actual gain value. An AGT greater than 1.0, when converted, indicates how much higher than the likely actual gain value the reported gain may be. As well, if the source reactance is very low, then multiplying the AGT numerical value by the reported source resistance will closely approximate the likely actual source resistance. (However, when the reactance grows higher, this latter corrective gradually fails.)

El. Dia. Inches	El. Length Inches	Source Impedance R +/- jX Ohms	AGT Relative	dB
#16 Single	+/- 204.900	72.10 - j 0.006	1.0	0.0
#16 Split	+/- 204.874	72.17 + j 0.006	1.0	0.0
0.5" Single	+/- 202.408	71.92 + j 0.001	1.0	0.0
0.5" Split	+/- 202.350	71.95 + j 0.003	1.0	0.0
1.0" Single	+/- 201.122	71.88 - j 0.006	1.0	0.0
1.0" Split	+/- 201.040	71.89 - j 0.001	1.0	0.0
1.5" Single	+/- 200.168	71.89 - j 0.003	1.0	0.0
1.5" Split	+/- 200.060	71.86 - j 0.005	1.0	0.0

With segment lengths varying from 9.53" to 9.99", these simple models give a fair account of NEC-4 modeling (and by extension, NEC-2, since nothing in them presses any of the problem areas in the earlier version of NEC). The difference in resonant length between the single and split feed versions of the model are most likely due to the additional segment needed to center the split source. As expected, such simple models show no calculable departure from a perfect AGT value.

The next table attaches to the center of the 41-segment model a 450-Ohm, velocity-factor=1.0 transmission line that is 421.531" long. It terminates in a perfect/lossless 1 segment wire that is about 2" long and has 1 segment. We place the source on this wire. The transmission line uses the TL facility of NEC. This facility creates non-physical, non-radiating mathematical lines that are lossless. (Perhaps future versions of NEC may replace this system with lossy line calculations by introducing the proper algorithms and allowing the user to introduce appropriate loss values.) Hence, the transmission line wires do not create any effects that would alter the radiation pattern. If the source wire is sufficiently small and distant from the dipole itself, it will have a completely negligible effect on the radiation pattern. The following table lists the resultant values for these runs. See models 65-3a through 65-3d.

El. Dia. Inches	El. Length Inches	Source Impedance R +/- jX Ohms	AGT Relative	dB
#16 Single	+/- 204.900	72.10 - j 0.063	1.0	0.0
0.5" Single	+/- 202.408	71.92 - j 0.061	1.0	0.0

1.0" Single	+/- 201.122	71.88 - j 0.068	1.0	0.0
1.5" Single	+/- 200.168	71.89 - j 0.063	1.0	0.0

These tests introduce a systematic decrease in the source reactance of about 0.06 Ohm. The most likely cause is imprecision in the length of the transmission line. Other than this one change, the transmission line alters nothing else.

These results are exactly what we should have expected. Indeed, they comprise one reason why NEC modelers use the TL facility for most modeling enterprises involving transmission lines, including the modeling of LPDAs.

Finally, we are ready to model the dipole using physical wires for the transmission line. If you think that I expect difficulties, you are correct. However, in a test, we let those difficulties emerge where they might rather than imposing any preconceptions upon them.

The first transmission line consists of two parallel AWG #16 wires separated vertically by 1.084". The dipole consists of two halves, each joining one of the transmission line wires at a 90-degree angle. The far end of the transmission line has a 1-segment wire connecting the two wires. The source is placed on this wire.

For the 4 element diameters, we obtained the following NEC-4 results. Note that each entry shows at least two levels of segmentation. The smaller numbers follow the segmentation of the simple dipole models, using about 42 segments per half wavelength. This condition results in two segments—one on each transmission line adjacent to the source wire/segment—that are radically different in length than the source segment. NEC recommendations call for segments each side of the source segment having lengths about the same as each other and as the source segment. Therefore, the second entry shows the entire assembly segmented to produce segments about 1" long. We shall discuss procedures used for the 1.5" diameter elements after reviewing the overall results. See models 65-4a through 65-4d.

El. Dia. Inches	El. Length Inches	Source Impedance R +/- jX Ohms	AGT Relative	dB
#16 21/42/1	+/- 204.900	57.64 + j 0.909	1.251	0.97
#16 205/421/1	+/- 204.900	77.38 - j 2.812	0.933	-0.30
0.5" 21/42/1	+/- 202.408	60.65 + j 0.511	1.185	0.74
0.5" 205/421/1	+/- 202.408	105.5 - j 1.382	0.684	-1.65
1.0" 21/42/1	+/- 201.122	63.24 + j 0.291	1.135	0.55
1.0" 205/421/1	+/- 201.122	151.2 - j 2.821	0.477	-3.22
1.5" 21/42/1	+/- 200.168	65.87 + j 0.060	1.089	0.37
1.5" 205/421/1*	+/- 200.168	137.4 - j 4.17	0.524	-2.81
1.5" 133/281/1	+/- 200.168	170.7 - j 2.836	0.421	-3.76

* See text for an explanation of why this entry has a special difficulty.

This table calls for a number of comments:

1. *The 1.5" diameter case*: The program warned of a condition that many modelers overlook and under-appreciate: the penetration at an angular junction of the surface of one wire into the center of another wire. See **Fig. 65-3**.

The 1.5" wire surface penetrates along the last segment of the #16 wire for 0.75". With a segment length of about 1", the surface of the large element extends beyond the center of the #16-wire segment. The core itself does not stop the run, even though this condition is considered highly problematical to any model.

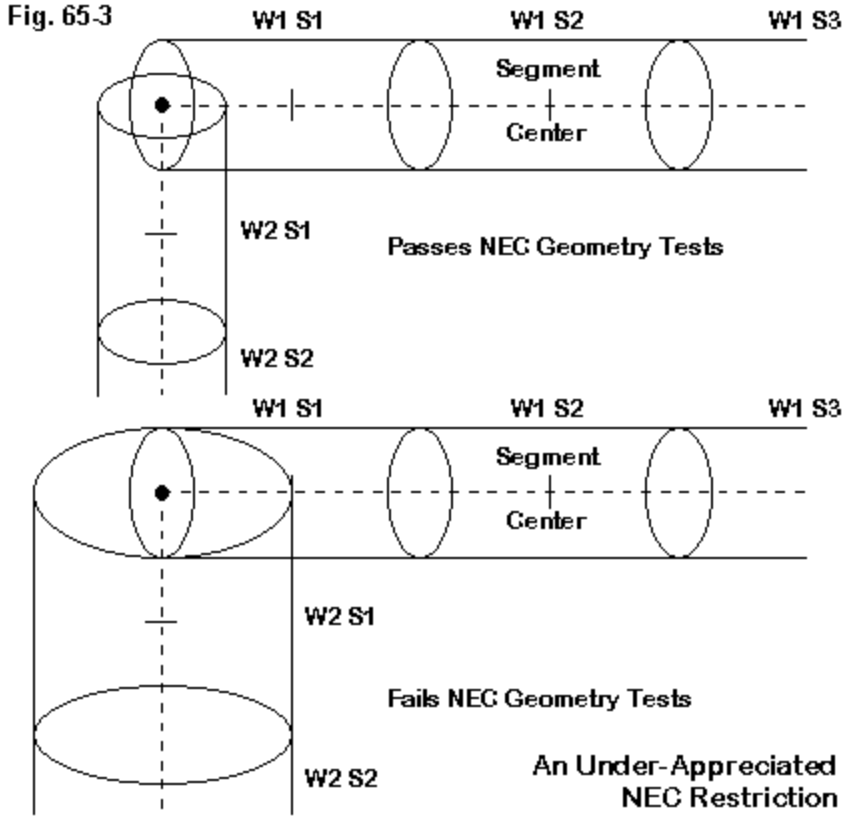

As a result, I developed the segmentation in the third line, keeping the segment lengths of the dipole and the transmission line roughly equal and using the shortest segment length that would avoid the warning. Indeed, the segment length in the transmission line wires is just over 1.50".

2. *Angular junctions of wires having dissimilar diameters*: Once we go past the #16 wire model, we begin to see a pattern of results that reveals another shortcoming of NEC. NEC-2 produces worse results than NEC-4, but the NEC-4 results show that the models are highly unreliable. In some circumstances, an AGT value less than 0.95 or greater than 1.05 is considered beyond the realm of reliability, while in other situations, the limits might be set as 0.99 and 1.01. In almost all cases where we have a ratio of diameters greater than about 2:1, the AGT value falls outside of virtually any set of limits.

The situation has an interesting abnormality relative to our usual expectations for convergence testing. In a normal situation, we anticipate increasing the number of segments until we reach a reasonable level of convergence between one level of segmentation and the next. Once we achieve this goal, we consider the model converged and that the results will be as reliable as possible.

In the case of angular junctions of wires having dissimilar diameters, we encounter a reverse convergence situation. The lower the level of segmentation, the more accurate the results are relative to an actual antenna using the physical counterparts of the modeled wires. However, since we do not have, in most modeling exercises, the external standard against which to measure the adequacy of the results, we must rely upon the AGT. In this case, the values are wholly beyond the limits of confidence.

3. *The case of #16 wire*: The reported values for the model composed wholly of #16 wire show better AGT ratings for the highly segmented model than for the model using fewer segments. Indeed, the larger model has a uniform diameter throughout, segment lengths very close to the length of the source segment, very adequate segment length to wire diameter ratios, and generally no other perceptible problems. However, the AGT rating of the “205/421/1” model is only 0.933. Something must be amiss.

NEC does have a sensitivity to closely spaced wires. We obtain the highest accuracy when we perfectly align the segment junctions, as is the case in the present model. However, the core is not perfectly comfortable with the parallel run of 1/2-wavelength wires. Exactly what constitutes the “imperfect comfort” I do not know except that it represents a limitation of NEC models.

The upshot of the exercise is this point: NEC models attempting to employ physical wires for both the elements and connecting transmission lines are likely to be less accurate than those using the TL facility available within the program. This point applies not only to cases like the dipole with the remote source at the end of a transmission line, but as well to LPDAs and other phased arrays.

Before we depart NEC models of dipoles with 1/2-wavelength transmission lines, let's briefly pause to look at the second type of line: one that splits the element but leaves it on a single plane. The gap created is once more 1.084" for our #16 450-Ohm line that is 1/2 wavelength or 421.531" long. Although we do not have to concern ourselves with the touching overlap of element wire ends, the results may be useful as a comparison in other respects with the vertically oriented transmission line. See models 65-5a through 65-5d.

El. Dia. Inches	El. Length Inches	Source Impedance R +/- jX Ohms	AGT Relative	dB
#16 21/42/1	+/- 204.900	56.00 - j 3.970	1.282	1.08
#16 205/421/1	+/- 204.900	76.29 - j 7.717	0.947	-0.25
0.5" 21/42/1	+/- 202.408	58.89 - j 3.310	1.216	0.85
0.5" 205/421/1	+/- 202.408	99.49 - j 6.399	0.723	-1.41
1.0" 21/42/1	+/- 201.122	61.14 - j 3.184	1.170	0.68
1.0" 205/421/1	+/- 201.122	131.3 - j 7.628	0.547	-2.62
1.5" 21/42/1	+/- 200.168	63.32 - j 3.164	1.129	0.53
1.5" 205/421/1	+/- 200.168	135.8 - j 8.688	0.528	-2.77

In all cases, the AGT values are very comparable to those we met when looking at the vertically oriented transmission line. Making the transmission line horizontal does not overcome any of the difficulties previously encountered. We may add to those difficulties—for both types of transmission line—that for the 1" and the 1.5" diameter elements, using the higher level of segmentation, the segment length to wire diameter ratio is deficient. The 1" element yields a ratio of 0.98:1, while the 1.5" element shows a ratio of 0.65:1. Both of these cases are above the absolute minimum ratio of 0.5:1, but a well into the region of growing unreliability.

The interesting phenomenon with these models is the systematic increase in capacitive reactance. The models all use the same lengths as the ones we found to be resonant in the single-feed simple models. Still, they show up as short. Before we attribute the shortness to any particular cause, we should review other models, namely, ones that we might develop using MININEC 3.13, the public domain version of the alternative core.

Some MININEC Tests

Raw MININEC 3.13 would be wholly inadequate to the task of modeling a dipole with a 1/2-wavelength transmission line and a remote feedpoint/source. However, the core-calculating program has undergone extensive modification by a number of implementers. Perhaps the most thoroughgoing set of modifications belongs to the Antenna Model package by Terisoft. The program has revised the algorithms to overcome limitations involving sharp angle at wire junctions, closely spaced wires, and increasing frequency. Over a set of models for which NEC-4 has known accuracy, Antenna Model has closely matched the reported outputs.

Like all MININEC programs, Antenna Model lacks the NEC TL facility and the Sommerfeld-Norton ground calculating system. The latter want has no relevance to the present set of tests, but the former absence does limit the number and type of tests that we may perform. **Fig. 65-4** shows the three tests that we can perform.

The simplest set of models is a single-wire dipole fed at its center and resonated to the standards used for the NEC models. Since MININEC counts pulses, which occur at segment junctions and specified ends, we require 42 segments to feed that dipole at the exact center. As a check on the adequacy of the segmentation, we shall also increase the number of segments by 50% to 64. The following table provides the results of our initial work.

Test Configurations for a Dipole and Transmission Line
MININEC Models

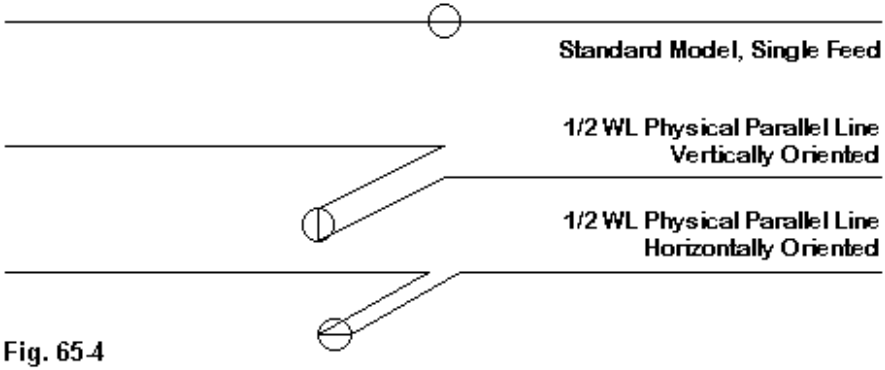

Fig. 65-4

El. Dia. Inches	El. Length Inches	Source Impedance R +/- jX Ohms	AGT Relative	dB
#16 42 Segs	+/- 204.9185	72.11 + j 0.002	0.9991	-0.004
#16 64 Segs	+/- 204.9185	72.18 + j 0.247	0.9994	-0.003
0.5" 42 Segs	+/- 202.475	72.02 - j 0.001	0.9981	-0.008
0.5" 64 Segs	+/- 202.475	72.11 + j 0.252	0.9985	-0.007
1.0" 42 Segs	+/- 201.231	72.06 - j 0.004	0.9974	-0.011
1.0" 64 Segs	+/- 201.231	72.15 + j 0.243	0.9979	-0.009
1.5" 42 Segs	+/- 200.280	72.14 + j 0.005	0.9966	-0.015
1.5" 64 Segs	+/- 200.280	72.23 + j 0.202	0.9973	-0.012

The simple dipole models appear to be sufficiently well converged to be useful for our further tests. The increase in segmentation yields a systematic increase in the feedpoint resistance and in the reactance in an inductive direction. Improve-

ments in the AGT values are completely marginal. (All values would be 1.0 if carried out to only 2 decimal places.)

Based on the resonant lengths of the dipoles, we may now construct vertically oriented transmission lines using AWG #16 (0.0508" diameter) wire space 1.084". The lines will be 1/2 wavelength long or 421.531". We shall use three levels of segmentation for all tests. 21/42/2 indicates that each side of the dipole has 21 segments, each transmission line wire has 42 segments, and the connecting feedpoint wire has 2 segments in order to center the source. We shall also use a 42/84/2 scheme to check convergence. Finally, we shall use a 205/421/2 scheme to provide a high segmentation level. In MININEC, it is recommended that adjacent segments have no more than a 2:1 length ratio, which this scheme achieves.

However, we have limitations using the 1" and the 1.5" diameter elements. The recommended minimum segment length should not be less than 1.25 times the diameter of the wire. To achieve this standard, it was necessary to perform revised tests for maximum segmentation. The 1" diameter element used a 160/421/2 scheme, while the 1.5" diameter element used a 106/421/2 scheme. The results appear in the following table.

El. dia.	El. Length	Source Impedance	AGT	
Inches	Inches	R +/- jX Ohms	Relative	dB
#16 21/42/2	+/- 204.9185	72.05 - j 21.69	0.9991	-0.004
#16 42/84/2	+/- 204.9185	72.15 - j 9.874	0.9995	-0.002
#16 205/421/2	+/- 204.9185	72.24 - j 0.867	0.9998	-0.001
0.5" 21/42/2	+/- 202.475	71.98 - j 16.71	0.9981	-0.008
0.5" 42/84/2	+/- 202.475	72.06 - j 7.456	0.9989	-0.005
0.5" 205/421/2	+/- 202.475	72.21 - j 0.176	0.9994	-0.003
1.0" 21/42/2	+/- 201.231	72.03 - j 15.38	0.9974	-0.011
1.0" 42/84/2	+/- 201.231	72.11 - j 6.779	0.9984	-0.007
1.0" 205/421/2	+/- 201.231	72.24 - j 0.256	0.9989	-0.005
1.0" 160/421/2	+/- 201.231	72.24 - j 0.220	0.9989	-0.005
1.5" 21/42/2	+/- 200.280	72.11 - j 14.70	0.9966	-0.015
1.5" 42/84/2	+/- 200.280	72.16 - j 6.578	0.9979	-0.009
1.5" 205/421/2	+/- 200.280	72.28 - j 0.456	0.9985	-0.007
1.5" 106/421/2	+/- 200.280	72.24 - j 0.533	0.9985	-0.007

Violating the length to diameter recommendation turns out to have no significance for the tests run here. More significant is the overall segmentation used. Segmentation levels that approach a level that allows the source wire segment to maintain the recommended margin with the segment lengths on the transmission line yield the most accurate results, using the simple dipole tests as a standard. Inadequate segmentation tends to introduce growing values of capacitive reactance into the source impedance and to yield slightly lower AGT values.

Overall, at every level of element diameter, the corrected MININEC algorithms yield highly usable results when we create dipoles with attached wire transmission lines. Unlike the NEC results, which strongly suggest that we avoid this route to modeling the dipoles (and by extension, other phased arrays with elements and transmission lines), an adequately corrected MININEC can easily and adequate model these situations. The AGT values strongly suggest—without guarantees, since the test is a necessary but not a sufficient condition of model adequacy—that the resulting models will be highly adequate in free space.

The NEC models showed enough deficiencies that they were unable to answer the initial question of this investigation. Does the overlap of element diameters that only touch at their ends create any danger of jeopardizing the adequacy of a model? The table above shows no signs that such problems will arise in MININEC. The 1.5" elements yield results that fall very exactly in the progression of values for the element diameters that do not have any end touching. For this class of cases, the touching of the inner element ends—where a wire junction does not form—appears to have no effect upon the outcome. Since MININEC uses pulses (appropriate segment ends) as the current centers, the special penetration problem that appears in NEC does not re-appear here.

Before we leave MININEC and our dipole tests, we should also test a horizontally oriented transmission line model. As with the NEC models, we shall split the dipole element and separate the two halves with a transmission line using #16 wire and a spacing of 1.084". The remaining dimensions of the model will be the same as in the previous model. As well, we shall employ the same set of segmentation levels as used previously. Here are the results.

El. Dia. Inches	El. Length Inches	Source Impedance R +/- jX Ohms	AGT Relative	dB
#16 21/42/2	+/- 204.9185	71.72 - j 27.85	0.9992	-0.003
#16 42/84/2	+/- 204.9185	71.83 - j 15.54	0.9996	-0.002
#16 205/421/2	+/- 204.9185	71.90 - j 6.654	0.9998	-0.001
0.5" 21/42/2	+/- 202.475	71.63 - j 21.66	0.9981	-0.008
0.5" 42/84/2	+/- 202.475	71.72 - j 11.91	0.9989	-0.005
0.5" 205/421/2	+/- 202.475	71.84 - j 4.699	0.9994	-0.003
1.0" 21/42/2	+/- 201.231	71.66 - j 19.89	0.9974	-0.011
1.0" 42/84/2	+/- 201.231	71.74 - j 10.83	0.9984	-0.007
1.0" 205/421/2	+/- 201.231	71.88 - j 4.164	0.9989	-0.005
1.0" 160/421/2	+/- 201.231	71.86 - j 4.178	0.9989	-0.005
1.5" 21/42/2	+/- 200.280	71.73 - j 18.89	0.9966	-0.015
1.5" 42/84/2	+/- 200.280	71.78 - j 10.34	0.9979	-0.009
1.5" 205/421/2	+/- 200.280	71.89 - j 4.034	0.9985	-0.007
1.5" 106/421/2	+/- 200.280	71.85 - j 4.124	0.9985	-0.007

Between the horizontal and vertical transmission line models, there is scarcely a change in any of the AGT values. The significant changes appear in the reactance at the source for each type of model. The higher the level of segmentation, the closer the model approaches resonance.

Perhaps the most comparable models between the NEC and the MININEC set are the highly segmented #16 AWG models using physical transmission lines. The following small table compares the NEC and MININEC models for horizontal transmission lines.

El. Dia. Inches	El. Length Inches	Source Impedance R +/- jX Ohms	AGT Relative	dB
MININEC				
#16 205/421/2	+/- 204.9185	71.90 - j 6.654	0.9998	-0.001
NEC				
#16 205/421/1	+/- 204.900	76.29 - j 7.717	0.947	-0.25

Both models show the remnant capacitive reactance. In the NEC model, there is a modifying algorithm that handles the effects of a feedpoint gap wherever one

places a source. That calculation is not a part of the separation of the element wire halves when we place a transmission line in the picture. The gap adjustment occurs at the remote source. It is possible that the difference creates the resulting capacitive reactance in the source impedance of the models, although I am at present uncertain whether there is a comparable calculation present in the MININEC algorithms.

The MININEC model achieves a higher AGT value, largely as a result of the corrections for closely spaced wires. At present, NEC cores do not have a correction or adjustment for errors that may creep in due to the close spacing of long wire runs.

Conclusion

Our foray into modeling dipoles and transmission lines has turned up a number of interesting facets of modeling in both NEC and MININEC. All of the results are relevant to modeling any set of elements and associated transmission lines. The pursuit of an answer to a single question gradually yielded at least partial answers to a larger set of questions.

Although we focused the exercise on a single question, the general procedure is relevant to any complex modeling task that may press one or more of the limitations inherent in the available modeling cores. Wherever a model type is complex and the modeling strategies approach the fringes of the core capabilities, it is worthwhile to develop a test procedure to assess in advance the adequacy of the strategy. The results can save us from inadvertent misrepresentations of the potentials of an antenna design. As well, they may also give us fuller confidence in a particular strategy that passes all of our tests. Either way, testing modeling techniques in advance with relevant but simplified models is a worthwhile enterprise.

* * * * *

Models included: 65-1a through 65-5d. (.NEC and .NWP model dimensions in meters; .EZ model dimensions in inches. Due to the variability of systems used to save a MININEC model, only NEC models can be supplied with this volume.)

66. State of the Art?

The following notes represent a set of ruminations on the state of development of both NEC and MININEC from their inception to the present. My interest as a user is not in the actual algorithms inside the calculating core, but rather with the efforts that have gone into developing the cores to their fullest potentials for accurate modeling of difficult antenna geometries.

An Initial Limitation

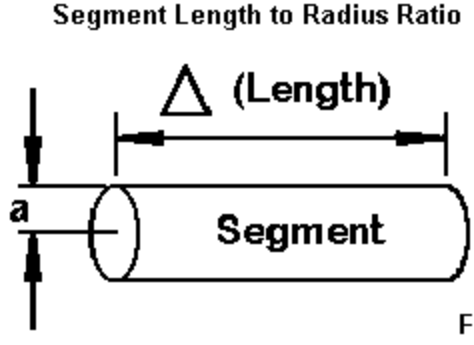

Fig. 66-1

Both NEC and MININEC are wire-modeling programs at root (even though NEC has a surface patch capability). Hence, we likely should accept the limitations imposed by a necessary segment-length-to-wire-radius value: this limitation, suggested in **Fig. 66-1**, will ultimately not be eliminated without changing the entire basis of the modeling core. The core uses a thin-wire calculation scheme, and hence, the radius can only be enlarged so far before one exceeds the limits of the thin-wire equations.

This limitation has consequences related to the maximum frequency for which one may model accurately. For a true wire size within the normal range of construction, there will be a frequency frontier or region at which the wire radius increases toward the segment length so that results become untrustworthy. I call this region a frontier because it appears to be dependent upon at least two variables: the wire radius and the complexity of the geometric structure. The more complex the structure, the more segments per wavelength are required to converge results.

Of course, we have a work-around for those willing to do the detailed modeling required. We may use very thin wires and simulate solid wires with cylindrical wire-grid structures. Under usual modeling conditions, the amount of effort required to create the cylindrical substitute and finding the most reliable means of giving the resulting antenna a source will together make this work-around untenable in practical terms.

Both NEC and MININEC are subject to this initial limitation. Hence, it is likely that there will always be an upper frequency limit—variable though it may be—for both types of cores. Above that limit, other modeling core techniques become dominant.

However, NEC-2 and MININEC 3.13 are both public domain software cores. Hence, both find a place in inexpensive entry-level software. Hence, they are both in very wide use—and that is part of the story.

Other Limitations

When MININEC 3.13 became available out of the work of Rockway and Logan and entered public domain use, it became the core of choice for early DOS-based commercial programs, such as MN by Brian Beezley and ELNEC by Roy Lewallen. When NEC-2, developed largely under the leadership of Jerry Burke at LLNL, finally became public domain (as NEC-3 and NEC-4 supplanted it at LLNL), it entered commercial programs such as NECWires by Beezley and EZNEC by Lewallen. These DOS-based programs eventually took a back seat to Windows-based program, as EZNEC converted to Windows and NSI's NEC-Win Pro and Plus appeared. Windows versions of MININEC began to appear in both free and commercial ware, such as NEC4WIN by Orion and most recently Antenna Model by Terisoft.

Before we assess some of the significance of these progressions of software, let's make a short listing of some of the limitations that each core suffers in its native form.

MININEC 3.13 Limitations

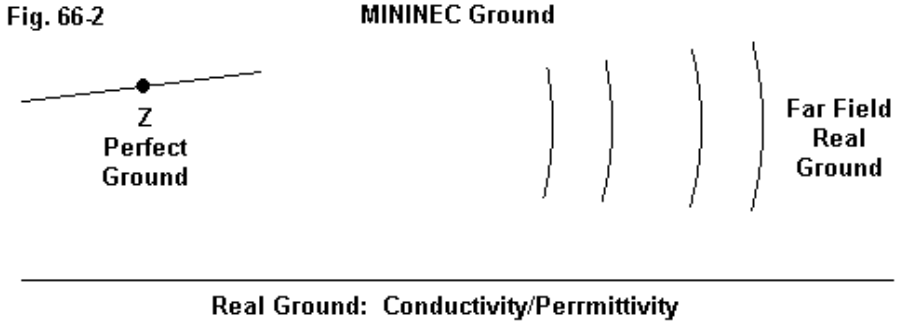

MININEC 3.13 uses a simplified ground system, as suggested in **Fug. 66-2**. It makes use of a reflection coefficient to determine the effects of ground on the far field. However, the reported source impedance is always taken over perfect ground—and that value may or may not be sufficiently accurate for a given modeling task. (In contrast, NEC-2 accesses a Sommerfeld-Norton ground calculation scheme that provides in NEC-2 very accurate result within a few wire radii of the ground. NEC-4, of course, permits buried wires, that is, wire below Z=0.)

MININEC 3.13 has what some call a frequency bias, that is, an error factor that increases with frequency. At VHF and higher, the error is significant. MN provided a correction for this bias. MININEC 3.13 also has a closely spaced wire problem in its native form. ELNEC provided a corrective for this difficulty. MININEC 3.13 also showed errors when wires met at angle from a right angle down to very small angles. Two routes were generally used to overcome this problem. Since the initial MININEC was limited in the number of total segments that a model might have—a limit removed in Windows versions that usually code in C (however many the following + signs)—one technique was the system of length tapering used in ELNEC. This

system ensured that the segment lengths at the angular corner were very short, thus eliminating the clipping effect that results from the use of pulses (at segment junctions) to form the center of current. Core modifications were a second route to overcoming this limitation. Early attempts at corrections have evolved into a rather sophisticated scheme in Antenna Model that produces very accurate results.

NEC-2 does not suffer the angular junction problem until the angles between wires become very small—small enough that the center of the joined wires interpenetrate. In the most general terms, the middle third of a wire segment is critical to model accuracy, and all junction penetrations should fall outside this area. The thinner the wire and the longer the segment, the narrower the angle may be without incurring model inaccuracies that show up on an average gain test.

MININEC has one more limitation relative to NEC-2/-4: it runs very slowly for a model of a given size relative to the comparable model in NEC. The latest core revisions and Windows programming languages have not yet allowed MININEC to catch up in speed to NEC. Indeed, for very large models, it is not even a race.

Unlike NEC-2 and -4, MININEC 3.13 does not have a "TL" or transmission line facility. This forces one to model all transmission lines as real (potentially radiating) wires, which can become a tedious task for arrays such as a very large and well-populated LPDA. However, the junctions between the thinner phase-line wires and the fatter element wires present no problems—as they would for NEC-2 and -4.

We should note in passing that Rockway and Logan have moved on to a complete revision of MININEC to overcome a number of the limitations of 3.13. The result is a sequence of programs called generally "Expert MININEC." Since the programs are proprietary and have considerable cost for versions that permit a high segment count, I do not have a current version and hence must exclude these developments from consideration here. However, a relatively full description of the program foundations has been available at the EM Scientific web site (http://www.emsci.com/).

NEC-2 Limitations

NEC-2 (and -4) place the center of current in the mid-segment region and thus are subject to limitations quite unlike those of MININEC 3.13. The original program-

ming is in Fortran, which has seen a number of run-speed improvements as those implementing the core make use of the latest compilers. With the increase in computer speed and RAM size as adjuncts to these speed improvements, the need for using the fast or reflection-coefficient ground calculation system has largely passed, and the S-N ground system is generally recommended for all antenna models requiring placement over ground. As well NEC calculates the source impedance of a model over the actual ground specified in the model, whichever type of ground that the user selects.

There are two ways to look at NEC-2 limitations. One is by way of comparison with what MININEC 3.13 does well. The other is by way of comparison with what NEC-4 does better. To be fair, we shall have to make both types of comparisons.

Fig. 66-3

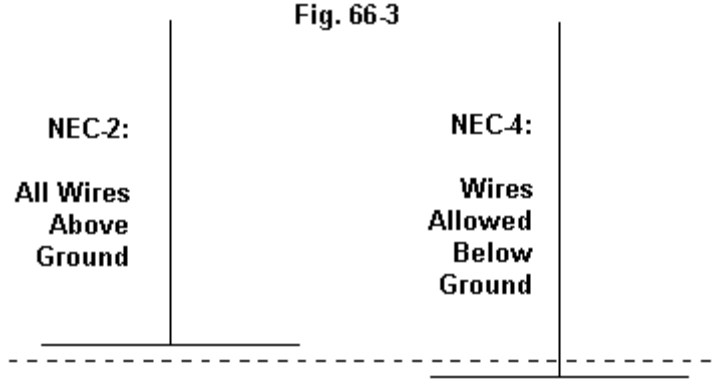

The primary example of a comparison between NEC-2 and NEC-4 is perhaps the ability of the latter version to handle wires placed below ground, as noted in **Fig. 66-3**. Although numerous modelers have tried to determine vertical monopole performance by placing NEC-2 ground radials very close to the ground, modeling the same structures in NEC-4 with buried radials have shown these approximations to be very limited.

NEC-4 also offers a few possibilities included in neither MININEC 3.13 nor NEC-2. An obvious example is the NEC-4 control card IS, that allows the user to evaluate a wire having an insulated sheath with a user-specifiable thickness, conductivity, and dielectric constant.

NEC-4 improvements over NEC-2 range from the well advertised to the relatively unknown. In the latter group belongs an emergent frequency offset between NEC-2 and NEC-4 as one goes into and through the UHF range. In general, NEC-4 is considered more accurate in this regard. It also appears that NEC-4 handles tight angles between joined wires, especially in radial sets and similar structures, somewhat better than NEC-2.

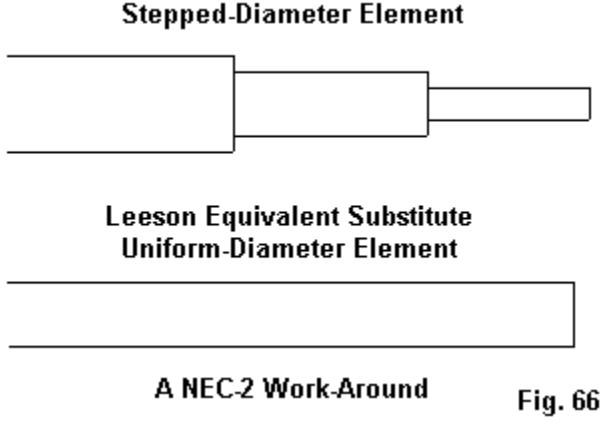

Fig. 66-4

The most widely advertised improvement in NEC-4, suggested in **Fig. 66-4**, is the ability to handle with reasonable accuracy antenna elements composed of stepped-diameter model wires, a common feature of upper HF arrays. NEC-2 models of such elements are wholly unreliable. There emerged some schemes for overcoming this limitation. The one used in both EZNEC and NEC-Win Plus involves the Leeson corrections. Essentially, the program calculates a uniform-diameter

element of the correct length and diameter to serve as a substitute for the stepped-diameter element. The calculations have restrictions, for example, the requirements that the element be symmetrical (if not a monopole touching the ground) and that all sources and loads be at the element center (or monopole base). Since these restrictions are no problem for Yagi, LPDA, and similar upper HF elements, the substitute uniform-diameter work-around has performed very successfully.

However, even the work-around has limitations. There will be a difference in the reported NEC-2 output for such an element with uniform segmentation vs. one with highly variable segmentation, especially if the segment lengths differ close to the source.

NEC-4 requires no substitute elements, as it handles stepped-diameter directly. However, the core does not yield identical results with those of substitute uniform-diameter elements, and the more radical the stepping of the original elements, the further NEC-4 results depart from those obtained by Leeson substitutes. In contrast, Leeson substitute elements correlate very precisely with the native stepped-diameter element directly handled by MININEC. MININEC 3.13 does not suffer the large limitation of NEC-2 and the smaller one of NEC-4, and hence yields accurate results without correction factors (other than those notes earlier for frequency and the like).

Related to the stepped-diameter element limitation is another, suggested in **Fig. 66-5**: NEC yields erroneous result when there are junctions of wires having dissimilar radii. As one might expect, the difficulty is worse in NEC-2 than in NEC-4. However, a well-corrected MININEC program produces more accurate results in such cases than even NEC-4.

Fig. 66-5

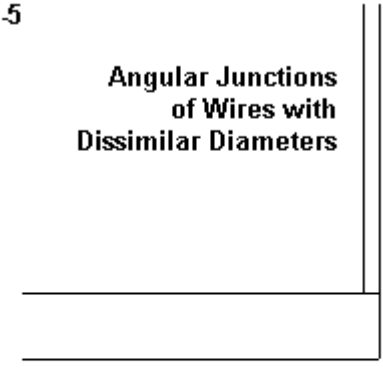

Angular Junctions
of Wires with
Dissimilar Diameters

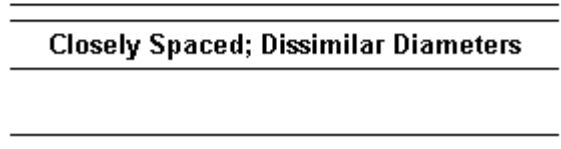

Closely Spaced; Dissimilar Diameters

Both NEC-2 and -4 require for greatest accuracy that closely spaced wires have the best possible segment-junction alignment. However, even adhering to this condition yields erroneous results if the wires—even though not touching—have dissimilar diameters and the error increases as the wires are brought closer to each other. The degree of divergence from accuracy tends to show clearly in average gain tests. Once more, a well-corrected MININEC 3.13 does not share this difficulty. However, note the qualification that the MININEC core must be well corrected. With suitable correction, MININEC will show poor accuracy with closely spaced wires of any diameter, including standard folded dipoles.

NEC-2 and -4 do have a TL or transmission line facility that enables the user to construct non-radiating lines of virtually any characteristic impedance and length.

However, despite having been around since at least the early 1980s, the TL facility remains restricted to lossless lines, with no way of handling real lossy lines. At the same time, constructing real-wire simulations of transmission lines to account for losses in them falls prey either to NEC's difficulty with very closely spaced wires or to its inability (without massive and mostly impractical wire-grid constructs) to handle concentric coaxial cables. Only NEC-4 would be able to handle the dielectric within a coaxial cable, if one tried to create such a cable as a wire-grid structure.

Some Common Limitations

Both NEC and MININEC permit the user to place resistance-reactance or resistance-inductance-capacitance loads on a modeled wire. In both cases, the loads are non-radiating or, in other terms, mathematical only. As such, they are, like transmission lines, most accurate when placed at current maximums, where the current at both ends of the loaded segment is roughly equal. Placed away from these positions, the current at one end of the load differs from the current at the other end, and the load less accurately reflects the performance of a real component. An inductor, for example, performs as almost solely an inductor only so far as the current at each end is equal. Any differential will show up in the form of the wire acting partly as a length of the antenna wire. The non-radiating loads of modeling programs cannot show this non-inductive activity of a load placed on a wire in a region of significantly changing current level.

Fig. 66-6

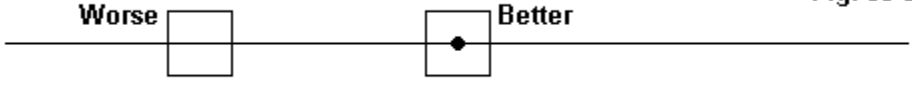

Load and Transmission Line Placement

MININEC 3.13 has another limitation in its native form, suggested by **Fig. 66-6**. It permits load and source placement only at the wire ends or at the center. Some implementations of MININEC, such as ELNEC, have overcome this limit, while others have not. Although the models—by judicious subdivision of an element into separate wires—can overcome the limitation, its persistence does complicate modeling.

As we have noted, of the cores under consideration, only NEC-4 permits the use of wires lower than Z=0. For a perfect ground, a monopole just touching ground will yield virtually identical results in both MININEC 3.13 and NEC-2. However, if we assign the ground values of conductivity and relative dielectric constant (permittivity), we obtain considerably different results. In general, NEC-2 results are without merit. MININEC 3.13 results are usable, but with limitations that have not been appreciated until comparisons were made between those results and the outputs obtained in NEC-4 with buried radial fields of various sizes. The resulting correlations were spotty at best. The usefulness of the MININEC ground had been sufficiently superior to use of either form of NEC-2 ground to encourage EZNEC to provide that ground system as an addition to the ones within the NEC-2 core.

However, in the end, the adequacy of using a MININEC ground with vertical monopoles and variants depends in large part on the degree of accuracy required by the modeling task. There is a vast difference in the demands placed on a modeling system when we desire precision from those we impose when we are looking a general trends. As well, the MININEC system has been misused in the analysis of monopole arrays where one or more of the elements is sloping. Any horizontal component to the radiation of the element, when the elements is in whole or part less than 0.2 wavelengths above ground will result in errors. Still, the results may be only as erroneous as those produced on a simulated buried field in NEC-2 that is composed of wires close to ground—assuming that a buried radial field is the actuality to be modeled.

I Am Surprised. . .

The sum of this incomplete review of MININEC 3.13 and NEC limitations is not what one might initially expect. The point is not at all to compare the two core types in an effort to assess superiority. As previous columns have suggested, which core is superior depends to a very great extent on the parameters of the modeling task.

Rather, my ruminations on the limitations of the cores bear an element of surprise that more has not been done in certain directions of potential development.

1. *MININEC 3.13*: The MININEC core lacks three things achieved by NEC-2: speed of run-time, the presence of the S-N ground calculation system, and the presence of the TL facility. In terms of the user's encounter with the best of current

MININEC 3.13 implementations, these shortcomings are the most pronounced. I cannot say what the future may hold for speeding up MININEC runs and for adding the two facilities to the programs available to the user. However, having noted these hoped-for developments, let's turn to the other side of the coin.

Since its release as a public domain program, MININEC 3.13 has been under continuous development by a number of individuals. Corrections have emerged for most of the geometry-related and frequency-related aspects of core performance. As well, initial segmentation limits have disappeared in Windows implementations of the cores so that now computer memory is the chief limiting factor in model size.

While user interfaces have emerged to ease both the input side of modeling and to make the output side more readable and interesting, the bottom line remains this one: the core itself has undergone considerable evolution in the decades since it became public domain.

2. *NEC-2*: NEC-2 is no less a public domain core than is MININEC 3.13. The code is readily available. Indeed, there have been a few core modifications to customize it for use with various interfaces, if for no other purpose than to set the maximum limit on the number of allowable segments in a model.

However, most of the major work of commercial developers has been in the region of the input and output interfaces. Input systems have become sophisticated, even to allowing modeling by equation in NEC-Win Plus or modeling in MathCAD, as in SuperNEC. Model viewing—with accessible geometry data—is commonplace, and modeling with a reliable transfer from a graphic to a wires table is not far off. Output tables and graphics have grown more numerous and content-rich, and the NEC outputs gradually become more easily accessed and transferred to a medium of preference.

However, the NEC-2 core has remained relatively inviolate. For example, EZNEC permits the specification of TL physical lengths and velocity factors. However, what enters the core is a pre-calculation of the electrical length. The core remains as is. Similarly for EZNEC and NEC-Win Plus Leeson corrections. The core uses the substitute element, but has not been altered internally to better handle stepped-diameter elements.

NEC-4 has emerged as the best of NEC, but even it has limitations, such as those suggested earlier. Although it is proprietary, its remaining limitations seem significant enough to encourage developers to work with the public domain NEC-2 core to yield a core that is as accurate as MININEC is in the regions where its accuracy is both known and high. Curiously, such developments have either not occurred or not been made public—even in the form of an improved commercial implementation of NEC-2. Improved versions of NEC-2 either rest on improved run times or upon improved user interface facilities.

I do not know if the existence of NEC-4—however proprietary it may remain—discourages wrestling with NEC-2 to improve it. Likely such development would have only limited commercial attractiveness within the U.S., where NEC-4 is readily available to those who can pay for both the license and the software. However, since NEC-4 still has export restrictions, refinement of the NEC-2 core seems to be a task that might appeal to developers outside the U.S.

It may well be that many of those who might be capable of undertaking the further development of NEC cores are awaiting a NEC-5. There have been hints from time to time of emergent cores using the method of moments in conjunction with a different set of algorithms.

So the state of the art is that NEC users either work with a 20-year old core having severe limitations or that they qualify to work with a decade-old core that is not limitation-free. MININEC 3.13 users face equal limitations in the absence of certain features that NEC users enjoy, despite continuous and intensive development efforts over the years.

Little wonder that I am surprised.

* * * * *

Models included: none

67. Wire Grids 1: Plane and Simple

Except for the use of surface patches—which are not generally available on entry level NEC software—the method of simulating a solid or closely meshed surface is through the use of wire grids. Note that I am including closely spaced meshes—such as window screening—along with solid planar surfaces in the wire-grid pool. **Fig. 67-1** gives us the initial story.

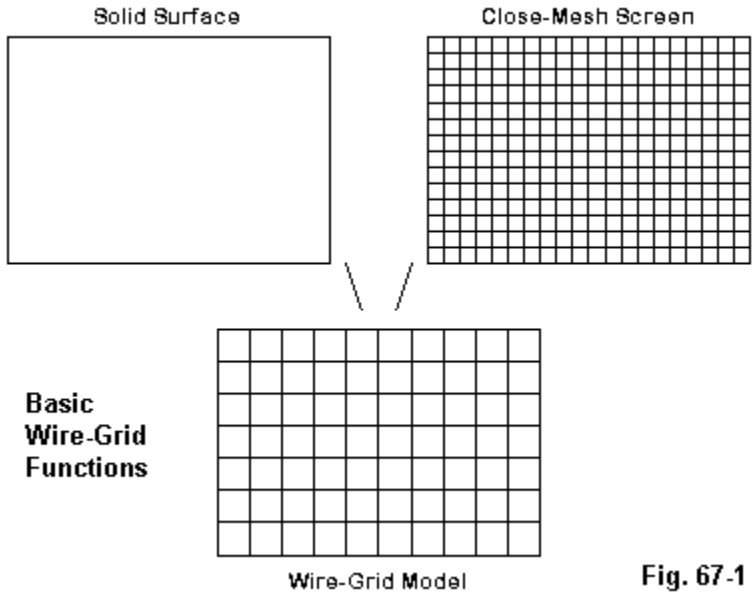

Fig. 67-1

NEC is based upon round conductors and thus cannot directly model a flat surface. This limitation shows up vividly in UHF modeling, where NEC has difficulty simulating integrated antenna elements and transmission lines composed of flat thin strips of copper on a glass or similar substrate. At lower frequencies, from VHF downward, we can simulate flat planes by constructing a grid of interconnected wires having the same outline area as the solid surface. In fact, for basic modeling of rectangular surfaces, some entry-level software—such as NEC-Win Plus and EZNEC Pro—provide semi-automated systems. The user inputs certain dimensions and the program creates the requisite wires and intersections for the plane in the form of a set of wires or GW entries.

In fact, the two software packages just cited illustrate two different ways in which we can go about creating a wire grid. **Fig. 67-2** illustrates the difference.

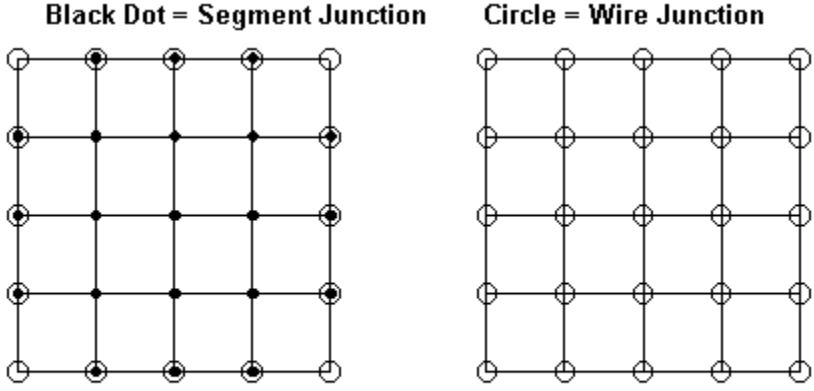

Alternative Methods for Constructing Wire-Grids

Fig. 67-2

On the left, we find a small number of wires, just enough to populate the two directions of the plane. The intersections of the grid, except for the 4 corners, consist either wholly of segment junctions or of combinations of wire and segment

junctions. Although beginning modelers are often cautioned to use a wire junction for every crossing pair of wires that touch, it is legal to NEC's rules to have wires joined at segment junctions.

The advantage of this systems revolves around the fact that the run time for a model depends upon both the number of segments in the model and the number of wires. Although the total number of segments in the left construct equals the number of segments in the construct to the right, the number of wires is considerably lower—and the run time is accordingly shorter. However, the advantage is accompanied by a disadvantage. If we move either end coordinate of any one of the wires, the entire set of junctions along the wire (except for the unmoved end) becomes a set of either non-junctions or illegal wire crossings at other than a wire end or a segment junction.

For this reason, one might equally create the same wire grid using the system at the right. Here, every junction is a wire end. The result is somewhat greater flexibility in model revision. We can take a given wire and move it a bit. Then we need only revise the end coordinates of a few other wires (from 1 to 3) to restore the integrity of the grid. We can take a simple rectangle and fold down the corners or make other simple geometric revisions with fair ease. The price that we pay for this flexibility is to have as many wire as we have segments, thus extending the run time for the core.

Wire grids are subject to some rules—actually, more like some rules of thumb. For example, the most common wire/segment length used in most wire grids is 0.1 wavelength. This value is about twice as long as the recommended length for a segment in a dipole (about 0.05 wavelength). Wherever the current levels are high or change rapidly from one wire-grid element to the next, the modeler should use a shorter segment length. However, when wire grids simulate planes that are not very active in the antenna system, that is, they have relatively low and nearly uniform currents, some modelers have used segments lengths longer than 0.1 wavelength. Even the 0.1-wavelength baseline segment length yields a sizable model, since the number of segments in the wire grid will be about 220 times the area of the plane when measured in square wavelengths.

Ideally, the surface area of the grid should approximate the surface area of the plane being modeled. This often leads to the use of fairly "fat" wires, since the grid

wire diameter should equal the grid spacing or segment length divided by PI. Obviously, the more wires in a grid of a certain set of outside dimensions, the smaller the segment length becomes and hence, the smaller the wire diameter needs to be.

These basic rules of thumb are subject to numerous variations according to the kind of surface that we are trying to simulate with a wire grid. A screen mesh may vary in its opening size and may not need the wire diameter required by a simulation of a flat plane. Likewise, a plane with a very coarse surface may more adequately model with thinner wires or longer segments. There is no simple infallible route to wire-grid modeling.

In this episode, we shall restrict ourselves to relatively simple wire grids that we can create using automated wire-grid facilities within modeling programs. All of our examples will focus on rectangular planes. In fact, all will serve as reflectors for various kinds of arrays. We shall eventually return to wire grids used to create other types of shapes. But in the beginning, simple planes or combinations of planes will alert us to some fundamentals of wire-grid modeling.

A Corner Reflector

One of the simplest high-performance arrays available for UHF service is the corner reflector. The antenna consists of a dipole and two flat surfaces joined along one edge. The apex of the tent-like reflector is behind the dipole at a certain distance that is largely a matter of the desired feedpoint impedance. Performance is a periodic function of the reflector dimensions, with larger reflector planes (up to a point) yielding higher gain. The corner reflector array is a wide-band antenna with stable performance values for a 25% bandwidth (at least). Some designers have used fan dipoles and other geometries to further increase the operating bandwidth.

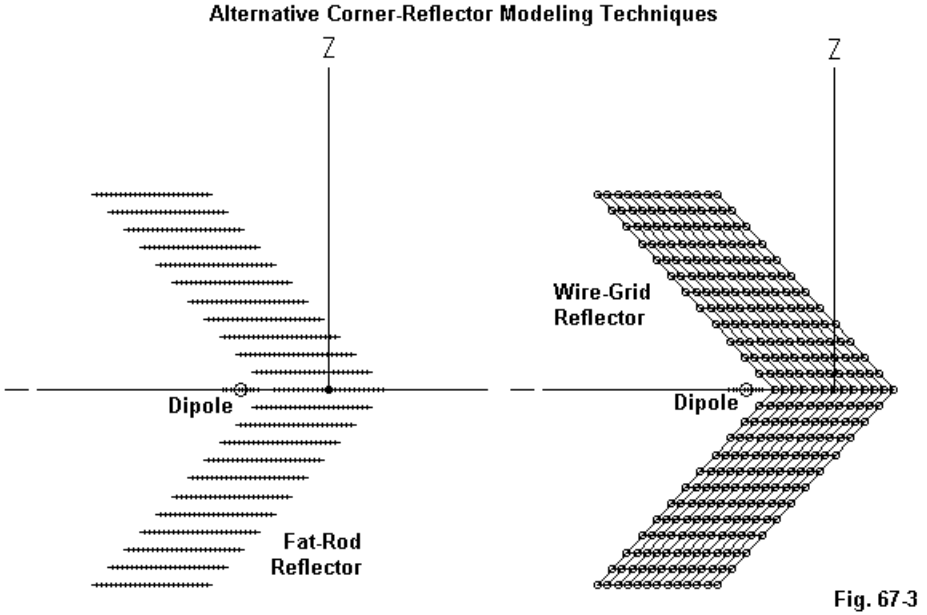

Fig. 67-3 shows two model outlines for a corner reflector. They correspond to typical ways of constructing the antenna. One style of construction uses a series of rods or tubes arranged to simulate a flat plane, with each rod being considerably longer than the dipole element and in the same plane. The other style of construction makes use of either a solid surface or a rigid screen to form the reflector planes. A screen tends to show less wind resistance than a solid surface and is popular in larger reflectors used at lower frequencies.

There is a tendency on the part of modelers to use the rod model as a substitute for the wire-grid version. The rod model uses (in this particular case) only 24 wires and 586 segments. The wire-grid version, for reflector planes having an identical overall area as the rod-planes, requires 613 wires and 622 segments. See models

67-1 and 67-2. (The slightly higher segment count is a function of the dipole using several segments in its single wire, while each element of the wire grids uses 1 segment per wire.)

When joining two independently created planes along one edge, be sure to delete the duplicate edge wire at the junction.

In this example, whether or not the rod model can substitute for the wire-grid model depends on the degree of refinement we require for the output data. The following brief table will illustrate the point. It presents the reported performance figures for the two models, which use identical dipoles at identical distances from the apex of the two planes of the reflector, each plane having the same outer dimensions.

Model	FS Gain dBi	180-Deg F-B dB	Feedpoint Impedance R +/- j X Ohms
Rod	11.25	29.90	92.6 - j 4.0
Wire-Grid	11.80	30.52	88.2 - j 0.3

For many purposes, the output data of each model is adequate. However, we can notice some difference. Note that each model is most likely adequate as a model of the particular construction type that it simulates. The question we posed was whether the simpler rod model might suffice as a model of a solid surface corner reflector that the wire-grid simulates. In general, the answer seems to wobble on a fence.

The wire grid used in our initial comparison employed 0.1-wavelength segments. So we might also ask whether that model is adequate or whether we should use a reflector model with shorter segment lengths, perhaps 0.05 wavelength. **Fig. 67-4** illustrates the difference between the low-density and high-density planes. Compare models 67-2 and 67-3.

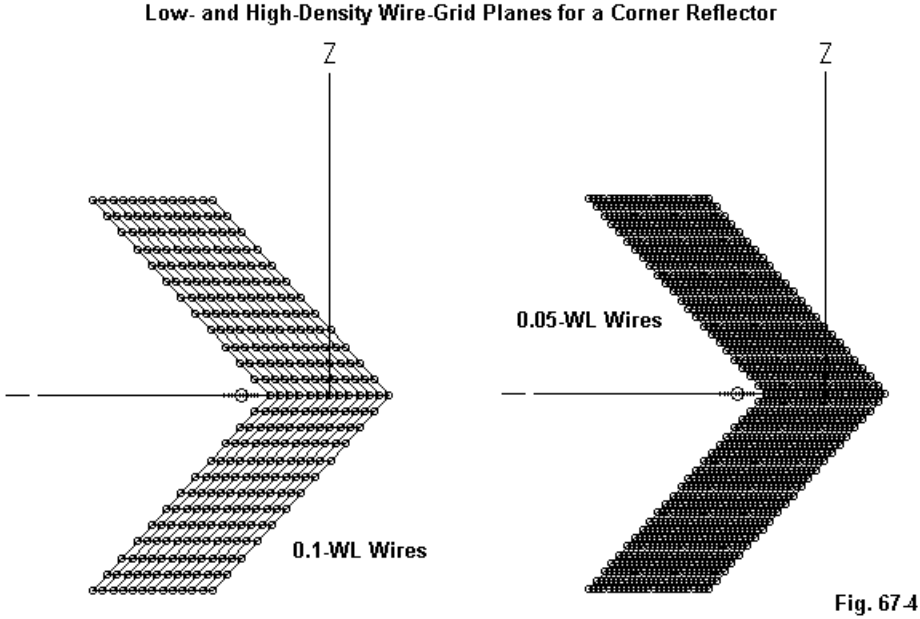

Fig. 67-4

While the low-density model required 613 wires and 622 segments, the new model demands 2279 wires and 2289 segments. Doubling the segment density results in a total wire count that is 4 times the original, minus some segments for the edges. Obviously, one's software must have a segment capacity able to handle the number of segments and wires.

Let's compare the performance results.

Model	FS Gain dBi	180-Deg F-B dB	Feedpoint Impedance R +/- j X Ohms
Low Density	11.80	30.52	88.2 - j 0.3
high Density	11.71	31.62	88.4 - j 0.8

For this particular application, increasing the segment density yielded no significant change in results. Unfortunately, about the only way to determine whether we need to use a wire grid with shorter segments is to actually model the antenna using both density levels. Of course, once you have the larger model, you might as well use it.

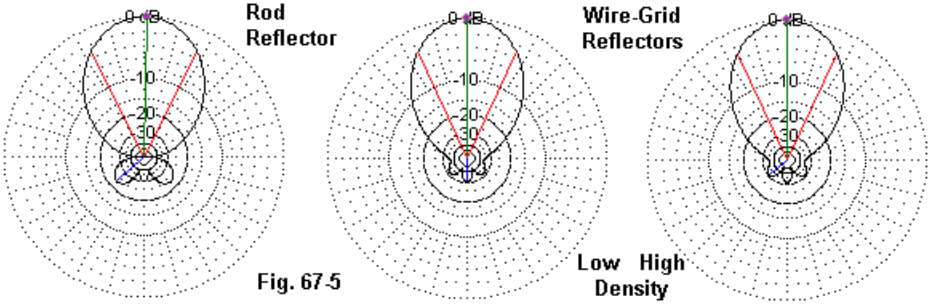

Free-Space E-Plane Patterns for Equal-Size Corner Reflectors

Fig. 67-5 shows the design-frequency E-plane patterns for the three models. It is clear that the two wire-grid models have very similar patterns. However, there are noticeable differences in the rearward portions of the pattern for the rod model. Although they make only a slight difference in this case, let's not forget them as we look at further examples.

A Flat Plane Reflector with a Double-Quad Driver

Although it has a fairly long history, the double quad has re-emerged as a high-performance UHF antenna when placed ahead of a flat-plane reflector. Fed across a gap at the center, the antenna is capable of a 50-Ohm impedance, convenient for conventional coax feeding. However, the exact impedance is also a function of the double-quad dimensions and the spacing from the reflector without much alteration of performance. Like the case of the corner reflector, the antenna is more sensitive to the size of the reflector plane.

<p>As we did for the corner reflector, let's create both a rod and a wire-grid reflector. All we need is a single plane, so our work is much simplified. We shall use identical outside dimensions for both types of reflector planes. The modeling results appear in sketch form in **Fig. 67-6**.

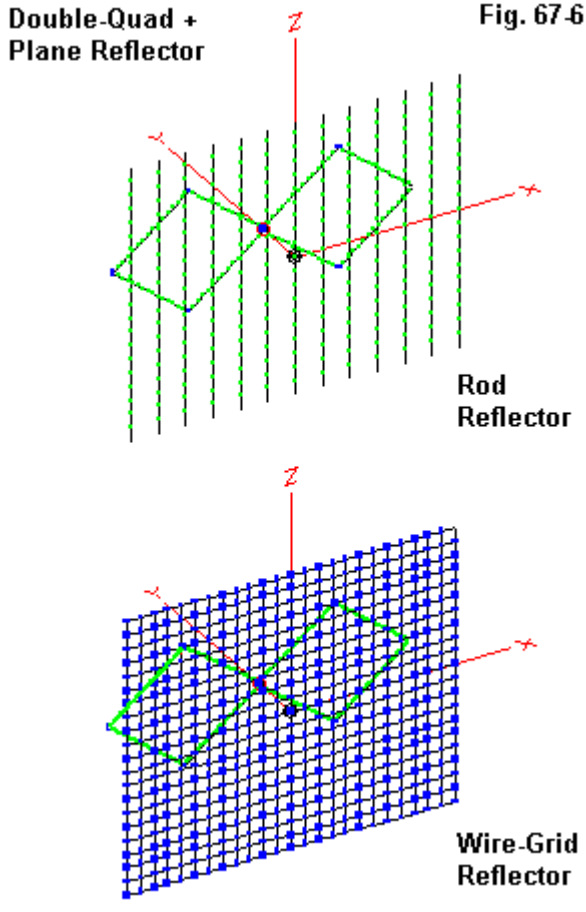

Neither reflector is optimally sized necessarily. For our purposes, it is only necessary that we make them the same size, use the same double quad, and place the driven element the same distance from the reflector. The rod model shows vertical rods, since the double quad is essentially a side-driven pair of quads in parallel. Compare models 67-4 and 67-5.

The next step, of course, is to compare the reported outputs from NEC-4.

Model	FS Gain dBi	180-Deg F-B dB	Feedpoint Impedance R +/- j X Ohms
Rod Ref. D-Q	10.10	21.59	55.5 - j 3.4
W-G Ref. D-Q	10.06	29.48	48.6 - j 10.7

Whether or not differences in gain and impedances reports are significant or trivial depends upon the modeling task at hand. What is undeniable is the very large difference in the reported front-to-back ratio—about 8 dB. We may wish to ask why there is so much larger a difference in the front-to-back ratios for this case and so little for the corner reflector.

The answer lies in the nature of the driven elements. The corner reflector used a dipole that was aligned with the rods in the reflector. However, our double-quad array uses a driven element that is not polarized wholly in a plane parallel to the rods. The side-fed quad loop has only a dominant vertical component (if we take a perspective on the antenna as if it were above a ground surface), but retains a small but significant amount of radiation with a horizontal component. Hence, the wholly vertical reflector rods are less effective than the full mesh of a screen or a solid surface reflector.

My goal in presenting this particular model is to make a simple point. Just because a simplified rod model (22 wires, 381 segments for the double quad) is adequate for some cases, we may still require the bulkier wire-grid model (1013 wires, 1245 segments of 0.05-wavelength for the double quad) in other cases. One must always analyze the nature of the driving antenna rather than assuming the a smaller rod model is “good enough.”

Fig. 67-7 displays the E-plane patterns for the two models. The differences in rearward performance show up clearly.

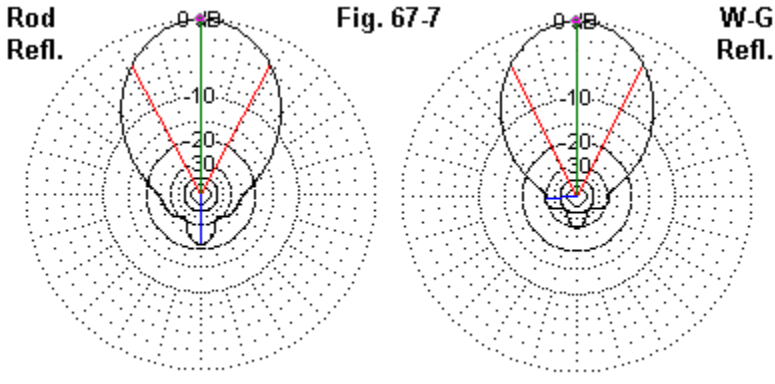

E-Plane Patterns: Double-Delta + Plane Reflector

A Tri-Plane Reflector Array

The tri-plane reflector is only sparingly used, although it has some interesting properties. Not the least of these properties is the fact that it uses a monopole driven element, where one plane of the reflector is also the "ground plane" for the monopole. A second interesting feature is that the main lobe of the antenna emerges in a direction roughly equidistant angularly from each of the reflecting surfaces.

The interesting part of these phenomena for the modeler is how to obtain a model over ground of the antenna when we aim it so that the signal is a parallel to the ground as possible. Let's make the game more interesting by desiring to have a version that is horizontally polarized and a version that is vertically polarized. **Fig. 67-8** shows the steps in the set of transitions. Let's see how we moved from one to the next. Compare models 67-6, 67-7, and 67-8.

Evolution of a 3-Sided Corner Reflector Fig. 67-8

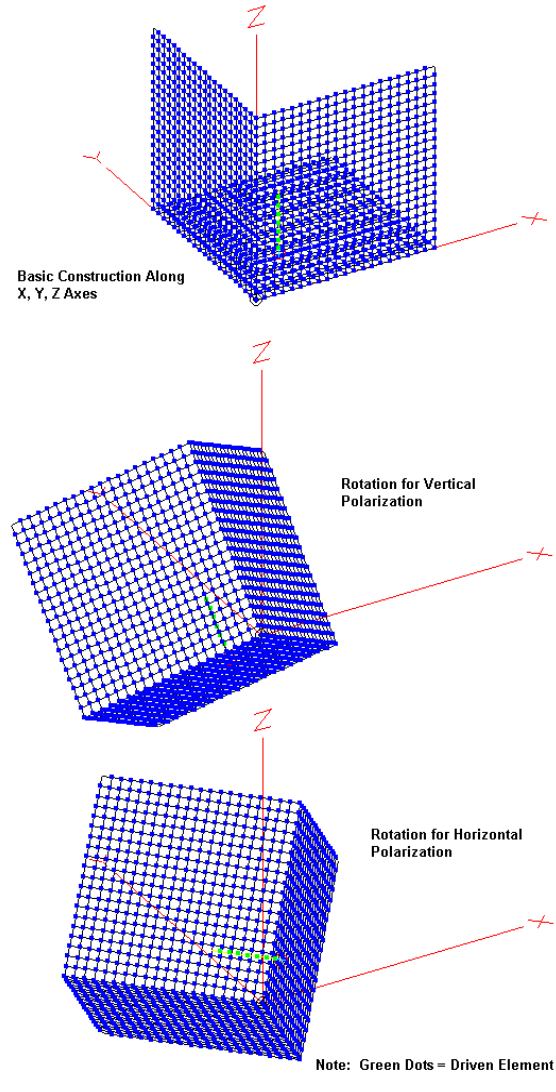

In any automated system of wire grid generation, it is usually easiest to develop a set of rectangular planes by using the axes of the coordinate system as one of the edges. Hence, the initial set of three sides for the tri-plane reflector are oriented in this manner, as shown in the top sketch of the three views. The driven monopole shows faintly inside the reflector as the line connecting the green segment-junction dots. Since 3-sided corner reflector theory is based upon reflector and monopole dimensions given in terms of wavelengths, I constructed the model in these terms. The grid wires are 0.1 wavelength, and the overall dimensions of each side of the reflector are 2.0 by 2.0 wavelengths. The model used 2461 wires and 2468 segments, with an 8-segment monopole driven element.

The performance of the array is somewhat better than that of a corner reflector with its reflector planes optimized. The free-space gain is about 16.2 dBi, with a front-to-back ratio of 35.7 dB. **Fig. 67-9** provides the E-plane pattern of the array.

The more important performance feature for this exercise is the fact that the direction of radiation at its maximum is about 45 degrees from any of the 3 planes. Since I had constructed the planes in a positive direction from the coordinate center (0, 0, 0), the pattern in **Fig. 67-9** is taken at a phi (azimuth) and a theta (elevation) angle of 45 degrees.

The original wire grid structure emerged from the EZNEC system. However, if I wanted to have vertically and horizontally polarized version of the antenna for use over ground, I would have had to build the array from scratch for each orientation. Instead, I converted the model into a standard .NEC format file and imported it into NEC-Win Plus. There, I used the rotation capabilities to rotate the entire array to the correct positions. Then, in order to have three corresponding patterns. I re-opened the file in EZNEC Pro. (Version 4 of EZNEC should contain complete wire rotation and translation facilities, making this maneuver unnecessary in the future.)

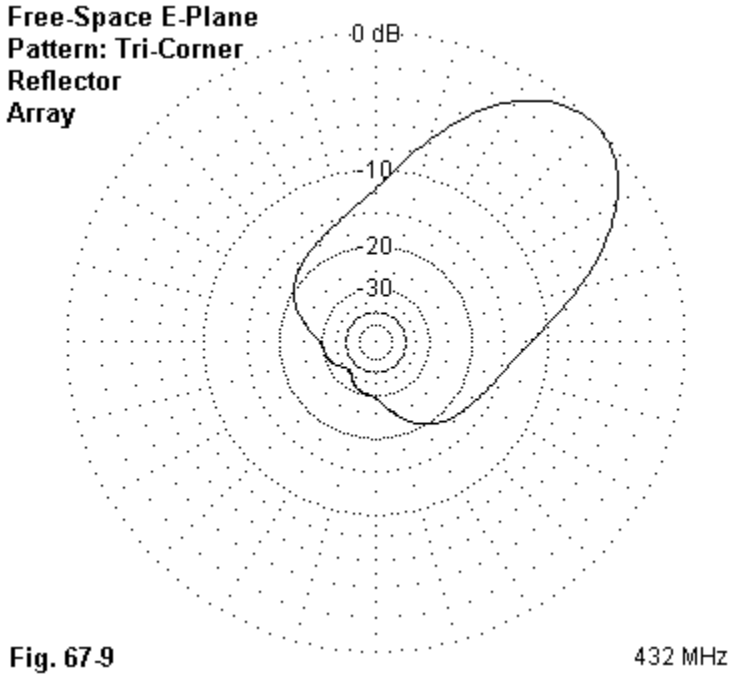

The two lower figures show the resulting models. The driving monopole will not be parallel to the Z-axis for the vertically polarized model. The driver is parallel to one of the seams of the reflector, and hence will be at a 45-degree angle to the Z-axis. Likewise, the horizontally polarized version shows a driver that is at 45 degrees to the axis along which we find the maximum radiation.

The point of using the tri-plane reflector array as an example in this context is to alert you to the fact that various modeling programs have different facilities for manipulating the collection of wires that form wire-grid planes. In this case, by some judicious exportations and importations, I was able to easily re-develop the array

wire-grid structure to a favorable orientation within the strictures of entry-level programs that use only the GW or basic wire creation input for the task.

Those using a more generalized NEC core may lack some of the automated wire-grid building features, but these users have a powerful feature absent in the entry-level programs. After building a single plane, one may use the GM input—described in past columns—to replicate and re-orient the initial plane to form and place the 3 sides of the overall reflector. The caution to exercise here is to omit the edge wire along one side of the initial plane. When you create a new plane with the GM card, be sure that its edge with a missing wire (or wire set) meets the next plane along an edge having the wire (set) in place. When you have the entire set of 3 planes constructed, fill in any missing wire edges with a final wire or wires. In general, this procedure is simpler than trying to remove duplicate wires later. As well, it is normally easier to create one plane, replicate it twice, with rotation to set the joining edges together, and finally to rotate the entire structure to the final desired position than it is to build the entire structure in its final orientation. To go from a horizontally polarized to a vertically polarized version of the array requires only changes to the final GM input line.

Other Planar Structures

The last of our examples, the tri-plane reflector, is, of course, half a cube. Extending our development to produce a solid cube 2 wavelengths along any edge would require about 4500-4800 wires and segments, using a wire or segment length of 0.1 wavelength.

Many wire-grid structures do not demand such densities. Many buildings require that we model only the conductive steel frames. However, when doing such modeling, it is important to keep in mind basic NEC requirements. We should strive for equal-length adjacent segments, especially those having higher current levels or rapid changes of current level from one segment to the next. As well, the wire diameter used in each wire of the grid should be about the same as the wire in any adjacent wire. This latter requirement is more stringent in NEC-2 than in NEC-4. However, even NEC-4 has limitations with respect to the amount of stepping in wire diameter along a straight line and at angular junctions. Finally, be certain not to use wire diameters and segment lengths such that an angular wire junction will let one wire penetrate too far into the center area of the other wire.

Wire-grid planes have proven highly effective in modeling solid and closely meshed surfaces well into the UHF range. We have only sampled one use of the wire-grid, namely, to model reflector planes. However, this simple introduction to wire-grid structures has given us a platform from which to remind beginning wire-gridders of some of the restrictions on such structures and some of the software facilities available for creating and manipulating wire grids.

Advanced wire-grid development is a special talent requiring both a drafting and an antenna background. There are detailed wire-grid models of exceedingly complex structures, such as ships, airplanes, helicopters, ground vehicles, and even human bodies. Most of these models are proprietary; that is, they are privately held by the firms that developed them for various antenna and EMI/RF compatibility studies. Nonetheless, some of the principles and the difficulties of modeling complex structures can be organized into some useful tips. That is for next time.

As well, there are software packages that can ease the process of developing a wide variety of common shapes. For example, making a wire-grid horn or parabola can be a very time-consuming task unless one has a program that synthesizes the shape and needs only some basic data, such as certain critical dimensions. Similar remarks apply to generalized vehicle shapes, even if we do not require all of the fine detail of an in-house proprietary model. For many purposes, we can evaluate antenna placements on a vehicle using a generic shape, such a the shape of a van, an SUV, or a pick-up truck, each having correct main dimensions.

In a future column, we shall return to wire grids as we move from the plane and simple to the angular and awkward.

* * * * *

Models included: 67-1 through 67-8. (.NEC and .NWP model dimensions in meters; .EZ model dimensions in inches.)

68. Wire Grids 2: Angular and Awkward

In the last episode, we looked at some simple rectangular wire-grid structures in order to set forth some of the rules of thumb that guide wire-grid construction. We saw that there are guides, but no completely firm rules for the process, although we always have the AGT and convergence tests that we may apply to the entire model in order to assess its adequacy.

In this episode, I want to look at more advanced wire-grid construction. We shall examine both very specific structures and more generic structures, and when each may be applicable to a modeling task. However, we shall have to speak in far more general terms than those used in the previous discussion. The more detailed and complex the wire-grid structure, the less absolute are the rules of construction.

Fig. 68-1 illustrates with clip-art a number of the types of structures that engineers have had to wire-grid. Some structures, like buildings, only need their skeletons modeled, since the remainder may be largely non-conductive. By far, the largest wire-gridding enterprise encompasses the many types of transportation devices to which we attach antennas or which may play a role in RF compatibility studies. If the Navy (or merchant marine) has a new vessel on the drawing boards, then antenna placement—including interactions among antennas—is a prime concern. It is no less a concern for the Saturday sailor who may directly or indirectly use part of his rigging for his antennas. Aircraft—both winged and helicopters—present new challenges to antenna placement as a function of both the use of new materials and the development of new RF-based services. Land motor vehicles ranging from compact cars to personal SUVs to medium and large carrier trucks remain a prime target for wire-grid construction. Some investigators are even wire-gridding the human body—with special attention to the head—in their studies of the effects of new communications technologies on human health.

The elements of **Fig. 67-1** would be more vivid had I been able to present samples of wire-grid structures capturing at least a sample of each type of subject. However, most of the very specific wire-grid models belong to the companies within which they have been created. Hence, unlike models of Yagis, quads, and other common

antenna types, there are few available and meaningful samples of the wire-gridder's art.

Specific Wire-Grid Models

The development of an adequate wire-grid model of any structure requires a number of skills and knowledge bases. First, one must have an intimate knowledge of the structure itself. The size and composition of the elements of the structure determine to a very large degree the parameters of the wire-grid model. One must also understand how RF energy interacts with the structure in order to place grid elements correctly, especially in areas likely to have high or changing currents. Indeed, the construction of a wire-grid model of a complex structure, like a war ship, may require more than one iteration before the model is fully adequate to its use in reliable analyses.

Some argue persuasively that wire-gridding is an art, since it resembles in many ways the production of a realistic sculpture of a given subject. The modeler must decide what is significant and how to go about ensuring that what is significant is prominent in the model. To illustrate the point crudely, let's examine a few steps in the process, using 2-D graphics to illustrate (inadequately) what essentially is a 3-D task.

Fig. 68-2

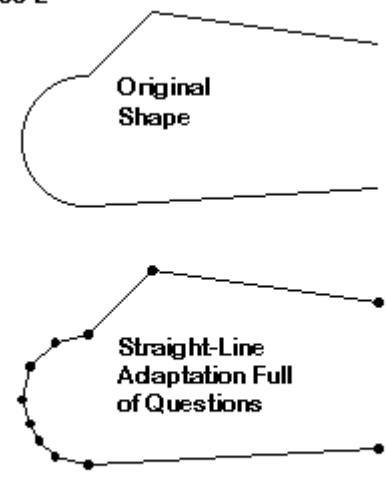

A Partial 2-D Simulation of the Questions Faced in Wire-Gridding a Complex Object

Fig. 68-2 gives us one type of starting point. We see a planar shape of modest complexity composed of curves and lines, where the lines are not parallel. A wire-grid model of the shape must use straight lines, for example, those connecting the dots in the lower part of the sketch. These points will not necessarily have the same distance from adjacent points throughout the model. Hence, the wire-gridder is faced

from the outset with decisions concerning segment length inequalities and their consequences upon the adequacy of the final model.

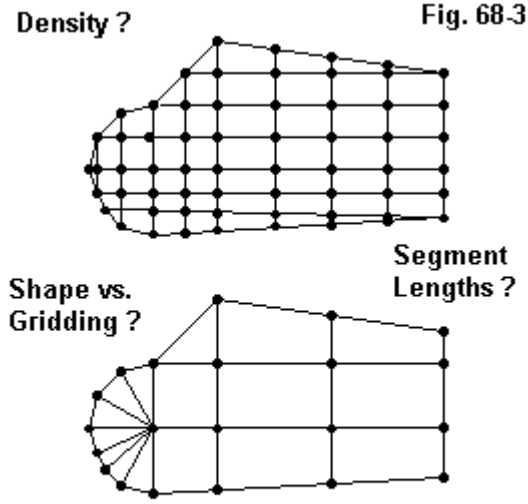

A Partial 2-D Simulation of the Questions Faced in "Filling In" a Wire-Grid Model

Even with a 2-D shape, we must fill in the model with wires and their junctions to simulate (in this example) a solid surface. **Fig. 68-3** shows a few of the questions we must answer. The density of segmentation will determine to a large degree the final model size. A very complex structure may occupy 10s of thousands of segments. The higher the frequency of the RF, the shorter that we must necessarily make the segments, at least in areas that we might classify as sensitive.

How we fill in the structure is as important as specific segment lengths, since the angles of the wires may play a role in how well the model serves as a tool for the

specific analyses tasks at hand. In some cases, like a wire-gridding El Greco, the modeler may have to distort the model relative to the real structure in order for it to perform its function. Each case of wire-gridding, a specific structure presents its unique challenges.

We have not addressed issues such as wire diameter and conductivity (and permeability). A building skeleton may consist of many different sizes of conductive frame members. Yet, NEC works best when adjacent wire segments have the same diameter. The requirement is relatively critical to NEC-2, although even NEC-4 requires close scrutiny when wire diameters of adjacent segments change too abruptly. As well, each wire in the assembly requires in many cases of very specific modeling its own conductivity (and permeability) value. Although steel vehicles and aluminum aircraft still abound, modern materials scattered in the latest designs have complicated both the real and modeled structures. (Note that we are not speaking here of minor conductivity differentials among materials, such as those among steel, aluminum, and copper. Instead, composites can be engineered for virtually any level of conductivity, and that value may differ as we change positions along a structure.)

Except for relatively straightforward cases of creating wire-grid structures, the modeler requires fully featured software for developing the final model. The core segmentation limit must be adequate to the model (rather than letting the segment limit drive the model size). If the conductivity issue is complex, then the software must allow for individual assignment of those values to each wire or group of wires.

Those who are heavily engaged in wire-grid work use a variety of adjunct software. Perhaps the most common type is some form of CAD software so that one can construct the model as a drawing—in 3 dimensions, of course. The output of the CAD file—perhaps in .DXF or a proprietary format—can then be transferred to a NEC input system and result in the requisite set of GW entries to form the model. Unless the adjunct software is very much customized, the modeler will still need to assign conductivity values (LD5 inputs) within the framework of NEC. As well, one must also introduce the frequency parameters, one or more sources, any R-X or R-L-C loads, and appropriate output requests in order to complete the model. As well, one may need to add further wires to the model to count as antennas placed upon the structure.

Finally (at least for this brief description), the modeler must place the structure within its operating environment. Sea-going vessels, of course, are among the simplest to place, as are buildings—IF they are composed of solid conductive exterior surfaces. However, even these examples may present occasional problems. A building frame with many sub-basements—sometimes filled with parked cars, sometimes not—may not show a working ground level that corresponds to the land surface within which the building stands. If the building frame has an earth ground, it may consist of the lowest level of construction, while an antenna on the roof may show its far field performance relative to the surface ground. Whether these features make a difference is usually not completely assured in advance of actually modeling and running the entire model.

The wire-grid model is therefore not completed just by developing a set of wires to create a structural framework in NEC-model form. Diagnostic analyses of the model, using whatever data may be available from real tests, is as much a part of the process as any other step.

We have described in outline form some of the parameters of the wire-grid art and science when applied to critical analyses of very specific structures. The challenges are sufficient that there should be little wonder that advanced wire-gridders hold their techniques close to the vest. As well, the subjects of these models may include proprietary designs, such as future automobiles, or security-sensitive designs, such as new weapons platforms or vehicles. Hence, the general modeler should not expect to see many of these advanced wire-grid structures being shared among modelers.

More Generic Wire-Grid Models

Many tasks that require wire-grid structures need not have all of the detail demanded by the most highly refined models that we have been discussing. A generic model of a vehicle, building, or other shape may suffice to yield adequate data for a given design of analysis project. To that end, modelers can benefit from adjunct software already available. For example, a South African firm produced Wiregrid, which they characterize as “a graphical interface for NEC.” More recently, Nittany-Scientific released its NEC-Win Synth software for graphically creating wire-grid structures, either free-hand or using a number of pre-set general shapes. Whether such packages are suitable to a particular modeling project is always a user-deci-

sion based in part upon the task specifications. However, for a large number of investigations, such software aids can be very useful. Let's focus on one such package—NEC-Win Synth—in order to see what may be involved in creating wire-grid structures using such aids. We shall be as interested in the limitations as in the opportunities afforded by the software.

NEC-Win Synth produces only a set of wires, that is, ultimately a set of GW input lines to a NEC file. The output is directly accessible in the proprietary .NWP format used in NEC-Win Plus, but may also be saved in .NEC format for use with other software packages. As well, the user may also create a wire table that can be imported by the EZNEC wire table facility. However, in all of these cases, one must keep track of the total wire and segment count to ensure that the package used to run the final NEC model will handle the wire-grid structure and its supplements.

Fig. 68-4 shows the main screen that is available for the user if he wishes to create his own wire grid by specifying the wires involved. The graphic display area is available for checking the model at every step, which consists of adding wires, one at a time. Note that the user specifies not only the wire end coordinates, but the number of segments and wire diameter as well. For the model as a whole, the user sets a design frequency and the unit of measure.

Although this screen is available, its largest use is perhaps to construct adjunct structures to one or more of the pre-set shapes available within the program. How one handles a pre-set shape is quite different from building a wire-grid one wire at a time.

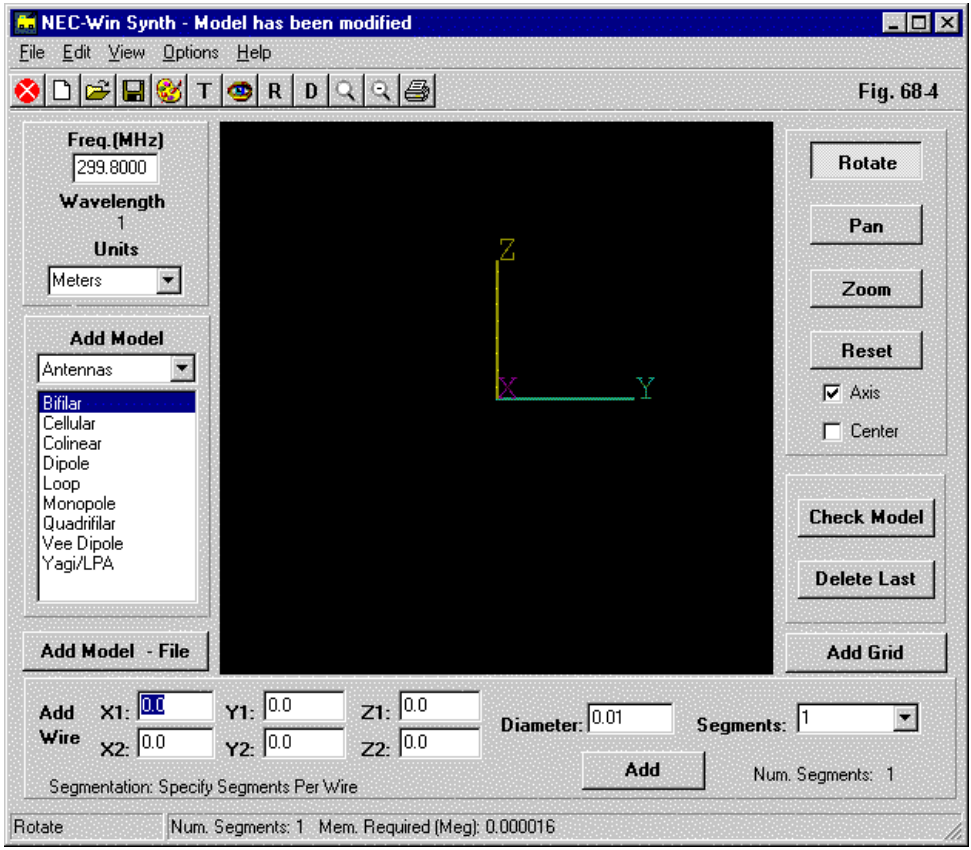
NEC-Win Synth - Model has been modified
File Edit View Options Help
Fig. 68-4
Freq.(MHz)
299.8000
Wavelength
1
Units
Meters
Add Model
Antennas
Bifilar
Cellular
Colinear
Dipole
Loop
Monopole
Quadrifilar
Vee Dipole
Yagi/LPA
Add Model - File
Z
X
Y
Rotate
Pan
Zoom
Reset
Axis
Center
Check Model
Delete Last
Add Grid
Add Wire
X1: 0.0
Y1: 0.0
Z1: 0.0
X2: 0.0
Y2: 0.0
Z2: 0.0
Diameter: 0.01
Segments: 1
Add
Num. Segments: 1
Segmentation: Specify Segments Per Wire
Rotate
Num. Segments: 1 Mem. Required (Meg): 0.000016

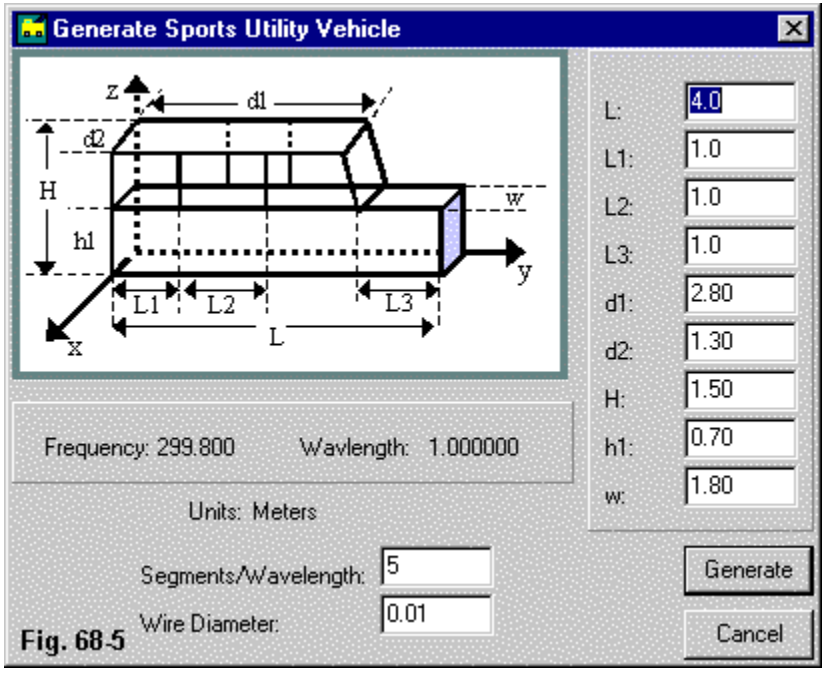

Fig. 68-5 displays one of the full pre-set screens available, in this case, an SUV. Like modeling from scratch, the user establishes a design frequency, along with the number of segments per wavelength and the wire diameter for the wire grid. However, the program itself determines how many wires it will use and where they are placed. The user inputs critical dimensions—in the selected units of measure—from a chart to the right. If one is perhaps trying to decide where to place antennas on a new SUV, then he needs only a tape measure to obtain the relevant dimensions. As with all construction projects, measure twice and enter once.

The NEC-Win Synth system of wire-grid creation uses segment junctions wherever relevant for wire intersections. The system reduces the ultimate file size and run time relative to wire grids that use a separate wire between each junction. However, the user will almost always need to go back to the Synth software to create a new model from scratch if he desires to revise features of the initial wire-grid structure. Not to take this step can all too easily result in a collection of unjoined or illicitly joined wires. Due to format limitations. The following model description lines are each broken into two parts.

```
CE Generated by NEC-Win Synth 1.0
CE
GW   1  6  0.0000000000  0.0000000000  0.0000000000  0.0000000000  1.0000000000
0.0000000000 0.0050000000
GW   2  6  0.0000000000  0.0000000000  0.1750000000  0.0000000000  1.0000000000
0.1750000000 0.0050000000
GW   3  6  0.0000000000  0.0000000000  0.3500000000  0.0000000000  1.0000000000
0.3500000000 0.0050000000
GW   4  6  0.0000000000  0.0000000000  0.5250000000  0.0000000000  1.0000000000
0.5250000000 0.0050000000
GW   5  6  0.0000000000  0.0000000000  0.7000000000  0.0000000000  1.0000000000
0.7000000000 0.0050000000
GW   6  4  0.0000000000  0.0000000000  0.0000000000  0.0000000000  0.0000000000
0.7000000000 0.0050000000
GW   7  4  0.0000000000  0.1666666667  0.0000000000  0.0000000000  0.1666666667
0.7000000000 0.0050000000
GW   8  4  0.0000000000  0.3333333333  0.0000000000  0.0000000000  0.3333333333
0.7000000000 0.0050000000
GW   9  4  0.0000000000  0.5000000000  0.0000000000  0.0000000000  0.5000000000
0.7000000000 0.0050000000
GW  10  4  0.0000000000  0.6666666667  0.0000000000  0.0000000000  0.6666666667
0.7000000000 0.0050000000
GW  11  4  0.0000000000  0.8333333333  0.0000000000  0.0000000000  0.8333333333
0.7000000000 0.0050000000
GW  12  4  0.0000000000  1.0000000000  0.0000000000  0.0000000000  1.0000000000
0.7000000000 0.0050000000
GW  13  6  1.8000000000  0.0000000000  0.0000000000  1.8000000000  1.0000000000
0.0000000000 0.0050000000
GW  14  6  1.8000000000  0.0000000000  0.1750000000  1.8000000000  1.0000000000
0.1750000000 0.0050000000
GW  15  6  1.8000000000  0.0000000000  0.3500000000  1.8000000000  1.0000000000
0.3500000000 0.0050000000
GW  16  6  1.8000000000  0.0000000000  0.5250000000  1.8000000000  1.0000000000
0.5250000000 0.0050000000
```

```
GW 17 6 1.8000000000 0.0000000000 0.7000000000 1.8000000000 1.0000000000
0.7000000000 0.0050000000
GW 18 4 1.8000000000 0.0000000000 0.0000000000 1.8000000000 0.0000000000
0.7000000000 0.0050000000
GW 19 4 1.8000000000 0.1666666667 0.0000000000 1.8000000000 0.1666666667
0.7000000000 0.0050000000
GW 20 4 1.8000000000 0.3333333333 0.0000000000 1.8000000000 0.3333333333
0.7000000000 0.0050000000
```

I have presented the resultant wire table only through wire #20, since the entire model of the SUV has 253 wires. The segment count is in the 1500 range at 5 segments per wavelength, with no antennas yet added. A higher segment density will increase the model size exponentially.

The user will have to add applicable antennas, wire conductivities, model frequency scanning limits, and output requests before running it through the NEC core. Some of the operations can be handled as block operations in some programs, so the finishing time is not excessive by any means. As well, compared to modeling an SUV from scratch, wire by wire, or even by combining semi-automated wire-grid planes, the model construction time is very small.

Nevertheless, the model does have limitations. The vehicle has a shape that reflects the general shape of an SUV having the same dimensions. However, it does not have all of the bumps and indents that are typical of specific SUV models. For most general modeling, these differences between reality and model will make little or no difference. However, they might make a difference in some particular investigation. Hence, the modeler should never assume without evaluation whether or not the synthesized model is adequate to any particular modeling task.

A modeler need not employ a pre-set shape for a particular object when creating a wire grid. The program contains a number of interesting geometric shapes, as illustrated in **Fig. 68-6**.

The illustration exhibits only 3 shapes. The conic section and the circular section, of course, can be combined in a single file to create a radiating ice cream cone—or anything else having that shape. Since the circular cap can be oriented as the user desires, he can cap either end of the cone.

The closed cylinder has been used in a number of cases to simulate each half of a very fat dipole. Another form develops an open-ended cylinder, allowing the modeler to cap the ends with circular sections. The caution each modeler must observe in combining shapes is to be certain that overlapping shape-edge wires are reduced to a single wire in each case.

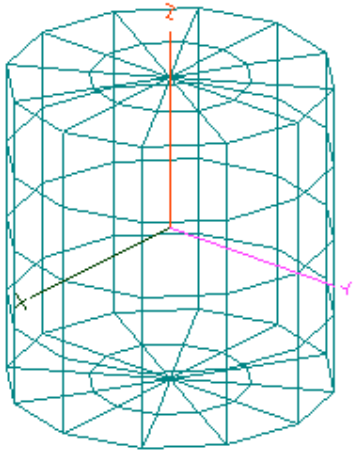

Closed Cylinder

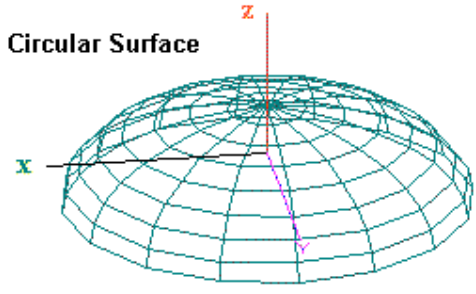

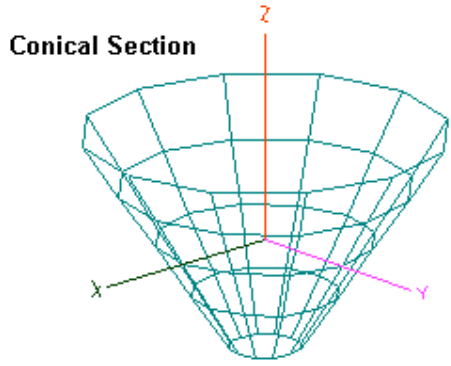

Some Useful Geometric Shapes: Use Alone or in Combination

Fig. 68-6

Fig. 68-7 illustrates some shapes that are useful for UHF and microwave antenna work. The corner reflectors used as illustrations in the preceding episode can now be fabricated—in model form—more simply, with the apex already set as a

single wire. The horn and parabola are of obvious use. Indeed, if one pre-calculates the parabola's geometry to yield a set of dimensions, forming one is simple. However, the wire spreadsheet accompanying the graphical user interface also has provision for modeling by equation, so that a modeler can set up the parabola with variables and revise its shape from within the synthesizing program. Which generation scheme works best depends upon the user's needs.

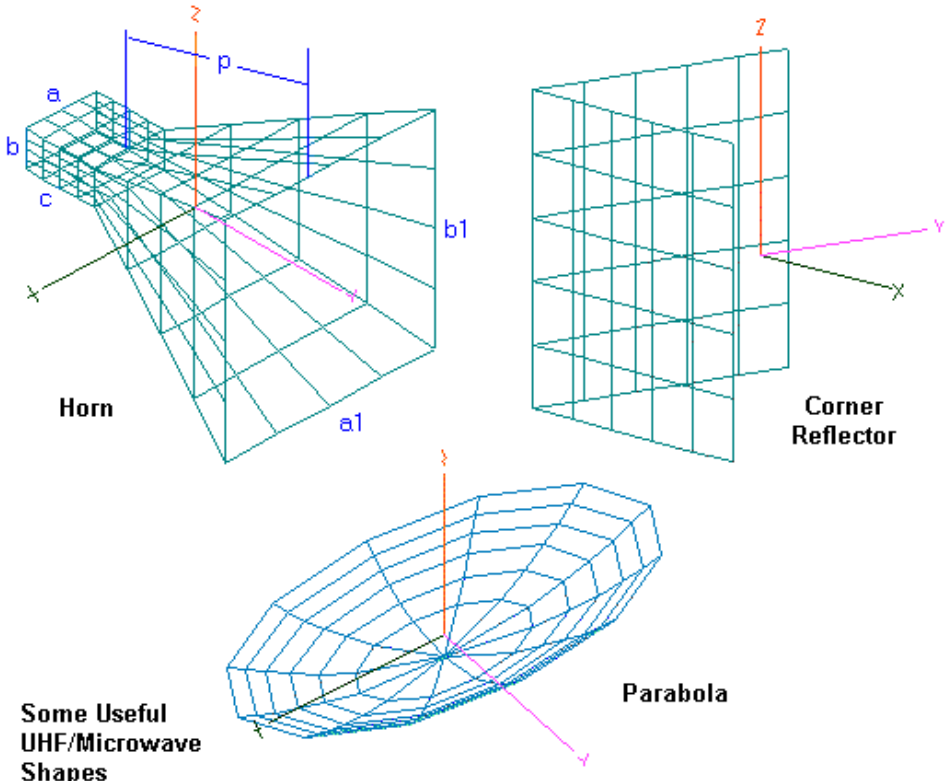

Fig. 68-7

Our final illustration, **Fig. 68-8**, shows the currently available vehicle shapes in terms of the necessary dimensional inputs necessary to fabricate a desired wire-grid model.

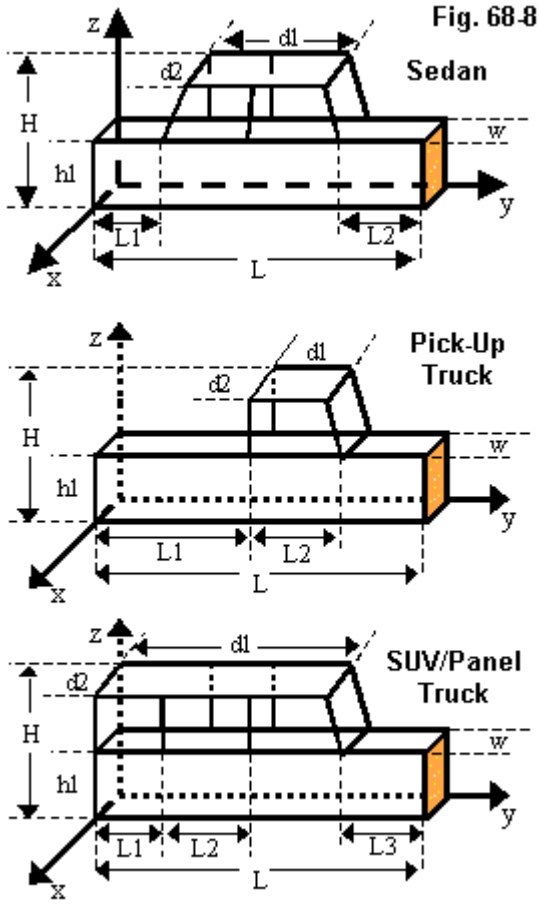

Some Generic Vehicle Shapes

Note that the collection does not include generic tanks, planes, ships, or helicopters. What the future may hold for additional pre-set models I cannot say at this time. However, the modeler is not left solely to wire-by-wire modeling of such structures in wire-grid form. Rather, one can combine preset wire-grid shapes—especially the geometric shapes—and develop specialized constructs in less time than a wire-by-wire technique would yield. However, the process is likely slower than other techniques to which I referred earlier, such as the use of CAD drawings exported as NEC wires lists.

Conclusion

In many ways, this episode has been cursory and vague, providing only a general idea of what advanced wire-gridding requires. At the same time, I see no way around this situation, since wire-gridding requirements cover such a wide span of purposes and needs. Whether one views wire-grid construction as an inviting challenge or a daunting necessary evil depends as much upon individual temperament as upon the nature of the specific task at hand. There are aids to wire-gridding, such as the program that we sampled, and these can assist one to get started into complex shapes, even if only at the generic level. However, the inveterate wire-gridder combines a wide variety of skills in developing the most refined structures that yield the most accurate analyses. Developing those skills takes time and energy and more than a little talent.

* * * * *

Models included: none

69. 4-8-16-Infinite Sided Loops

Suppose that we have a conventional quad loop, that is a square (in either the flat or diamond configuration) loop of approximately 1-wavelength circumference at resonance. In fact, such a square will be considerably larger than 1 wavelength, although the exact resonant circumference will depend upon the wire size as measured in fractions of a wavelength.

A question posed every now and again is what circumference is required if we use a circular form. Since most loops have taken a square form, the question is usually asked in terms of the adjustment needed, if any, to transform the loop into a circle and still be resonant.

Actually, the question is often set out in the context of a multi-element parasitic beam. However, the number of variables involved in an answer to a beam question is initially too great to deal with. We need a simpler starting point, and a single loop is the reasonable initial focus of inquiry. Here, we can eventually use near-resonance (plus or minus a very few Ohms of reactance) to determine that a given circle is the counterpart of a square or vice versa. Since we tend to measure loops by their circumference, we have a means of direct comparison and the possibility of coming up with an “adjustment factor.”

Once we establish that two loops are counterparts, we can also determine the gain of each shape for a direct comparison. Theoretically, a circular loop form has a higher gain than a symmetrical square—indeed, a higher gain than any regular polygon. However, we rarely hear how much gain. Hence, it is difficult to know whether it is worth the effort of fabricating a circular loop in preference to the fairly easy construction associated with the square.

Antenna modeling software provides us with a means of exploring the questions that we have listed. However, NEC and MININEC cannot take us all the way to a circle. Every curved geometric shape must consist of straight wires. So the best that we can do is approximate a circle with a suitable complex polygon. Some say that a hexagon is good enough; others prefer an octagon. Still others think that a

hexadecagon or 16-sided polygon is required. Therefore, let us begin with a little geometry and trigonometry.

Geometry and Trigonometry

Finding counterpart polygons and circles with equal circumferences is mostly a matter of finding appropriate counterpart dimensions. Circumference will be one of those dimensions. We need another, and we shall call it a focal line. A focal line is a line drawn from the center of a figure to its outermost point. In the case of a polygon, that point will be a corner. For a circle, the line is a radius.

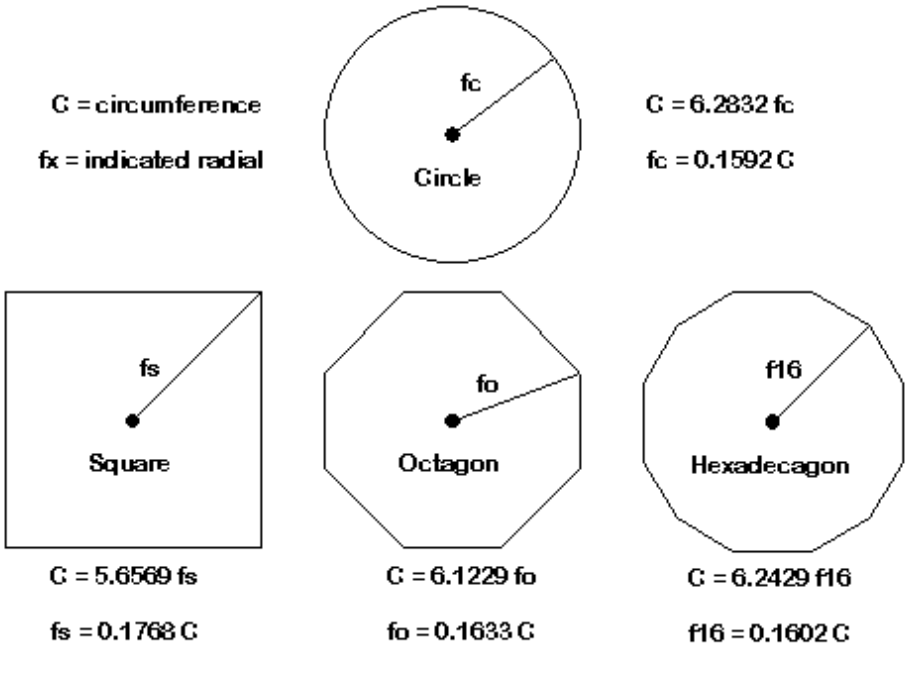

How Well Polygons Approximate a Circle Fig. 69-1

Fig. 69-1 shows a circle, a square, an octagon, and a 16-sided polygon. These will be the members of our progression of polygons that ever more closely approximate a circle, in 2:1 steps in terms of the number of sides. The 16-side limit is appropriate, since it limits the complexity of the models we use and it fairly closely approaches a circle as determined by the ratio of the circumference to the length of the focal line.

The figure shows the relationship of C to fn (where n may be an s for a square, an o for an octagon, and 16 for the 16-sided figure) for each of our polygons. The ratio of C to Fs is only 0.9003 of the ratio of C to fc (or r for radius). However, the ratio of C to f16 is 0.9936 of the ratio for the circle. Hence, although we cannot attain a true circle, we can approach it well within 1 percent geometrically with the most complex of our polygons.

We can calculate the ratios between C and fn simply by knowing the angle between 2 adjacent focal lines. Obviously, the square has 90-degree angles. The octagon has 45-degree angles, and the 16-sided polygon has 22.5-degree angles: simple arithmetic that is a function of the 2:1 ratio of sides in our set of polygons.

Fig. 69-2 helps us calculate the ratio of circumference to focal line length for any of our polygons. If we set one side of the polygon vertical, as in the figure, then a line bisecting the angle between adjacent focal lines will create a right triangle. The angle of concern is now 1/2 the total angle, and the sine of that angle times the length of the focal line will give us 1/2 the length of the side. Twice that length times the number of sides gives us the circumference or sum of the lengths of all sides. The inverse of that number gives us the length of the focal line as a function of the circumference.

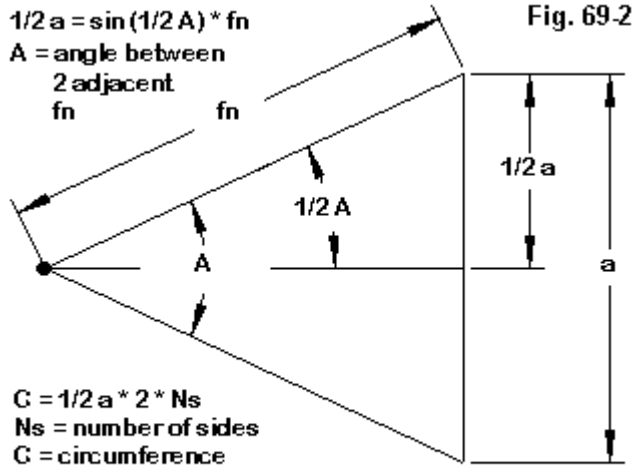

Relating a Focal Line to the Circumference of a Polygon

Hence, we may use circumference as an initial measure that two figures are counterparts, that is, they have the same circumference. From the circumference comes the length of the relevant focal line, and combining that value with the sine and cosine of the half-angle between focal lines, we can derive all of the necessary coordinates to create a model of our polygon. (The 16-sided polygon will need the sine and cosine of either one or two intermediate angles, but that is a small matter.)

Modeling the Loops

Our interest in the basic questions and the project that they inspire lies in the modeling issues associated with trying to derive an answer using NEC or MININEC. We shall restrict ourselves to entry-level software, where only the GW input line is

accessible for creating our polygons. In advanced software that makes available all of the NEC input possibilities, we might set up a single wire and then complete the circle using the GM input to replicate and move new wires. We might also use the GA (arc) input line. However, anything that we can do with those inputs, we can also do with GW lines—and a little more manual labor in the set-up. Indeed, going through the exercise of using an input line per wire may be useful in giving modelers with programs like NEC-Win Pro or GNEC some ideas for simplifying the process—or at least the appearance of the input file. (Unless we invoke symmetry—the GX input—NEC will treat each internally generated wire resulting from the GM or GA lines as a segmented wire, and the total run time will not materially change. So it will be largely a matter of showing a given amount of set-up work within the model or hiding that same amount of work, used in the pre-modeling stage, behind a shorter input file. One might well debate, as we shall not do here, which is better: an elegantly short input file that is far from self-explanatory or a full input file that one might read at a glance.)

We shall begin with the square loop as the most conventional shape. Indeed, our selection of starting points has a second rationale. We have a perfectly good calculating program that will determine the dimensions of a single loop to near resonance solely by entering the design frequency and the wire diameter in the units of measure used in the model. **Fig. 69-3** shows the equations and wire set-up screen for this model. This model is available from the Nittany Scientific web site (http://www.nittany-scientific.com) and is a NEC-Win Plus model. Alternative calculation programs are available for the same results, although they would require manual entry to create a model.

Since the question of square vs. circular loops arises almost exclusively in VHF antenna design, we shall use 146 MHz as our standard frequency. To limit the number of models that we need to examine, we shall use the following wire diameters in inches: 0.0625, 0.125, and 0.25. 0.0625" is close to the diameter of AWG #14 wire, while 0.25" is a useful diameter for soft copper tubing that we might press into quad-loop use. 0.125" is close to the diameter of AWG #10 wire. As with the sequence of polygons, the wire sizes step in 2:1 ratios. See model 69-1.

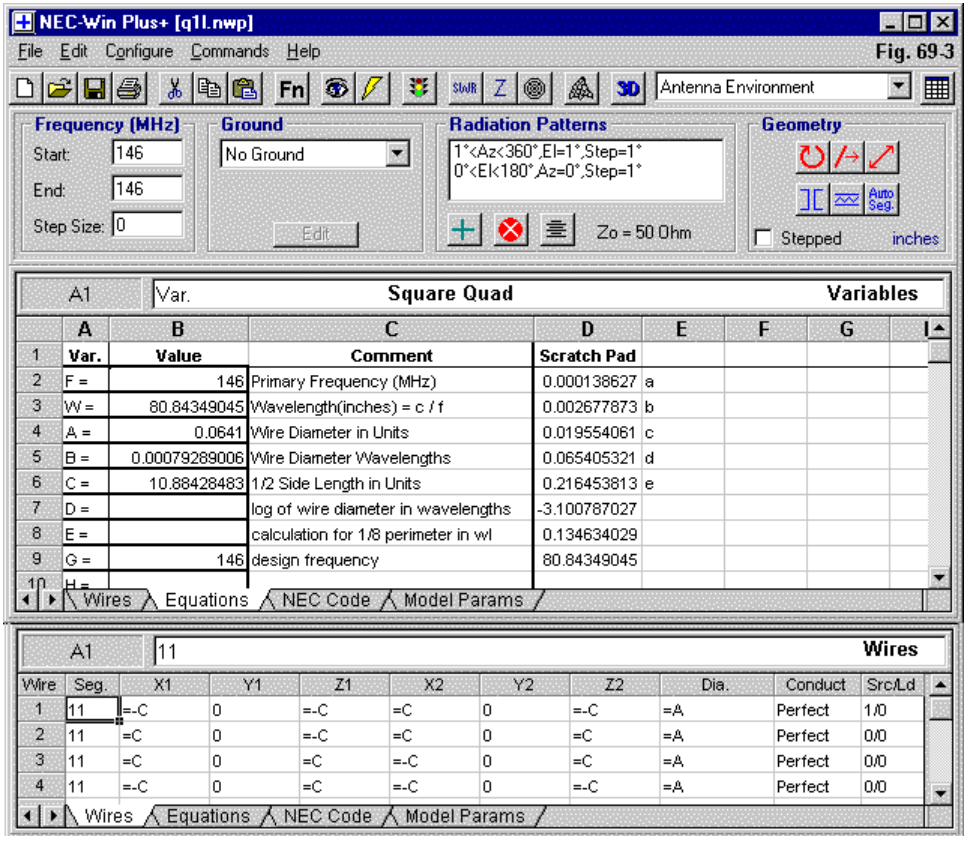

The square quad loop model automates the generation of dimensions for the first step in our trials. However, we need models for the other polygons. If we externally calculate the length of the focal line for each of them, using the circumference of the square version as a starting value, then we can construct a simplified equation-based model for the more complex polygons (again, using NEC-Win Plus as our platform).

Fig. 69-4 shows the variables and wire set-up needed for the octagon. See model 69-2. By making the starting side parallel the Z-axis, we can use the sine and cosine of 22.5 degrees to determine the coordinates of the corners, adding plus and minus signs as necessary for the quadrant within which the coordinates lie. With allowances for those signs, the set-up work is simply repetitious.

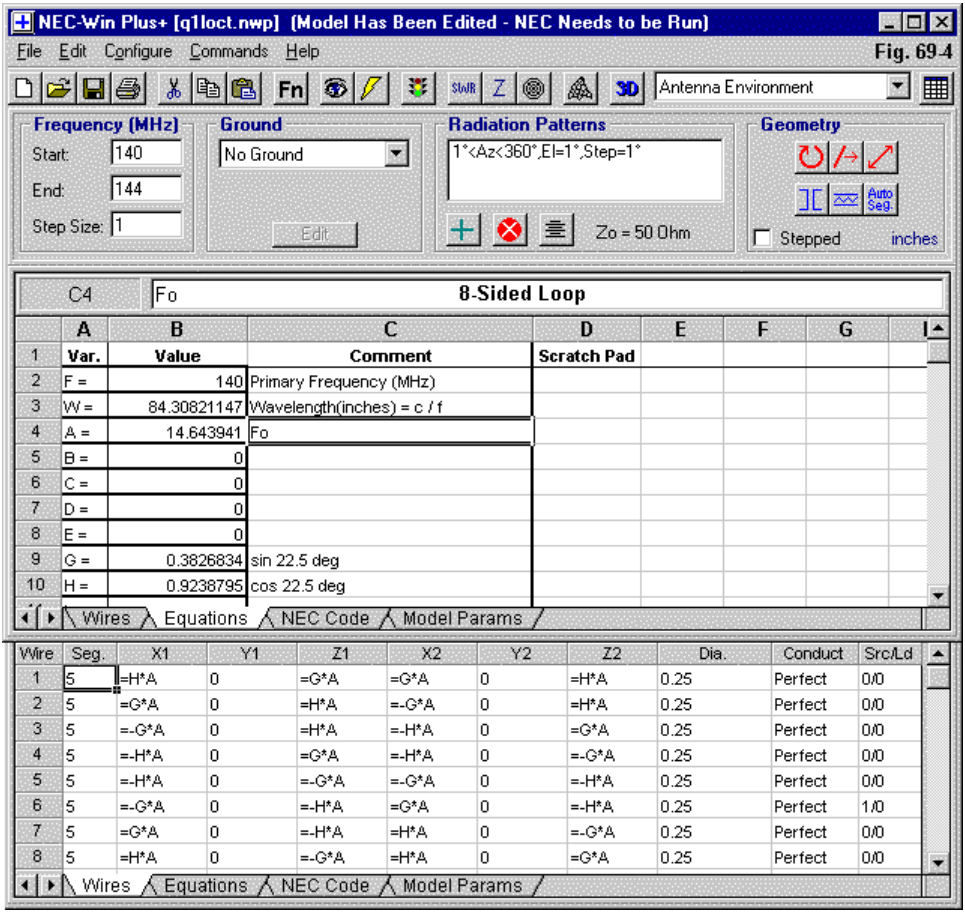

Fig. 69-5

NEC-Win Plus+ [q1l16.nwp] (Model Has Been Edited - NEC Needs to be Run)

File Edit Configure Commands Help

Antenna Environment

Frequency (MHz) Start: 144 End: 148 Step Size: 1

Ground No Ground — Edit

Radiation Patterns 1°<Az<360°,El=1°,Step=1° — Zo = 50 Ohm

Geometry Auto Seg. — Stepped — inches

C4 | F16 | **16-Sided Loop**

	A	B	C	D	E	F	G
1	**Var.**	**Value**	**Comment**	**Scratch Pad**			
2	F =	144	Primary Frequency (MHz)				
3	W =	81.96631671	Wavelength(inches) = c / f				
4	A =	13.942268	F16				
5	B =	0					
6	C =	0					
7	D =	0					
8	E =	0					
9	G =	0.3826834	sin 22.5 deg/cos 67.5 deg				
10	H =	0.9238795	cos 22.5 deg/sin 67.5 deg				
11	I =	0.7071068	sin/cos 45 deg				

Wires | Equations | NEC Code | Model Params

Wire	Seg.	X1	Y1	Z1	X2	Y2	Z2	Dia.	Conduct	Src/Ld
1	3	=A	0	=0	=H*A	0	=G*A	0.0625	Perfect	0/0
2	3	=H*A	0	=G*A	=I*A	0	=I*A	0.0625	Perfect	0/0
3	3	=I*A	0	=I*A	=G*A	0	=H*A	0.0625	Perfect	0/0
4	3	=G*A	0	=H*A	=0	0	=A	0.0625	Perfect	0/0
5	3	=0	0	=A	=-G*A	0	=H*A	0.0625	Perfect	0/0
6	3	=-G*A	0	=H*A	=-I*A	0	=I*A	0.0625	Perfect	0/0
7	3	=-I*A	0	=I*A	=-H*A	0	=G*A	0.0625	Perfect	0/0
8	3	=-H*A	0	=G*A	=-A	0	=0	0.0625	Perfect	0/0
9	3	=-A	0	=0	=-H*A	0	=-G*A	0.0625	Perfect	0/0
10	3	=-H*A	0	=-G*A	=-I*A	0	=-I*A	0.0625	Perfect	0/0
11	3	=-I*A	0	=-I*A	=-G*A	0	=-H*A	0.0625	Perfect	0/0
12	3	=-G*A	0	=-H*A	=0	0	=-A	0.0625	Perfect	1/0
13	3	=0	0	=-A	=G*A	0	=-H*A	0.0625	Perfect	0/0
14	3	=G*A	0	=-H*A	=I*A	0	=-I*A	0.0625	Perfect	0/0
15	3	=I*A	0	=-I*A	=H*A	0	=-G*A	0.0625	Perfect	0/0
16	3	=H*A	0	=-G*A	=A	0	=0	0.0625	Perfect	0/0

Wires | Equations | NEC Code | Model Params

In **Fig. 69-5**, we find the comparable information for the 16-sided figure. To minimize the number of trig functions, this model places a focal line along the X-axis. Hence, we may reuse the sine and cosine of 22.5 degrees and only need to add the sine/cosine of 45 degrees to complete the variable set for the model. The wire set-up reflects the change of orientation. See model 69-3.

The square quad loop uses 11 segments per wire for a total of 44. The octagon uses 5 segments per wire for a total of 40. The 16-sided figure uses 3 per wire, for a total of 48. NEC, of course, requires an odd number of segments per wire if we wish to center the source on a given wire. Once we settle on the segmentation of the source wire, it is a good habit to make all of the segments in the model as close to the same length as possible. In the case of regular polygons, achieving that goal is simple. As well, when comparing models of different shapes but very comparable sizes, it is normally useful to have similar segment lengths in all of the compared models. However, these rules of thumb are no substitute for performing convergence and average gain tests on each model of a sequence.

Fig. 69-6 shows the numerical values for the coordinates of the 16-sided figure using the alternative set-up. You may locate the value of f16 by looking at the very first end-1 X coordinate. In some cases, having the points arranged so that they parallel the coordinate system axes may be inconvenient. In that event, you may set up the figure in the same manner that we used for the octagon. You will need the sines and cosines of 11.25, 33.75, 56.25, and 78.75 degrees. However, in terms of variables, we may reduce the set to a pair of angles, because 11.25 and 78.75 degrees form one pair whose sines and cosines reverse, while 33.75 and 56.25 degrees form the second pair with the same property. See model 69-4.

NEC-Win Plus+ [1lq161.nec] (Model Has Been Edited - NEC Needs to be Run)

File Edit Configure Commands Help Fig. 69-6

Antenna Environment

Frequency (MHz) Start: 144 End: 148 Step Size: 1

Ground: No Ground — Edit

Radiation Patterns: 1°<Az<360°,El=1°,Step=1° — Zo = 50 Ohm

Geometry — Stepped — inches

A1 | 3 | Coordinates of a 16-Sided Polygon as Set Up in Fig. 5

Wire	Seg.	X1	Y1	Z1	X2	Y2	Z2	Dia.	Conduct	Src/Ld
1	3	14.119018	0	0	13.044271	0	5.4031138	0.125	Perfect	0/0
2	3	13.044271	0	5.4031138	9.9836536	0	9.9836536	0.125	Perfect	0/0
3	3	9.9836536	0	9.9836536	5.4031138	0	13.044271	0.125	Perfect	0/0
4	3	5.4031138	0	13.044271	0	0	14.119018	0.125	Perfect	0/0
5	3	0	0	14.119018	-5.4031138	0	13.044271	0.125	Perfect	0/0
6	3	-5.4031138	0	13.044271	-9.9836536	0	9.9836536	0.125	Perfect	0/0
7	3	-9.9836536	0	9.9836536	-13.044271	0	5.4031138	0.125	Perfect	0/0
8	3	-13.044271	0	5.4031138	-14.119018	0	0	0.125	Perfect	0/0
9	3	-14.119018	0	0	-13.044271	0	-5.4031138	0.125	Perfect	0/0
10	3	-13.044271	0	-5.4031138	-9.9836536	0	-9.9836536	0.125	Perfect	0/0
11	3	-9.9836536	0	-9.9836536	-5.4031138	0	-13.044271	0.125	Perfect	0/0
12	3	-5.4031138	0	-13.044271	0	0	-14.119018	0.125	Perfect	1/0
13	3	0	0	-14.119018	5.4031138	0	-13.044271	0.125	Perfect	0/0
14	3	5.4031138	0	-13.044271	9.9836536	0	-9.9836536	0.125	Perfect	0/0
15	3	9.9836536	0	-9.9836536	13.044271	0	-5.4031138	0.125	Perfect	0/0
16	3	13.044271	0	-5.4031138	14.119018	0	0	0.125	Perfect	0/0

Wires | Equations | NEC Code | Model Params

An alternative procedure is to accept the model as is initially and then to rotate it by 11.25 degrees. **Fig. 69-7** shows the results of global rotation around the Y-axis. See model 69-5.

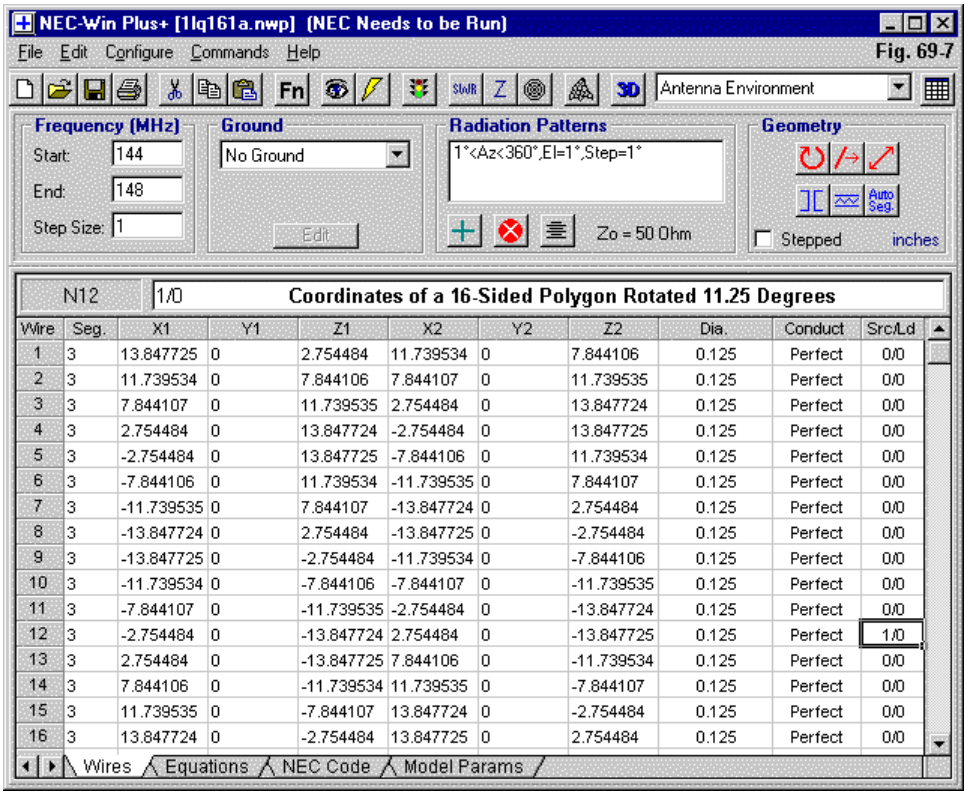
NEC-Win Plus+ [1lq161a.nwp] (NEC Needs to be Run)

File Edit Configure Commands Help

Fig. 69-7

Antenna Environment

Frequency (MHz) Start: 144 End: 148 Step Size: 1

Ground: No Ground, Edit

Radiation Patterns: 1°<Az<360°,El=1°,Step=1°, Zo = 50 Ohm

Geometry: Stepped, inches

N12 | 1/0 | Coordinates of a 16-Sided Polygon Rotated 11.25 Degrees

Wire	Seg.	X1	Y1	Z1	X2	Y2	Z2	Dia.	Conduct	Src/Ld
1	3	13.847725	0	2.754484	11.739534	0	7.844106	0.125	Perfect	0/0
2	3	11.739534	0	7.844106	7.844107	0	11.739535	0.125	Perfect	0/0
3	3	7.844107	0	11.739535	2.754484	0	13.847724	0.125	Perfect	0/0
4	3	2.754484	0	13.847724	-2.754484	0	13.847725	0.125	Perfect	0/0
5	3	-2.754484	0	13.847725	-7.844106	0	11.739534	0.125	Perfect	0/0
6	3	-7.844106	0	11.739534	-11.739535	0	7.844107	0.125	Perfect	0/0
7	3	-11.739535	0	7.844107	-13.847724	0	2.754484	0.125	Perfect	0/0
8	3	-13.847724	0	2.754484	-13.847725	0	-2.754484	0.125	Perfect	0/0
9	3	-13.847725	0	-2.754484	-11.739534	0	-7.844106	0.125	Perfect	0/0
10	3	-11.739534	0	-7.844106	-7.844107	0	-11.739535	0.125	Perfect	0/0
11	3	-7.844107	0	-11.739535	-2.754484	0	-13.847724	0.125	Perfect	0/0
12	3	-2.754484	0	-13.847724	2.754484	0	-13.847725	0.125	Perfect	1/0
13	3	2.754484	0	-13.847725	7.844106	0	-11.739534	0.125	Perfect	0/0
14	3	7.844106	0	-11.739534	11.739535	0	-7.844107	0.125	Perfect	0/0
15	3	11.739535	0	-7.844107	13.847724	0	-2.754484	0.125	Perfect	0/0
16	3	13.847724	0	-2.754484	13.847725	0	2.754484	0.125	Perfect	0/0

Wires | Equations | NEC Code | Model Params

The rotation gives us the same result as setting up the polygon with sides parallel to the X- and Z-axes. **Fig. 69-8** shows the difference.

Why select one orientation over the other? The procedure that results in **Fig. 69-7** is a bit quicker to develop. However, in some cases, one may wish to have a source that is centered within a wire and also on a wire parallel to the ground—if one were to further develop the models to place them over a ground surface.

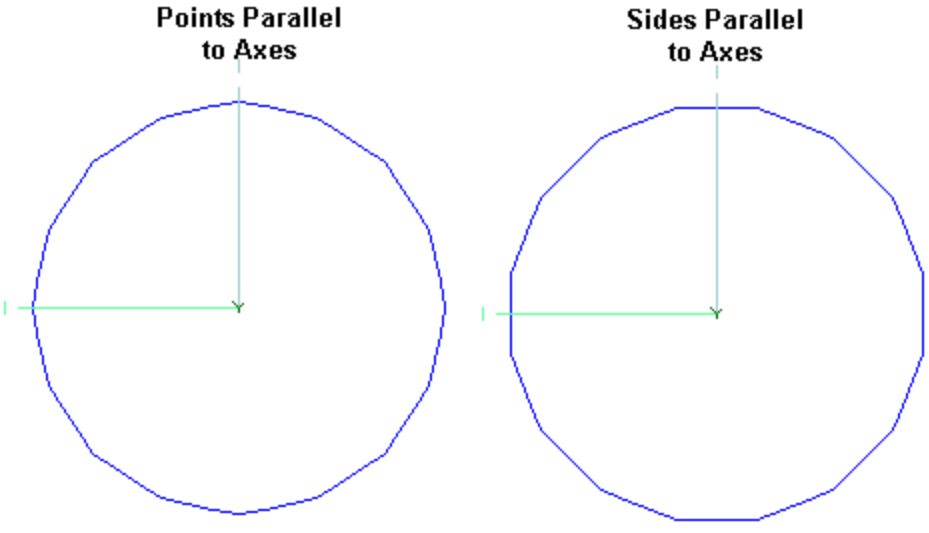

16-Sided Polgons Using Alternate Orientations

Fig. 69-8

For any model, we can check the circumference. In the case of the square and the octagon, the absolute value of the second end-1 X coordinate is also the length of a half-side. Hence, the circumference of the square is 8 times that values and the circumference of the octagon is 16 times its half-side value. The initial 16-sided polygon uses the full length of the focal line as an X coordinate, so its circumference is 6.2428903 times that value (to be spuriously precise). The alternate or rotated 16-sided figure uses the same calculation as the square and the octagon.

Almost all of the set-up steps may also be accomplished with Multi-NEC, AC6LA's NEC adjunct program. As well, Antenna Model—among well-corrected MININEC implementations—would allow much the same set up, but with an even number of segments per source wire.

Some Sample Results

The initial values for the 8- and 16-sided figures do not yield resonance. Indeed, the more sides that we add, the lower the self-resonant frequency. However, once we obtain the self-resonant frequency, we may re-scale the loop to 146 MHz. We must take care to return the scaled wire size to its original value and recheck the impedance at 146 MHz to assure ourselves that it is within reasonable limits, since we wish to know by how much a resonant near-circle circumference differs from the circumference of a resonant square.

In fact, the ratio of loop circumferences is also the ratio of the initial resonant frequency to 146 MHz, the design frequency.

In all cases, I performed an average gain test (AGT) on each test model to assure myself that the result would be comparable. The AGT values ranges from 0.998 to 1.005, for a range of gain errors totalling 0.03 dB. The worst case AGT value was 1.005, which is equivalent to a gain error of 0.02 dB. The resistive component of the feedpoint impedance would be off in this case by 1/2 of 1%. Since most builders work with perhaps 1% tolerances, the AGT margins are well within limits. All models used perfect or lossless wire, but the differences in outcome for copper or aluminum would be insignificant.

The following table summarizes the results of the test models, with all values for 146 MHz and all dimensions in inches. Gain values are free space. The tests and re-scaling were performed using NEC-4 (in this instance, EZNEC Pro/4).

Model Test Results for 4-, 8-, and 16-Sided Loops

0.0625" Diameter Wire (0.00077 wavelength)				
# Sides	Gain dBi	Feed Z R+/-jX Ohms	Circumference Inches	Ratio/Square
4	3.35	128.0 + j 0.3	87.040	——
8	3.59	137.2 + j 0.2	85.579	0.9832
16	3.63	139.4 - j 0.2	85.043	0.9771
Gain increase:	0.28			

0.125" Diameter Wire (0.00155 wavelength)				
# Sides	Gain dBi	Feed Z R+/-jX Ohms	Circumference Inches	Ratio/Square
4	3.39	130.2 + j 2.5	88.143	——

```
 8              3.62       139.1 + j 1.9   86.453          0.9808
16              3.66       141.2 + j 1.5   85.849          0.9740
Gain increase:  0.27

0.25" Diameter Wire (0.00309 wavelength)
# Sides         Gain       Feed Z          Circumference   Ratio/Square
                dBi        R+/-jX Ohms     Inches
 4              3.45       133.3 + j 4.2   89.664          ——
 8              3.67       141.9 + j 3.3   87.699          0.9781
16              3.71       143.9 + j 2.9   87.023          0.9705
Gain increase:  0.26
```

There are several characteristics of the progressions worth noting.

1. As we approach a true circle, the gain increases over that of a square quad loop. However, the increase is less than 0.3 dB, which is operationally unnoticeable. In a multi-element array, this gain will not accrue to each added element, but instead will represent the total gain increase for the entire array. Hence, if moving from a square to a circular element quad invokes considerable construction complexities, it may not be worth the effort.

2. As we approach a true circle from the square starting point, the near-resonant feedpoint impedance increases. The increase is between 7% and 8%. Although not a truly serious increase, it is sufficient to bring a note of caution relative to SWR curves based on calculations for a square loop starting point. The change may also require some re-optimizing of multi-element quads that move from square to circular elements.

3. As is well known among quad builders, the larger the element diameter, the larger the required loop circumference for resonance. This fact does not change as we move from square elements to circular ones.

4. The fatter the wire diameter, the greater the adjustment required in the loops. Using the 16-sided polygon as a reasonable approximation of a circle, it requires a circumference nearly 98% of the size of a square loop with 0.0625" diameter wire but only about 97% of the square's circumference when the wire is 0.25" in diameter.

A Caution

The adjustment factors developed based on models through 16 sides apply only to independent loop elements. For this situation, simple re-scaling is a sufficient technique for returning the loop to resonance as we increasingly round it.

However, multi-element parasitic beams have other considerations that make the situation far more complex. Establishing resonance through loop adjustment may not suffice to ensure that the performance of the array replicates a square-quad original. Element spacing may require changes. As well, one must consider not only centering the impedance or SWR curve at the design frequency, but as well the curves for the forward gain and the front-to-back ratio.

A 16-sided polygon is within 1% of being a good approximation of a circle, considering the ratio of the circumference to the length of a focal line. Hence, for individual quad loops, the adjustment factors developed by the models should be quite reliable. As the figures derived from octagons show, the 8-sided figure may not be as reliable as a guide to circularizing elements. As well, in the adjustment of loops from a square original to a circular final product, the change in resonant impedance may be as important as the loop circumference. On the other hand, it is unlikely that the gain differential will ever be noticed.

In terms of modeling approximations of circles, the polygon that we select for the approximation depends upon the degree of precision that we require. For tracking some general trends or where we know in advance that there are features of the physical antenna that we cannot model, even a hexagon may serve as an approximation (where the circumference C equals 6 times fh, the hexagon focal line length). Increasing requirements for precision, however, makes the 16-sided figure a very adequate choice in most cases. Even if we cannot model a true circle in NEC or MININEC, we may still come very close. The answer to whether “very close” is “satisfactorily close” is always a task-driven judgment.

* * * * *

Models included: 69-1 through 69-5. (All dimensions in inches. Because models 69-1 through 69-3 involve modeling by equation, the set is available only in the .NWP format.)

70: Refining Physical Transmission-Line Models

There are numerous occasions when we need to model transmission lines as physical-wire or GW entries. The advantage of physically modeling a transmission line is the fact that it will show the losses found in reality. Using the TL facility produces lossless or ideal lines. (Perhaps some future version of NEC will modify the core to accept loss factors to expand the utility of this facility.)

However, for most purposes, the modeler is faced with certain limitations. **Fig. 70-1** shows one example.

Fig. 70-1

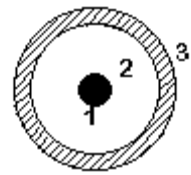

Coaxial Cable

Coaxial cables are likely to defy physical modeling for almost all applications. The close spacing of the wires within the most common coax cables (such as RG-8, -8X, -11, -17, -28, -58, etc.) even makes impractical modeling a cylinder with another wire along the center. For NEC-4, the dielectric between the wire and the cylinder is perhaps the smallest part of the problem, given the IS control entry.

However, it is possible to model physically many types of 2-wire parallel transmission lines. With a vacuum or dry air dielectric between and around the wires, parallel transmission lines answer to the equation

$$Z_o = 120 \cosh^{-1}\frac{S}{d} = 120 \ln\left(\frac{S}{d} + \sqrt{\left(\frac{S}{d}\right)^2 - 1}\right) \qquad (1)$$

Z is the characteristic impedance of the line, S is the center-to-center spacing of the wires, and d is the diameter of the wire. **Fig. 70-2** illustrates the elements of the calculation. If the two wires have different diameters, some references replace the element d with the square root of the product of the two individual diameters.

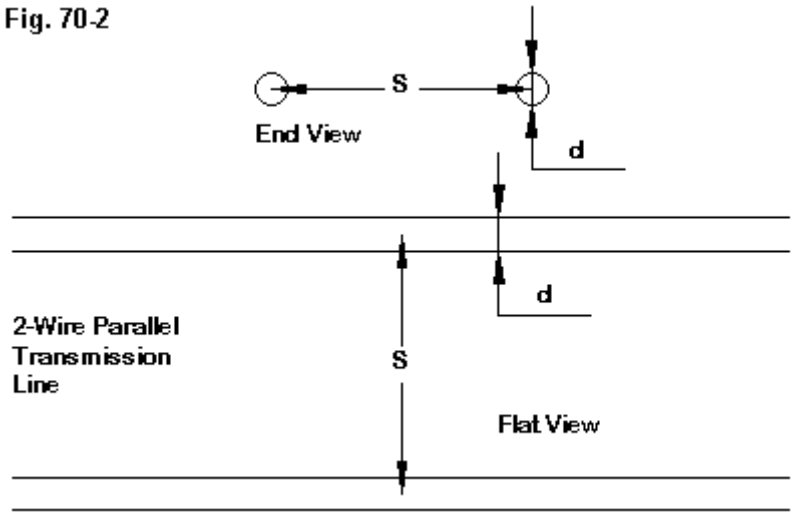

If we create a parallel transmission line from 2 AWG #14 (0.0641" diameter) wires, calculations show a spacing of 1.367" for a 450-Ohm line. We can model this transmission line and check the calculation against NEC reports. We shall use NEC-4.1 in the program GNEC for the illustrations in this set of notes.

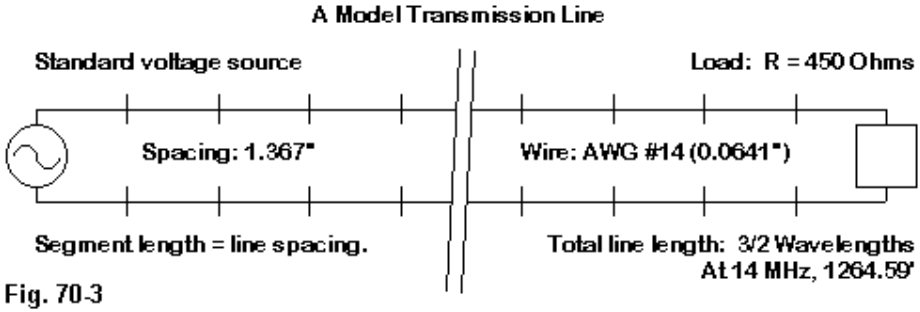

Fig. 70-3

We must pay reasonably careful attention to the model that we use for correlating NEC to standard calculations. First, as suggested by **Fig. 70-3**, the segment lengths should all be about 1.367" to correspond with the short source and load wires at the end of the transmission line. Second, the end wires do change the overall effective line length by a small amount. Therefore, the length selected for the check is 3/2-wavelengths, which minimizes the amount of error per half wavelength. For a test frequency of 14 MHz, the resulting model has 1852 segments.

The source is a standard voltage source of 1 volt at 0-degrees phase angle. The load is 450 Ohms and is purely resistive. At exactly 3/2 wavelengths, the source impedance should be exceptionally close to the load impedance if the model captures adequately the standard calculation method for parallel transmission lines.

The standard calculation for the relationship among the line characteristic impedances and the key physical line dimensions makes no reference to wire losses. Therefore, the initial trial of the model used a perfect or lossless line. The resulting source impedance was 450.003 + j 0.466 Ohms. Replacing the ideal wire with copper yielded an impedance reports of 450.979 + j 1.349 Ohms.

Since this is an exercise, I have reported the results using all decimal places provided by the program. In an exercise, there are no task-related specifications of the required precision, so using all of the data seems appropriate. However, it does

appear that differences in the CPU and/or the operating system used in a computer may result in slight variations in reports. Most of these variations are confined to the second, third, or later decimal places. For practical purposes, the differences make no difference. However, they can be disconcerting to one experiencing them for the first time when moving from one computer to another, even when using the same program.

Even with copper wire, the modeled result is within about 0.2% of the calculated value. The obvious conclusion is that for purely air-dielectric lines, a physical model is quite adequate, so long as one does not try to bring the wires too close to each other.

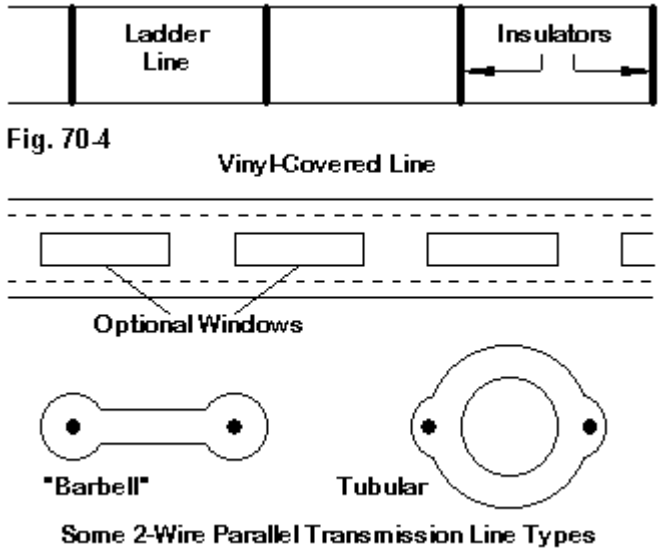

Fig. 70-4
Some 2-Wire Parallel Transmission Line Types

The type of transmission line so far modeled at best reflects the actual parallel line that we call ladder line. This style of line consists of two wires held parallel by

periodic spacers that are too small to create a significant velocity factor (VF), where a factor becomes significant as it grows lower than 1.0. Ladder line is but one of many styles of parallel transmission line, a few of which appear in **Fig. 70-4**.

Far more commonly used by radio amateurs and general consumers are vinyl-covered lines, such as those shown in the lower part of **Fig. 70-4**. TV twin lead usually has a characteristic impedance (Zo) of 300 Ohms. The cheaper sorts use a solid flat area between the wires. To reduce losses, some varieties use a tubular form with air in the center hollow area. Since the strongest fields exist directly between wires, the tubular line tends to have a higher VF than the common type, perhaps 0.9 vs. 0.8. Another technique used to raise the VF is to cut windows in the flat vinyl area between wires. The technique also tends to raise the VF to about 0.9 and is most common in 400-450-Ohm lines.

Physically modeling a transmission line is limited to crude approximations unless it can also model the line's velocity factor. Many transmission line sections occur as parts of antennas, and the dimensions of those parts often account for the velocity factor of the line used in the assembly. Hence, an accurate model should be able to replicate or approximate the line's VF.

NEC-2 is limited to modeling parallel lines in an air/vacuum environment only. NEC-4, however, includes the IS (Insulated Sheath) control input that allows the user to specify for any given wire in the model an insulated covering. We explored the basics of using the IS input in column #50. Essentially, we specify a radius greater than that of the wire, along with a conductivity and a relative permittivity (dielectric constant).

Suppose that we wished to develop a 450-Ohm transmission line having a VF of 0.90. The development process begins with the fact that a physical wavelength of line will be 0.90 times the electrical wavelength. So we may take our original 3/2-wavelengths test transmission line and shorten it to 1.35 wavelengths. At 14 MHz, our test frequency, the length is 1138.13". Of course, to maintain the correct segment lengths, we shall reduce the number of segments on each long wire from 925 down to 833.

Before we make any other changes to the model, we may check the source impedance at the new length. The report was 493.005 - j 35.816 Ohms.

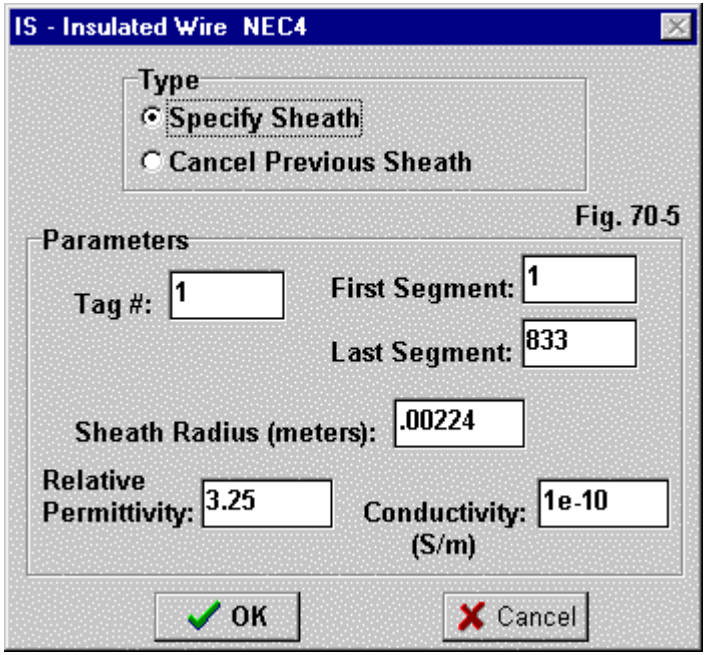

Fig. 70-5 shows the GNEC assist screen with labels upon all of the required entries. Perhaps the one entry that initially catches most modelers is the radius number. Although we were able to specify the wire coordinates in inches and then use a scaling entry (GS) to convert those coordinates into meters, as required by the core, control cards require direct entry in meters. Hence, the radius, which will be in the general vicinity of 0.09", must be entered in terms of meters, that is, about 0.002286. The entry shown is a bit smaller (0.882").

Assuming that we have an excellent insulating material, we may enter 1E-10 for the conductivity (0.0000000001 S/m). For single wires, there is little change in the performance of wires with conductivities from 1E-10 down to 1E-7 S/m. Much more

influential on the performance will be the relative permittivity or relative dielectric constant. The value shown, 3.25, falls in the general range for vinyl plastics (2.5 to 3.5) in the HF range.

The following two brief model descriptions in ASCII entry form show the difference between the pre-insulated (VF = 1.0) and post-insulated (VF = 0.9) condition of the long transmission-line wires. Note that we have insulated only the long wires, leaving the source and load wires bare. See models 70-1 and 70-2.

```
CM Parallel 450-Ohm TL Simulation
CM cu AWG #14 wire
CE
GW 1 925 0 0 0 0 0 1264.59 .03205
GW 2 1 0 0 1264.59 0 1.367 1264.59 .03205
GW 3 925 0 1.367 1264.59 0 1.367 0 .03205
GW 4 1 0 1.367 0 0 0 0 .03205
GS 0 0 .02540
GE 0
EX 0 4 1 0 1 0
LD 4 2 1 1 450 0 0
LD 5 1 1 925 5.8001E7
LD 5 2 1 1 5.8001E7
LD 5 3 1 925 5.8001E7
LD 5 4 1 1 5.8001E7
FR 0 1 0 0 14 0
RP 0 1 361 1000 90 0 1 1
EN

CM Parallel 450-Ohm TL Simulation
CM cu wire + .9 VF via IS cards GW 1 & 3
CE
GW 1 833 0 0 0 0 0 1138.13 .03205
GW 2 1 0 0 1138.13 0 1.367 1138.13 .03205
GW 3 833 0 1.367 1138.13 0 1.367 0 .03205
GW 4 1 0 1.367 0 0 0 0 .03205
GS 0 0 .02540
GE 0
```

```
EX 0 4 1 0 1 0
LD 4 2 1 1 450 0 0
LD 5 1 1 833 5.8001E7
LD 5 2 1 1 5.8001E7
LD 5 3 1 833 5.8001E7
LD 5 4 1 1 5.8001E7
IS 0 1 1 833 3.25 1e-10 .00224
IS 0 3 1 833 3.25 1e-10 .00224
FR 0 1 0 0 14 0
RP 0 1 361 1000 90 0 1 1
EN
```

The rest of the development effort is to find—using a constant conductivity value—a radius and a permittivity value that together bring the transmission line to resonance at, hopefully, 450 Ohms. In fact, any number of combinations will do the job as well as it can be done by this method. The following table shows eligible combinations of sheath radius and permittivity that yield reasonably close tallies. Remember that the length is preset to 90% of the air-dielectric length, so that the only changes being made are to the two IS entries.

IS Radius and Permittivity Values for a 450-Ohm, 0.90-VF Line

Sheath Radius		Relative	Source Impedance
inches	meters	Permittivity	(R+/-jX Ohms)
0.09	0.002286	3.1	452.431 - j 0.967
0.09	0.002286	3.15	452.462 + j 0.461
0.882	0.002240	3.25	452.437 - j 0.617
0.88	0.002235	3.25	452.430 - j 1.033
0.88	0.002235	3.3	452.456 + j 0.237
0.878	0.002230	3.3	452.446 - j 0.186
0.866	0.00220	3.4	452.442 - j 0.342
0.858	0.00218	3.5	452.454 + j 0.153

The inverse relationship between the sheath radius and the permittivity value is readily apparent. Somewhat less noticeable is the fact that the resonant (more accurately, the near-resonant) condition of the source resistance is about 2 Ohms higher than for the air-dielectric case. (Again, more precisely, about 2.5 Ohms higher

than the perfect-conductor model and about 1.5 Ohms higher than the copper-wire case. The present model also uses copper wire.)

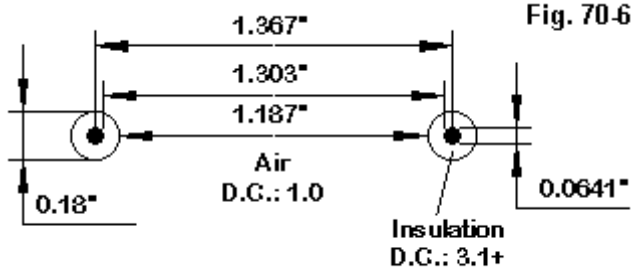

Fig. 70-6

A 0.9-VF, 450-Ohm Transmission-Line Model

Fig. 70-6 illustrates the situation. We have a combination of insulated sheathing plus an air dielectric between the wires. The greater part of the spacing uses an air dielectric, but the insulated sheathing of the wires is sufficient to change the Zo of the line itself. In a more complete form, the equation for calculating the characteristic impedance of a parallel transmission line is

$$Z_o = \frac{120}{\sqrt{\epsilon}} \cosh^{-1} \frac{S}{d} = \frac{120}{\sqrt{\epsilon}} \ln\left(\frac{S}{d} + \sqrt{\left(\frac{S}{d}\right)^2 - 1} \right) \qquad (2)$$

The added factor is the square root of the relative permittivity of the material between and around the lines. Hence, the Zo of the line is slightly different from our originally calculated 450 Ohms. However, since most of the space is air, we are only off by about 0.5%, with is close enough for most purposes. Nevertheless, further development can refine the characteristic impedance, if necessary.

For our purposes in this exercise, I shall declare that we are close enough. Our goal was to establish a means by which to model transmission lines having a desired velocity factor (0.90) and a selected characteristic impedance (450 Ohms).

By the correct selection of a radius and a relative permittivity for a parallel transmission line, we can develop the necessary model within reasonably close tolerances.

If we need a lower value for the velocity factor, we shall find that the required IS entry—keeping the conductivity constant at 1E-10 S/m—requires nearly a doubling of both the sheath radius and the relative permittivity. For our sample line, a radius of 0.0039 m (0.1535") and a permittivity of 7.0 yielded a source impedance of 454.316 - j 0.353 Ohms. The new source value continues to climb by another 2 Ohms. However, the doubling is not quite linear, since we obtained resonance with a 0.90 VF with a permittivity of 3.5 and a sheath radius of 0.00218 m (which would have yielded, if doubled, 0.00436 m).

Indeed, the non-linearity shows more clearly if we take the wire radius into account, since it is the sheath thickness—and not simply its outer radius—that is effective in establishing a given velocity factor. The thickness of the 3.5-permittivity sheath for a 0.90 VF was 0.00137 m, while the thickness of the 7.0-permittivity sheath for a 0.80 VF is 0.00309 m. See model 70-3.

Nevertheless, the exercise does provide some guidance in the development of lines with any desired velocity factor. At least it does so by a trial-and-error method within the modeling software.

We have used a sample transmission line consisting of a pair of AWG #14 (0.0641" diameter) wires spaced 1.367" center-to-center. The use of this sample is not without reason. The wire size and spacing fall well within the ability of the NEC-4 core to model accurately if the segment junctions are well aligned. Of course, with parallel wires, we may obtain perfect alignment simply by assigning the same number of segments to each wire. With a segment length that is equal to the wire spacing, we assure that the source and load wires adjoin segments of the same length.

A further reason for using the specified sample line stems from the fact that the transmission line wire diameter can be the same as the diameter of the antenna wire to which it might be attached in a sample antenna + transmission line model. AWG #14 copper or copperweld wire is a very common value used in many installations, especially those designed for use in the amateur HF bands. However, if all we were concerned with was the feed line for a center-fed doublet, then we would not

require all of the effort to establish a line velocity factor. We might with greater ease use the TL facility and externally adjust the required physical line length to achieve a set of electrical conditions.

Not all uses of transmission lines in antenna systems are so simple as modeling the main feedline of a center-fed doublet. Let's look at a different application and see what the modeling opportunities and limitations might be.

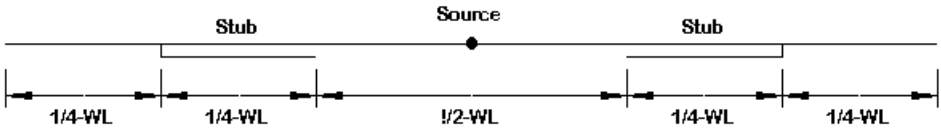

Sample Application of a Transmission Line Within an Antenna Fig. 70-7

Fig. 70-7 shows the basic outlines of a 3/2-wavelengths center-fed doublet for the 20-meter amateur band. The difference between this antenna design and an ordinary doublet is the use in the center region of each half-element a 1/4-wavelength shorted stub, where the short occurs 1/2-wavelength from the feedpoint.

The interesting question surrounding the design proposal concerned the effects of the stubs on the pattern and gain of the antenna. The top portion of **Fig. 70-8** shows the pattern of the same antenna treated simply as a 3/2-wavelength doublet. At the prescribed length of 99', the antenna shows a typical 6-lobe pattern with a maximum strength of about 8.4 dBi, as modeled at an elevation angle of 14 degrees, based on its height of 50' above average ground. The antenna uses AWG #14 copper wire and extends left-to-right (or right-to-left) across the pattern plot.

The center section of the figure shows the azimuth pattern when we create the parallel transmission-line stub using AWG #14 wire. The model for this azimuth pattern uses the very type of transmission line sampled earlier in the exercises, but with no insulated sheath. Hence, the velocity factor is very close to 1.0. As the pattern shows, there is a slight shift in the power distribution among lobes. The strongest lobes are now—by a slight margin—the 4 angling lobes relative to the wire, with a small reduction in the broadside lobes. By dividing power among 4

lobes, the overall maximum gain decreases fractionally to about 8.2 dBi, using the same elevation angle.

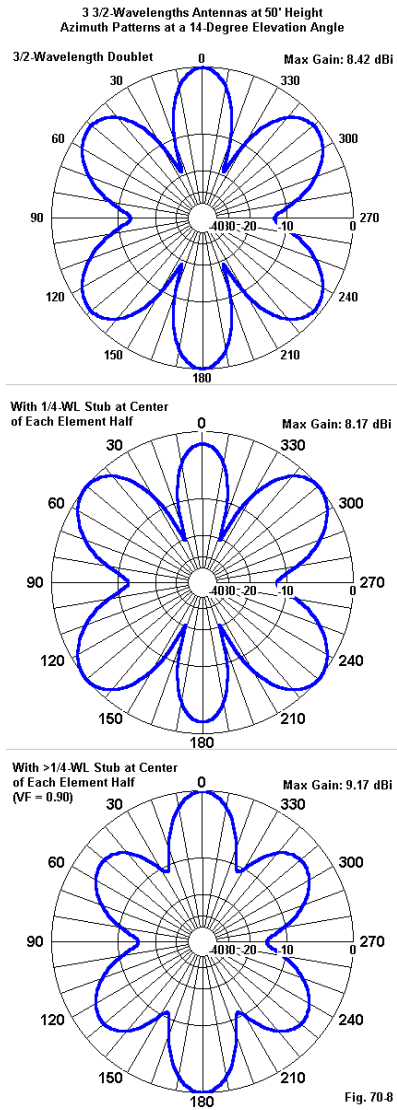

Fig. 70-8

In the design proposal, however, the 1/4-wavelength stub section used material having a velocity factor of about 0.8. Hence, it seemed appropriate to investigate whether the antenna performance would change by assigning a velocity factor less

than 1.0 to the modeled stub section. One stage in the modeling insulated the stub wires with insulation radii and permittivities consistent with the 0.9-VF line shown earlier. The result was the pattern in the lowest portion of **Fig. 70-8**. This pattern changes the relative strength of the lobes to increase the power in the broadside lobes and decrease it in the angling lobes, resulting in a maximum gain of about 9.2 dBi. Among the models tried, this one yields the strongest broadside lobe strength.

At best, the models in this series suggest some trends in performance, none of which offer much optimism that going to the extra lengths of construction complexity for the antenna will yield a comparable improvement in performance as compensation. However, the models—as limited as they are, do suggest trends and hence fall among a whole class of modeling efforts that I tend to classify as "suggestive" rather than definitive. Since they are not a decisive confirmation or refutation of the claimed principles of construction, they do not qualify as "proof-of-principle" models. Each of these categories of models has utility in a domain of modeling that is well shy of a definitive "analytical" model or a definite "design" model. Each category of model has functions within a task-defined set of limitations.

One of the limitations inherent to the evaluation of the design proposal is the fact that the physical antenna uses coaxial cable as the shorted stubs. Its physical length is as specified in the model, which means that its velocity factor makes the stubs—as stubs—electrically longer than the physical length.

The key factor of variance between the model and the physical antenna is the fact that when a shorted stub is not exactly 1/4-wavelength long, the reactance differs between a 50-Ohm stub and a 450-Ohm stub by a 9:1 ratio. Since the shorted stubs are longer than 1/4-wavelength, the reactance is capacitive, indicating a resonant or 1/4-wavelength frequency well below the 14-MHz test frequency. **Fig. 70-9** provides some graphic data on the reactance of shorted stubs from 10 through 80 degrees of electrical length.

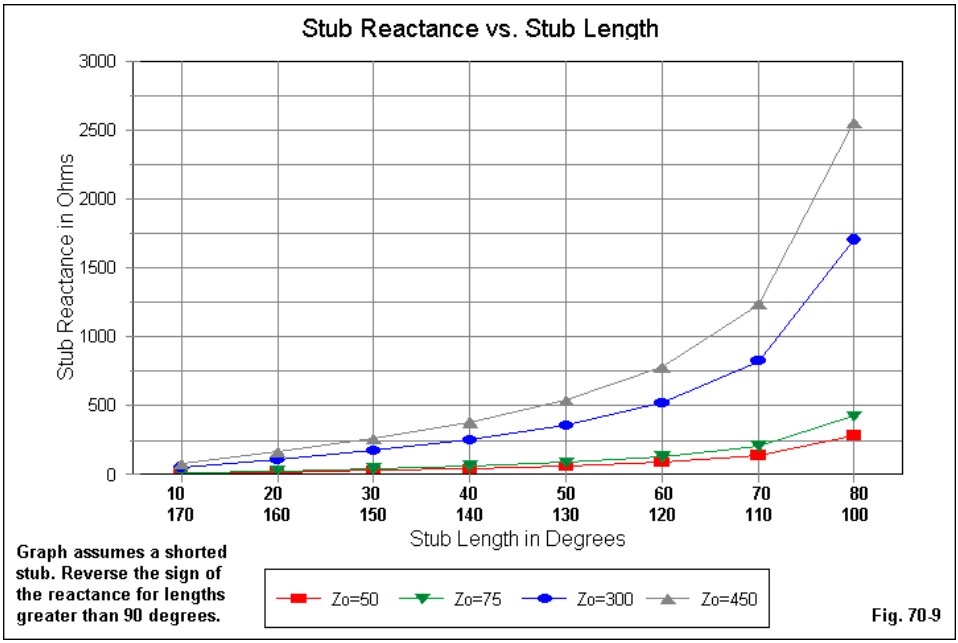

Fig. 70-9

The proposed antenna was to operate at a variety of frequencies, some far removed from the 14-MHz test frequency. Hence, it is not possible in the simplified exercise to substitute the 450-Ohm line—at any VF supplied by the use of an insulated sheath—for the coax line at all frequencies.

Had the antenna been differently designed, the differences reported by using the 450-Ohm line stub with and without an insulated sheath would have been far more dramatic. Let's move the short from the outer ends of the stubs to the inner ends. Now the distance from the center feedpoint to the far end of the stub—the open end—is about 1/2-wavelength, while the inner end is about 1/4-wavelength distant from the feedpoint. Then let's repeat our experiment of modeling the stub

sections without sheathing—giving us a VF close to 1.0—and with a sheathing corresponding to the 0.9-VF transmission line sample.

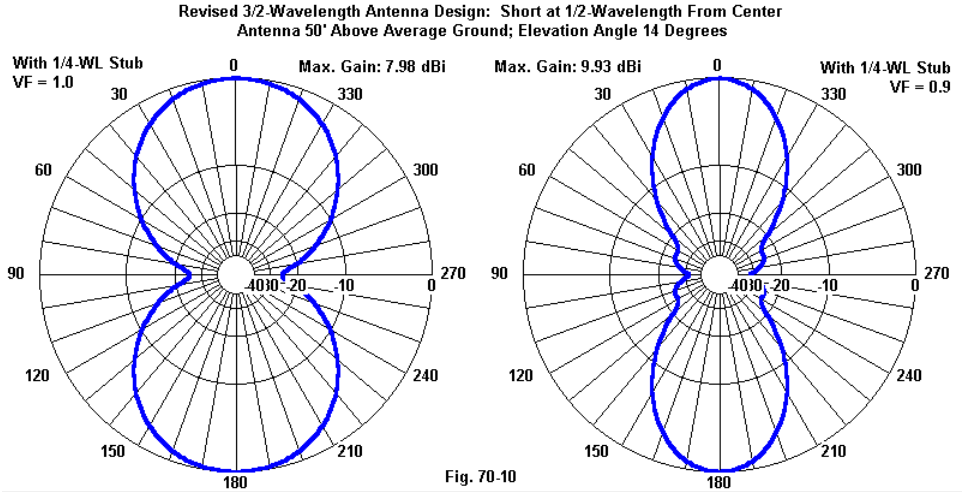

Fig. 10 shows the results. In this case, there is almost a full 2-dB increase in gain and a corresponding narrowing of the beamwidth for the sheathed version. As in the first version, we cannot claim that we have a definitive model, but we may be moving from a suggestive to a proof-of-principle model, relative to using transmission-line sections—even of coax—to tailor the performance of a wire antenna.

What principle applies to this particular antenna lies beyond the scope of the exercise. We have examined the use of the IS or insulated sheath control input of NEC-4 to simulate a transmission line with a velocity factor other than 1.0. There may be modeling occasions on which it is worthwhile to use this facility in more than a haphazard way to check out an actual design, the principles of a design, or the trends that would likely emerge from design variations. So long as we do not overstate the claims from a model, all of these goals are worthwhile.

* * * * *

Models included: 70-1 through 70-3. (Because the sequence uses the IS command, these models are available only in .NEC format.)

71: The Average Gain Test Revisited

In column 20, we examined the basic parameters of the Average Gain Test (AGT) as a test for model adequacy. This test is built into such commercial implementations of NEC as EZNEC and NEC-Win Plus, and has been adapted to the Antenna Model implementation of MININEC 3.13. However, a number of modelers do not use these programs, but instead use one of the public domain versions of the NEC-2 core. Hence, they must set up their own AGT, a fairly simple but elusive process unless one has some detailed instructions. Let's begin by reviewing some basic information from the earlier column.

AGT Basics

Essentially, we only need two numbers to perform the test: the input power and average radiated power. For a lossless antenna, the input power and the average radiated power should be equal in an ideal model. Whatever the gain in one or more favored directions, it will be offset by nulls in other directions. Over the entire sphere of free space, the total amount of radiated power can never exceed the power supplied to the antenna, and if the antenna is lossless, can never be lower than the input power. Hence, the ratio of average radiated power to supplied power should be 1. If the ratio differs by more than a small amount from 1, then the model may be considered suspect.

The conditions under which an adequate model will show an Average Power Gain (G_{ave}) of 1 also establish the conditions for performing the Average Gain test. The model is set in free space. (We shall look at setting the model over perfect ground in a moment.) The wire material must be perfect or lossless. All "real" or resistive parts of loads, networks, and transmission lines must also be set to zero.

For test purposes, the model is run by taking a regular sample of the radiation pattern every few degrees, and the results are averaged. (Note: for these tests, the sample is taken as a power and not as a power ratio, although one can be easily converted to the other.) The result is a fair reading of the average radiated power. To calculate the average power gain, we simply apply the following simple equation:

$$G_{AVE} = \frac{kP_{RAD}}{P_{IN}}$$

where P_{rad} is the radiated power as averaged and P_{in} is the input power as calculated from source information.

What about k? For a free space model, k = 1. However, if the test lossless model is placed over perfect ground, then k = 2.

The results will not vary by much if the only loss in the antenna is wire loss for high conductivity materials of reasonably large diameters. However, for the most reliable figure of merit, the test is best run on a wholly lossless version of the model being tested.

The average gain figure that results from the test may be higher or lower than 1.0. One proposed gradation of model merit uses the following dividing points:

G_{ave} Value Range	Significance
0.95 - 1.05	Model is considered to have passed the test and is likely to be highly accurate.
0.90 - 0.95 and 1.05 - 1.10	Model is quite usable for most purposes.
0.80 - 0.90 and 1.10 - 1.20	Model may be useful, but adequacy can be improved.
<0.80 and >1.20	Model is subject to question and should be refined.

The user may develop more strict limits for the adequacy of a model based on the specific tasks within which the model plays a role.

Most models that deviate in the test from an average gain of 1 show an inverse correlation between errors in gain and in the resistive component of the source impedance. As the gain climbs, the source impedance decreases, and vice versa. For limited purposes, the average gain value derived from the test can be used to correct both figures, using the following equations:

$$\textbf{Corrected Input Resistance} = \frac{\textbf{Computed}R_{IN} \times G_{AVE}}{k}$$

and

$$\textbf{Corrected Gain} = \frac{\textbf{Computed Gain} \times k}{G_{AVE}}$$

Obviously, an average gain value that is greater than 1 will increase the input resistance and decrease the gain. Values less than 1 will do the opposite. One may simplify the gain correction by converting the AGT value into an equivalent value in dB:

$$Gain_{dB} = 10\log(Gain_{AVE})$$

If the resulting value in dB is positive, it is an amount by which the model reports are high and must be subtracted from the reports. If the converted gain value in dB is negative, it is the amount by which the reports are low and its absolute value must be added to the reports.

The list of suggested categories of adequacy of a model place the most ideal models in the AGT range from 0.95 to 1.05. An AGT value of 1.05 yields a conversion value of 0.21 dB, while a value of 0.95 converts to -0.22 dB. For some purposes, these differentials may be well within task limits, while for others, they may fall outside task limits. Hence, whether we use raw NEC report data or corrected values—even for quite adequate models—remains a user responsibility based upon the nature of the modeling task at hand.

The key limitations in the use of the correctives are two. First, if the AGT value is very high or very low, then the corrections are unlikely to give more than a suggestion of the corrected gain. The closer to a perfect value, the more likely the corrections will yield values that are reliable relative to a physical implementation of the modeled antenna.

The utility of the AGT test in warning of on inadequate model are obvious for large departures from the ideal values of 1.0 for a free-space run and 2.0 for a monopole array set over perfect ground. Large departures from the ideal call for a careful inspection of both the model and the many published limitations of NEC in order to detect and correct errors in the model. There are many conditions leading to error which the core will not call attention to by stopping its run. As well, some of these conditions may not be detected by the error-detection systems in commercial implementations of NEC. For example, closely spaced wires that do not inter-penetrate may have misaligned segments that will create errors in the NEC results. Ultimately, it is up to the modeler (and not the software) to develop the most reliable possible model and to establish that reliability.

Second, the corrective to the source impedance is reliable only if the reactance is very low. In other words, the antenna must be at or relatively close to resonance if the AGT value is to yield a reasonably accurate value for the source resistance. When reactance is high at the source segment, the source resistance correction may be suggestive, but is inadequate to be treated as reliable.

When AGT values are close to ideal, but depart by more than a very few percent from the ideal, individual models are often presented as yielding actual values of gain and impedance. In a perfect world, the reports should be adjusted by reference to the AGT, but usually, the differences are too small to make a significant difference for either analysis or for translating a model design into a physical reality. Unmodeled “lumps and bumps” in the physical antenna normally swamp such small variations between corrected and uncorrected model results.

However, reference to AGT values may be important in several types of modeling enterprises. For example, when modeling a series of related antennas for certain comparisons, it is wise to determine the AGT value of each model to ascertain that trends in gain and impedance are accurate, with no anomalous values that result from variations in the AGT values for the sequence of models. As a second type of example, I recently had occasion to compare the same model(s) using NEC and using MININEC. The initial results, using raw report data, produced gains over a half-dB apart, with similar differences in the source impedance. However, for the models in question, NEC AGT values were systematically high (averaging about 1.06), while MININEC results were equally systematically low (averaging about 0.94).

When I compared corrected gain and source impedance values, they fell within 1% of each other.

Setting Up an Average Gain Test

Obtaining an AGT value is matter of reviewing the existing model and then setting up an RP 0 (Request for Pattern) input as a substitute for whatever other output request might be made. Suppose that we start with the following simple dipole model. See model 71-1.

```
CM Simple dipole antenna in Free Space
CM Optimized for resonance at 300 MHz
CE
GW 1 9 0 -.2418 0 0 .2418 0 .0001
GS 0 0 1
GE 0 -1 0
EX 0 1 5 0 1 0
FR 0 1 0 0 300 1
RP 0 181 1 1000 -90 0 1 1
RP 0 1 360 1000 90 0 1 1
EN
```

The model has already eliminated all resistive loading. Indeed, there are no load (LD) entries at all. As well, the model is in free space. However, it still retains its requests for E-plane and H-plane patterns (AZ/phi and EL/theta patterns in modeling terms). It is not necessary to remove these lines or other properly structured output requests from a model to obtain an AGT value. However, for clarity, we shall substitute the requisite RP 0 entry for the ones in the initial simple model. See model 71-2.

```
CM Simple dipole antenna in Free Space
CM Optimized for resonance at 300 MHz
CE
GW 1 9 0 -.2418 0 0 .2418 0 .0001
GS 0 0 1
GE 0 -1 0
EX 0 1 5 0 1 0
```

```
FR 0 1 0 0 300 1
RP 0 181 361 1002 0 0 1 1
EN
```

Now let's extract the RP0 line and explore its necessary and optional properties.

```
RP   0    181      361    1002   0      0      1      1
    Type  # theta  # phi  XNDA   theta  phi    theta  phi
          angles   angles see    start  start  incr.  incr.
                          text
```

The XNDA entry differs from the most common far-field pattern request only in the last or "A" integer. (In an RP request, the first 4 numeric entries are integers, and the remaining are floating decimals. XNDA is therefore not a single number, but a set of 4 integer entries in one.) A "0" indicates no request for averaging, while a "1" or a "2" request averaging. The difference between "1" and "2" is that the latter suppresses printing to the output file of the individual values making up the total field defined by the phi and theta entries, while a "1" yields a sizable table of values. Which you choose depends upon the need for those values.

There are two dimensions to the theta and phi entries: their formulation and the increment used within that formulation. Let's look at them individually, beginning with the number of angles.

Fig. 71-1 shows what we wish to obtain from each azimuth increment: an "orange" slice that samples each increment for theta from the zenith to its polar opposite. The number of theta angles will thus for a semicircle, and each new phi angle increment will produce another "orange" slice until we have sampled the entire free-space sphere.

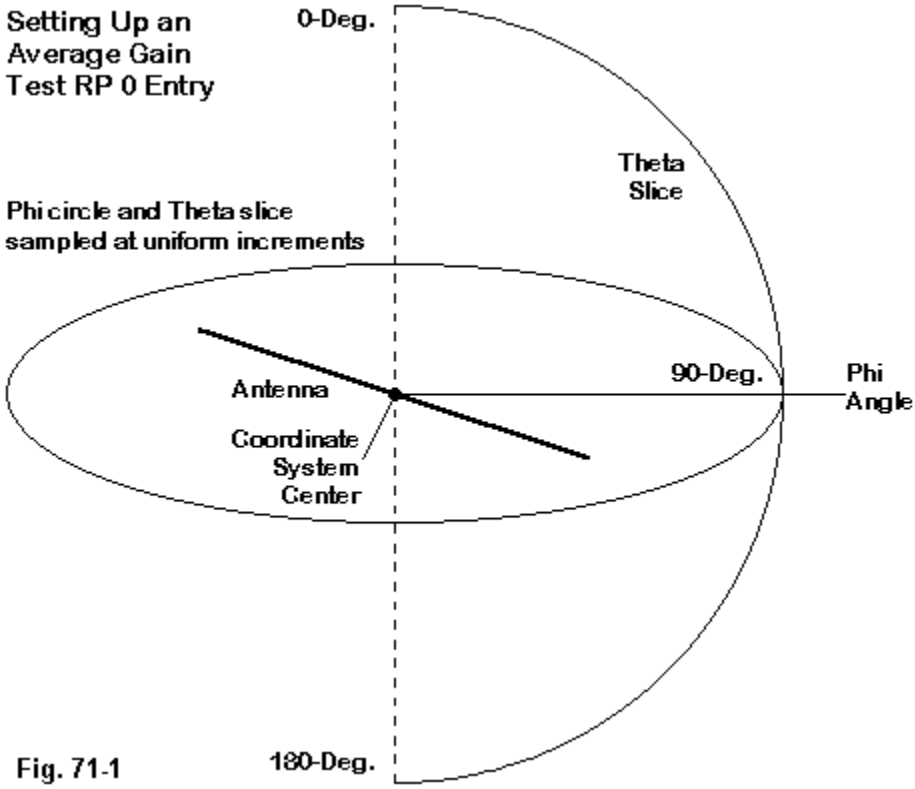

Fig. 71-1

For the sample line, we have chosen 1-degree increments for our fair sample. We might have chosen 91 theta angles and 181 phi angles, using a 2-degree increment in the last floating-decimal positions. Equally, we might have selected 0.5 as the angular increment, resulting in 361 theta angles and 721 phi angles. The object is always to create a complete sphere without repetition of angles, a problem that

will cause erroneous results by counting some samples more than once. You may compare the results of the suggested line with another that simply doubles the theta angles from 181 to 361 to see what error might emerge. (The extra "1" is to ensure that we include both points at the limits of the slice.)

For a hemisphere, used when evaluating monopole arrays over perfect ground, use a theta value of half that required for a full sphere. Be sure to include the extra point for example (91 instead of 90) to include both end points. By starting with theta = zero, you assure that the hemisphere will just reach the perfect ground surface.

In fact, the selection of sampling increments (and the consequent number of sampled angles) does make a small difference in the AGT value—so small as to be numerically but not operationally interesting. For antennas with highly varied pattern shapes, very narrow beamwidths, many secondary lobes, etc., changing the sampling increment may make a much bigger difference than it does for our simple dipole with its "figure-8" pattern.

AGT Values as a Function of the Number of Samples
Test Dipole: 9 Segments

Angular Increment	Reported AGT	Common Form
2 Degree (Phi/Theta)	9.95720E-01	0.9957
1	9.95696E-01	0.9957
0.5	9.95690E-01	0.9957

In general, the smallest increment that the modeler can use yields the most accurate figure for the AGT and for any correctives used in the analysis of multiple models. However, for simple geometric shapes, a 1 or 2 degree angle is quite adequate in virtually all cases. In the days of slow PCs, one often heard the advice to use the largest angle applicable to the beamwidth of the antenna. As well, those slower days suggested making use of antenna pattern symmetry to reduce number of sampling points and the run time for an average gain test pattern, especially when recording the sampling point values. However, since the amount of time required for an AGT test of the simple dipole by the current generation of PCs is under 30 seconds on an "old" 400-MHz P-2 machine for the smallest increment in the table above, there is little reason not to use small angles for all antennas. The more

complex the antenna geometry, the smaller will be the percentage of run time devoted to the AGT pattern, with or without a print-to-file of the sampled positions.

As a reference, here is the sort of report lines that you will receive from a NEC-4 output file (reduced to only the AGT lines) for an 11-segment dipole.

```
AVERAGE POWER GAIN= 9.97119E-01
      SOLID ANGLE USED IN AVERAGING=( 4.0000)*PI STERADIANS.

POWER RADIATED ASSUMING RADIATION INTO 4*PI STERADIANS =
6.91679E-03 WATTS


                - - - POWER BUDGET - - -

             INPUT POWER   = 6.93677E-03 WATTS
```

Make sure that the solid angle used in the averaging is equal or very close to 2*pi steradians for a hemisphere over perfect ground or equal or very close to 4*pi steradians for a full free-space sphere. (Including both limits is essential in obtaining a true 2.0 or 4.0 value for the solid angle.) NEC-2 does not yield the radiated power report entry. However, I have listed the Power Budget Input Power line, which is actually a rounded (by 1 place) version of the power reported by the Antenna Input Parameters power entry. Multiplying the Average Power Gain times the Input Power will provide the Power Radiated value.

There is one more set of numbers that is interesting before we leave our overkill of AGT. Our initial dipole was modeled using 9 segments. Let's see what happens as we increase the number of segments, each time moving the source position to center it.

AGT Values as a Function of Segmentation
Test Dipole: 1-Degree Increments

Number of Segments	Reported AGT	Common Form
9	9.95696E-01	0.9957

11	9.97119E-01	0.9971
15	9.98451E-01	0.9985
21	9.99212E-01	0.9992
31	9.99640E-01	0.9996
51	9.99871E-01	0.9999
71	9.99937E-01	0.9999
101	9.99973E-01	1.0000

For some tasks, the differences will make no difference. For others, up to a point, increased segmentation may be advisable when measured against the parameters of a modeling task. However, note the decrease in the rate of increasing AGT value toward 1.0 with the higher levels of segmentation. Hence, even for the most exacting modeling task, there will be a cut-off, beyond which increasing the number of segments—even on this model with a very thin wire (radius = 0.1 mm) relative to total length (about 0.484 m)—will yield nothing useful.

In this regard, remember that there is a convergence test that is also useful in evaluating the adequacy of a model. With NEC, there is a region of segmentation density that yields the least change in output report values as we increase and decrease the density by small increments. For most purposes, this region represents the converged model. In the end, balancing the two tests provides the best measure of an adequate model.

However, there are two limitations in this generalization. First, not all models that yield close-to-ideal AGT numbers will converge, and not all models that converge will yield close-to-ideal AGT values. Second, there are models that will neither converge nor yield a satisfactory AGT value. Both tests represent necessary but not sufficient conditions of model adequacy. Hence, the final responsibility for producing an adequate model within the much-published limitations of the core software remains squarely on the shoulders of the modeler.

* * * * *

Models included: 71-1 through 71-2. (Because the sequence requires access to the structure of the RP0 command, these models are available only in .NEC format.)

72. The GX or Symmetry Geometry Input

NEC-2 and NEC-4 have a useful geometry input card labeled GX. Often called the Symmetry Card, its actual title is “Reflection in Coordinate Planes.” A typical input line suggests extreme simplicity:

```
GX      5       110
        I1      I2
```

Note that there are no floating decimal positions for this input. The I1 entry indicates by how much to increment the tag numbers for each new construct created by the card. This maneuver helps prevent overlapping tag numbers for the wires of the model. The next entry is actually three binary entries, one each for the X, Y, and Z axes around which a reflection would occur: a “1” means “yes, reflect in this plane (across this axis),” and a “0” means “do not reflect.”

A reflection is a symmetrical replication of the existing structure created by GW and other entries preceding the GX card. Since the sample line has reflections in two planes, we shall end up with 3 new constructs for a total of 4 constructs and 4 times the total number of wires and segments as are in the geometry preceding the GX line. The 3 planes in the I2 entry indicate the X-, Y-, and Z-axes. However, replication or reflection occurs in reverse order. In this case, we have no Z-axis replication. The Y-axis “1” creates a replica on the “other” side of the Y-axis. Then, the X-axis “1” creates a reflection of the two structures on the other side of the X-axis. Obviously, to use this card effectively requires careful planning to avoid ending up with a tangled jungle of illicitly overlapping and intersecting wires.

The user’s question is obvious: what do we get for all of our careful planning? The answer is a reduction of the core run-time. The NEC manuals provide a chart of the relative run-times for the matrix storage, fill-time, and factor-time elements of the core run, but the bottom line is that a single reflection can reduce a run-time to about half of the same model created by other means. Two reflections cut the time to about a fourth, and 3 reflections to about an eighth. The values show up most graphically on very large models (several thousands of segments), where the over-

head for pre- and post-matrix work is a very small part of the total run-time. Hence, most advanced modelers save the GX card for very large models.

A Working Example: 3 Ways to Analyze a Square of 4 Yagis

Any account of the GX card faces a problem. Either the illustrations will be too large to print in this column, and the run-time improvements will be easy to see; or the models will be small, but the run-time differences will be hardly significant. Since these notes aim to orient the newer modeler to the use of the GX card, we shall use the small-model avenue and look at run-times in more detail later on.

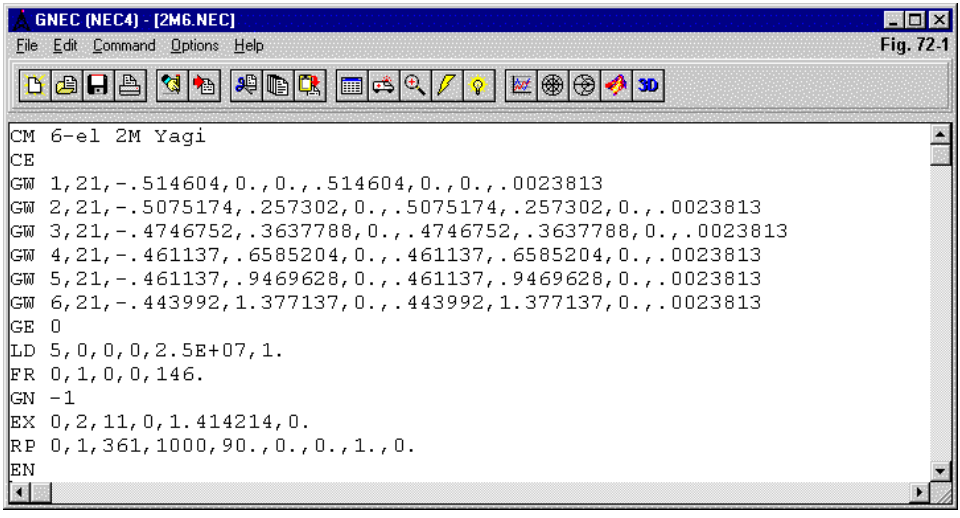

Let's begin with a simple 6-element Yagi designed for 146 MHz, where a wavelength is about 80.84" or 2.0533 meters. The total model, with all dimensions in meters, appears in **Fig. 72-1**. We shall stay in free space for this exercise, since eventually we shall want to create a GX version with symmetry relative to the X and the Z axes. For simplicity throughout this exercise, we have modified the LD5 (material load) line so that it always encompasses all segments, no matter how many

wires segments we add to the model by any of the means that we shall explore. The vital NEC output report data for this little antenna appears in the following table. See model 72-1.

Single 6-Element 146-MHz Yagi

Gain dBi	Front-to Back Ratio dB	Feedpoint Impedance R +/- j X Ohms	Run-Time Sec
10.23	35.39	49.97 + j 9.53	1.20

The only unusual bit of data in the listing is the core run-time taken from the NEC output report. It encompasses all core operations, which include the modification of values for the conductivity of aluminum and the E-plane or azimuth/phi pattern request as well as the matrix work.

This is our base-line data against which we shall make comparisons as we modify the model to create a square array of 4 such beams with their booms separated by 1 wavelength in each direction. (We do not here have to concern ourselves as to whether the spacing is optimal, so the convenient measures will work well for us.)

There are at least 3 ways to create our square of 4 models. The method that is available on entry-level programs is simply to replicate the first Yagi 3 more times and to space each one at the required distances apart to make the square. Using copy and move functions for blocks of GW or wire entries simplifies the process somewhat, but the final model is somewhat large visually and not too easy to scan rapidly. **Fig. 72-2** verifies this fact. See model 72-2.

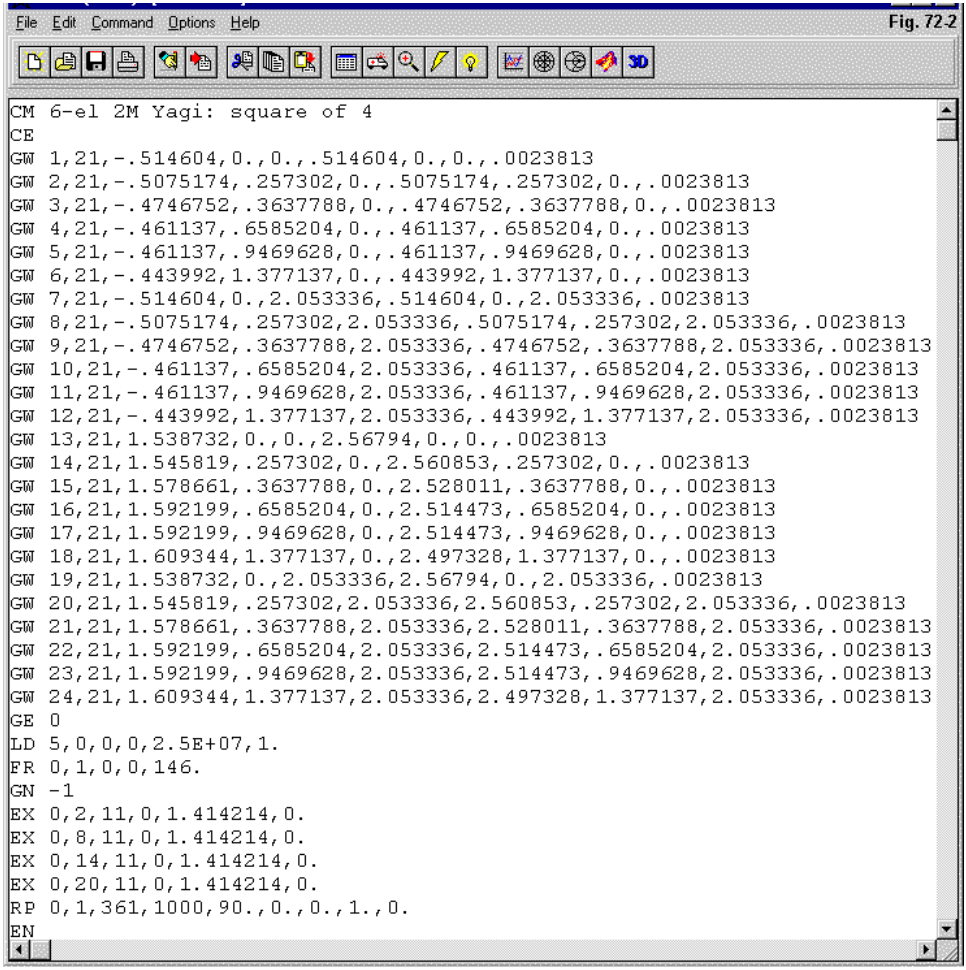


```
CM 6-el 2M Yagi: square of 4
CE
GW 1,21,-.514604,0.,0.,.514604,0.,0.,.0023813
GW 2,21,-.5075174,.257302,0.,.5075174,.257302,0.,.0023813
GW 3,21,-.4746752,.3637788,0.,.4746752,.3637788,0.,.0023813
GW 4,21,-.461137,.6585204,0.,.461137,.6585204,0.,.0023813
GW 5,21,-.461137,.9469628,0.,.461137,.9469628,0.,.0023813
GW 6,21,-.443992,1.377137,0.,.443992,1.377137,0.,.0023813
GW 7,21,-.514604,0.,2.053336,.514604,0.,2.053336,.0023813
GW 8,21,-.5075174,.257302,2.053336,.5075174,.257302,2.053336,.0023813
GW 9,21,-.4746752,.3637788,2.053336,.4746752,.3637788,2.053336,.0023813
GW 10,21,-.461137,.6585204,2.053336,.461137,.6585204,2.053336,.0023813
GW 11,21,-.461137,.9469628,2.053336,.461137,.9469628,2.053336,.0023813
GW 12,21,-.443992,1.377137,2.053336,.443992,1.377137,2.053336,.0023813
GW 13,21,1.538732,0.,0.,2.56794,0.,0.,.0023813
GW 14,21,1.545819,.257302,0.,2.560853,.257302,0.,.0023813
GW 15,21,1.578661,.3637788,0.,2.528011,.3637788,0.,.0023813
GW 16,21,1.592199,.6585204,0.,2.514473,.6585204,0.,.0023813
GW 17,21,1.592199,.9469628,0.,2.514473,.9469628,0.,.0023813
GW 18,21,1.609344,1.377137,0.,2.497328,1.377137,0.,.0023813
GW 19,21,1.538732,0.,2.053336,2.56794,0.,2.053336,.0023813
GW 20,21,1.545819,.257302,2.053336,2.560853,.257302,2.053336,.0023813
GW 21,21,1.578661,.3637788,2.053336,2.528011,.3637788,2.053336,.0023813
GW 22,21,1.592199,.6585204,2.053336,2.514473,.6585204,2.053336,.0023813
GW 23,21,1.592199,.9469628,2.053336,2.514473,.9469628,2.053336,.0023813
GW 24,21,1.609344,1.377137,2.053336,2.497328,1.377137,2.053336,.0023813
GE 0
LD 5,0,0,0,2.5E+07,1.
FR 0,1,0,0,146.
GN -1
EX 0,2,11,0,1.414214,0.
EX 0,8,11,0,1.414214,0.
EX 0,14,11,0,1.414214,0.
EX 0,20,11,0,1.414214,0.
RP 0,1,361,1000,90.,0.,0.,1.,0.
EN
```

Note that we need not add any new LD5 inputs, since the I1 and I2 entries cover all segments in the total model. Otherwise expressed, everything is aluminum. However, we did add new EX lines so that each beam has a source. **Fig. 72-3** shows the NEC-Vu graphic of the square.

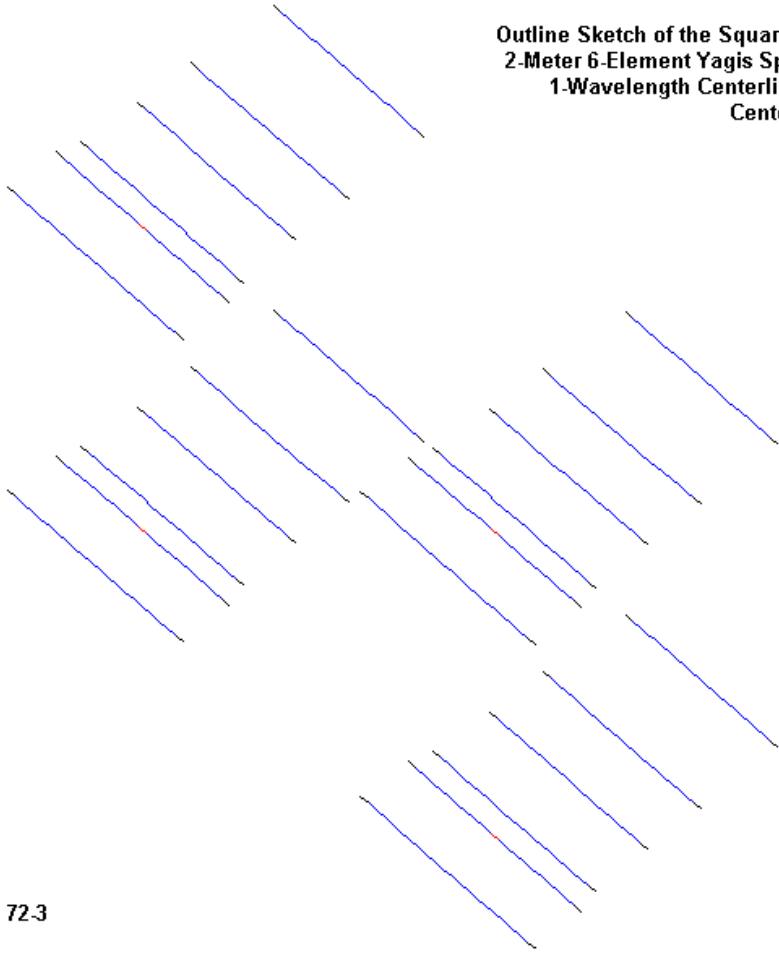

Fig. 72-3

The output data appears in the following table.

```
                Square of 4 6-Element 146-MHz Yagis:  GW Construct

  Gain          Front-to Back          Feedpoint Impedance          Run-Time
  dBi           Ratio dB               R +/- j X Ohms               Sec
  16.25         26.23                  50.96 + j 7.29 (x4)          9.50
```

The performance is interesting, but the run-time is the more crucial figure to examine. The run-time is 7.9 times longer than for the single Yagi.

A second formation technique is available to the user of more advanced programs, such as NEC-Win Pro (NEC-2) or GNEC (NEC-4). Instead of replicating with modifications all of the GW lines, we may employ the GM or Coordinate Transformation card instead. So let's reuse our 6 GW lines for a single Yagi and then make the moves indicated by the GM lines that follow in **Fig. 72-4**. See model 72-3.

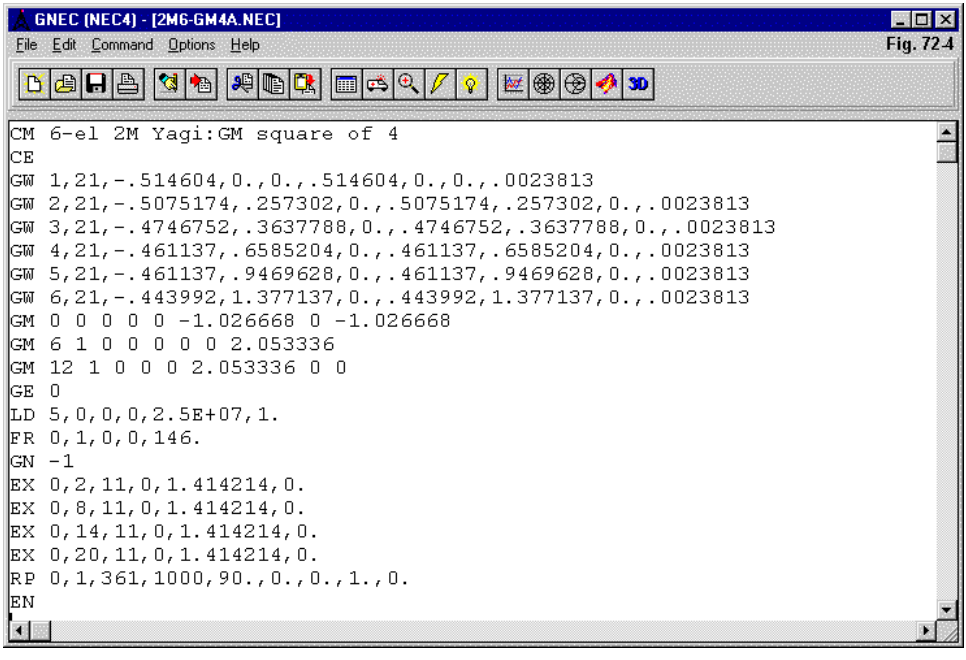

The first GM line moves the existing Yagi into the -X and -Z region. The amount of each move is 1/2 wavelength, as indicated by the 1.026668 (meter) values. This move will simplify the required moves for both this and the third alternative square.

The second GM line creates a second Yagi 1 wavelength above the first one and assigns it tag numbers 7-12.

The third GM line creates a new pair of Yagis 1 wavelength in the +X direction and assigns them the tag numbers 13-24.

We end up with the same square of Yagis that we viewed in **Fig. 72-3**. The output report appears in the following table.

```
              Square of 4 6-Element 146-MHz Yagis:  GM Construct

 Gain         Front-to Back          Feedpoint Impedance          Run-Time
 dBi          Ratio dB               R +/- j X Ohms               Sec
 16.25        26.23                  50.96 + j 7.29 (x4)          9.45
```

The only difference in the reported data is the run-time. In this instance, it is 0.05 seconds shorter than the run-time for the GW construct. However, such times will show natural variations for the individual models that are larger than the difference in the two recorded values, depending upon the myriad of variables within the computer.

If we know how to read the GM cards, the GM model is simpler to scan. Although the model uses NEC-4, it will also run in NEC-2, at least using the version of NEC-2 employed by NEC-Win Pro. The Imov entries may be missing if we are moving or replicating the entirety of the structure that so far exists. However, because there are so many cores of various ages and variation, if you are using something like Multi-NEC with a public domain core, be certain that you adhere to that core's requirements for setting up the GM lines.

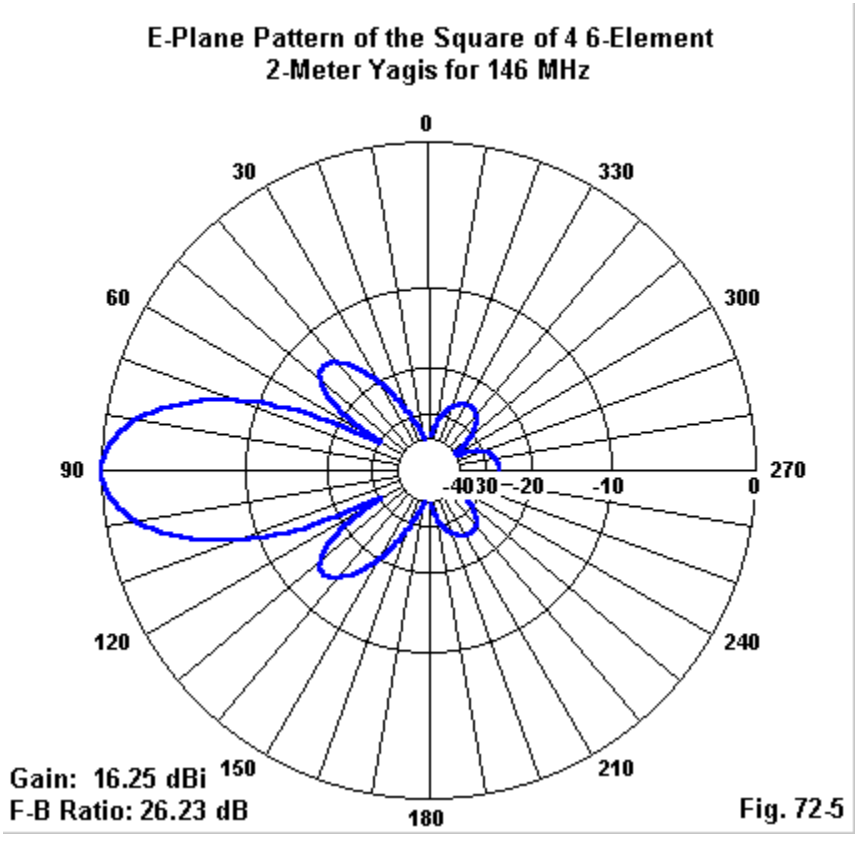

Fig. 72-5 records the E-plane (phi) pattern for the free-space square of 4 Yagis. Since the output reports for the two different models are identical, the pattern applies equally to both.

Now let's create the same models with mirrors but no smoke, that is, with the GX reflection input. We shall add a GM card to move the initial Yagi into the same -X, -Z position that we used with the GM construct. However, this time, we shall create the other 3 Yagis with a single GX line, as shown in **Fig. 72-6**.

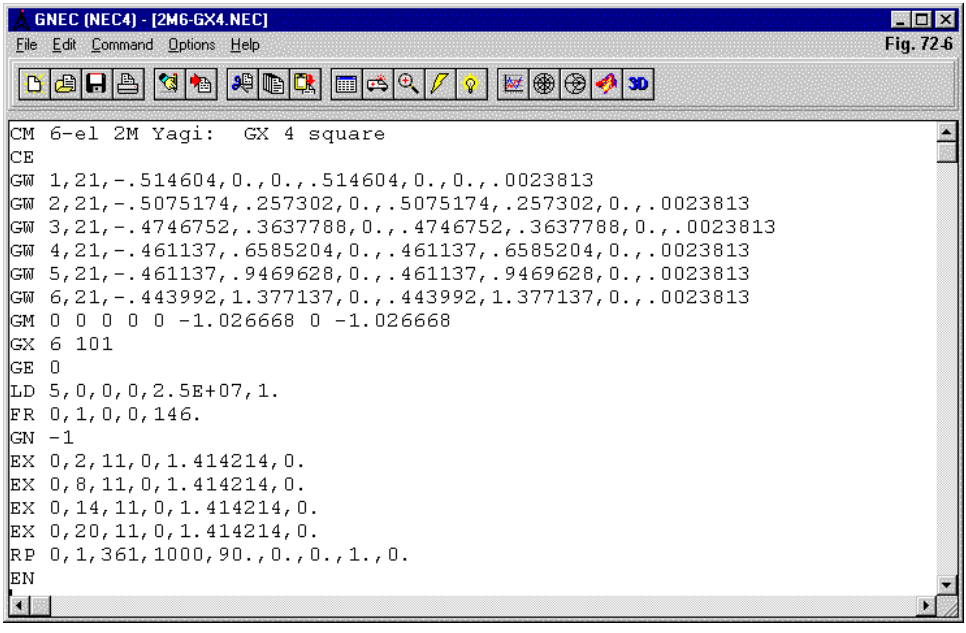

Note that by incrementing the tag numbers by 6, we shall create a total of 24 tags. The GX line indicates replication across the Z-axis and then total replication across the X-axis. The NEC-Vu result is identical to the square of Yagis shown in **Fig. 72-3**. We also have added the EX lines to make sure that we have a source for each reflection. So why does the resulting pattern emerge as shown in **Fig. 72-7**? See model 72-4.

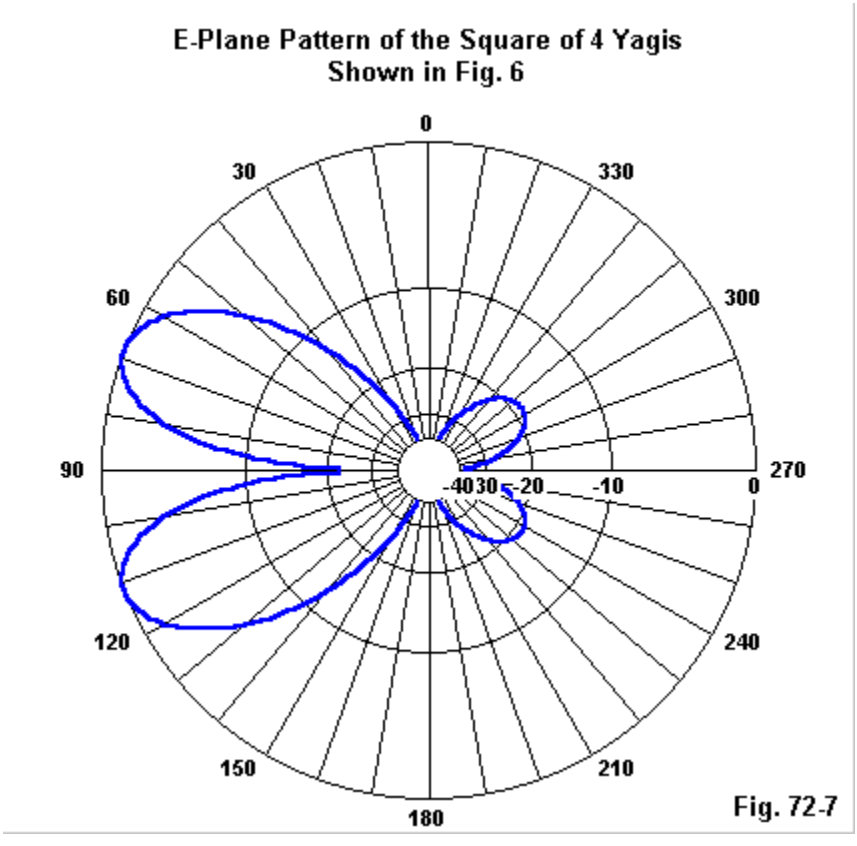

Fig. 72-7

The answer lies in how NEC creates reflections in coordinate planes. The new structures are indeed mirror images. The following abbreviated table compares the first and last segments of each of the 4 reflector wires from the GM construct (which is identical to the GW construct) and from the GX construct, as recorded in the Segmentation Data in the NEC output file.

```
                Partial Segmentation Tables From NEC-4 Output Files
2m6-GM4a:  GM Construct

  SEG.   COORDINATES OF SEG. CENTER     SEG.     ORIENTATION ANGLES    WIRE
CONNECTION DATA   TAG
  NO.       X         Y         Z       LENGTH     ALPHA     BETA      RADIUS
I-   I    I+    NO.
     1  -1.51677   0.00000  -1.02667   0.04901    0.00000   0.00000   0.00238
0    1    2      1
    21  -0.53657   0.00000  -1.02667   0.04901    0.00000   0.00000   0.00238
20   21    0      1

   127  -1.51677   0.00000   1.02667   0.04901    0.00000   0.00000   0.00238
0  127  128      7
   147  -0.53657   0.00000   1.02667   0.04901    0.00000   0.00000   0.00238
146  147    0      7

*  253   0.53657   0.00000  -1.02667   0.04901    0.00000   0.00000   0.00238
0  253  254     13
*  273   1.51677   0.00000  -1.02667   0.04901    0.00000   0.00000   0.00238
272  273    0     13

*  379   0.53657   0.00000   1.02667   0.04901    0.00000   0.00000   0.00238
0  379  380     19
*  399   1.51677   0.00000   1.02667   0.04901    0.00000   0.00000   0.00238
398  399    0     19

2m6-GX4:  GX construct

  SEG.   COORDINATES OF SEG. CENTER     SEG.     ORIENTATION ANGLES    WIRE
CONNECTION DATA   TAG
  NO.       X         Y         Z       LENGTH     ALPHA     BETA      RADIUS
I-   I    I+    NO.
     1  -1.51677   0.00000  -1.02667   0.04901    0.00000   0.00000   0.00238
0    1    2      1
    21  -0.53657   0.00000  -1.02667   0.04901    0.00000   0.00000   0.00238
20   21    0      1

   127  -1.51677   0.00000   1.02667   0.04901    0.00000   0.00000   0.00238
0  127  128      7
   147  -0.53657   0.00000   1.02667   0.04901    0.00000   0.00000   0.00238
146  147    0      7

*  253   1.51677   0.00000  -1.02667   0.04901    0.00000 180.00000   0.00238
0  253  254     13
```

```
*  273   0.53657   0.00000  -1.02667   0.04901    0.00000 180.00000   0.00238
272  273    0     13

*  379   1.51677   0.00000   1.02667   0.04901    0.00000 180.00000   0.00238
0  379  380     19
*  399   0.53657   0.00000   1.02667   0.04901    0.00000 180.00000   0.00238
398  399    0     19
```

If we compare the entries for the 3rd and 4th reflectors, which emerge from translations or from reflections across the X-axis, we can see that the order from first to last segment is reversed in the GX construct. As well, the beta orientation angle is not 0, but 180 degrees. However, if we return to **Fig. 72-6**, the model description, and examine the EX lines, we set up all four sources with the same phase angles: 1.414 real and 0 volts imaginary. The result is a square of four Yagis with the left pair fed out of phase with the right pair.

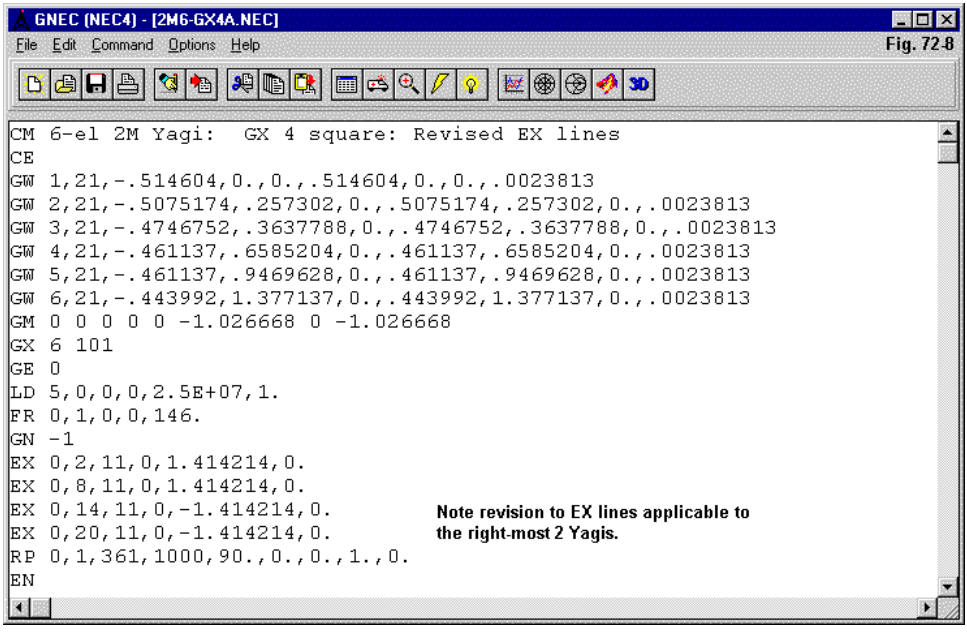

To restore the in-phase feed for the two pair of Yagis, we need to reverse the phase of the right-most beam sources or EX entries (or, alternatively, of the left-

most pair). We achieve this simply by adding a minus sign to the real component of the voltage at the source, as shown in **Fig. 72-8**.

When we make the change, the following data emerge from the model after running the core.

```
              Square of 4 6-Element 146-MHz Yagis:  GX Construct

  Gain        Front-to Back          Feedpoint Impedance         Run-Time
  dBi         Ratio dB               R +/- j X Ohms              Sec
  16.25       26.23                  50.96 + j 7.29 (x4)         4.40
```

Obviously, almost nothing changes relative to the GW and GM constructions, except for the run-time. In this trivial-sized model, the run-time is about half that of the other two models, and most of that time is taken up in pre- and post-matrix calculations and file generation. A truly large model would show a far greater reduction in core run-time.

A Different Type of Reflection Model

A second type of example may better illustrate the run-time savings that symmetry yields. We shall develop a simple doublet at 15 MHz, where a wavelength is close to 20 meters. We shall use segments close to 1-meter long so that there are about 20 segments per wavelength. The first model uses 2001 segments in a 2000-meter length. The second uses 4001 segments and twice the length of the first model. The third model uses 2001 segments with the same lengths as the first model. However, we set the 2001 segments from a position of Y=-2000 to Y=0. Then we set the GX input as follows.

```
GX  1  010
```

This entry creates a reflection across the Y-axis. The reflection runs from Y=+2000 to Y=0. The result is a single continuous wire-pair running 2000 meters each side of Y=0. To center the source, we create two EX lines, each in the segment closest to Y=0. The sum of the two source impedance reports should equal the impedance we would achieve in the 4001-segment model at the same overall length (4000 meters). The values will not be precisely the same, because the sources are located in a low current, high voltage region of the antenna, where the impedance changes rapidly in a very small distance. However, we are here less interested in

the output reports for the models—except to ensure that each model is accurately constructed—and more interested in the run times. **Fig. 72-9** shows the two large models. The half-size initial doublet is simply the left half of the lower sketch without a GX card and with only one source centered (segment 1001).

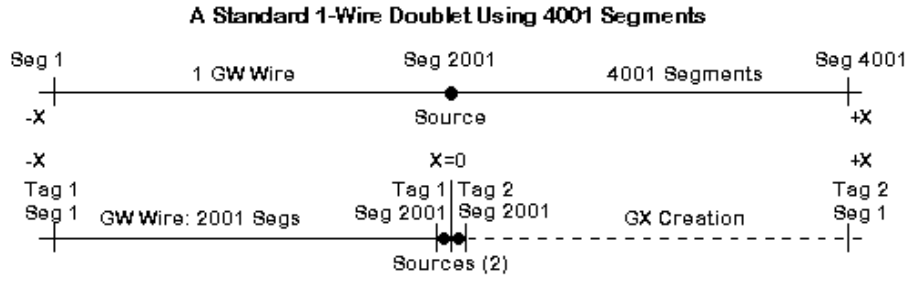

Alternative Ways to Create Large Models **Fig. 72-9**

Fig. 10 is a composite of all three models. (If you test them, use only one at a time.) See models 72-6, 72-7, and 72-8.

The following table summarizes the run times with double-precision NEC-4 on a 1.8-GHz machine running under XP. The parameters were set so that the entire operation in each case required no file-swapping to the hard drive.

Larger Model Run Times

Model	Run-Time
D2001 (2001 segments)	27.73 seconds
D4001 (4001 segments)	179.01 seconds
D4002GX (2001 segments + GX)	55.43 seconds

The models are perhaps medium-size and simple enough not to require excessive run-times regardless of the method of construction. However, they are large enough that the overhead becomes insignificant compared to the matrix time. Hence, their relative times are useful in developing an expectation of run times on models of this size and larger. A single reflection requires about twice the run-time of virtually

the same model without the reflection. However, the GW version of the same model requires over 3.2 times the run-time of the GX version of the same wire antenna. The run-times shown are averages of runs of the same models after various periods of computer operation. However, in this case, the times varied by less than 0.1 second per model.

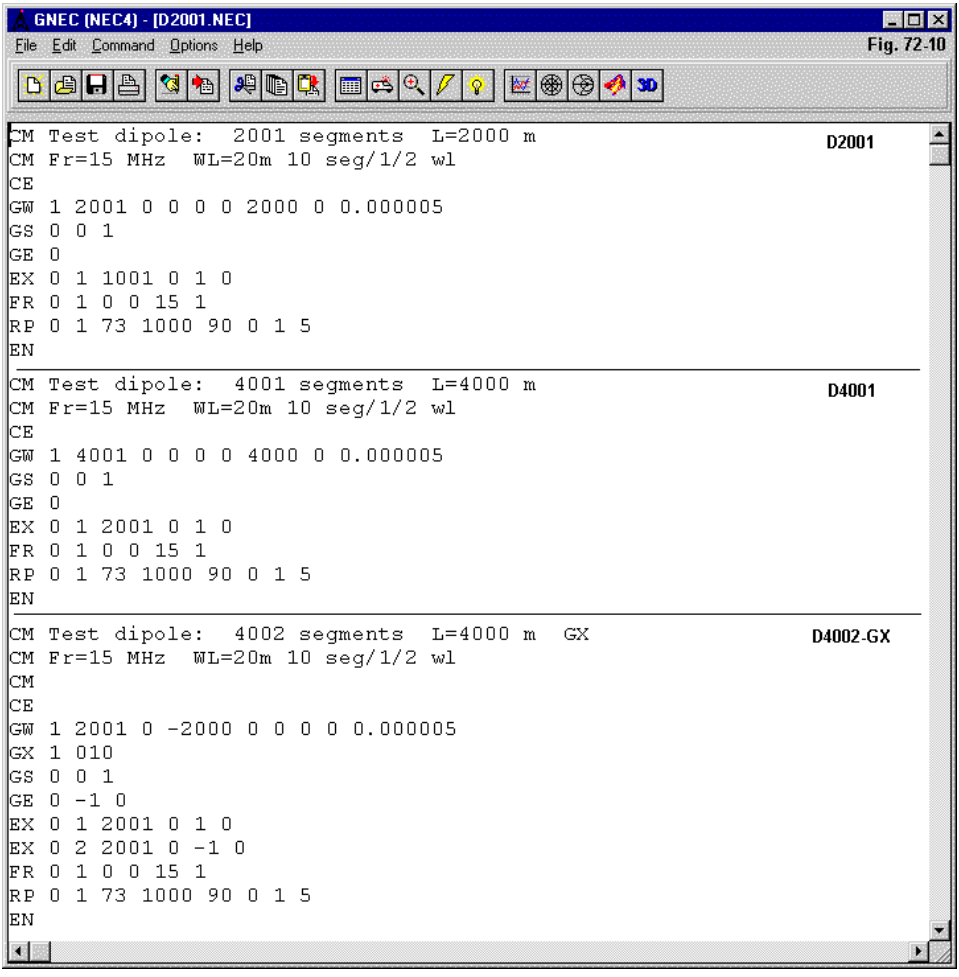

The doubling of the number of segments in the two GW-only models results in a 6.45 increase in run-time. Reducing that time to merely double the smaller-model run-time represents a considerable saving, especially when extrapolated (roughly) to even larger models. Since I did not exclude to the degree possible all overhead time, these numbers will be imprecise relative to all of the possible variations in model construction. But they do provide an indication of the orders of savings possible whenever a GX input is relevant to a large model.

Run-times are not the only notable feature of the model. The ability to bring a wire to a zero value, that is, to a position on an axis, can be multiplied indefinitely within the limits of array dimensions allowed by the core and the operating system. Hence, one might build 1/2 of a wire-grid ship, plane, or ground vehicle and create the other half via the GX entry. Similarly, a free-space sphere may begin with 1/8th of the structure and reach completion via the GX entry specifying reflection in all three planes. An oval may require only 1/4 of the structure for completion in two reflections.

Some GX Cautions

Here are some cautions in using the GX card.

1. Do not locate segments in the plane (axis-value=0) or crossing the plane around which the reflection occurs. The result will be intersecting or overlapping wire segments, an illicit NEC condition.

2. Do not add a wire or patch after the GX card; that is, do not add on a GW, GH, CW, or SP entry. Such additions will destroy at least one plane of symmetry, and the program will reset to whatever symmetries may exist prior to the ruined one (or more).

3. Do not use a GM card with a number of new structures greater than zero, or symmetry will be destroyed. As well, a GM card acting on only part of a structure will also destroy symmetry.

4. Avoid second GX entries, since they will negate the symmetry established by the prior GX entry. A following GR (Generate Cylindrical Structure) card will also negate the symmetry of a prior GX card.

5. If the GE card indicates a ground plane by setting I1 to 1 or to -1, then symmetry across the Z-axis (otherwise expressed, symmetry parallel to the X-Y plane) will be destroyed, although any other specified symmetry will be used. As a practical example, if one wishes to use symmetry for the square of 4 Yagis, but above a real ground, then the most direct way to accomplish this goal is to set a vertical pair of Yagis either as a pair of GW constructs or a GW + GM construct, and then to use the GX card to create the second pair across (in our examples) the X-axis. A following GM card may be used to rotate a structure about the Z-axis, so long as it includes the entire structure and does not create new structures.

Most of the listed cautions or limitations on the GX entry reset the core to either non-symmetry or to the highest level of symmetry allowable in light of the fault. There are other conditions, such as placing non-symmetrical lumped loads (LD1 through LD4) on the structure, that simply destroy symmetry without any resetting of the core. However, non-radiating networks (NT or TL entries) will not adversely affect a symmetry specification.

For the novice to the use of the GX card, making it the last entry prior to the geometry end (GE) card is perhaps the wisest route. Like sources (EX), one must also specify lumped loads in separate lines in the model. During the learning curve, it may prove useful to develop an over-simplified model having the same essential features as the eventual complex or very large model to ensure that you have introduced no symmetry-destroying features. Further information on the GX entry appears in the user-sections of the NEC-2 and NEC-4 manuals.

Our foray into the GX card has been to introduce both its features and its restrictions. In general, for small to medium size models, it is likely best to avoid using the card, since the time saved on the current crop of 1- to 2-GHz machines is small. However, for exceedingly complex and large models, symmetry may be the only course to take to achieve acceptable run-times.

* * * * *

Models included: 72-1 through 72-8. (Because the sequence requires access to the GX command, these models are available only in .NEC format.)

73. Source-to-Feedline Matching Techniques

With most antenna designs that we model, the source segment is as far as we need to model to fairly represent the characteristics of the antenna. If the source impedance does not match the characteristic impedance of a proposed feedline, we leave the matching network for calculations external to the actual modeling process. In most cases, the addition of the matching network has no affect upon the properties of the antenna itself as a radiating system.

There are simple matching systems that we can incorporate into the antenna model. However, more complex matching networks may lie beyond the modeler's experience or the facilities built into entry-level implementations of NEC-2. Some of these programs do not make available the NT or network facility. As well, the NT facility calls for values of shunt admittance (conductance plus or minus susceptance), and calculating these values calls for a bit of external effort relative to one's initial modeling experience with series impedance (resistance plus or minus reactance) loads. Finally, the shunt admittance values that we may insert into an NT command are fixed and do not change with frequency.

For this reason, modelers are sometimes interested in seeing if there is a way to create matching networks at the ostensible antenna source using LD load values that we may insert as series (or parallel) R-L-C values. These values are frequency nimble, changing their reactance with frequency changes assigned to the model.

In fact, there is a fairly straightforward technique for accommodating standard matching networks to the ostensible antenna source. (I used the qualifier "ostensible" because in the process of adding these networks, we shall change the location of the source segment.) To arrive at the general network solution, we shall have to review a few modeling fundamentals relative to sources, transmission lines, and loads.

A Few Source-Load-Transmission-Line Basics

Fig. 73-1 shows the standard diagram that describes the relationship among sources (EX0), lumped loads (LD0 through LD4), and transmission lines (TL). EX0 is a voltage source and here covers the implementation of current sources in programs like EZNEC and NEC-Win Plus. LD4 loads are impedance specifications in terms of resistance and reactance. LD0 through LD3 are lumped R-L-C loads in series or parallel form.

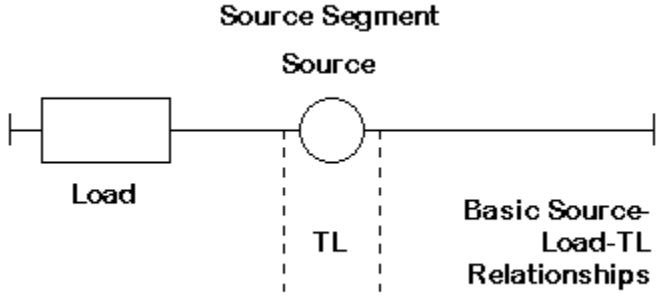

Fig. 73-1

We are working with EX, LD, and TL commands that we assign to the same segment. The key relationships to note in **Fig. 73-1** are these. First, an LD load is always in series with both a source and a transmission line assigned to the segment. This applies no matter how short the segment or where we may locate it. (I sometimes receive questions as to why a load assigned to the terminating wire of a TL transmission line does not significantly affect any antenna parameter, including the source impedance value. If we created a stub with a terminating wire, any load we assign to the terminating wire falls outside the region that we might represent as the portion of the wire between the transmission line wires. The only way to place a load between the wires is to create a transmission line from parallel (GW) wires and place the load on the physical wire (GW) that connects the two wires at their termination.)

Second, a voltage source (EX0) always is in series with the segment to which we assign it. In essence, it creates a mathematical gap in the segment and places the assigned source voltage and the resultant current in series with the segment wire. (Hence, any assigned lumped load falls outside the "gap.") So the source will be in series with any load.

Third, a TL transmission line is also in series with the segment to which we assign it, and it will be in series with a load and in parallel with a source placed on the same segment. All TL transmission lines are non-radiating structures, that is, they are not represented by geometry commands that add to the radiating structure of the model. As well, such lines are lossless. The fact that a TL is in parallel with a source and in series with a load opens the way to both potentials and to limitations.

The Simplest Matching Situation

The simplest case of matching that faces a modeler is bringing a non-resonant source impedance, that is, one containing reactance, to a resonant condition. If we make a center-fed doublet (actually, a redundant expression) that is too long or too short for some designated frequency of operation, the source impedance will appear as a resistance plus or minus a reactance. We may bring the doublet to resonance by inserting on the source segment a load with a reactance that is equal in magnitude but opposite in type to the reactance reported for the source.

We sometimes forget what we are doing relative to the model, because the technique is so simple and because we tend to express what we are doing in physical terms, such as "adding a loading coil." However, the coil has an inductance, which we may convert at the operating frequency to a reactance. NEC gives us the option of inserting either an LD0 series R-L-C load in which we specify the inductance or an LD4 load in which we specify the reactance. LD0 (and the counterpart parallel LD1) loads have the advantage of changing reactance with frequency and so give more accurate results for the progression of
source impedance values across a frequency sweep.

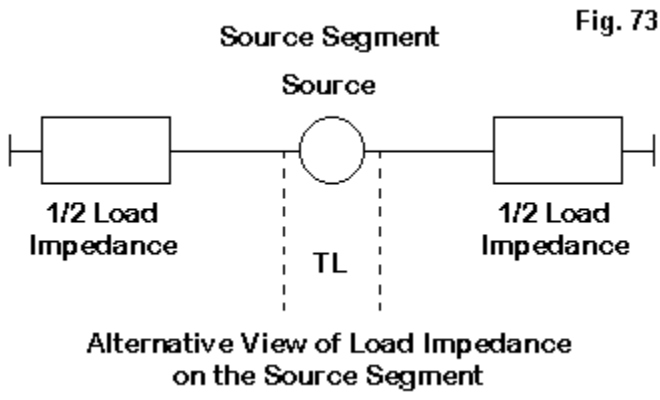

It is significant to understand that **Fig. 73-2** is an appropriate reformulation of **Fig. 73-1**. For inductive loads added to the source segment, the source and any TL that we may add are mathematically at the center of whatever physical structure we may use to implement them in a real antenna. Therefore, we may assume that the source is at the middle turn of a loading coil. Likewise, we may physically implement each half of the loading inductance with a shorted transmission line stub and each side of the physical feedpoint. We call such implementations of center loading "linear loads," and they are subject to fields of the antenna itself that may slightly disrupt the equal magnitude but opposite polarity currents we assume for transmission lines. Hence, it is normally most accurate to model linear loads using physical wires rather than the TL facility, which cannot show the influences of the radiated fields.

If our doublet is too long, it shows an inductive reactance at the feedpoint. In a model, we may add a capacitive reactance or a capacitor value in an LD load on the source segment to bring the doublet to resonance, that is, to a source impedance that is solely resistive. Our physical implementation of the load in most wire antennas would involving placing capacitance at the feedpoint assembly, between the antenna wire ends at the feedpoint gap and the transmission line ends. Since we are dealing with a series reactance situation, we may wish to use equal value ca-

pacitors, one for each side of the feedpoint gap. Each capacitor will need to provide half of the series reactance, which means choosing capacitors with twice the capacitance of the value specified in a single load assigned to the model source segment.

The Beta or Hairpin Match

A common system of matching a low (20-30-Ohm) Yagi feedpoint impedance to a 50-Ohm main feedline involves the use of a beta or hairpin match. A beta match is not only a simple matching system, it is also easily modeled. See **Fig. 73-3**. See model 73-1.

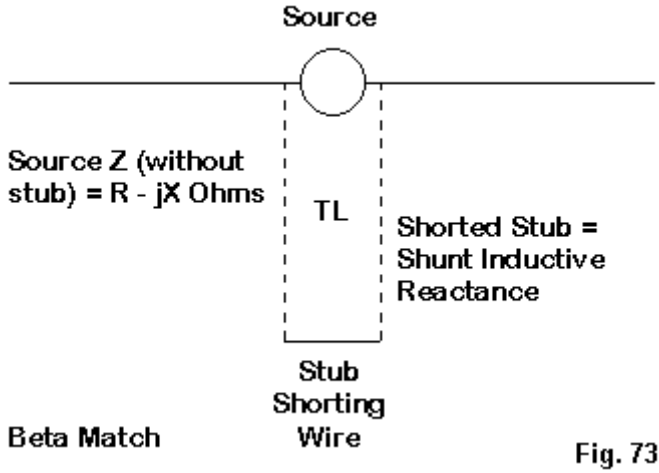

Fig. 73-3

In most cases, we set the length of the driver element—the element that we model with a source—slightly short of resonance. Hence, the source impedance prior to matching will show a resistance plus a degree of capacitive reactance. Note that the source impedance specification is in the form of a series circuit value of R - jX. In effect, the reactance is the equivalent of a component in series with the resistive component of the impedance.

From the perspective of the feedline, we are trying to match the higher feedline characteristic impedance to a low resistive impedance at the antenna. An L-network that will achieve this goal consists of a shunt or parallel inductive reactance on the

higher-impedance side and a series capacitive reactance on the low impedance side. We already have the series capacitive reactance built into the feedpoint segment. All that we need to do is to add the appropriate inductive reactance across the feedpoint.

In modeling terms, this means placing an inductive reactance across the source gap. Of course, we cannot directly achieve this with an LD load, since it will always be in series with the source. (If we are willing to highly segment the antenna structure, we can create a wire bridge across the source segment/wire, and insert the required inductive reactance or an inductor having that reactance at the design frequency on the bridge wire. If the segment lengths are very short relative to a wavelength, the bridge wire construct will not materially affect the array performance. The need for high segmentation arises not only because we must keep the bridge-wire construct very small, but as well because the segments adjacent to the source segment need to be the same length as the source segment for highest NEC report accuracy. See model 73-2.)

The beta inductive reactance can be either in the form of a coil or a shorted transmission line stub, so long as each has the correct value of inductive reactance. In fact, the hairpin match received its name from the shape of a shorted transmission line stub using parallel transmission line. Since a TL line is in parallel with the source, we may model a beta match using a shorted TL stub placed on the source segment. All that we need to do is to calculate the required stub length. (Depending upon the implementation of NEC-2, the program may create a “hidden” stub terminating wire or it may require that the user create his own terminating wire and values of admittance for a short circuit. A TL is actually a form of NT or network set up to simulate transmission lines.)

We often forget that the terms of a down-converting L-network are reversible. We may use a series inductive reactance in combination with a parallel or shunt capacitive reactance to achieve the very same goal. I have used this technique to match phased arrays showing series inductive reactance but a low resistive component at the feedpoint to common coaxial cable. In this case, the physical implementation was a capacitor across the feedpoint terminals, but the model used an open TL stub with a length to yield the same capacitive reactance.

Equivalent Single-Ended and Balanced Networks

We have worked our way through simple and specialized matching situations toward a more general solution to the feedline matching and modeling problem. Many of the networks that we physically implement are unbalanced or single-ended. In fact, their names are derived from unbalanced forms of the network: the L, the PI, and the Tee, to name the most common ones. (Of course, we may create more complex combinations of these networks, such as the PI-L, once common in vacuum tube power amplifiers. However, we must remember that the PI and the Tee are simply L-networks back-to-back.)

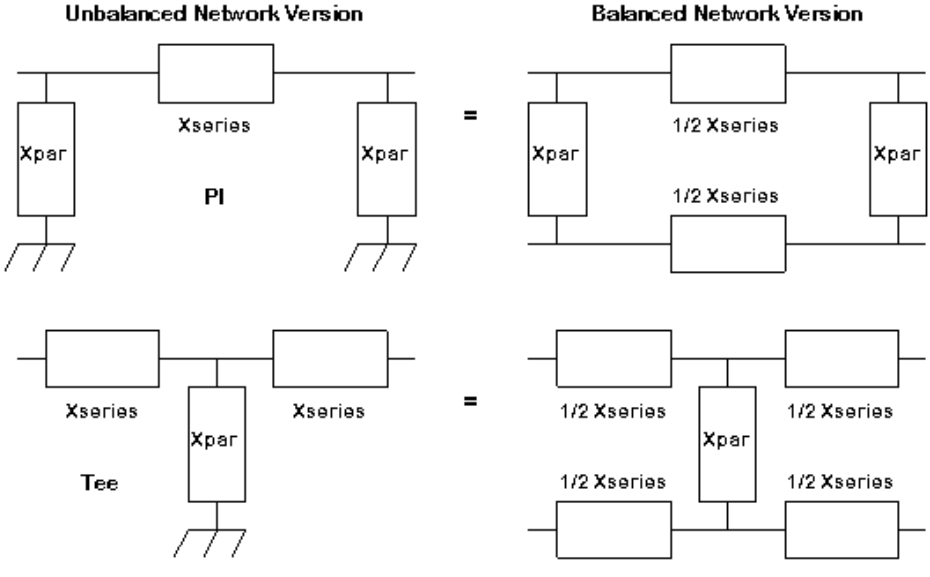

Fig. 73-4 Equivalent Networks

As noted in **Fig. 73-4** for the PI and the Tee unbalanced networks, every single-ended network has a balanced equivalent. We calculate the values using the single-

ended equations, which appear in a myriad of utility programs to save us the hand-calculator work. Then, we simply divide the reactances for the series elements in half, place one portion in each of the two lines of the balanced system.

Converting networks into balanced forms relieves us of a major limitation relative to NEC and single-ended networks. An unbalanced network presumes a virtually lossless ground buss to terminate components, as well as a source and a load (the old antenna feedpoint) that also run between the "hot" line and ground. NEC has a limitation in this regard. Simply bringing a wire to Z=0, except for a perfect ground, will not achieve a virtually lossless interconnection with other wires brought to Z=0 unless they all terminate at the same point. Two wires connected to a real ground (Sommerfeld or reflection coefficient) at any distance will always show a resistance between the two Z=0 points. In most instances, this limitation precludes modeling a single-ended network in NEC.

A balanced network is independent of any ground connection. We can implement Ls, PIs, and Tees in balanced form without regard to ground and arrive at relatively accurate modeled results. All that we need to do is to figure out how to attach our network to the antenna's former feedpoint. After all, we have a single segment with the former source point at its center, but two terminals of a 4-terminal network.

The TL Connection

The creation of a network using LD0, LD1, or LD4 loads for the reactive components requires that we construct a grid of wires matching the network needs. **Fig. 73-5** shows such a network for a balanced PI network. For the moment, let's concentrate on the wire grid in the lower portion of the graphic.

Because the network terminating components of the balanced PI are shunt reactances, each end of the grid shows a bridge section of only wires connected on one end to a cross wire to which the TL is joined and at the other network end to a bridge wire to which we assign the source. Had we used a balanced Tee network, the "empty legs" of the parallel parts of the wire grid would hold LD loads, and we would need one less crossing section for shunt or parallel components. An L-network would also be smaller, since we would need only a single pair of series components across from each other and a single shunt component.

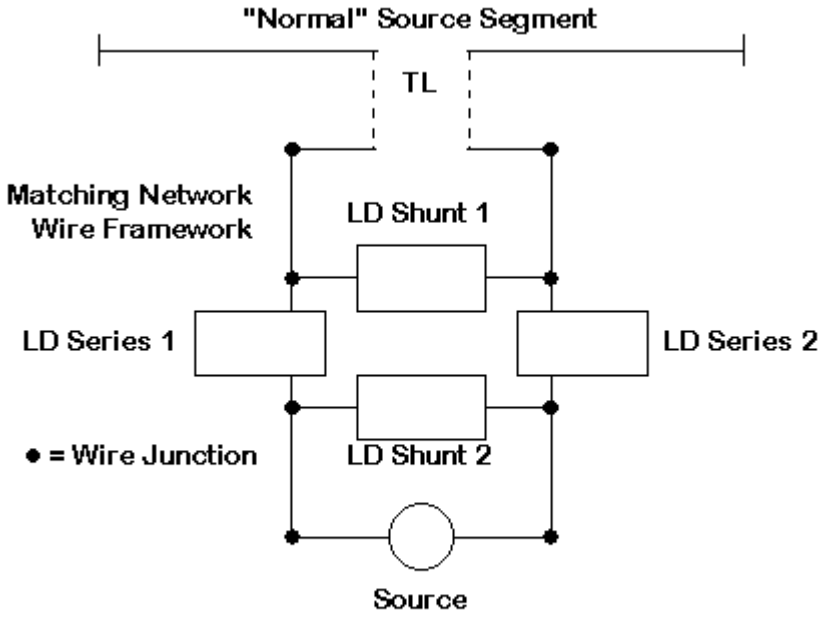

The Matching Network Assembly

Fig. 73-5

The point is to make the wire-grid no large than it has to be to hold the components and to establish the parallel connection to the grid of both the source (on one end) and the TL (on the other). As well, make the grid as small as possible. By using extremely thin lossless wire for the grid, we can shorten the length of the individual grid wires to the limits of NEC—about .001 wavelength. Each wire in the grid—contrary to the graphic—whether crossing of parallel—should be exactly the same length.

Now we are ready to examine the upper portion of the graphic. We want the physical structure of the grid to be as far distant as feasible from the antenna wires in the model. The goal is minimal influence on the network grid by the antenna's radiation. However, we want to have the grid as electrically close as is feasible to

the former source segment. The TL facility allows us to achieve this goal. We may place the grid wires anywhere we wish in terms of the cartesian coordinates that specify the physical structure. However, the electrical length of the transmission line depends upon the entry that we make for it, regards of the location of the terminals of the line.

The TL acts like a source in that it creates a series connection to a wire segment. Hence, we may specify only one segment for each end of the TL line (or any other NT command). We may set the wire-grid end a few or many wavelengths from the antenna wire. We specify the electrical length of the TL to something very short—perhaps an inch or less in the upper HF range.

The best characteristic impedance (Zo) to use for the TL is the feedpoint impedance (resistive component) of the antenna prior to adding the TL and the wire grid. Almost any Zo will do, since the impedance transformation for the line length will normally not by significant. However, the higher the reactive component of the impedance, the shorter we need to make the line and the more critical the value of Zo.

Once we have set up the antenna structure, the TL, and the wire grid for the intended network, all that we need to do is to calculate the network values or to obtain them by trial and error.

Does This System Really Work?

Let's set up a model and see if this system of feedpoint matching in models really works. Our worked example will consist of a near-resonant folded dipole made from lossless AWG #18 wire with a spacing of 3" between wires on a frequency of 28.5 MHz. For the folded dipole in question, in free space, with a total length of 196", the reported source impedance is 286.7 + j 0.6 Ohms.

What I wish to obtain is a match to 50-Ohm feedline. So I shall implement a balanced L-network in the model. Calculations show the required antenna-side shunt capacitor to be 42.4 pF (-j 131.7 Ohms) and the required pair of series inductors to be 0.304 uH (+j 54.4 Ohms). Now we can create the total model, with the wire grid about 1000" or more in any direction from the model. I chose "up." The

result resembles **Fig. 73-6**, although the folded dipole and the network grid are not in scale, since I combined two separate views to make this one.

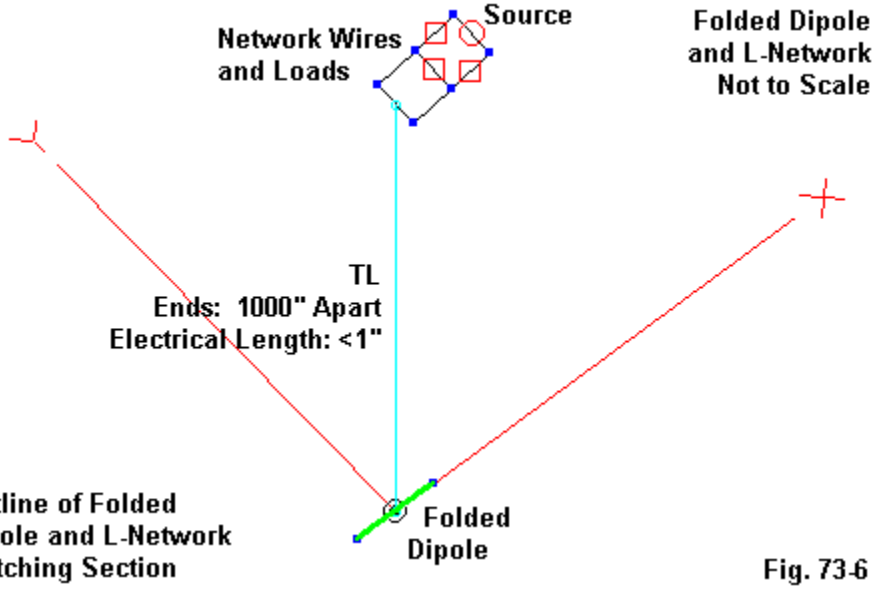

Fig. 73-6

The red circle represents the source location, while the red squares indicate the load locations. The wires in this grid are 1" long, or about 0.0012-wavelength at 28.5 MHz. They also use lossless AWG #18 wire (0.0403" diameter). The 290-Ohm transmission line is 0.1" long electrically, despite the 1000" separation of the network from the antenna wires. The following table shows the EZNEC model description for anyone wishing to replicate the exercise. See model 73-3.

```
                        EZNEC/4 ver. A4.0

Folded Dipole                                      Frequency = 28.5  MHz.

Wire Loss: Zero

                 ———————— WIRES ————————
Wire Conn.— End 1 (x,y,z : in)  Conn.— End 2 (x,y,z : in)  Dia(in) Segs

1   W4E2 -98.000,  0.000,  0.000  W2E1  98.000,  0.000,  0.000    # 18   99
2   W1E2  98.000,  0.000,  0.000  W3E1  98.000,  0.000,  3.000    # 18    1
3   W2E2  98.000,  0.000,  3.000  W4E1 -98.000,  0.000,  3.000    # 18   99
4   W3E2 -98.000,  0.000,  3.000  W1E1 -98.000,  0.000,  0.000    # 18    1
5   W7E2   0.000, -1.000,1000.00  W6E1   0.000,  1.000,1000.00    # 18    1
6   W5E2   0.000,  1.000,1000.00  W8E2   1.000,  1.000,1000.00    # 18    1
7   W8E1   1.000, -1.000,1000.00  W5E1   0.000, -1.000,1000.00    # 18    1
8   W9E2   1.000, -1.000,1000.00 W10E1   1.000,  1.000,1000.00    # 18    1
9  W11E1   2.000, -1.000,1000.00  W7E1   1.000, -1.000,1000.00    # 18    1
10  W6E2   1.000,  1.000,1000.00 W11E2   2.000,  1.000,1000.00    # 18    1
11  W9E1   2.000, -1.000,1000.00 W10E2   2.000,  1.000,1000.00    # 18    1

                 ———————— SOURCES ————————
Source    Wire      Wire #/Pct From End 1    Ampl.(V, A)  Phase(Deg.)  Type
          Seg.     Actual      (Specified)

1           1    11 / 50.00   ( 11 / 50.00)      1.000       0.000       I
               ———————— LOADS (RLC Type) ————————
Load   Specified Pos.     Actual Pos.       R          L          C      Type
       Wire #  % From E1  % From E1  Seg    (ohms)     (uH)       (pF)
1       9       50.00      50.00     1      Short      0.27       Short  Ser
2      10       50.00      50.00     1      Short      0.27       Short  Ser
3       8       50.00      50.00     1      Short      Short      42.2   Ser

                  ——— TRANSMISSION LINES ———
Line  Wire #/% From End 1   Wire #/% From End 1    Length    Z0   Vel Rev/
      Actual  (Specified)   Actual  (Specified)              Ohms Fact Norm

1     1/50.0  (  1/50.0)    5/50.0  (  5/50.0)    0.100 in   290.0  1.00  N

Ground type is Free Space
```

Note that the values of inductance and capacitance do not precisely coincide with the calculated values. We shall examine the variables in the system in a moment. However, with the values shown, the reported source impedance is 49.5 + j 0.1 Ohms.

The system does work—but within limits. Here are some of those limits based on the fact that the wires in the grid will interact with each other.

1. Wire size will make a difference to the results, although the affect tends to be small compared to some other affects. #12 wire yielded an impedance of 49.1 - j 0.9 Ohms, while #22 gave 49.6 + j 1.0 Ohms.

2. The TL Zo for the very short (0.1") line can vary considerably without significant change in the new source impedance value. Values between 250 and 300 Ohms occasioned no change in the reported impedance within the decimal limits shown here. As well, extending the line length from 0.1" to 1.0" also produced no source impedance change.

3. Grid wire length makes a large difference to the adjusted network values to achieve a near-50-Ohm source impedance. Doubling the wire length in both directions to 2" required 0.24-uH coils and a 40.9-pF capacitor. A second doubling to 4" wires required 0.155-uH coils and a 39.8-pF capacitor. The progression is clear, and the smallest feasible wire grid yields results closest to calculated values.

4. The wire grid presses NEC limits. Hence, it is essential to obtain an Average Gain Test value and to correct the reported system gain accordingly. The free-space folded dipole reported a gain of 2.14 dBi and an AGT of 1.0. The version with the matching network yielded a gain of 2.26 dBi, but with an AGT value of 1.029. Correcting the gain requires a 0.12 dB subtraction, for a net gain of 2.14 dBi. With the calculated values of matching network components, the reported impedance was 49.3 + j 12.7 Ohms. The resistive component corrected (AGT * reported value) is 50.7 Ohms, although the reported reactance is not accounted for by any known corrective measures.

Note that the LD values make no assumption about coil Q, although this factor may be important in some (but not necessarily all) models. I purposely used lossless wire and components to be able to compare the results with standard L-network computations. In general, the series inductance is more sensitive to Q-changes than the shunt capacitor (or, properly speaking, their respective reactance values).

Nevertheless, since component measuring techniques rarely surpass +/-5% for gear outside of precision laboratories, the modeled values are certainly within the limits of what is measurable by most experimenters. With due modeling of known cases, one can calibrate a given wire grid structure at a design frequency to know in advance the modeling offset.

The benefit of this technique, of course, is that it permits the use of R-L-C loads and hence returns relatively accurate results as one checks the performance across a frequency span. The limitation of the technique is that the requirements for maximum load accuracy are at odds with the limits of NEC itself for a perfect AGT value. Longer wire grid wires reduces the AGT variation, but create sufficient wire interaction to throw off the network values by much more significant amounts.

In the End. . .

There likely is no perfect or limitless method for replicating networks used to match a given antenna feedpoint impedance to a given feedline characteristic impedance. However, this one comes as close as I have so far been able to develop for using standard series R-L-C loads that are frequency nimble in a way that closely approximates calculated values for such networks. Used within its limits, it may be of service in a variety of applications.

The remote wire-grid network technique is, of course, adaptable to many configurations, even to adding a component in parallel to a series component and source situation. Not all configurations will require a full grid of the sort used with L-circuits and PI-networks. However, the same general rules of formation and the same limitations should be observed for all such structures.

* * * * *

Models included: 72-1 through 72-8. (.NEC and .NWP dimensions in meters; .EZ dimension in meters or in inches.)

74. Some Numerical Green's Function Rudiments

Suppose that you need to use a geometric structure over and over, each time varying some relatively simple appurtenance. We might have a wire-grid model of a ship, plane or ground vehicle and wish to know the best type of antenna and placement for a certain purpose. We might even have a fixed-size reflector—again constructed as a wire-grid assembly—and wish to find the best drive element for it, as well as the best place to put the driver.

We always have the option of running new models of the entire geometric structure composed of GW, GM, etc. entries. Very often, we can make the necessary changes using cut and paste methods within whatever ASCII editor we happen to use to create .NEC files. However, each run takes the same amount of time, plus or minus a little for variations in the new model sections that we introduce.

There is a better way—at least better in the sense of saving some time. How much time we save will vary not only with our computer speed, but as well with certain ratios between the size of what we create to use many times and the size of what we add to the model. The modeling technique involves Numerical Green's functions, which pre-calculate certain portions of the modeling problem and then use the results as substitute elements in the final set of matrix solutions. Mathematical details appear (for NEC-4) in section 6.3 of the program description and theory portion of the manual. NEC-2 handles these functions in essentially the same way as NEC-4. However, the feature is only available on advanced version of implementing programs and is generally omitted from entry level programs.

For the user, the task is a double one: first, learning the rudiments of incorporating Green's functions into a model. And second, learning when it is useful to employ them. If we take first things first, then we need to start with a little big model, that is, a model eligible for Green's function treatment, but small enough to handle within the confines of these notes.

A Planar Reflector and a Double-Diamond-Quad Driver

If we begin with a complete model, we can then more easily sort out the elements of a Green's function version of it. So let's begin with a double-quad driver in front of a planar reflector. The reflector uses a wire-grid in standard ways. **Fig. 74-1** shows a portion of the model: the driver and the start and end of the reflector. See model 74-1.

The first nine GW lines of the model describe the double-quad driver assembly. The short vertical wire across the center—where the diamonds join—is the source segment. Its length determines the segment lengths in the remaining parts of the structure so that we obtain maximum accuracy. All wires from GW 10 onward are portions of the reflector.

The model also shows the commands necessary to complete the model. For simplicity, I have set all of the wires to the same conductivity in one LD5 line. The ground setting is for free space. The frequency (FR) is 435 MHz only. The pattern request (RP0) is a simple azimuth or phi request at 0-degrees elevation or 90-degrees theta. If I run this example, I obtain the pattern shown in **Fig**. **74-2**.

My sample has only 450 wires and 678 segments, so it is not all that large. It took 22.03 second for the core run on my slower machine. The model shows 11.25 dBi forward gain and a 180-degree front-to-back ratio of 21.28 dB, with a source impedance (at the center of the diamonds) of 45.11 - j 6.40 Ohms. I cite these reference figures only for comparison with those that we get from running the model in a different way: the Green's function way.

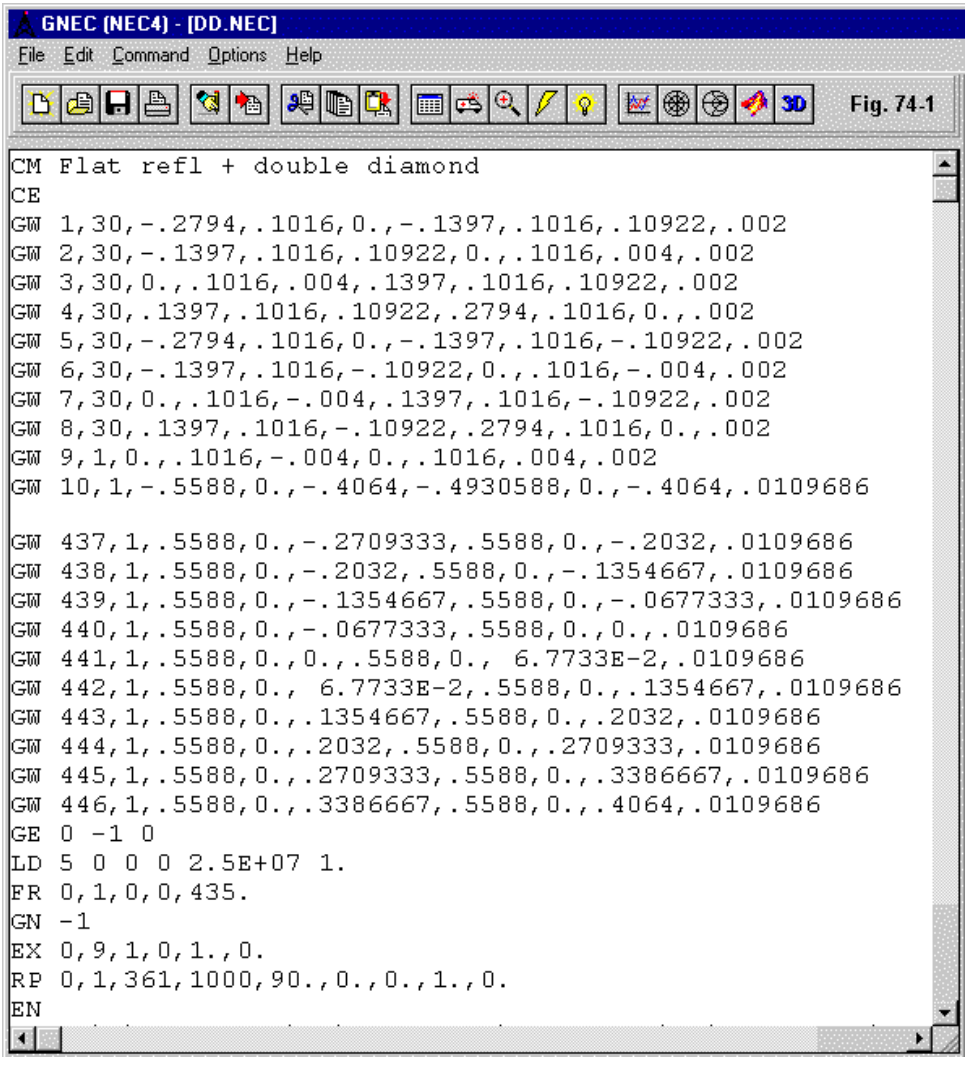
GNEC (NEC4) - [DD.NEC]
File Edit Command Options Help
3D
Fig. 74-1
CM Flat refl + double diamond
CE
GW 1,30,-.2794,.1016,0.,-.1397,.1016,.10922,.002
GW 2,30,-.1397,.1016,.10922,0.,.1016,.004,.002
GW 3,30,0.,.1016,.004,.1397,.1016,.10922,.002
GW 4,30,.1397,.1016,.10922,.2794,.1016,0.,.002
GW 5,30,-.2794,.1016,0.,-.1397,.1016,-.10922,.002
GW 6,30,-.1397,.1016,-.10922,0.,.1016,-.004,.002
GW 7,30,0.,.1016,-.004,.1397,.1016,-.10922,.002
GW 8,30,.1397,.1016,-.10922,.2794,.1016,0.,.002
GW 9,1,0.,.1016,-.004,0.,.1016,.004,.002
GW 10,1,-.5588,0.,-.4064,-.4930588,0.,-.4064,.0109686
GW 437,1,.5588,0.,-.2709333,.5588,0.,-.2032,.0109686
GW 438,1,.5588,0.,-.2032,.5588,0.,-.1354667,.0109686
GW 439,1,.5588,0.,-.1354667,.5588,0.,-.0677333,.0109686
GW 440,1,.5588,0.,-.0677333,.5588,0.,0.,.0109686
GW 441,1,.5588,0.,0.,.5588,0., 6.7733E-2,.0109686
GW 442,1,.5588,0., 6.7733E-2,.5588,0.,.1354667,.0109686
GW 443,1,.5588,0.,.1354667,.5588,0.,.2032,.0109686
GW 444,1,.5588,0.,.2032,.5588,0.,.2709333,.0109686
GW 445,1,.5588,0.,.2709333,.5588,0.,.3386667,.0109686
GW 446,1,.5588,0.,.3386667,.5588,0.,.4064,.0109686
GE 0 -1 0
LD 5 0 0 0 2.5E+07 1.
FR 0,1,0,0,435.
GN -1
EX 0,9,1,0,1.,0.
RP 0,1,361,1000,90.,0.,0.,1.,0.
EN

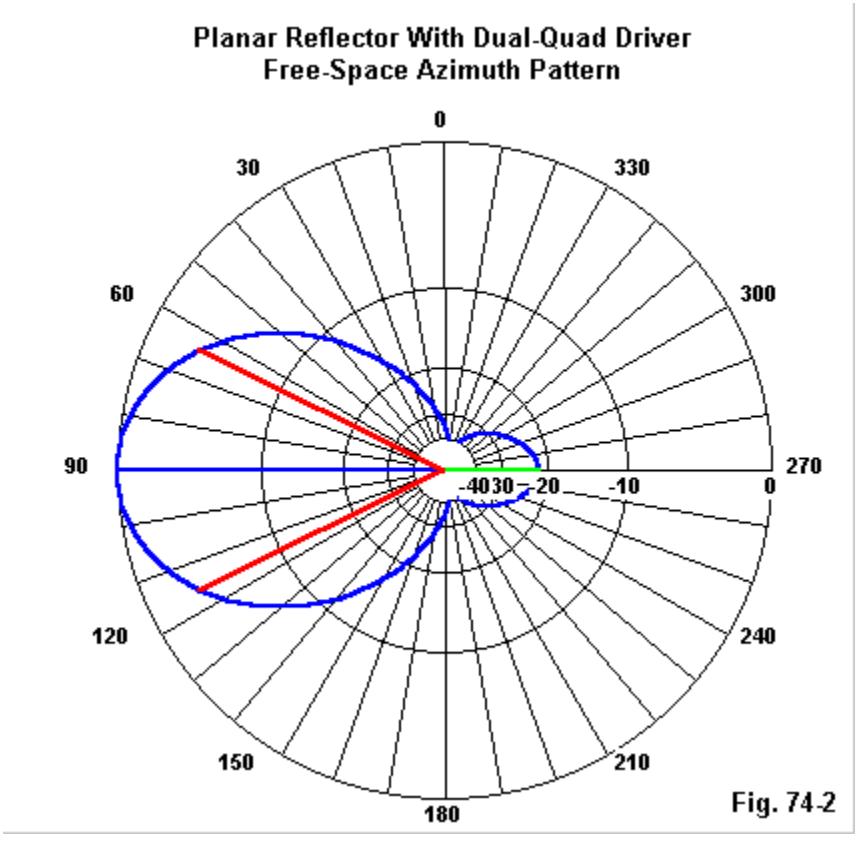
Planar Reflector With Dual-Quad Driver
Free-Space Azimuth Pattern
0
30
330
60
300
90
270
120
240
150
210
180
-40
-30
-20
-10
0

Fig. 74-2

Green's Functions: the File

Operationally, there are two steps to using Green's functions in a model: the structure for which we create a file and the model that calls up the file so that we can get a final result. We shall take them one at a time.

In our example, the portion of the model that we may wish to use many times is the wire-grid reflector that runs from GW 10 through GW 446. So we shall include those lines in the file part of the Green's function model without even changing the wire numbers. You can see an abbreviated portion of the structure in **Fig. 74-3**. See model 74-2.

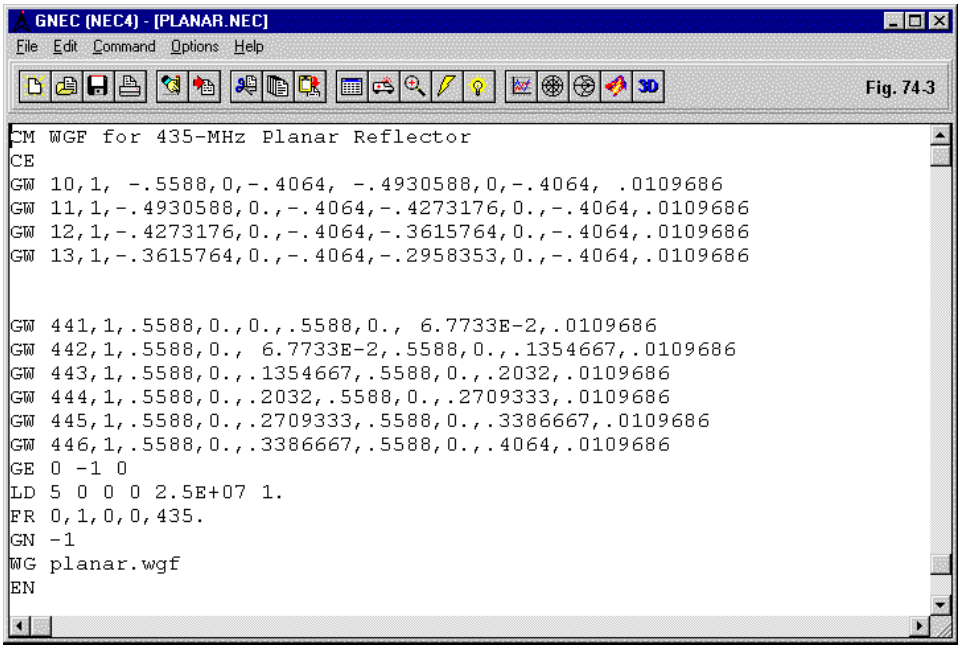

The file portion of our work must also include a few other items. If we wish to assign a conductivity to the wire-grid wires, then we must have an LD5 entry in this unit. As well, we specify the frequency, the FR entry. (A Green's file may not use multiple frequencies.) Since lumped loads, networks, and transmission lines do not affect the basic matrix calculations done within the file that we are creating, we may omit them. The file created would only ignore such entries anyway. We also specify ground conditions (GN) (or free-space, as in this example) within the file part of the effort.

The last line (before EN) in this example is a request to write the result to a file. We can specify any filename, but the .WGF extension is what the core recognizes as a Green's file. If there are other output requests, such as RP, NE, or NH, they come after the WG (write Green's file) command. However, in most cases, the modeler will save such requests for the other part of the modeling process.

Note: early versions of NEC-2 do not permit the addition of a user-created filename. Rather, the earliest—unmodified—versions of the core automatically assigned the file the name TAPE20. NEC-2 Programs such as NEC-Win Pro have added the ability of the user to specify filenames, since one may wish to maintain a collection of Green's files for any number of modeling tasks.

When we run this model, that we can save as a regular .NEC model file, we may discover no noticeable return. That is, we created a .WGF file, but not a complete model. The process is not a storage of what the modeler has written, but a filling and factoring of the matrix for the structure, along with a reservation of array space in memory for the matrix in subsequent runs when the users calls the file. That is step two.

Green's Functions: the Model

To use the Green's function file that we just created, we must create one or more models that call on the file. The file will consist of a GF entry to call up the file, followed by whatever else we may add to complete the model. **Fig. 74-4** shows the model file for our complete planar reflector and double-diamond-quad driver. See model 74-3.

In the new model, we begin (after the CM and CE lines) with a GF, a call for the Green's file that we have created. Note that besides mentioning the filename, the line also has a zero. That zero indicates a call for normal printing in the NEC output file. A 1 in this position would have been a call for a list of wire ends, in case we wanted to join a new wire to a wire within the Green's file structure. We do not need that feature for our examples, since our driver elements do not make contact with the wire-grid reflector.

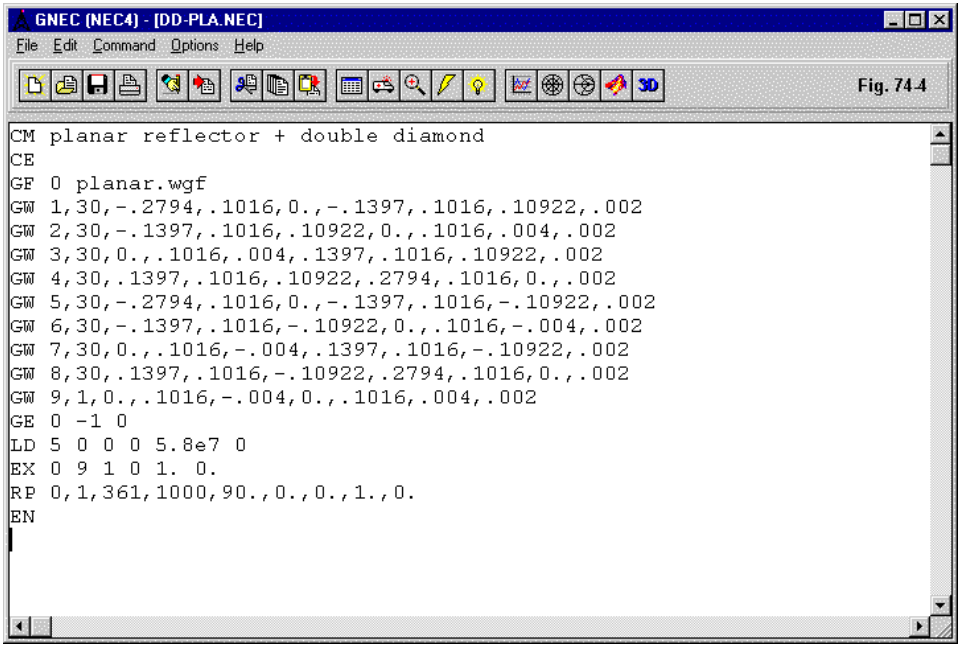

Note: early versions of NEC-2 do not permit the addition of a user-created filename. Rather, the earliest—unmodified—versions of the core automatically assigned the file the name TAPE20. Therefore, be sure to use the procedure that applies to the core that you are using.

Following the GF entry, we add whatever geometric structure we may need to complete the full antenna model. In this case, we enter the 9 lines that form the double-diamond-quad driver assembly. It does not matter whether the GW tag numbers precede or follow the tag numbers in the Green's function file, so long as the numbers are unique.

The new modeling file does not contain either frequency (FR) or ground (GN) commands. When the model runs, it will take these commands from the Green's file.

In this file, we need to add an LD5 entry if we wish the wires in the GW lines to have a different conductivity from those in the Green's file. I arbitrarily assigned copper values to these lines. Even though the LD5 card specifies all wires in the model, an LD in this part of the model will not reflect back into the Green's file, where the wires are aluminum.

No matter where we may place the Excitation (EX), it goes into this part of the model. The last major entry is the output request, in this case, a simple RP0 phi-pattern request. We may use any of the legitimate output requests within the model. As well, if we had any lumped loads (LD0 - LD4), networks (NT), or transmission lines (TL), we would place them in this portion of the total model.

Once we have our model complete, let's run it. If we do, again using my slow machine, we obtain 11.25 dBi free-space gain, 21.28 dB 180-degree front-to-back ratio, and 45.06 - j 6.44 Ohms source impedance. The slight difference in source impedance results from the change of material conductivity that I imposed to illustrate the separation of file and model values. Otherwise, the result is identical. If you look into the NEC output file, you will see all segments listed, with the notation "241 new unknowns."

The double-diamond-quad driver has so many segments because the source segment is very short as it forms a common link between the two quad loops. But we still have the same total number of wires (450) and the same total number of segments (678) that we had in our single model containing everything in one file. The total number of new unknowns does have an important consequence: the total run time for the model was 19.88 seconds, just a bit over two seconds shorter than the run time for the single complete model.

With that sort of run time, one might well ask why one should use a Green's function file. For this small model, where overhead, patterns requests, etc. occupy a significant portion of the run time, it may make no great sense to use a Green's file. However, we have only begun to scratch the surface of NGF use.

Re-Using the .WGF File

The total structure of the double-diamond-quad plus planar reflector looks like the views shown in **Fig. 74-5**.

Fig. 74-5

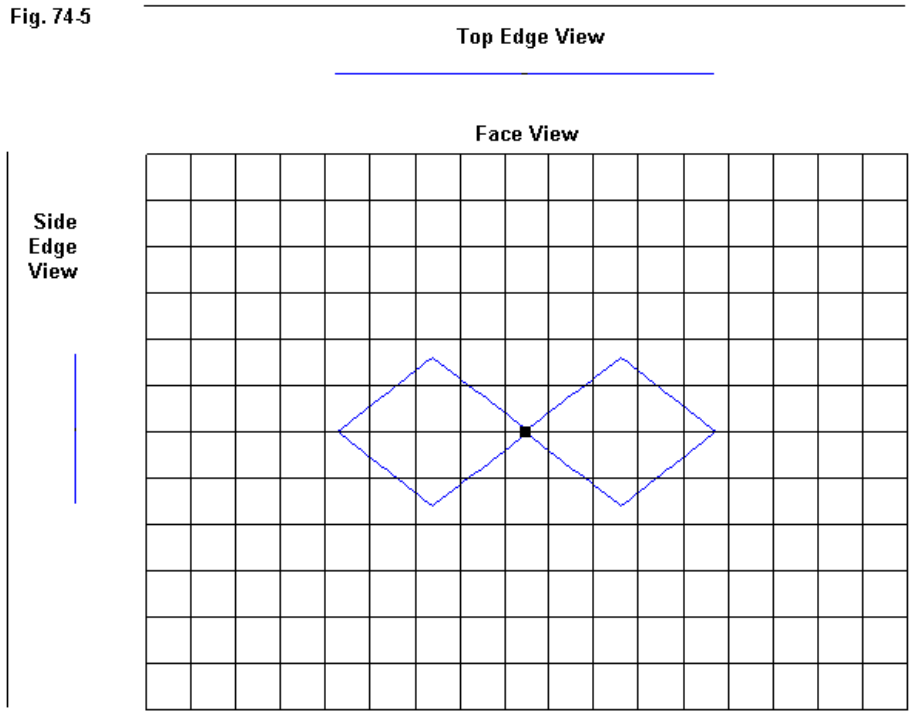

A Wire-Grid Planar Reflector With a Double-Diamond-Quad Driver

If we wish to look at other candidates for antennas using planar reflectors, we might well wish to save the wire-grid structure and simply replace the driver portion of the overall model. (The antenna view is actually for the original full model because in many systems, the antenna view facility may not show the contents of the Green's file.)

Fig. 74-6

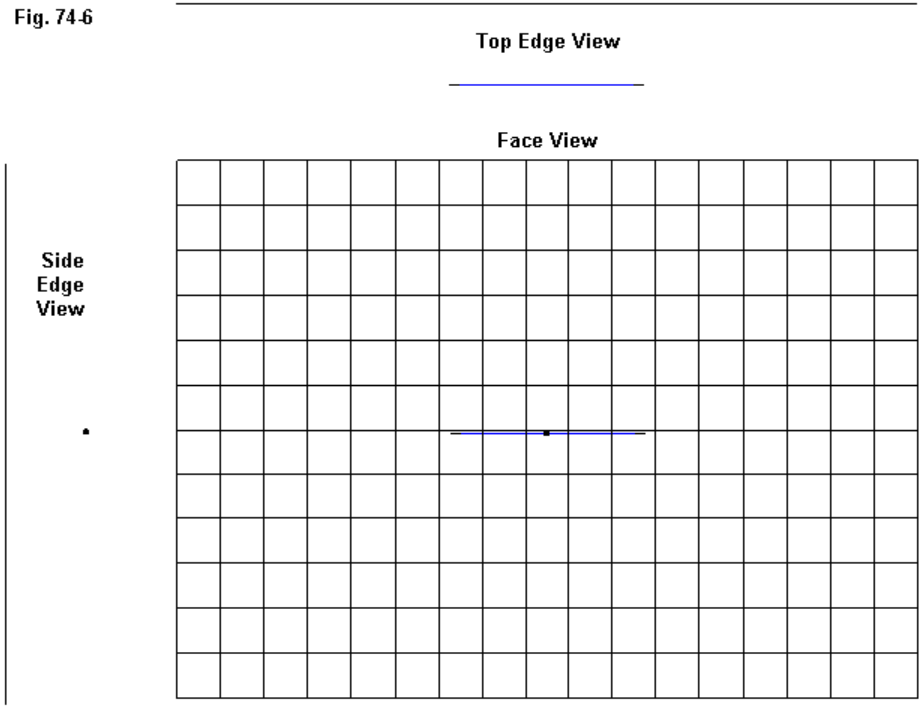

A Wire-Grid Planar Reflector With a Simple Dipole Driver

Suppose that I wished to find out how well a horizontal dipole might perform ahead of the given planar reflector. (In the real world, I would recognize that the double-diamond-quad driver is vertically polarized and also that the optimal size for a planar reflector may vary with the driver in front of it. However, in this context, we may by-pass such matters.) Suppose that I select a wire radius. I still have to find the right length so that the dipole is nearly resonant (or perfectly resonant, if I am lucky or patient). As well, I shall set myself the task of finding a dipole length and position ahead of the reflector so that the source impedance is very close to 50 Ohms at resonance. My final model will look like **Fig. 74-6**. The face view is slightly tipped, since the dipole lines up with the center horizontal wires in the reflector structure.

The model for the dipole plus planar reflector appears in **Fig. 74-7**. Note that we simply re-use the Green's file. In fact, I re-used that file about a dozen times before arriving at this final model, since the X and Y coordinates required considerable shifting to achieve our goals. See model 74-4.

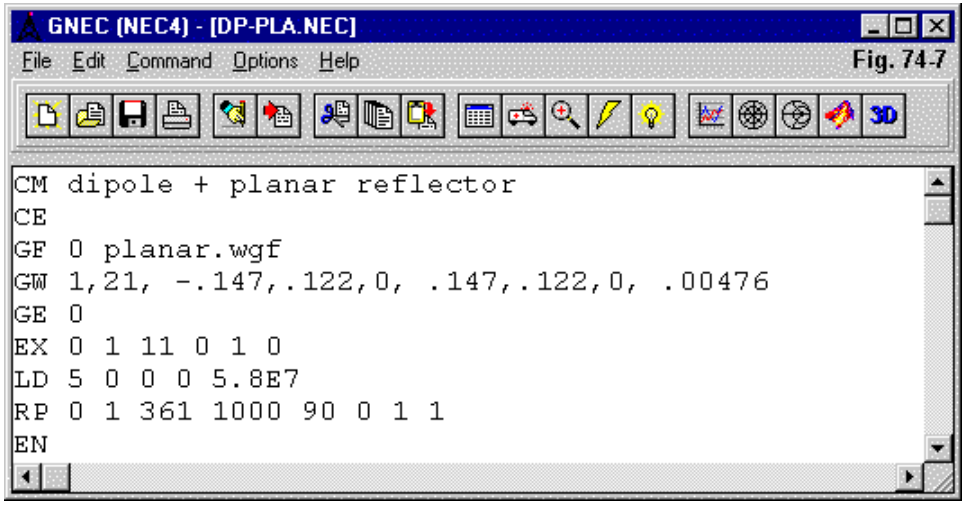

The model showed a free-space gain of 8.83 dBi, with a 180-degree front-to-back ratio of 24.14 dB. The reported source impedance was 49.93 + j 1.53 Ohms. The run time for this model was 4.12 seconds.

Two aspects of the model and its run time are important here. First, the model has 458 segments, of which only 21 represent new unknowns—the 21 segments of the dipole. Note the much larger ratio of total segments to new unknowns than we found in our double-diamond model.

The second important aspect of the model is called to our attention by creating a full model of the antenna using only GW entries for the wires. You need not always create such a check model, but for this column, I had no choice. He who cites time must take time to run the models.

The non-Green's-file model reported 8.83 dBi free-space gain, 24.14 dB 180-degree front-to-back ratio, and 49.95 + j 1.55 Ohms impedance. However, the full model had all aluminum wires, whereas the Green's version used a copper dipole. Hence, we obtained a 0.02 difference in both resistance and reactance at the source. (Of course, these differences are not operationally significant, but in this exercise, we are comparing calculation results for the sake of establishing confidence in the modeling technique.)

The run time for the non-Green's version was 13.95 seconds. The Green's version took less than 30% of that amount of time to run. If I had had to make my dozen or so runs to zero in on the targets of the modeling design exercise, it would have taken me well over 3 times as long per run.

Fig. 74-8 shows the phi pattern for the dipole plus planar reflector, not at all a bad pattern for such a simple antenna. Although 2.5 dB lower in gain that the double-diamond, the dipole version may be that much easier to construct. Turned the other way for vertical polarization and translated into the region just below a GHz, the antenna might be suitable for use in a back-to-back pair of passive repeating antennas for use when one's phone site is in a hollow or other area shielded from normal line-of-sight contact with the cell tower. (Of course, the vertical positioning of the antenna will show a wider beamwidth.)

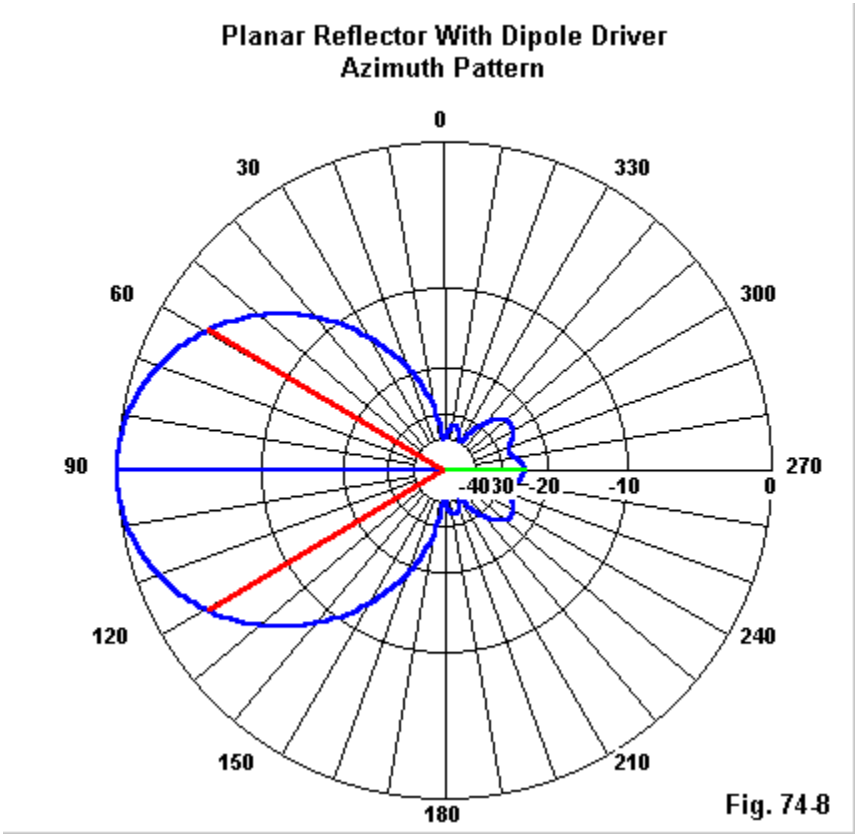

Fig. 74-8

Some Potentials and Some Cautions

The use of a Green's functions file can save time in model formation. Instead of using cut and paste methods to patch a set of GW lines into a model, we merely need to repeat the GF or file call line of the model. The resulting model, as the

dipole example illustrates, is very much easier to read, since the added structure is so much simpler than the full model. In addition, the load, source, and output request lines are more immediately at hand. For example, it was easy for me to see that I had initially placed my source on the wrong segment of the dipole model. Separating the dipole GW line from the EX line by 400+ other lines of model might have made the error search a longer one.

However, with every potential comes a caution. If the added structure is to contact the structure within the Green's file, it may be important to print the wire-end file. The error to avoid is either having no contact when one is desired or having the new wire intersect an existing wire in the Green's file at other than a segment or wire junction. There is always a big difference between saving time and becoming careless. The latter often requires much more time in the hunt for the errant entry.

The use of a Green's file may also save run time for the model. However, as we saw from the two examples, the relative time that we save appears to be a function of how much we can pack into the Green's file and how little is left over for the variable new structures that we wish to test. The lower the number of new unknowns relative to the total number of segments in a model, the more run time that we are likely to save, all other aspects of our model being equal.

Of course, there is no objection to having a collection of Green's files and calling them up sequentially in certain types of tests. For example, with our planar reflector, we might have up to a dozen or more wire-grid reflector files, each with a different shape or size. To find the one closest to optimal for a given driver system, we need only change the GF line of the model. The utility of the collection depends in part on having a constant test frequency for all of the members of our collection so that moving from one file to the next yields reliable results.

Do not expect to build up a collection of multiple-use Green's files overnight—unless you have a graduate student or other indentured servant to whom you can assign the task. (And if your work based on these models results in a publication, at least give the grad student a footnote, if not co-authorship.) The collection will emerge with time. Hence, it pays to think from the first use of such models what the test frequency should be for the most profitable work. Then, design each Green's file for that frequency. As well, from the start, give some thought to properly descriptive

filenames so that you can sort out the files and know at a glance what is in each of them.

Green's files are especially useful where an overall structure may have a symmetrical portion and another portion that is non-symmetrical. For example, one may use symmetry (the GX entry) to create ships, planes, and ground vehicles with half the wires, using a centerline and symmetry to complete the overall structure. Placing this structure in a Green's file gives you the ability to place—in the model that calls the file—an antenna of any shape anywhere on or about the structure without harming the symmetry. In fact, we can place structures that are mostly, but not completely, symmetrical into two files, the Green's file for the symmetrical portion, and a regular modeling file with a GF line for the portions that are not symmetrical. We can then evaluate such structures not only for antenna placement using voltage sources, but as well using plane-wave excitation to see the consequences for the structure.

The use of Green's functions is not a means of increasing the overall number of segments in a model. MAXSEG needs to be set at or above the total number of segments, including those held in the Green's file. As well, a Green's file does not relinquish the memory space needed by the model. Although it omits the fill and factor times, it retains the matrix storage time—and the memory space needed for that function.

(As an aside, the key limiting factor for model size is not the NEC-4 core itself. The core can be and has been modified by various implementations to expand the number of allowable segments in a model. Moving the region reserved for SP entries from above 10,000 to above 80,000 theoretically raises the number of allowable segments beyond anything that almost any modeler might imagine. However, it appears that the 32-bit Windows operating system is limited to about 4 GB, divided between system operations and applications. Hence, the practical limit for the number of segments on a Windows platform with about 2GB maximum available memory for a run that does not involve file-swapping with the hard drive is just above 11,000 (if there are no surface patches). The run time for hard-drive file swapping depends on the input and output speeds of the drive—as the slowest procedure in the process—and may take 10 or more times as long as runs wholly within memory. The ability of a machine to handle such runs varies with the machine set-up, what may be running in the background, and a host of other factors outside the control of an

implementing program for NEC-4. NEC-2, which handles Green's files in the same way as NEC-4, tends to be limited at most to 10,000 segments or less by most implementations of the core.)

Wisely used, Green's function files may save a modeler both time and error-hunting energy. These notes are designed only to introduce the rudiments of the process of using them. Modeler task assignment and creativity will, in the end, determine if they are worth the development time.

* * * * *

Models included: 74-1 through 74-4. (Models available in .NEC format only. You must run model 74-2 in order to use models 74-3 and 74-4.)

75. NEC: Power Efficiency vs. Radiation Efficiency

There seems to be a semi-pervasive mystery about what NEC may report by way of "efficiency" with respect to an antenna under test. So let's examine what the NEC output report may tell us in this regard. We shall use a series of simple examples to illustrate the information.

Power and Radiation Efficiency Reports and Calculations

First, every NEC output report provides a Power Budget report. The general form of the budget looks something like the following (without regard to the specific model that generated the numbers involved).

```
INPUT POWER   = 6.8603E-02 WATTS
RADIATED POWER= 5.6868E-02 WATTS
WIRE LOSS     = 1.1735E-02 WATTS
EFFICIENCY    =  82.89 PERCENT
```

The input power is a calculation based upon the source level (normally, voltage magnitude at 0-degrees phase angle) and the calculated source impedance. The radiated power is the input power minus the sum of all losses. Wire losses include losses due to the material conductivity (LD5) assigned to the models wires as well as losses associated with lumped loads (LD0 - LD4). A category of loss not present in the given model are the "NETWORK LOSSES," that is, losses associated with network (NT) and transmission line (TL) commands. In all cases, losses are calculated relative to the resistive portion of any impedances (or, for networks, the conductive portion of any admittances). The example allows a simple subtraction of the loss from the input power to arrive at the radiated power.

Power efficiency (as we shall call it here) is simply (Radiated Power / Input Power) * 100, and is given as a percentage.

Numerous modelers are also interest in another figure, a radiation efficiency. This value would give a measure of some sort for the effectiveness of the antenna as a radiator within the actual operating environment. Hence, if there are ground losses associated with the antenna, radiation efficiency (again, as we shall call it) would take them into account. A number of experimenters try many techniques to arrive at this value, ignoring the fact that NEC will yield such a value with the correct output call.

Of course, the NEC report will be limited in the same way that any other output data are limited. NEC will use level ground, and the only objects within the field of the antenna will be those modeled by the program user. On the other hand, these limitations may also become an advantage, since one may compare antenna radiation efficiencies under conditions in which all "other" things are equal.

The required call is an RP0 (far-field) request for the same sort of pattern that we need for an Average Gain Test. We set the XNDA entry to either 1001 (if we wish the pattern data to appear in the output report) or 1002 (if we are interested only in the required information for calculating the radiation efficiency). There are two cases of note: free space (no ground) and all other cases having a ground that may range from perfect to very lossy (using either the refection coefficient or Sommerfeld ground systems). We set up the RP0 request to fairly sample the sphere or hemisphere at reliably constant intervals in degrees. So the two possible lines will look something like the following ones:

```
Free Space @ 5-degree Intervals       RP 0 37 73 1002 -90 0 5 5
Over any ground @ 5-degree intervals  RP 0 19 73 1002 -90 0 5 5
```

In both cases, we have suppressed the printing (to file) of the radiation pattern. However, one may uses this data for generating a surface or 3-D pattern for the antenna model in question. The angles follow the phi and theta conventions, which may differ from azimuth/elevation starting points that may be built into an implementation of NEC.

The 5-degree interval may not always be sufficient to track precisely the pattern undulations of a given far-field pattern. In such cases, one may reduce the interval for both phi and theta to 2 degrees or even 1 degree. The number of steps for theta (37 for free space) and phi (73 for free space) will increase accordingly, reaching

181 and 361, respectively, for 1 degree intervals. However, it will be rare that we need a value for radiation efficiency that approaches that level of precision.

As noted, we must calculate the value of radiation efficiency. We base what amounts to a super-simple calculation on the data that emerges when we set the final digit of XNDA to 1 or 2, both of which request "gain averaging." The raw data line has the following appearance at the end of the RP0 request portion of the NEC output report.

```
   AVERAGE POWER GAIN= 4.99152E-01       SOLID ANGLE USED IN
AVERAGING=( 2.0000)*PI STERADIANS.
```

First, examine the solid angle data. For free space, the value within (—) will be 4. If that is the case, the radiation efficiency will be the value of the average power gain * 100 and will be a percentage. In this case, which applies to the case of a hemisphere created over any ground type, the value in (—) is 2. For all such cases, the radiation efficiency is the (average power gain / 2) * 100 %. Since the reported power gain is 0.4992, the radiation efficiency is 24.96% (using at least 1, if not 2, too many decimal places for most purposes).

There are some shortcuts to arrive at the desired average power gain for patterns of known symmetries. However, on modern computers, using the RP0 calls shown will not create delays for most model runs.

Some Case Studies

When we wish to give weight to a set of examples, we re-name them "case studies." Let's look at a few and see what we get for our efforts by way of reports. We shall begin with a vertical monopole with 4 radials, all of AWG #12 wire. We shall set the base of the monopole and its radials at 5' above ground level. The set-up has the outline shown in **Fig. 75-1**.

Fig. 75-1

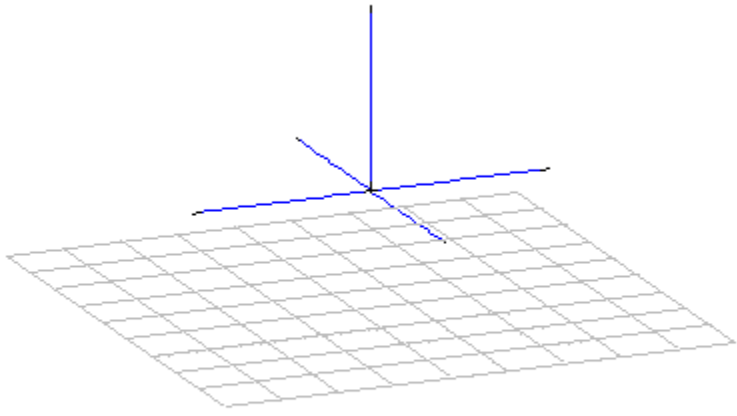

General Outline of Test Antenna
28.5-MHz AWG #12 Copper Monopole + 4 Radials
5' Above Specified Ground

Initially, we shall use perfect or lossless wire, no loads, and a perfect ground to run out test. The model appears in the following lines. See model 75-1.

```
CM radiation efficiency test vertical/4 radials
CM full length
CM perfect conductor
CM perfect ground
CM no loads
CE
GW 1 21 0 0 13.7 0 0 5 0.0033695
GW 2 21 0 0 5 8.7 0 5 0.0033695
GW 3 21 0 0 5 0 8.7 5 0.0033695
```

```
GW 4 21 0 0 5 -8.7 0 5 0.0033695
GW 5 21 0 0 5 0 -8.7 5 0.0033695
GS 0 0 .3048
GE 1 -1 0
GN 1
EX 0 1 21 0 1 0
FR 0 1 0 0 28.5 1
RP 0 19 73 1002 -90 0 5 5
EN
```

The relevant power and average gain report data follows.

```
                - - - POWER BUDGET - - -
              INPUT POWER   = 1.7441E-02 WATTS
              RADIATED POWER= 1.7441E-02 WATTS
              WIRE LOSS     = 0.0000E+00 WATTS
              EFFICIENCY    = 100.00 PERCENT

AVERAGE POWER GAIN= 1.94882E+00        SOLID ANGLE USED IN
AVERAGING=( 2.0000)*PI STERADIANS.
```

Using our handy calculation method, we obtain a radiation efficiency of 97.45%. One would think that we should obtain 100%, since there are no losses anywhere in the model. However, we did not sample the hemisphere at close intervals. The perfect-ground pattern for the monopole appears in **Fig. 75-2**.

Note the lobe structure near the zenith angle. It varies rapidly—more rapidly than our 5-degree interval can precisely track. The two small peaks (actually, circles of peak value on a true hemispherical display) occur between our 5-degree sampling intervals. So our rule of thumb must be this: the more irregular the pattern shape, the smaller the required interval between sampling steps.

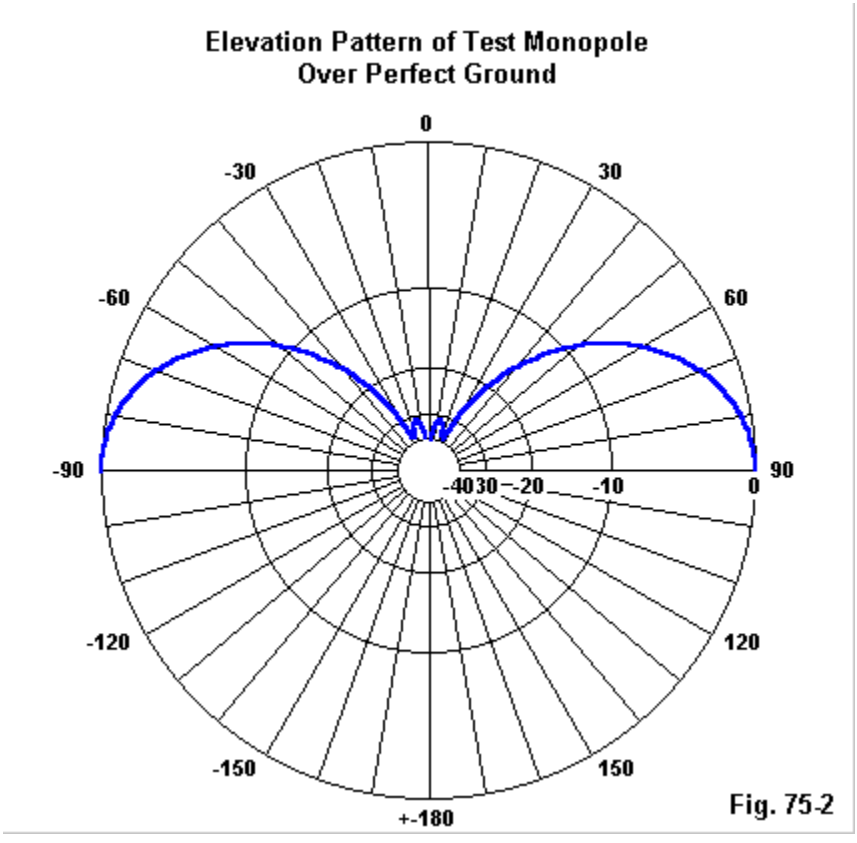

Fig. 75-2

Now let's add wire loss to the model by inserting an LD5 line into the model. See model 75-2.

```
LD 5 0 0 0 5.8e7 0
```

Now our report takes the following appearance.

```
                    - - - POWER BUDGET - -
                  INPUT POWER   = 1.7119E-02 WATTS
                  RADIATED POWER= 1.6890E-02 WATTS
                  WIRE LOSS     = 2.2951E-04 WATTS
                  EFFICIENCY    =  98.66 PERCENT

AVERAGE POWER GAIN= 1.92198E+00         SOLID ANGLE USED IN
AVERAGING=( 2.0000)*PI STERADIANS.
```

The power efficiency is 98.66%, due to the small losses of copper for the antenna elements. Our radiation efficiency is 96.10%, again off the mark by virtue of the sampling interval.

It is now time to revise the GN (ground specification) entry to place the antenna over a real ground. We shall use the standard default values for average ground (conductivity = 0.005 S/m, permittivity = 13). (Some programs call these values "good" ground.) The required revised GN line appears below.

```
GN 2 0 0 0 13 .005
```

After running NEC (-4 for these examples), the resulting report appears.

```
    - - - POWER BUDGET - - -
                  INPUT POWER   = 1.8126E-02 WATTS
                  RADIATED POWER= 1.7858E-02 WATTS
                  WIRE LOSS     = 2.6748E-04 WATTS
                  EFFICIENCY    =  98.52 PERCENT

AVERAGE POWER GAIN= 5.72269E-01         SOLID ANGLE USED IN
AVERAGING=( 2.0000)*PI STERADIANS.
```

The power efficiency changed slightly as a function of the fact that the source impedance upon which the power calculations are based also changed with the revision to the ground beneath the antenna. The average power gain over average ground is 0.5723, for a radiation efficiency of 28.62%. (Given the number of small

influences on the values that result from calculations, it is usually most profitable to take radiation efficiencies as whole numbers, even though this exercise shows them to 2 decimal places.)

Now let's change the antenna. I shall arbitrarily alter the length of the monopole to 5' (at 28.5 MHz), but retain all other properties. Eventually, I want to check out the radiation efficiencies of two ways of loading the antenna inductively to near resonance. The two ways appear in **Fig. 75-3**.

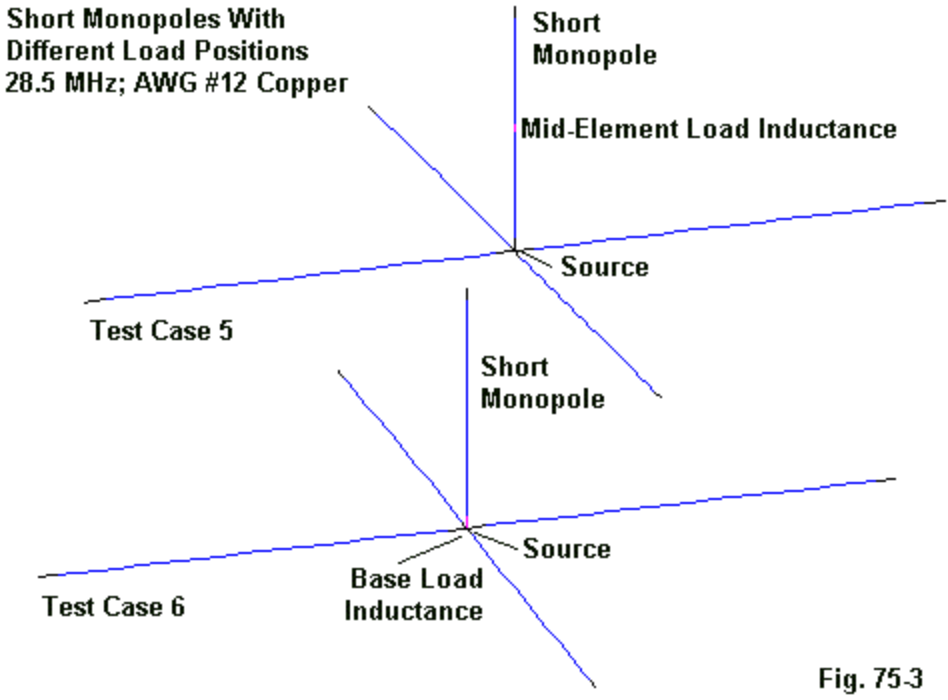

Fig. 75-3

Before we add either a mid-element or base loading inductor, let's run our revised model that has no loading at all. The model (75-4) has this structure:

```
CM radiation efficiency test vertical/4 radials
CM short length
CM copper conductor
CM SN-Ave ground
CM no loads
CE
GW 1 21 0 0 10 0 0 5 0.0033695
GW 2 21 0 0 5 8.7 0 5 0.0033695
GW 3 21 0 0 5 0 8.7 5 0.0033695
GW 4 21 0 0 5 -8.7 0 5 0.0033695
GW 5 21 0 0 5 0 -8.7 5 0.0033695
GS 0 0 .3048
GE 1 -1 0
GN 2 0 0 0 13 .005
LD 5 0 0 0 5.8e7 0
EX 0 1 21 0 1 0
FR 0 1 0 0 28.5 1
RP 0 19 73 1002 -90 0 5 5
EN
```

When we run NEC, we obtain this report.

```
                - - - POWER BUDGET - - -
              INPUT POWER   = 3.0774E-05 WATTS
              RADIATED POWER= 2.9852E-05 WATTS
              WIRE LOSS     = 9.2238E-07 WATTS
              EFFICIENCY    =  97.00 PERCENT

AVERAGE POWER GAIN= 5.79608E-01        SOLID ANGLE USED IN
AVERAGING=( 2.0000)*PI STERADIANS.
```

For a copper wire short monopole with full-length radials over average ground, our power efficiency has dropped by merely 1.5%. Since the average power gain is 0.5796, the radiation efficiency has actually increased (allowing for sampling inter-

val error) to 28.98%. (Actually, the difference is not supportable without a much tighter sampling interval.) If you revise this model and the full-length monopole that preceded it, you will discover that the gain difference is also not too significant (0.72 dBi at 20 degrees elevation for the full-length monopole, 0.69 dBi at 21 degrees for the short model).

Next, let's add a mid-element loading coil to bring the short monopole to near resonance. The required new LD4 line shows an R-X load of 1.89 + j 568 Ohms. In this and the next example, I shall use inductive reactances with a Q of 300.

```
LD 4 1 11 11 1.89 568
```

By adding the loading coil, we obtain near resonance, but show the following power and radiation efficiencies. See model 75-5.

```
                - - - POWER BUDGET - - -
           INPUT POWER   = 3.8337E-02 WATTS
           RADIATED POWER= 3.2516E-02 WATTS
           WIRE LOSS     = 5.8202E-03 WATTS
           EFFICIENCY    =  84.82 PERCENT

AVERAGE POWER GAIN= 4.99152E-01        SOLID ANGLE USED IN
AVERAGING=( 2.0000)*PI STERADIANS.
```

Wire loss now includes not only the copper material losses, but also the mid-element loading coil losses. Our power efficiency is 84.82%. The average power gain is 0.4992, for a radiation efficiency of 24.96%. The loading coil has cost us only 4% in radiation efficiency, but about 2/3-dB in gain. The antenna shows a gain of -0.04 dBi at 21 degrees elevation.

There is a wide-spread mythology that mid-element loading improves antenna performance properties by noticeable amounts over a base loading coil. There is an improvement in feedpoint impedance (in these examples, from 7 Ohms to about 13 Ohms), but the jury is out on performance until we look at the models. First, let's replace the mid-element LD4 line with an alternative base-loading line.

```
LD 4 1 21 21 1.06 318.05
```

The required inductive reactance to bring the initial short monopole to resonance is j 318.05 Ohms. The corresponding series resistance for a Q of 300 is 1.06 Ohms. With all other factors unchanged, we obtain the following efficiency reports. See model 75-6.

```
        - - - POWER BUDGET - - -
INPUT POWER   = 6.8603E-02 WATTS
RADIATED POWER= 5.6868E-02 WATTS
WIRE LOSS     = 1.1735E-02 WATTS
EFFICIENCY    =  82.89 PERCENT

AVERAGE POWER GAIN= 4.95310E-01          SOLID ANGLE USED IN
AVERAGING=( 2.0000)*PI STERADIANS.
```

The power efficiency has dropped 2 percentage points. However, the radiation efficiency has dropped only 0.2 percentage points to 24.77% (based on an average power gain of 0.4953). As well, the gain dropped only from -0.04 dBi to -0.06 dBi at 20-degrees elevation. What most folks overlook in the comparison of base loading and mid-element loading is that a mid-element loading coil must be considerably larger than a base loading coil, and for the same value of Q, that means an increase in the series resistance as well. Hence, except for the differential in feedpoint impedance—which can be useful in itself—the performance difference falls in the range of the operationally unnoticeable.

We have noted that there is no great correlation over small ranges of change between directional gain and radiation efficiency. Here, directional gain applies at least in the theta plane for our omni-directional monopole. The following table compares reported gain and radiation efficiencies of the base-loaded monopole as we change the soil type beneath it.

Soil Type	Cond. S/m	Perm.	Far-Field Gain dBi	Ave. Pwr Gain	Rad. Eff. %
Very Good	0.0303	20	+0.04	0.4766	23.83
Average	0.005	13	-0.06	0.4953	24.77
Poor	0.002	13	+0.13	0.5209	26.05
Very Poor	0.001	5	-0.42	0.4931	24.66

There are mathematical accounts for the changes shown in the table, but the values defy glib or simplistic generalizations.

To avoid any misimpression that the determination of radiation efficiency involves only vertical antennas, let's set up a horizontal dipole at 1 wavelength above ground, as shown in **Fig. 75-4**. We shall use AWG #12 copper wire for the antenna and select a near-resonant length. See model 75-7.

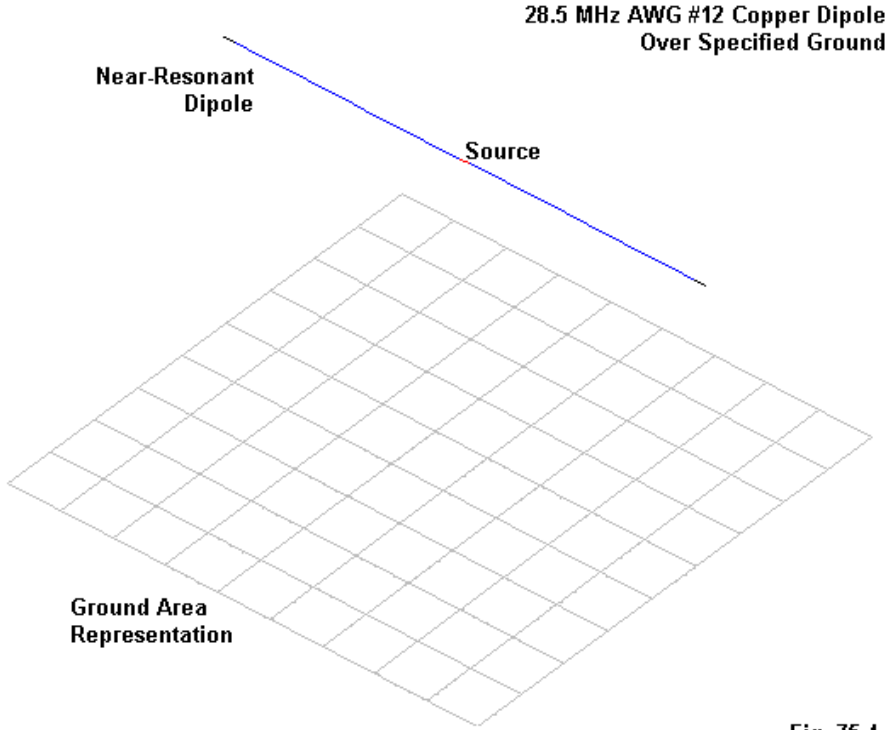

Fig. 75-4

Before we establish the antenna over ground, we shall first check it in free space. The free-space model has this appearance.

```
CM Copper #12 Dipole
CM Free Space
CE
GW 1 41 0 -100 420 0 100 420 0.0404331
GS 0 0 .02540
GE 0
EX 0 1 21 0 1 0
LD 5 1 1 41 5.8001E7
FR 0 1 0 0 28.5 1
RP 0 37 73 1002 0 0 5 5
EN
```

Note that we employ the RP0 call for a complete sphere of samples to arrive at the average power gain.

```
                    - - - POWER BUDGET - - -
                INPUT POWER   = 6.9136E-03 WATTS
                RADIATED POWER= 6.8595E-03 WATTS
                WIRE LOSS     = 5.4029E-05 WATTS
                EFFICIENCY    =  99.22 PERCENT

AVERAGE POWER GAIN= 9.92175E-01        SOLID ANGLE USED IN
AVERAGING=( 4.0000)*PI STERADIANS.
```

The power efficiency is 99.22%, allowing for the loss involved in using copper wire. The average power gain is 0.9922. Since we used a complete sphere, the radiation efficiency is 99.22%. We show no variance between power and radiation efficiencies, because the free-space pattern of a dipole is so regular. Next, let's place the dipole 35' (1 wavelength at 28.5 MHz) above average ground. Our model changes in several respects. See model 75-8.

```
CM Copper #12 Dipole
CM Average Ground
```

```
CE
GW 1 41 0 -100 420 0 100 420 0.0404331
GS 0 0 .02540
GE 1 -1 0
GN 2 0 0 0 13 .005
EX 0 1 21 0 1 0
LD 5 1 1 41 5.8001E7
FR 0 1 0 0 28.5 1
RP 0 19 73 1002 -90 0 5 5
EN
```

Besides changes in the GN entry, we also have a different RP0 call, since we shall now work with a hemisphere of samples. Here is the report that we obtain.

```
                    - - - POWER BUDGET - - -
                INPUT POWER   = 7.0811E-03 WATTS
                RADIATED POWER= 7.0243E-03 WATTS
                WIRE LOSS     = 5.6826E-05 WATTS
                EFFICIENCY    =  99.20 PERCENT

AVERAGE POWER GAIN= 1.47681E+00       SOLID ANGLE USED IN
```

The power budget remains essentially unchanged, despite the slight change in the source impedance that yields slightly different input and radiated power values. However, our average power gain is 1.4768, for a radiation efficiency of 73.84%. Unlike the vertical monopole, the horizontal dipole shows much more regular changes of radiation efficiency with changes of soil type, ranging from 80.01% over very good soil to 65.93% over very poor soil.

Conclusion

NEC will indeed yield a value for radiation efficiency, if we set up the proper RP0 call and select a sampling interval adequate to the level of precision that we may require from the report and subsequent calculation. The values produced may be surprising to some modelers, because for many types of analysis and design tasks, we are normally unconcerned over radiation efficiency. However, in the design of

vertical monopoles and arrays, as well as in the design of "mini-antennas," radiation efficiency may be a more important concept.

Depending upon the antenna design, there may be slight differences in the reports yielded by NEC-2 and NEC-4. All of the examples used here used NEC-4. The procedures remain the same in both programs, and the NEC models used here will run in NEC-2, but slight mathematical differences in the outputs may occur. So far, I have encountered none that reach the level of being significant relative to other data we may derive from our models.

Correlating radiation efficiency values to directional gain reports, soil type, and other data derived from models is neither simple nor automatic. Hence, the interpretation of relatively small changes in radiation efficiency (in contrast to very large changes) is the responsibility of the investigator and should rest upon appropriate considerations in addition to the data reports that emerge from the models.

At most, these notes show you how to get a radiation efficiency report. They do not show you what to do with it.

* * * * *

Models included: 75-1 through 75-8. (Models available in .NEC format only.)

Appendix: Antenna Models

This volume—the third of the 3 projected volumes—of antenna modeling notes comes with 100 antenna models, almost all of which have text references (Model xx-x). I have included most of the models in 3 different formats: .EZ for users of EZNEC, .NWP for NEC-Win Plus users, and .NEC for NEC-Win Pro, GNEC, and generic NEC-2 core users. The folder (directory) structure simply follows this scheme.

N:\models\ez	for EZNEC format files
N:\models\nec	for generic ASCII NEC files
N:\models\nwp	for NEC-Win Plus format files

I recommend that you copy the most relevant set of files into your hard drive for use. NEC-Win Plus, for example, will store its output files in the same directory as the basic model file, and that requires a space to which the computer can write. Each file name follows the text by starting with the column number, followed by the model number within the chapter. So Model 54-3 is the third model used in conjunction with column #54.

The files are not likely to add to your collection of models in the sense of providing new or interesting antenna designs. For that purpose, I have assembled collections of interesting models from my own storehouse. These collections are available from *antenneX*. The files that go with this volume of antenna modeling notes are those referenced in the text. As such, they are illustrations of the principles discussed in the text. Hence, you may read along with your own modeling software active and investigate further the model under discussion.

You will find some discrepancy between many of the model outputs and the performance figures cited in the text. This situations has a number of sources, all related to the fact that I began the series in the last century (the late 1990s). In some cases, I simply could not find the file used for a column, and so I had to reconstruct as best I could the model under discussion. Sometimes, the text did not provide complete modeling data, so I approximated the text model as closely as

possible. Although the exact figures may not jive between text and model, the trends certainly do.

In other cases, software developments are the source of slight numerical deviance between the model as used when I wrote and the same model when you run it on your current software. When I began the series of columns, EZNEC was a DOS program, and now uses Windows. NEC-Win Plus did not yet exist. In the course of time and software development, the NEC cores have undergone customizing and enhancement for speed—with special reference to the latest Fortran compilers. In the process, there have been changes in the order of operations and rounding conventions, enough to create slight output differences. With respect to guiding construction, showing performance trends, or yielding reliable analysis, the changes make no noticeable difference relative to older outputs. However, in order to show trends as sensitively as possible, many parts of the output data cited in the text will be overly precise. That fact will create an illusion of difference where no operationally significant difference exists.

Models for columns that deal with advanced commands—such as GC, GH, GM, GX, and WGF—require the use of a raw core or a program that includes the complete command set. Hence, they appear only in .NEC format.

I regret that I cannot include in this collection samples of MININEC files. I have and use several MININEC programs, including ELNEC, AO, MMANA, NEC4WIN, and the most recent and able version, Antenna Model. Each version uses a different file format, and there are few means of converting a MININEC file from one format to another except by writing the model from scratch. In contrast, I was able to convert files from one to another of the NEC formats. Conversion is not perfect, and so some EZNEC files given in English measures will appear in metric form in the generic NEC and NEC-Win Plus formats.

With these limitations in mind, I hope that the attached files enhance your safari through the topical jungle within this volume of antenna modeling notes.

Other Publications

We hope you've enjoyed this third in a series of several volumes of the **Antenna Modeling Notes.** Along with volumes 1 and 2, you'll find many other very fine books and publications by the author L.B. Cebik, W4RNL in the ***antenneX Online Magazine BookShelf*** at the web site shown below.

A Publication by
antenneX Online Magazine
http://www.antennex.com/
POB 271229
Corpus Christi, Texas 78427-1229
USA

Copyright © 2004 by **L. B. Cebik** jointly with ***antenneX Online Magazine***. All rights reserved. No part of this book may be reproduced or transmitted in any form, by any means (electronic, photocopying, recording, or otherwise) without the prior written permission of the author and publisher jointly.

ISBN: 1-877992-62-3